McGraw-Hill PROFESSIONAL ENGINEERING

- New pipe materials: profile-wall polyethylene & more
- New standards from ASTM, AWWA, ASHTTO & TRB
- New safety section for installation specifications
- More design examples

Buried Pipe Design

SECOND EDITION

A. P. Moser

Buried Pipe Design

A. P. Moser, Ph.D.
Mechanical Engineering
Utah State University
Logan, Utah

Second Edition

McGraw-Hill
New York Chicago San Francisco Lisbon London Madrid
Mexico City Milan New Delhi San Juan Seoul
Singapore Sydney Toronto

0-07-141801-6

The material in this eBook also appears in the print version of this title: 0-07-043503-0

DOI: 10.1036/0071418016

Contents

This page intentionally left blank.

Preface to Second Edition

In American cities, piping systems are complex and marvelous. But the average city dweller does not know of, and could not care less about, buried pipes and simply takes them for granted. This person cannot contemplate the consequences if these services were to be disrupted. City managers and pipeline engineers are sobered by the present-day reality of deteriorating pipe systems. The problem is almost overwhelming. Engineers who deal with piping systems will be key in helping to solve this problem. The First (1990) Edition of this book was well received and hopefully has been of some help to the various practitioners who deal with buried piping systems. It is also hoped that this Second Edition will be helpful in designing, installing, replacing, and rehabilitating buried pipe systems.

There has been progress and changes in the 11 years since the First Edition was published. Thus there are many expansions of and additions to the material in this new edition. Most of the material that appeared in 1990 is also included here, resulting in a book almost twice the size. In addition, there have been many small changes, such as corrections of the errors that were pointed out by readers. For this kind help, I offer my sincere thanks.

Following is a list of the subjects covered in each chapter, with special mention of new material.

Chapter 2, External Loads. Methods are given for the determination of loads that are imposed on buried pipes, along with the various factors that contribute to these loads.

The following topics have been added to this Second Edition: minimum soil cover, with a discussion of similitude; soil subsidence; load due to temperature rise; seismic loads; and flotation.

Chapter 3, Design of Gravity Flow Pipes. Design methods that are used to determine an installation design for buried gravity flow pipes are described. Soil types and their uses in pipe embedment and backfill are discussed. Design methods are placed in two general classes, rigid pipe design and flexible pipe design. Pipe performance limits are given, and recommended safety factors are reviewed. The powerful tool of the finite element method for the design of buried piping systems is discussed.

The following topics have been added: compaction techniques, *E´* analysis, parallel pipes and trenches, and analytical methods for predicting performance of buried flexible pipes.

Chapter 4, Design of Pressure Pipes. This chapter deals with the design methods for buried pressure pipe installations. Included in this chapter are specific design techniques for various pressure piping products. Methods for determining internal loads, external loads, and combined loads are given along with design bases.

The following topics have been added: corrected theory for cyclic life of PVC pipe, and strains induced by combined loading in buried pressurized flexible pipe.

Chapter 5, Rigid Pipe Products. This chapter deals with generic rigid pipe products. For each product, selected standards and material properties are listed. The standards are from standards organizations such as the American Water Works Association (AWWA) and American Society for Testing and Materials (ASTM). Actual design examples for the various products are given.

The following topics have been added: the direct method, design strengths for concrete pipe, and SPIDA (soil-pipe interaction design and analysis).

Chapter 6, Steel and Ductile Iron Flexible Pipe Products. This chapter deals with generic steel and ductile iron pipe products. For each product, selected standards and material properties are listed. The standards are from standards organizations such as AWWA and ASTM. Actual design examples for the various products are given.

The following topics have been added: three-dimensional FEA modeling of a corrugated steel pipe arch, tests on spiral ribbed steel pipe, test on low-stiffness ribbed steel pipe, and testing of ductile iron pipe.

Chapter 7, Plastic Flexible Pipe Products. This chapter deals with generic rigid pipe products. For each product, selected standards and material properties are listed. The standards are from standards organizations such as AWWA and ASTM. Actual design examples for the various products are given.

The following topics have been added: long-term stress relaxation and strain testing of PVC pipes, frozen-in stresses, cyclic pressures and elevated temperatures, the AWWA study on the use of PVC, long-term ductility of PE, the ESCR and NCTL tests for PE, and full-scale testing of HDPE profile-wall pipes.

Chapter 8, Pipe Installation and Trenchless Technology. The material in this chapter is entirely new to this book. It includes information on pipe handling and trenching as well as some safety aspects. The "Trenchless Technology" section contains information for the fast-growing trenchless methods for installing and rehabilitating pipelines.

A. P. Moser, Ph.D.

This page intentionally left blank.

Acknowledgments

Truly, piping system theory and application has been largely developed starting with Marston's premiere paper on loads, published in 1913, and Spangler's paper on flexible pipe, published in 1941. One could say that we are where we are today because we have been carried on the backs of giants who went before us. As the author of this book, I realize how much I am indebted to others who had the foresight and a desire to obtain answers where sometimes there were only questions. As an undergraduate student, I had the opportunity to work for Dr. R. K. Watkins on his buried structures projects. He had worked with Prof. Spangler. After obtaining a Ph.D. degree and returning to Utah State University (USU), I again worked with Dr. Watkins, this time as a colleague. It was at this time, in 1967, that USU, under the direction of Dr. Watkins, constructed the large pipe testing facility, under a contract from the American Iron and Steel Institute (AISI). Those on the technical committee of AISI at the time were people whom I consider to be giants in their profession, engineers with great foresight. Much of the material in this book is tied in some way to these individuals. I am indebted (indeed, we are all indebted) to them. In the testing facility archives, I found photographs of the committee taken at USU about 1967. Also in the photos are some USU personnel. (See Figs. P.1 and P.2.)

In the preparation of this Second Edition, I have drawn greatly from the First Edition. Also, source material is used from various standards and handbooks. Acknowledgment is given throughout the book where this material is used.

I express my deepest appreciation to those who helped to make this edition possible. I am indebted to:

Dr. Mohammad Najafi of Missouri Western State College, who provided much of the material on trenchless technology found in Chap. 8. Thanks goes to Dr. Najafi and others who helped with the publications he supplied. His works with his coauthors are found in the References of Chap. 8.

Figure P.1 AISI committee with newly completed test cell. (Photograph taken about 1967.)

Figure P.2 AISI committee and some USU personnel in a USU conference room. (Photograph taken about 1967.)

Dr. Reynold K. Watkins (Professor Emeritus) of Utah State University, for his many years of help and encouragement.

The many sponsors of pipe research and testing who, over the years, have allowed me to gain both theoretical and practical knowledge, understanding, and insight into problems and solutions pertaining to buried piping systems. This understanding forms the foundation of this book.

The many publishers who graciously gave permission to use their materials.

My staff assistants at Utah State University, Andrea and Janet, for their tremendous help.

My wife Kay for proofreading the manuscript, and for her general patience and understanding during the preparation of this new edition.

This page intentionally left blank.

Chapter

1

Introduction and Overview

Underground conduits have served to improve people's standard of living since the dawn of civilization. Remnants of such structures from ancient civilizations have been found in Europe, Asia, and even the western hemisphere, where some of the ancient inhabitants of South and Central America had water and sewer systems. These early engineering structures are often referred to as examples of the art of engineering. Nevertheless, whether art or science, engineers and scientists still stand amazed at these early water and sewer projects. They seem to bridge the gap between ancient and modern engineering practice. The gap referred to here is that period known as the "dark ages" in which little or no subsurface construction was practiced—a time when most of the ancient "art" was lost.

Today, underground conduits serve in diverse applications such as sewer lines, drain lines, water mains, gas lines, telephone and electrical conduits, culverts, oil lines, coal slurry lines, subway tunnels, and heat distribution lines. It is now possible to use engineering science to design these underground conduits with a degree of precision comparable with that obtained in designing buildings and bridges. In the early 1900s, Anson Marston developed a method of calculating the earth load to which a buried conduit is subjected in service. This method, the Marston load theory, serves to predict the supporting strength of pipe under various installation conditions. M. G. Spangler, working with Marston, developed a theory for flexible pipe design. In addition, much testing and research have produced quantities of empirical data which also can be used in the design process. Digital computers, combined with finite element techniques and sophisticated soil models, have given the engineering profession design tools which have produced, and will undoubtedly continue to produce, even more precise designs.

Engineers and planners realize that the subsurface infrastructure is an absolute necessity to the modern community. It is true we must "build down" before we can "build up." The underground water systems serve as arteries to the cities, and the sewer systems serve as veins to carry off the waste. The water system is the lifeblood of the city, providing culinary, irrigation, and fire protection needs. The average man or woman on the street takes these systems for granted, being somewhat unaware of their existence unless they fail. In the United States today, people demand water of high quality to be available, instantaneously, on demand. To ensure adequate quality, the distribution systems must be designed and constructed so as not to introduce contaminants.

Sewage is collected at its source and carried via buried conduits to a treatment facility. Treatment standards and controls are becoming continually more stringent, and treatment costs are high. Because of these higher standards, the infiltration of groundwater or surface water into sewer systems has become a major issue. In the past, sewer pipe joining systems were not tight and permitted infiltration. Today, however, tight rubber ring joints or cemented joints have become mandatory.

Even though septic tanks and cesspools are still widely used today, they are no longer accepted in urban or suburban regions. Only in the truly rural (farm) areas are they sanctioned by health departments. Today, more sewer systems are being installed. This produces a demand for quality piping systems. Thus, the need for water systems that deliver quality water and for tight sanitary sewers has produced a demand for high-quality piping materials and precisely designed systems that are properly installed.

Old and deteriorating conduits frequently fail. These failures can cause substantial property damage that results in tremendous cost, inconvenience, and loss of public goodwill. Utilities have programs to replace or rejuvenate deteriorating pipes to minimize failures and associated costs. In urban areas, trenching to remove the old and install the new can be very difficult and extremely expensive. Relining and microtunneling are viable options in certain situations where it is difficult and extremely disruptive to construct an open trench.

Soil Mechanics

Various parameters must be considered in the design of a buried piping system. However, no design should overlook pipe material properties or the characteristics of the soil envelope surrounding the pipe.

The word *soil* means different things to different people. To engineers, soil is any earthen material excluding bedrock. The solid particles of which soil is composed are products of both physical and chemical action, sometimes called weathering of rock.

Soil has been used as a construction material throughout history. It is used for roads, embankments, dams, and so forth. In the case of sewers, culverts, tunnels, and other underground conduits, soil is important, not only as a material upon which the structure rests, but also as a support and load-transfer material. The enveloping soil transfers surface and gravity loads to, from, and around the structure. Much has been written about soil mechanics and soil structure interaction. Such variables as soil type, soil density, moisture content, and depth of the installation are commonly considered. If finite element analysis is used, many soil characteristics are required as input to the mathematical soil model. These soil properties are usually determined from triaxial shear tests.

Standards organizations such as the American Association of State Highway and Transportation Officials (AASHTO) and the American Society for Testing and Materials (ASTM) issue standard test methods for classifying soil and for the determination of various soil properties. Of the various methods of soil classification, the Unified Soil Classification System (USCS) is most commonly used in the construction industry. Complete details on this system can be found in any textbook or manual of soils engineering. (For example, see *Soils Manual MS-10,* The Asphalt Institute, College Park, Md., 1978.)

Soils vary in physical and chemical structure, but can be separated into five broad groups:

Gravel. Individual grains vary from 0.08 to 3 in (2 to 75 mm) in diameter and are generally rounded in appearance.

Sand. Small rock and mineral fragments are smaller than 0.08 in (2 mm) in diameter.

Silt. Fine grains appear soft and floury.

Clay. This very fine-textured soil forms hard lumps when dry and is sticky to slick when wet.

Organic. This is peat.

Soils are sometimes classified into categories according to the ability of the soil(s) to enhance the structural performance of the pipe when installed in the particular soil. One such classification is described in ASTM D 2321, "Standard Practice for Underground Installation of Flexible Thermoplastic Sewer Pipe."

The project engineer often requires a soil survey along the route of a proposed pipeline. Information from the survey helps to determine the necessary trench configuration and to decide whether an imported soil will be required to be placed around the pipe. Soil parameters such as soil type, soil density, and moisture content are usually considered in a design. Soil stiffness (modulus) is an extremely important soil property and is the main contributor to the pipe-soil system performance. Experience has shown that a high soil density will ensure a high soil stiffness. Therefore, soil density is usually given special importance in piping system design.

Economy in any design is always a prime consideration. The engineer must consider the cost of compaction compared to the cost of bringing in a select material such as pea gravel which will flow into place in a fairly dense state. For piping systems, a compacted, well-graded, angular, granular material provides the best structural support. However, such is not always required. In selecting a backfill material, the designer will consider such things as depth of cover, depth of water table, pipe materials, compaction methods available, and so forth.

Strength of Materials

There are many types of piping materials on the market today, ranging from rigid concrete to flexible thermal plastic. Proponents of each lay claim to certain advantages for their material. Such things as inherent strength, stiffness, corrosion resistance, lightness, flexibility, and ease of joining are some characteristics that are often given as reasons for using a particular material.

A pipe must have enough strength and/or stiffness to perform its intended function. It must also be durable enough to last for its design life. The term *strength* as used here is the ability to resist stress. Stresses in a conduit may be caused by such loadings as internal pressure, soil loads, live loads, differential settlement, and longitudinal bending, to name a few. The term *stiffness* refers to the material's ability to resist deflection. Stiffness is directly related to the modulus of elasticity of the pipe material and the second moment of the cross section of the pipe wall. Durability is a measure of the pipe's ability to withstand environmental effects with time. Such terms as *corrosion resistance* and *abrasion resistance* are durability factors.

Piping materials are generally placed in one of two classifications: rigid or flexible. A *flexible* pipe has been defined as one that will deflect at least 2 percent without structural distress. Materials that do not meet this criterion are usually considered to be *rigid.* Claims that a particular pipe is neither flexible nor rigid, but somewhere in between have little importance since current design standards are based either on the concept of a flexible conduit or on the concept of a rigid conduit. This important subject will be discussed in detail in subsequent chapters. See Fig. 1.1.

Concrete and clay pipes are examples of materials which are usually considered to be rigid. Steel and plastic pipes are usually considered to

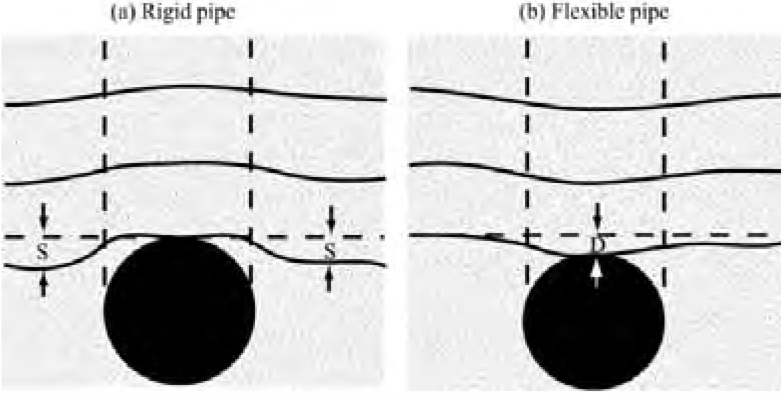

Figure 1.1 The effect of soil settlement on (*a*) rigid and (*b*) flexible pipes. Here S represents settlement of backfill for a rigid pipe; D represents vertical deflection of a flexible pipe as it deflects under earth pressure. (*Reprinted, by permission, from AWWA Manual M-11, Steel Pipe Design and Installation, American Water Works Association, 1964.*)

be flexible. Each type of pipe may have one or more performance limits which must be considered by the design engineer. For rigid pipes, strength to resist wall stresses due to the combined effects of internal pressure and external load is usually critical. For flexible pipes, stiffness may be important in resisting ring deflection and possible buckling. Each manufacturer or industry goes to great lengths to establish characteristics of its particular product. These parameters are readily available to the design engineer. The desire to have products with high strength has given rise to reinforced products such as steel-reinforced concrete and glass-reinforced thermal setting plastic. For such products, other performance limits often arise such as a strain limit to prevent cracking. For a thermal plastic pipe, such as PVC pipe, strength is measured in terms of a long-term hydrostatic design hoop stress. Thus, it can be seen that not all installations of all products will be designed in exactly the same manner. The engineer must be familiar with design criteria for the various pipe products and know where proper design parameters can be obtained.

Pipe Hydraulics

The field of study of fluid flow in pipes is often referred to as *hydraulics*. Designers of water or sewer systems need some knowledge of pipe hydraulics.

Flow in pipes is usually classified as *pressure flow* for systems where pipes are flowing full or *open-channel flow* when pipes are not flowing full. Water systems are pressure systems and are considered to be flowing full. On the other hand, sewer systems, for the most part, are open-channel systems. The exception to this is forced sewer mains where lift pumps are used to pump sewage under pressure. The relatively small concentration of solids found in sanitary or storm sewage is not sufficient to make it behave hydraulically significantly differently from water. Thus, sewage is accepted to have the same hydraulic flow characteristics as water. Of course, the design engineer must be aware of the possibility of the deposition of solids and hydrogen sulfide gas generation in sanitary sewers. These considerations are not within the scope of this text.

In either case, pressure flow or open-channel flow, the fluid encounters frictional resistance. This resistance produces head loss, which is a function of the inside surface finish or pipe roughness. The smoother the inside surface, the better the flow. Many theories and empirical equations have been developed to describe flow in pipes. The solution of most flow problems requires experimentally derived coefficients which are used in conjunction with empirical equations. For pressure flow, the Hazen-Williams equation is widely accepted. Another equation that has a more theoretical basis is attributed to Darcy and Weisback. For open-channel flow, the *Manning equation* is normally used. These equations, or others, are used to calculate head loss as a function of flow or vice versa.

Water Systems

Water systems are lifelines of communities. They consist of such items as valves, fittings, thrust restraints, pumps, reservoirs, and, of course, pipes and other miscellaneous appurtenances. The water system is sometimes divided into two parts: the transmission lines and the distribution system. The transmission system is that part of the system which brings water from the source to the distribution system. Transmission lines have few, if any, interconnections. Because of this, flow in such a line is usually considered to be quasi-steady with only relatively small transients. Such lines are normally placed in fairly shallow soil cover. The prime design consideration is internal pressure. Other design considerations include longitudinal stresses, ring deflection, buckling, and thrust restraints.

The distribution piping system distributes water to the various users. It includes many connections, loops, and so forth. The design is somewhat similar to that of transmission lines except that a substantial surge allowance for possible water hammer is included in the pressure design. Also, greater care is usually taken in designing the backfill for around the pipe, fittings, and connections. This is done to prevent longitudinal bending and differential settlement. Distribution systems are made up of an interconnected pipe network. The hydraulic analysis of such a system is almost impossible by "hand" methods, but is readily accomplished using programming methods via digital computers.

Wastewater Systems

A sewage system is made up of a collection system and a treatment system. We are concerned only with the collection part. For the most part, sanitary sewers and storm (street) sewers are separate. However, there are a few older cities in North America which use *combined sewers*. The ills of these combined sewers have been recognized by modern engineers, and such systems are no longer designed. Most state and regional engineering and public works officials and agencies no longer permit installation of these dual-purpose lines. Unfortunately, many combined sewers are used throughout the world, and some still exist in the United States.

Some sanitary sewers are pressurized lines (sewer force mains), but most are gravity flow lines. The sanitary sewer is usually buried quite deep to allow for the pickup of water flow from basements. Due to this added depth, higher soil pressures, which act on the pipe, are probable. To resist these pressures, pipe strength and/or pipe stiffness become(s) important parameters in the design. Soil backfill and its placement and compaction also become important to the design engineer. The installation may take place below the water table so construction procedures may include dewatering and wide trenching. For such a system, the pipe should be easy to join with a tight joint that will prevent infiltration. The soil-pipe system should be designed and constructed to support the soil load. The pipe material should be chemically inert with respect to soil and sewage, including possible hydrogen sulfides. The inside wall should be relatively smooth so as not to impede the fluid flow.

Storm sewer design conditions are not as rigorous as they are for sanitary sewers. Storm sewers are normally not as deep. The requirements for the joining system are often very lax and usually allow exfiltration and infiltration. Because of the above, loose joining systems are often acceptable for storm sewers. The design life for any sewer system should also be 100 years minimum.

Design for Value

The piping system must be strong enough to withstand induced stresses, have relatively smooth walls, have a tight joining system, and be somewhat chemically inert with respect to soil and water. The piping systems must be designed to perform for an extended period.

The normal design life for such systems should be 50 years minimum. However, 50 years is not long enough. Government and private agencies cannot afford to replace all the buried pipe infrastructures on a 50-year basis. A 100-year design life should be considered minimum. Pipe manufacturers warrant their products to be free from manufacturing defects, but cannot guarantee the pipe will perform for a given length of time. This is because the life of the pipe, after it is installed, is not just a function of the pipe material, but is largely a function of the loading conditions and the environment to which it is subjected. It is the design engineer's responsibility to assess all factors and formulate a design with a predicted design life. The cost of the system should be based on life considerations, not just initial cost.

Most piping system contracts are awarded to the lowest bidder. Contractors will usually bid materials and construction methods which allow for the lower initial cost with little thought to future maintenance or life of the system. Even for the owner, the lowest initial cost is often the overriding factor. However, the owner and the engineer should insist on a design based on value. For engineers, economics is always an important consideration; any economic evaluation must include more than just initial cost. Annual maintenance and life of the system must also be considered.

Initial cost may include such things as piping materials, trenching, select backfill, compaction, site improvements and restoration, and engineering and inspection. Pipe cost is related to pipe material and to pipe diameter. Diameter is controlled by the design flow rate and pipe roughness. That is, a smaller diameter may be possible if a pipe with a smooth interior wall is selected. Annual maintenance cost includes cleaning, repair, and replacement due to erosion, corrosion, and so forth. Life is directly related to durability and is affected by such things as severe loading conditions, corrosion, erosion, and other types of environmental degradation. It is important to design the installation to minimize detrimental effects.

The question is not whether the pipe will last, but how long it will perform its designed function. Generally, metals corrode in wet clayey soils and corrode at an accelerated rate in the presence of hydrogen sulfide sewer gas. Concrete-type structures are also attacked by hydrogen sulfide and the resulting sulfuric acid. Care should be taken when selecting a pipe product for any service application and installation conditions to ensure that environmental effects upon the life of the system have been taken into consideration. The system should be designed for value.

Chapter

2

External Loads

Loads are exerted on buried pipes by the soil that surrounds them. Methods for calculating these loads are given in this chapter. Marston's theory for loads on buried conduits is discussed along with the various factors which contribute to these loads. Underground pipes are placed in tunnels, buried under highways, buried under railways, and buried under airports. Methods are given for the determination of loads which are imposed on pipes in these and other applications.

Soil Pressure

The subject of soil structure interaction has been of engineering interest since the early 1900s. The horseless carriage had its volume-production start with the Oldsmobile in 1902, and the need for improved roads was immediately apparent. Many projects for road drainage were begun using clay tile and concrete drain tile. One major problem existed, however. There was no rational method of determining the earth load these buried drains would be subjected to. As a result, there were many failures of pipelines.

The loads imposed on conduits buried in the soil depend upon the stiffness properties of both the pipe structure and the surrounding soil. This results in a statically indeterminate problem in which the pressure of the soil on the structure produces deflections that, in turn, determine the soil pressure.

When designing rigid pipes (for example, concrete or clay pipes), it is customary to assume that the pipe is affected mainly by a vertical pressure caused by soil and traffic; a horizontal reacting pressure is either nonexistent or negligible. For flexible pipes, the vertical load causes a deflection of the pipe, which in turn results in a horizontal supporting soil pressure. If the horizontal soil pressure and vertical pressure are close to being equal, the load around the pipe approximates a hydrostatic load. The stresses in the pipe wall are then mainly circumferential (hoop) compressive stresses, and for deep burial will give rise to buckling.

Rigid pipe

Marston load theory. Anson Marston, who was dean of engineering at Iowa State University, investigated the problem of determining loads on buried conduits. In 1913, Marston published his original paper, "The Theory of Loads on Pipes in Ditches and Tests of Cement and Clay Drain Tile and Sewer Pipe."[15] This work was the beginning of methods for calculating earth loads on buried pipes. The formula is now recognized the world over as the Marston load equation. More recently, demands to protect and improve our environment and rising construction costs have produced research that has substantially increased our knowledge of soil structure interaction phenomenon. However, much of this knowledge has yet to be applied to design practice. Many questions are as yet unresolved.

Anson Marston

Trench condition. The Marston load theory is based on the concept of a prism of soil in the trench that imposes a load on the pipe, as shown in Fig. 2.1. A trench (ditch) conduit as defined by Marston was a relatively narrow ditch dug in undisturbed soil. Marston reasoned that settlement of the backfill and pipe generates shearing or friction forces at the sides of the trench. He also assumed that cohesion would be negligible since (1) considerable time would have to elapse before cohesion could develop and (2) the assumption of no cohesion would yield the maximum load on the pipe.

The vertical pressure V at the top of any differential volume element $B_d(1)\,dh$ is balanced by an upward vertical force at the bottom of the element $V + dV$ (see Fig. 2.1). The volume element is B_d wide, dh tall, and of unit length along the axis of the pipe and trench. The weight of the elemental section is its volume times its unit weight, expressed as

$$w = B_d\,(dh)\,(1)\,\gamma$$

where $(B_d)(dh)(1)$ is volume of the element and γ is the specific weight density.

The lateral pressure P_L at the sides of the element at depth h is

$$P_L = \frac{\text{active lateral unit pressure}}{\text{vertical unit pressure}} \times (\text{vertical unit pressure})$$

or

$$P_L = K\,(\text{Rankine's ratio}) \times \frac{V}{B_d}$$

The shearing forces per unit length F_s on the sides of the differential element, induced by these lateral pressures, are $F_s = K(V/B_d)(\mu')\,dh$ where μ' = coefficient of friction. The vertical forces on the element are summed and set equal to zero.

$$F_v = 0$$

Or, the upward vertical forces are equal to the downward vertical forces. Thus, for equilibrium, vertical force at bottom + shear force at sides = vertical force at top + weight of the element, or

$$(V + dV) + \frac{2K\mu'\,V}{B_d\,dh} = V + \gamma B_d\,dh$$

(dimensionally, force per length) or

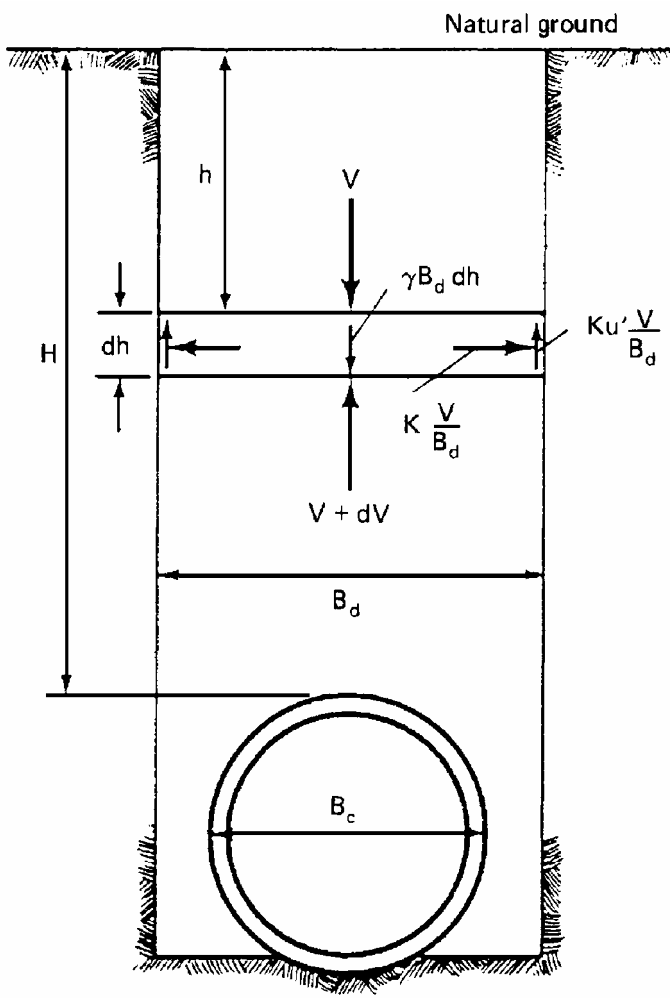

Figure 2.1 Basis for Marston's theory of loads on buried pipe. W_d = load on conduit per unit length along conduit in pounds per linear foot; e = base of natural logarithms; γ = unit weight of backfill, i.e., pounds per cubic foot; V = vertical pressure on any horizontal plane in backfill, in pounds per unit length of ditch; B_c = horizontal breadth (outside) of conduit, in feet; B_d = horizontal width of ditch at top of conduit, in feet; H = height of fill above top of conduit, in feet; h = distance from ground surface down to any horizontal plane in backfill, in feet; C_d = load coefficient for ditch conduits; $\mu = \tan \varphi$ = coefficient of internal friction of backfill; $\mu' = \tan \varphi$ = coefficient of friction between backfill and sides of ditch; K = ratio of active lateral unit pressure to vertical unit pressure. (*Reprinted from Spangler and Handy, Soil Engineering, 4th ed., Harper & Row, 1982, by permission of the publisher.*)

$$0 = \left(B_d - \frac{2K\mu' V}{B_d}\right)\frac{dh}{dV} \tag{2.1}$$

The solution to the differential Eq. (2.1) is

$$V = \frac{\gamma B_d^{\,2}}{2K\mu'}\left(1 - e^{-2K\mu'(hB_d)}\right) \tag{2.2}$$

Substituting $h = H$, we get the total vertical pressure at the elevation of the top of the conduit. How much of this vertical load V is imposed on the conduit is dependent upon the relative compressibility (stiffness) of the pipe and soil. For very rigid pipe (clay, concrete, heavy-walled cast iron, and so forth), the sidefills may be very compressible in relation to the pipe, and the pipe may carry practically all the load V. For flexible pipe, the imposed load will be substantially less than V since the pipe will be less rigid than the sidefill soil (see Fig. 2.3). The maximum load on ditch conduits is expressed in Eq. (2.2) with $h = H$. For simplicity and ease of calculation, the load coefficient C_d is defined as

$$C_d = \frac{1 - e^{-2K\mu'(H/B_d)}}{2K\mu'} \tag{2.3}$$

Now the load on a rigid conduit in a ditch is expressed as

$$W_d = C_d \gamma B_d^{\,2} \tag{2.4}$$

The function

$$C_d = \frac{1 - e^{-2K\mu'(H/B_d)}}{2K\mu'}$$

is then plotted as H/B_d versus C_d for various soil types as defined by their $K\mu'$ values, where $K\mu'$ is a function of the coefficient of internal friction of the fill material (see Fig. 2.2). The values of K, μ, and μ' were determined experimentally by Marston, and typical values are given in Table 2.1.

Example Problem 2.1 What is the maximum load on a very rigid pipe in a ditch excavated in sand? The pipe outside diameter (OD) is 18 in, the trench width is 42 in, the depth of burial is 8 ft, and the soil unit weight is 120 lb/ft^3.

1. Determine C_d. From Table 2.1 for sand, $K\mu = K\mu' = 0.165$.

$$\frac{H}{B_d} = \frac{8\text{ ft}}{42\text{ in}} \times \frac{12\text{ in}}{1\text{ ft}} = 2.29$$

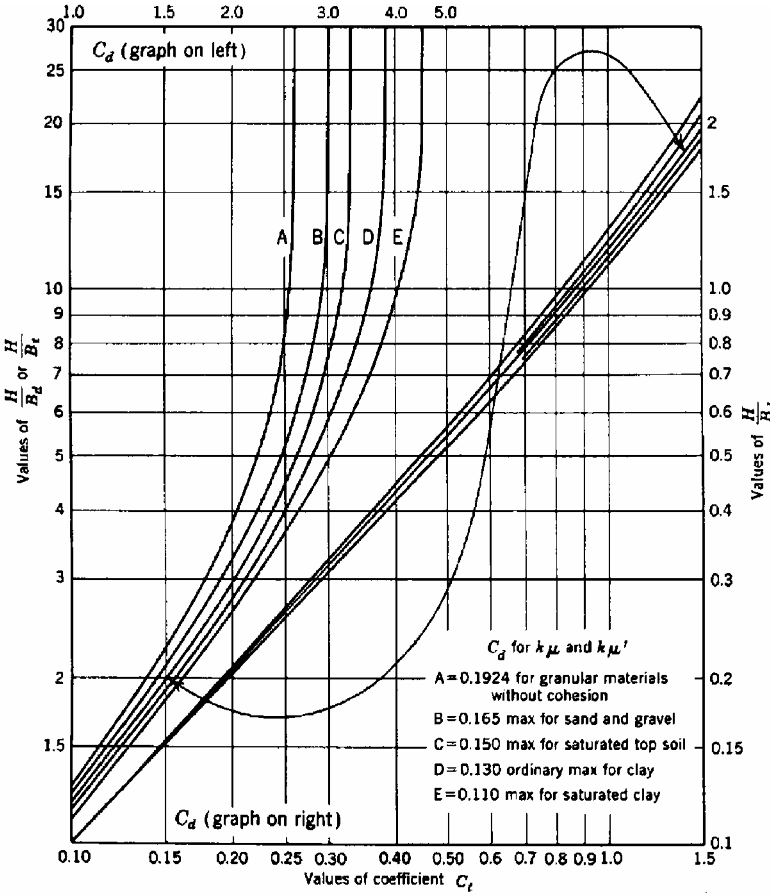

Figure 2.2 Computational diagram for earth loads on trench conduits completely buried in trenches. (*Reprinted, by permission, from Gravity Sanitary Sewer Design and Construction, Manuals & Reports on Engineering Practice, No. 60, American Society of Civil Engineers, and Manual of Practice, No. FD-5, Water Pollution Control Federation, 1982, p. 170.*)

From Fig. 2.2, $C_d = 1.6$.

2. Calculate the load from Eq. (2.4):

$$W_d = C_d \gamma B_d^{\,2} = 1.6\,(120)\left(\frac{42}{12}\right)^2 = 2352 \text{ lb/ft}$$

Embankment conditions. Not all pipes are installed in ditches (trenches); therefore, it is necessary to treat the problem of pipes buried in embankments. An embankment is where the top of the pipe

TABLE 2.1 Approximate Values of Soil Unit Weight, Ratio of Lateral to Vertical Earth Pressure, and Coefficient of Friction against Sides of Trench

Soil type	Unit weight, lb/ft^3	Rankine's ratio K	Coefficient of friction μ
Partially compacted damp topsoil	90	0.33	0.50
Saturated topsoil	110	0.37	0.40
Partially compacted damp clay	100	0.33	0.40
Saturated clay	120	0.37	0.30
Dry sand	100	0.33	0.50
Wet sand	120	0.33	0.50

is above the natural ground. Marston defined this type of installation as a positive projecting conduit. Typical examples are railway and highway culverts. Figure 2.4 shows two cases of positive projecting conduits as proposed by Marston. In case I, the ground at the sides of the pipe settles more than the top of the pipe. In case II, the top of the pipe settles more than the soil at the sides of the pipe. Case I was called the projection condition by Marston and is characterized by a positive settlement ratio r_{sd}, as defined in Fig. 2.4. The shear forces are downward and cause a greater load on the buried pipe for this case. Case II is called the ditch condition and is characterized by a negative settlement ratio r_{sd}. The shear forces are directed upward in this case and result in a reduced load on the pipe.

In conjunction with positive projecting conduits, Marston determined the existence of a horizontal plane above the pipe where the shearing forces are zero. This plane is called the *plane of equal settlement*. Above this plane, the interior and exterior prisms of soil settle equally. The condition where the plane of equal settlement is real (it is located within the embankment) is called an incomplete projection or an incomplete ditch condition. If the plane of equal settlement is imaginary (the shear forces extend all the way to the top of the embankment), it is called a complete ditch or complete projection condition.

All the above discussed parameters affect the load on the pipe and are incorporated in Marston's load equation for positive projecting (embankment) conduits

$$W_c = C_c \gamma B_c^2 \tag{2.5}$$

where

$$C_c = \frac{e^{\pm 2K\mu(H/B_c)} - 1}{\pm 2K\mu} \tag{2.6}$$

or

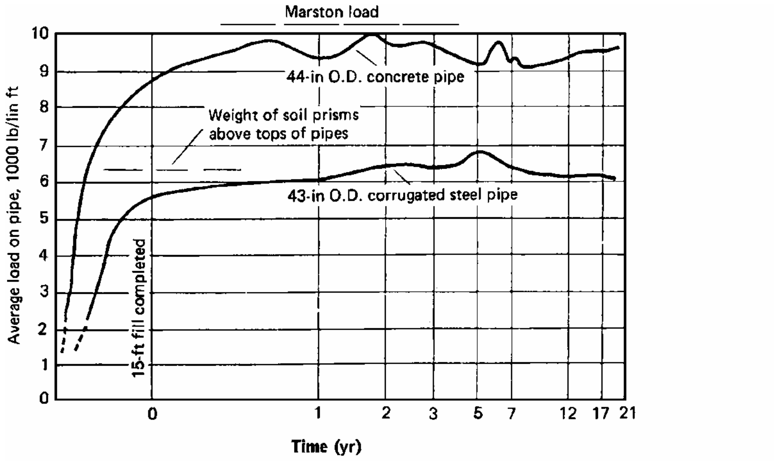

Figure 2.3 Measured loads on rigid and flexible pipe over a period of 21 years. (*Reprinted from Spangler and Handy, Soil Engineering, 4th ed., Harper & Row, 1982, by permission of the publisher.*)

$$C_c = \frac{e^{\pm 2K\mu(H_e/B_c)} - 1}{\pm 2K\mu} + \left(\frac{H}{B_c} - \frac{H_e}{B_c}\right) e^{\pm 2K\mu(H_e/B_c)} \tag{2.7}$$

Equation (2.6) is for the complete condition. The minus signs are for the complete ditch, and the plus signs are for the complete projection condition. Equation (2.7) is for the incomplete condition, where the minus signs are for the incomplete ditch and the plus signs are for the incomplete projection condition. And H_e is the height of the plane of equal settlement. Note that if $H_e = H$, the incomplete case of Eq. (2.7) becomes the complete case and Eq. (2.6) applies for C_c.

Although the above equations are difficult and cumbersome, they have been simplified and can be found in graphical form in many references.

Note that value C_c is a function of the ratio of height of cover to pipe diameter, the product of the settlement ratio and projection ratio, Rankine's constant, and the coefficient of friction.

$$C_c = f\left(\frac{H}{B_c}, r_{sd}p, K, \mu\right)$$

The value of the product $K\mu$ is generally taken as 0.19 for the projection condition and 0.13 for the ditch condition. Figure 2.5 is a typical diagram of C_c for the various values of H/B_c and $r_{sd}p$ encountered. Table 2.2 gives the equations of C_c as a function of H/B_c for various values of $r_{sd}p$ and $K\mu$.

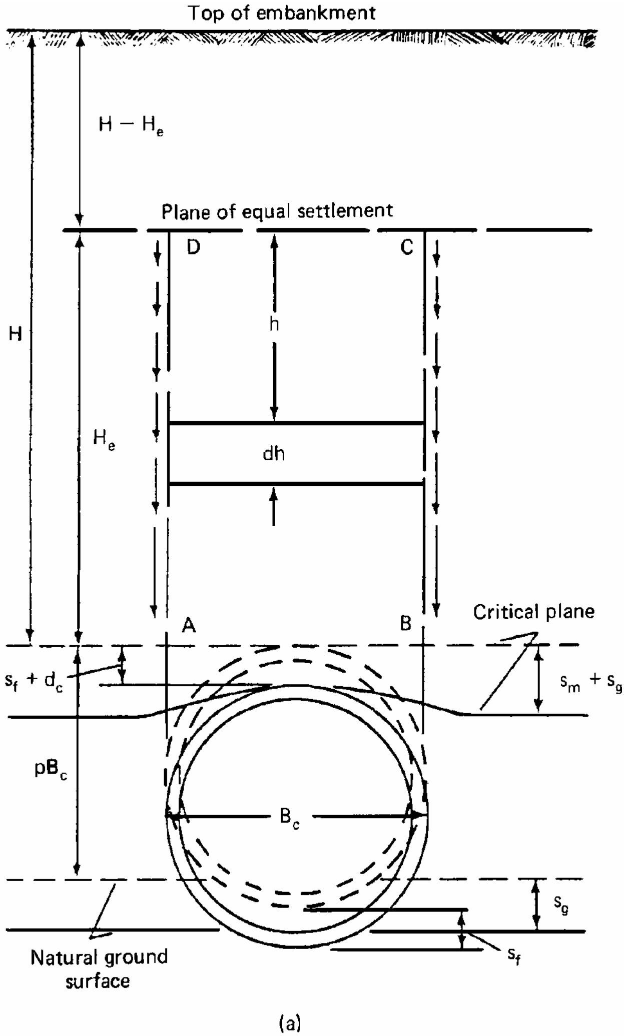

Figure 2.4 Comparison of positive projecting conduits: (*a*) Projection conditions; (*b*) ditch condition. $r_{sc} = [(S_m + S_g) - (S_f + d_c)]/S_m$; r_{sd} = settlement ratio; s_m = compression of soil at sides of pipe; s_g = settlement of natural ground surface at sides of pipe; s_f = settlement of foundation underneath pipe; d_c = deflection of the top of pipe. (*Reprinted from Spangler and Handy, Soil Engineering, 4th ed., Harper & Row, 1982, by permission of the publisher.*)

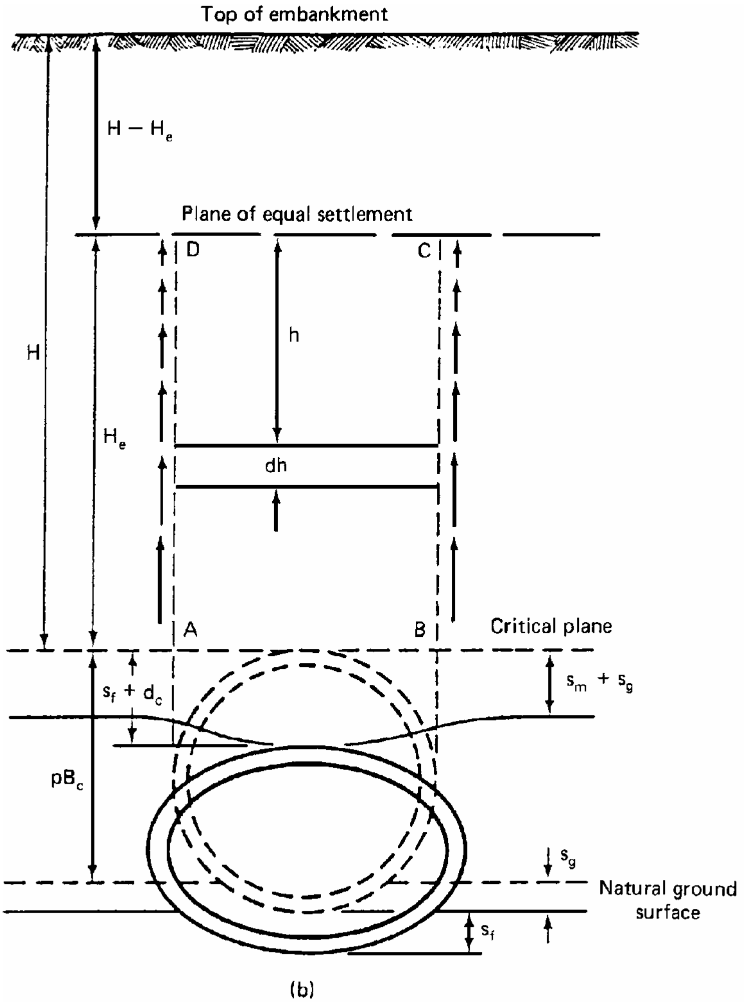

Figure 2.4 *(Continued)*

The settlement ratio r_{sd} is difficult, if not impossible, to determine even empirically from direct observations. Experience has shown that the values tabulated in Table 2.3 can be used with success. Note that when $r_{sd}p = 0$, $C_c = H/B_c$ and $W_c = H\gamma B_c$. This is the prism load (i.e., the weight of the prism of soil over the top of the pipe). When $r_{sd} = 0$, the plane at the top of the pipe called the critical plane settles the

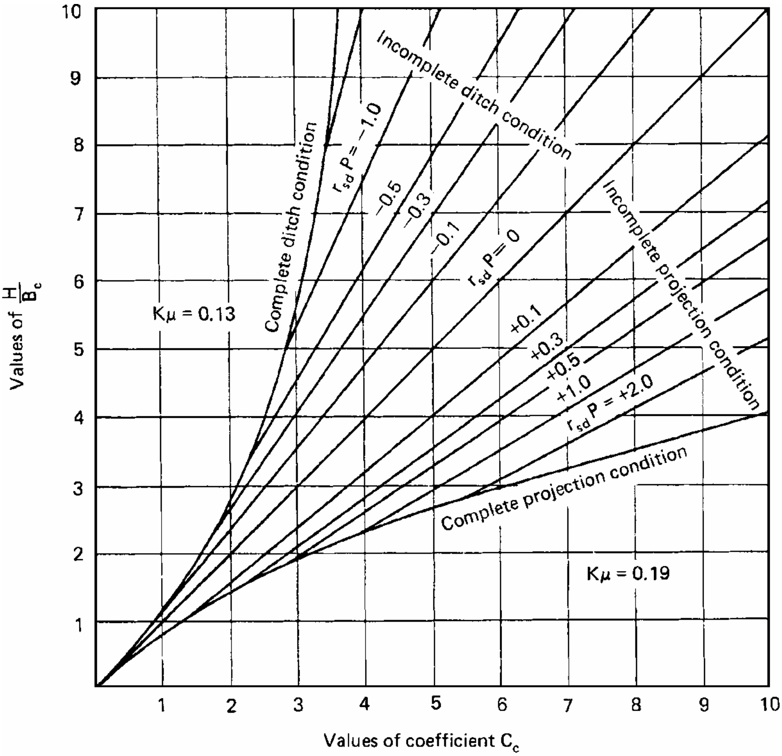

Figure 2.5 Diagram for coefficient C_c for positive projecting conduits. (*Reprinted from Spangler and Handy, Soil Engineering, 4th ed., Harper & Row, 1982, by permission of the publisher.*)

TABLE 2.2 Values of C_c in Terms of H/B_c

Incomplete projection condition $K\mu = 0.19$		Incomplete ditch condition $K\mu = 0.13$	
$r_{sd}p$	Equation	$r_{sd}p$	Equation
+0.1	$C_c = 1.23\, H/B_c - 0.02$	−0.1	$C_c = 0.82\, H/B_c + 0.05$
+0.3	$C_c = 1.39\, H/B_c - 0.05$	−0.3	$C_c = 0.69\, H/B_c + 0.11$
+0.5	$C_c = 1.50\, H/B_c - 0.07$	−0.5	$C_c = 0.61\, H/B_c + 0.20$
+0.7	$C_c = 1.59\, H/B_c - 0.09$	−0.7	$C_c = 0.55\, H/B_c + 0.25$
+1.0	$C_c = 1.69\, H/B_c - 0.12$	−1.0	$C_c = 0.47\, H/B_c + 0.40$
+2.0	$C_c = 1.93\, H/B_c - 0.17$		

SOURCE: Reprinted from Spangler and Handy, *Soil Engineering,* 4th ed., Harper & Row, 1982, by permission of the publisher.

TABLE 2.3 Design Values of Settlement Ratio

Conditions	Settlement ratio
Rigid culvert on foundation of rock or unyielding soil	+1.0
Rigid culvert on foundation of ordinary soil	+0.5 to +0.8
Rigid culvert on foundation of material that yields with respect to adjacent natural ground	0 to +0.5
Flexible culvert with poorly compacted side fills	−0.4 to 0
Flexible culvert with well-compacted side fills*	−0.2 to +0.8

*Not well established.

SOURCE: Reprinted from Spangler and Handy, *Soil Engineering,* 4th ed., Harper & Row, 1982, by permission of the publisher.

same amount as the top of the conduit (see Fig. 2.4). The settlement ratio is defined as

$$r_{sd} = \frac{(S_m + S_g) - (S_f + d_c)}{S_m} \tag{2.8}$$

Critical plane settlement $= S_m$ (strain in side soil) + S_g (ground settlement). Settlement of the top of the pipe $= S_f$ (conduit settlement) + d_c (vertical pipe deflection). If $S_m + S_g = S_f + d_c$, then $r_{sd} = 0$.

When a pipe is installed in a narrow, shallow trench with the top of the pipe level with the adjacent natural ground, the projection ratio p is zero. The distance from the top of the structure to the natural ground surface is represented by pB_c.

The question may be asked, Is Marston's equation for the earth load on a rigid pipe in a ditch valid regardless of the width of the trench? The answer to this question was given by W. J. Schlick, a colleague of Marston, in 1932.[21] Schlick found that Marston's equation, Eq. (2.4), for W_d was valid until the point where the ditch conduit load W_d was equal to the projection conduit load W_c. That is, the load will continue to increase according to Eq. (2.4) for an increasing trench width until the ditch load is equal to the embankment load. Once this point is reached, the correct load must be calculated by Eq. (2.5). The trench width at which this occurs is called the *transition width.* Figure 2.6 is a plot of values of H/B_c and $r_{sd}p$ that give B_d/B_c values that represent the transition width. That is, $W_c = W_d$. It is generally suggested that an $r_{sd}p$ value of 0.5 be used to determine the transition width.

If the calculation of B_d/B_c is:

- Greater than that of Fig. 2.6, use W_d.
- Less than that of Fig. 2.6, use W_c.
- Equal to that of Fig. 2.6, then $W_c = W_d$.

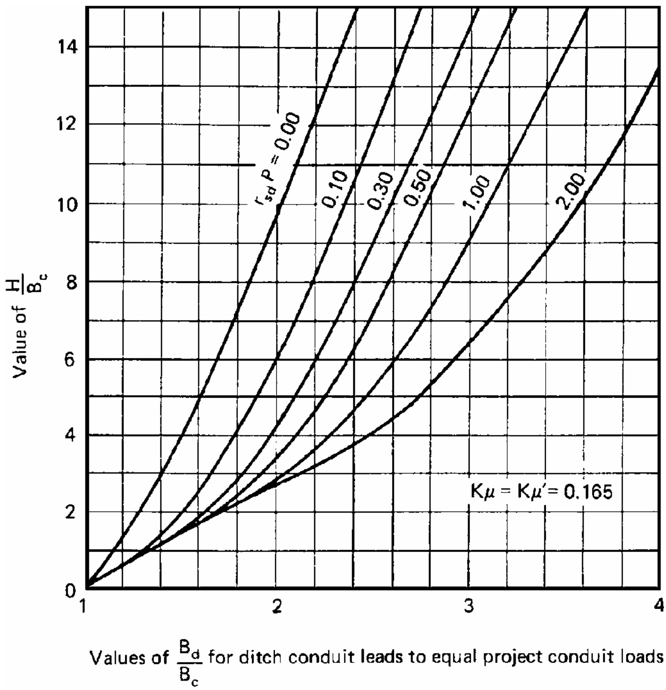

Figure 2.6 Curves for transition-width ratio. (*Reprinted from Spangler and Handy, Soil Engineering, 4th ed., Harper & Row, 1982, by permission of the publisher.*)

Example Problem 2.2 What is the transition width for a 12-in pipe buried 6 ft deep?

$$\frac{H}{B_C} = \frac{6 \text{ ft}}{12 \text{ in}} \times \frac{12 \text{ in}}{1 \text{ ft}} = 6$$

From Fig. 2.6,

$$\frac{B_d}{B_c} = 2.35$$

$$r_{sd}p = 0.5$$

$$B_d \text{ (transition)} = \frac{B_d}{B_c} B_c = 2.35 \text{ (1 ft)} = 2.35 \text{ ft}$$

Tunnel construction. Marston's theory may be used to determine soil loads on pipes that are in tunnels or that are jacked into place through undisturbed soil. The Marston tunnel load equation is

$$W_t = C_t B_t (\gamma B_t - 2C) \tag{2.9}$$

where W_t is the load on the pipe in pounds per linear foot and γ is specific weight. The load coefficient C_t is obtained in the same way that C_d was determined (see Fig. 2.2). And B_t is the maximum tunnel width; or if the pipe is jacked, B_t is the OD of the pipe. The coefficient C is called the *cohesion coefficient* and is, dimensionally, force per unit area (lb/ft^2).

Equation (2.3) can be used in calculating C_t as well as C_d. This equation indicates that for very large values of H/B, C_t approaches a limiting value of $1/(2K\mu')$. Thus, for very deep tunnels, the load can be closely estimated by using the value of $1/(2K\mu')$ for C_t.

It is readily apparent that the theory for loads on pipes in tunnels or being jacked through undisturbed soil is almost identical to the theory for loads on pipes in trenches. The tunnel load will be somewhat less because of the soil cohesion. It is also apparent from Eq. (2.9) that C is very important in determining the load. Unfortunately, values of the coefficient C have a wide range of variation even for similar soils. The value of C may be determined by laboratory tests on undisturbed samples. Conservative values of C should be used in design to account for possible saturation of the soil. It has been suggested that about one-third of the laboratory determined value should be used for design. The Water Pollution Control Federation (WPCF) *Manual of Practice,* No. FD-5, recommends the use of values given in Table 2.4 if reliable laboratory data are not available or if such tests are impractical. It is also suggested that this coefficient be taken as zero for any zone subjected to seasonal frost and cracking or loss of strength because of saturation. The factor $\gamma B_t - 2C$ cannot be negative. Therefore, $2C$ cannot be larger than γB_t.

Flexible pipe

A flexible pipe derives its soil-load-carrying capacity from its flexibility. Under soil load, the pipe tends to deflect, thereby developing passive soil support at the sides of the pipe. At the same time, the ring deflection relieves the pipe of the major portion of the vertical soil load which is picked up by the surrounding soil in an arching action over the pipe. The effective strength of the flexible pipe-soil system is remarkably high. For example, tests at Utah State University indicate that a rigid pipe with a three-edge bearing strength of 3300 lb/ft buried in class C bedding will fail by wall fracture with a soil load of about 5000 lb/ft. However, under identical soil conditions and loading, a PVC sewer pipe deflects only 5 percent. This is far below the deflection that would cause

TABLE 2.4 Recommended Safe Values of Cohesion *C*

Material	Values of C	
	kPa	lb/ft^2
Clay, very soft	2	40
Clay, medium	12	250
Clay, hard	50	1000
Sand, loose, dry	0	0
Sand, silty	5	100
Sand, dense	15	300

damage to the PVC pipe wall. Thus the rigid pipe has failed, but the flexible pipe performed successfully and still has a factor of safety with respect to failure of 4 or greater. Of course, in flat-plate or three-edge loading, the rigid pipe will support much more than the flexible pipe. This anomaly tends to mislead some engineers because they relate low flat-plate supporting strength with in-soil load capacity—something one can do for rigid pipes but cannot do for flexible pipes.

Marston load theory. For the special case when the sidefill and pipe have the same stiffness, the amount of load V that is proportioned to the pipe can be found merely on a width basis. This means that if the pipe and the soil at the sides of the pipe have the same stiffness, the load V will be uniformly distributed as shown in Fig. 2.7. By simple proportion the load becomes

$$W_c = \frac{W_d B_c}{B_d} = \frac{C_d \gamma B_d^{\,2} B_c}{B_d}$$

or

$$W_c = C_d \gamma B_c B_d \tag{2.10}$$

Pipe stiffness versus soil compressibility. Measurements made by Marston and Spangler revealed that the load on a flexible pipe is substantially less than that on a rigid pipe (see Fig. 2.3). The magnitude of this difference in loads may be a little shocking. The following analogy will help us to understand what happens in the ground as a flexible pipe deflects. Suppose a weight is placed on a spring. We realize the spring will deform, resisting deflection because of its spring stiffness. When load versus deflection is plotted, we find that this relationship is linear up to the elastic limit of the spring (Fig. 2.8). When a load is placed on a flexible pipe, the pipe also deflects and resists deflection because of its stiffness. It is even possible to think of soil as

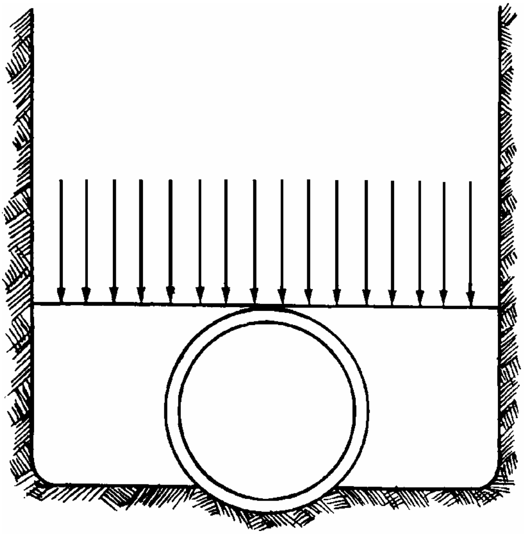

Figure 2.7 Load proportioning according to Marston's theory for a flexible pipe.

being a nonlinear spring that resists movement or deflection because of its stiffness (Fig. 2.9).

When we draw an analogy between a rigid pipe represented by a stiff spring in comparison to soil at its sides, represented by more flexible springs, and then place a load or weight on this spring system representing a rigid pipe in soil, we can easily visualize the soil deforming and the pipe carrying the majority of the load (see *a* in Fig. 2.10). If the situation is reversed and we place a flexible spring between two springs which are much stiffer, representing the soil, we can again picture the pipe deflecting as a load is applied and the soil in this case being forced to carry the load to a greater extent (see *b* in Fig. 2.10).

When a flexible pipe is buried in the soil, the pipe and soil then work as a system in resisting the load (Fig. 2.11). The system is statically indeterminate. That is, the deflection of the pipe is a function of the load on the pipe, but the load on the pipe is a function of the deflection. The reduction in load imposed on a pipe because of its flexibility is sometimes referred to as *arching*. However, the overall performance of a flexible pipe is not just due to this so-called arching, but is also due to the soil at the sides of the pipe resisting deflection (see Fig. 2.12).

Equation (2.10) has become known as the Marston load equation for flexible pipes. It should be remembered, however, that the assumption of soil friction resisting the downward movement of the central soil

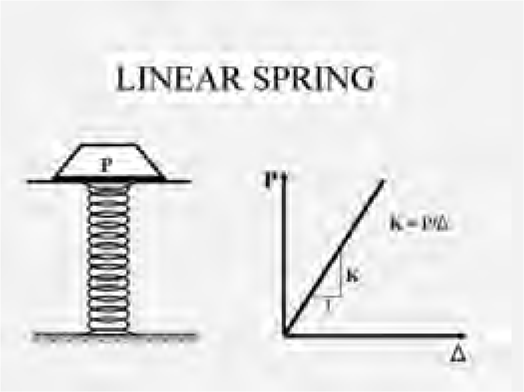

Figure 2.8 Graphic of linear spring.

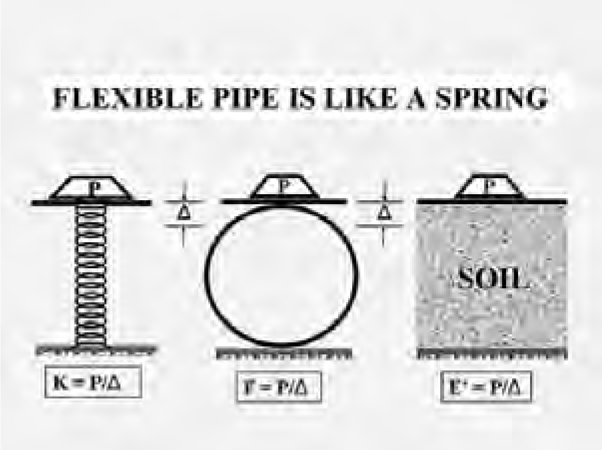

Figure 2.9 Graphic of spring, pipe, and soil.

prism has been used in its development, and that it should not be used merely because a pipe is flexible. The maximum loads on rigid and flexible pipes as predicted by the Marston equations, (2.4) and (2.10), do not take place instantaneously and may not occur for some time. In certain cases the initial load may be 20 to 25 percent less than the maximum load predicted by Marston, and the long-term load may be greater than that predicted.

Example Problem 2.3 For Example Problem 2.1, what would be the load if the pipe and side soil had approximately the same stiffness?

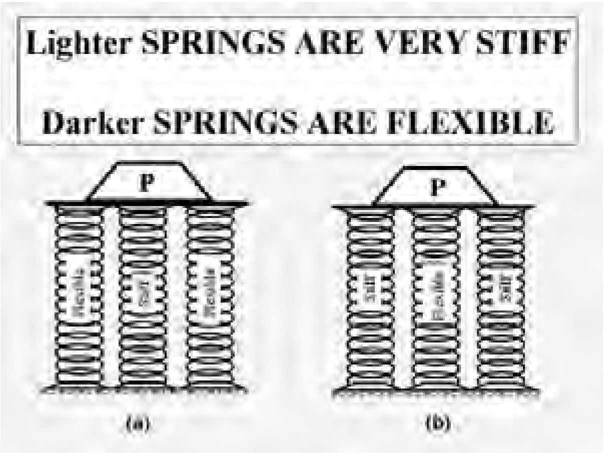

Figure 2.10 Flexible and stiff springs working together.

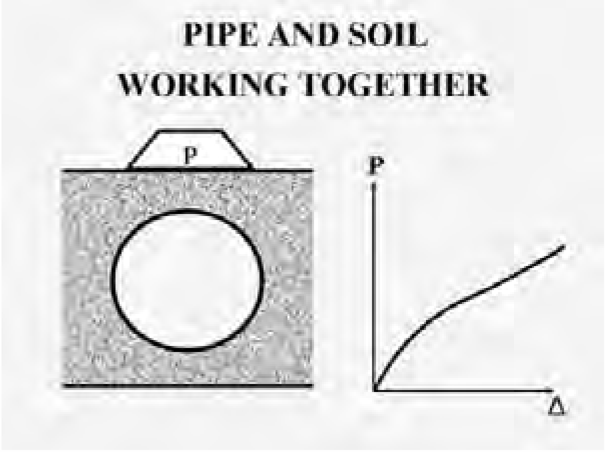

Figure 2.11 Graphic of pipe and soil working together as a system.

$$W_c = C_d \gamma B_c B_d = 1.6\,(120)\left(\frac{42}{12}\right)\left(\frac{18}{12}\right) = 1008 \text{ lb/ft} \tag{2.10}$$

Prism load. Again, Eq. (2.4) represents a maximum-type loading condition, and Eq. (2.10) represents a minimum. For a flexible pipe, the maximum load is always much too large since this is the load acting on a rigid pipe. The minimum is just that, a minimum. The actual load will lie somewhere between these limits.

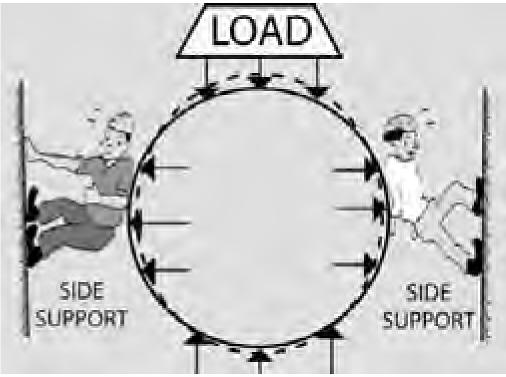

Figure 2.12 Graphic showing the contribution of sidefill soil in the performance of a flexible pipe.

A more realistic design load for a flexible pipe would be the prism load, which is the weight of a vertical prism of soil over the pipe. Also, a true trench condition may or may not result in significant load reductions on the flexible conduit since a reduction depends upon the direction of the frictional forces in the soil. Research data indicate that the effective load on a flexible conduit lies somewhere between the minimum predicted by Marston and the prism load. On a long-term basis, the load may approach the prism load. Thus, if one desires to calculate the effective load on a flexible conduit, the prism load is suggested as a basis for design. The prism or embankment load is given by the following equation (see Fig. 2.13):

$$P = \gamma H \tag{2.11}$$

where P = pressure due to weight of soil at depth H
γ = unit weight of soil
H = depth at which soil pressure is required

Example Problem 2.4 Assume an 8-in-OD flexible pipe is to be installed in a 24-in-wide trench with 10 ft of clay soil cover. The unit weight of the soil is 120 lb/ft^3. What is the load on the pipe?

For the Marston load, use Eq. (2.10) for minimum W:

$$W_d = C_d \gamma B_c B_d$$

where C_d = 2.8, from Fig. 2.2
γ = 120 lb/ft^3
B_d = trench width = 2 ft
B_c = OD = 8 in = $^2/_3$ ft

$$\text{Marston load} = W_d = (2.8)\,(120)\,(2)\,(^2/_3) = 448 \text{ lb/ft}$$

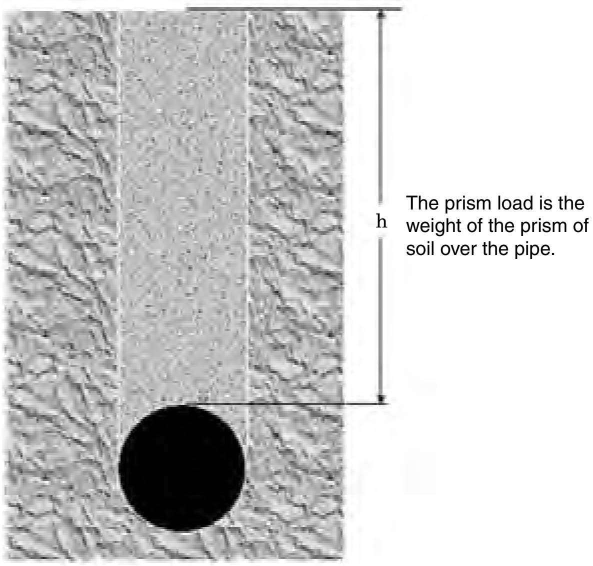

Figure 2.13 Graphic depiction of the prism load on a pipe.

For the prism load, use Eq. (2.11):

$$P = \gamma H = 120\ (10) = 1200\ \text{lb/ft}^2$$

To obtain load in pounds per foot, multiply the above by the pipe OD in feet:

$$W = 1200\ (^2/_3) = 800\ \text{lb/ft}$$

The Marston load for this example is 56 percent of the prism load and is unconservative for design. Again, for flexible conduits, the prism load theory represents a realistic estimate of the maximum load and is slightly conservative.

Trench condition. The Marston-Spangler equation for the load on a flexible pipe in a trench is given by Eq. (2.10). The load coefficient C_d is obtained from Fig. 2.2. One may ask, Under what conditions, if any, will the prism load and the ditch (trench) load be equal?

$$\text{Prism load } P = \gamma H \qquad \text{lb/ft}^2$$

$$\text{Marston load } W_d = C_d \gamma B_d B_c$$

Multiply the prism load by B_c (to express in pounds per foot, as in the Marston load) and set it equal to the Marston load.

$$PB_c = \gamma HB_c = W_d = C_d \gamma B_d B_c$$

Solve for

$$C_d = \frac{H}{B_d}$$

Thus the prism load is a special case of the Marston-Spangler trench load. In Fig. 2.2, $C_d = H/B_d$ is plotted as a straight 45° line. One of the advantages of the prism load is that it is independent of trench width.

Embankment condition. The load on a flexible pipe in an embankment may be calculated by the Marston-Spangler theory via Eq. (2.5).

$$W_c = C_c \gamma B_c^2$$

This equation does not include a trench width term since a trench is not involved. Again it is interesting to set this load equal to the prism load.

$$\text{Prism load} \times B_c = PB_c = \gamma HB_c$$

$$\text{Marston embankment load } W_c = C_c \gamma B_c^2$$

Equating the two loads,

$$\gamma HB_c = C_c \gamma B_c^2$$

or

$$C_c = \frac{H}{B_c}$$

and C_c can be determined from Fig. 2.5. The above equation plots as a straight 45° line on Fig. 2.5. This is the line shown for $r_{sd}p = 0$. Thus for an embankment, the prism load is the same as the Marston load for $r_{sd}p = 0$.

Tunnel loadings. There are few documented data dealing with loads on flexible pipes placed in unsupported tunnels. However, since a flexible pipe develops a large percentage of its load-carrying capacity from passive side support, this support must be provided, or the pipe will tend to deflect until the sides of the pipe are being supported by the sides of the tunnel.

When a flexible pipe is jacked into undisturbed soil, the load may be calculated by either the prism load, Eq. (2.11), or Eq. (2.9).

$$B_t = B_c$$

$$W_p = PB_t = \gamma HB_t \tag{2.11}$$

$$W_t = C_t B_t (\gamma B_t - 2C) \tag{2.9}$$

The prism load in this case will be very conservative because it neglects not only friction but also the cohesion of the soil. If C_t is taken as H/B_t and the cohesion coefficient is zero, then the two methods of calculating loads give the same results.

Longitudinal Loading

Certain types of pipe failures which have been observed over the years are indicative of the fact that only under ideal conditions is a pipeline truly subjected to only vertical earth loading. There are other forces that in some way produce axial bending stresses in the pipe. These forces can be large, highly variable, and localized and may not lend themselves to quantitative analysis with any degree of confidence. Some of the major causes of axial bending or beam action in a pipeline area are

1. Nonuniform bedding support
2. Differential settlement
3. Ground movement for such external forces as earthquakes or frost heave

Nonuniform bedding support

A nonuniform bedding can result from unstable foundation materials, uneven settlement due to overexcavation and nonuniform compaction, and undermining, such as might be produced by erosion of the soil into a water course or by a leaky sewer.

One of the advantages of a flexible conduit is its ability to deform and move away from pressure concentrations. The use of flexible joints also enhances a pipe's ability to yield to these forces and reduces the risk of rupture. These advantages, coupled with good engineering and a proper installation, virtually eliminate axial bending as a cause of failure in a flexible pipe. The examples which follow in Figs. 2.14, 2.15, and 2.16 give an indication of the magnitude of bending moments that might be induced.

Axial bending of a long tube in a horizontal plane will produce vertical ring deflection ($\Delta y/D$) due to the bending moments created. Reissner[20] has amplified the work of others in this area, and the following formula results from his work on pure bending of a long pressurized tube:

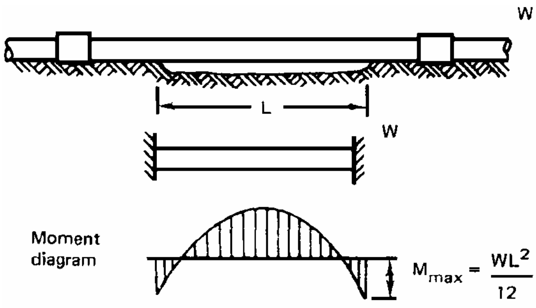

Figure 2.14 Longitudinal bending of conduits.

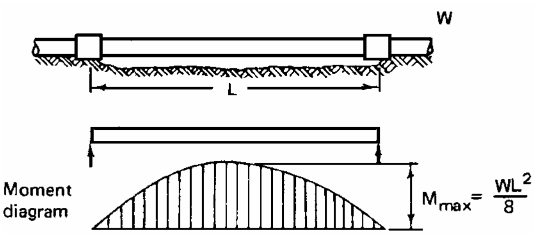

Figure 2.15 Longitudinal bending of conduits.

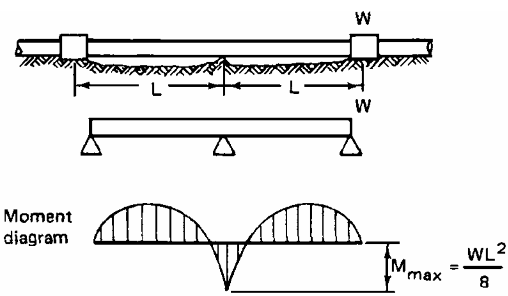

Figure 2.16 Longitudinal bending of conduits.

$$\frac{\Delta y}{D} = \frac{1}{16}\left(\frac{D}{t}\right)^2\left(\frac{D}{R}\right)^2 \tag{2.12}$$

where D = nominal pipe diameter
t = pipe thickness
R = radius of curvature of longitudinally deflected pipe
$\frac{\Delta y}{D}$ = ring deflection

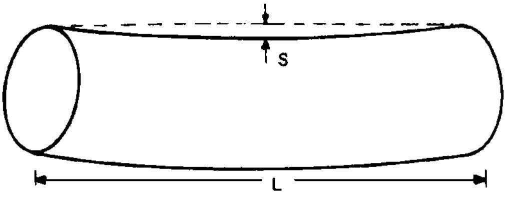

$$\frac{\Delta y}{D} = \frac{1}{16}\left(\frac{D}{t}\right)^2\left(\frac{D}{R}\right)^2 \qquad \frac{D}{R} \approx \frac{8SD}{L^2}$$

Example: rpm pipe D/t = 60, L = 20 ft, D = 24 in

S	$\Delta y/D$
2 in	1.2%
3 in	2.7%
4 in	4.8%

Longitudinal bending

Buckling radius of curvature R_b

$$R_b = \frac{D}{1.12\ t/D}$$

Figure 2.17 Ring deflection due to axial bending.

Although Reissner's derivation included internal pressure, it has been omitted from Eq. (2.12) because the nonpressure case is the more critical for ring deflection (see Fig. 2.17). This type of bending frequently occurs when pipes are bent around corners.

Differential settlement

Differential settlement of a manhole or other structure to which the pipe is rigidly connected can induce not only high bending moments, but also shearing forces. These forces and moments are set up when the structure and/or the pipe moves laterally with respect to the other. Quantitatively, these induced stresses are not easily evaluated. Effort should be made during design and during construction to see that differential settlement is eliminated or at least minimized. This can be accomplished by the proper preparation and compaction of foundation and bedding materials for both the structure and the connecting pipe.

Ground movement

Certain types of soils (mostly expansive clays) are influenced by moisture content. Such soil may be subjected to seasonal rise and fall due to changes in moisture. Good practice does not allow pipes to be embedded directly in such soils. Nevertheless, such shifting by adjacent soil can and will affect a pipeline. Normally these movements are relatively small but may be large enough to adversely affect the pipe performance.

To mitigate such adverse effects for rigid pipe, short lengths are used with flexible joints. In the case of flexible pipe, the pipe's natural flexibility tends to allow the pipe to conform to these movements without structural distress. In this case, both longitudinal flexibility and diametrical flexibility are important.

Tidal water may also cause ground movement. These movements may be designed for as described above.

Wheel Loading (Live Loads)

Boussinesq solution

Here, live loads mean static or quasi-static surface loads. Buried conduits may be subjected to such applied loads produced by ground transportation traffic. The French mathematician Boussinesq calculated the distribution of stresses in a semi-infinite elastic medium due to a point load applied at its surface. This solution assumes an elastic, homogeneous, isotropic medium, which soil certainly is not. However, experiments have shown that the classical Boussinesq solution, when properly applied, gives reasonably good results for soil.

Figure 2.18 compares the percent of a surface load that is felt by a buried pipe as a function of depth of burial as calculated by the Boussinesq equation and as found from measurements.

Hall and Newmark integrated the Boussinesq solution to obtain load coefficients. The integration developed by Hall for C_s is used for calculating concentrated loads (such as a truck wheel) and is given in the following form:

$$W_{sc} = \frac{C_s P F'}{L} \tag{2.13}$$

where W_{sc} = load on pipe, lb/unit length
P = concentrated loads, lb
F' = impact factor (see Table 2.5)
L = effective length of conduit (3 ft or less), ft
C_s = load coefficient which is a function of $B_c/(2H)$ and $L/(2H)$, where H = height of fill from top of pipe to ground surface, ft; and B_c = diameter of pipe, ft

The integration developed by Newmark for C_s is used for calculating distributed loads and is given in the form

$$W_{sd} = C_s p F' B_c \tag{2.14}$$

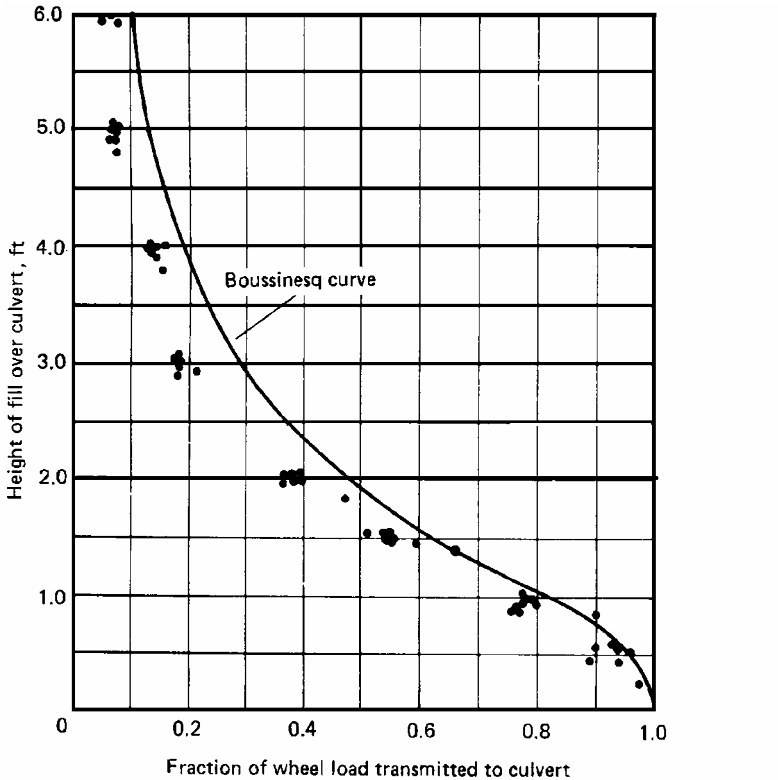

Figure 2.18 Distribution of surface live loads versus loads on a plane at depths of cover. Boussinesq solutions versus actual measurement. (*Reprinted from Spangler and Handy, Soil Engineering, 4th ed., Harper & Row, 1982, by permission of the publisher.*)

TABLE 2.5 Impact Factor *F*' versus Height of Cover

	Installation surface condition			
Height of cover, ft	Highways	Railways	Runways	Taxiways, aprons, hardstands, run-up pads
0 to 1	1.50	1.75	1.00	1.50
1 to 2	1.35	*	1.00	†
2 to 3	1.15	*	1.00	†
Over 3	1.00	*	1.00	†

*Refer to data available from American Railway Engineering Association (AREA).

†Refer to data available from Federal Aviation Administration (FAA).

SOURCE: Reprinted from *Uni-Bell Handbook*[26] by permission.

where the only new term is p, which is the intensity of the distributed load in pounds per square foot. The load coefficient C_s is a function of $D/(2H)$ and $M/(2H)$, where D and M are the width and length, respectively, of the area over which the distributed load acts. The values of the impact factor F' can be determined from Table 2.5 and the load coefficient C_s from Table 2.6.

Highway and railway loads

Figure 2.19 is a plot of an H-20 live load, prism earth load, and the sum of the two. An H-20 loading is designed to simulate a highway load of a 20-ton truck. Figure 2.14 includes a 50 percent impact factor to account for the dynamic effects of the traffic.

Figure 2.20 is a plot of an E-80 live load, prism earth load, and the sum of the two. An E-80 loading is designed to represent a railway load, and again this includes a 50 percent impact factor.

An H-20 load consists of two 16,000-lb concentrated loads applied to two 18-in by 20-in areas, one located over the point in question and the other located at a distance of 72 in away. It is interesting to note (Fig. 2.19) that for the example considered, the minimum total load would occur at about $4^1/_2$ ft of cover. Also, it is evident from Fig. 2.19 that live loads have little effect on pipe performance except at shallow depths. Thus, design precautions should be taken for shallow installations under roadways. If the live load is an impact-type

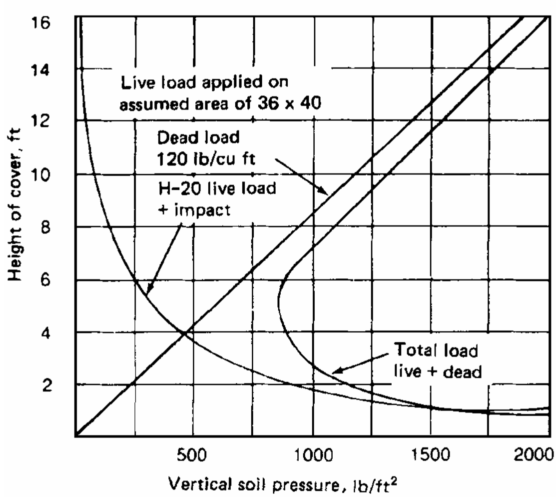

Figure 2.19 Combined H-20 highway live load and dead load is a minimum at about 1.5 m (5 ft) of cover. Live load is applied through a pavement 305 mm (1 ft) thick.

TABLE 2.6 Values of Load Coefficients C_S for Concentrated and Distributed Superimposed Loads Vertically Centered over Conduit*

$D/(2H)$ or	$M/(2H)$ or $L/(2H)$													
$B/(2H)$	0.1	0.2	0.3	0.4	0.5	0.6	0.7	0.8	0.9	1	1.2	1.5	2	5.0
0.100	0.019	0.037	0.053	0.067	0.079	0.089	0.097	0.103	0.108	0.112	0.117	0.121	0.124	0.128
0.037		0.072	0.103	0.131	0.155	0.174	0.189	0.202	0.211	0.219	0.229	0.238	0.244	0.248
0.053		0.103	0.149	0.190	0.224	0.252	0.274	0.292	0.306	0.318	0.333	0.345	0.355	0.360
0.400	0.067	0.131	0.190	0.241	0.284	0.320	0.349	0.373	0.391	0.405	0.425	0.440	0.454	0.460
0.500	0.079	0.155	0.224	0.284	0.336	0.379	0.414	0.441	0.463	0.481	0.505	0.525	0.540	0.548
0.600	0.089	0.174	0.252	0.320	0.379	0.428	0.467	0.499	0.524	0.544	0.572	0.596	0.613	0.624
0.700	0.097	0.189	0.274	0.349	0.414	0.467	0.511	0.546	0.584	0.597	0.628	0.650	0.674	0.688
0.800	0.103	0.202	0.292	0.373	0.441	0.499	0.546	0.584	0.615	0.639	0.674	0.703	0.725	0.740
0.900	0.108	0.211	0.306	0.391	0.463	0.524	0.574	0.615	0.647	0.673	0.711	0.742	0.766	0.784
1.000	0.112	0.219	0.318	0.405	0.481	0.544	0.597	0.639	0.673	0.701	0.740	0.774	0.800	0.816
1.200	0.117	0.229	0.333	0.425	0.505	0.572	0.628	0.674	0.711	0.740	0.783	0.820	0.849	0.868
1.500	0.121	0.238	0.345	0.440	0.525	0.596	0.650	0.703	0.742	0.774	0.820	0.861	0.894	0.916
2.000	0.124	0.244	0.355	0.454	0.540	0.613	0.674	0.725	0.766	0.800	0.849	0.894	0.930	0.956

*Influence coefficients for solution of Hall and Newmark's integration of the Boussinesq equation for vertical stress.

SOURCE: *Gravity Sanitary Sewer Design and Construction,* Manuals & Reports on Engineering Practice, No. 60, American Society of Civil Engineers, and Manual of Practice, No. FD-5, Water Pollution Control Federation, 1982, p. 190. Reprinted by permission.

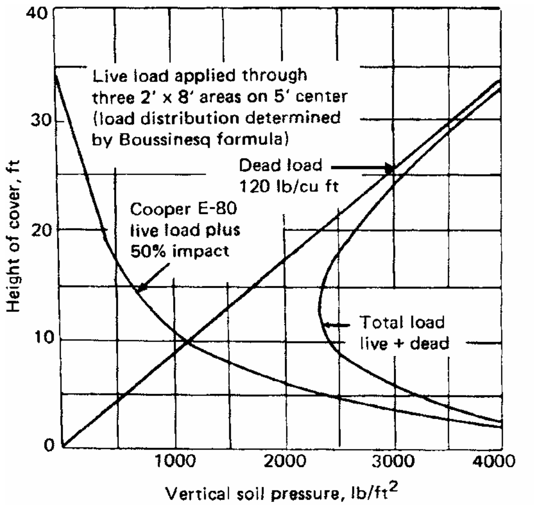

Figure 2.20 Cooper E-80 live loading. (*Reprinted from Handbook of Steel Drainage and Highway Construction Products,*[2] *by permission of the American Iron and Steel Institute, Washington, D.C.*)

load, it can be as much as twice the static surface load. However, from a practical standpoint, the impact factor will usually be less than 1.5. At extremely shallow depths of cover, a flexible pipe may deflect and rebound under dynamic loading. Special precautions should be taken for shallow burials in roadways to prevent surface breakup.

The effect of heavy loads at the soil surface, such as highway traffic, railroad, or structures built above buried pipe, is often controlled in design practice by providing a minimum depth of cover above the pipe. Indeed,[8] the pressure P_p applied on the pipe wall from a concentrated surface load P_s placed right above the pipe decreases as the square of the height of cover H

$$P_p = \frac{3P_x}{2\pi H^2 \, [1 + (d_s/H)^2]^{5/2}}$$

where P_p = pressure transmitted to pipe wall, lb/in^2
P_s = concentrated load at surface, above pipe, lb
H = height of cover, in
d_s = offset distance from pipe to line of application of surface load, in

The design of water piping for surface loads is provided in AWWA C101 (cast iron), AWWA C150, C151, and C600 (ductile iron), AWWA M11 (steel), AWWA M45 (fiberglass), and AWWA M23, C605, and C900 (PVC). In all cases, the depth of cover is to be established by the engineer on the basis of earth and surface load formulas to calculate the demand, and pipe stress and deflection limits to calculate the capacity. Minimum depth of cover is provided in AWWA M45 for fiberglass pipe.

In civil engineering applications, the *Handbook of Steel Drainage and Highway Construction Products* (American Iron and Steel Institute) applies to low-pressure, large-*D/t* buried pipes. In this case, the minimum cover for surface live loads is established on the basis of experience. The minimum cover specified is one-eighth (*D*/8) for highway conduits, *D*/4 and *D*/5 for railway conduits, but not less than 12 in. Deeper covers may be needed during construction for traffic of heavy equipment.

Where surface loads are of an impact nature, such as the impact of wheels on uneven roads, an impact factor is added to the surface load. For gas and liquid pipelines, a minimum depth of cover is usually used in place of detailed design analysis or encasement of the pipe. Minimum depths of cover for ductile iron gas pipelines follow the rules of AWWA C150.

Aircraft loads

Design live loads for modern airports may be very large. Airports are often designed for wheel loads of aircraft which have not yet been designed. Table 2.7 lists live loads for an aircraft loading of 180,000-lb dual-tandem gear assembly.

In the design for live loads on pipe buried under runway pavement, the impact factor is taken as 1.0. This is because the load is partially taken by the aircraft's wings when the aircraft is landing. For taxiways, aprons, and so on, an impact factor may be necessary (see Table 2.5). The design engineer should seek current data available from the Federal Aviation Administration.

Minimum soil cover

Figure 2.19 is copied from AISI graphs of vertical pressures on buried pipes (*Handbook of Steel Drainage and Highway Construction Products*[2]). As soil cover decreases, live load pressure on a buried pipe increases. There exists a minimum height of soil cover. If the soil cover is less than the minimum, the surface live load may damage the pipe. Less obvious is a minimum height of soil cover for dead load (weight of soil only). Each of these cases is discussed for rigid and flexible rings.

TABLE 2.7 Live Loads

Live load transferred to pipe, lb/in*				Live load transferred to pipe, lb/in*			
Height of cover, ft	Highway H-20†	Railway E-80*	Airport‡	Height of cover, ft	Highway H-20†	Railway E-80*	Airport‡
1	12.50	—	—	14	§	4.17	3.06
2	5.56	26.39	13.14	16	§	3.47	2.29
3	4.17	23.61	12.28	18	§	2.78	1.91
4	2.78	18.40	11.27	20	§	2.08	1.53
5	1.74	16.67	10.09	22	§	1.91	1.14
6	1.39	15.63	8.79	24	§	1.74	1.05
7	1.22	12.15	7.85	26	§	1.39	§
8	0.69	11.11	6.93	28	§	1.04	§
10	§	7.64	6.09	30	§	0.69	§
12	§	5.56	4.76	35	§	§	§
				40	§	§	§

*Simulates 80,000 lb/ft railway load + impact.
†Simulates 20-ton truck traffic + impact.
‡180,000-lb dual-tandem gear assembly, with 26-in spacing between tires and 66-in center-to-center spacing between fore and aft tires under a rigid pavement 12 in thick + impact.
§Negligible live-load influence.
SOURCE: Reprinted from *Uni-Bell Handbook*[26] by permission.

TABLE 2.8 Minimum Depth of Cover for Fiberglass Pipe (AWWA M45-1996)

Condition	Minimum cover, in
High-stiffness soils with crushed rock and gravel with < 15% sand and 75% fines (soil stiffness category SC1), with AASHTO-20 live load	24
Lower-stiffness soils (SC2 to 4) with AASHTO-20 live loads	36
Use of hydrohammer for compaction	48
Other conditions	Established by engineer

NOTE: The H-20 load assumes two 16,000-lb concentrated loads, one over the pipe, the other 72 in away, corresponding to a 20-ton truck load.

Only cohesionless soil is considered because vehicles are unable to maneuver on poor soil such as wet cohesive soil.

Notation

A = cross-sectional area of pipe wall per unit length of pipe

c = distance from neutral surface of pipe wall cross section to most remote fiber

D = mean diameter of pipe

E = modulus of elasticity of pipe material

H' = installed height of soil cover (see Fig. 2.24)

H = rutted height of soil cover

I = centroidal moment of inertia of pipe wall cross-sectional area per unit length of pipe

M = moment in wall due to ring deformation

P = vertical soil pressure at level of top of pipe due to a surface load distributed over a rectangular area

r = mean radius of pipe

S = compressive strength of pipe wall

T = circumferential thrust in ring

W = weight of a surface load

γ = unit weight of soil

ρ = soil density in percent standard Proctor (AASHTO T-99, ASTM D 698) for granular soil cover and embedment

σ_y = yield stress of pipe

σ = ring compression stress

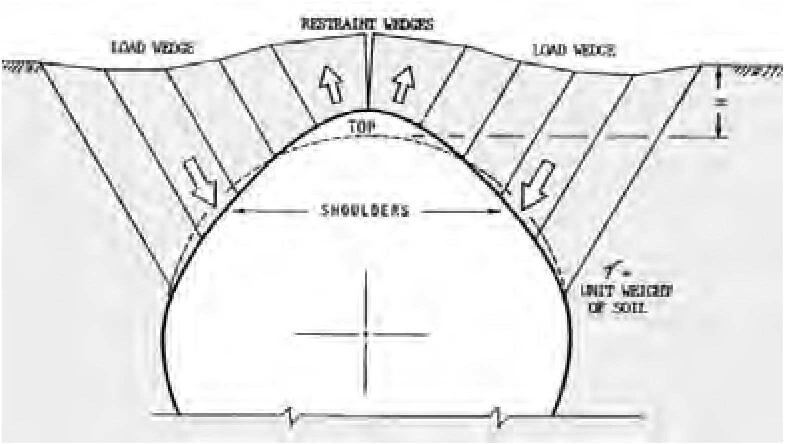

Figure 2.21 Flexible ring in the process of collapse under minimum dead load soil cover showing the load wedges advancing against the ring, and lighter restraint wedges being lifted.

Dead load. Cohesionless soil cover is minimum if the pipe is unable to resist the variation in soil pressure. This concept is shown in Fig. 2.21, where top pressure is γH but shoulder pressure is greater than γH. If the pipe cannot resist the difference in pressures, shoulder wedges slide in against the pipe, deforming the ring which lifts the top wedges. Collapse of the pipe is catastrophic. If the pipe is rigid (brittle), collapse is fragmentation. If the pipe is flexible, equations of equilibrium of soil wedges provide values of minimum soil cover. For typical granular backfill, based on analysis confirmed by tests, minimum cover is about $H = D/10$. An often specified minimum allowable is $H = D/6$, but this applies to a perfectly flexible ring. In fact, pipes have ring stiffness and so provide resistance to dead load collapse.

Pyramid/cone soil stress. The Boussinesq and Newmark procedures for calculating live load pressure on a buried pipe are based on the assumption that soil is elastic. The assumption does not apply to minimum-cover analysis. Pipe damage due to surface loads on less-than-minimum cover occurs after a truncated soil pyramid or cone is punched through. Figure 2.22 shows a truncated pyramid and cone. If the loaded surface area is circular, a truncated cone is punched through. If the loaded surface area is a rectangle, a truncated pyramid is punched through. Pyramids are imperfect because sharp corners do not form. Nevertheless, using a conservative pyramid slope θ, the analysis is applicable. The tire print of dual wheels is nearly rectangular.

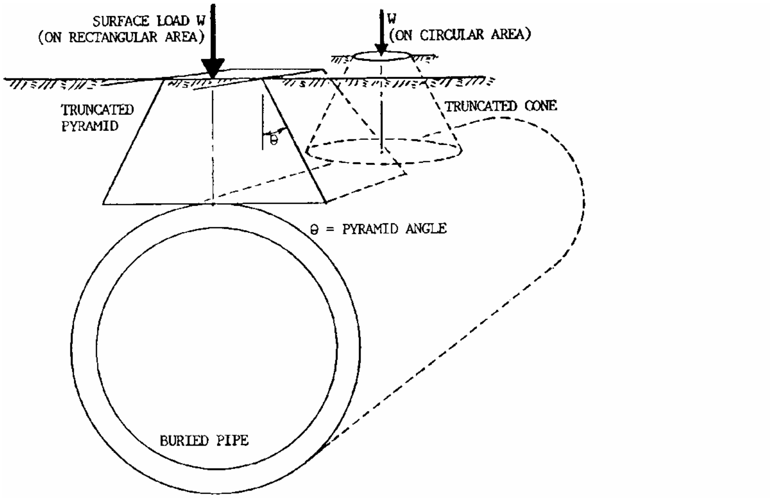

Figure 2.22 Soil stress models for minimum cover are free-body diagrams of truncated pyramid and cone showing shear planes on slope θ at "punch-through."

Figure 2.23 shows a surface live load W on a rectangular area (tire print) of breadth B and length L. If W is great enough to punch through granular soil and damage the pipe, then shear planes must form in the soil, isolating a truncated pyramid—a pedestal that supports the load.

The total load on the pipe is surface load W plus the weight of the pyramid of soil. The weight of the soil is ignored because it is small compared to any surface load great enough to punch through. The vertical soil pressure on the pipe is load W divided by the base area of the pyramid. The angle θ which the shear planes make with the vertical is the pyramid angle $\theta = 45° - \varphi/2$, where φ is the soil friction angle. From tests on cohesionless soil, the pyramid angle is roughly 35°, for which $\tan \theta = 0.5$, and the base area is approximately $(B + H)(L + H)$. The precision is as good as can be justified for typical installations. Analysis is conservative. At punch-through, the pressure on the pipe is the pressure at the base of the pyramid, i.e.,

$$P = \frac{W}{(B + H)\,(L + H)} \tag{2.15}$$

For H-20 dual-wheel load on a firm surface, $B = 180$ mm (7 in) and $L = 560$ mm (22 in) if tire pressure is 7 MPa (105 lb/in^2).

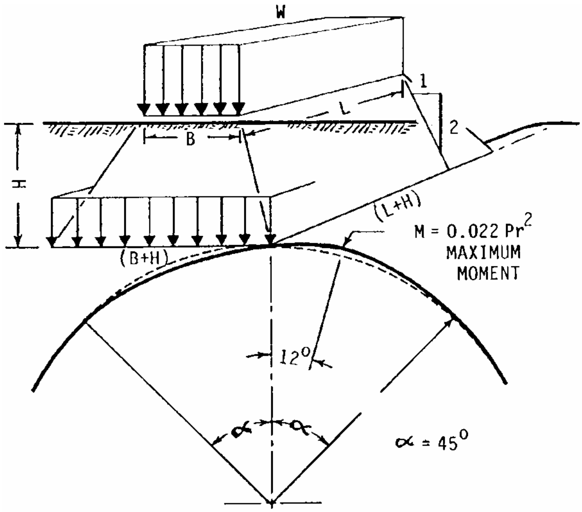

Figure 2.23 Truncated pyramid punched through a minimum soil cover H by an approaching wheel load W. Shear planes form on a 1:2 slope. Typical angles α are less than 45°. Pressure is approximately $P = W/[(B + H)(L + H)]$.

Live load. Minimum height of soil cover can be found by solving Eq. (2.15) for H if the surface load W is known and if the allowable pressure P on the pipe can be evaluated for any given pipe and for any given performance limit, such as inversion or ring compression at yield. Evaluation of allowable pressure P must include ring compression strength, ring stiffness, and the critical location of the load.

An unsuspected problem in the minimum-cover analysis is the definition of the height of soil cover. For paved highways, the height of soil cover remains constant during passes of live loads. But during construction, a heavy load leaves ruts. See Fig. 2.24. In fact, successful passes of the load may increase the depth of the ruts. If the depth of ruts approaches a limit as the number of passes increases, the pipe-soil system is stable. But if the depth of ruts continues to increase with each pass of the surface load, it is obvious that the pipe may be in the process of inversion. Whatever the ultimate damage may be, a performance limit has been exceeded. Minimum soil cover is defined as that soil cover H less than which the pipe-soil system becomes unstable upon multiple passes of surface load W. The height of cover to be used in Eq. (2.15) for soil stress on the pipe is H *after* the ruts have reached their maximum depth.

For rigid pipes, failure is fracture of the pipe and possible fragmentation. Critical load is located either symmetrically over the pipe,

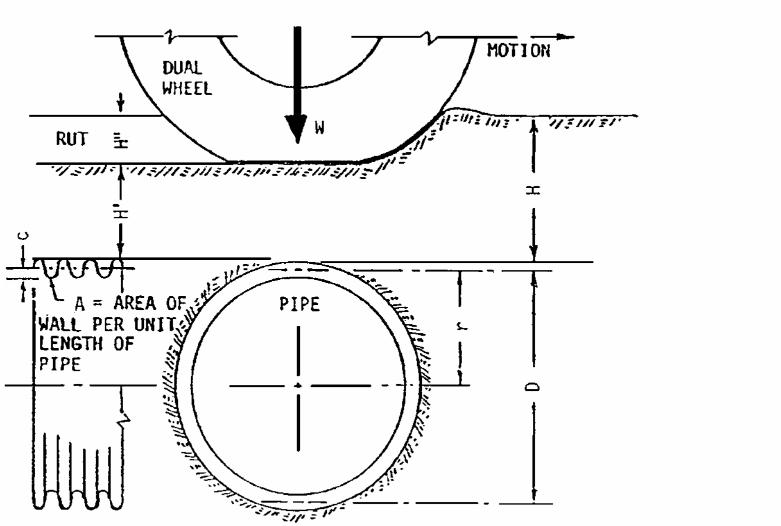

Figure 2.24 Sketch of a surface wheel load passing over a pipe buried in loose soil.

shown in Fig. 2.22, or, less often, on approach, shown in Fig. 2.23. For flexible pipes, failure is ring inversion as live load approaches, shown in Fig. 2.23. The leading edge of the base area of the truncated pyramid is at the crown of the pipe. From observations of granular soil cover, the inversion angle is $\alpha = 30°$ to $40°$, or, to be conservative, assume $\alpha = 45°$.

Analysis entails evaluation of the maximum moment caused by the live load. Dead load is neglected. The weights of soil wedges are small compared to the live load. Shear between wedges and between pipe and soil is neglected. The ring is fixed at both ends of the collapse arch. See Fig. 2.25. Vertical soil pressure P becomes radial P on a flexible ring. Castigliano's equation is used to find the reactions, the maximum moment M, and thrust T. Maximum M is located by equating its derivative to zero. If wall crushing is critical, thrust T is pertinent.

If circumferential stress is of interest,

$$\sigma = \frac{T}{A} + \frac{Mc}{I} \qquad \text{elastic limit} \tag{2.16}$$

The thrust term T/A is usually so small compared to the moment term that it can be neglected. And $T = \gamma Hr$ = circumferential thrust due to

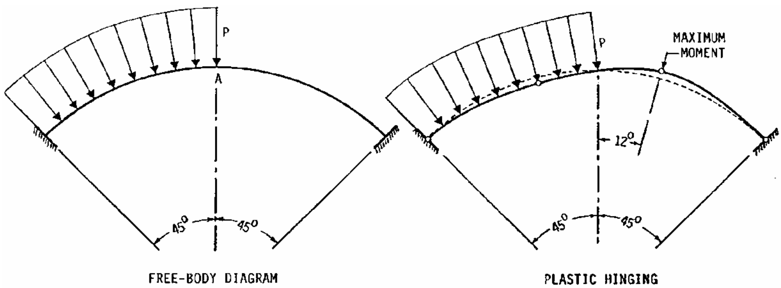

Figure 2.25 Free-body diagram of the inversion arch for finding maximum moment M in terms of pressure P due to a surface wheel load W approaching a pipe with minimum soil cover H. Locations of four potential plastic hinges are shown as circles. Hinging starts at the location of maximum moment.

deadweight of the soil cover on the right side of the crown. It is more likely that the performance limit is inversion at plastic hinging. As hinging progresses, four hinges develop and isolate a three-link mechanism. See Fig. 2.25. For plain pipes and corrugated pipes, the moment at plastic hinging (by plastic analysis) is approximately 3/2 times the elastic moment at yield stress. Therefore,

$$\sigma = \frac{2Mc}{3I} \qquad \text{plastic hinging} \tag{2.17}$$

Live load soil pressure is constant radial pressure P over 45° left of the crown, point A. From Castigliano's equation, the maximum moment occurs at the point of minimum radius of curvature, about 12° to the right of the crown A, and is

$$M = 0.022Pr^2$$

For design of pipes based on flexural yield stress σ_f, the minimum required section modulus I/c is

$$\frac{I}{c} = (0.022Pr^2)\,\frac{\text{sf}}{\sigma_f} \qquad \text{elastic limit} \tag{2.18}$$

$$\frac{I}{c} = (0.015Pr^2)\,\frac{\text{sf}}{\sigma_f} \qquad \text{plastic hinging} \tag{2.19}$$

where sf is the safety factor and I/c is the required section modulus of the pipe wall cross section per unit length of pipe. For plain pipe, $I/c = t^2/6$. It can be found from tables of values for corrugated metal pipes and can be calculated for other pipes. Tests show that I/c from these equations is conservative. A safety factor of 1.5 is usually adequate, and it does not need to be greater than 2 for highway culverts. With M and T known, Eq. (2.16) can be solved for the maximum stress whenever stress (or strain) is of concern, as in the case of bonded linings in pipes. And H does not appear in Eqs. (2.18) and (2.19) because the weight of the soil is negligible.

Example Problem 2.5 Find the minimum cover of granular soil over corrugated polyethylene pipe with 460-mm (18-in) inside diameter (ID). The polyethylene is HDPE (high-density polyethylene). The soil cover is compacted to 85 percent density (AASHTO T-99, ASTM D 698). The yield strength of HDPE at sudden inversion is 21 MPa (3 ksi). The surface load is a highway truck dual wheel for which the area of the tire print is 180 mm (7 in) by 560 mm (22 in). The procedure is to substitute values of P from Eq. (2.15) into Eq. (2.18). By including values of r and I/c for 460-mm (18-in) HDPE pipe, the resulting equation becomes a quadratic, $(H + 14.5 \text{ in})^2 = 56.25 \text{ in}^2 + 25W \text{ in}^2/\text{kip}$. Solutions are as follows:

W, kN (kips)	25 (5.5)	31 (7)	48 (9)	71 (16)
H, mm (in)	−15 (−0.6)	18 (0.7)	58 (2.3)	175 (6.9)

W = dual-wheel load of 70 kN (16 kips = H-20 load)

H = rutted soil cover—no surface pavement

A safety factor of 2 is often applied to H because loads are dynamic—not static. Some specifications require a minimum cover of 1 ft of compacted granular backfill. The negative $H = -15$ mm at $W = 25$ kN indicates that soil cover is not needed for such a light load. The pipe can carry a 25-kN dual-wheel even though the top of the pipe is exposed. Of course, enough soil cover should be provided to allow for rutting, prevent surface rocks from denting the pipe, and prevent crushing of corrugations. This example is confirmed by field tests. A similar analysis for 610-mm (24-in) HDPE pipes is almost identical. Apparently manufacturers provide equivalent properties for their pipes in both sizes. Installation techniques are about the same for 460-mm (18-in) and 610-mm (24-in) corrugated HDPE pipes.

Flotation. When pipes are buried in soil under water, the minimum height of soil cover to prevent flotation of an empty pipe is about $H = D/2$. But the soil should be denser than the critical density in order to prevent liquefaction. Because a safety factor is advisable, specifications often call for minimum $H = D$.

Rigid pipe. Two performance limits for buried rigid pipes subjected to surface loads are longitudinal fractures and broken bells. Circumferential fractures can occur, but less frequently. They occur at midlength of a pipe acting as a simply supported beam under a heavy load at midspan.

Longitudinal fractures. Longitudinal fractures occur if vertical pressure P exceeds the ring strength. Generally, the worst location of the surface load is directly above the pipe, as shown in Fig. 2.22. Minimum soil cover H is based on punch-through of a pyramid or cone. Longitudinal fractures occur at 12 and 6 o'clock and 9 and 3 o'clock. This is not collapse of the pipe. Many gravity flow pipes serve even when cracked. The soil envelope holds the ring in nearly circular shape. But for some rigid pipes, such as pressure pipes, longitudinal cracks are unacceptable. Occasionally one longitudinal hairline crack occurs—at 12 o'clock, or possibly at 6 o'clock if the pipe is on a rigid bedding. If the embedment is compacted select soil, a crack at 12 o'clock might be caused either by a surface wheel load or by a conscientious installer who compacts the first layer above the pipe directly against the pipe. It is prudent to compact sidefills; however, one should leave the first layer uncompacted over the pipe within one pipe diameter. For many buried rigid pipes, longitudinal cracks are not the performance limit. Good embedment holds the pipe in shape such that the pipe is in ring compression—not flexure. It performs in the same way as brick sewers with no mortar. Brick sewers function structurally, but are not leakproof.

The vertical pressure is $P = P_l + P_d$ where the live load pressure P_l is found by the pyramid/cone theory. For minimum cover analysis, dead load pressure P_d is negligible. The live load pressure P_l is a function of height of cover H. Minimum cover can be found from equating $P_{cr} = P_l$, where critical pressure P_{cr} is a function of class of bedding and class of pipe. Values are published for each class.

Broken bells. If a pipe section acts as a beam, the performance limit may be signaled a broken bell. Under heavy live load and minimum soil cover, rigid pipes require support under the haunches. If soil is not deliberately placed under the haunches, a void remains. See Fig. 2.26. If the angle of repose of the embedment is $\varphi' = 40°$, the void is wider than one-half the outside diameter [0.643(OD)]. Live load on the pipe could cause the top of the pipe to move downward either by cracking the pipe or by pressing the pipe into the bedding. Under the haunches, loose soil at its angle of repose offers little resistance. As a pipe section deflects downward, it becomes a simply supported beam with reactions at the ends of the pipe section. See Fig. 2.27. It is this reaction Q that fractures the bell. Clay pipes and nonreinforced concrete pipes are vulnerable because of low tensile strength. The maximum tensile stress is in the bell near the spring line. Once it is cracked, a shard forms roughly one diameter in length, as shown in Fig. 2.27. An approximate analysis is done by equating the Q that can be withstood by the bell to the Q reaction caused by the surface load on the pipe section acting as a beam.

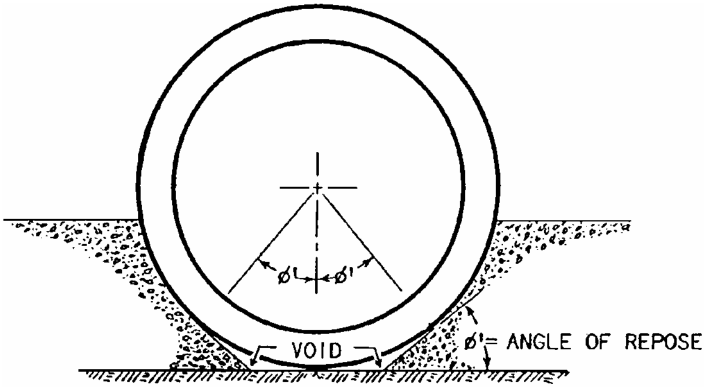

Figure 2.26 Rigid pipe cross section showing how voids are left if soil is not deliberately placed under the haunches.

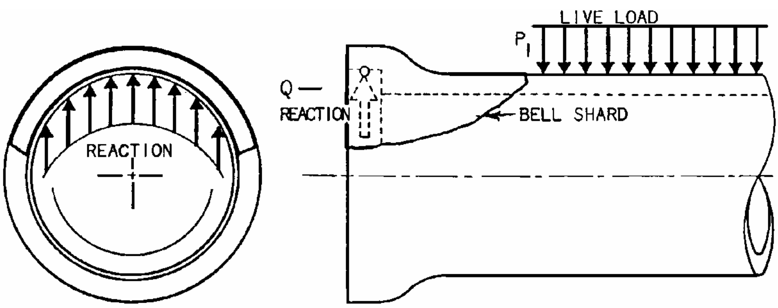

Figure 2.27 Bell end of a section of rigid pipe subjected to live load pressure, but acting as a simply supported beam. Reactions Q at the ends are provided by contiguous pipe sections.

Example Problem 2.6 A nonreinforced concrete pipe, with ID of 380 mm (15 in), bell and spigot, C-14, class 3, is to be used as a storm drain. The outside diameter is OD = 480 mm (19 in). What is the minimum cover H if the fracture is a broken bell? The length of nonreinforced pipes is L = 2.4 m (8 ft). Assume (estimate) that the cross-sectional area of the thin part of the bell is A = 3230 mm^2 (5 in^2). Tensile stress at the spring lines is $\sigma = Q/(2A)$, from which maximum $Q = 2A\sigma_f$, where σ_f = tensile strength of the concrete. Reaction Q at fracture is $Q = 2A\sigma_f$ = 44.5 kN (10 kips). But Q is the reaction to pressure P_l on the pipe which is caused by surface live load W. From the punch-through cone analysis, $P_l = 4W/[\pi(32 \text{ in} + H)^2]$. Conservatively, it can be assumed that W is located at midspan, and that reaction Q = $0.5P(\text{OD})(32 \text{ in} + H)$. Substituting for P and equating the two Q values give

$$\frac{W\,(\text{OD})}{\pi\,(32 \text{ in} + H)} = A\sigma_f \tag{2.20}$$

From Eq. (2.20), the minimum soil cover is $H = 724$ mm (28.5 in). In this analysis, the pipe section is a simply supported beam (no support from the soil). Minimum cover is 724 mm (28.5 in). This is an upper limit.

It is prudent to specify good bedding and embedment, and to require a minimum cover of 0.9 m (3 ft) for the impact loads of heavy construction equipment. To place and compact embedment under the haunches, a windrow of soil along the pipe can be shoved into place by laborers with J-bars working on top of the pipe, by flushing the windrow under the haunches with a water jet, or by mechanical compactors. Some installers pour soil cement or slurry under the haunches. The slump should be about 10 in, and the strength should be low—maybe 100 lb/in^2.

Example Problem 2.7 What is the minimum cover H for the pipe in the above examples based on maximum longitudinal tensile stress $\sigma = Mc/I$ in the bottom of a simply supported beam? With a uniform load w at midspan, $M = wL^2/8$, where w is the load per unit length of beam; that is, $w = P(\mathrm{OD}) = 4W/[\pi(32 \text{ in} + H)^2]$. And $I/c = (\pi/32)[(\mathrm{OD})^4 - (\mathrm{ID})^4]/\mathrm{OD}$. If tensile strength is $\sigma_f = 7$ MPa (1 ksi), substituting values into the equation $\sigma_f = M/(I/c)$ gives $H = 665$ mm (26.2 in). Failure by a broken bell is slightly more critical.

Similitude. Engineering is basically design and analysis with attention paid to cost, risk, safety, etc. In this section, the design considered is a buried pipe. Analysis is a model that predicts performance. Performance must not exceed performance limits. Mathematical models are convenient. Physical, small-scale models are better for complex pipe-soil interaction. The most dependable models are full-scale prototypes. Mathematical models are often written to describe prototype performance because it is impractical to perform a full-scale prototype study for every buried pipe to be installed. The set of principles upon which a model can be related to the prototype for predicting prototype performance is called *similitude.* Similitude applies to all models—mathematical, small-scale, and prototype.

There are three basic steps in achieving similitude.

1. Fundamental variables (FVs) are all the variables that affect the phenomenon. All the FVs must be uniquely interdependent. However, no subset of FVs can be uniquely interdependent. For example, force, mass, and acceleration of gravity cannot all be used as fundamental variables in a more complex phenomenon, because force equals mass times acceleration. Therefore the subset is uniquely interdependent. Only two of the three fundamental variables could be used in the phenomenon to be investigated.

2. Basic dimensions (BDs) are the dimensions in which the FVs can be written. The basic dimensions for buried pipes are usually force F, distance L, and sometimes time T and temperature.

3. Pi terms are combinations of the FVs that meet the following three requirements: (*a*) The number of pi terms must be at least the number of FVs minus the number of BDs. (*b*) The pi terms must all be dimensionless. (*c*) No subset of pi terms can be interdependent. This is ensured if each pi term contains a fundamental variable not contained in any other pi term.

Pi terms can be written by inspection.

Example Problem 2.8 Write a set of pi terms for investigating the maximum wheel load W that can pass over a buried flexible pipe without denting the top of the pipe. See Fig. 2.28 for a graphical model and Fig. 2.29 for the laboratory test for the determination of soil modulus E'. Following the three pi-term requirements yields the following:

FVs	BDs
W = wheel load	F
EI = wall stiffness	FL
H = height of soil cover	L
P = all pressures	FL^{-2}
D = pipe diameter	L
E' = soil modulus	FL^{-2}
γ = soil unit weight	FL^{-3}

7 FVs − 2 BDs = 5 pi terms required

Here are the pi terms:

$(W/E'D^2)$ π_1

(EI/D^3) π_2

(H/D) π_3

(P/E') π_4

$(\gamma D/E')$ π_5

This set of five pi terms, by inspection, is not the only possible set. If this set is not convenient for investigating the phenomenon, a different set can be written. For these pi terms, the maximum wheel load is given by the mathematical function

$$\pi_1 = f(\pi_2, \pi_3, \pi_4, \pi_5) \tag{2.21}$$

This functional relationship of pi terms needs to be found. Principles of physics provide one possibility. Prototype studies allowing the writing of empirical best-fit equations of graphs of data are another option. If small-scale model studies are to be used, Eq. (2.21) must describe the performance of both model and prototype. Therefore, the model must be designed such that corresponding pi terms on the right side of Eq. (2.21) are equal for both model and prototype. This can be accomplished, even for small-scale models, because pi terms are dimensionless and therefore have no feel for size—or any other dimension, for that matter. If the subscript m designates model, in order to design the model, the design conditions (DCs) are $(\pi_m)_2 = (\pi_2)$, etc.:

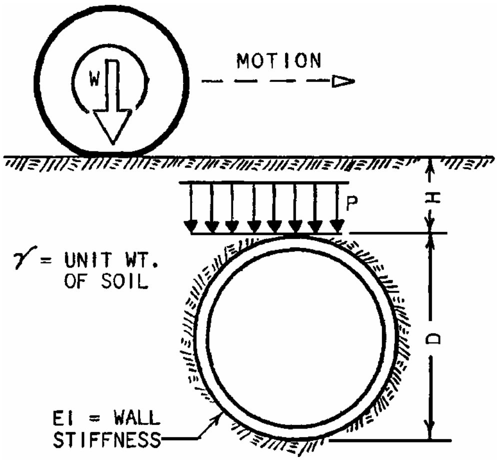

Figure 2.28 Sketch of a physical model for evaluating the wheel load passing over a buried flexible pipe that dents the top of the pipe.

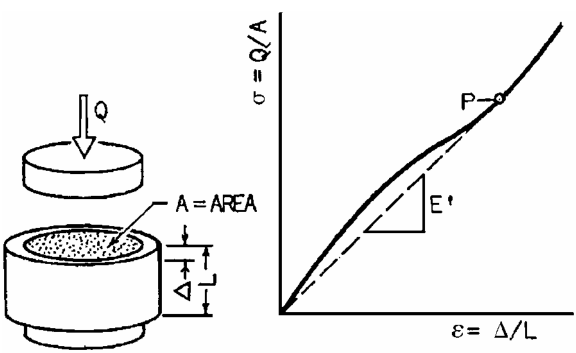

Figure 2.29 Confined compression soil test.

1. $(EI/D^3)_m = (EI/D^3)$
2. $(H/D)_m = (H/D)$
3. $(P/E')_m = (P/E')$
4. $(\gamma D/E')_m = (\gamma D/E')$

Using subscript r to represent the ratio of prototype to model, each of the design conditions can be met according to the following:

1. $(EI)_r = (D_r)^3$ where D_r is length scale ratio
2. $(H_r) = (D_r)$ geometric similarity

3. $(P_r) \ = (E_r{}')$
4. $(\gamma_r) \ = (E_r{}')/(D_r)$

Because soil is a complex material, it would be convenient if the same soil could be placed and compacted in the same way in both model and prototype. The results are $E_r{}' = 1$ and $\gamma_r = 1$. But now design conditions 3 and 4 are not met. From design condition 3, $P_r = 1$. Therefore, all pressures P must be the same in the model as at corresponding points in the prototype. For example, tire pressures must be the same in model and prototype. The soil pressure must be the same at corresponding depths in the model and prototype. But this is impossible for a small-scale model if the soil has the same unit weight. One remedy is to test the model in a long-arm centrifuge such that centrifugal force plus gravity increases the effective unit weight of the soil in the model. Another approximate remedy is to draw seepage stresses down through the model (air or water if the soil is to be saturated) in order to increase the effective unit weight of the model soil. For most minimum soil cover studies, the effect of soil unit weight is negligible, so DC 4 is ignored. From tests on the model, weight W can be observed when the buried pipe is dented.

The prediction equation (PE) is the equation of pi terms on the left sides of Eq. (2.21) for model and prototype, i.e.,

$$(W/E'D^2) = (W/E'D^2)_m$$

If $E_r{}' = 1$, then the prediction equation is

$$W = W_m\ (D_r)^2$$

where D_r is the length scale ratio of prototype to model. If the length scale ratio is 5 (that is, 5:1 prototype to model), the load W on the prototype that will dent the buried pipe is 25 times the load W_m that dents the model pipe.

In order to write a mathematical equation (model) for the phenomenon, enough tests must be made to provide graphs of data for $\pi_1 = f(\pi_2)$ with π_3 held constant and for $\pi_1 = f'(\pi_3)$ with π_2 held constant. From the best-fit graphs plotted through the data, an equation of combination can be written for $\pi_1 = f(\pi_2, \pi_3)$. This becomes a mathematical model.

In fact, neglecting dead load, design condition 3 is met when tire pressures are the same in model and prototype. Then the mathematical model is simply the equation of the best-fit graph of $\pi_1 = f(\pi_2)$. It can be written in terms of the original fundamental variables.

Soil Subsidence

Buried pipe is typically routed in competent soil and installed in a compacted trench. These precautions provide reasonable assurance that the soil will not deform, and therefore this effect is rarely included in design. Where the potential for natural soil subsidence is real or, more often, when subsidence has occurred, the buried line is analyzed to assess its integrity. The soil movements are applied to the buried pipe, either through soil springs or by directly deforming the pipe as a beam following the soil contour. Stresses or strains are calculated. In the case of a simple longitudinal pull of a straight buried pipe, as would occur, e.g., at the interface between a buried pipe and a building penetration as the building settles, the axial stress imposed on the pipe end would be

$$\sigma = \sqrt{\frac{2Ef\Delta}{A}}$$

where E = Young's modulus of pipe, lb/in^2
Δ = building movement pull along pipe axis, in
A = cross section of pipe wall, in^2
f = pipe-soil longitudinal friction, lb/in

In certain cases, designers prefer to evaluate strains based on the deformed shape. However, there is no consensus standard specifying allowable strains for permanent deformation such as sustained from soil subsidence.

Loads due to Temperature Rise

Buried pipelines are often operated at temperatures that do not significantly differ from the surrounding soil temperature. In these cases, there will be little or no differential expansion and contraction between the pipe and soil, and a thermal design analysis is not required. In cases where the fluid is hot or cold, stresses are generated as the pipe expansion is constrained by the surrounding soil.[9] For long sections of straight pipelines, the resulting longitudinal stress is

$$S_L = E\alpha\,(T_2 - T_1) - \nu S_h$$

where S_L = longitudinal compressive stress, lb/in^2
E = modulus of elasticity of steel, lb/in^2
α = coefficient of thermal expansion, 1/°F
T_2 = maximum operating temperature, °F
T_1 = installation temperature, °F

ν = Poisson's ratio
S_h = hoop stress due to fluid pressure, lb/in^2

At changes in direction, such as bends and tees, the soil-to-pipe friction may not be sufficient to prevent expansion of the pipe relative to the soil. As a result of the pipe movement relative to the soil, the pipe is subject to bending stresses in addition to the longitudinal stress S_L. In these cases, the current practice would be to account for the thermal bending stresses in one of two ways:

1. By using formulas such as provided in Appendix VII of ASME B31.1.
2. By a pipe-soil spring model to which the temperature rise is applied. Special-purpose PC-based computer codes have been developed to perform these calculations.

Seismic Loads

In certain critical zones, large ground movement associated with an earthquake may be devastating to a pipeline. These critical zones are primarily those where high differential movement takes place such as a fault zone, a soil shear plane, or transition zones where the pipe enters a structure. Also certain soils will tend to liquefy during the earthquake vibration, and buried pipelines may rise or tend to float. On the other hand, most buried flexible pipelines can survive an earthquake. Again, a more flexible piping material with a flexible joint will allow the pipe to conform to the ground movement without failure. In practice, the design of buried pipe for seismic loads is limited to critical applications. In earthquake-prone areas, seismic design is a consideration for piping that must perform an essential function (such as providing fire protection water) or prevent the release of toxic or flammable contents (such as from a gas leak). A large body of data on the behavior of buried pipe during earthquakes has been collected in the last 20 years. The data point to a few critical characteristics that govern the seismic integrity of buried pipe (O'Rourke, FEMA): In general,

1. Modern (post-1930s) pipelines constructed with full-penetration shielded arc welds and proper weld examination performed well.
2. Segmented construction (nonwelded segments assembled by mechanical joints) have experienced damage in large earthquakes.
3. Failures are more often due to soil failures (liquefaction, landslides, fault movement) than to the transient passage of seismic waves.
4. Seismic damage of storage tanks (sliding, rupture, buckling, or foundation settlement) has caused failures in connected buried pipe.

5. Buried pipe made of ductile materials [steel, or more recently polyvinyl chloride (PVC) and high-density polyethylene (HDPE)] performed well.

Understanding this track record is important when developing design criteria, to emphasize the positive characteristics and avoid those that resulted in failures.

An earthquake may affect the integrity of a buried pipe in two possible ways: through wave passage (transient ground deformation) and through permanent ground deformation.

Wave passage

The passage of seismic waves in the soil generates compressive, tensile, and bending strains in a buried pipe. Extensive research in the seismic performance of buried pipelines points to the fact that wave passage alone does not seem to fail arc-welded steel pipe or polyethylene pipe.[19] Older buried piping assembled with oxyacetylene welds or with mechanical joints is more susceptible to transient seismic ground movements due to wave passage. Techniques do exist to analyze the effects of seismic wave passage on a buried pipe (ASCE). This analysis can be carried out with several levels of complexity.

In the simplest of cases, the pipe strain is set equal to the soil strain and compared to a strain limit. The value of the strain limit is not standardized. Compressive strain limits to avoid wrinkling of the pipe wall on the order of $0.4t/D$ or $2.42(t/D)^{1.6}$ have been proposed.[27] In the 1970s Hall and Newmark[12] had proposed strain limits of 1 to 2 percent. Tensile strain limits on the order of 3 to 6 percent have been used for modern steel pipeline construction.

In a more detailed analysis, the soil is modeled as three-directional springs around the pipe. The soil strain is applied to the model, and the axial and bending stresses are computed and compared to an allowable. In this case, two difficulties remain to be solved: the choice of a stress equation (and stress intensification factor) and the allowable stress. Unintensified stress limits of S_y (ISO/DIS 13623) and intensified elastically calculated stress limits of $2S_y$ have been proposed by Bandyopadhyay.[9] As a shortcut for applying the soil strain to the model, the seismic problem may be approached as a thermal expansion problem: The soil strain is converted to an equivalent temperature rise, which is applied to the pipe.[10]

A more detailed analysis would include finite element models of the pipe and the soil and would subject the model to time-history input motions. The waves would be applied at several angles of incidence relative to the buried pipe. Strain or plastic stress criteria have been used in these cases.

In light of the many uncertainties associated with the initiating earthquake, the soil response, and the pipe behavior, it is often necessary to perform sensitivity analyses where key parameters are varied around a best-estimate value to ensure that the design is safe, accounting for uncertainties.

Permanent ground deformation

Ground deformation from earthquakes includes lateral spread of sloped surfaces, liquefaction, and differential soil movement at fault lines. Ideally, the routing of a buried pipe is selected to avoid these seismic hazards. Where this is not possible, the effects of postulated ground motions are considered in design.[15]

The first step is to establish the seismic hazard, or design basis earthquake, and predict the corresponding ground movement.

The second step is to establish the performance requirement for the buried pipe. For example:

1. The pipe may need to remain serviceable and allow, e.g., the passage of pig inspection tools.
2. The pipe may need to remain operational, with valves opening on demand to deliver flow or closing to isolate a hazardous material.
3. The pipe may only need to retain its contents, without being operational following the earthquake.

Based on the performance requirement, an allowable stress or strain limit is established.

The third step is to analyze the pipe response to the postulated movement, and the resulting tensile, bending, and compressive loads applied to the buried pipe. This may be done very easily by hand calculations to the extent that the deformations are small. For large deformations, preferably the calculations should be done by finite element analysis of the soil-pipe interaction. Finally, the computed stresses or strains are compared to allowable limits established earlier based on the required performance of the pipe following the earthquake.

The design for seismic loads and deformations associated with buried piping depends on the accuracy of the predicted ground movement and soil properties as well as the accuracy of the pipe-soil interaction model. Parametric variations of the input and model are usually necessary to bound the problem. Costs are therefore incurred in (1) developing the range of soil and pipe properties used in analysis and (2) conducting the parametric analyses, which may be linear for small displacements or nonlinear for large displacements. A cost-benefit decision must therefore be made regarding the seismic design of buried pipe. To help in the process, the designer may turn to the lessons learned from actual earthquakes.

Frost Loading

When freezing atmospheric conditions exist continuously for several hours, ice layers or lenses form as shallow soil moisture freezes. As the frost penetrates downward, additional small volumes of water freeze. This freezing has a drying effect upon the soil since the water is no longer available to satisfy the soil's attraction for capillary water. Thus, groundwater from below the frost layer is attracted by capillary action to the area of lower potential. This water also freezes as it reaches the frost, and the process continues until equilibrium is reached. The freezing of ice below existing ice layers causes pressure to develop because of the expansion due to growth (volume increase) of ice.

It has been shown that this expansive pressure can substantially increase vertical loads on buried pipes. A paper authored by W. Harry Smith (*AWWA Journal,* December 1975) indicates almost a doubling of load during the deepest frost penetration. For this study, the test pipe setup was essentially nonyielding.

The test pipe was split longitudinally in two halves, and load cells were placed inside the pipe (see Fig. 2.30) such that the load cell was between the two halves. The maximum deflection of the load cells was 0.003 in. The test pipe simulated an extremely rigid pipe. Due to this rigidity, the load increase was greatly magnified. The previously discussed spring analogy can be applied here. In this case, the test pipe is represented by a very stiff spring, and the soil sidefills by softer springs. It is clear that the stiffer spring will take most of the load.

The increase in load, due to frost penetration, is less pronounced for flexible pipes. For example, plastic pipes such as PVC may have a small increase in deflection without any structural distress. Normally, designs require pipes to be placed 1 or 2 ft below the frost line. The design engineer should be aware that frost action may increase loads on a rigid pipe.

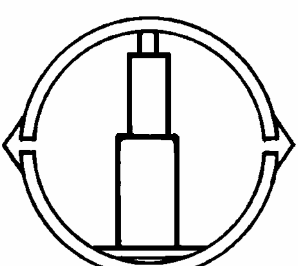

Figure 2.30 Schematic of split pipe with supporting load cell.

Loads due to Expansive Soils

Expansive soils were mentioned briefly in the "Longitudinal Loading" section concerning possible ground movement. Certain soils, primarily bentonite clays, expand and contract severely as a function of moisture content. Soil expansion can cause an increase in soil pressure just as frost can cause an increase in soil pressure. This rise in pressure is directly due to expansion and is a function of confinement. Tremendously high pressures can result if such soils are confined between nonyielding surfaces. However, data are lacking concerning such forces which may be induced on buried conduits. This lack of data can probably be attributed to design practices that do not allow such soils to be placed directly around the pipe. Also, in the case of gravity sewers, designs usually require such material to be removed for certain depths below the pipe if moisture content is variable at such depths. The primary reason for this requirement is to ensure that the grade is maintained. The design engineer should be cognizant that expansive soils do pose certain potential problems. He or she should seek advice from a component soils (geotechnical) engineer and then take appropriate steps in the installation design to mitigate adverse effects of expanding soils.

Flotation

Buried pipes and tanks are often placed below the water table. High soil cover can prevent flotation, but in shallow cover, holddowns, weights, etc., may be required to prevent flotation. Reinforced concrete pavement over a pipe helps to resist flotation. Holddowns require anchors—a concrete slab or deadmen. When the water table is a problem, soil at the bottom of the excavation is so wet that a concrete slab is used as a platform on which to work. In some cases, two longitudinal footings (deadmen) may be adequate anchors. Straps are sometimes used to tie the pipe or tank to the anchors.

Soil wedge

If the embedment is granular and compacted, a floating pipe must lift a soil wedge. See Fig. 2.31. If the buoyant force of the pipe exceeds the pipe weight and the effective weight of the soil wedge, anchors must restrain the difference.

Example Problem 2.9 Suppose that a large-diameter steel pipe is buried under 2 ft of soil cover. Is any anchorage required if the pipe is empty when the water table rises to or above the ground surface?

Steel pipe: $D = 105$ in

$$\text{Pipe weight} = 580 \text{ lb/ft}$$

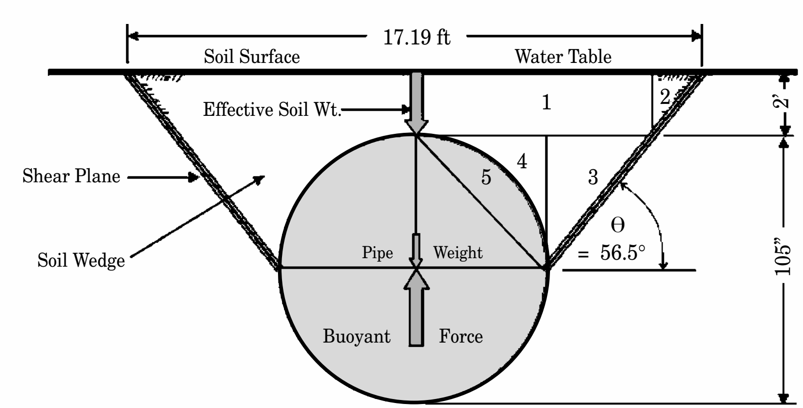

Figure 2.31 Sketch of 105-in-diameter buried pipe with water table at the soil surface. Sketch shows acting vertical forces—the buoyant force, the effective soil resistance, and the pipe weight. The pipe is empty.

Soil:

$$\gamma_d = 110 \text{ lb/ft}^3 = \text{dry unit weight of soil}$$

$$e = 0.52 = \text{void ratio}$$

$$\gamma_b = 69.0 \text{ lb/ft}^3 = \frac{\gamma_d - \gamma_w}{1 + e}$$

$$\varphi = 23° = \text{soil friction angle from lab tests}$$

$$\theta_f = 56.5° = \text{soil slip angle} = 45° + \frac{\varphi}{2}$$

$$H = 3.0 \text{ ft} = \text{soil cover}$$

$$G = \frac{(1 + e)\,110}{62.4} = 2.68 = \text{specific gravity of soil grains}$$

The specific gravity of most soil is in the range of 2.65 to 2.7.

Will the pipe float? To calculate, first find the volume of the soil wedge per foot of pipe. This is the area of the soil wedge in Fig. 2.31.

$$\text{Total area } A = 2\,(A_1 + A_2 + A_3 + A_4)$$

$$A_1 = hR + \frac{hR}{\tan\theta}$$

$$A_2 = \frac{1}{2} hb_2 = \frac{1}{2}\,\frac{hh}{\tan\theta} = \frac{1}{2}\,\frac{h^2}{\tan\theta}$$

$$A_3 = \frac{1}{2}\,\frac{R^2}{\tan\theta}$$

$$A_4 = \frac{1}{2}R^2 - A_5 = 0.215R^2$$

$$A_5 = \frac{1}{4}\pi R^2 - \frac{1}{2}R^2 = R^2\left(\frac{1}{4}\pi - \frac{1}{2}\right) = 0.285R^2$$

Then

$$\text{Total area } A = 2\left[hR + 0.215R^2 + \frac{1}{2}\,\frac{(h+R)^2}{\tan\theta}\right]$$

$$\Delta W = W_w - W_s - W_p$$

where W_w = 3.752 kips/ft = buoyant uplift force per unit length of tank. This is the weight of water per foot displaced by the pipe. $\pi R^2 (\gamma_w) = \pi\,(52.5/12)^2\,(62.4)$

W_s = 3.631 kips/ft = effective soil wedge (ballast) on top per unit length at $\theta_f = 45° + \varphi/2$
$= A\gamma_b$
$= 52.63\,(69) = 3631$ lb/ft^3 for this example

W_p = 0.580 kip/ft = weight of steel pipe

ΔW = −0.459 kip/ft = net downward force

Thus, if the 17.19-ft soil wedge forms, as supposed, the pipe will not float. However, tests show that planes are well established near the tank, but are not well established at the ground surface. In fact, the "plane" may be more nearly a spiral cylinder that breaks out on the ground surface at a width less than the 17.19 ft shown. In design, a factor of safety is required and should be at least 2.0. That is, the downward forces (soil and pipe) should be at least 2 times the buoyant uplift force.

Liquefaction

If there is any possibility of soil liquefaction, flotation will be a major concern and additional considerations are required. Soil can liquefy if it is saturated and shaken, and if the density is less than about 80 percent modified Proctor density (AASHTO T-180). The shaking can be a result of seismic activity. If the soil is completely saturated to ground level and the pipe is empty, there will be little resistance to flotation and the empty pipe will rise through the liquid soil.

The concept of liquefaction is as follows: Pour loose sand into a quart jar to the top, then carefully fill to the top with water. Put on the lid and shake the soil-water mixture. Remove the lid and turn the jar upside down, and the liquefied soil will run out. Now repeat the process, but this time carefully compact the sand in layers. The density must be greater than 80 percent modified Proctor. Another way of saying this is that *the void ratio must be less than the critical void ratio.* After the jar is completely full with compacted sand, again care-

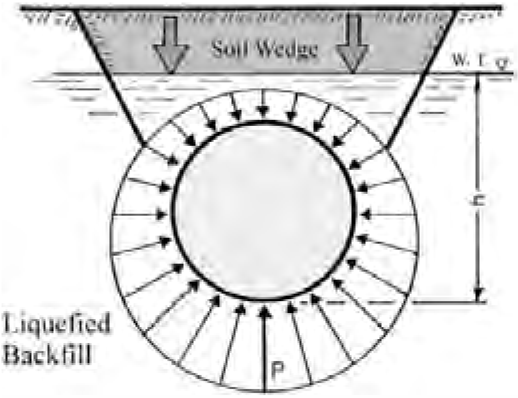

Figure 2.32 Pressure distribution on a pipe in a liquefied soil. Buckling at bottom is possible.

fully fill the jar to the top with water. Replace the lid and shake as before; remove the lid and turn upside down. The wet sand will stay in the jar because it has not liquefied.

If the embedment liquefies when a circular pipe is empty, the ring may be subjected to the hydrostatic pressures shown in Fig. 2.32. If somehow flotation is prevented, catastrophic collapse may occur from the bottom according to the classical buckling equation

$$\frac{Pr^3}{EI} = 3 \qquad \text{or} \qquad h = \left(\frac{E}{4\gamma}\right)\left(\frac{t}{r}\right)^3 \qquad \text{for plain pipe}$$

Example Problem 2.10 What is the height h of the water table above the bottom of a steel pipe in embedment so loose that it can liquefy and cause catastrophic ring collapse?

Pipe: $D = 105$ in

$t = 0.5$

$\frac{r}{t} = 105$

Soil: $\gamma = 125\ \text{lb/ft}^3$ saturated

h = height of water table above invert

$P = h\gamma$

Solving yields $h = \left(\frac{E}{4\gamma}\right)\left(\frac{t}{r}\right)^3 = \frac{30 \times 10^6}{4\ (125/1728)}\ (0.00952)^3 = 89.6\ \text{in} = 7.46\ \text{ft}$

The pipe is 8.75 ft in diameter, so the water does not even have to be to the top of the pipe. Thus, if a water table can rise in the embedment, the importance of densifying the embedment soil, including soil under the haunches, is evident. If the soil does not liquefy, the soil gives support to the pipe and prevents buckling. Then the buckling equation is

$$P_{cr} = h\gamma = 1.15\sqrt{P_b E'}$$

where $P_b = (2E/1 - \nu^2)(t/D)^3$
$P_{cr} = h\gamma$
E' = soil modulus
E = pipe modulus of elasticity
ν = pipe Poisson's ratio

Soil bearing

An empty pipe below the water table may rise through the soil by the means of penetration if the soil's bearing capacity is too low. This may be more critical than the soil wedge for resisting flotation.

Example Problem 2.11 In the previous example, suppose that the soil is so poor that the bearing capacity is only 300 lb/ft². Soil resistance is W_s = (105/12 tank diameter)(300 lb/ft²) = 2.625 kips/ft, where

W_w = 3.752 kips/ft = buoyant uplift force per unit length of tank

W_s = 2.625 kips/ft = effective bearing capacity

W_p = 0.580 kip/ft = weight of steel pipe

$\Delta W = W_w - W_s - W_p$

= +0.543 kip/ft and is a net upward force

The pipe will rise through the soil by penetration because of a low bearing capacity. To prevent this, a better soil with higher bearing capacity must be used, or the pipe must never be allowed to be empty.

Internal vacuum

For a pipe with an internal vacuum, treat the vacuum as a positive external pressure and add it to any acting external water pressure before making the buckling analysis. The performance limit for internal vacuum and/or external soil pressure only is ring inversion. Embedment usually prevents total collapse. Critical vacuum p is sensitive to the radius of curvature. Ring deflection reduces critical vacuum. Because vertical radius of curvature r_y is greater than r, ring stiffness EI/r_y^3 is less than EI/r^3 and the vacuum at collapse is less for a deflected ring than for a circular ring.

References

1. *Autopipe Pipe Stress Analysis* [software manual], App. D. Walnut Creek, Calif.: Rebis, 1999.
2. American Iron and Steel Institute. 1971. *Handbook of Steel Drainage and Highway Construction Products,* 5th ed. Chicago.
3. American Railway Engineering Association. *Manual of Recommended Practice,* REA Spec 1-4-28. Chicago.
4. American Society of Civil Engineers. 1984. *Guidelines for the Seismic Design of Oil and Gas Pipeline Systems.* New York.
5. American Society of Civil Engineers. 1984. *Structural Analysis and Design of Nuclear Plant Facilities.*
6. American Society of Civil Engineers and Water Pollution Control Federation. 1982. *Gravity Sanitary Sewer Design and Construction.* New York.
7. American Water Works Association. *Thickness Design of Ductile Iron Pipe,* AWWA C150-96. Denver.
8. Antaki, G. A. 1997. A Review of Methods for the Analysis of Buried Pressure Piping. *Welding Research Council Bulletin* 425. New York.
9. Bandyopadhyay, K., et al. 1995. *Seismic Design and Evaluation Guidelines for the Department of Energy High-Level Waste Storage Tanks and Appurtenances,* BNL-52361.
10. Federal Emergency Management Agency. 1992. *Earthquake Resistant Construction of Gas and Liquid Fuel Pipeline Systems Serving, or Regulated by, the Federal Government,* FEMA-233. Washington, D.C.
11. Goodling, E. C. 1983. Buried Piping—An Analysis Procedure Update. *ASME PVP.*
12. Hall, W. J., and N. M. Newmark. 1977. Seismic Design Criteria for Pipelines Facilities. In *Proceedings of the Conference on the Current State of Knowledge of Lifeline Earthquake Engineering.* American Society of Civil Engineers. New York.
13. Honegger, D. G. 1997. Evaluating Pipeline Performance for Earthquake Induced Lateral Spread Ground Movement. *ASME PVP.*
14. ISO/DIS 13623, draft, 1998.
15. Marston, Anson, and A. O. Anderson. 1913. The Theory of Loads on Pipes in Ditches and Tests of Cement and Clay Drain Tile and Sewer Pipe. *Bulletin* 31. Ames: Iowa Engineering Experiment Station.
16. Moser, A. P., R. K. Watkins, and O. K. Shupe. 1976. Design and Performance of PVC Pipes Subjected to External Soil Pressure. Logan: Buried Structures Laboratory, Utah State University.
17. Newmark, N. M. 1942. Influence Charts for Computation of Stresses in Elastic Foundations. *Bulletin* 338. University of Illinois: Engineering Experiment Station.
18. O'Rourke, M. J., and J. Liu. 1998. Seismic Loading Behavior of Buried Pipelines. *ASME PVP.*
19. Piping Systems Institute. 1980. *Course Notebook.* Logan: Utah State University.
20. Reissner, E. 1959. On Final Bending of Pressurized Tubes. *Journal of Applied Mechanics* (*Trans. ASME*). September, pp. 386–392.
21. Schlick, W. J. 1932. Loads on Pipe in Wide Ditches. *Bulletin* 108. Iowa State Engineering Experiment Station.
22. Spangler, M. G. 1941. The Structural Design of Flexible Pipe Culverts. *Bulletin* 153. Ames: Iowa Engineering Experiment Station.
23. Spangler, M. G., and R. L. Handy. 1982. *Soil Engineering,* 4th ed., New York: Harper & Row.
24. Stephens, D. R., et al. 1991. *Pipeline Monitoring—Limit State Criteria,* Batelle Report NG-18 no. 188 for AGA.
25. Terzaghi, K., and R. B. Beck. 1967. *Soil Mechanics in Engineering Practice.* Wiley.
26. Uni-Bell PVC Pipe Association. 1982. *Handbook of PVC Pipe Design and Construction.* Dallas.
27. Watkins, R. K., and L. R. Anderson. 2000. *Structural Mechanics of Buried Pipes.* New York: CRC Press.
28. Watkins, R. K., and A. P. Moser. 1971. Response of Corrugated Steel Pipe to External Soil Pressures. *Highway Research Record,* 373:88–112.
29. Watkins, R. K., and A. P. Moser. 1998. Soil and Surface Loads on Buried Pipes Including Minimum Cover Requirements. *ASME PVP,* 360.

This page intentionally left blank.

Chapter

3

Design of Gravity Flow Pipes

Design methods which are used to determine an installation design for buried gravity flow pipes are described in this chapter. Soil types and their uses in pipe embedment and backfill are discussed. Design methods are placed in two general classes—rigid pipe design and pressure pipe design. Pipe performance limits are given, and recommended safety factors are reviewed.

The finite element method for design of buried piping systems is relatively new. The use of this powerful tool is increasing with time. A detailed discussion of this method is included.

Soils

The importance of soil density (compaction) and soil type in contributing to buried pipe performance has long been recognized by engineers. The pipe-zone backfill, which is often referred to as the *soil envelope* around the pipe, is most important. An introduction and a brief discussion of embedment soils are presented in Chap. 1. In this chapter, additional information on soil classification and soil-pipe interaction is provided.

Soil classes

Professor Arthur Casagrande proposed a soil classification system for roads and airfields in the early 1940s. This system, now called the Unified Soil Classification System (USCS), has been adopted by many groups and agencies, including the Army Corps of Engineers and the Bureau of Reclamation. The American Society for Testing and Materials (ASTM) version of the USCS is entitled "Classification of Soils for Engineering Purposes" and carries the designation D 2487.

The USCS is based on the textural characteristics for those soils with a small amount of fines such that the fines have little or no influence on behavior. For those soils where fines affect the behavior, classification is based on plasticity-compressibility characteristics. The plasticity-compressibility characteristics are evaluated by plotting the plasticity chart. The position of the plotted points yields classification information. The following properties form the basis of soil classification and identification:

1. Percentages of gravel, sand, and fines [fraction passing 0.75-mm (no. 200) sieve]
2. Shape of grain-size distribution curve (see Fig. 3.1)
3. Plasticity and compressibility characteristics (see Fig. 3.2)

A soil is given a descriptive name and letter symbol to indicate its principal characteristics. (See ASTM D 2487 or any text on soil mechanics.)

Embedment materials listed here include the soil types defined according to the USCS and a number of processed materials. ASTM D 2321, "Underground Installation of Flexible Thermoplastic Sewer Pipe," breaks down embedment materials into five classes. These classes along with the USCS letter designation and description are given in Table 3.1.

Class I comprise angular, $^1/_4$- to $1^1/_2$-in (6- to 40-mm) graded stone, including a number of fill materials that have regional significance such as coral, slag, cinders, crushed shells, and crushed stone. *Note:* The size range and resulting high voids ratio of class I material make it suitable for use to dewater trenches during pipe installation. This permeable characteristic dictates that its use be limited to locations where pipe support will not be lost by migration of fine-grained natural material from the trench walls and bottom, or migration of other embedment materials into the class I material. When such migration is possible, the material's minimum size range should be reduced to finer than $^1/_4$ in (6 mm) and the gradation properly designed to limit the size of the voids.

Class II comprises coarse sands and gravels with maximum particle size of $1^1/_2$ in (40 mm), including variously graded sands and gravels containing small percentages of fines, generally granular and noncohesive, either wet or dry. Soil types GW, GP, SW, and SP are included in this class.

Sands and gravels that are clean or borderline between clean and with fines should be included. Coarse-grained soils with less than 12 percent but more than 5 percent fines are neglected in ASTM D 2487 and the USCS and should be included. The gradation of class II material influences its density and pipe-support strength when loosely

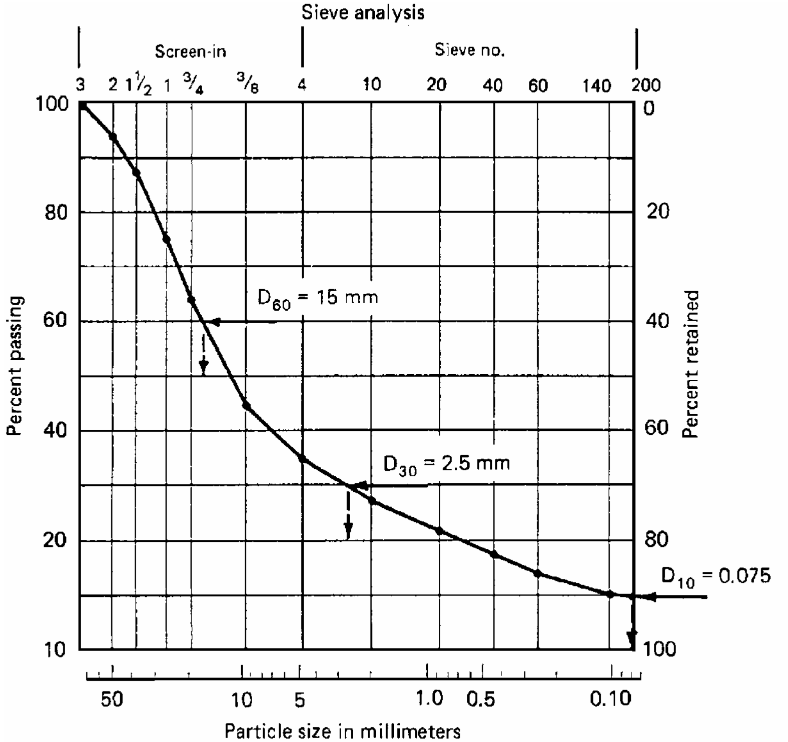

Figure 3.1 Grain-size distribution curve for a particular soil. (*Reprinted, by permission, from ASTM D 2487, Fig. 4.*)

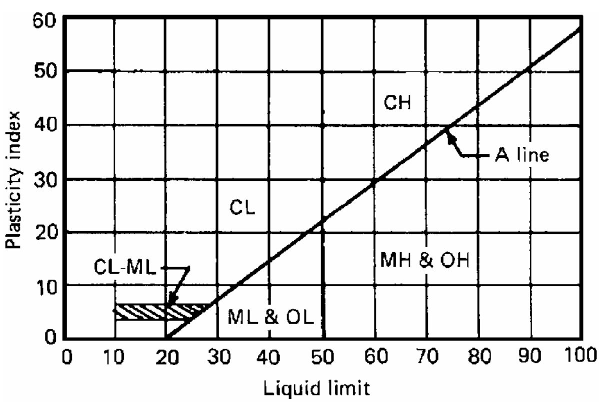

Figure 3.2 Plasticity chart. (*Reprinted, by permission, from Asphalt Institute Soils Manual.*[1])

TABLE 3.1 Description of Embedment Material Classifications

Soil class	Soil type	Description of material classification
Class I soils*	—	Manufactured angular, granular material, $^1/_4$ to $1^1/_2$ in (6 to 40 mm) in size, including materials having regional significance such as crushed stone or rock, broken coral, crushed slag, cinders, or crushed shells.
Class II soils†	GW	Well-graded gravels and gravel-sand mixtures, little or no fines. 50 percent or more retained on no. 4 sieve. More than 95 percent retained on no. 200 sieve. Clean.
	GP	Poorly graded gravels and gravel-sand mixtures, little or no fines. 50 percent or more retained on no. 4 sieve. More than 95 percent retained on no. 200 sieve. Clean.
	SW	Well-graded sands and gravelly sands, little or no fines. More than 50 percent passes no. 4 sieve. More than 95% retained on no. 200 sieve. Clean.
	SP	Poorly graded sands and gravelly sands, little or no fines. More than 50% passes no. 4 sieve. More than 95% retained on no. 200 sieve. Clean.
Class III soils‡	GM	Silty gravels, gravel-sand-silt mixtures. 50% or more retained on no. 4 sieve. More than 50% retained on no. 200 sieve.
	GC	Clayey gravels, gravel-sand-clay mixtures. 50% or more retained on no. 4 sieve. More than 50% retained on no. 200 sieve.
	SM	Silty sands, sand-silt mixtures. More than 50% passes no. 4 sieve. More than 50% retained on no. 200 sieve.
	SC	Clayey sands, sand-clay mixtures. More than 50% passes no. 4 sieve. More than 50% retained on no. 200 sieve.
Class IV soils	ML	Inorganic silts, very fine sands, rock flour, silty or clayey fine sands. Liquid limit 50% or less. 50% or more passes no. 200 sieve.
	CL	Inorganic clays of low to medium plasticity, gravelly clays, sandy clays, silty clays, lean clays. Liquid limit 50% or less. 50% or more passes no. 200 sieve.
	MH	Inorganic silts, micaceous or diatomaceous fine sands or silts, elastic silts. Liquid limit greater than 50%. 50% or more passes no. 200 sieve.
	CH	Inorganic clays of high plasticity, fat clays. Liquid limit greater than 50%. 50% or more passes no. 200 sieve.
Class V soils	OL	Organic silts and organic silty clays of low plasticity. Liquid limit 50% or less. 50% or more passes no. 200 sieve.
	OH	Organic clays of medium to high plasticity. Liquid limit greater than 50%. 50% or more passes no. 200 sieve.
	PT	Peat, muck, and other highly organic soils.

*Soils defined as class I materials are not defined in ASTM D 2487.
†In accordance with ASTM D 2487, less than 5 percent pass no. 200 sieve.
‡In accordance with ASTM D 2487, more than 12 percent pass no. 200 sieve. Soils with 5 to 12 percent pass no. 200 sieve fall in borderline classification, e.g., GP-GC.
SOURCE: Reprinted by permission. Copyright ASTM.

placed. The gradation of class II material may be critical to the pipe support and stability of the foundation and embedment if the material is imported and is not native to the trench excavation. A gradation other than well-graded, such as uniformly graded or gap-graded, may permit loss of support by migration into void spaces of a finer-grained natural material from the trench wall and bottom.

Class III comprises fine sand and clayey (clay-filled) gravels, including fine sands, sand-clay mixtures, and gravel-clay mixtures. Soil types GM, GC, SM, and SC are included in this class.

Class IV comprises silt, silty clays, and clays, including inorganic clays and silts of low to high plasticity and liquid limits. Soil types MH, ML, CH, and CL are included in this class. *Note:* Caution should be used in the design and selection of the degree and method for compaction for class IV soils because of the difficulty in properly controlling the moisture content under field conditions. Some class IV soils with medium to high plasticity and liquid limits greater than 50 percent (CH, MH, CH-MH) exhibit reduced strength when wet and should only be used for bedding, haunching, and initial backfill in arid locations where the pipe embedment will not be saturated by groundwater, rainfall, and/or exfiltration from the pipeline system. Class IV soils with low to medium plasticity and with liquid limits lower than 50 percent (CL, ML, CL-ML) also require careful consideration in design and installation to control moisture content, but need not be restricted in use to arid locations.

Class V includes the organic soils OL, OH, and PT as well as soils containing frozen earth, debris, rocks larger than $1\frac{1}{2}$ in (40 mm) in diameter, and other foreign materials. These materials are not recommended for bedding, haunching, or initial backfill.

Soil-pipe interaction

Design of a buried conduit has a basic objective of adequate overall performance at minimum cost. Overall performance includes not only structural performance, but also service life. Minimum cost analysis should consider all costs including lifetime maintenance.

Initial cost is often broken down into piping material cost and installation cost. Various pipe products have differing strengths and stiffness characteristics and may require differing embedment materials and placement techniques depending on the in situ soil and depth of burial. Products which allow for minimum initial or installation costs may not be the lowest-cost alternative when consideration is given to total lifetime cost. Soil-structure interaction influences pipe performance and is a function of both the pipe properties and embedment soil properties, and therefore impacts total system costs. The design engineer should consider soil-structure interaction in the installation design and lifetime cost estimates.

The soil-pipe system is highly statically indeterminate. This means that the interface pressure between the soil and pipe cannot be calculated by statics alone—the stiffness properties of both soil and pipe must also be considered. The ratio of pipe stiffness to soil stiffness (PS/E') determines to a large degree the load imposed on the conduit. For example, a "rigid pipe" will have a much greater load than a "flexible pipe" installed under the same or similar conditions.

Soil to be placed in the pipe zone should be capable of maintaining the specified soil density. Also, to eliminate pressure concentrations, the soil should be uniformly placed and compacted around the pipe.

Various placement methods can be used depending upon system parameters such as soil type, required density, burial depth, pipe stiffness, and pipe strength. The following are suggested as methods which will achieve desirable densities with the least effort (see Table 3.2).

Certain manufactured materials may be placed by loose dumping with a minimum of compactive effort. These materials must be angular and granular such as broken coral, crushed stone or rock, crushed shells, crushed slag, or cinders and have a maximum size of $1\frac{1}{2}$ in (40 mm). Care should be taken to ensure proper placement of these materials under pipe haunches.

With coarse-grained soils containing less than 5 percent fines such as GW, GP, SW, SP, GW-GP, and SW-SP, the maximum density will be obtained by compacting by saturation or vibration. If internal vibrators are used, the height of successive lifts or backfill should be limited to the penetrating depth of the vibrator. If surface vibrators are used, the backfill should be placed in lifts of 6 to 12 in (150 to 300 mm). This material may also be compacted by hand tamping or other means, provided that the desired relative density is obtained.

Coarse-grained soils which are borderline between clean and those with fines containing between 5 and 12 percent fines, such as GW-GM, SW-SM, GW-GC, SW-SC, GP-GM, SP-SM, GP-GC, and SP-SC, should be compacted either by hand or by mechanical tamping, saturation or vibration, or whichever method meets the required density.

Coarse-grained soils containing more than 12 percent fines, such as GM, GC, SM, SC, and any borderline cases in the group (that is, GM-

TABLE 3.2 Bedding Factors

Bedding class	Load factor
A	2.8–3.4
B	1.9
C	1.5
D	1.1

SM), should be compacted by hand or by mechanical tamping. The backfill should be placed in lifts of 4 to 6 in (100 to 150 mm). Fine-grained soils such as MH, CH, ML, CL, SC-CL, SM-ML, and ML-CL should be compacted by hand or by mechanical tamping in lifts of 4 to 6 in (100 to 150 mm).

Embedment

Soil is a major component of the soil-pipe interaction system and is actually part of the structure that supports the load. The following are some basic rules of thumb that may be of use in the evaluation of buried pipe structures.

1. A common installation is a narrow trench with only enough side clearance to align the pipe and to permit placement of embedment. A trench should never be so narrow that it is difficult to place and compact soil in the haunch zone of the pipe.
2. The arching action of the soil helps to support the load. The soil acts like a masonry arch. No cement is needed because the soil is confined in compression. Soil protects the pipe. The sidefill is the soil arch. It must be compacted up and over the pipe in order to create a soil arch. Bedding provides abutments for the soil arch so the bedding must be compacted.
3. If mechanical compactors are used, the soil arch should be compacted in lifts of less than 1 ft on alternate sides of the pipe, so that the compaction surfaces are at the same elevation. Soil should not be compacted directly on top of the pipe. Compaction right over the pipe creates a load concentration and can produce a worst-case Marston load.
4. Very good buried pipe installations are those which disturb the native soil the least. A bored tunnel of exact pipe OD, into which the pipe is inserted, would cause the least disturbance. Microtunneling, with a bore slightly greater than the inserted pipe, is used successfully.
5. In saturated soil, most pipes tend to float rather than sink.
6. All voids in the backfill should be eliminated. Voids can cause pressure concentrations against the pipe and may become channels for groundwater flow along the pipe (under the haunches). Full contact of embedment against the pipe should be achieved.
7. Soil density is the most important soil property to ensure that the soil will provide the structural support for the pipe. Its importance cannot be overemphasized—in actual tests, the ring deflection of flexible pipes 3 ft in diameter, in an embedment of loose silty sand, was reduced to approximately one-half by merely stomping soil under the haunches. For many soils the required density can only be achieved by mechanical compaction. For select embedment such as pea gravel, compaction can be achieved by merely moving the gravel into place in

contact with the pipe. Crushed angular stone provides ideal support but often requires vibration or compaction to move the stone under the haunches and in contact with the pipe.

Below the water table, soil density is extremely important. At void ratios greater than the critical void ratio, the addition of water will cause relative shifting of soil particles and tends to “shake down” the soil grains into a smaller volume. When a loose soil is saturated, the volume decrease and the voids left are occupied by only the noncompressible water that cannot support stresses. The soil mass becomes liquefied, and the pipe may collapse. If the soil has initially been placed at a density greater than the critical density (void ratio less than critical), under disturbance (vibration) the soil volume tries to increase but is confined, and cannot increase. For many soils, the critical density is fairly high and is in the range of 88 to 92 percent standard Proctor density.

Compacting techniques

Select embedment. Carefully graded select soils, such as pea gravel and crushed stone, fall into place at densities greater than critical density. The only requirement is to actually move the soil in against the pipe especially under the haunches, to provide intimate contact between embedment and pipe.

Mechanical compaction. Mechanical compaction of the soil in lifts (layers) is an effective method for densifying soils. Mechanical compactors densify the soil by rolling, kneading, pressing, impacting, vibrating, or any combination. Instructions are available on mechanical compactors and on procedures such as optimum heights of soil lifts and moisture content. Efficiencies of various compactors in various soils have been studied. In most cases, density tests are required to ascertain that the specified density is being achieved. Heavy equipment (compactors, loaders, scrapers, etc.) must not operate close to the structure—especially flexible structures, since misalignment, deflection, and high induced stress may occur.

Vibration. Loose soil can be compacted by vibrating it with vibroplates and vibrating rollers on each soil lift. Some compaction of the embedment can be achieved by vibrating the pipe itself. Concrete vibrators are effective in the placement of embedment around pipes if enough water is mixed with the soil to form a viscous, concretelike mix. The contractor may saturate a lift of sidefill and then settle it with concrete vibrators. This technique places, but does not compact, the soil. Saturated soil is noncompressible, therefore, *noncompactible.* If such a method is used, the soil must be free-draining. Also no load (soil on top of pipe) should be placed until, after vibration, the soil has drained and has developed its strength. If the soil is not free-draining, particles flow into place, but settle only under buoyant weight. The result is the same as ponding. The soil gradation must be controlled just as concrete aggregate is controlled. Flotation must be avoided.

Flooding (ponding). A lift of free-draining soil is placed up to the spring line of the pipe, then the soil is irrigated. A second lift to the top of the structure is often specified. Enough water must be applied that the lift of soil is saturated. The soil should be free-draining and must be dewatered to settle the soil. The compaction mechanism is downward seepage stress which compacts the soil. Soil is washed into voids and under the haunches of the pipe. The pipe must not float out of alignment. This is the least effective method (yet often adequate) for compaction.

Jetting. Soil density greater than critical can be achieved by jetting. This technique is particularly attractive for soil compaction around large buried structures. Soil is placed in high lifts, such as 3 to 5 ft, or to the spring line (midheight) of large-diameter pipes. A *stinger* pipe (1-in diameter and 5 or 6 ft long, attached to a water hose) is injected vertically down to near the bottom of the soil lift. A high-pressure water jet moves the soil into place at a density greater than critical if the soil is free-draining and immediately dewatered. Jet injections are made on a grid every few feet. Five-foot grids have been used successfully for 5- or 6-ft lifts of cohesionless soil. Gangjets can be mounted on a tractor. They can be injected into a lift of sidefill up to the spring line. To fill the holes left when jets are withdrawn, the stingers are vibrated. A second lift up to the top is jetted in a similar manner. The technique works well in sand. As with vibration, no load (soil on top of pipe) should be placed until, after the jetting of the soil around the pipe, the soil has drained and has developed its strength. Pipe overdeflection and pipe failures have been reported when soil, several feet in depth, was placed on the pipe before jetting took place. In such a case, jetting causes the soil to collapse and liquefy around the pipe, giving no support to the pipe and no arching to help support the soil on the pipe. In any compaction technique, it is absolutely essential that the required pipe zone density be achieved before overburden is placed on the pipe.

Flushing. Soil densities greater than critical can be achieved if a high-pressure water jet is used to flush soil into place against the pipe. A high-pressure water jet plays the stream onto the inside slope of the windrow of soil on the trench bank until a soil slide develops. This soil slide can be directed by the jet into place against the pipe with enough energy to fill in the voids. Windrows are added on both sides simultaneously in order to keep the soil in balance. Of course, the water must drain out rapidly for best compaction.

Slurry and flowable fill. Under some circumstances, the best way to ensure support under the haunches is by flowable fill (soil cement or slurry). The pipe is aligned on mounds. Flowable fill is poured into the haunch area on one side of the pipe. If flowable fill is required to a depth greater than the flotation depth, it can be poured in lifts. Full contact is ensured when the flowable fill rises on the other side of the pipe. Flowable fill should not shrink excessively. Some agencies specify compressive strength of 200 lb/in^2. Less strength (40 lb/in^2) may be desirable to reduce stress concentration and to facilitate subsequent excavations. Recommended slump is about 10 in.

High-velocity impact. Soil compaction can be achieved by dropping from a sufficient height, blowing, slinging, etc. Better control is achieved if the embedment is "shot-creted" into place or if dry soil is blown or slung into place.

Trench Width

Trenches are kept narrow for rigid pipes. The Marston load on a pipe is the weight of backfill in the trench reduced by frictional resistance of the trench walls. The narrower the trench, the lighter is the load on the pipe. The pipe has to be strong enough to support the load. The trench only needs to be wide enough to align the pipe and to place embedment between the pipe and trench wall. If ring deflection is excessive, or if the pipe has less than minimum soil cover when surface loads pass over, the soil at the sides can slip. Ring inversion is incipient. If there is any possibility of soil liquefaction, the embedment should be denser than critical density. Ninety percent standard density (AASHTO T-99 or ASTM D 698) is often specified. In loose saturated soil, liquefaction can be caused by earth tremors. Soil compaction may or may not be required depending upon the quality of the embedment. For example, gravel falls into place at densities greater than 90 percent. Loss of embedment by washout of soil particles by groundwater flow (piping) should be prevented. Spangler observed that a flexible ring depends upon support from sidefill soil. His observation led to the inference that if the trench is excavated in poor soil, the trench walls cannot provide adequate horizontal support. The remedy appeared to be wider trenches, especially in poor native soil. Both principles of stability and experience show a wide trench is seldom justified.

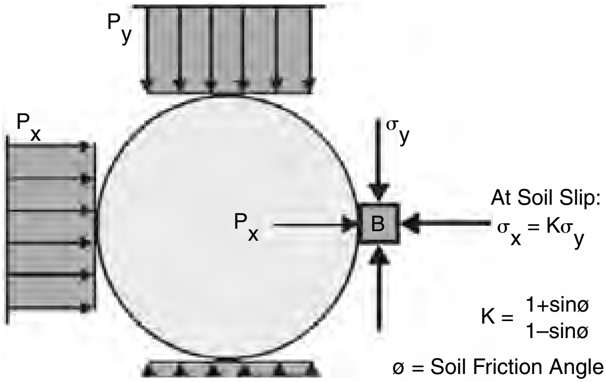

Figure 3.3 Infinitesimal soil cube B. Conditions for soil slip are $P_x = K\sigma_y$.

For small deflection (5 percent or less), theoretically, the embedment needs little horizontal strength. Good sidefill soils add a margin of safety. See Fig. 3.3, where the infinitesimal soil cube is in equilibrium as long as the pipe pressure does not exceed sidefill soil strength σ_x. For stability, $P < \sigma_x = K\sigma_y$.

As long as the pipe is nearly circular, in poor native soils, the pipe depends little on the side support from the trench wall and the trench does not need to be wider than half a diameter on each side for both rigid and flexible pipes. If ring deflection of a flexible pipe is no more than 5 percent, the effect of ring deflection can be neglected. On a rigid pipe, P_d is the Marston load.[24] On a flexible pipe, P_d is more nearly the prism load γH.[41,42]

The height of soil cover H is not a pertinent variable in the analysis of trench width. As soil load is increased, the pressure on the pipe increases; but the strength of the sidefill soil increases in direct proportion.

Rules of thumb for required trench width for flexible pipes

1. Trench must be wide enough for proper soil placement.
2. In poor soil, specify a minimum width of sidefill of one-half a diameter $D/2$ from the pipe to the walls of the trench, or from the pipe to the windrow slopes of the embedment in an embankment.
3. In good soil, the width of sidefill can be less, provided that the embedment is placed at adequate density.

Some concerns for embedments

Wheel loads over a pipe with less than minimum soil cover

Water table above the pipe and/or vacuum in the pipe

Migration of soil particles out of the embedment

Voids left by a trench shield or sheet piling

Heavy equipment near pipe

Wheel loads

(See the section "Minimum Soil Cover" in Chap. 2.) Sidefill soil strength must support the pipe under a live load. However, minimum cover of compacted granular soil is about $H = 1$ ft for HS-20 dual-wheel, and $H = 3$ ft for the single wheel of a scraper. Manufacturers of large steel pipes with mortar linings recommend that a margin of safety of 1.5 ft be added to the minimum cover. Recommended minimum cover is 2.5 ft for HS-20 loads and 4.5 ft for scraper wheel loads. With soil cover greater than minimum, wheel load pressure is less than $P_l = W/(2H^2)$. Trench width could be critical if the sidefill embedment were so poor that it could not support wheel loads anyway.

Water table

(See the section "Flotation" in Chap. 2.) When the water table is above the pipe, sidefill soil strength is effective (buoyant) strength $\sigma_x = K\sigma_y$. The effective vertical soil stress is $(\sigma_y)_{\text{eff}} = \sigma_y - u$, where u is the pore water pressure; that is, $u = \gamma_w h$, where γ_w is the unit weight of water and h is the height of the water table (head) above the spring line of the pipe. If the pipe tends to float, for analysis, P is the hydrostatic buoyant pressure on the bottom of the pipe, $P = \gamma_w(h + r)$, rather than soil pressure on top.

Soil particle migration

ASTM D 2321 has some rules to follow concerning soil particle size and possible soil particle migration. In general, open-grained coarser material should not be used for foundation and bedding if finer materials are used in haunching and initial backfill. In such a case, the finer material can migrate down in the coarser material, and pipe support can be lost. Also, groundwater flow may wash trench wall fines into the voids in coarser embedments.

Wheel loads and earth tremors may shove or shake coarser particles from the embedment into the finer soil of the trench wall. If fines migrate from the trench wall into the embedment, the trench wall may settle, but the pipe is unaffected. If embedment particles migrate into the trench wall, the shift in sidefill support may allow slight ring deflection. This could occur only if the trench wall soil is loose enough, or plastic enough, that the embedment particles can migrate into it.

Soil particle migration is unusual, but must be considered. Remedies include: (1) embedment with enough fines to filter out migrating particles in groundwater flow and (2) trench liners. Geotextile liners may be required under some circumstances.

Voids in the embedment

Soil should be in contact with the pipe in order to avoid piping (channels of groundwater flow) under the haunches. Voids are avoided if the embedment is flowable fill—a good idea when trench widths are too narrow for placement of soil under the haunches. Trench boxes and sheet piling should be designed so that the tips of the piles or shield are above the spring lines of the pipe. If they are designed and used properly, voids left by the withdrawal of sheet piling or trench shield will not affect the performance of the pipe.

Heavy equipment

If the buried structure has a low inherent strength or is so flexible that heavy compactors can deform it, then only light compactors can be used close to it. Heavy compactors must remain outside of planes tangent to the structure and inclined at an angle less than $45° + \phi/2$ from horizontal. Soil cover H greater than minimum is required above the structure. The heavy equipment zone is often specified and is usually 2 ft or $D/2$, whichever is greater. Operators should be reminded that a large structure gives a false illusion of strength. It achieves its strength and stability only after the embedment has been placed about it. Because the structure cannot resist high sidefill pressures during soil placement, operators should think, "If it were not there, how far back from the edge of the sidefill would I keep this equipment in order not to cause a soil slope failure?" The answer is found from experience and from the tangent plane concept. A margin of safety is usually applied to the $45° + \phi/2$ plane by specifying a 45° tangent plane. The minimum cover H_{min} for various types and weights of equipment can be determined by the methods suggested in Chap. 2. As a rule of thumb, the minimum soil cover should not be less than 3 ft for H-20 truck loads, D8 tractors, etc. For scrapers and super-compactors, 5 ft of soil may be a more comfortable minimum.

Rigid Pipe Analysis

Three-edge bearing strength

Rigid nonpressure pipes are of four general types and are covered by four ASTM specifications. Asbestos-cement pipe is governed by ASTM

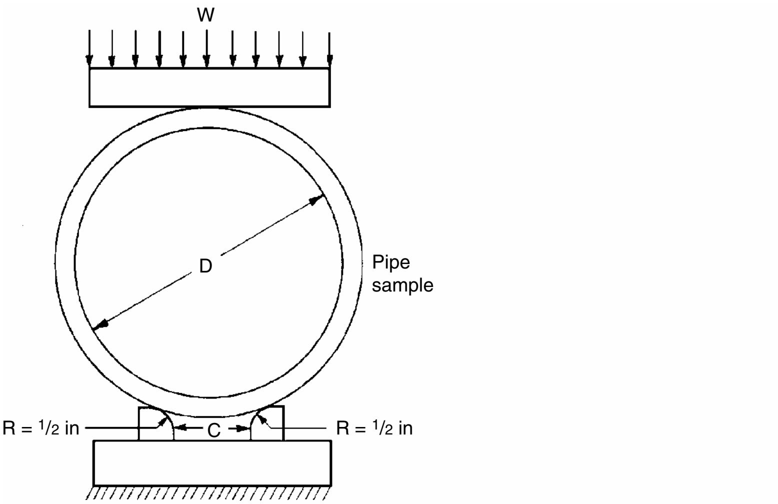

Figure 3.4 Three-edge bearing (wood block) schematic.

C 428. Vitrified clay pipe is specified in two strength classes by ASTM C 700. Nonreinforced concrete pipe is covered by ASTM C 14. Reinforced concrete nonpressure pipe is specified by its so-called *D* load strength as given in ASTM C 76. The *D* load is the three-edge bearing strength divided by diameter. Designs of the various types of rigid pipe for nonpressure applications to resist external loads require knowledge of available pipe strengths as well as the construction or installation conditions to be encountered.

Rigid pipe is tested for strength in the laboratory by the three-edge bearing test (see Fig. 3.4 for diagram of test). Methods for testing are described in detail in the respective ASTM specifications for the specific pipe product. The three-edge bearing strength is the load per length (usually pounds per foot) required to cause crushing or critical cracking of the pipe test specimen. This strength is the load at failure in a testing machine. It is not necessarily the load that will cause failure in the soil.

Bedding factors and classifications

In Chap. 2 we learned that for rigid pipe, the soil load can be calculated by Marston's equation $W_d = C_d \gamma B_d^2$. Experience has shown that the Marston load, to cause failure, is usually greater than the three-edge bearing strength and depends on how the pipe was bedded (Fig. 3.4).

The Marston load that causes failure is called the *field strength*. The ratio of field strength to three-edge bearing strength is termed the *bedding factor* since it is dependent upon how the pipe was bedded (installed). The term *bedding factor* as used by Marston is sometimes called the *load factor.* The two terms refer to the same parameter and may be used interchangeably.

$$\text{Bedding factor} = \frac{\text{field strength}}{\text{three-edge bearing strength}} \tag{3.1}$$

Major pipe manufacturing associations recommend bedding factors that correspond to those listed in the Water Pollution Control Federation Manual of Practice, No. FD-5, *Gravity Sanitary Sewer Design and Construction.*

These bedding types (classes) are shown in Fig. 3.5, and corresponding bedding factors (load factors) are given in Table 3.2.

Installation design

Equation (3.1) may be solved for the three-edge bearing strength as follows:

$$\text{Three-edge bearing strength} = \frac{\text{field strength}}{\text{bedding factor}} \tag{3.2}$$

The field strength is the Marston load that will cause failure in the field. Most designers and specifications require a factor of safety in the design. Thus the required strength is as follows:

$$\text{Required three-edge bearing strength} = \frac{\text{design load} \times \text{factor of safety}}{\text{bedding factor}} \tag{3.3}$$

A design procedure to select the appropriate pipe classification or strength is outlined as follows:

1. Determine the earth load.
2. Determine the live load.
3. Select the bedding requirement.
4. Determine the load factor.
5. Apply the safety factor.
6. Select the appropriate pipe strength.

The following example will illustrate the use of the six design steps and basic rigid pipe principles in selecting the appropriate pipe. It is not within the scope of this text to discuss pipe material design [i.e., how much material (reinforcing steel, asbestos fiber, cement, and so forth) is required to meet a specific crush strength is not included].

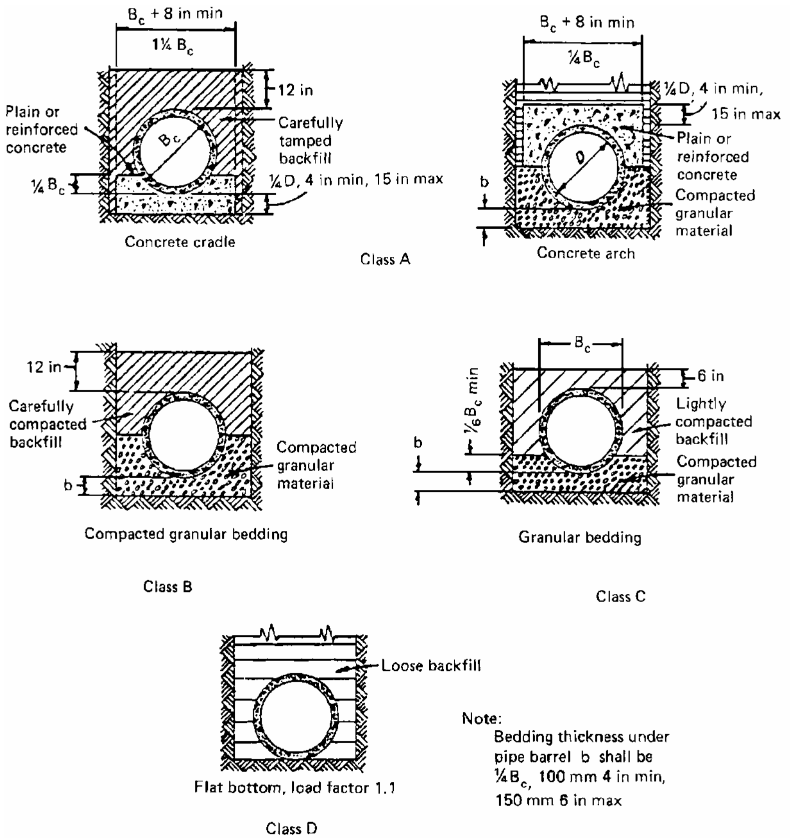

Figure 3.5 Class of bedding for rigid sewer pipes. [*Note:* In rock trenches, excavate at least 6 in below bell. In unstable material, such as peat or expansive material, remove unstable material and replace with a select fill material (consult competent soils engineer).] (*Reprinted with permission of Water Pollution Control Federation.*)

Since ASTM specifies minimum crush strengths, these will be used as a beginning point for design in the discussion here.

Example Problem 3.1 A 15-in-diameter sanitary sewer line is to be installed 14 ft deep in native material, which is sand. If the trench width is 3.0 ft, what pipe and bedding classes should be selected?

1. Determine the earth load.

$$\frac{H}{B_d} = 14/3 = 4.67$$

$$K\mu = 0.165 \qquad \text{sand}$$

From Fig. 2.2, $C_d = 2.4$, so

$$W_d = C_d \gamma B_d^{\,2} = 2.4\,(120)\,(3.0)^2 = 2592 \text{ lb/ft}$$

2. Determine the live load (assume H-20 highway loading). From Fig. 2.21, note that the live load is negligible for 14 ft of cover.

3. Select bedding. Economic and practical engineering judgment is required. Compare classes D, C, and B (Fig. 3.4).

4. Determine the load factor. From Table 3.2

Class D	BF = 1.1
Class C	BF = 1.5
Class B	BF = 1.9

5. Apply the safety factor.

Recommendations:	
Concrete (ACPA)	SF = 1.25–1.5
Reinforced concrete (ACPA)	SF = 1.0 based on 0.01-in crack
Clay (CPI)	SF = 1.0–1.5
Asbestos cement (ACPPA)	SF = 1.0–1.5

6. Select pipe strength.

$$W_{\text{3-edge}} = W_c \times \frac{\text{SF}}{\text{BF}}$$

$$W_{D\text{ load}} = W_c \times \frac{\text{SF}}{\text{BF}} \times D$$

$$W_{\text{3-edge}} = 2592\,\frac{\text{SF}}{\text{BF}}$$

$$W_{D\text{ load}} = 2074\,\frac{\text{SF}}{\text{BF}}$$

Minimum Required Strength for SF = 1.5

Bedding class	Three-edge, lb/ft	*D* load, (lb/ft)/ft
B	2046	1637
C	2592	2074
D	3535	2828

Choice may be based on job details including economic consideration of pipe versus bedding cost. Choose a strength class that equals or exceeds strengths given in the table above.

Example Problem 3.2 Suppose the trench width of 3.0 ft cannot be maintained at the top of the pipe in Example Problem 3.1. What are the required strengths if the transition trench width is reached?

1. Determine transition width.

$$\frac{H}{B_c} = \frac{14}{1.25} = 11.20$$

$$r_{sd}p = 0.5$$

From Fig. 2.6, $B_d/B_c = 2.9$ and

$$B_d \text{ (transition)} = \frac{B_d}{B_c B_c} = 2.9\left(\frac{15}{12}\right) = 3.6 \text{ ft}$$

2. Determine the earth load.

$$\frac{H}{B_d} = \frac{14}{3.6} = 3.9$$

$$K\mu = 0.192 \qquad \text{granular}$$

From Fig. 2.2, $C_d = 2.0$ and

$$W_d = C_d \gamma B_d^{\,2} = 2.0\,(120)\,(3.6)^2 = 3110 \text{ lb/ft}$$

Alternately,

$$\frac{H}{B_c} = \frac{14}{1.25} = 11.20$$

$$r_{sd}p = 0.5$$

From Table 2.2,

$$C_c = \frac{1.5\,H}{B_c} - 0.07 = 16.73 \approx 16.7$$

$$W_c = C_c \gamma B_c^{\,2} = 16.7\,(120)\,(1125)^2 = 3131 \text{ lb/ft}$$

At the transition width $W_c \approx W_d$

$$W_{\text{3-edge}} = 3131\,\frac{\text{SF}}{\text{LF}}$$

$$W_{D\text{ load}} = 2505\,\frac{\text{SF}}{\text{LF}}$$

Minimum Required Strength for SF = 1.5

Bedding class	Three-edge, lb/ft	*D* load, (lb/ft)/ft
B	2472	1977
C	3131	2505
D	4270	3416

Flexible Pipe Analysis

Installation design

Three parameters are most essential in the design or the analysis of any flexible conduit installation:

1. Load (depth of burial)
2. Soil stiffness in pipe zone
3. Pipe stiffness

The design load on the pipe is easily calculated using the prism load theory, as discussed in Chap. 2. This load is simply the product of the soil unit weight and the height of cover. Research has shown that the long-term load on a flexible pipe approaches the prism load. Thus, if this load is used in design, the deflection lag factor should be taken as unity.

The soil stiffness is usually expressed in terms of E' (effective soil modulus, lb/in^2). Effective soil modulus E' is dimensionally the load per square inch. The soil modulus E' is a function of soil properties such as soil density, soil type, and moisture content. Experience has shown that soil density is the most important parameter influencing soil stiffness.

For flexible pipes, pipe stiffness rather than crush strength is usually the controlling pipe material property. Pipe stiffness may be expressed in terms of various parameters as follows:

Pipe stiffness terminology

$$\text{Stiffness factor} = EI$$

$$\text{Ring stiffness} = \frac{EI}{r^3} \qquad \left(\text{or sometimes } \frac{EI}{D^3}\right)$$

$$\text{Pipe stiffness} = \frac{F}{\Delta y} = 6.7\,\frac{EI}{r^3}$$

where E = modulus of elasticity, lb/in^2
I = moment of inertia of wall cross section per unit length of pipe, in^4/in = in^3
r = mean radius of pipe, in
D = mean diameter of pipe, in
F = force, lb/in
Δy = vertical deflection, in

The most commonly used terminology is *pipe stiffness* ($F/\Delta y$). For a given pipe product, this term is readily determined in the laboratory by a parallel-plate loading test. In this test, a pipe sample is placed between two horizontal parallel plates in a testing machine. A compressive load is applied and increased until the vertical deflection Δy reaches 5 percent of the diameter. And $F/\Delta y$ is the load at 5 percent divided by the sample length and divided by the vertical deflection Δy. Typical units for $F/\Delta y$ are pounds per square inch. This is evident from the third equation, as it is clear that $F/\Delta y$ has the same units as the modulus of elasticity E.

In summary, the three most important parameters for flexible pipe analysis and design are (1) load, (2) soil stiffness, and (3) pipe stiffness. Any design method that does not include a consideration of these three parameters is incomplete.

For a flexible pipe, vertical deflection is the variable that must be controlled by proper installation design. This deflection is a function of the three parameters discussed above.

Spangler's Iowa formula

M. G. Spangler, a student of Anson Marston, observed that the Marston theory for calculating loads on buried pipe was not adequate for flexible pipe design. Spangler noted that flexible pipes provide little inherent stiffness in comparison to rigid pipes, yet they perform remarkably well when buried in soil. This significant ability of a flexible pipe to support vertical soil loads is derived from (1) the redistribution of loads around the pipe and (2) the passive pressures induced as the sides of the pipe move outward against the surrounding earth. These considerations, coupled with the idea that the ring deflection may form a basis for flexible pipe design, prompted Spangler to study flexible pipe behavior to determine an adequate design procedure. His research and testing led to the derivation of the Iowa formula, which he published in 1941.[42]

Spangler incorporated the effects of the surrounding soil on the pipe's deflection. This was accomplished by assuming that Marston's theory of loads applied and that this load would be uniformly distributed at the plane at the top of the pipe. He also assumed a uniform pressure over part of the bottom, depending upon the bedding angle. On the sides, he assumed the horizontal pressure h on each side would be proportional to the deflection of the pipe into the soil. The constant of proportionality was defined as shown in Fig. 3.6 and was called the *modulus of passive resistance* of the soil. The modulus would presumably be a constant for a given soil and could be measured in a simple lab test. He derived the Iowa formula through analysis as follows:

$$\Delta X = \frac{D_L K W_c r^3}{EI + 0.061 e r^4} \tag{3.4}$$

M. G. Spangler

where D_L = deflection lag factor
K = bedding constant
W_c = Marston's load per unit length of pipe, lb/in
r = mean radius of pipe, in
E = modulus of elasticity of pipe material, lb/in^2
I = moment of inertia of pipe wall per unit length, in^4/in = in^3
e = modulus of passive resistance of sidefill, lb/(in^2) (in)
ΔX = horizontal deflection or change in diameter, in

Equation (3.4) can be used to predict deflections of buried pipe if the three empirical constants K, D_L, and e are known. The bedding constant K accommodates the response of the buried flexible pipe to the opposite and equal reaction to the load force derived from the bedding under the pipe. The bedding constant varies with the width and angle of the bedding achieved in the installation. The bedding angle is shown in Fig. 3.7. Table 3.3 contains a list of bedding factors K dependent upon the bedding angle. These were determined theoretically by Spangler and published in 1941. As a general rule, a value of $K = 0.1$ is assumed.

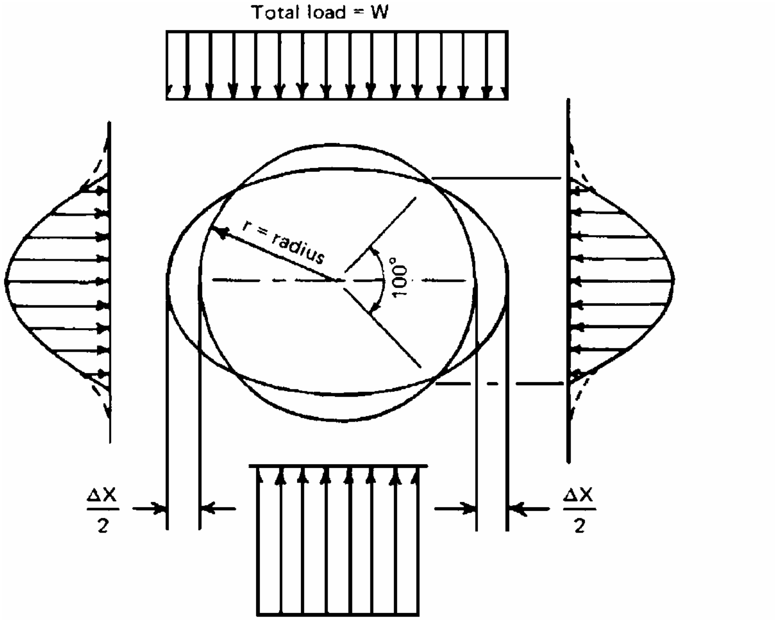

Figure 3.6 Basis of Spangler's derivation of the Iowa formula for deflection of buried pipes. $\Delta X = D_L K W_c r^3/(EI + 0.061er^4)$ (the Iowa formula), where $e = 2h/\Delta X$, $2r = D$ = pipe diameter, K = bedding constant, D_L = deflection lag factor, and EI = stiffness factor (related to pipe stiffness). (*Reprinted with permission of Utah State University.*)

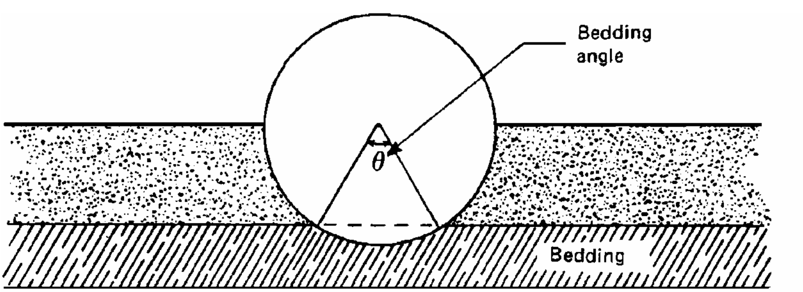

Figure 3.7 Bedding angle.

In 1958, Reynold K. Watkins, a graduate student of Spangler, was investigating the modulus of passive resistance through model studies and examined the Iowa formula dimensionally.[52] The analysis determined that e could not possibly be a true property of the soil in that its dimensions are not those of a true modulus. As a result of Watkins'

TABLE 3.3 Values of Bedding Constant K

Bedding angle, deg	K
0	0.110
30	0.108
45	0.105
60	0.102
90	0.096
120	0.090
180	0.083

effort, another soil parameter was defined. This was the *modulus of soil reaction* $E' = er$. Consequently, a new formula called the modified Iowa formula was proposed. This equation is also often referred to as *Spangler's equation* or the *Iowa formula* and may be so referenced in this text.

$$\Delta X = \frac{D_L K W_c r^3}{EI + 0.061E'r^3} \tag{3.5}$$

Two other observations from Watkins' work are of particular note. (1) There is little point in evaluating E' by a model test and then using this modulus to predict ring deflection, as the model gives ring deflection directly. (2) Ring deflection may not be the only performance limit.

Another parameter that is needed to calculate deflections in the Iowa formula is the deflection lag factor, D_L. Spangler recognized that in soil-pipe systems, as with all engineering systems involving soil, the soil consolidation at the sides of the pipe continues with time after installation of the pipe. His experience had shown that deflections could increase by as much as 30 percent over a period of 40 years. For this reason, he recommended the incorporation of a deflection lag factor of 1.5 as a conservative design procedure. However, recall that the load proposed by Spangler was the Marston load for a flexible pipe. For most sewer pipe installations, the prism load is at least 1.5 times greater than the Marston load (see Chap. 2 for soil loads on pipe). If the prism load is used for design, a design deflection lag factor D_L = 1.0 should be used.

Soil modulus E' analysis. The remaining parameter in the modified Iowa formula is the soil modulus E'. Spangler's Iowa formula predicts ring deflection based on elastic pipe and elastic soil. Spangler, a soil engineer, included a horizontal elastic soil modulus E' which he called the modulus of passive resistance of soil. In fact, horizontal passive resistance is $K\sigma_y$, where $K = (1 + \sin\phi)/(1 - \sin\phi)$. Soil slip planes occur at $45° - \phi/2$—not at 45°.

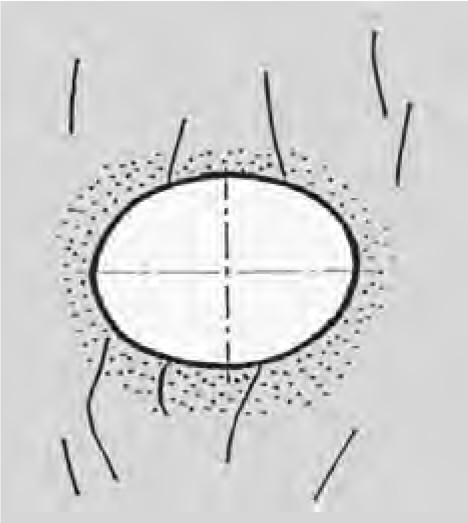

Figure 3.8 Soil slip planes in an embankment of sand compacted to 85 percent standard Proctor density.

Eventually (at a high enough load), general soil shear will occur. By Mohr's circle analysis, horizontal soil resistance is $K\sigma_y$. Accordingly, soil slip planes should occur at spring lines at angle $45° - \phi/2$ with the horizontal. The analysis is conservative. The soil friction angle ϕ is not constant. It varies with depth of cover and ring deflection. In a controlled test, planes of soil slip were observed in the sand embedment of a flexible ring. See Fig. 3.8.

Soil modulus E' may vary as the depth of cover (confining pressure increases). In a confined compression test of soil, the slope of the stress-strain (load-deflection) curve increases as the load increases. That is, the load-deflection curve is concave upward. Thus, the slope of the curve increases with load or depth. There have been suggestions that a pipe buried in the soil performs in the same manner. Therefore, E' should increase with depth (degree of confinement). If such were true, then the slope of the load-deflection curve of a buried pipe should increase with depth of cover, and the load-deflection curve should be concave upward. In fact, only in select fills such as crushed stone is this true. In other soils, the load-deflection curves are concave downward and usually have a knee that is a function of the preconsolidation occurring because of soil compaction in the pipe zone.

A pipe buried in soil is not like a confined compression test. The pipe effectively introduces a hole in the soil which in turn introduces pressure concentration. And in the case of a flexible pipe, the soil is not

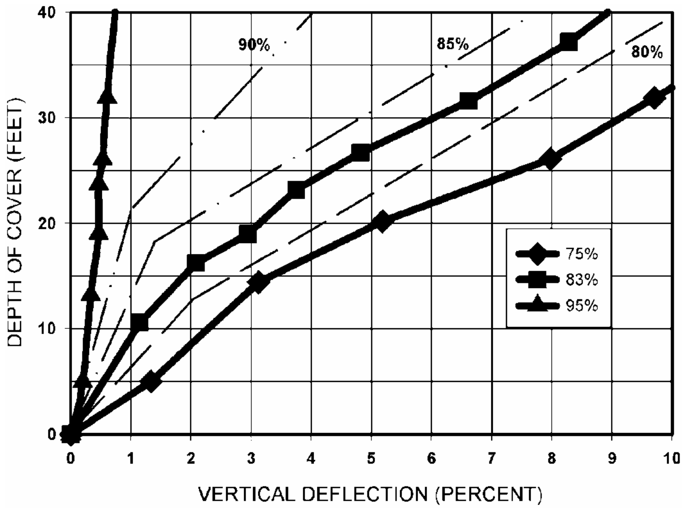

Figure 3.9 Vertical deflection curves for 60-in HDPE pipe at various soil densities. Solid lines are actual test data, and the dashed lines are approximated curves for intermediate densities. For the most part, curves are concave downward. The 95 percent curve could be approximated by a straight line. All curves could be approximated by bilinear lines.

confined but deflects with the pipe and may actually slide on the pipe surface. Soil is not elastic and cannot take tension. (It is not attached to the pipe.) The net effect of the deflection is the formation of micro shear planes in the soil. The effective soil modulus decreases because of the failing soil along the shear planes.

Figures 3.9 and 3.10 are load-deflection curves for steel and polyethylene pipes which are flexible pipes. One can see in these figures that the curves are concave downward, indicative of a decreasing soil modulus because of micro shear failure in the soil. Also one can see the knees in the curves that result from the preconsolidation of the soil.

Many research efforts have attempted to measure E' without much success. The most useful method has involved the measurement of deflections of a buried pipe for which installation conditions are known, followed by a back calculation through the Iowa formula to determine the effective value of E'. This requires assumed values for the load, the bedding factor, and the deflection lag factor. Inconsistent assumptions have led to a variation in reported values of E'.

One attempt to acquire information on values of E' was conducted by Amster K. Howard of the U.S. Bureau of Reclamation.[11] Howard

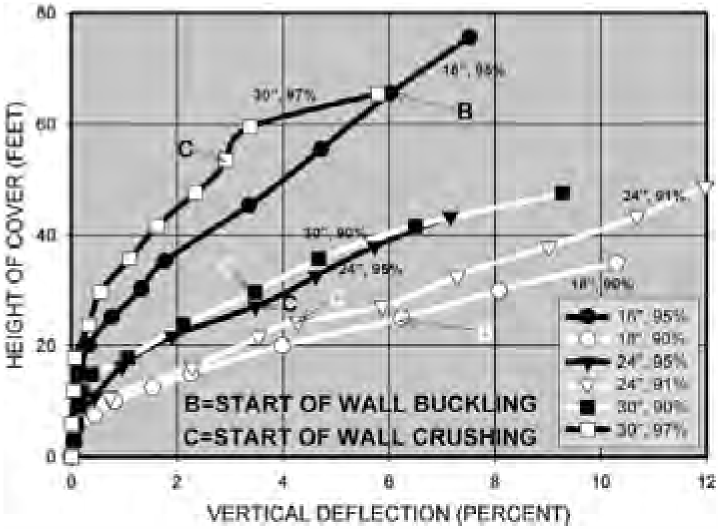

Figure 3.10 Vertical deflections for the six load-deflection tests on steel pipe. Note that the curves are concave downward and have knees corresponding to preconsolidation (compaction) of the soil.

used data from laboratory and field tests to compile a table of average E' values for various soil types and densities (see Table 3.4). He assigned values to E', K, and W_c and then used the Iowa formula to calculate a theoretical value of deflection. This theoretical deflection was then compared with actual measurements. By assuming the E' values of Table 3.4 and a bedding constant $K = 0.1$, Howard was able to correlate the theoretical and empirical results to within ±2 percent deflection when he used the prism soil load. This means that if theoretical deflections using Table 3.4 were approximately 5 percent, measured deflections would range between 3 and 7 percent. Howard is reported to have used a deflection lag factor $D_L = 1.5$ in his calculations. However, if the prism load were used as reported, a lag factor $D_L = 1.0$ would have to have been used to be theoretically correct. In any case, the data in Table 3.4 are consistent with field and laboratory data taken over a 20-year period at Utah State University if the prism load is used along with a value of 1.0 for the deflection lag factor. Although the vast majority of data from Howard's study were taken from tests on steel and reinforced-plastic mortar pipe with diameters greater than 24 in, they do provide some useful information to guide designers of all flexible pipe, including PVC pipe, since the data help to give an understanding of the Iowa deflection formula.

TABLE 3.4 Average Values of Modulus of Soil Reaction *E′* (for Initial Flexible Pipe Deflection)

Soil type-pipe bedding material (Unified Soil Classification System*)	E' for degree of compaction of bedding, lb/in^2			
	Dumped	Slight, <85% Proctor, <40% relative density	Moderate, 85–95% Proctor, 40–70% relative density	High, >95% Proctor, >70% relative density
Fine-grained soils (LL > 50)† Soils with medium to high plasticity CH, MH, CH-MH	No data available. Consult a competent soils engineer; otherwise, use $E' = 0$			
Fine-grained soils (LL < 50) Soils with medium to no plasticity CL, ML, ML-CL with less than 25% coarse-grained particles	50	200	400	1000
Fine-grained soils (LL < 50) Soils with medium to no plasticity CL, ML, ML-CL with more than 25% coarse-grained particles Coarse-grained soils with fines GM, GC, SM, SC containing more than 12% fines	100	400	1000	2000
Coarse-grained soils with little or no fines GW, GP, SW, SP‡ containing less than 12% fines	200	1000	2000	3000
Crushed rock	1000	3000	3000	3000
Accuracy in terms of percentage of deflection§	±2	±2	±1	±0.5

*ASTM D 2487, USBR E-3.
†LL = liquid limit.
‡Or any borderline soil beginning with one of these symbols (i.e., GM-GC, GC-SC).
§For ±1 percent accuracy and predicted deflection of 3 percent, actual deflection would be between 2 and 4 percent.

NOTE: Values applicable only for fills less than 50 ft (15 m). Table does not include any safety factor. For use in predicting initial deflections only, appropriate deflection lag factor must be applied for ling-term deflections. If bedding falls on the borderline between two compaction categories, select lower E' value or average the two values. Percentage Proctor based on laboratory maximum dry density from test standards using about 12,500 ft·lb/ft^3 (598,000 J/m^3)(ASTM D 698, AASHTO T-99, USBR E-11). 1 lb/in^2 = 6.9 kN/m^2.

SOURCE: Amster K. Howard, U.S. Bureau of Reclamation, Denver, "Modulus of Soil Reaction (E') Values for Buried Flexible Pipe," *J. Geotech. Eng. Div.*, January 1977, pp. 33–43. Reprinted with permission from American Society of Civil Engineers.

Use of the constrained soil modulus for flexible pipe design

In design of buried flexible pipe, the soil stiffness has traditionally been modeled using the modulus of soil reaction E'. This is a semiempirical parameter required as input to the Iowa formula for predicting the deflection of buried pipe. An alternate would be to use the one-dimensional constrained modulus M_s. The relationship between E' and M_s has often been discussed in the literature, with a few researchers concluding that the two parameters are interchangeable. Design values for M_s as used in finite element programs are derived using the hyperbolic model for Young's modulus developed by Duncan. The development of the hyperbolic soil model[5,38,39] provides a nonlinear soil model that has been used successfully in finite element analyses of buried pipe. Thus, the hyperbolic model is incorporated in most finite element programs that are used in buried pipe analysis. Examples are CANDE and PIPE5.

The Iowa formula, as proposed by Spangler, predicted the change in the horizontal diameter of the pipe due to soil placed over the top of the pipe. Watkins and Spangler[52] proposed the use of the modulus of soil reaction E' with units of force per length squared. Later Watkins, Spangler, and others showed that the vertical and horizontal deflections were about equal for small deflection. They also showed that the vertical deflection was the better predictor relating to pipe performance. While the Iowa formula has been criticized by some, it remains the best known simplified method for computing deflections.

Howard's E' values (Table 3.4), back-calculated from measured vertical deflections of many flexible pipe installations, are conservative. For the back-calculation, he had to assume the bedding factor and the lag factor. Some have proposed an increasing soil modulus with depth of cover, but Howard found no correlation between E' and depth of fill. His data were limited to 50 ft of cover, so he stated that his proposed values of E' may not be valid for cover greater than 50 ft.

As noted, many researchers have attempted to correlate the modulus of soil reaction E' with other true soil properties that can be evaluated by test. The most common parameter used in these efforts is the constrained modulus M_s, which is the soil stiffness under three-dimensional strain, where strain is assumed to be zero in two of the dimensions because of restraint (Fig. 3.11).

Hooke's law for σ_z in three dimensions is as follows:

$$\sigma_z = \frac{E}{1+\nu}\left[\varepsilon_z + \frac{\nu}{1-2\nu}(\varepsilon_x + \varepsilon_y + \varepsilon_z)\right]$$

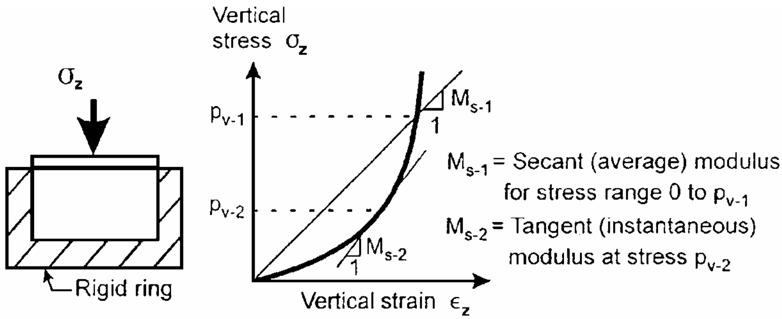

Figure 3.11 Constrained compression test schematic.

where E is the elastic soil modulus (Young's modulus) and ν is Poisson's ratio.

For the constrained compression test (Fig. 3.11), both ε_x and ε_y are assumed to be zero. In this case, Hooke's law above takes on the following form:

$$\sigma_z = \left[\frac{E\,(1 - \nu)}{(1 + \nu)\,(1 - 2\nu)} \right] \varepsilon_z$$

The term in brackets is the effective modulus and is called the constrained modulus M_s.

Thus, M_s is related to Young's modulus for the soil E_s and Poisson's ratio ν by the following equation:

$$M_s = \frac{E_s\,(1 - \nu)}{(1 + \nu)\,(1 - 2\nu)} \tag{3.6}$$

where M_s = constrained soil modulus
E_s = Young's modulus of soil, MPa, lb/in^2
ν = Poisson's ratio of soil

Typically, values for M_s are computed as the slope of the secant from the origin of the stress-strain curve to the stress level on the curve that represents the free field soil stress at the side of the pipe (the average modulus in Fig. 3.11).

Krizek et al.[21] reported that M_s could vary from 0.7 to 1.5 times E'. Hartley and Duncan[9] and McGrath[26] proposed a direct substitution, that is, $E' = M_s$. In developing an elasticity model for a pipe embedded in uniform soil mass, Burns and Richard[3] used the constrained modulus as the soil property most representative of soil behavior in the ground. For purposes of buried pipe installations, the precision of the design models is sufficiently low that an approximate relationship is acceptable.

TABLE 3.5 Suggested Design Values for Constrained Soil Modulus M_s

Stress level, kPa	Soil type and compaction condition, MPa								
	SW95	SW90	SW85	ML95	ML90	ML85	CL95	CL90	CL85
7	13.8	8.8	3.2	9.8	4.6	2.5	3.7	1.8	0.9
35	17.9	10.3	3.6	11.5	5.1	2.7	4.3	2.2	1.2
69	20.7	11.2	3.9	12.2	5.2	2.8	4.8	2.4	1.4
138	23.8	12.4	4.5	13.0	5.4	3.0	5.1	2.7	1.6
275	29.3	14.5	5.7	14.4	6.2	3.5	5.6	3.2	2.0
413	34.5	17.2	6.9	15.9	7.1	4.1	6.2	3.6	2.4

1 MPa = 145 lb/in^2.

The constrained modulus can be derived directly from the hyperbolic soil model. Two constants are required to define the behavior of an elastic material. The hyperbolic model uses Young's modulus and the bulk modulus as the parameters. The bulk modulus K in terms of E and ν is as follows:

$$K = \frac{E}{3\,(1 - 2\nu)}$$

If both K and E are known, ν can be calculated as follows:

$$\nu = \frac{1}{2} - \frac{E}{6K}$$

Thus, the constrained modulus M_s can be calculated if the E and K values for the hyperbolic model are known.

McGrath[26] has suggested design values for M_s, for use as a soil stiffness parameter. These suggested values are proposed for use in the Iowa formula for deflection of buried pipe and other design equations that had adopted the use of E'. The proposed values are secant moduli and are listed in Table 3.5.

Deflection lag and creep

The length of time that a buried flexible pipe will continue to deflect after the maximum imposed load is realized is limited. This time is a function of soil density in the pipe zone. The higher the soil density at the sides of the pipe, the shorter the time during which the pipe will continue to deflect, and the total deflection in response to the load will be less. Conversely, for lower soil densities, the creep time is longer, and the resulting deflection due to creep is larger.

After the trench load reaches a maximum, the pipe-soil system continues to deflect only as long as the soil around the pipe is in the process of densification. Once the embedment soil has reached the density required to support the load, the pipe will not continue to deflect.

The full load on any buried pipe is not reached immediately after installation unless the final backfill is compacted to a high density. The increase in load with time is the largest contribution to time-dependent deflection. However, for a flexible pipe, the long-term load will not exceed the prism load. Therefore, for design, the prism load should be used, which effectively compensates for the time-dependent increase in load with trench consolidation and the resulting time-dependent deflection. Thus, when deflection calculations are based on the prism load, the deflection lag factor D_L should be 1.0.

Creep is normally associated with the pipe material and is defined as continuing deformation with time when the material is subjected to a constant load. Most plastics exhibit creep. As temperature increases, the creep rate under a given load increases. Also, as stress increases, the creep rate for a given temperature increases. Materials that creep are also subject to stress relaxation. *Stress relaxation* is defined as the decrease in stress, with time, in a material held in constant deformation. Figure 3.12 shows stress relaxation curves for PVC pipe samples held in a constant deflection condition. It is evident that stresses in PVC pipes do relax with time.

Figure 3.13 shows long-term data for buried PVC pipe. Long-term deflection tests were run at Utah State University by imposing a given soil load that was held constant throughout the duration of the test. PVC pipe material creep properties have little influence on deflection lag, but soil properties such as density exhibit great influence.

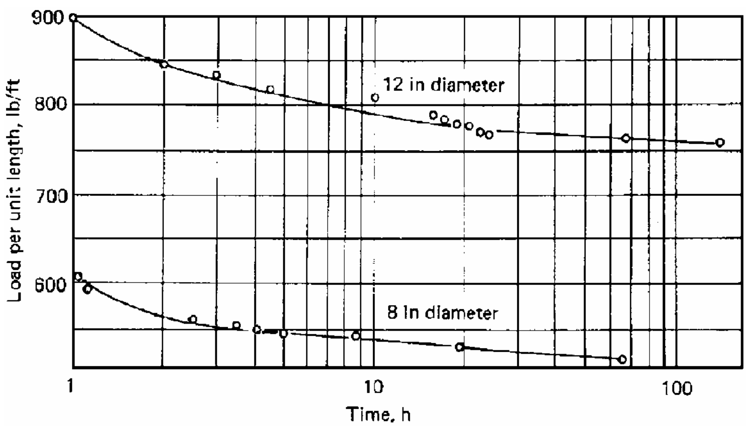

Figure 3.12 Stress relaxation curves.

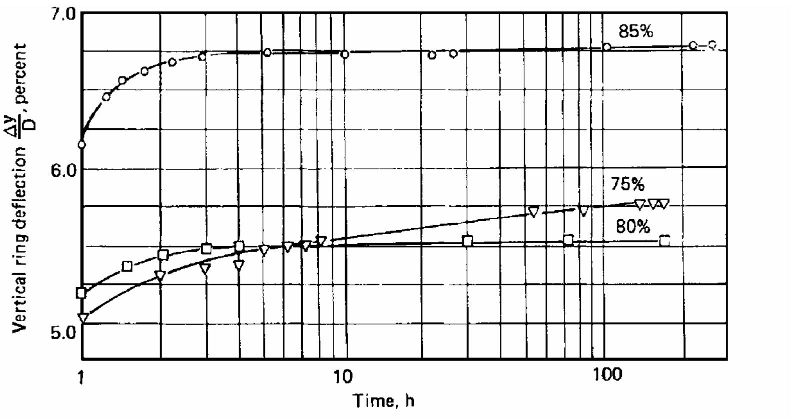

Figure 3.13 PVC pipe creep response.

Temperature-controlled tests of buried PVC pipe were run to determine the temperature effect on the long-term behavior. Data from these tests are given in graphical form in Fig. 3.14. The following procedures were used in conducting these tests. The pipe to be tested was placed in the load cell. It was then embedded in soil which was compacted to the specified percentage of Proctor density. The load on the soil was increased until the desired starting vertical deflection of the pipe was reached. At this point, the load as well as the temperature was held constant, and the resulting time-dependent deflection was determined. The starting deflections are somewhat arbitrary. Four of these tests were begun at about 4.75 percent deflection, and two were begun between 9 and 9.5 percent deflection. The loads required to produce these deflections were different in each case.

Note that for the temperature range tested, an equilibrium state is reached, and the pipe does not deflect beyond that point. The limiting deflection and the time required to reach it are largely controlled by the soil density. However, it is interesting to note in Fig. 3.14 for tests at different temperatures with the same soil density:

1. The equilibrium deflection is slightly larger for higher temperatures because the effective pipe stiffness is lower.
2. The time for equilibrium to be reached is shorter for higher temperatures since the soil-pipe system can interact at a faster rate in achieving equilibrium.

The above-described long-term tests were carried out in a soil cell. The imposed load on a pipe in a soil cell is almost instantaneous

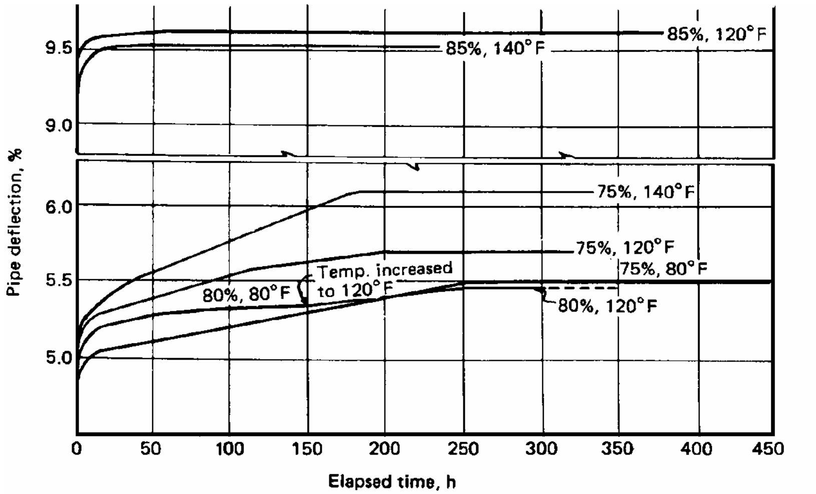

Figure 3.14 Time deflection curves in temperature-controlled soil cell test.

because the loading plane is only about 30 in above the pipe. This provides a significant advantage over tests in either trench or embankment conditions. In both the trench and the embankment, it takes substantial time for the full load to reach the pipe—months and years have been reported. When long-term tests are carried out in trenches and embankments, the change in deflections with time is due to increasing loads and soil consolidation. Figure 3.15 shows long-term deflection curves for PVC pipe buried in an embankment.

During September 1975, an embankment installation reaching a depth of cover of 22 ft was constructed over four test pipe sections that extended radially from a single access manhole. The test site became known as the mole hole and provided an excellent opportunity to easily monitor buried performance of PVC pipes for a 14-year period. In the fall of 1989, the test pipes were excavated for a posttest examination. The test site was part of a gravel pit where the in situ soil is a fine blow sand with 18 percent silt. The soil is moisture-sensitive and is subject to soil collapse when saturated. Except in dry years, the site itself experiences seasonal groundwater level changes which place the pipe below the water table in the spring months and above the water table in summer and most winter months.

Pipes were made of two different PVC compounds. Two samples were 12364B cell class per ASTM D 1784. They have a calcium carbonate filler content of 30 parts per 100 to each 100 parts per 100 resin by weight. Two other samples were foamed PVC with a specific

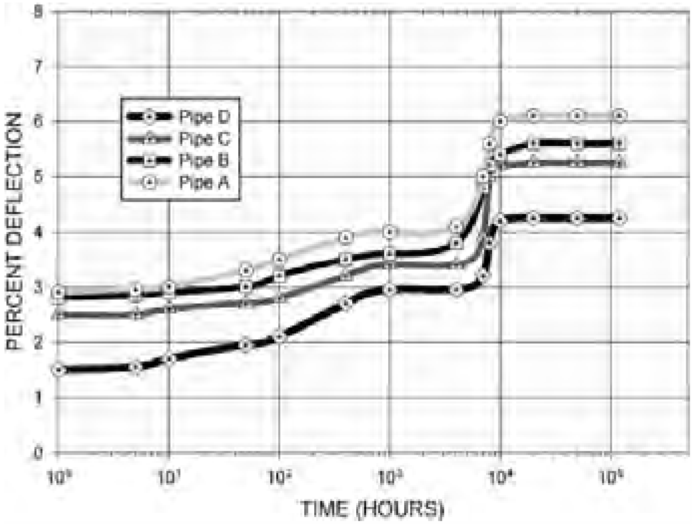

Figure 3.15 Deflection versus time for 10-in-diameter PVC sewer pipe (22-ft-deep embankment).

gravity of 1.2. Tables 3.6 and 3.7 provide basic dimensions and property data for the test pipe. Typical properties for unfilled, unfoamed PVC cell class 12454B are also given in Table 3.6 for comparison purposes.

Long-term deflection data. In-ground vertical deflection data were taken for 14 years and are plotted in Fig. 3.15. A stable deflection period was reached at 40 days (960 h) after installation, and was constant until the first instance of the groundwater table reaching the level of the pipe zone bedding. During the first spring season at about 150

TABLE 3.6 Basic Properties of Pipe Samples

Compound	Cell class*	Pipe stiffness, lb/in^2	Thickness, in	SDR, OD/t_{min}	E, lb/in^2	Sp. gravity
Filled	12364B	45–50	0.327–0.331‡	39–41	630,000	1.62
Foamed	Exp.†	32–36	0.381–0.417	31–32	218,000	1.2
Unfilled/ unfoamed	12454B	46 min.	0.320	35	400,000	1.4

*Per ASTM D 1784.
†Experimental (not classified).
‡t_{min} was varied to produce pipes with the same pipe stiffness.

TABLE 3.7 Test Pipe Parameters

Pipe	$F/\Delta y$, lb/in^2	Soil density (% std. Proctor)
A	34	82
B	45	83
C	38	85
D	50	87

days (3600 h) following installation, the groundwater table rose above the level of the pipe. This groundwater condition caused the soil to consolidate and the load to increase. This caused a somewhat rapid increase in deflection for all pipe samples during this period. A new stable or equilibrium deflection level was reached at about 400 days (9600 h). The water table continued to fluctuate on an annual basis for the 14-year test period. These subsequent water table movements influenced deflection readings only slightly since the initial saturation of the pipe zone.

Again, the soil around these pipes was a silty fine sand. For this soil, over 92 percent standard Proctor density is necessary to ensure a void ratio less than the critical value. The installed densities were less than 92 percent, resulting in void ratios greater than the critical. Thus, when the water table rose into the pipe zone, soil consolidation took place and caused pipe deflections to increase. This indicates that for pipe installation below the groundwater table, additional deflection control can be obtained if the density is such that the void ratio is below the critical value. The test site area was also subjected to small earthquake tremors during the test period. Any effects are included in the deflection results.

The change in deflection, with respect to time, for this embankment condition is greater than that measured in soil cell tests. This time-dependent deflection is due to the increasing load that is taking place in the embankment tests, whereas in the soil cell tests the load is applied to soil just over the pipe and is held constant. The equilibrium deflections, being approached by the curves in Fig. 3.15, are the same deflections which would result if similar pipes were tested in the soil cell at the same soil pressure, with the same initial soil density, and with the addition of water.

Postevaluation of buried samples. Pipe samples excavated from the site were examined visually, and no signs of cracking, crazing, or other polymer damage were evident. Specific gravity, pipe stiffness, and wall thickness measurements were taken for each sample and are given in Table 3.8. Notably, the pipe stiffness for the foamed samples varied from 34 to 38 lb/in^2 initially and ranged from 36 to 40 lb/in^2 after 14

TABLE 3.8 Postexcavation Properties of Embankment Pipe Samples

Pipe sample designation	Compound type	Thickness average, in	Specific gravity	Pipe* stiffness, lb/in^2	60% flattening
A	Foamed	0.381	1.2	36.8	No cracking
B	Filled	0.327	1.6	44.0	No cracking
C	Foamed	0.417	1.2	40.5	No cracking
D	Filled	0.331	1.6	49.0	No cracking

*Postevaluation pipe stiffness per ASTM D 2412.

years. The filled pipe samples varied from 45 to 50 lb/in^2 initially and measured 44 to 49 lb/in^2 after 14 years of buried service. These small variations are probably within the expected experimental error, and no change in the pipe's capacity to resist deflection occurred over this time period.

These pipes were each subjected to a 60 percent deflection test prescribed in D 3034, F 789, F 798, F 784, etc., to determine ductility. Each sample sustained that deflection level without cracking.

Additional mole hole data. After the above pipes were excavated, four new PVC pipes were installed in the same location in an embankment installation with 22 ft of cover. This installation was completed on October 20, 1989. Deflections were monitored for the next 7 years. The 2 years following this installation were fairly dry years, and groundwater did not rise into the pipe zone during these years. The winter of 1991–1992 was fairly wet. During the mountain snowmelt period in the spring of 1992, after the pipes had been in the ground for 30 months, groundwater rose above the pipe and saturated the pipe zone soils.

In-ground vertical deflection data are plotted in Fig. 3.16. It can be seen that the deflection became almost stable after about 10 months and was totally stable after 20 months. For the silty sand, the critical density is about 92 percent of standard Proctor density. Thus, the pipe that was installed at 88 percent had an increase in density when the soil became saturated and became more dense. The two pipes that were installed in dumped gravel showed a small increase in deflection. This shows that the water serves as a lubricant for the gravel particles and allow some densification. The pipe that was installed in silty sand compacted to 93 percent standard Proctor density had almost no increase in deflection. This is a direct indication that pipe should be installed in soils compacted to densities higher than critical if deflection control is pertinent.

A new stable or equilibrium deflection level was reached at about 32 months. The water table continued to fluctuate on an annual basis for the remaining test period. These subsequent water table movements had no measurable influence on the deflection readings.

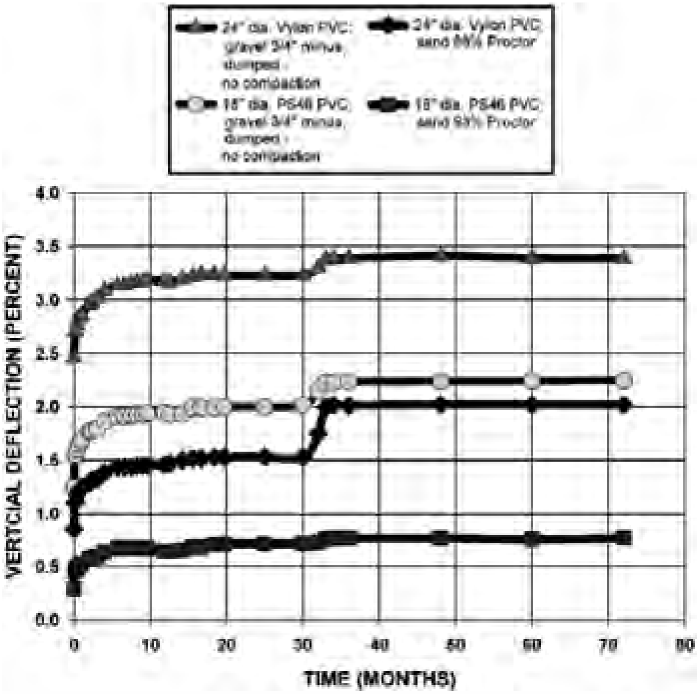

Figure 3.16 Embankment data for pipes installed 22 ft deep. Note the increase when groundwater rose above the top of pipes 30 months after installation.

This test location became a victim to progress. Thirty months after installation, a subdivision moved into the area. The access pipe was removed and homes now stand over the pipes which are 22 ft down.

Extensive research has established that any buried flexible pipe (i.e., steel, fiberglass, or plastic) will continue to deflect as long as the surrounding soil consolidates. Thus, as previously stated, the creep properties of pipe materials have little effect on the long-term deflection behavior of flexible pipe when buried in soil, and in most cases, a deflection lag factor D_L of 1.5 conservatively accounts for long-term effects due to time-dependent load increases and due to consolidation of soil in the pipe zone. Alternatively, design can be based upon the anticipated prism load and a D_L of 1.0.

PVC versus steel. Time-versus-deflection curves for pipe under constant load in a soil test cell are given in Fig. 3.17. The two pipes are from totally different materials (steel and PVC) but have exactly the

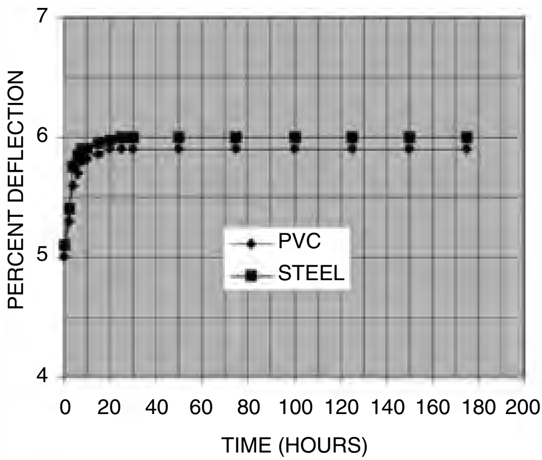

Figure 3.17 Steel and PVC pipes with the same pipe stiffness ($F/\Delta y = 46$ lb/in^2) and installed in the same manner with 85 percent standard Proctor density in silty sand soil.

same pipe stiffness ($F/\Delta y = 6.7EI/r^3 = 46$ lb/in^2). Both pipes are installed in the same soil (silty sand) compacted to the same soil density (85 percent standard Proctor density). For these constant-load tests, equilibrium is achieved in about 25 h. This shows that the basic material properties of the pipe have little to do with overall performance of the pipe. For instance, PVC creeps at a much higher rate than does steel, but this difference in creep properties has no effect on performance. Also, the modulus of elasticity of steel is 75 times that of PVC. The two most important properties that have the principal influence on the performance of a buried pipe are first and foremost, *soil density,* second, *pipe stiffness.*

In very simple terms, the soil stiffness is primarily a function of soil density, and the soil stiffness and the pipe stiffness work together in supporting the imposed loads. Thus, the two contribute directly to the overall pipe performance.

Watkins's soil-strain theory

A number of variations of Spangler and Watkins's modified Iowa formula have been proposed. All can be represented in simple terms as follows:

$$\text{Deflection} = \frac{\text{load}}{\text{pipe stiffness} + (\text{constant})\,(\text{soil stiffness})} \tag{3.7}$$

Upon analyzing data from many tests, Watkins wrote the Iowa formula in terms of dimensionless ratios as follows:

$$\frac{\Delta y}{D} = \frac{PR_s}{E_s AR_s + B} \tag{3.8}$$

where P = vertical nominal pressure at the top of pipe level, lb/in², and R_s = stiffness ratio. (This is the ratio of soil stiffness E_s to pipe-ring stiffness EI/D^3. This quantity includes all the properties of materials, soil as well as pipe.) Since for a solid wall pipe of constant cross section $I = t^3/12$, then

$$R_s = 12\,\frac{E_s D^3}{Et}$$

where
E_s = slope of stress-strain curve for soil at load in question in a one-dimensional consolidation test
$= P/\varepsilon$
ε = vertical soil strain
A, B = empirical constants which include such terms as D_L and K of the Iowa formula

Through transposition, Eq. (3.8) can be restated as

$$\frac{\Delta y}{D\varepsilon} = \frac{R_s}{AR_s + B} \tag{3.9}$$

In this form, the above equation represents a simple relationship between two dimensionless variables: ring deflection ratio $\Delta y/(D\varepsilon)$ and stiffness ratio R_s. Figure 3.18 represents the design curve that can be used for predicting ring deflection. It is based on current theoretical as well as empirical data generated in Europe and the United States.

In most flexible pipe installations, the pipes are relatively flexible compared to recommended sidefill. Thus, the pipe follows the soil down, and the deflection ratio approaches unity. The stiffness ratio R_s is usually greater than 300, which is to the right of the plot of Fig. 3.18. Even if R_s is usually greater than 300, it is conservative to assume $(\Delta y/D)/\varepsilon = 1$. So the ring deflection becomes

$$\frac{\Delta y}{D} = \varepsilon \tag{3.10}$$

This demonstrates that a flexible pipe is deflected down about as much as the sidefill settles. The vertical soil strain in the fill depends upon the soil compressibility and the nominal load (Fig. 3.19). Curves shown in Fig. 3.20 relate soil strain to the soil pressure.

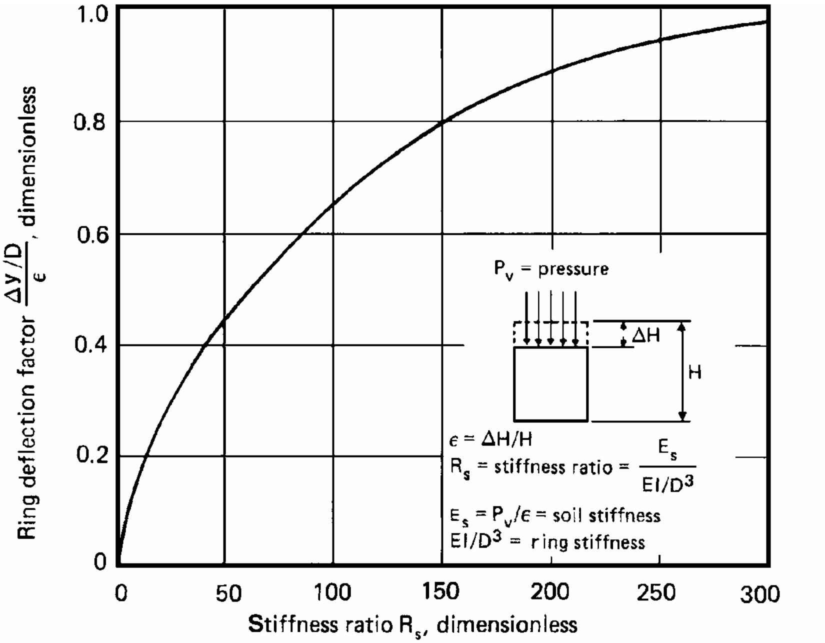

Figure 3.18 Ring deflection factor as a function of stiffness ratio.

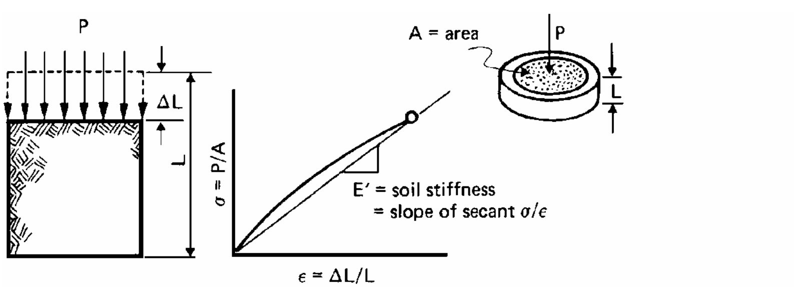

Figure 3.19 Concept for predicting settlement of soil by means of stress-strain compression data from field or laboratory.

The use of soil strain to predict pipe deflection then becomes a simple exercise. The ratio of pipe deflection to soil strain can be determined from Fig. 3.18. This value will usually be unity for most flexible pipe installations. The load on the pipe is calculated using the prism (embankment) load theory, and the soil strain can be determined from Fig. 3.20.

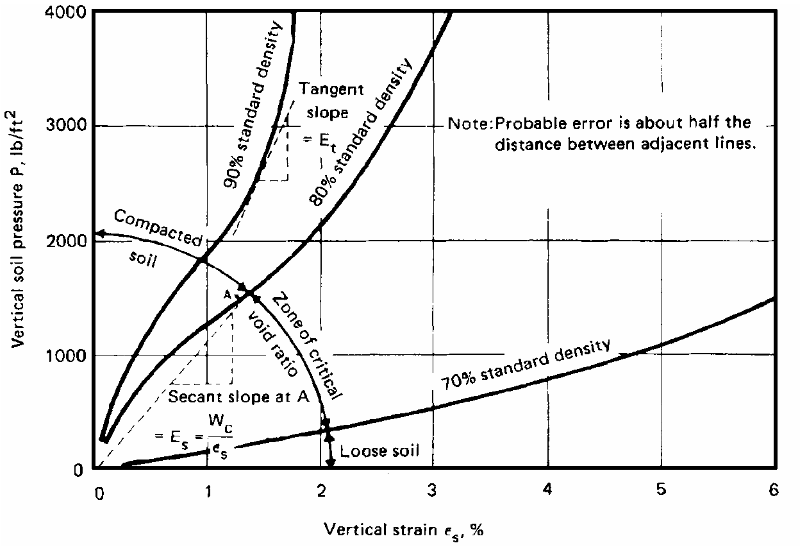

Figure 3.20 Plot of vertical stress-strain data for typical trench backfill (except clay) from actual tests.

For the soil to be used as embedment, a series of simple laboratory tests can be run to produce data similar to those shown in Fig. 3.20. However, experience has shown that data given in Fig. 3.20 are representative of most soils and can be used for design. Thus it is evident that soil density is the most important parameter in limiting pipe deflection.

Empirical method

Each of the methods discussed so far for determining load and deflection has a theoretical basis, and except for the prism load theory, all require experimental investigation to determine the unknown constants. In the past several years, techniques have evolved whereby a model or prototype pipe is tested until failure occurs and the total performance of the pipe is studied. Suppose a pipe is to be designed with a certain earth cover in an embankment. Without a pipe in place, no arching occurs, and the soil pressure at any height is easily calculated (the prism theory load at that depth). When a pipe having good flexibility is in place, the static pressure will not be greater than the prism load pressure applied. Trying to calculate the actual pressure has frustrated researchers for years. If a pipe is installed in a prism load condition (e.g., soil cell), the resulting deformation can be monitored without the need to calculate the actual static pressure.

This procedure has been used with great success at various research laboratories such as at Utah State University under the direction of Reynold K. Watkins and at the U.S. Bureau of Reclamation under the direction of Amster K. Howard. Data obtained in this manner can be used directly in the design of soil-pipe systems and in the prediction of overall performance. The possibility of buckling, overdeflection, and wall crushing is evaluated simultaneously by actual tests. No attempt to explain the soil-pipe interaction phenomenon is necessary in the use of this method, and the end results leave nothing to be estimated on the basis of judgment.

For example, if tests show that for a given soil compaction at 25 ft (7.6 m) of cover a flexible pipe deflects 3 percent, and in every other way performs well, the actual load on the pipe and the soil modulus are academic. Thus, a pipe installation can be designed with a known factor of safety provided that enough empirical test data are available. In collection of these data, pipe was installed in a manner similar to that used in actual practice, and the height of cover was increased until performance levels were exceeded. The procedure was repeated many times, and a reliable empirical curve of pipe performance versus height of fill was plotted. The use of these empirical curves or data eliminates the need to determine the actual soil pressure since the pipe performance as a function of height of cover is determined directly. Equally good empirical approaches to study of the deflection mechanism are

- The study of actual field installations
- The simulation of a large enough earth cover in a soil test box to exceed the performance limits of the pipe

To avoid the problem of having to establish design data for the infinite variety of installations and bedding conditions that are found in the field, the following design bases have been chosen:

- The embankment condition is selected as critical. (The results are conservative for other than embankment conditions.)
- Time lag or settlement of the embankment is included by analyzing long-term values of deflection.

An added advantage of this system is that by a single test, not only can ring deflection be determined, but also performance limits such as ring crushing, strain, and wall buckling can be noted and analyzed. The use of such data may be considered the most reliable method of design and is recommended when available. Some of the pipe products for which empirical test data have been determined are as follows:

Asbestos-cement (AC) pipe

Corrugated steel pipe

Ductile iron pipe

Fiberglass-reinforced plastic (FRP) pipe

Polyethylene (PE) pipe

Polyvinyl chloride (PVC) pipe

Reinforced-plastic mortar (RPM) pipe

Steel pipe (CMC-CML)

Substantial data are available for PVC sewer pipe made in accordance with ASTM D 3034 with minimum pipe stiffness of 46 lb/in^2 and have been compiled by researchers at the Buried Structures Laboratory, Utah State University. The results of many measurements are categorized in Table 3.9 according to soil type, soil density, and height of cover. Deflections presented in Table 3.9 represent the largest deflections encountered under the conditions specified. Data presented in this manner are designed to provide various options for design engineers. Their use, in most cases, will show that several engineering solutions may be available, and economic inputs may suggest a proper solution.

For example, suppose PVC sewer pipe (ASTM D 3034 DR 35) with a minimum pipe stiffness of 46 lb/in^2 is to be installed where the native soil is a class IV clay. Ninety percent of the line will be at depths as great as 20 ft. The engineer has selected 7.5 percent deflection as his design limit. According to Table 3.9, the native class IV material could be used for that portion of the pipeline with less than 14 ft of cover if compacted to 75 percent of standard Proctor, thereby ensuring deflections less than 7.5 percent. However, groundwater conditions may make compaction difficult, even impossible, or may result in subsequent reduction in soil strength. If this is the case, class I, II, or III material may be imported and used with appropriate embedment procedures to limit deflection to 7.5 percent. The choice will be based on availability, convenience, and consequently, cost. For the deep portion of the line, class III material compacted to 85 percent, class II material compacted to 80 percent, or class I material without compaction could be used successfully.

Pipe Design Criteria

Design methods for installation design have been discussed. However, no design can be effected without performance criteria. Performance criteria are usually established by the design engineer based upon

TABLE 3.9 Long-Term Deflections of PVC (SDR 35) Pipe (Percent)*†

ASTM embedment material classifications‡	Density (Proctor) AASHTO T-99, percent	Height of cover, ft 3	5	8	10	12	14	16	18	20	22	24	26	28	30
Manufactured (class I) granular angular		0.2	0.3	0.4	0.5	0.6	0.7	0.9	1.0	1.1	1.2	1.3	1.4	1.5	1.6
Clean sand (class II)	90	0.2	0.3	0.5	0.7	0.8	0.9	1.1	1.2	1.3	1.4	1.6	1.7	1.8	2.0
and gravel	80	0.9	1.4	2.3	3.2	3.6	4.1	5.0	5.5	6.0	6.4	7.3	7.7	8.2	9.1
Sand and gravel (class III)	90	0.2	0.4	0.6	0.8	0.9	1.1	1.2	1.4	1.6	1.7	1.9	2.1	2.2	2.83
with fines	85	0.7	0.9	1.7	2.2	2.6	3.0	3.5	3.9	4.3	4.8	5.2	5.6	6.0	6.5
	75	1.1	1.8	2.9	3.8	4.5	5.5	6.8	8.5	9.9	11.3	12.7	14.1	15.5	16.8
	65	1.3	2.4	3.6	4.7	5.5	6.8	8.5	9.6	11.4	13.0	14.5	16.0	17.3	18.0
Silt and clay (class IV)	85	0.65	0.9	1.7	2.2	2.6	3.0	3.5	3.9	4.3	4.8	5.2	5.6	6.0	6.5
	75	1.3	2.3	3.3	4.3	5.0	6.5	7.8	9.5	10.6	12.2	13.5	15.0	16.3	17.0
	65	1.3	2.4	3.6	4.7	5.5	8.0	10.5	12.5	15.0	17.6	20.0	22.0	24.0	26.0

*Test data indicate no length of pipe installed under conditions specified will deflect more than is indicated; the pipe will deflect less than the amount indicated if specified density is obtained.

†Listed deflections are those caused by soil loading only and do not include initial out-of-roundness, etc.

‡Embedment material classifications are per ASTM D 2321, Underground Installation of Flexible Thermoplastic Sewer Pipe.

SOURCE: Data obtained from Utah State University report.

required performance and capabilities of specified products. When a capability of a product is reached or exceeded, it is said that a performance limit has been reached. Each product will exhibit one or more performance limits for each application. Performance limits are established for each product to prevent conditions that may interfere with the design function, including the life of the product.

Performance limits

For buried pipes, as for most structures, performance limits are directly related to stress, strain, deflection, or buckling. It is not implied that stress, strain, deflection, and buckling are independent, but only convenient parameters on which to focus attention. For a particular product, certain performance limits are not considered because others will always occur first. The following is a list of performance limits that are often considered in design and could be thought of as possible responses to soil pressure:

Wall crushing (stress)
Wall buckling
Reversal of curvature (deflection)
Overdeflection
Strain limit
Longitudinal stresses
Shear loadings
Fatigue
Delamination

Wall crushing. *Wall crushing* is the term used to describe the condition of localized yielding for a ductile material or cracking failure for brittle materials. This performance limit is reached when the in-wall stress reaches the yield stress or the ultimate stress of the pipe material. The ring compression stress is the primary contributor to this performance limit. (See Fig. 3.21.)

$$\text{Ring compression} = \frac{P_v D}{2A} \qquad (3.11)$$

where P_v = vertical soil pressure
D = diameter
A = cross-sectional area per unit length

However, wall crushing can also be influenced by the bending stress.

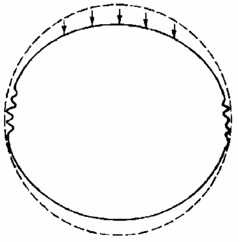

Figure 3.21 Wall crushing at the 3 and 9 o'clock positions.

$$\text{Bending stress} = \frac{Mt/2}{I} \tag{3.12}$$

where M = bending moment per unit length
t = wall thickness
I = moment of inertia of wall cross section per unit length

Wall crushing is the primary performance limit or design basis for most "rigid" or brittle pipe products. This performance limit may also be reached for stiffer flexible pipes installed in highly compacted backfill and subjected to very deep cover. A quick check for this performance limit can be made by comparing the ring compression stress with yield and/or ultimate strengths.

Wall buckling. Buckling is not a strength performance limit, but can occur because of insufficient stiffness. The buckling phenomenon may govern design of flexible pipes subjected to internal vacuum, external hydrostatic pressure, or high soil pressures in compacted soil. (See Fig. 3.22.)

The more flexible the conduit, the more unstable the wall structure will be in resisting buckling. For a circular ring in plane stress subjected to a uniform external pressure, the critical buckling pressure is

$$P_{cr} = \frac{3EI}{R^3} \tag{3.13}$$

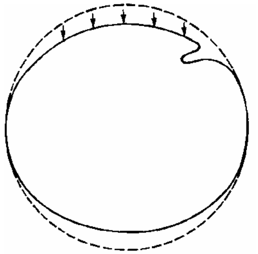

Figure 3.22 Localized wall buckling.

For a long tube in plane strain, E must be replaced by

$$E = \frac{E}{1 - \nu^2}$$

Also, I may be replaced by

$$I = \frac{t^3}{12} \times 1$$

in Eq. (3.13). Then

$$P_{\mathrm{cr}} = \frac{Et^3}{4\,(1 - \nu^2)\,R^3} \tag{3.14}$$

For buckling in the inelastic range (materials with pronounced yield points), the critical buckling pressure in terms of the yield point σ_y is

$$P_{\mathrm{cr}} = \frac{t}{R}\,\frac{\sigma_y}{1 + \sigma_y R^2/(Et^2)} \tag{3.15}$$

The limiting value of the above equation as the pipe thickness becomes small is

$$\frac{Et^3}{4R^3}$$

which is less than Eq. (3.14). In fact, in all cases Eq. (3.15) is less than

$$\frac{\sigma_y t}{R}$$

or less than the pressure corresponding to the yield point stress. The above equations apply only to a hydrostatic condition, i.e., for a conduit completely submerged in a medium that has zero shear strength. The above equations would therefore be valid for checking the buckling resistance of a pipeline used for a river crossing, for a liner pipe, for a pipe in a saturated soil, or for a line subjected to an internal vacuum. This analysis does not include the initial ellipticity of the conduit.

Most conduits are buried in a soil medium that does offer considerable shear resistance. An exact rigorous solution to the problem of buckling of a cylinder in an elastic medium would call for some advanced mathematics, and since the performance of a soil is not very predictable, an exact solution is not warranted. Meyerhof and Baike developed the following formula for computing the critical buckling force in a buried circular conduit:[25]

$$P_{cr} = \frac{2}{R}\sqrt{\frac{KEI}{1-\nu^2}} \tag{3.16}$$

If the *subgrade modulus* K is replaced by the soil stiffness E'/R, we have

$$P_{cr} = 2\sqrt{\frac{KE'}{1-\nu^2}\left(\frac{EI}{R^3}\right)} \tag{3.17}$$

In both Eqs. (3.16) and (3.17), initial out-of-roundness is neglected, but this reduction in P_{cr} because of this is assumed to be no greater than 30 percent. As a result, it is recommended that a safety factor of 2 be used with the above formula in the design of a flexible conduit to resist buckling. The Scandinavians have rewritten the above formula for critical buckling pressure as follows:

$$P_{cr} = 1.15\sqrt{P_b E'} \qquad P_b = \frac{2E}{1-\nu^2}\left(\frac{t}{D}\right)^3 \tag{3.18}$$

Actual tests show that while the above equations work fairly well for steel pipe, the equations are conservative for either plastic pipe or fiberglass-reinforced plastic pipe. However, one of the above equations should be used for design, keeping in mind that the predicted buckling pressure will be on the conservative side for most plastic pipe.

A more exact approach to buckling follows:

The summation of external loads should be equal to or less than the allowable buckling pressure. The allowable buckling pressure q_a may be determined by the following:

$$q_a = \frac{1}{FS}\left(32\, R_w B' E' \frac{EI}{D^3}\right)^{1/2}$$

where q_a = allowable buckling pressure, lb/in²

FS = design factor

$$= \begin{cases} 2.5 & \text{for } \dfrac{h}{D} \geq 2 \\ 3.0 & \text{for } \dfrac{h}{D} < 2 \end{cases}$$

h = height of ground surface above top of pipe, in

D = diameter of pipe, in

R_w = water bouyancy factor

$$= 1 - 0.33\,\frac{h_w}{h} \qquad 0 \leq h_w \leq h$$

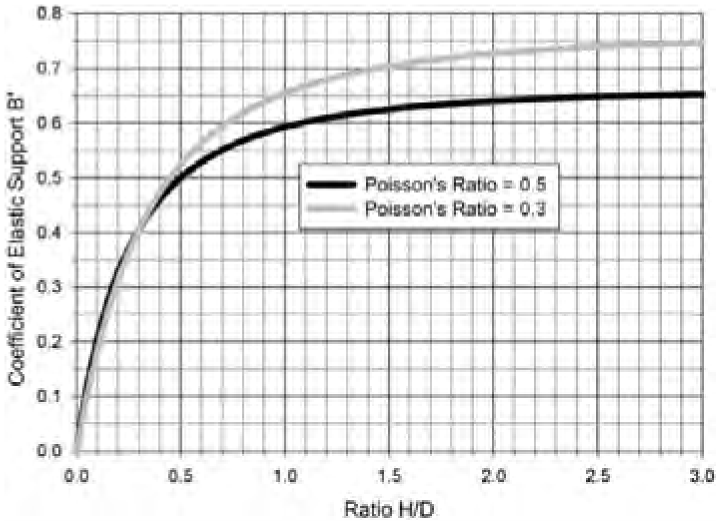

Figure 3.23 Coefficient B' as a function of H/D, where H is height of cover over top of pipe and D is diameter.

h_w = height of water surface above top of pipe, in
B' = empirical coefficient of elastic support (dimensionless)

Coefficient B' was given by Luscher in 1966. The equation is as follows:

$$B' = \frac{4\,(h^2 + Dh)}{(1 + \nu)\,[\,(2h + D)^2 + D^2\,(1 - 2\nu)\,]}$$

Coefficient B' has some dependence on Poisson's ratio for the soil. However, this effect is small, as is shown in Fig. 3.23. The above equation simplifies when the value for Poisson's ratio is taken as $^1/_2$. This equation is conservative and should be used for the calculation of B'.

$$B' = \frac{4\,(h^2 + Dh)}{1.5\,(2h + D)^2}$$

Buckling for typical pipe installations. For determination of external loads in normal pipe installations, use the following equation:

$$\gamma_w h_w + R_w \frac{W_c}{D} + P_v \le q_a$$

where h_w = height of water above conduit, in
γ_w = specific weight of water (0.0361 lb/in^3)

P_v = internal vacuum pressure, lb/in^2
= atmospheric pressure less absolute pressure inside pipe, lb/in^2
W_c = vertical soil load on pipe per unit length, lb/in

In some situations, it may be appropriate to consider live loads as well. However, simultaneous application of live load and internal-vacuum transients need not be considered. Therefore, if live loads are also considered, the buckling requirement is satisfied by

$$\gamma_w h_w + R_w \frac{W_c}{D} + \frac{W_L}{D} \leq q_a$$

where W_L = live load on the conduit (lb/lin in of pipe).

Extreme caution should be used when considering large-diameter pipes. The above equations assume the external pressure (or internal vacuum) to be essentially constant around the pipe. This condition is not met when a very large pipe is placed in shallow burial below the water table. In this case, the hydrostatic pressure can vary substantially from the top to the bottom of the pipe.

Overdeflection. Deflection is a design parameter for flexible pipes and *semirigid* or *semiflexible* pipes. It is rarely, if ever, considered in the design of rigid pipe installations.

Flexible pipe products will have a deflection design limit (Fig. 3.24). This design limit is not a performance limit, but is often based on a performance limit with a safety factor. For example, PVC pipes will not start a reversal of curvature until about 30 percent deflection. (See Fig. 3.25.) Thus a design deflection of 7.5 percent is based on a safety factor of 4.

Not all design deflections are based on reversal of curvature. For cement-lined steel and ductile iron pipe, the design deflections are based on deflection limits (performance limits) which produce substantial cracking in the cement lining. Other products have deflection

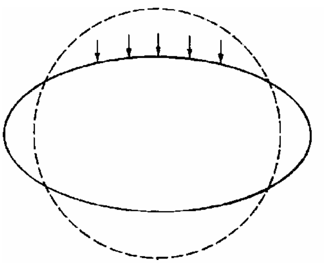

Figure 3.24 Ring deflection in a flexible pipe.

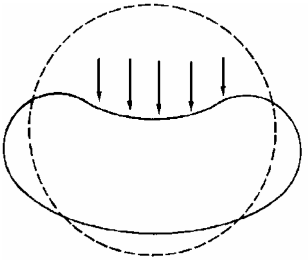

Figure 3.25 Reversal of curvature due to overdeflection.

limits to limit bending stresses or strains. The design engineer must be aware of each product's limitations for design calculations and to assess adequate safety.

The semirigid and semiflexible products depend on their deflection capability to carry the imposed soil load—just as all flexible products do. Thus, a deflection consideration must be made in design. For such products, bending stress and bending strain may also become limiting performance criteria. Such products are often cited as having only the positive attributes of both rigid and flexible pipe. However, tests have shown that these same products can and do exhibit the combination of performance limits of both rigid and flexible pipes which makes design analysis more complicated.

The calculated design deflection should always be equal to or less than the design deflection limit for the particular product. The design deflection is calculated by one of the methods described under the flexible pipe analysis section of this chapter. Traditionally, Spangler's Iowa formula has been used. Finite element methods are starting to be used and will be the method of the near future.

Reversal of curvature. Reversal of curvature is a deflection phenomenon and will not occur if deflection is controlled. A reverse curvature performance limit for flexible steel pipe was established shortly after publication of the Iowa formula. It was determined that corrugated steel pipe would begin to reverse curvature at a deflection of about 20 percent. Design at that time called for a limit of 5 percent deflection, thus providing a structural safety factor of 4.0. From this early design consideration, an arbitrary design value of 5 percent deflection was selected.

Buried PVC sewer pipe (D 3034 DR 35), when deflecting in response to external loading, may develop recognizable reversal of curvature at a deflection of 30 percent. This level of deflection has been commonly designated as a conservative performance limit for PVC sewer pipe. Research at Utah State University has demonstrated that the load-carrying capacity of PVC sewer pipe continues to increase even when deflections increase substantially beyond the point of reversal of curvature. With consideration of this performance characteristic of PVC sewer pipe, engineers generally consider the 7.5 percent deflection limit recommended in ASTM D 3034 to provide a very conservative factor of safety against structural failure.

Strain limit. The strain must be limited in certain pipe materials, such as some fiberglass-reinforced pipes. This limit is necessary to prevent strain corrosion. Strain corrosion is an environmental degradation of the pipe material which takes place in a finite time only after the pipe wall strain is greater than some threshold strain. Proper design calls for the design strain to be lower than this strain limit with some safety factor.

Strain is related to deflection. Therefore, most manufacturers of such products will propose installation techniques for their particular product which will limit deflection and thus limit the strain. Usually only brittle, composite, or highly filled materials have installation designs which are controlled by strain.

Strain described in this section refers to total circumferential strain, which is made up of bending strain, ring compression strain, hoop strain due to internal pressure, and strain due to Poisson's effect. For gravity sewer pipe, the bending strain is largest, and other components may be small in comparison.

Bending strain. The bending strains can be calculated by using the following equation. The equation requires ring deflection $\Delta y/D$ and the dimension ratio D/t. The equation is based on the pipe's deforming into an elliptical shape. The assumption of an elliptical shape has been shown to be a very close approximation for most solid wall pipe.

$$\varepsilon = \pm \frac{t}{D} \frac{3\,\Delta y/D}{1 - 2\,\Delta y/D} \tag{3.19}$$

where ε = maximum strain in pipe wall due to ring bending (can be assumed to occur at crown or invert of pipe)
t = pipe wall thickness
D = pipe diameter
Δy = vertical decrease in diameter

For example, if $t = 0.132$, $d = 4$, and the ring deflection is 10 percent, the bending strain is calculated as follows:

$$\varepsilon = \pm \frac{0.132}{4} \frac{3\,(0.10)}{1 - 2\,(0.10)} = 0.0124 \quad \text{or 1.24 percent strain}$$

The following simplified equation for calculating maximum strain due to ring deflection has been proposed.

$$\varepsilon_b = 6\,\frac{t}{D}\,\frac{\Delta y}{D} \tag{3.20}$$

This equation predicts strains that are too high for low ring deflections and does not work well for solid wall pipes. However, it is the preferred equation for profile wall pipes. The two equations predict the same bending strain when $\Delta y/D$ is 0.25.

Ring compression strain

$$\varepsilon_c = \frac{P_v D}{2tE} \tag{3.21}$$

Hoop strain (due to internal pressure)

$$\varepsilon_p = \frac{PD}{2tE} \tag{3.22}$$

Poisson's circumferential strain

$$\varepsilon = -\nu\ (\text{longitudinal strain}) \tag{3.23}$$

where ε_b = bending strain
ε_c = ring compression strain
ε_p = internal pressure strain
ε = circumferential Poisson's strain
t = wall thickness
D = diameter
Δy = vertical deflection
P_v = vertical soil pressure
E = Young's modulus
p = internal pressure
ν = Poisson's ratio

Longitudinal stresses. Installation design and construction should be such that longitudinal stresses are minimized. Rigid pipe products and many flexible pipe products are not designed to resist high longitudinal stresses. Longitudinal stresses are produced by

1. Thermal expansion (contraction) (major design consideration in welded steel lines)
2. Longitudinal bending
3. Poisson's effect (due to internal pressure)

Thermal stresses in welded steel lines are often produced by welding the pipe during the high-temperature period in the day. Cooling later can cause extremely high tensile stresses. These stresses can be minimized by providing closure welds during cool temperatures or by the use of expansion joints.

Some of the major causes of longitudinal bending or beam action in a pipeline area are

1. Differential settlement of a manhole or structure to which the pipe is rigidly connected
2. Uneven settlement of pipe bedding or undermining, e.g., erosion of the soil below it into a water course or leaky sewer
3. Ground movement associated with tidal water
4. Seasonal rise and fall of soil effected by changes in moisture content (e.g., most expansive clays)
5. Nonuniformity of the foundation
6. Tree-root growth pressure

This type of bending frequently occurs when pipes are bent to conform to direction changes. Such bending can cause ring buckling. Reissner has also provided an equation for calculating the radius of curvature that will cause ring buckling as follows:

$$R_b = \frac{D}{1.12\, t/D} \tag{3.24}$$

Shear loadings. Shear loadings often accompany longitudinal bending. The cause can usually be attributed to nonuniform bending or differential settlement. Forces can be large, highly variable, and localized and may not lend themselves to quantitative analysis with any degree of confidence. For this reason, shear force must be eliminated or minimized by design and proper installation.

Fatigue. The fatigue performance limit may be a necessary consideration in both gravity flow and pressure applications. However, normal operating systems will function in such a manner as not to warrant consideration of fatigue as a performance limit, although some fatigue failures have been reported in forced sewer mains.

Pipe materials will fail at a lower stress if a large number of cyclic stresses are present. Pressure surges due to faulty operating equipment and resulting water hammer may produce cyclic stress and fatigue. Cyclic stresses from traffic loading are usually not a problem except in shallow depths or burial. The design engineer should consult the manufacturer for applications where cyclic stresses are the norm.

Delamination. Reinforced and laminated products may experience delamination when subjected to ring deflection. Delamination is caused by radial tension and interlaminar shear. In the design of reinforced products, the radial strength is often neglected and radial reinforcement is omitted. However, the resulting radial strength may be adequate if deflections are controlled. Radial tension is given by

$$\sigma_r = T/[t\,(R + y)]$$
$$T = \int_{-c}^{y} \sigma \, da$$

where σ_r = radial tension stress
t = wall thickness
R = radius
y = distance from neutral axis to point in question
c = $t/2$
σ = stress in tangential direction as function of position in wall (My/I)
da = dy (unit length)

A discussion of radial tension in curved members can be found in most advanced solid mechanics texts.

Delamination may also be caused by chemical action. A prime example is the corrosion of reinforcing steel. When corrosion takes place, corrosion products produce interlaminar pressure which can result in delamination. Reinforcement is usually protected and will not corrode except in the case of product misapplication.

Safety factors

The need for selecting a design load that is less than the performance limit load arises mainly from uncertainties. These uncertainties exist in service conditions, loads, uniformity in materials, and assumptions made in design. Thus, a reduction factor is needed and is usually referred to as a safety factor or factor of safety.

Rigid pipe. The safety factor for rigid pipe is usually based on the performance limit of injurious cracking.

W_f = load to cause failure (cracking)

W_w = safe working load

$$W_w = \frac{W_f}{\text{SF}}$$

SF = safety factor

The acceptable safety factor is

$$SF = 1.5$$

Thus, if a load of 2000 lb/ft will cause cracking, the safe design load should be 2000/1.5 = 1333 lb/ft.

Flexible pipe. Performance limits for flexible pipes are usually deflection-related. Safety factors are then often based on deflection instead of on load. For example, if a cement-lined pipe has injurious cracking at 3 percent deflection, a design deflection of 2 percent would be based on a safety factor of 1.5. The design engineer has the responsibility to design the installation (pipe, bending, backfill, and so forth) so that the calculated design deflection does not exceed 2 percent.

Each product will exhibit different performance limits, and the factor of safety is usually 1.5 or greater. For flexible products which exhibit only deflection as a performance limit, the design deflection is 7.5 percent, and the factor of safety is 4 or greater.

The inexperienced design engineer should consider each possible performance limit, in succession, until the performance limit which occurs at the lowest load or deflection is arrived at. The factor of safety is then based on that performance limit. Literature published by the pipe manufacturer is very helpful in assessing the capabilities and limitations of pipe products.

When a pipe deflects under load, bending strains are induced in the pipe wall. These strains vary linearly through the pipe wall. Somewhere within the wall section (usually about the center) these bending strains will be zero.

Profile-wall pipes are designed and manufactured to minimize the use of material by increasing the section modulus of the pipe wall. *Profile-wall* is a relatively new designation, but the concept is not new. Corrugated steel pipe is truly a profile-wall pipe. Some of the newer plastic products introduced in the last several years are of this type. That is, the plastic is placed primarily at the inside and outside walls or in ribs for greater pipe stiffness. Many of these products have been shown to perform with the profile section acting as a unit as designed. For adequate safety, for any such product, the design should include sufficient plastic between the inner and outer walls and/or between the ribs to carry shear and to ensure that the profile section indeed acts as a unit.

The placement of a rigidlike filler material between walls as a substitute will impart a brittlelike behavior to the pipe and will interfere with the pipe's ability to deflect without cracking. Such pipes often deflect as a flexible pipe and have a brittle behavior and crack under deflection. Some pipes manufactured in this manner are sometimes referred to as semirigid. This is simply a misnomer. Many solid wall PVC and ductile iron pipes are actually more rigid and still behave as flexible pipes.

Parallel Pipes and Trenches

When buried pipes are installed in parallel, principles of analysis for single pipes still apply. Soil cover must be greater than minimum. However, the design of parallel buried pipes requires an additional analysis for heavy surface loads. Consider a free-body-diagram of the pipe-clad soil column between two parallel pipes. See Fig. 3.26. Section AA is the minimum cross section. This column must support the full weight of the soil mass, shown crosshatched, plus part of the surface load *W* shown as a live load pressure diagram. The soil column is critical at its minimum section AA at the spring lines.

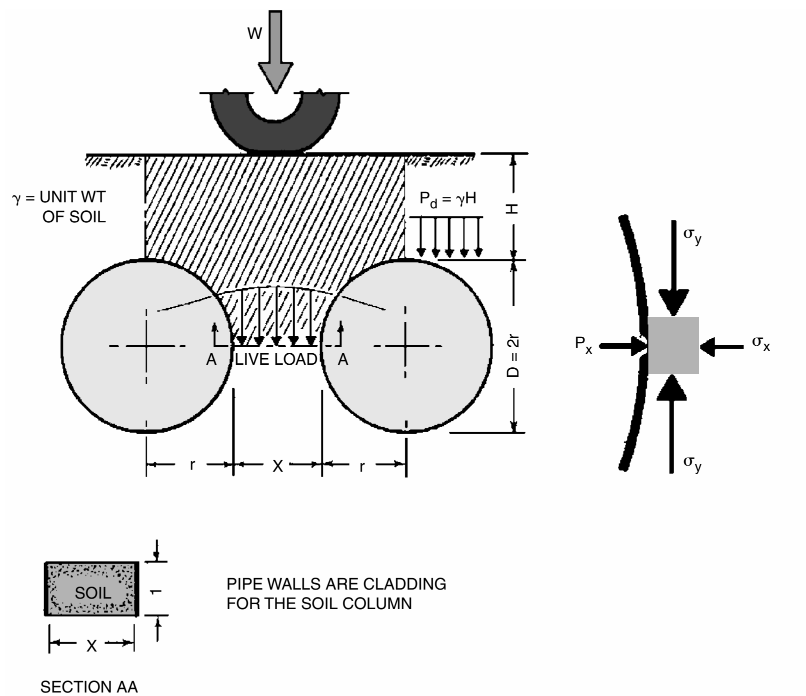

Figure 3.26 Soil column between parallel pipes showing minimum section AA. This section must be able to resist the entire live load plus part of the dead load.

Definitions of terms

D = outside diameter of pipe = $2r$

A = pipe wall area per unit length of pipe

σ_f = ring compression strength of wall

σ_t = ring compression stress in wall

SF = safety factor

W = live load on surface

γ = unit weight of soil

w = load per length of pipe

w_d = dead load per length of pipe

w_l = live load per length of pipe

P = vertical pressure = w/D or V/D

σ_y = vertical soil stress on section AA

S' = vertical soil compression strength

X = width of section AA between pipes

V = total vertical load per length on section AA = $w_d + w_l$

V' = $V - \gamma HD$ = vertical load per length supported by soil at section AA = total vertical load reduced by load that is supported by pipe walls

H = height of soil cover over pipe

For design, the strength of the column at section AA must be greater than the vertical load. Failure (a performance limit) occurs if either of the following happens.

1. Thrust in the pipe wall exceeds the ring compression strength.
2. The vertical soil stress at section AA exceeds the compressive strength (vertical resistance) of the soil.

The ring compression strength of the pipe wall is usually the yield strength. For rigid pipes, σ_f is the crushing strength of the wall. The value for σ_f can be obtained from the pipe manufacturer.

The strength of the soil is found as follows. Assume that the embedment is granular and compacted. Soil strength is vertical stress σ_y at slip. Horizontal soil stress is provided by the pipe walls. Approximate soil strength may be found from triaxial soil tests in which interchamber pressure is equal to the horizontal pressure P_x of the pipe against the soil. For circular, flexible pipes at soil slip, $P_x = P_d = \gamma H$.

Stresses in the pipe and soil are each calculated independently. This is because the bond between soil and pipe can be assumed to be zero. The bond cannot be ensured because of fluctuations in temperature, moisture, loads, etc., all of which tend to break down the bond at the soil-pipe interface.

The pipe must be adequate. Therefore, before the soil column is analyzed, design starts with the ring compression equation

$$\frac{PD}{2A} = \frac{\sigma_f}{\mathrm{SF}}$$

For worst-case ring compression, the live load W is directly above the pipe where $P = P_l + P_d$. The live load effect P_l can be found by the Boussinesq equation (see Chap. 2). If W is assumed to be a point load directly over the pipe, the Boussinesq equation reduces to

$$P_l = \frac{0.477W}{H^2} \tag{3.25}$$

If live load W is assumed to be a distributed surface pressure, the Newmark integration can be used. Soil cover must be greater than minimum by the pyramid/cone analysis of Chap. 2. After an adequate pipe has been selected, the soil column can be designed.

The following analysis is for flexible pipes. The vertical load supported by the two flexible pipe walls at section AA is no less than $2PD/2 = PD$. So, in the design of the soil column, it is assumed, conservatively, that the pipe wall cladding takes a vertical load of PD. The remainder of the load must be supported by the soil. The greatest load on the soil occurs when the heavy live load W is centered above section AA—centered between the two pipes. At this location, not only is the live load pressure on the soil maximum, but also the portion supported by the pipe walls is minimum. Pipe walls carry dead load $P_dD = \gamma HD$. The live load P_l on the pipes is small enough to be neglected. The live load on section AA cannot be neglected. This is the Boussinesq soil stress σ_y, and it must be less than strength S'. Vertical stress is soil load per length divided by the distance between pipes X:

$$\sigma_y = \frac{V'}{X} = \frac{S'}{\mathrm{SF}}$$

Per unit length of pipe, V is the sum of the deadweight of the cross-hatched soil mass w_d and that portion w_l of the surface live load W that reaches section AA. See Fig. 3.26. The dead load w_d per unit length of pipe is the soil unit weight times the crosshatched area, i.e.,

$$w_d = \left[(X + 2r)\,(H + r) - \frac{\pi r^2}{2} \right] \gamma \tag{3.26}$$

The live load w_l is the volume under the live load pressure diagram of Fig. 3.26 at section AA. It is calculated by means of the Boussinesq live load w_l per unit length.

$$w_l = \frac{0.477WX}{(H + r)^2}$$

Example Problem 3.3 What is the vertical soil stress at section AA of Fig. 3.26? The pipes are 24-in-diameter DR 35 PVC. There is 12 in of soil between the two at the spring line. Soil cover is 1.5 ft of soil at a unit weight of 120 lb/ft^3. A surface wheel load of $W = 20$ kips is anticipated. Thickness $t = 24/35 = 0.686$ in.

1. Find the maximum ring compression stress in the pipe wall.
2. Evaluate the soil stress at section AA.

The pressure on pipe due to dead load is

$$P_d = \gamma H = 120 \times 1.5 = 180 \text{ lb/ft}^2$$

or

$$P_d D = 180\ (2) = 360 \text{ lb/ft}$$

For live load on pipe, use the Boussinesq equation:

$$w_l = \frac{0.477WD}{H^2} = \frac{0.477 \times 20{,}000 \times 2}{(1.5)^2} = 8480 \text{ lb/ft}$$

$$P_l = \frac{w_l}{D} = \frac{8480}{2} = 4240 \text{ lb/ft}^2$$

$$P = P_d + P_l = 180 + 4240 = 4420 \text{ lb/ft}^2$$

Total vertical load (per length) on pipe $V = w_d + w_l = 360 + 8480 = 8840$ lb/ft $= 737$ lb/in. The ring compression stress is

$$\sigma_t = \frac{PD}{2t} = \frac{V}{2t} = \frac{737}{2\ (0.686)} = 537 \text{ lb/in}^2$$

The pipe wall will not crush. It is interesting to note that the total load of 4420 lb/ft^2 is equivalent to a static load of about 37 ft of cover for soil weighing 120 lb/ft^2. Thus, the soil in the pipe zone should be compacted to a density required for 37 ft of cover.

For the dead load on section AA, use Eq. (3.26),

$$w_d = \left[(X + 2r)\,(H + r) - \frac{\pi r^2}{2}\right]\gamma$$

$$= \left[(1 + 2)\,(1.5 + 1) - \frac{\pi}{2}\right]120$$

$$= 712 \text{ lb/ft (dead load on section AA)}$$

or $$P_d = \frac{w_d}{X} = \frac{712}{1} = 712 \text{ lb/ft}^2$$

For live load on section AA, the live load w_l can be evaluated by the Boussinesq equation, (3.25), where

$$P_l = 0.477\frac{W}{H^2} = \text{total live load on section AA}$$

where W = wheel load on surface and H = 2.5 ft, which is the depth to section AA = 1.5 ft + 1 ft. So

$$P_l = 0.477\frac{W}{H^2} = \frac{0.477\,(20{,}000)}{(2.5)^2} = 1526 \text{ lb/ft}^2$$

The soil pressure on section AA is

$$P' = P - \gamma H = P_d + P_l - \gamma H = 712 + 1526 - 120(1.5) = 2058 \text{ lb/ft}^2$$

where γHD is the load supported by the pipe walls. Vertical soil stress on section AA is $\sigma_y = P' = 2058$ lb/ft^2.

The maximum pressure σ_x at the side of the pipe should be no greater than the vertical load at the top of the pipe. That is, σ_x should be less than or equal to $\gamma H = 180$ lb/ft^2. If σ_x is greater than γH, the pipes may collapse inward from the sides. And σ_x is related to σ_y by the following equation:

$$\sigma_x = \frac{\sigma_y}{K}$$

where

$$K = \frac{1 + \sin\phi}{1 - \phi} = 3$$

where K is Rankine's lateral pressure ratio and ϕ is the soil friction angle, and for this soil $\phi = 30°$.

Thus, the pipe must be able to support a horizontal load of $\sigma_y/3 = 2058/3 = 686$ lb/ft^2, but it will only support 180 lb/ft^2 (vertical dead load on top of pipe). To remedy the situation, one could:

1. More than triple the space between the parallel pipes.

2. Place the pipes deeper to diminish the live load, and increase the vertical dead load.
3. Place a concrete slab on the soil surface to distribute the live load.

Example Problem 3.4 What is the vertical soil stress at section AA of Fig. 3.26? The pipes are 72-in-diameter HDPE profile-wall pipe. There is 24 in of soil between the two at the spring line. Soil cover is 1.5 ft of soil at a unit weight of 120 lb/ft^3. A surface wheel load of $W = 20$ kips is anticipated. This is similar to the last.

$$\text{Area per unit length} = \text{effective thickness} = 0.675 \text{ in}$$

$$\text{Stiffness } F/\Delta y = 18 \text{ lb/in}^2$$

$$\text{Tensile strength} = 1000 \text{ lb/in}^2$$

$$\text{Compression strength} = 3000 \text{ lb/in}^2$$

1. Find the maximum ring compression stress in the pipe wall.
2. Evaluate the soil stress at section AA.

The pressure on pipe due to dead load is

$$P_d = \gamma H = 120\,(1.5) = 180 \text{ lb/ft}^2$$

or

$$P_d D = 180(6) = 1080 \text{ lb/ft}$$

For live load on pipe, use the Boussinesq equation:

$$w_l = \frac{0.477WD}{H^2} = \frac{0.477 \times 20{,}000 \times 6}{(1.5)^2} = 25{,}440 \text{ lb/ft}$$

$$P_l = \frac{w_l}{D} = \frac{25{,}440}{6} = 4240 \text{ lb/ft}^2$$

Total vertical load on pipe

$$V = w_d + w_l = 1080 + 25{,}440 = 26{,}520 \text{ lb/ft} = 2210 \text{ lb/in}$$

or

$$P = \frac{V}{D} = \frac{26{,}520}{6} = 4420 \text{ lb/ft}^2$$

Ring compression stress

$$\sigma_t = \frac{PD}{2t} = \frac{V}{2t} = \frac{2210}{2\,(0.675)} = 1637 \text{ lb/in}^2$$

As in the previous example, the pipe wall will not crush, but this stress is more than one-half of the compressive strength. There may be local buckling. It is interesting to note that the total load of 4420 lb/ft^2 is equivalent to a static load of about 37 ft of cover for soil weighing 120 lb/ft^2. Thus the soil in the pipe zone should be compacted to a density required for 37 ft of cover.

For the dead load on section AA, use Eq. (3.26):

$$w_d = \left[(X + 2r)\,(H + r) - \frac{\pi r^2}{2} \right] \gamma$$

$$= \left[(2 + 6)\,(1.5 + 3) - \frac{9\pi}{2} \right] 120$$

$$= 2624 \text{ lb/ft (dead load on section AA)}$$

or

$$P_d = \frac{w_d}{X} = \frac{2624}{2} = 1312 \text{ lb/ft}^2$$

Live load on section AA can be evaluated by the Boussinesq equation (3.25):

$$P_l = \frac{0.477W}{H^2} = \text{total live load on section AA}$$

$$W = \text{wheel load on surface}$$

$$H = 4.5 \text{ ft (which is the depth to section AA)} = 1.5 \text{ ft} + 3 \text{ ft}$$

so $$P_l = \frac{0.477W}{H^2} = \frac{0.477\,(20{,}000)}{(4.5)^2} = 471 \text{ lb/ft}^2$$

The soil pressure as section AA is

$$P' = P - \gamma H = P_d + P_l - \gamma H = 1312 + 471 - 120(1.5) = 1603 \text{ lb/ft}^2$$

And γH is the load supported by the pipe walls. Vertical soil stress on section AA is $\sigma_y = P' = 1603$ lb/ft^2.

The maximum pressure σ_x at the side of the pipe should be no greater than the vertical load at the top of the pipe. That is, σ_x should be less than or equal to $\gamma H = 180$ lb/ft^2. If σ_x is greater than γH, the pipes may collapse inward from the sides. And σ_x is related to σ_y by the following equation:

$$\sigma_x = \frac{\sigma_y}{K} \qquad \text{where} \qquad K = \frac{1 + \sin\phi}{1 - \sin\phi} = 3$$

Thus, the pipe must be able to support a horizontal load of $\sigma_y/3 = 1603/3 = 534$ lb/ft^2, but it will only support 180 lb/ft^2. To remedy the situation one could

1. Increase the space between the parallel pipes.

2. Place the pipes deeper to diminish the live load, and increase the vertical dead load.
3. Place a concrete slab on the soil surface to distribute the live load.

Rigid pipes

For a rigid pipe, the pipe wall will take almost the entire load because of the great difference between the modulus of elasticity of the pipe wall and the modulus of elasticity (compressibility) of the soil. Unlike flexible pipes, rigid pipes do not exert pressure $P_x = P$ against the soil. Total load Q is supported by the pipe walls in ring compression and by the soil in vertical passive resistance.

Safety factors

Safety factors for live load analysis may be close to unity. In the above analyses, the arching action of the soil cover was neglected, and thus the analyses are very conservative.

Parallel trench

In 1968, parallel-trench research was conducted at the Buried Structure Laboratory at Utah State University. This research was conducted under the direction Reynold K. Watkins with the primary objective to answer questions that had arisen concerning embedment stability when a trench is excavated parallel to an existing buried flexible pipe. Questions such as these were posed:

1. What is the stability of the trench?
2. At what minimum separation between the pipe and the parallel trench will the pipe collapse?
3. Compacted soil at the sides supports and stiffens the top arch. What happens to a buried flexible pipe when some of or all the side support is removed in a parallel excavation?
4. What are the variables that influence collapse?

Answers to these questions as determined by Watkins are summarized here.

In order to reduce the number of variables, ring stiffness was assumed to be zero. Results were conservative because no pipe has zero ring stiffness. For the most flexible plain steel pipes, D/t is less than 300. For the test pipes, D/t was 600 in an attempt to approach zero stiffness. It was necessary to hold the pipes in shape on mandrels during placement of the backfill.

Vertical trench walls

Figure 3.27 shows the cross section of a buried flexible pipe with an open-cut vertical trench wall parallel to it. If trench wall *AB* is cut back closer and closer to the buried pipe, side cover *X* decreases to the point where the sidefill soil is no longer able to provide the lateral support required to retain the flexible ring. The ring deflects, thrusting out a soil wedge, as indicated in Fig. 3.28. As the ring deflects, a soil prism breaks loose directly over the ring. The soil prism collapses the flexible ring. In order to write pi terms to investigate this phenomenon, the pertinent fundamental variables must be identified. Ring stiffness is ignored because the ring is flexible. In fact, at zero ring deflection, the ring stiffness has no effect anyway. The remaining fundamental variables are as follows:

Fundamental variables	Basic dimensions
X = minimum side cover (minimum horizontal separation between pipe and trench at collapse)	L
D = pipe diameter	L
H = height of soil cover over top of pipe	L
Z = critical depth of trench in vertical cut (vertical sidewalls)	L

Critical depth Z is a convenient measure of soil strength. It is defined as the maximum depth of a trench at which the walls stand in vertical cut. At greater depths the trench walls slip or cave in.

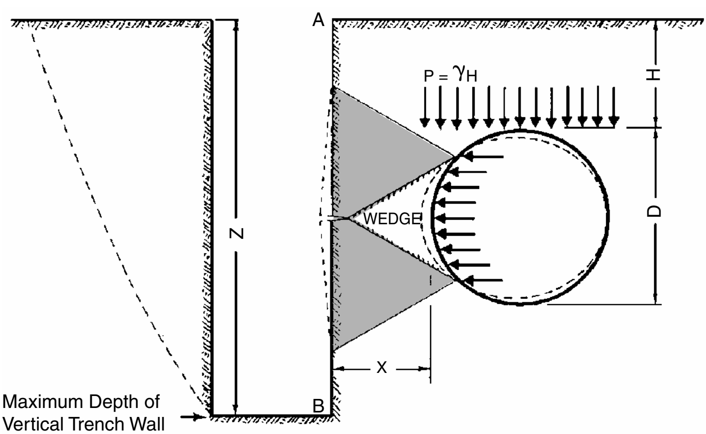

Figure 3.27 Vertical trench wall parallel to a buried flexible pipe showing the soil wedge and shear planes that form as the pipe collapses.

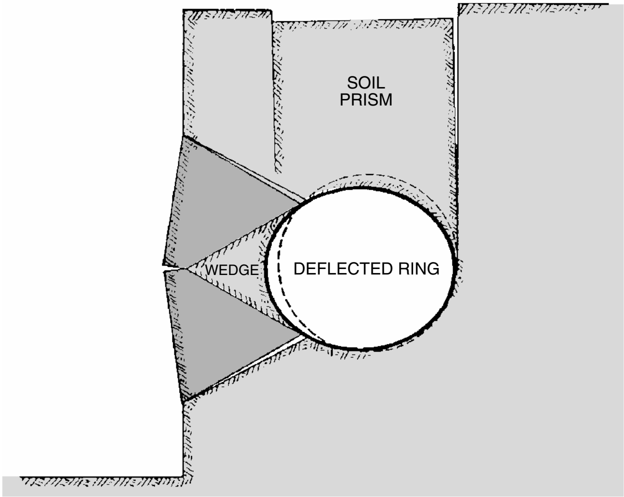

Figure 3.28 Formation of a soil prism on the pipe as a collapse mechanism forms.

Critical depth Z may be determined by excavation in the field, or it may be calculated from the dimensionless stability number $Z\gamma/C$. See Fig. 3.31.

$$\frac{2C}{\gamma Z} = \tan\left(45° - \frac{\phi}{2}\right) \tag{3.27}$$

where Z = critical depth of trench in vertical cut
γ = unit weight of soil, lb/ft^3
C = soil cohesion, lb/ft^2
ϕ = soil friction angle of trench wall

Depth Z can be found from Eq. (3.27) if soil properties γ, C, and ϕ are provided by laboratory tests.

To investigate the four fundamental variables, three pi terms are required. One possible set is X/D, H/D, and H/Z. Tests show that H/D is not pertinent. Only X/D and H/Z remain as pertinent pi terms.

For a vertical trench wall excavated parallel to a flexible pipe:

1. If the ring has some stiffness, and if soil cover H is not great enough to collapse the ring, soil may slough off the pipe into the trench. This is not considered failure because the soil can be replaced during backfilling.

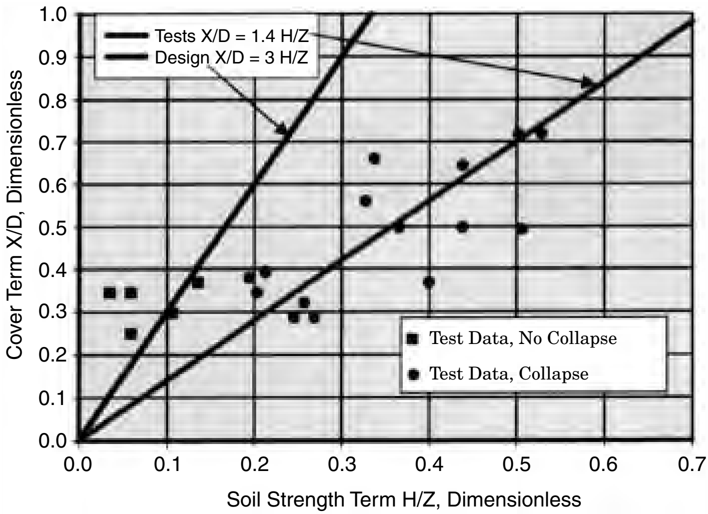

Figure 3.29 Cover term X/D as a function of the soil strength term H/Z for a vertical trench wall excavated parallel to a very flexible pipe.

2. The ring collapses under a free-standing prism of soil that breaks loose on top of the pipe.
3. Failure is sudden and complete collapse.

Test data are plotted in Fig. 3.29, which shows X/D as a function of H/Z. The best-fit straight-line equation is $X/D = 1.4H/Z$. The probable error in X/D is ±0.1, so the probable error in side soil cover X is roughly $\pm D/10$. Because field conditions may be less reliable than laboratory conditions, the safety factor should be 2. Therefore, the minimum side cover X might be specified as

$$\frac{X}{D} = \frac{3H}{Z} \tag{3.28}$$

Of interest in Fig. 3.29 are the data points indicated by squares. These do not represent collapse. The ring stiffness for the test pipes was great enough that part of the shallow soil cover merely sloughed off the pipes after the soil wedge fell into the trench. If ring stiffness were to be included as a fundamental variable, ring deflection would have to be included. Then the coefficient of friction between pipe and soil should also be included as a fundamental variable.

If the pipe has significant ring stiffness, the height of soil cover that it can support without collapse can be found for uniform vertical pressure with no side support.

$$\text{Moment } M = \frac{Pr^2}{4} \qquad \text{Stress } \sigma = \frac{Mc}{I}$$

For pipes, at yield stress, based on elastic theory,

$$P_y = \frac{4\sigma_y}{r^2}\frac{I}{c} = \frac{16\sigma_y}{D^2}\frac{I}{c} \tag{3.29}$$

where P = vertical soil pressure
I = moment of inertia of wall cross section
D = pipe diameter = $2r$
c = distance to wall surface from neutral surface = $t/2$ for plain pipes
t = wall thickness of plain pipes
σ_y = yield strength of pipe
DR = dimension ratio D/t for plane pipes

$$P_y = \frac{8\sigma_y}{3}\left(\frac{t}{D}\right)^3 \quad \text{for plain pipes} \tag{3.30}$$

For plain pipes, the moment that produces a fully plastic hinge is 1.5 times the moment that produces yielding. Therefore the fully plastic load is

$$P_{\text{fp}} = 4\sigma_y\left(\frac{t}{D}\right)^3 \tag{3.31}$$

The approximate vertical ring deflection at plastic hinging can be calculated as follows:

$$\frac{\Delta y}{D} \approx \frac{0.02P_{\text{fp}}D^3}{EI}$$

where $\Delta y/D$ = ring deflection
P = vertical pressure on ring
D = circular pipe diameter
EI = wall stiffness per unit length of pipe

Sloped trench walls

Figure 3.30 shows a flexible pipe in cohesionless soil for which the slope is the angle of repose $\approx \phi$. Pressure distribution on the ring is triangular, as shown. Maximum moment at A can be found by

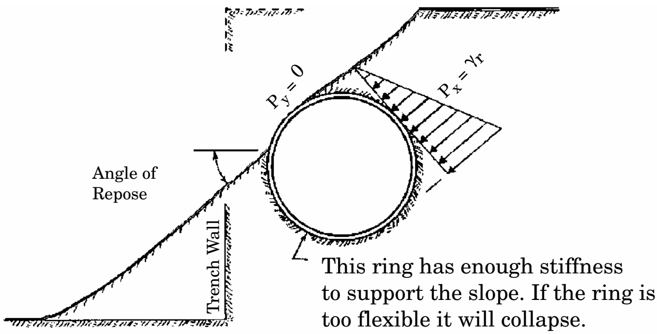

Figure 3.30 Trench wall sloped at the angle of repose (soil is stable). The flexible pipe requires sufficient pipe stiffness or minimum cover to prevent collapse.

Castigliano's equation. However, it is sufficiently accurate to find the equivalent moment $M_A = Pr^2/4$ for average uniform pressure $P_x = r\gamma$.

Excavation

Depth of the excavation must include *overexcavation* required to remove unstable subbase material. It should be replaced by approved bedding material. Some tank manufacturers consider soil to be unstable if the cohesion is less than $C = 750$ lb/ft^2 based on the unconfined compression test or if the bearing capacity is less than 3500 lb/ft^2. In the field, bearing capacity is adequate if an employee can walk on the excavation floor without leaving footprints. A muddy excavation floor can be choked with gravel until it is stable. These are conservative criteria for soil stability.

Of greater concern are OSHA safety requirements for retaining or sloping the walls of the trench. Excavations for tanks are usually short enough that OSHA trench requirements leave a significant margin of safety. Longitudinal, horizontal soil arching action is significant.

These criteria for bearing capacity and cohesion are equivalent to a vertical trench wall over 20 ft deep. Bearing capacity of 3500 lb/ft^2 can support more than 29 ft of vertical trench depth at soil unit weight of 120 lb/ft^3. Cohesion of 750 lb/ft^2 can support a vertical open-cut trench wall that is more than 20 ft deep.

Critical depth of vertical trench wall. Granular soil with no cohesion cannot stand in vertical cut. Much of the native soil in which pipes and tanks are buried has cohesion. Therefore, the wall of the excavation can stand in vertical open cut to some critical depth Z. See Fig. 3.31

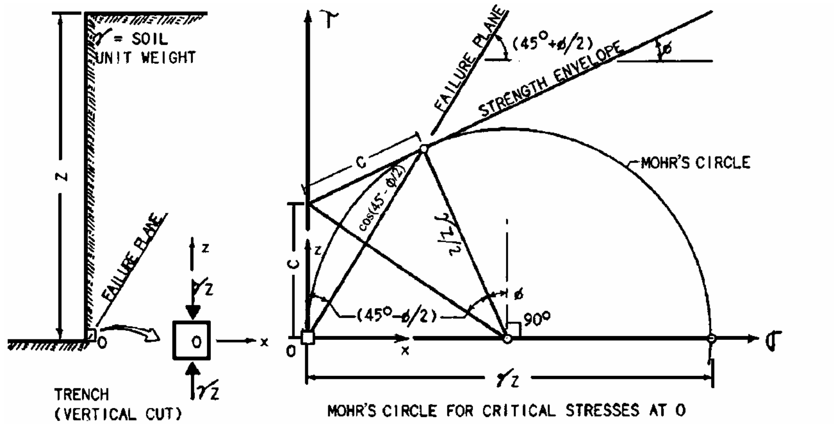

Figure 3.31 Mohr's circle analysis for finding critical depth Z for a vertical trench wall in a brittle soil cohesion C and a soil friction angle ϕ, where $2C/(\gamma Z) = \tan(45° - \phi/2)$.

(left). Greater depth will result in a "cave-in" starting at the bottom corner O, where the slope of the failure plane is $45° + \phi/2$. For a two-dimensional trench analysis, the infinitesimal soil cube O is subjected to vertical stress γZ, where

γ = soil unit weight

Z = critical depth of vertical trench wall

ϕ = soil friction angle

C = soil cohesion

Mohr's circle is shown in Fig. 3.31. The orientation diagram (x-z) of planes on which stresses act is superimposed, showing the location of the origin O. The strength envelope slopes at soil friction angle ϕ from the cohesive strength C. At soil slip, Mohr's stress circle is tangent to the strength envelope. From trigonometry,

$$\tan\left(45° - \frac{\phi}{2}\right) = \frac{2C}{\gamma Z}$$

This is the critical depth, Eq. (3.31).

From tests, Eq. (3.27) provides a reasonable analysis for brittle soil. If the soil is plastic, soil slip does not occur until shearing stresses reach shearing strength C. Consequently, in plastic soil, the critical depth equation is $2C/(\gamma Z) = 1$. Below the water table, critical depth is essentially doubled.

Example Problem 3.5 What is the critical depth Z of a vertical, open-cut trench wall if $C = 600$ lb/ft^2, $\gamma = 120$ lb/ft^3, and $\phi = 30°$?

Substituting into Eq. (3.27) gives $Z = 17.3$ ft. This is a lower limit if the soil has some plasticity (is not brittle).

Example Problem 3.6 Suppose that a sloped trench wall exposes a pipe as shown in Fig. 3.30. Pressure P_x must be resisted by ring stiffness. What is the required pipe stiffness for a 72-in HDPE pipe to prevent buckling?

Assume the soil is granular with unit weight of 120 lb/ft^3. Since there is no soil on one side of the pipe, assume the pipe is unsupported and must be able to withstand the pressure $P_x = \gamma r$. From Eq. (3.14),

$$P_{cr} = \frac{3EI}{(1 - \nu^2)\, R^3} = \gamma r$$

Assume the following:

$$E = 110{,}000 \text{ lb/in}^2 \qquad \nu = 0.4$$

and solve for EI/R^3.

$$\frac{EI}{R^3} = \frac{\gamma r\,(1 - \nu^2)}{3} = \left(\frac{120\ 1\text{ ft}^3}{1728\text{ in}^3}\right)36\,(0.84) = 2.1 \text{ lb/in}^2$$

Pipe stiffness is

$$\frac{f}{\Delta y} = 6.7\,\frac{EI}{R^3} = 14 \text{ lb/in}^2$$

It is possible the bending stress will exceed the yield strength before buckling takes place. The maximum moment in the ring is $M = (P_x r^2)/4$, and bending stress is given by

$$\sigma_y = \frac{Mc}{I} = \frac{M}{I/c}$$

Solve for I/c.

$$\frac{I}{c} = \frac{M}{\sigma_y}$$

$$M = \frac{(\gamma r)\, r^2}{4} = \frac{\gamma r^3}{4} = \left(\frac{120}{1728}\right)\frac{(36)^3}{4} = 810 \text{ in} \cdot \text{lb/in}$$

Assume the following:

$$\sigma_y = 110{,}000 \text{ lb/in}^2$$

$$c = \text{distance from neutral axis to outer fiber} = 1.7 \text{ in}$$

$$\frac{I}{c} = \frac{810}{110{,}000} = 7.36 \times 10^{-3}$$

Therefore,

$$I = 7.36 \times 10^{-3}\,(1.6) = 1.18 \times 10^{-2}\ \frac{\text{in}^4}{\text{in}}$$

Thus, a little ring stiffness makes a big difference in the stability of a flexible ring on a sloped trench wall (sidehill).

For most pipes, the ring stiffness required for installation is adequate if it complies with the familiar rule of thumb according to which minimum cover is $D/2$. For a pipe parallel to a sloped trench wall in cohesionless soil, *minimum cover is one-half a diameter to the sloped surface of the trench wall.*

Analytical Methods for Predicting Performance of Buried Flexible Pipes

Introduction

There are various methods for predicting the structural behavior of flexible conduits. Included here is an in-depth analysis of the various methods, pointing out strengths and weaknesses with emphasis on large-diameter profile-wall HDPE pipes. Comparisons of test data with predictions from the various theoretical methods are made. Methods discussed include (1) full-scale testing, (2) semiempirical equations (such as the Iowa formula), (3) closed-form analytical method (such as the Burns and Richard elastic solution), (4) finite element methods, and (5) model testing (with dimensional analysis).

The Burns and Richard solution and the Iowa formula are both linear elastic theories. Both assume the soil and the pipe structure to be linear elastic materials. The assumption that the soil is elastic can lead to large errors. The Burns and Richard solution allows for a nonlinear soil modulus correction to account for overburden pressure. With the same soil modulus or the same modulus correction, these two methods are shown to produce almost identical results. For large-diameter PE pipes, the Burns and Richard method, although still in error, offers some advantages over the Iowa formula. It produces results such as strain, horizontal deflection, and thrust that are not directly available from the Iowa formula. The presently used soil modulus correction in the Burns and Richard solution is shown to be incorrect.

Flexible pipe design and analysis

Installation design. Traditionally there were three parameters that were considered most essential in the design or the analysis of any flexible conduit installation. A fourth needs to be added to the list:

1. Load (depth of burial)
2. Soil stiffness in pipe zone
3. Pipe stiffness
4. For profile-wall pipe, the profile itself

Load. The design load on a flexible pipe is easily calculated using the prism load theory. This load is simply the product of the soil unit weight and the height of cover. Research has shown that the long-term load on a flexible pipe can approach the prism load.[29,42] This load is conservative. Thus, if this load is used in design, the deflection lag factor should be taken as unity. A design procedure that calls for a load that is less than the prism load should also incorporate an appropriate lag factor in the procedure.

Soil stiffness. The soil stiffness is usually expressed in terms of the parameter E', where E' is a soil modulus term and is, dimensionally, the load per unit area (normally MPa or lb/in^2). The soil modulus E' is a function of soil properties such as soil density, soil type, and moisture content. Experience has shown that soil density is the most important parameter influencing soil stiffness.[32,40,52] As discussed early in this chapter, the secant modulus from a constrained soil test may be used in place of E' with some acceptable error.

Pipe stiffness. The most commonly used terminology is pipe stiffness ($F/\Delta y$). For a given pipe product, this term is readily determined in the laboratory by a parallel-plate loading test

$$\text{Pipe stiffness} = \frac{F}{\Delta y} = \frac{6.7\, EI}{r^3}$$

Profile of the pipe wall. When a pipe deflects under load, bending strains are induced in the pipe wall. These strains vary through the pipe wall. Profile-wall pipes are designed and manufactured to minimize the use of material by increasing the section modulus of the pipe wall. The concept of a profile-wall pipe is not new since corrugated steel pipe is truly a profile-wall pipe and has been available for many years. Some of the newer plastic pipe products are of this type. That is, the plastic is placed primarily at the inside and outside walls or in ribs for greater pipe stiffness. Many of these products have been shown to perform with the profile section acting as a unit as designed. For adequate safety, for any such product, the design should include sufficient plastic between the inner and outer walls and/or between the ribs to carry shear and to ensure that the profile section indeed acts as a unit. Also, the cross-sectional area per unit length and the individual wall component thickness should be sufficient to resist localized buckling.

Long-term properties of plastic. In a finite element program, an incremental analysis with a decreasing pipe modulus shows that using the so-called long-term modulus has little influence on the overall behavior. Thus, inclusion of the viscoelastic properties of the pipe in the analysis is not justified. Error caused by imprecision in the soil terms totally masks any benefit gained by a viscoelastic analysis.

As previously stated in this book, in both the trench and the embankment, it takes substantial time for the full load to reach the pipe, and changes in deflections with time are due to increasing loads and soil consolidation—not due to creep in the pipe material. Thus, as previously stated, the creep properties of pipe materials have little effect on the long-term deflection behavior of flexible pipe. Note that for some profile-wall pipes, controlling vertical deflection may not control localized buckling as a performance limit.

Methods for predicting pipe performance

Full-scale testing. Full-scale testing has been used with great success at various research laboratories such as at Utah State University, the U.S. Bureau of Reclamation, and Ohio University. Techniques have evolved whereby a prototype pipe is tested until failure occurs, and then the total performance of the pipe is studied.

Model testing. Model testing is as described above but often involves smaller-scale pipes. Dimensional analysis is used to predict the performance of larger pipes. Pipe models are sometimes put in centrifuges where g forces are generated to simulate high depths of cover. Model testing has been used with some success, but centrifuge testing has its problems and has not been universally accepted.

Spangler's Iowa formula. This equation is discussed earlier in this chapter.

$$\Delta x = \Delta y = \frac{D_L K W}{EI/r^3 + 0.061E'}$$

Spangler assumed symmetry about the vertical centerline but did not assume symmetry about the horizontal centerline. A review of the derivation of the Iowa formula shows that it has an excellent theoretical foundation. The derivation uses the exact relations of moment, shear, and thrust in the pipe ring. It is an excellent linear theory.

Burns and Richard's elastic solution.[3,8] Burns and Richard published their solution at the Symposium on Soil-Structure Interaction at the University of Arizona in 1964. There was little interest shown in their solution, since it is an elasticity solution. In fact, it was largely ignored until the mid-1990s when some renewed attention was given to this solution. This solution is nothing more than an adaptation of the theory of elasticity solution published by Michell in 1899. Michell's solution is for a circular hole in a semi-infinite isotropic elastic medium. Burns and Richard modified the Michell solution by placing a circular isotropic elastic shell in the hole and used thin-shell theory to match boundary conditions between the circular hole and circular shell. This solution is linear. It assumes both the soil and the pipe structure to be linear elastic materials. The elastic assumption for the pipe structure is acceptable for most pipe materials. However, in this solution and in the Iowa formula, the assumption that the soil is elastic can lead to large errors.

Burns and Richard used only a constant elastic modulus for the soil. The possibility for the soil modulus to change as the depth of cover increases has been added to the linear elastic theory proposed by Burns and Richard. In this modified version, the effective soil modulus increases as the soil height over the top of the pipe is increased. This is sometimes called the *overburden-dependent* soil modulus. Again, this overburden-dependent soil modulus was not proposed by Burns and Richard but was added later. The justification for an increasing modulus with depth of cover comes from the confined compression test for soil. In such a test, the stress-strain curve is concave upward. The slope of the line (modulus) increases with increasing stress. However, in a buried flexible pipe situation, the soil next to the pipe is not confined and the load-deflection curve is concave downward.

It has been shown that when the overburden-dependent model is applied to steel, solid wall PVC, FRP, RPM, or HDPE pipes, the predicted vertical deflection is often in large error. The primary difficulty lies in having the proper soil modulus to make the solution work. The assumed increase in the effective soil modulus with depth of cover usually does not take place for flexible pipes, but may be valid for rigid pipes. If the overburden-dependent feature is not used, the Burns and Richard solution produces almost identical results to those produced by the Iowa formula. Also, if the same overburden-dependent modulus is used in both the Iowa formula and the Burns and Richard solution, then the calculated vertical deflections are essentially the same from either theory. A PC version of the Burns and Richard solution is available on a spreadsheet.

The advantages of the Burns and Richard solution are that

1. It has been programmed on a spreadsheet and is easy to use.
2. It produces pipe wall thrust and strain, and horizontal deflection directly.
3. It allows for full slip or no slip at the soil-pipe interface.

The greatest shortcomings of the Burns and Richard solution are that

1. The solution assumes double symmetry. That is, it assumes that the soil-pipe system is symmetric about both the horizontal and the vertical axes. It is normal to assume symmetry about the vertical axes; however, both test results and finite element methods show that symmetry about the horizontal axis is not the norm. Spangler recognized (based on tests) that symmetry about the horizontal axes was not present and provided for nonsymmetry about that axis in his semiempirical method.

2. As the solution is used by some, with the overburden soil modulus, results will be nonconservative for flexible pipe installations. Whereas this correction may work for rigid pipe, it should not be used for flexible pipe. The solution itself, without the overburden-dependent soil modulus, does not require the pipe to be rigid. However, it is for the small-displacement theory which does require small displacements.

Finite-element methods.[18,22] A more complete discussion of the finite element analysis (FEA) technique is given later in this chapter.

The FEA method has been shown to be successful in predicting the behavior of buried flexible pipes.[40] In particular, recent research at Utah State University has shown that the FEA method is the most successful method in the prediction of the behavior of large-diameter HDPE pipes. However, the user must be forewarned that the FEA results are only as good as the ability to model the behavior of soil-structure interaction.

The addition of the geometric nonlinear analysis has been included by modifying the nodal coordinates of each node at the end of each loading increment. This procedure has essentially removed the concern that the small-strain theory used in FEA programs was inducing some inaccuracies in the results for flexible pipes.

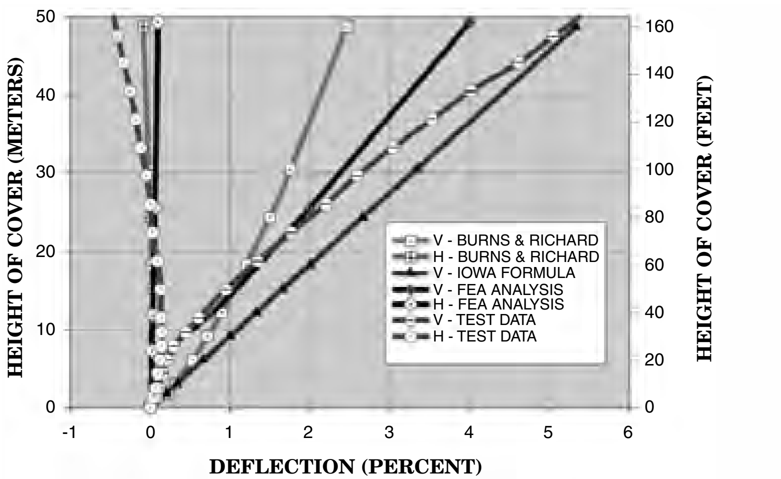

Figure 3.32 Comparison of test results with various analytical methods for a 48-in-diameter HDPE pipe buried in silty-sand soil compacted to 85 percent standard Proctor density.

Comparison of results. In the following figures, height of cover is calculated by dividing the vertical soil pressure by an assumed unit weight of soil. For these figures, a unit weight of 19.1 kN/m^3 (120 lb/ft^3) has been used. Figure 3.32 shows a comparison of the various analytical methods with test data for 48-in-diameter HDPE pipe. The soil was silty sand compacted to 97 percent standard Proctor density. The E' value used in the solutions is 27.56 MPa (4000 lb/in^2). Note that the finite element analysis solution most closely represents the actual test data. Also, note that the slope of the load-deflection of the test data approaches the slope of the Iowa formula. With the overburden correction, the Burns and Richard (B&R) solution produces a concave-upward curve which does not match results. It is interesting to note that for vertical deflection, the Iowa formula and the B&R solution agree at very low cover heights. This is before the overburden correction becomes effective in the B&R solution.

Figure 3.33 shows a similar comparison for a 48-in-diameter HDPE pipe installed in silty sand compacted to 85 percent standard Proctor density. The value for E' used in the solutions is 3.45 MPa (500 lb/in^2). Again, the deviation of the B&R solution is due to the incorrect overburden correction on the soil modulus. Again, the FEA results most closely match the test results. For details of the FEA program and the mesh used in the analyses, see Refs. 29 and 40.

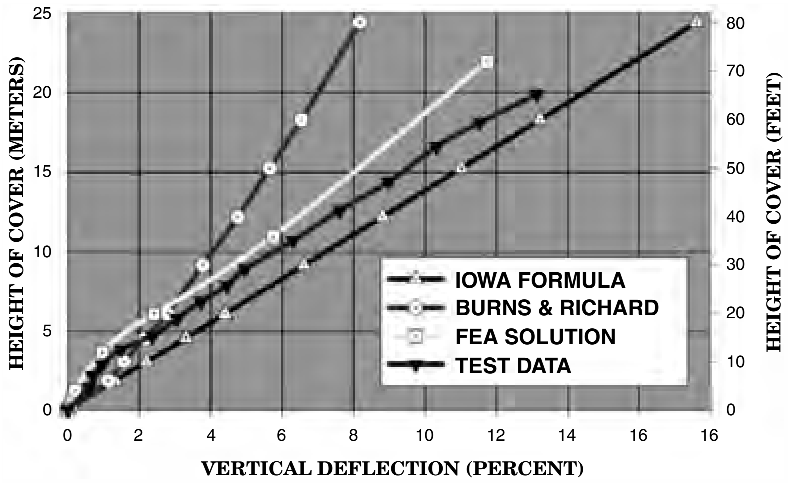

Figure 3.33 Comparison of test results with various analytical methods for a 48-in-diameter HDPE pipe buried in silty-sand soil compacted to 97 percent standard Proctor density.

Overburden-dependent modulus. The overburden correction used in the Burns and Richard solution is as follows:

$$E'_{\text{eff}} = \begin{cases} E' & \text{for } H < 6 \text{ ft} \\ E' \, [1 + 0.15\,(H - 6)^{0.5}] & \text{for } H \geq 6 \text{ ft} \end{cases}$$

where E' = traditional soil modulus
E'_{eff} = effective soil modulus
H = height of cover

If the same overburden correction is used in both the Iowa formula and the B&R solution, the predicted vertical deflections are very similar. Figure 3.34 shows the two theories for the 48-in-diameter HDPE pipe installed in a material with $E' = 11.02$ MPa (1600 lb/in^2). Note that the two solutions agree almost perfectly up to about 25 m of cover. And of course, both are incorrect because they are concave upward over the entire range of covers. Figure 3.35 gives similar curves showing close agreement of the two theories if the same overburden-dependent soil modulus is used in both theories.

There are real problems with the overburden-dependent modulus as used in the Burns and Richard solution that require further investigation. Load-deflection curves for buried pipe are normally plotted with the soil load on the vertical axis and deflection on the horizontal axis, as shown in Fig. 3.32. The overburden dependence of the

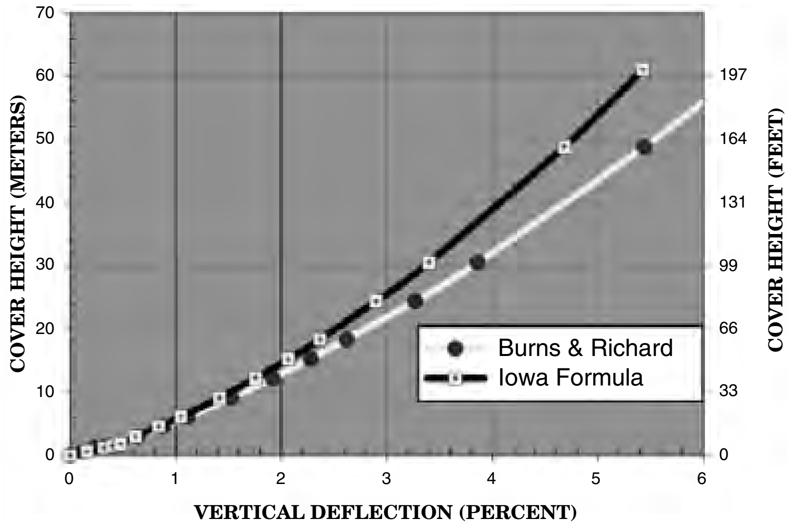

Figure 3.34 Comparison of the Burns and Richard solution with the Iowa formula for the case when the same overburden-dependent soil modulus is used in both solutions. Initial E' is 11.02 MPa or 1600 lb/in^2.

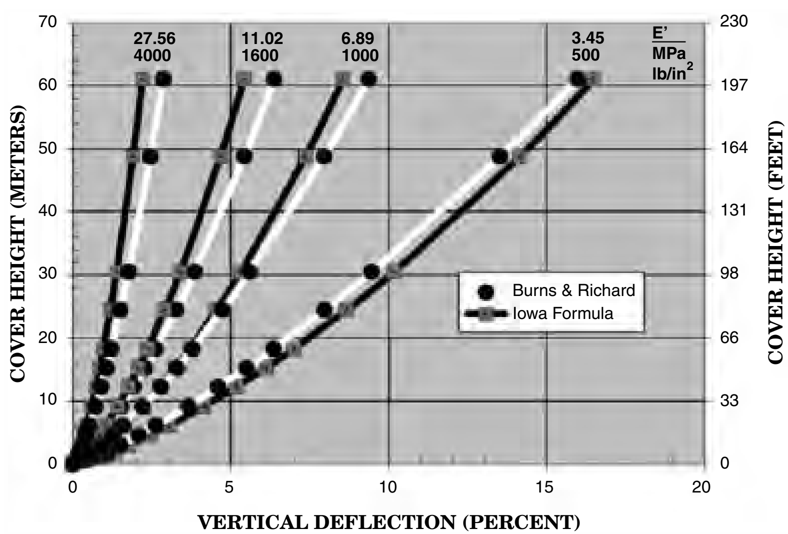

Figure 3.35 Comparison of the Burns and Richard solution with the Iowa formula for the case when the same overburden-dependent soil modulus is used in both solutions for various initial E' values.

modulus produces curves that are concave upward, as shown in Fig. 3.35. This is rarely the case for actual load-deflection curves—they are normally concave downward, as can be seen for the test data curve shown in Figs. 3.32 and 3.33. The slope of the load-deflection curve for the overburden-dependent modulus is the smallest at very low heights of cover. In actual tests, the steepest part of the curve occurs at very low height of cover (see Fig. 3.33). This is especially true for compacted soils. The initial steepness of the load-deflection curves is due to the working of the backfill soil (sometimes called precompaction, or preconsolidation).

Compaction simulation. In a flexible pipe installation, when the overburden is applied, the pressure in the soil must reach the effective precompaction pressure (essentially reloading) before the soil deforms with a slope of the initial soil modulus. The increase in modulus in the upper part of the stress-strain curve, as predicted via a simple confined compression test, does not take place in the load-deflection curve of a flexible pipe installation. The placement of a pipe in the soil introduces stress concentrations that are not present in a confined compression test. The combination of high stress and pipe deformation causes shear failures to take place in the soil. This negates the increase in soil modulus that occurs as the soil is compressed by the increase in overburden.

Therefore, a modulus correction is needed that allows for precompaction and will allow for the slope of the load-deflection curve to approach that of the Iowa formula. Load-deflection curves were analyzed for hundreds of tests of flexible pipes made from many different materials. It was determined that the load-deflection data are represented fairly accurately with a bilinear curve. A modulus correction that will produce the desired results is as follows:

The effective modulus is actually a soil-structure interaction term and is dependent on both the soil and the pipe. Thus, the break point may be different for different pipe products.

$$E'_{\text{eff}} = \begin{cases} 2.5\,E' & H \le b \\ \dfrac{2.5\,E'H}{[b + 2.5\,(H - b)]} & H > b \end{cases}$$

E'_{eff} = effective soil modulus

E' = traditional soil modulus

H = height of cover

b = break height (where the curve changes slope)

Proctor density, percent	Soil modulus E'	Break point b
80	1.73–3.45 MPa (250–500 lb/in^2)	1 m (3 ft)
85	3.45–4.82 MPa (500–700 lb/in^2)	1.5 m (5 ft)
90	4.82–6.89 MPa (700–1000 lb/in^2)	3 m (10 ft)
97	6.89–11.02 MPa (1000–1600 lb/in^2)	9 m (30 ft)

When the above modulus corrections are used in the Burns and Richard and Iowa theories, they produce almost identical results and these results closely follow FEA results and test data. Curves for the two analytical methods, FEA results, and test data are compared in Fig. 3.36.

The Iowa formula versus the Burns and Richard solution. Since it has been shown here that both methods produce the same vertical deflection when applied with the same soil modulus, it no longer needs to be debated as to which solution is better. Both solutions are linear elastic solutions with theoretical bases. Both methods are in error when compared to test data and with finite element data but are easily corrected to give accurate results. However, the Burns and Richard method produces results such as strain, horizontal deflection, and thrust that are not directly available from the Iowa formula.

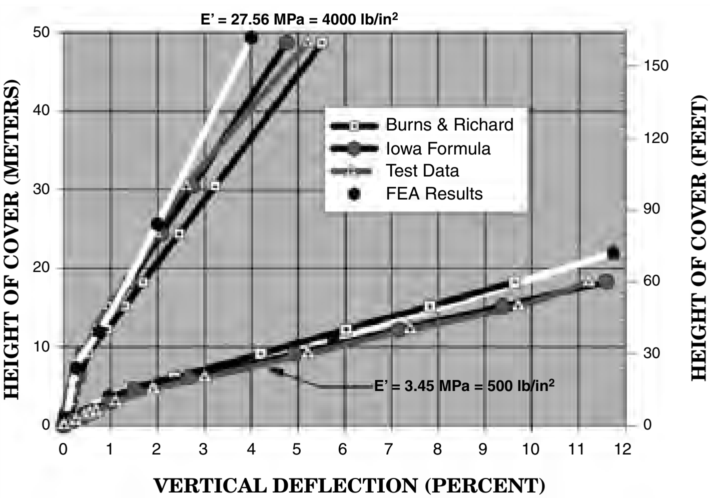

Figure 3.36 Comparison of the test results with various analytical methods for 48-in HDPE pipe. Soil modulus has been corrected for overcompaction, and a bilinear response is assumed for both the Iowa formula and the Burns and Richard solution.

Conclusions

1. The FEA method produces results that most closely represent test data.
2. Full-scale testing and finite element analysis used together are the preferred methods for research and product testing, evaluation, and qualification.
3. The overburden-dependent soil modulus that is presently used in the Burns and Richard solution is incorrect and should not be used in analysis, design, or evaluation of flexible pipe installations.
4. The Iowa formula and the Burns and Richard solution predict essentially the same vertical deflections when the same soil modulus and correction are used in each theory.
5. On a theoretical basis, both the Burns and Richard solution and the Iowa formula are incorrect since they assume an elastic soil. Further, the Burns and Richard solution assumes symmetry about the horizontal axes, which is usually not a valid assumption.
6. If a corrected soil modulus is used, results from either solution closely match test results. The corrected soil modulus is such that a bilinear load-deflection curve results.
7. With the corrected soil modulus, the Burns and Richard solution has advantages over the Iowa formula as it will directly produce horizontal deflection, stress, and strains.

Finite Element Methods

Introduction

The finite element analysis technique was developed primarily for the analysis of complex structural systems. The technique was developed to analyze structural responses to different loading conditions. Through the years, the technique has been extended through mathematical relationships and developed in other areas such as fluid mechanics, thermodynamics, geotechnical engineering, groundwater analysis, aerodynamics, and many other areas of science. The approach has evolved into a rather sophisticated mathematical analysis technique. It has proved to be a very useful tool in research and development as well as in everyday analysis.

One area of development for the use of FEA that has been promoted is in soil-structure interaction mechanics. One- and two-dimensional finite elements can be combined into a global matrix. Each element type may be defined with different stiffness properties. The modeling of the nonlinear stress-strain properties of soil has been accommodated through incremental analysis and an iterative solution scheme. This approach has been widely used in the past for the analysis of earth structures, buried pipes, and earth-retaining structures. It has allowed the development and use of some very large and/or complex structures. Various loading conditions, subsurface conditions, and structural properties can be modeled mathematically. This is an advantage over physical testing of such structures. However, the user must be forewarned that the FEA results are only as good as the ability to model the behavior of soil-structure interaction. Also, the finite element method often has to be calibrated by comparing FEA results with results from physical tests. Additional FEA limitations may include inaccurate input data, convergence, and roundoff error.

A study completed at Utah State University in 1985 addressed some of the problems of finite element modeling. The responses of flexible pipes under various loading conditions, compaction conditions, and groundwater conditions were analyzed. To calibrate the FEA technique, results from physical tests were used for comparison. The actual modeling of some of the different loading schemes brought out the need for additional development of FEA capabilities that had not been addressed in any previous research efforts. These developments have greatly increased the ability to more accurately model soil-structure interaction, particularly for very flexible pipes.

A computer code SSTIPN was obtained and modified by the Utah State University researchers. This program has a structure similar to the program SAP originally developed by Wilson.[54] Modifications to SAP to include soil modeling were implemented by Ozawa and Duncan.[35] Further enhancements including interface elements and improved soil models were included (Duncan et al.[5] and Wong and Duncan[55]). SSTIPN was modified to run on a VAX computer at Utah State University in 1982 and has since been significantly enhanced and is now available on a personal computer (PC).

The FEA research and program development that was performed included the addition of nonlinear geometric analysis; an improved iteration scheme; modifications to the soil model to include primary loading, unloading, and reloading analysis; and improved output files for pipe response analysis and plotting. Applications of the enhanced model included compaction simulation, initial ovalization of the pipe, unsymmetric compaction and bedding analysis, and pseudotime effects due to saturation and soil structure collapse.

Laboratory testing for the soil properties was also performed. The testing included grain-size analysis, Atterberg limits, compaction, confined compression, and triaxial testing for stress-strain properties of each soil type. The results of the triaxial testing were used to analyze the pipe response for several soil types on the enhanced version of SSTIPN. Due to the numerous modifications of the code to specifically accommodate pipe analysis, the code is now called PIPE. The PC version is called PIPE5.

Enhancements to the finite element program SSTIPN

Finite element method for stress analysis in solid mechanics is a mathematical technique whereby a continuum is idealized by dividing it into a number of discrete elements. These elements are connected to their adjacent elements at the nodes only.

Special shape functions are used to relate displacements along the element boundaries to the nodal displacements and to specify the displacement compatibility between adjacent elements. Once the continuum has been idealized, as shown in Fig. 3.37, an exact structural analysis of the system is performed using the stiffness method of analysis.

Equation (3.32) represents the equilibrium equations, in matrix form, for each node in the idealized system. After boundary conditions

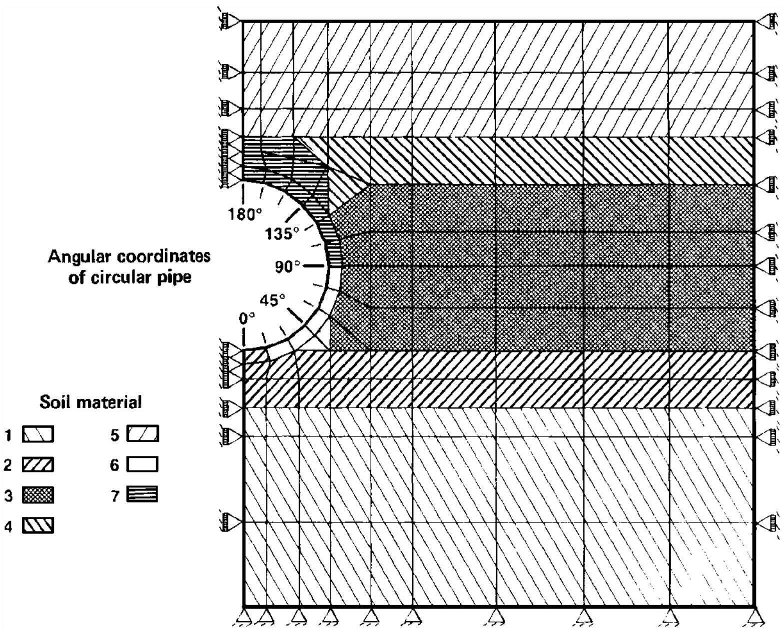

Figure 3.37 Finite element mesh for a buried pipe.

are applied (identifying nodes with fixed or restricted movement), the system of equations can be solved for the unknown nodal displacements. These displacements can in turn be used to evaluate element stresses and strains.

$$[K]\, d = \mathbf{f} \qquad (3.32)$$

where $[K]$ = global stiffness matrix
d = nodal displacement factor
$\mathbf{f}$ = nodal load vector

The stiffness matrix $[K]$ relates the nodal displacements to nodal forces and is a function of the structural geometry, the element dimensions, the properties of the elements, and the element shape functions.

Finite element analyses for soil-structure interaction problems vary in several ways from finite element analyses for simple linear elastic problems.

1. The soil properties are strain-dependent (nonlinear).
2. Different element types must be used to represent the structure (pipe in this case).
3. For flexible pipe, the structure may be geometrically nonlinear.
4. It may be necessary, in some instances, to allow movement between the soil and the walls of the pipe.

The stress-strain behavior of the soil is nonlinear; thus the solution procedure must follow the stress condition incrementally. The construction of the soil structure must be followed in steps, and the external loads must be added incrementally for the FEA program to follow the nonlinear stress-strain properties of the soil. This particular nonlinear behavior of the soil system has resulted in a special type of analysis that is commonly used in most soil mechanics FEA programs. The basic procedure followed is outlined below. The steps described are those that are used in PIPE and PIPE5.

In the finite element analysis of buried pipes, the pipe is modeled using beam elements. These elements are capable of accommodating shear, moment, and thrust. The nodes of the pipe elements are connected to the adjacent soil elements at their common nodal points. Slip between the pipe and soil can be accommodated in the finite element analysis by placing "interface" elements between the pipe nodes and the soil element nodes. These interface elements have essentially no size, but kinematically allow movement between nodes when a specified friction force is exceeded.

Analysis procedure

1. Initial estimates of the stresses and elastic parameters of the soil elements are assumed. Soil properties are nonlinear and are stress- and strain-dependent. Due to the soil nonlinearities, the solution procedure requires modeling that allows for incremental construction of the soil structure and the incremental addition of loads. Initial elastic parameters must be known or assumed to compute the stiffness matrix.
2. An incremental load vector is computed in one of two ways. If incremental construction is being modeled, the load vector is computed as the weight of the added soil and/or structure elements for the increment. Alternatively, the load vector may comprise external loads resulting from external forces.
3. Incremental nodal displacements are computed for the incremental load vector by solving the system of equations represented by Eq. (3.32).
4. The incremental element strains are computed from a strain-displacement matrix using the nodal displacements. The strain-displacement matrix is based on nodal coordinates of each element and the shape functions used to describe the element behavior. The element strains are then used to compute the element stresses using Hooke's law and the initial elastic parameters used in step 1 above. The total stresses, strains, and displacements in the element are computed by adding the incremental stresses, strains, and displacements from the previous increments. An iteration sequence is followed until convergence is achieved. The convergence criterion is that the computed stresses match the initial stresses used to compute the elastic parameters. The total stresses are used to evaluate new elastic parameters for the next loading increment.
5. Once convergence is achieved for a particular load construction increment, a new incremental load vector is computed, and the procedure outlined in steps 2 through 4 is again followed. This method of analysis is called the incremental loading method (or equivalent linear method) and is very common to most soil mechanics finite element analysis programs. The accuracy of the solution is dependent on the assumptions used to derive the stiffness matrix (including the mathematical representation of soil stress-strain response), the size of the loading increment, and many other factors.

The Utah State University research program included the development of a model and its calibration by comparing FEA results with actual physical test data. This FEA research has aided in the enhancement of the computer code. These enhancements have resulted in abilities to better model the actual conditions and predict actual responses.

The computer code PIPE

The computer program PIPE includes soil, beam, bar, and interface elements and nodal links. The program is structured for a computer that has limited available core storage and thus uses disk storage to store most of the data in up to 16 separate files. For example, the global stiffness matrix, incremental load vector, and displacement vector are each stored in separate files. The structure of the program is such that the individual arrays that are stored in separate files are brought into memory as they are needed in the analysis. Although this may cause the total elapsed time for a particular run to increase due to time needed to retrieve the information on the disk files, the structure of the program makes it easy to adapt for use on microcomputers, which have a limited core storage.

Soil model. The soil model that is used is commonly called the *Duncan soil model.* This soil model assumes that the stress-strain properties of soil can be modeled using a hyperbolic relationship. Figure 3.38 shows a typical nonlinear stress-strain curve and the hyperbolic transforma-

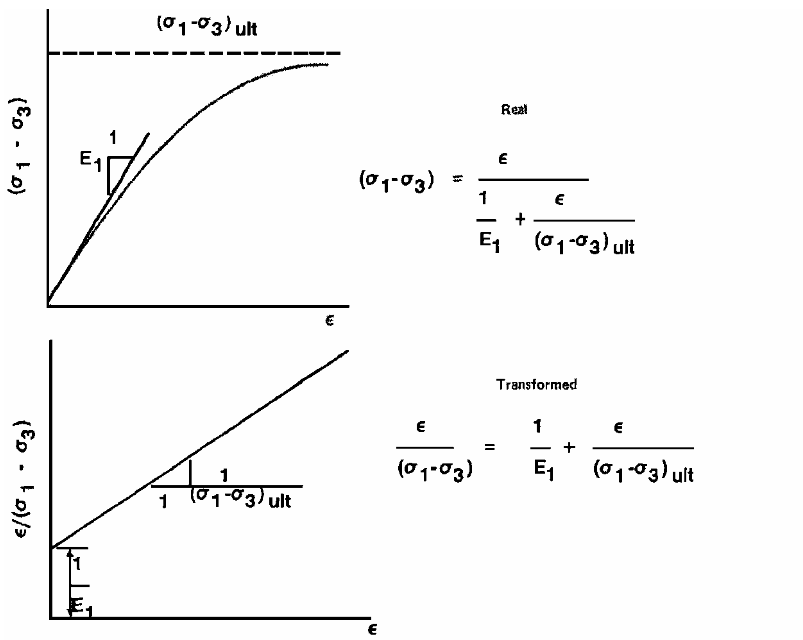

Figure 3.38 Hyperbolic presentation of a stress-strain curve. (*After Duncan et al.*[5])

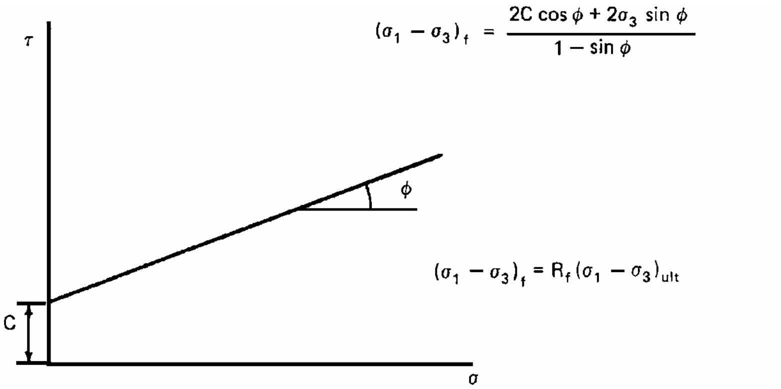

Figure 3.39 Variation of strength with confining pressure. (*After Duncan et al.*[5])

tion that is used. The value of the initial tangent modulus E_t is a function of the confining pressure. Also, the change in the tangent modulus that occurs as strain increases is shown. For a given constant value of confining pressure, the value of the elastic modulus is a function of the percent of mobilized strength of the soil, or the stress level. As the stress level approaches unity (100 percent of the available strength is mobilized), the value of the modulus of elasticity approaches zero.

The Mohr-Coulomb strength theory of soil indicates that the strength of the soil is also dependent on the confining pressure (see Fig. 3.39). Figure 3.40 shows the logarithmic relationship between the initial tangent modulus and confining pressure. The Duncan soil model combines the variation of initial tangent modulus with confining pressure and the variation of elasticity with stress level to evaluate the tangent modulus of elasticity at any given stress condition. The equation that is used to evaluate the modulus of elasticity as a function of confining pressure strength is

$$E_t = \left[1 - \frac{R_f(\sigma_1 - \sigma_3)(1 - \sin\phi)}{2C\cos\phi + 2\sigma_3\sin\phi}\right] KP_a\left(\frac{\sigma_3}{P_a}\right)^n$$

where E_t = tangent elastic modulus
P_a = atmospheric pressure used for dimensional purposes
K = an elastic modulus constant
n = elastic modulus exponent
σ_1 = major principal stress
σ_3 = minor principal stress (confining pressure)
R_f = failure ratio

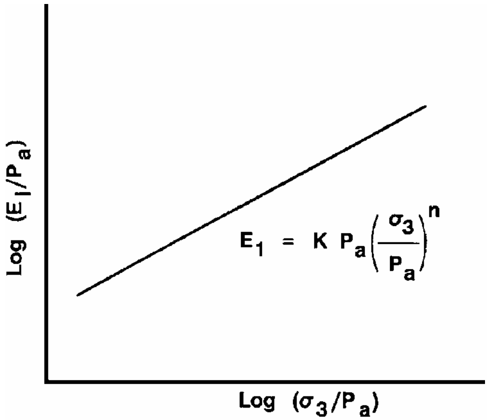

Figure 3.40 Variation of initial tangent modulus with confining pressure. (*After Duncan et al.*[5])

Modifications to the Duncan soil model as presented in Duncan et al.[5] use a hyperbolic model for the bulk modulus. The hyperbolic relationship for the bulk modulus is similar to the initial elastic modulus relationship where the bulk modulus is exponentially related to the confining pressure. Figure 3.41 shows the model of the variation of bulk modulus with confining pressure. This particular soil model does not allow for dilatancy of the soil during straining. The equation that is used to relate the bulk modulus to confining pressure is

$$B = K_b P_a \left(\frac{\sigma_3}{P_a}\right)^m$$

where B = bulk modulus
K_b = bulk modulus constant
m = bulk modulus exponent

The computer code uses the two equations given above to evaluate elasticity parameters that are required in the stiffness matrix. Poisson's ratio and the shear modulus are calculated by the computer using classical theory of elasticity. Limitations are put on the magnitudes of Poisson's ratio in order to remain within the allowable limits of the theory of elasticity. If Poisson's ratio is computed to be more than 0.495, it defaults to 0.495. Likewise, if it is computed to be less than 0.0, it again defaults to its lower limit, 0.0.

Shear failure is also tested by evaluating the stress level before the modulus of elasticity is computed. If the stress level is computed to be more than 0.95 of ultimate, the modulus of elasticity is computed

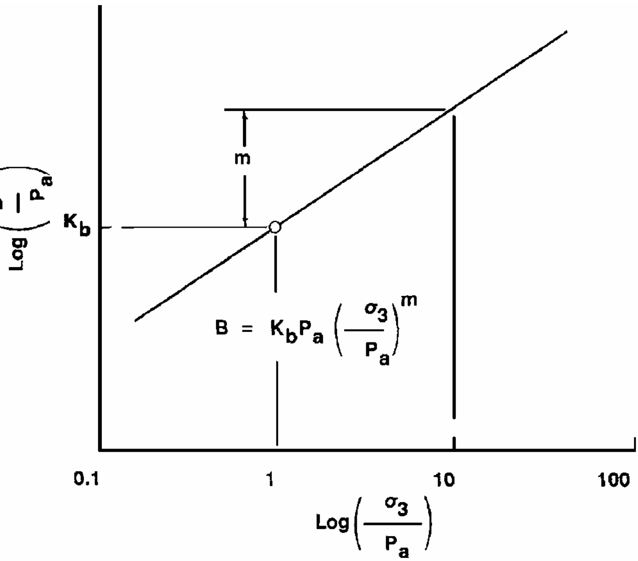

Figure 3.41 Variation of bulk modulus with confining pressure. (*After Duncan et al.*[5])

based on a stress level of 0.95. This results in a low modulus of elasticity. The bulk modulus is unaffected, thus modeling a high resistance to volumetric compression in shear. A test is also performed to evaluate if tension failure has occurred when computing the elastic parameters. If the confining pressure is negative, then the soil element is in tension failure. The elastic parameters are then set to very small values, thus simulating a tension condition. The bulk modulus is set to $0.01B_i$, where B_i is the initial bulk modulus. Poisson's ratio is set to 0.495, and the shear modulus is set to $0.0001B_i$. These constraints appear to be a reasonable approach to modeling soil under shear or tension conditions. The resulting output has been set up to identify the failed elements as the analysis progresses through the incremental loading.

Construction of the stiffness matrix. The stiffness matrix is composed of several parts. In the isoparametric soil elements that are used, the stiffness matrix is recomputed at every iteration. One component is a constitutive matrix relating stress to strain through the elasticity parameters. Another component relates element strains to nodal displacements through the strain-displacement matrix. This matrix is computed based on element types, shape functions, and nodal coordinates. It is not within the scope of this book to derive the above-mentioned relationships. The intent is merely to describe how the global stiffness matrix is computed during the analysis.

Beam, bar, and soil elements have their own particular stiffness matrices. A beam element is a three-force element, and a bar is a two-force element. Both beam and bar elements are called one-dimensional elements. For these elements, the strain-displacement matrix is derived based on the appropriate shape functions and their cross-sectional area, length, and angle of inclination of the element. A soil element is a two-dimensional element. It does not transmit moment stresses. The strain-displacement matrix is derived using the x and y coordinates of each node that comprise the element and the shape functions that are used to describe the deformation characteristics of the soil elements.

Small-displacement theory. The individual stiffness matrices are computed and stored on separate disk files. Beam and bar stiffnesses are computed only once, since their elastic properties are not strain-dependent, their shape function matrix is a definite integral, and it is assumed that the nodal coordinates do not change appreciably during the analysis (small-displacement theory). Since the soil elements are isoparametric elements, a numerical integration scheme is used to evaluate the strain-displacement matrix at each iteration; however, the nodal coordinates used are the initial coordinates since small-displacement theory is used. The elastic portion of the soil stiffness matrix is also recomputed during each iteration since soil elasticity is strain-dependent. During an individual iteration, the elastic matrix is evaluated for the soil elements and is combined with the solution of the strain-displacement matrix during the numerical integration. Once the stiffness matrix for the soil elements has been computed, an overall global stiffness matrix is formed by combining stiffness entries from adjacent elements having common nodes. A solution procedure is then followed, as discussed previously, where the nodal displacements are evaluated based on the incremental load vector and where the incremental load vector is the nodal force vector due to construction loads or external loads.

Large-displacement theory. The derivation of the global stiffness matrix is based on small displacement. However, due to the convenient structuring of the computer code that allows storing individual components of the stiffness matrix into separate disk files, modifications have been made to the code to accommodate large-displacement theory.

Execution of PIPE requires the user to prepare a data file that contains all the mesh information and material properties. The data that

TABLE 3.10 Summary of Required Soil Properties for the Hyperbolic Soil Model

Parameter	Name	Function
K, K_{ur}	Modulus number	Relate E_i and E_{ur} to σ_3
n	Modulus exponent	
c	Cohesion intercept	Relate $(\sigma_1 - \sigma_3)_f$ to σ_3
ϕ, $\Delta\phi$	Friction angle parameters	
R_f	Failure ratio	Relate $(\sigma_1 - \sigma_3)_{\text{ult}}$ to $(\sigma_1 - \sigma_3)_f$
K_b	Bulk modulus number	Value of B/P_a at $\sigma_3 = P_a$
m	Bulk modulus exponent	Change in B/P_a for 10-fold increase in σ_3

SOURCE: After Duncan et al.[5]

are required in the input file include nodal coordinates, element data, structural material and properties, soil material properties (Table 3.10 lists the parameters required for the soil model), construction sequence information, preexisting element stresses, strains, displacements, and external loading information. The data on the input file must be prepared according to specific formats given in the user's manual.

Preexisting stresses. A convenient feature of PIPE is the specification of preexisting elements. These elements may be soil, structure, or interface elements. The preexisting elements are elements already in place before any construction layers or external loading forces are analyzed. The preexisting elements must have initial stresses specified. Preexisting strains may also be input. For the nodes that are contained in the preexisting elements, any preexisting displacements may also be input. Structural forces may be input for any preexisting structural elements that are in place. Preexisting stresses in the interface elements can also be specified. The *preexisting stress* concept is very convenient when one is performing a series of analyses. The use of preexisting stresses, strains, and displacements essentially defines the stress condition for the preexisting elements. Construction sequences, therefore, need only be modeled once for a given mesh and soil configuration. The preexisting stresses resulting from that construction simulation can be input for the entire mesh, and the subsequent analyses can be performed by adding only combinations of external loads to the mesh. This can save on computer time if the user intends to analyze the mesh for different loading schemes without repeating the construction sequences.

External loads. External loads can be input as either concentrated loads or uniform loads. Each loading sequence must have the number of concentrated and uniform loads to be used. Concentrated loads are specified by denoting the node number that will receive the load and the x and y components of the point load. Uniform loads are specified for each element that will receive them. The two nodes of an element with a uniform load are specified along with nodal pressures. The magnitude of the nodal pressure is the acting uniform load. Trapezoidal loading can then be modeled by specifying different magnitudes of the uniform load at each node.

PIPE output. The results of the analysis of PIPE are contained on a data file specified by the user. The results contain all the input information. Element and node information, material properties, construction and load sequencing, preexisting element information, and initial stresses used for estimating the initial elastic parameters are listed. For each load construction increment, the user has an option concerning the amount of information that will be contained on the output. If the user does not specify that the results will be printed, the output indicates only the load or construction increment number and the nodal forces that were used in the load vector. If the user specifies that the results are to be printed, the output contains all the information for the nodal load vector, nodal displacements, structural response, soil element strains, and soil element stresses. Nodal displacements include the total displacements for the x, y, and rotation components and the incremental displacements and rotations for that particular increment.

The structural responses that are listed include the moment, shear, and thrust for each node of each structural member. The listing contains the incremental structural forces and the total structural forces from the accumulated incremental forces.

The soil element strain information includes the soil element strains in x and y directions and the shear strain. Element elastic moduli including elastic modulus, Poisson's ratio, shear modulus, and bulk modulus are also listed for each element. In addition, the principal strains for each element are enumerated.

Soil element stresses that are printed include the horizontal and vertical stresses, shear stresses, and principal stresses. The angle of orientation of the origin of planes with respect to the principal plane, the ratio of major to minor principal stress, and stress levels are also printed out for each element. The stress levels that are printed out indicate the stress condition of each element. If the stress level is greater than 1.0, the element has undergone a local shear failure, and the elastic parameters used were based on a stress level of 0.95. If the stress level is between 0.0 and 1.0, the element has not undergone either tension or shear failure, and the elasticity parameters that were computed were based on the indicated stress level. If the stress level is listed to be 1.0, the element has undergone a tension failure. The element elasticity parameters that were used for this condition were, as indicated in a previous section, very small to allow for the displacements that would occur for a soil element in tension.

Enhancements included in PIPE

The program PIPE is specifically designed for flexible buried pipe analysis, but can be used for rigid pipe analysis. Many of the changes have improved the cosmetics of the output and have improved the analysis of the pipe response without additional calculations. The changes to the code that are discussed involve inclusion of geometric nonlinear analysis; improvement of the soil model to include primary loading, unloading, and reloading; an expanded procedure to increase the number of iterations to convergence; a modified method to improve the stability of the solution on unloading and reloading and improve output for easier analysis of the pipe response and plotting; and subsequent analysis for preexisting stresses.

Geometric nonlinear analysis. Most finite element programs have been developed based on small-strain theory. In small-strain theory, it is assumed that during the FEA analysis, the resulting element strains and nodal displacements are too small to justify reevaluation of the stiffness matrix components that were derived based on the nodal coordinates. The stiffness matrix component that relies on the nodal coordinates is the strain-displacement matrix that is derived from the shape-function matrix. The isoparametric element that is used is one in which the shape-function matrix is evaluated at every iteration of the analysis by a numerical integration scheme. Its evaluation is partly based on the x and y coordinates of the element's nodes that define the size and shape of the element.

The strain-displacement matrix, as previously defined, relates the strains that occur in each element based on the displacements of each of the element nodes. In the bilinear element, the shape functions are linear, which results in constant magnitude of strain across each element. However, the magnitudes of strain vary from element to element. Thus, one could visualize a three-dimensional surface showing the x, y, or shear strain across each element and having discontinuous magnitudes of the element boundaries. Use of higher-order shape functions would result in a three-dimensional surface with a higher degree of continuity at the boundaries for each increase in degree of the shape function.

In the incremental loading procedure, the nodal coordinates are established at the initial execution of the program. Construction is modeled by adding rows of elements and solving for nodal displacements due to the weights of the newly added elements. However, as the construction sequence is followed, the displaced nodes are not recognized in the stiffness matrix. The assumption of small-strain theory has been investigated in other works and has been shown to provide acceptable results, especially in view of the other inaccuracies in the analysis.

The finite element analysis, which does evaluate the stiffness matrix based on deformed nodal coordinates, is defined as a geometric nonlinear analysis. Thus, one which includes both nonlinear stress-strain properties and large-displacement theory performs material and geometric nonlinear analysis.

There has been some concern that the small-strain theory that has been used in the FEA of flexible pipes was inducing some inaccuracies in the results. The addition of the geometric nonlinear analysis has been included by modifying the nodal coordinates of each node at the end of each loading increment. The elemental stiffness matrices of all elements need to be reevaluated at every loading increment due to the changing nodal coordinates. The stiffness matrices of the structural elements are developed partly on the basis of the element length and its inclination. Thus, the structural element stiffness matrix components are reevaluated based on the nodal deformations. Since the soil stiffness matrices are reevaluated at each iteration due to changing material elastic properties, an additional step to reevaluate the strain-displacement matrix (using deformed coordinates) is necessary.

The geometric nonlinear analysis has been used to help determine initial deflections by means of compaction simulation. Also, modifications have given the program the ability to model internal pressure loads and rerounding effects with incremental loading.

Enhanced soil model. The Duncan soil model, as described in a previous section, was developed to model deformation characteristics of soil as the confining pressure of the soil increases. Duncan et al.[5] gave a brief account of the behavior of soil on unloading and reloading. The Duncan soil model could accommodate unloading and reloading by identifying the elastic modulus constant K (defined previously) as the unloading and reloading modulus. A typical stress-strain curve of soil which has undergone primary loading, unloading, and reloading is shown on Fig. 3.42. It can be seen that the soil does not unload to a zero strain as the stress decreases, and that the unloading tangent modulus of elasticity (slope of the unloading stress-strain curve) is much higher than the slope of the primary loading curve. Duncan et al.[5] indicated that the unloading modulus is independent of stress level. Thus, the slope of the unloading stress-strain curve will not change if unloading is performed at any point on the primary stress-strain

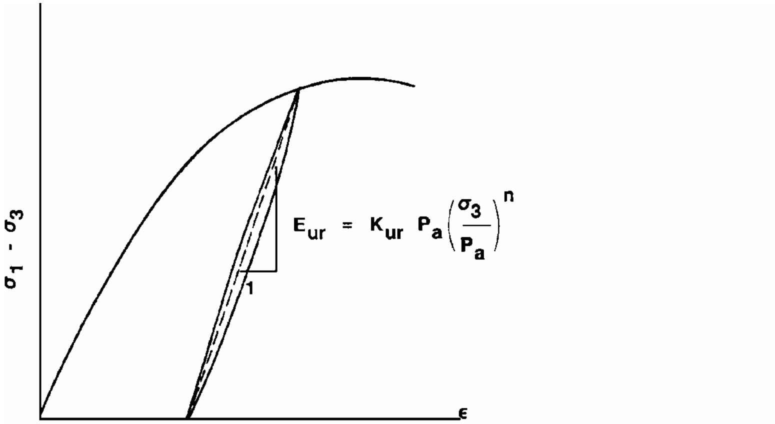

Figure 3.42 Unloading-reloading modulus. (*After Duncan et al.*[5])

curve. They also indicate that the unloading modulus is dependent only on confining pressure and that the bulk modulus is not a function of the stress history of the soil.

The equation that relates the unloading-reloading modulus to other soil properties is

$$E_{ur} = K_{ur} P_a \left(\frac{\sigma_3}{P_a}\right)^n$$

where K_{ur} is the unloading-reloading constant and E_{ur} is the unloading-reloading modulus.

In the original Duncan soil model, if one wanted to use the unloading modulus, the elastic modulus constant that was used for the soil parameters was the unloading constant K_{ur}. There was no mechanism to evaluate the stress history of the soil elements and determine the appropriate modulus if unloading was detected. Also, it was not possible to change the soil elasticity parameters during the analysis in order to simulate loading and unloading all within a single analysis. Additionally, it has been noted that some soil elements would not respond to unloading when a given external loading pattern causes a decrease in stress.

Determining the maximum stress. The most desirable condition is to provide a means of monitoring the stress history of each soil element and to use an unloading modulus when the soil stresses are detected to be less than a maximum previous stress. An improved soil model was developed which includes both primary loading parameters and unloading-reloading parameters. The stress condition of a soil element is uniquely determined by the values of the maximum and minimum principal stresses. For plane-strain analysis, the intermediate principal stress is assumed to be equal to the minimum principal stress. Several different schemes have been tested to monitor the stress history of each soil element: maximum deviator stress, maximum confining pressure, maximum principal stress, and maximum average stress.

The schemes were investigated in view of Mohr's circle analysis. These investigations show the best variable for testing the stress condition of the soil elements is the average stress (or the center of Mohr's circle). The center of Mohr's circle gives a general indication of the stress condition, dependent on both maximum and minimum principal stresses. If the position of the center of the circle is decreasing, an unloading modulus is in effect. The unloading-reloading modulus is also in effect until the position of the center of the circle exceeds a maximum position indicated by the stress history.

The average principal stress is monitored for each element and compared to its maximum average stress. The soil model uses an unloading modulus if the average stress is less than the maximum. A mechanism is provided to simulate maximum past pressures by inputting values for maximum stresses for each soil element, similar to the preexisting stress concept.

Behavior of other soil parameters. The discussion given by Duncan et al.[5] indicates that the only soil parameter that is a function of stress history is the elastic modulus constant. However, there appears to be an insufficient database to substantiate these remarks. Poisson's ratio ν is computed based on the bulk modulus B and elastic modulus E by

$$\nu = \frac{3B - E}{6B}$$

Duncan's recommendation is that the modulus of elasticity be from 1.2 to 3.0 times greater on unloading than on primary loading depending on the soil density. If the bulk modulus is invariant of stress history, the value of Poisson's ratio will become very small if the modulus of elasticity increases by a factor of 2 or 3. This would indicate that a soil will have very little lateral deformation with changing vertical stress if the soil has seen a stress condition greater than the existing stresses.

The behavior of the soil parameters on primary loading and unloading was investigated using triaxial soil tests at Utah State University. The results of this testing program indicate that the bulk modulus behavior is very unpredictable on loading and reloading. It is difficult to make any definite observations on the behavior of the bulk modulus. However, the elastic modulus exponent, in some cases, is dependent on stress history. Consequently, the soil model has been modified to use both the unloading elastic modulus constant and the unloading elastic modulus exponent.

Magnitude of unloading modulus constant. As mentioned, Duncan et al.[5] recommend that the unloading modulus constant be approximately 1.2 times higher than the primary loading constant for stiff soils and 3.0 times higher for soft soils. These approximate factors appear to work relatively well, in view of the results of the triaxial testing program. In fact, the modulus constant has been as much as 4 times higher on unloading than on primary loading. This leads to the phenomena of small or even negative values of Poisson's ratio.

Iteration procedure. The iteration procedure accommodates the changes in elastic moduli when they occur. The soil elements are monitored to test whether they are on the primary loading curve or on the unloading-reloading curve during the first iteration of the previous loading increment. If the results of the first iteration indicate that the soil element is changing from one curve to another, the element condition is flagged and the second iteration follows the same logic as the first, except that the correct modulus is used to evaluate the elastic parameters based on the stresses from the final iteration of the previous loading increment. The third iteration that follows uses the average stresses to compute new element properties and responses to the current loading increment. It appears that at least three iterations are required if soil unloading-reloading is to be included. However, since the results of the analysis reflect an equilibrium condition, neighboring elements to those that changed their stress condition at the first iteration may not have come to "equilibrium" at the end of the third iteration, particularly if the resulting stresses of the second (or later) iteration indicate that an element should change from one soil model to another. Changing soil models is only permitted on the first iteration. This may cause some difficulties in the strain compatibilities of the solution.

One of the inputs of the data file for PIPE includes a variable for the desired number of iterations. All analyses that have been subsequently performed using the soil unloading-reloading model have used four iterations. A sensitivity study has been performed to evaluate the number of iterations to be used. It appears that four iterations are the optimum when unloading-reloading is included.

PIPE output. The goal was to make the program more user-friendly with respect to easier analysis of the PIPE response. The elimination

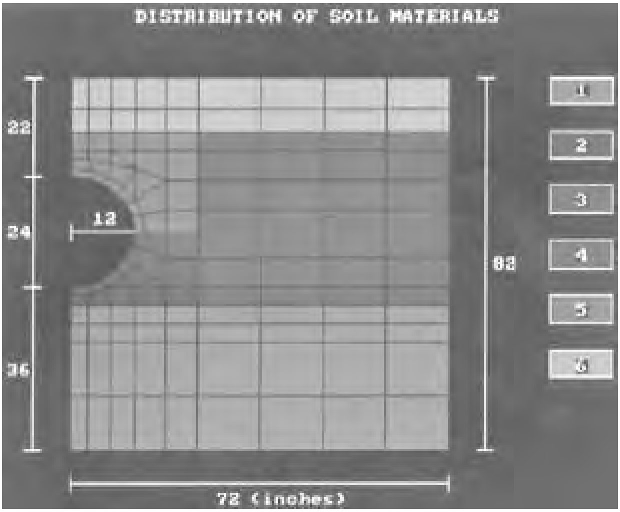

Figure 3.43 Photograph of a PC monitor display showing various soil types and/or compactions used in an FEA model.

of unnecessary output, the preparation of results for plotting, and the structuring of data files so that calculated stresses can be treated as preexisting stresses for a subsequent analysis are program enhancements that have been made. Also, computer graphics have been incorporated to help visualize the modeling process. Figures 3.43 through 3.46 are computer-generated displays produced by PIPE5.

Printed results. The output of SSTIPN, as discussed previously, consists of a single output file which contains all the results of a given analysis. So that the user can examine the results, the voluminous output must be printed, and the results of each loading increment that was printed must be examined. This procedure can be quite cumbersome, especially in production runs where only a few variables are needed to present the results. Additionally, the structural response is printed in terms of nodal forces (shears, moments, and thrusts) for each structural element. For example, the design criteria for the FRP pipe are pipe-wall strains, and the user must compute strains based on the nodal forces. The output of PIPE is such that computed strains due to thrust and bending are printed. Ring deflections are also printed in terms of percent vertical and percent horizontal deflection for the pipe. Thus, the printed output can easily be examined to evaluate the pipe response. The user may still wish to examine the other parameters, which are still included.

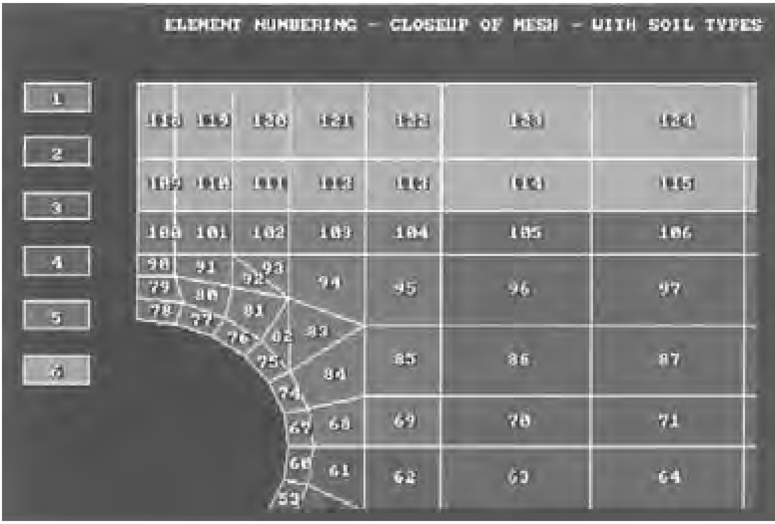

Figure 3.44 Printed output showing element numbering scheme of upper part of mesh in an FEA model.

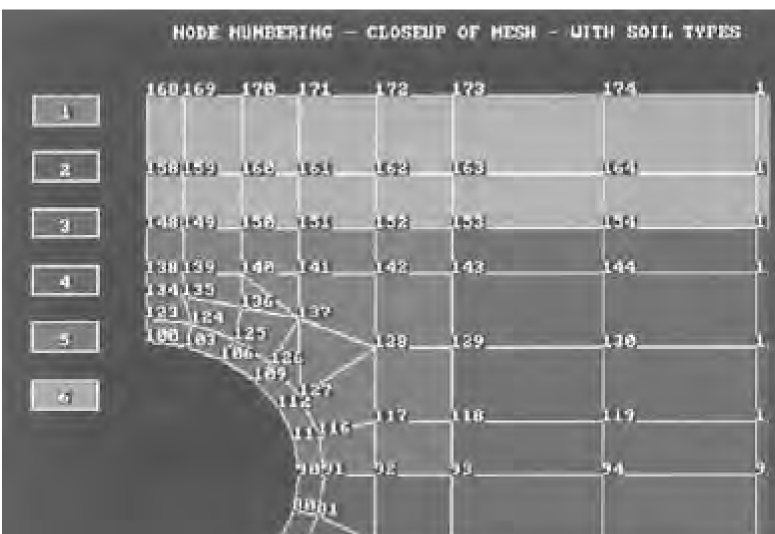

Figure 3.45 Printed output showing node numbering scheme of upper part of mesh in an FEA model.

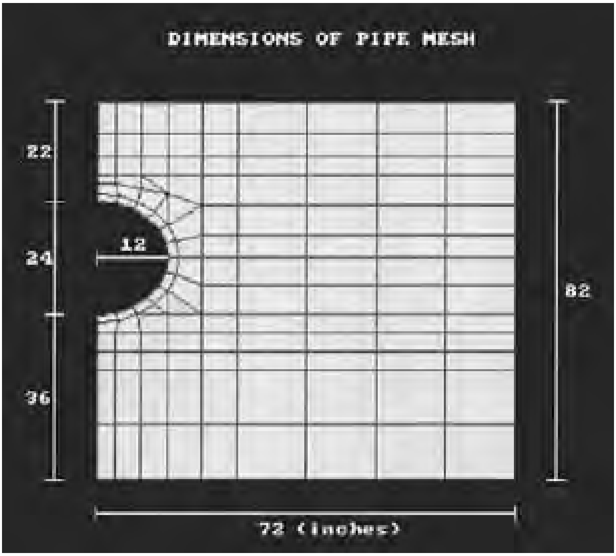

Figure 3.46 Photograph of a PC monitor display of the FEA mesh.

Also incorporated is a data check sequence where the element information is processed to test if the data have been input correctly. Element areas are computed based on the element nodes. If the nodes are not input in a counterclockwise manner, the element area is computed as a negative area, and the user can then identify input errors on the element data more easily. Soil elements which have been evaluated on the unloading model are identified by their stress level. Unloading and rebound elements have a negative stress level.

Additional output. There are several additional output files that have been included in PIPE to accommodate data processing. For each loading increment, the user has the option of having the results printed on separate files. The option includes having the stresses, strains, and displacements printed to separate output files. This allows the user to use the stresses, strains, and displacements as preexisting stresses for any subsequent runs.

In addition to having an option to print particular results to separate output files, an option is included to have the ring deflections separately printed to an output file. This option exists for every load increment. Combinations of ring deflection files and/or stress, strain, displacement files are included. Results of a given run can be easily viewed by examining the load-deflection curve; therefore, viewing the ring deflection file facilitates a much faster review of the results.

Plotting. Several output files have been created that are compatible with the plotting routines. The mesh information is stored on a separate file that has a compatible format with mesh plotting routines. Pipe strains are also printed out to a file that is used to plot the strains versus position of the pipe. The ring deflection file previously described is also used to plot the load-deflection curve for a given analysis. Thus, the results of a given run can be analyzed through the output files and presented graphically through plotting files that are used by the postprocessor plotting programs.

Example applications

Some results from applications of the FEA program PIPE are included here and are compared with measured responses from actual tests conducted in soil load cells at Utah State University (see Figs. 3.47 and 3.48). The comparisons that are shown are for pipe with a 10 lb/in^2 pipe stiffness. Test cell soil compaction conditions that are included for comparisons are

1. Ninety percent relative compaction with homogeneous conditions
2. Ninety percent relative compaction with poor haunches
3. Eighty percent relative compaction with homogeneous conditions

Soil parameters used in the FEA program are listed in Table 3.11.

In the buried pipe tests, every attempt was made to achieve homogeneous conditions when called for. However, the flexible nature of the pipe does not always allow for a high uniform compaction in the haunches and around the shoulders and crown of the pipe. Therefore, homogeneous conditions that are attempted in the test cell or for that matter in an actual installation will result in some variation in density. Of course, the FEA program can perfectly model the homogeneous soil condition. When a test pipe was installed in the soil box with poor haunches, no attempt was made to compact the soil in the haunch area. Finite element modeling of homogeneous and poor haunch conditions is well defined because numerically all soil elements in each homogeneous condition have identical stress-strain properties.

Comparisons of the FEA results with those of the soil box tests can be made using pipe-strain and load-deflection results. For the pipe-strain plots, tension bending strains on the outside fibers are considered positive. Thrust strains around the circumference of the pipe are also included. The load-deflection plots show the vertical and horizon-

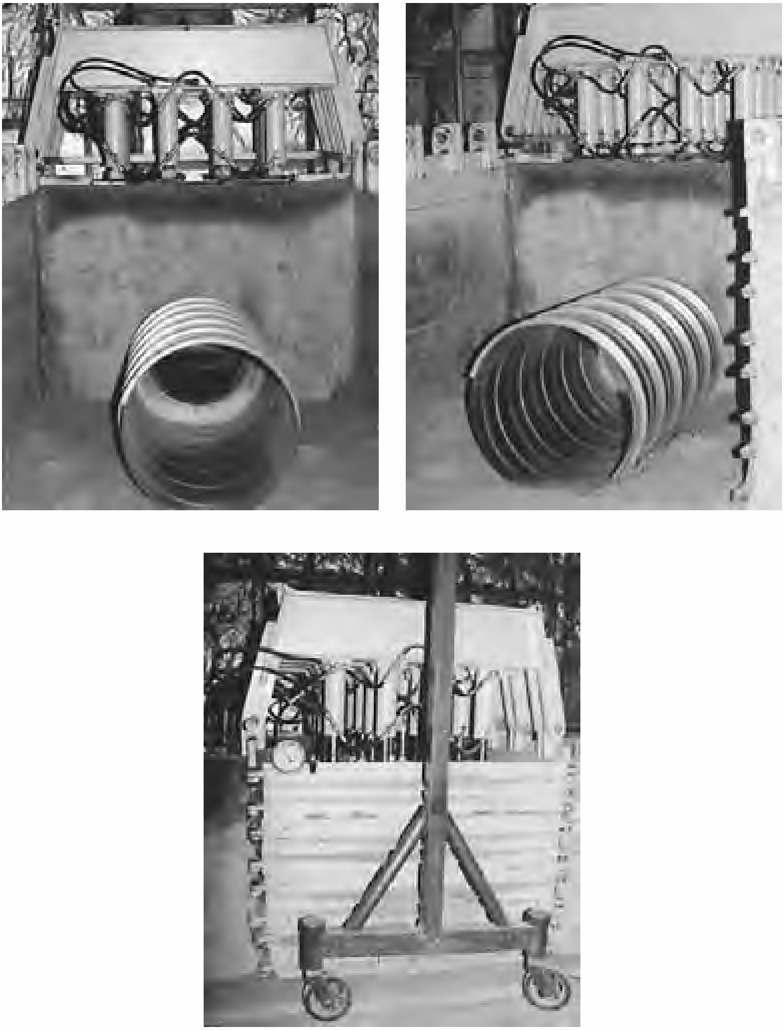

Figure 3.47 Small test cell at Utah State University.

tal ring deflections in terms of surcharge pressure. The zero point for the load-deflection plots for the load cell tests is referenced to the deformed state of the pipe after compaction. In the FEA plots, the zero reference for ring deflection is based on the initial undeformed condition. Thus, in the load-deflection illustrations, the zero point of deflection should be considered when direct comparisons are made between

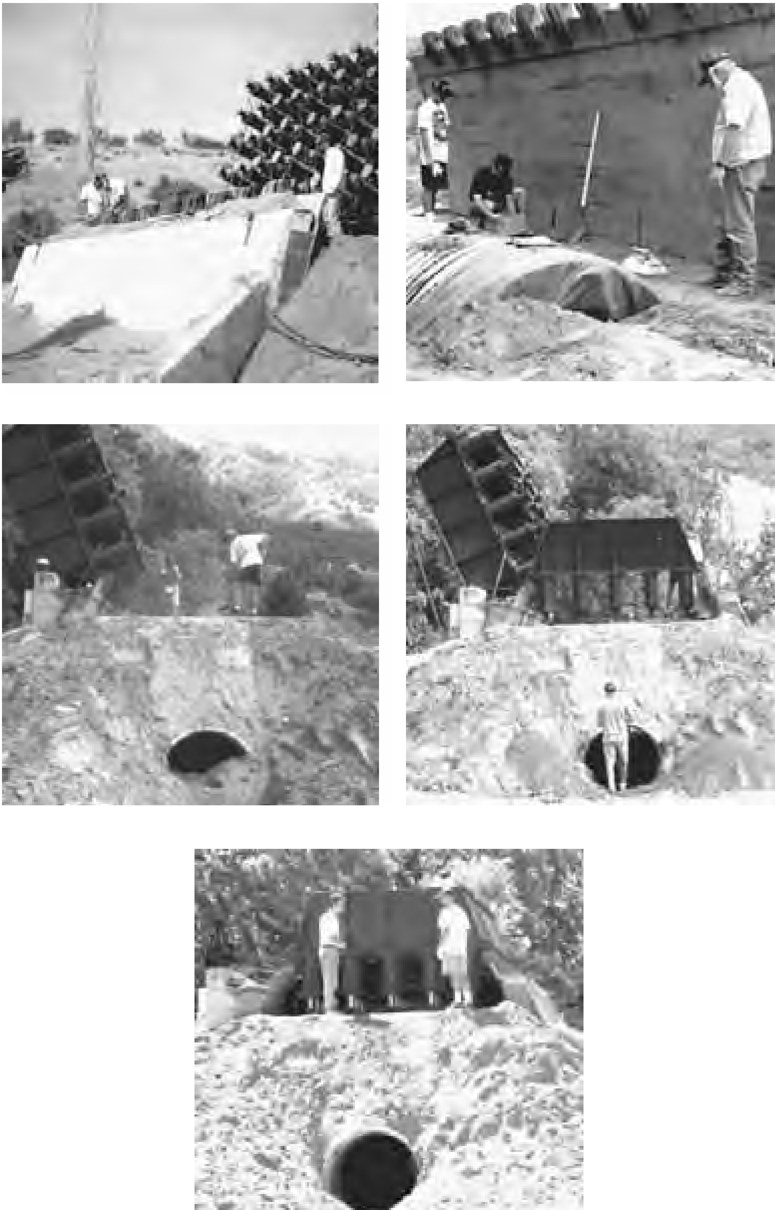

Figure 3.48 Large test cell at Utah State University.

TABLE 3.11 Soil Parameters for Silty Sand

Relative compaction standard, percent	Density, lb/in^3	ϕ, deg	Δ, deg	c, lb/in^2	K	n	R_f	K_b	m	K_0	K_{ur}	n_{ur}
90	0.065	30	0.	8.3	480	0.44	0.75	80	0.38	0.48	720	0.44
80	0.058	30	0.	3.5	350	0.28	0.89	15	0.40	0.37	525	0.28

NOTE: ϕ, friction angle; Δ, friction angle reduction for 10-fold increase in lateral pressure; C, cohesion intercept; K, elastic modulus constant; n, elastic modulus exponent; R_f, failure ratio; K_b, bulk modulus constant; m, bulk modulus exponent; K_0, earth pressure coefficient; K_{ur}, unload-reload modulus constant; n_{ur}, unload-reload modulus exponent.

results from the FEA and results from the soil test cell. Plots of pipe-wall strain for the soil test cell and for the FEA results are both referenced from the same unstrained condition. These plots show bending and thrust strain versus position on the pipe. The 0° position on the pipe is at the invert, the 90° position is at the spring line, and the 180° position is at the crown, as shown in Fig. 3.37. The values for pipe strain from 180° to 360° are symmetric with 0° to 180° for the FEA because the FEA mesh presented here used an axis of symmetry for the analysis of symmetric bedding.

Homogeneous installation at 90 percent relative compaction. Figures 3.49 and 3.50 show the soil box test results for a 10 lb/in^2 pipe installed with homogeneous compaction at 90 percent of standard Proctor maximum dry density. Physical pipe data are as follows:

	Curve	
Parameter	*A*	*B*
Stiffness, lb/in^2	10	10
Thickness, in	0.285	0.300
Surface pressure, lb/in^2	48.9	50.0
Vertical deflection, percent	5.53	4.82
Horizontal deflection, percent	3.74	2.52

Figure 3.49 shows the load-deflection curve, and Fig. 3.50 shows pipe strain versus position on the pipe for a surcharge pressure of 48.9 lb/in^2. Features of these results to note are the shape of the load-deflection curve, relative magnitudes between the horizontal and vertical ring deflections, and shape and magnitudes of bending and thrust strain. This condition was modeled with FEA in several ways. These illustrations also show the results from the FEA for a homogeneous 90 percent relative compaction with no compaction simulation. There is a marked similarity between the FEA and test data. The pipe-strain plot in Fig. 3.50 indicates that the magnitudes of pipe strain at a surface

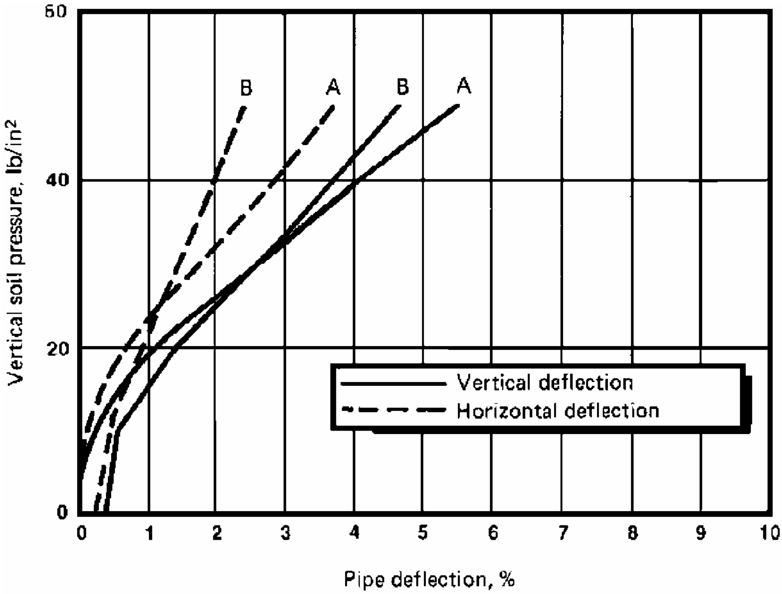

Figure 3.49 Vertical soil pressure versus pipe deflection. (*A*) Soil test cell data, 90 percent relative compaction; (*B*) FEA, no compaction simulation.

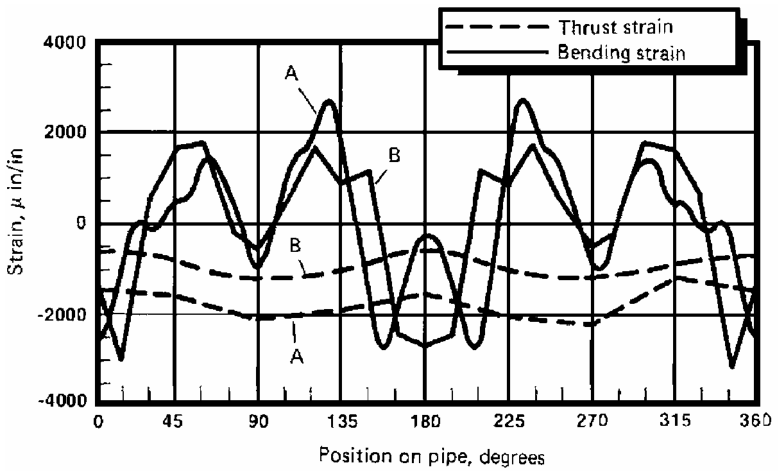

Figure 3.50 Pipe strain as function of circumferential position, conditions as in Fig. 3.49.

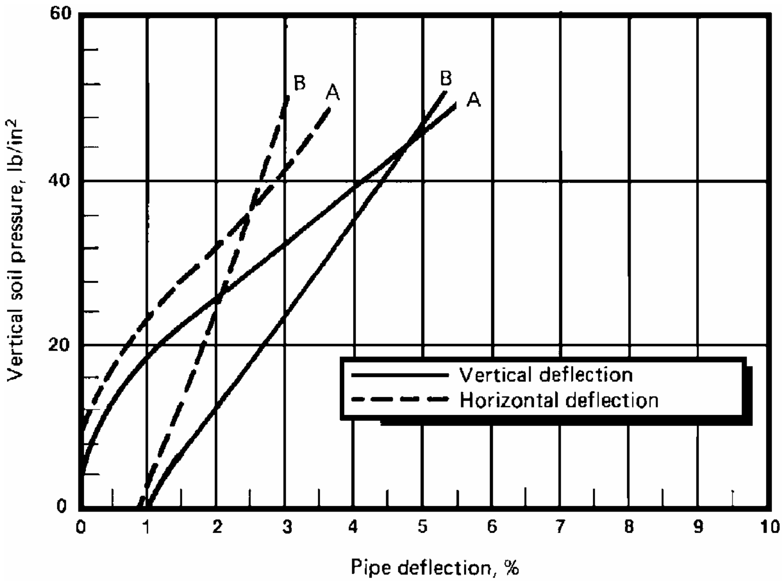

Figure 3.51 Vertical soil pressure versus pipe deflection. (*A*) Soil box data 90 percent relative compaction, silty sand; (*B*) FEA with compaction simulation.

pressure of 50.0 lb/in^2 are fairly comparable. The ring deflections determined from experiment and for FEA also compare quite closely.

Figures 3.51 and 3.52 show the results of the FEA for the homogeneous dense condition including compaction simulation during construction. The physical pipe data are as follows:

Parameter	Curve *A*	Curve *B*
Stiffness, lb/in^2	10	10
Thickness, in	0.285	0.300
Surface pressure, lb/in^2	48.9	50.0
Vertical deflection, percent	5.53	5.42
Horizontal deflection, percent	3.74	3.14

The compaction simulation load-deflection curve in Fig. 3.51 lost some of the initial steepness compared with Fig. 3.49. However, the difference between vertical and horizontal deflection is maintained. Deflections of Fig. 3.51 are similar in magnitude to those of Fig. 3.49.

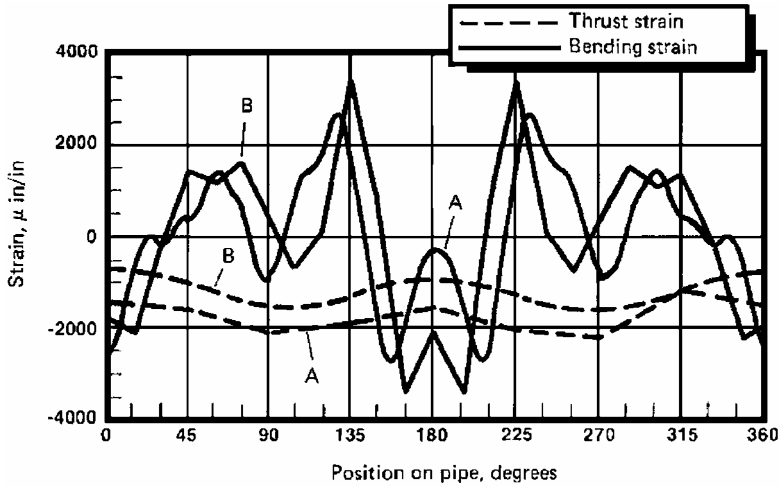

Figure 3.52 Pipe strain as function of circumferential position, conditions as in Fig. 3.51.

Figure 3.52 shows pipe-strain plots for compaction simulation and a surface pressure of 50.0 lb/in^2. A comparison of data in Fig. 3.52 with data in Fig. 3.50 shows that compaction simulation did improve the correlation between FEA and test results. The general shape, maxima, and magnitudes all compare very well.

Additional comparisons that were made with this condition included soft elements in the shoulder areas of the pipe. Because soil placement techniques do not allow compaction directly above the pipe, a completely homogeneous compaction is not obtained in an actual installation.

For a flexible pipe, the soil will be of a lesser density at the shoulders and crown of the pipe. One noticeable result with soft-crown analyses is that generally the pipe strain at the 135° position of the pipe (see Fig. 3.52) increased. This is due to the lowered stiffness of the soil in the shoulders, which allows for more bending deformation in the pipe. Compaction simulation for the soft-crown condition did decrease the bending strains and ring deflections because the soil would respond in the rebound range initially, thus inhibiting deformation at the low-pressure ranges. Because compaction simulation did not include adding loads directly over the pipe at the first construction increment, a soft-crown condition was actually created with the homogeneous case. This is because the soil at the crown was uncompacted and did not respond on the stiffer rebound modulus at the lower-pressure ranges as did the surrounding soil elements that had received the compaction loads directly.

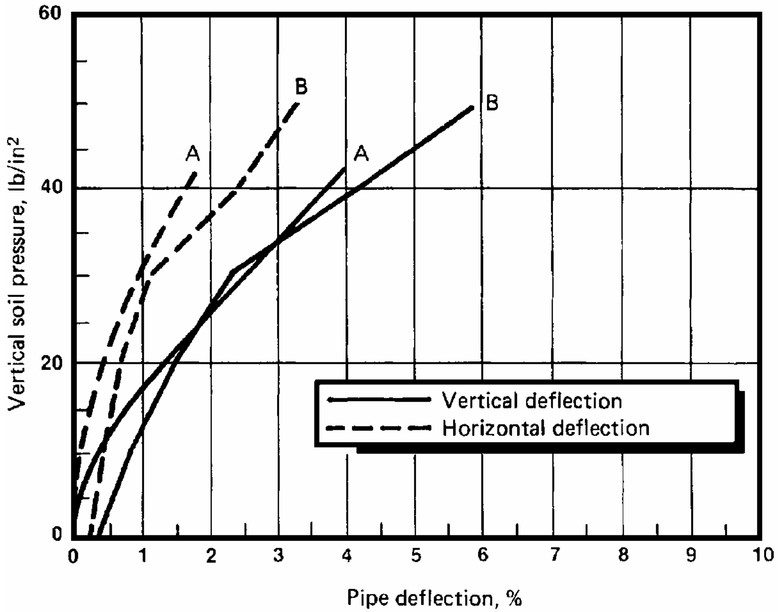

Figure 3.53 Vertical soil pressure versus pipe deflection. (*A*) Soil box data, 90 percent relative compaction, silty sand, and poor haunch support; (*B*) FEA, no compaction simulation, and poor haunch support.

Poor haunch installation at 90 percent relative compaction. Figures 3.53 and 3.54 show the results for the poor haunch installation with a silty sand soil. A poor haunch condition, as used here, occurs where soil is placed in the haunch areas but is not compacted. The physical pipe data are as follows:

Parameter	Curve *A*	Curve *B*
Stiffness, lb/in^2	10	10
Thickness, in	0.285	0.300
Surface pressure, lb/in^2	35.5	30.0
Vertical deflection, percent	3.14	2.21
Horizontal deflection, percent	1.30	1.09

Figure 3.53 shows the load-deflection response, and Fig. 3.54 shows the pipe strain around the pipe for a surface pressure of 35.5 lb/in^2. Again, the initial steepness of the load-deflection curve, the relative

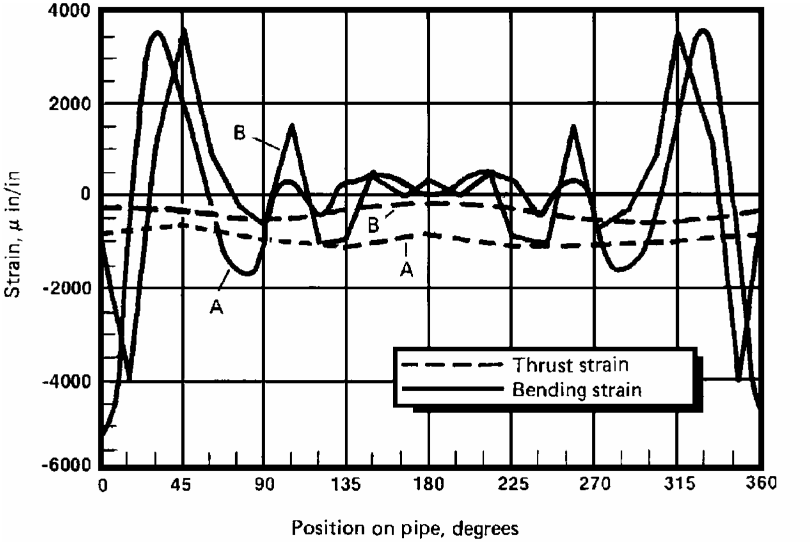

Figure 3.54 Pipe strain as function of circumferential position, conditions as in Fig. 3.53.

magnitudes between the vertical and horizontal deflections, and the shape and magnitude of the strain plots should be noted. The bending strains are higher than before at the 30° to 45° positions of the pipe because of the lack of support in the haunch area. Also, a comparison between the homogeneous installation and the poor haunch installation (Figs. 3.52 and 3.54, respectively) shows noticeable differences in the pipe-strain plots from soil box tests.

Figures 3.52 and 3.54 also show the FEA results for the poor haunch condition without compaction simulation. The load-deflection plots show similar behavior, yet the deformations are larger in the FEA results. The pipe-strain plots show very similar peaks of large strain at the 45° position and low strains from the spring line to crown.

Figures 3.55 and 3.56 show the FEA results for poor haunches with compaction simulation. In the load-deflection plots, the FEA indicates larger deflections. The pipe-strain plots show larger strains in the pipe from the spring line to the crown. However, the strain at the invert of the pipe with compaction simulation compared better with measured results. That is, FEA with compaction simulation seems to give a more accurate prediction of strain at the pipe invert as compared with FEA without compaction simulation. The physical pipe data for Figs. 3.55 and 3.56 are as follows:

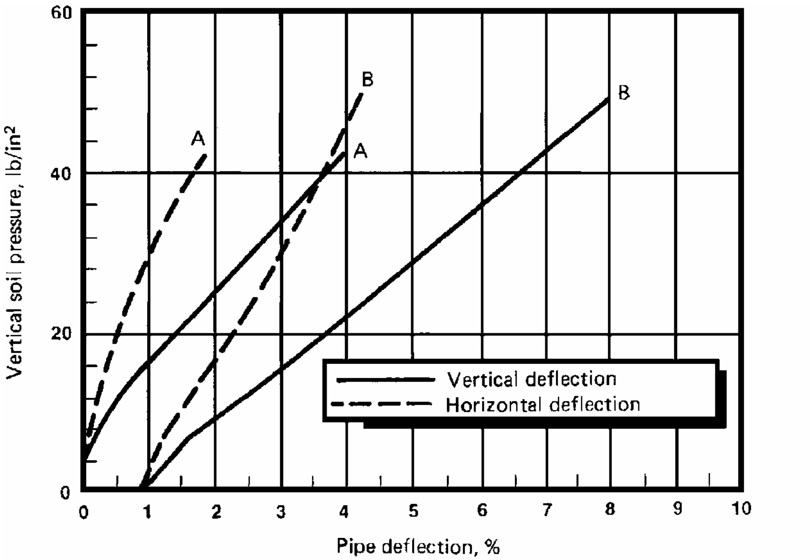

Figure 3.55 Vertical soil pressure versus pipe deflection. (*A*) Soil box data, 90 percent relative compaction, silty sand, and poor haunch support; (*B*) FEA with compaction simulation and poor haunch support.

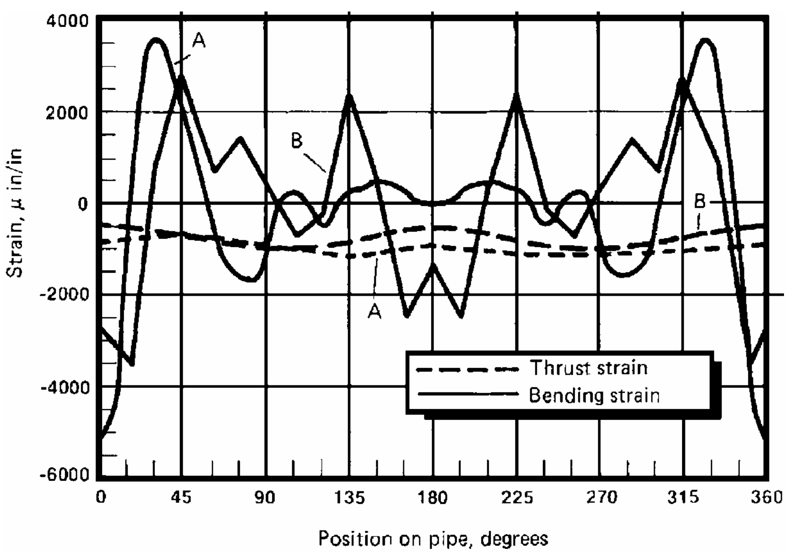

Figure 3.56 Pipe strain as a function of circumferential position, conditions as in Fig. 3.55.

Parameter	Curve A	Curve B
Stiffness, lb/in^2	10	10
Thickness, in	0.285	0.300
Surface pressure, lb/in^2	35.5	30.0
Vertical deflection, percent	3.14	5.14
Horizontal deflection, percent	1.30	2.92

Homogeneous installation with 80 percent relative compaction. Figures 3.57 and 3.58 show the test results for an 80 percent relative compaction homogeneous installation. The physical pipe data are as follows:

Parameter	Curve A	Curve B
Stiffness, lb/in^2	10	10
Thickness, in	0.285	0.300
Surface pressure, lb/in^2	14.6	15.0
Vertical deflection, percent	8.78	3.85
Horizontal deflection, percent	7.87	2.06

The vertical and horizontal deflections are very similar throughout the test, which indicates elliptical deformation as shown in Fig. 3.57. Figures 3.57 and 3.58 also show the results from the FEA for the 80 percent relative compaction homogeneous condition. Although the load-deflection curves show much greater deformation with the loose

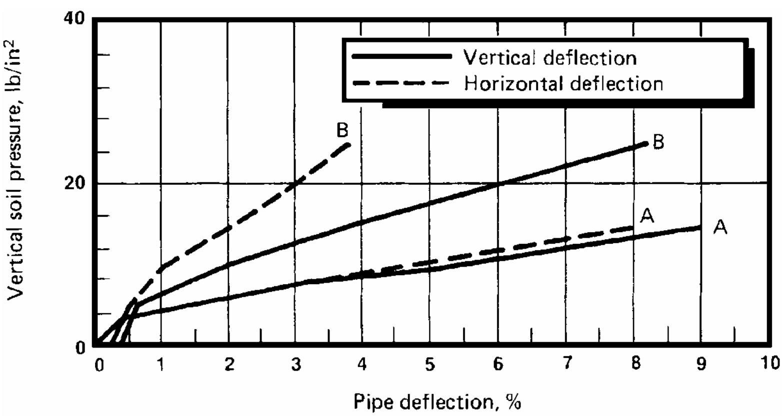

Figure 3.57 Vertical soil pressure versus pipe deflection. (*A*) Soil box data, 80 percent relative compaction; (*B*) FEA, no compaction simulation.

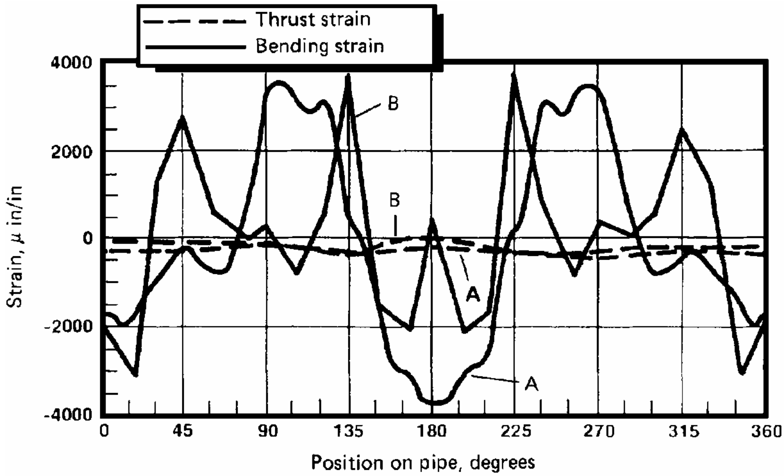

Figure 3.58 Pipe strain as function of circumferential position, conditions as in Fig. 3.57.

material than with the dense material, the actual comparison of soil box tests with FEA tests shows that the FEA does not compare quite as well for loose soil conditions. The pipe-strain plots shown in Fig. 3.58 also indicate a generally poorer correlation. In terms of magnitude of the maximum strain, there is some correlation, but the overall shape of the pipe-strain plot does not match the measured values as well as for the cases with 90 percent density.

Discussion of results. The incorporation of the compaction simulation for comparison of the response of the FRP pipe improved the comparison for the homogeneous condition for most cases that were attempted. For the nonhomogeneous installation conditions, the compaction simulation did not improve the correlation of FEA and test results. It is possible that nonhomogeneous conditions dominate the response, masking the compaction simulation response. This could be due to the nature of the compaction simulation sequence. Had the compaction sequence individually modeled the backfill condition (poor haunch, soft top, and so forth), the results might have improved. For most cases, the compaction simulation does not improve the results enough to justify the additional computational effort required.

The FEA data and experimental data generally correlated better for the dense installation conditions than for the loose conditions. This is probably due to a combination of numerical difficulties with the finite element method and difficulties in obtaining a uniform soil condition for low to medium density in the test cell. Entries in the stiffness matrix become sensitive to the magnitudes of the elastic and bulk modulus parameters at low stiffnesses. To achieve larger deflections, lower values of the bulk modulus parameters are required. This, however, can result in singular matrix warnings, which indicates that entries in the stiffness matrix will not produce reliable results. More work is needed in this area with respect to modeling soil behavior under loose conditions.

The geometric nonlinear analysis (where the formulation of the stiffness matrix accounts for the nodal deflections at each loading increment) does not significantly change the results for installation condition modeling. The inclusion of the geometric nonlinear analysis would generally predict somewhat higher deflections. For example, an analysis that did not include geometric nonlinearities might predict a vertical ring deflection of 4 percent. The same conditions including geometric nonlinearities would predict ring deflections of around 5 percent. However, for the other types of loading conditions (for instance, rerounding), the formulation of the stiffness matrix must reflect the shape of the pipe.

Summary and conclusions

Good correlation of finite element modeling of flexible pipes with test data requires modeling capabilities not readily available in most existing computer programs. Such capabilities include analysis of stress history of the soil elements to determine whether each element is in primary loading or in unloading and reloading, modification of the iteration scheme to better model the soil response when changing from one stress condition to another, and large-deflection theory by modifying nodal coordinates after each load increment. Additionally, postprocessing plotting routines are needed to graphically analyze the pipe response to each loading condition.

The development of these features has allowed for analysis of not only rigid pipe but also flexible pipe with compaction simulation, surcharge pressures, rerounding caused by internal pressurization, and various installation conditions. The results of the analysis of the various installation conditions have shown the effects of shoulder and haunch support on the pipe and suggest that these conditions be considered in pipe and installation design.

The results of this FEA development program at Utah State University have improved the modeling capability of flexible pipe systems. Moreover, an improved understanding of the behavior of the buried flexible pipe has been developed due to the ability to model various installation conditions. The results of the overall study, including the four soil types and various loading conditions, have shown a very good correlation between the FEA results and the measured responses from the physical model tests. This has given strong justification for the use of the finite element method to adequately model various installation conditions, soil materials, loading conditions, pipe sizes, and so forth, without the additional expense of performing extensive physical tests. However, calibration of the FEA model required the results from physical tests. Finite element analysis, along with experiments, has resulted in a better analytical tool for the evaluation of buried pipe performance. This tool is now available and is being used primarily for research and analysis. It is the design tool of the future.

References

1. Asphalt Institute. 1978. *Soils Manual for the Design of Asphalt Pavement Structures.* Manual Series No. 10 (MS-10). College Park, Md.
2. Bishop, R. R. 1981. Time Dependent Performance of Buried PVC Pipe. In *Proceedings of the International Conference on Underground Plastic Pipe,* pp. 202–212. New York: American Society of Civil Engineering Conference.
3. Burns, J. Q., and R. M. Richard. 1964. Attenuation of Stresses for Buried Cylinders. In *Proceedings of the Symposium on Soil Structure Interaction,* pp. 378–392. Tucson: University of Arizona.
4. Chambers, R. E., and F. J. Heger. 1975. *Buried Plastic Pipe for Drainage of Transportation Facilities.* Cambridge, Mass.: Simpson Gumpertz and Heger, Inc.
5. Duncan, J. M., P. Byrne, K. S. Wong, and P. Mabry. 1980. Strength, Stress-Strain and Bulk Modulus Parameters for Finite Element Analysis of Stresses and Movements in Soil Masses. Report No. UCB/GT/80-01. Berkeley: University of California Office of Research Services.
6. Dunn, I. S., L. R. Anderson, and F. W. Kiefer. 1980. *Fundamentals of Geotechnical Analysis,* 1st ed. New York: Wiley.
7. Gere, J. M., and W. Weaver. 1980. *Analysis of Framed Structures,* 2d ed. New York: Van Nostrand Reinhold Co.
8. Goddard, J. B. 1996. *An Analysis of Flexible Pipe Using the Burns & Richard Solution* [software]. Columbus, Ohio: Advanced Drainage Systems, Inc.
9. Hartley, J. P., and J. M. Duncan. 1987. *E′* and Its Variations with Depth. *Journal of Transportation Engineering, ASCE* 113(5):538–553.
10. Hild, J. W. 1975. Compacted Fill. In *Foundation Engineering Handbook,* 1st ed. Eds. H. F. Winterkorn and H. Y. Fang. New York: Van Nostrand Reinhold Co.
11. Howard, Amster K. 1977. Modulus of Soil Reaction (*E′*) Values for Buried Flexible Pipe. *Journal of the Geotechnical Engineering Division, ASCE* 103(GT), Proceedings Paper 127000.
12. Howard, A. K. 1996. *Pipeline Installation.* Lakewood, Colo.: Relativity Publishing.
13. Janbu, N. 1963. Soil Compressibility as Determined by Odometer and Triaxial Tests. In *Proceedings of European Conference on Soil Mechanics and Foundation Engineering,* pp. 19–25. Wiesbaden, Germany: Soil Mechanics Foundation.
14. Janson, Lars-Eric. 1981. Plastic Gravity Sewer Pipes Subjected to Constant Strain by Deflection. In *Proceedings of the International Conference on Underground Plastic Pipe,* pp. 104–116. New York: American Society of Civil Engineers.
15. Janson, Lars-Eric, and Jan Molin. 1981. Design and Installation of Underground Plastic Sewer Pipes. In *Proceedings of the International Conference on Underground Plastic Pipe,* pp. 79–88. New York: American Society of Civil Engineers.
16. Jensen, Brent M. 1977. Investigations of Strain Limits Proposed for Use in Designing PVC Pipe Subjected to External Soil Pressure. Master of Science thesis. Logan: Utah State University.

17. Katona, M. G., P. D. Vittes, C. H. Lee, and H. T. Ho. 1981. CANDE-1980: Box Culverts and Soil Models. Springfield, Va.: National Technical Information Service.
18. Katona, M. G., J. B. Forrest, F. J. Odello, and J. R. Allgood. 1976. CANDE—A Modern Approach for the Structural Design and Analysis of Buried Culverts. Report FHWA-RD-77-5. FHWA, U.S. Department of Transportation.
19. Knight, G. K., and A. P. Moser. 1983. The Structural Response of Fiberglass Reinforced Plastic Pipe under Earth Loadings. Logan: Buried Structures Laboratory, Utah State University.
20. Konder, R. L., and J. S. Zelasko. 1963. A Hyperbolic Stress-Strain Formulation of Sands. In *Proceedings of the Second Pan American Conference on Soil Mechanics and Foundation Engineering.* 1:209.
21. Krizek, R. J., R. A. Parmelee, N. J. Kay, and H. A. Elnaggar. 1971. Structural Analysis and Design of Buried Culverts. National Cooperative Highway Research Program Report 116. Washington: National Research Council.
22. Kulhawy, F. H., J. M. Duncan, and H. B. Seed. 1969. Finite Element Analysis of Stresses and Movements in Embankments during Construction. Report No. TE-69-4. Berkeley: Office of Research Services, University of California.
23. Kunz, Walter M. 1982. Mechanical Properties of Filled Poly Vinyl-Chloride. Master's thesis. Logan: Utah State University.
24. Marston, A. 1930. The Theory of External Loads on Closed Conduits in the Light of the Latest Experiments. *Bulletin* 96. Ames: Iowa Engineering Experiment Station.
25. Meyerhof, G. G., and L. D. Baike. 1963. Strength of Steel Culverts Sheets Bearing against Compacted Sand Backfill. *Highway Research Board Proceedings* 30.
26. McGrath, Timothy J. 1998. Replacing *E′* with the Constrained Modulus in Flexible Pipe Design. In *Proceedings of the Pipeline Division Conference.* San Diego: American Society of Civil Engineers.
27. McGrath, T. J., R. E. Chambers, and P. A. Sharff. 1990. Recent Trends in Installation Standards for Plastic Pipe. In *Buried Plastic Pipe Technology ASTM STP 1093,* eds. George S. Buczala and Michael J. Cassady. Philadelphia: American Society for Testing and Materials.
28. Molin, J. 1985. Long Term Deflection of Buried Plastic Sewer Pipes. *Advances in Underground Pipeline Engineering,* pp. 263–277. New York: American Society of Civil Engineers.
29. Moser, A. P. 1990. *Buried Pipe Design.* New York: McGraw-Hill.
30. Moser, A. P. 1974. Can Plastic Sewer Pipe Be Installed with 100% Confidence? Paper presented at the 68th Annual Meeting of the American Society of Sanitation Engineers in New Orleans.
31. Moser, A. P. 1981. Strain as a Design Basis for PVC Pipes? In *Proceedings of the International Conference on Underground Plastic Pipe,* pp. 89–103. New York: American Society of Civil Engineers Conference.
32. Moser, A. P., R. R. Bishop, O. K. Shupe, and D. R. Bair. 1985. Deflection and Strains in Buried FRP Pipe Subjected to Various Installation Conditions. Transportation Research Record 1008. Washington: Transportation Research Board.
33. Moser, A. P., R. K. Watkins, and O. K. Shupe. 1976. Design and Performance of PVC Pipes Subjected to External Soil Pressure. Logan: Buried Structures Laboratory, Utah State University.
34. Nyby, D. W. 1981. Finite Element Analysis of Soil Sheet Pipe Interaction. Ph.D. dissertation. Logan: Department of Civil and Environmental Engineering, Utah State University.
35. Ozawa, Y., and J. M. Duncan. 1973. ISBILD: A Computer Program for Analysis of Static Stresses and Movements in *e*=Embankments. Report no. TE-73-4. Berkeley: Office of Research Services, University of California.
36. Piping Systems Institute. 1980. *Course Notebook.* Logan: Utah State University.
37. Reissner, E. 1959. On Final Bending of Pressurized Tubes. *Journal of Applied Mechanics* (*Transactions of ASME*), pp. 386–392.
38. Selig, E. T. 1988. Soil Parameters for Design of Buried Pipelines. In *Pipeline Infrastructure—Proceedings of the Conference,* pp. 99–116. New York: American Society of Civil Engineers.

39. Selig, E. T. 1990. Soil Properties for Plastic Pipe Installations. *Buried Pipe Technology, ASTM STP 1093,* eds. George S. Buczala and Michael J. Cassady. Philadelphia: American Society for Testing and Materials.
40. Sharp, Kevan, L. R. Anderson, A. P. Moser, and R. R. Bishop. 1985. Finite Element Analysis Applied to the Response of Buried FRP Pipe due to Installation Conditions. Transportation Research Record 1008. Washington: Transportation Research Board.
41. Spangler, M. G., and R. L. Handy. 1982. *Soils Engineering,* 4th ed. New York: Harper & Row.
42. Spangler, M. G. 1941. The Structural Design of Flexible Pipe Culverts. *Bulletin* 153. Ames: Iowa Engineering Experiment Station.
43. Timoshenko, S. P. 1961. *Theory of Elastic Stability,* 2d ed. New York: McGraw-Hill.
44. Timoshenko, S. P. 1968. *Strength of Materials, Part II—Advanced Theory and Problems.* Princeton, N.J.: Van Nostrand Company.
45. Timoshenko, S., and D. H. Young. 1961. *Elements of Strength of Materials,* 4th ed. Princeton, N.J.: Van Nostrand Company.
46. Uni-Bell PVC Pipe Association. 1982. *Handbook of PVC Pipe Design and Construction.* Dallas.
47. Watkins, R. K. 1970. Design of Buried, Pressurized Flexible Pipe. Paper presented at ASCE National Transportation Engineering Meeting, July, in Boston, App. C.
48. Watkins, R. K., and L. R. Anderson. 2000. *Structural Mechanics of Buried Pipes.* New York: CRC Press.
49. Watkins, R. K., and A. P. Moser. 1971. Response of Corrugated Steel Pipe to External Soil Pressures. *Highway Research Record* 373:88–112.
50. Watkins, R. K., A. P. Moser, and R. R. Bishop. 1973. Structural Response of Buried PVC Pipe. *Modern Plastics,* pp. 88–90.
51. Watkins, R. K., and A. B. Smith. 1967. Ring Deflection of Buried Pipe. *Journal AWWA* 59(3).
52. Watkins, R. K., and M. G. Spangler. 1958. Some Characteristics of the Modulus of Passive Resistance of Soil—A Study in Similitude. *Highway Research Board Proceedings* 37:576–583.
53. White, H. C., and J. P. Layer. 1960. The Corrugated Metal Conduit as a Compression Ring. *Highway Research Board Proceedings* 39:389–397.
54. Wilson, E. 1971. Solid SAP, A Static Analysis Program for Three-Dimensional Solid Structures. SESM Report 71-19. Berkeley: Structural Engineering Laboratory, University of California.
55. Wong, K. S., and J. M. Duncan. 1974. Hyperbolic Stress-Strain Parameters for Nonlinear Finite Element Analysis of Stresses and Movements in Soil Masses. Report no. TE-74-3. Berkeley: Office of Research Services, University of California.
56. Zienkiewitcz, O. C. 1977. *The Finite Element Method,* 3d ed. New York: McGraw-Hill. 33–43. Reprinted with permission from American Society of Civil Engineers.

This page intentionally left blank.

Chapter

4

Design of Pressure Pipes

The design methods for buried pressure pipe installations are somewhat similar to the design methods for gravity pipe installations which were discussed in Chap. 3. There are two major differences:

1. Design for internal pressure must be included.
2. Pressure pipes are normally buried with less soil cover so the soil loads are usually less.

Included in this chapter are specific design techniques for various pressure piping products. Methods for determining internal loads, external loads, and combined loads are given along with design bases.

Pipe Wall Stresses and Strains

The stresses and resulting strains arise from various loadings. For buried pipes under pressure, these loadings are usually placed in two broad categories: internal pressure and external loads. The internal pressure is made up of the hydrostatic pressure and the surge pressure. The external loads are usually considered to be those caused by external soil pressure and/or surface (live) loads. Loads due to differential settlement, longitudinal bending, and shear loadings are also considered to be external loadings. Temperature-induced stresses may be considered to be caused by either internal or external effects.

Hydrostatic pressure

Lamé's solution for stresses in a thick-walled circular cylinder is well known. For a circular cylinder loaded with internal pressure only, those stresses are as follows:

Tangential stress: $$\sigma_t = \frac{P_i a^2\,(b^2/r^2 + 1)}{b^2 - a^2}$$

Radial stress: $$\sigma_r = \frac{P_i a^2\,(b^2/r^2 - 1)}{b^2 - a^2}$$

where P_i = internal pressure
a = inside radius
b = outside radius
r = radius to point in question

The maximum stress is the tangential stress σ_t, and it occurs at $r = a$ (Fig. 4.1). Thus,

$$\sigma_{\max} = (\sigma_t)_{r=a} = \frac{P_i a^2\,(b^2/a^2 + 1)}{b^2 - a^2}$$

or $$\sigma_{\max} = \frac{P_i\,(b^2 + a^2)}{b^2 - a^2} \tag{4.1}$$

For cylinders (pipe) where $a \approx b$ and $b - a = t$,

$$b^2 - a^2 = (b + a)(b - a) = \overline{D}t \tag{4.1a}$$

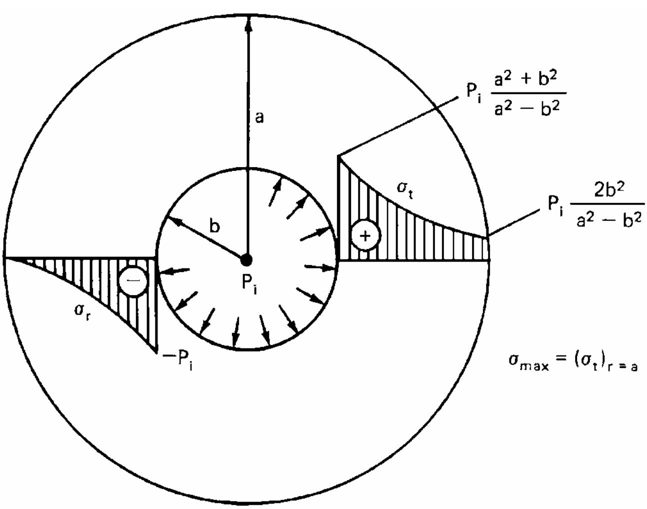

Figure 4.1 Thick-walled cylinder with internal pressure.

where $\overline{D}$ = average diameter = $b + a$ and t = thickness = $b - a$. Also,

$$(b + a)^2 = D^2 = b^2 + a^2 + 2ab \tag{4.1b}$$

Thus Eq. (4.2) can be rewritten using Eqs. (4.1*a*) and (4.1*b*) as follows:

$$\sigma_{\max} = \frac{P_i\,(\overline{D}^2/2)}{\overline{D}t} = \frac{P_i\,\overline{D}}{2t} \tag{4.2}$$

Equation (4.2) is recognized as the equation for stress in a thin-walled cylinder (Fig. 4.2). This equation is sometimes called the Barlow formula, but is just a reduction from Lamé's solution. This equation is the form most often recognized for calculating stresses due to internal pressure P_i.

If the outside diameter D_o is the reference dimension, Eq. (4.2) can be put into another form by introducing

$$\overline{D} = D_o - t$$

$$b^2 + a^2 = \overline{D}^2 - 2ab \approx \overline{D}^2 - 2r^2 = \overline{D}^2 - \frac{\overline{D}^2}{2}$$

That is, the average diameter is equal to the outside diameter minus thickness. Equation (4.2) becomes

$$\sigma_{\max} = \frac{P_i\,(D - t)}{2t} \tag{4.3}$$

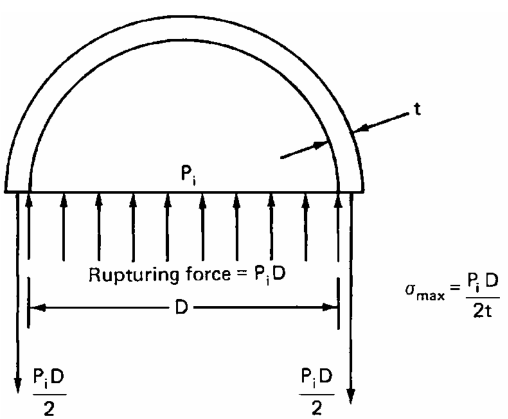

Figure 4.2 Free-body diagram of half-section of pipe with internal pressure.

Certain plastic pipe specifications refer to a dimension ratio (DR) or a standard dimension ratio (SDR), where

$$\mathrm{DR} = \frac{D_o}{t} \qquad \text{or} \qquad \mathrm{SDR} = \frac{D_o}{t}$$

Both DR and SDR are defined the same. However, SDR often refers to a preferred series of numbers that represents D_o/t for standard products. By introducing $D_o/t = \mathrm{SDR}$ into Eq. (4.3), it can be rewritten as follows:

$$\sigma_{\max} = \frac{P_i}{2}\,(\mathrm{SDR} - 1) \tag{4.4}$$

The above equation may be expressed as

$$\frac{2\sigma_{\max}}{P_i} = \mathrm{SDR} - 1 \tag{4.5}$$

Equation (4.5) is often referred to as the ISO (International Standards Organization) equation for stress due to internal pressure. However, this basic equation has been known to engineers for more than a century and was originally given by Lamé in "Leçons sur la theorie de l'elasticité," Paris 1852. Obviously, ISO is a relative newcomer and should not be given credit for Lamé's work.

To calculate these tangential stresses in the pipe wall produced by internal pressure, either Eq. (4.2) or Eq. (4.4) is often suggested by the manufacturer or by national standards. All forms are derived from Lamé's solution and will produce comparable results.

Surge pressure

Pressure surges are often divided into two categories: transient surges and cyclic surges. Cyclic surging is a regularly occurring pressure fluctuation produced by action of such equipment as reciprocating pumps, undamped pressure control valves or interacting pressure regulating valves, oscillating demand, or other cyclic effects. Cyclic surges may cause fatigue damage and should be designed out of the system.

Transient surges are just that—transient in nature, occurring over a relatively short time and between one steady state and another. A transition surge may occur, and the system then returns to the same steady state as before the surge. Transient surges are usually not cyclic in nature although they may be repetitive. A transient surge is often referred to as *water hammer.*

Any action in a piping system that results in a change in velocity of the water in the system is a potential cause of a water hammer surge.

A partial listing of some typical causes of water hammer is given below.

1. Changes in valve settings (accidental or planned)
2. Starting or stopping of pumps
3. Unstable pump or turbine characteristics

The magnitude of water hammer pressures generated by a given change in velocity depends on (1) the geometry of the system, (2) the magnitude of the change in velocity, and (3) the speed of the water hammer wave for the particular system. These variables are expressed quantitatively as

$$\Delta H = \frac{a}{g}\,\Delta V \tag{4.6}$$

where ΔH = surge pressure, ft of water
a = velocity of pressure wave, ft/s
g = acceleration due to gravity (32.17 ft/s^2)
ΔV = change in velocity of fluid, ft/s

The pressure rise, in pounds per square inch, may be determined by multiplying Eq. (4.6) by 0.43 lb/in^2 per foot of water as follows:

$$\Delta P = \frac{a}{g}\,\Delta V\,(0.43) \tag{4.7}$$

The wave speed is dependent upon

1. Pipe properties
   a. Modulus of elasticity
   b. Diameter
   c. Thickness
2. Fluid properties
   a. Modulus of elasticity
   b. Density
   c. Amount of air, and so forth

These quantities may be expressed as

$$a = \frac{12\sqrt{K/\rho}}{\sqrt{1 + (K/E)\,(D/t)\,C_1}} \tag{4.8}$$

where a = pressure wave velocity, ft/s
K = bulk modulus of water, lb/in^2
ρ = density of water, slug/ft^3

D = internal diameter of pipe, in
t = wall thickness of pipe, in
E = modulus of elasticity of pipe material, lb/in^2
C_1 = constant dependent upon pipe constraints ($C_1 = 1.0$ for pipe with expansion joints along its length)

For water at 60°F, Eq. (4.8) may be rewritten by substituting $\rho = 1.938$ slug/ft^3 and $K = 313{,}000$ lb/in^2.

$$a = \frac{4822}{\sqrt{1 + (K/E)\,(D/t)\,C_1}} \tag{4.9}$$

Equations (4.6), (4.7), and (4.8) can be used to determine the magnitude of surge pressure that may be generated in any pipeline. The validity of the equations has been shown through numerous experiments.

Figure 4.3 is a plot of the pressure rise in pounds per square inch as a function of velocity change for various values of wave speed. Tables 4.1 and 4.2 give the calculated wave speed according to Eq. (4.8) for ductile iron and PVC pipe, respectively. In general, wave speeds vary from 3000 to 5000 ft/s for ductile iron and from 1200 to 1500 for PVC pipes.

Example Problem 4.1 Determine the magnitude of a water hammer pressure wave induced in a 12-in class 52 ductile iron pipe and in a class 150 PVC pipe if the change in velocity is 2 ft/s.

solution From Tables 4.1 and 4.2 and Fig. 4.3:

Pipe	Wave speed, ft/s
Class 52 DI	4038
Class 150 PVC	1311

The resulting pressure surges are

Pipe	Surge pressure, lb/in^2
Class 52 DI	105
Class 150 PVC	35

Some appropriate rules of thumb for determining maximum pressure surges are listed below in pounds per square inch of surge per 1 ft/s change in velocity.

Pipe	Surge pressure rise, lb/in^2, per 1 ft/s velocity change
Steel pipe	45
DI (AWWA C150)	50
PVC (AWWA C900)	20
PVC (pressure-rated)	16

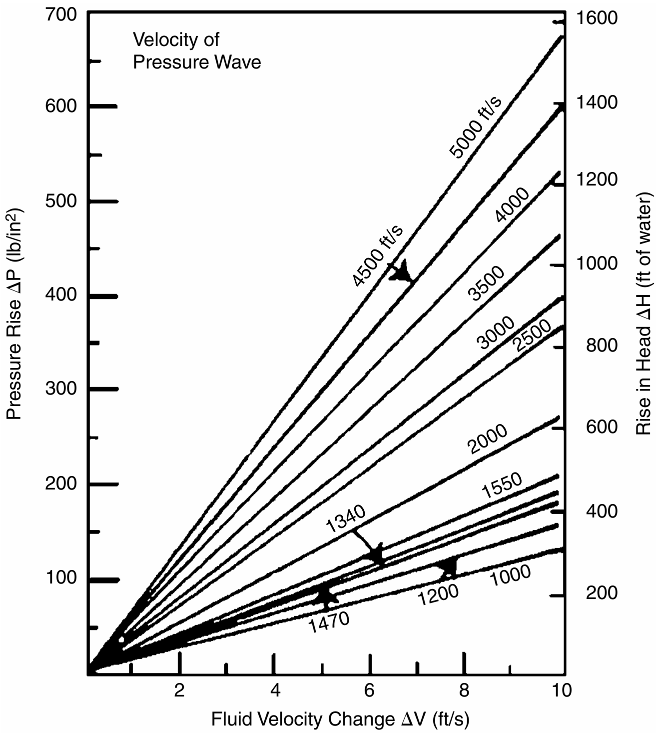

Figure 4.3 Water hammer surge calculation.

Since velocity changes are the cause of water hammer surge, proper control of valving may eliminate or minimize water hammer. If fluid approaching a closing valve is able to sense the valve closing and adjust its flow path accordingly, then the maximum surge pressure as calculated from Eq. (4.6) may be avoided. To accomplish this, the flow must not be shut off any faster than it would take a pressure wave to be initiated at the beginning of valve closing and returning again to the valve. This is called the *critical time* and is defined as the longest elapsed time before final flow stoppage that will still permit this maximum pressure to occur. This is expressed mathematically as

$$T_{cr} = \frac{2L}{a}$$

TABLE 4.1 Water Hammer Wave Speed for Ductile Iron Pipe, ft/s*

	Class						
Size	50	51	52	53	54	55	56
4	—	4409	4452	4488	4518	4544	4567
6	4206	4265	5315	4358	4394	4426	4454
8	4085	4148	4202	4248	4289	4324	4356
10	3996	4059	4114	4162	4205	4242	4276
12	3919	3982	4038	4087	4130	4169	4205
14	3859	3921	3976	4024	4069	4108	4144
16	3783	3846	3902	3952	3998	4039	4076
18	3716	3779	3853	3887	3933	4038	4014
20	3655	3718	3776	3827	3874	3917	3957
24	3550	3614	3671	3723	3771	3815	3855
30	3387	3472	3547	3615	3676	3731	3782
36	3311	3409	3495	3571	3638	3700	3755
42	3255	3362	3456	3539	3612	3678	3737
48	3207	3323	3424	3512	3590	3659	3721
54	3201	3320	3423	3512	3591	3599	3724

*AWWA C150; water at 60°F.

TABLE 4.2 Water Hammer Wave Speed for PVC Pipe, ft/s*

	(AWWA C900) Class			Pressure-rated PVC SDR			
Size	100	150	200	21	26	32.5	41
4	1106	1311	1496	1210	1084	967	859
6	1106	1311	1496	1210	1084	967	859
8	1106	1311	1496	1210	1084	967	859
10	1106	1311	1496	1210	1084	967	859
12	1106	1311	1496	1210	1084	967	859

*AWWA C150; water at 60°F.

where T_{cr} = critical time
L = distance within pipeline that pressure wave moves before it is reflected by a boundary condition, ft
a = velocity of pressure wave for particular pipeline, ft/s

Thus, the critical time for a line leading from a reservoir to a valve 3000 ft away for which the wave velocity is 1500 ft/s is

$$T_{cr} = \frac{2\,(3000)\text{ ft}}{1500\text{ ft/s}} = 4\text{ s}$$

Unfortunately, most valve designs (including gate, cone, globe, and butterfly valves) do not cut off flow proportionately to the valve-stem travel (see Fig. 4.4). This figure illustrates how the valve stem, in turning the last portion of its travel, cuts off the majority of the flow. It is extremely important, therefore, to base timing of valve closing on the

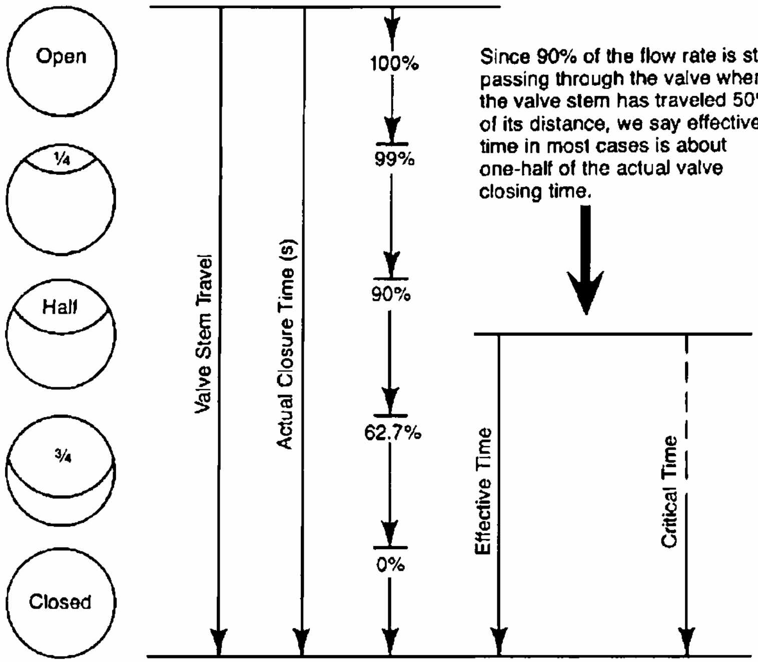

Figure 4.4 Valve stem travel versus flow stoppage for a gate valve.

effective closing time of the particular valve in question. This effective time may be taken as about one-half of the actual valve closing time. The effective time is the time that should be used in water hammer calculations. Logan Kerr[14] has published charts that allow calculation of the percent of maximum surge pressure obtained for various valve closing characteristics.

There is one basic principle to keep in focus in the design and operation of pipelines: Surges are related to changes in velocity. The change in pressure is directly related to the change in velocity. Avoiding sudden changes in velocity will generally avoid serious water hammer surges. Taking proper precautions during initial filling and testing of a pipeline can eliminate a great number of surge problems. In cases where it is necessary to cause sharp changes in flow velocity, the most economical solution may be a relief valve. This valve opens at a certain preset pressure and discharges the fluid to relieve the surge. Such valves must be carefully designed and controlled to be effective.

Surge tanks can also be designed to effectively control both positive and negative surges. In general, they act as temporary storage for excess liquid that has been diverted from the main flow to prevent overpressures, or as supplies of fluid to be added in the case of negative pressures.

External loads

External earth loads and live loads induce stresses in pipe walls. Methods for calculating these loads were discussed in Chap. 2, and design procedures for external loads were discussed in Chap. 3. These loads and their effects should be considered in pressure pipe installation design. Often stresses due to external loads are secondary in nature, but can be the primary controlling factor in design.

Rigid pipes. Stresses due to external loads on rigid pipes are usually not directly considered. Strength for rigid pipe is determined in terms of a *three-edge* test load (see Chap. 3).

Flexible pipes. Stresses in the wall of a flexible pipe produced by external loads can be easily calculated if the vertical load and resulting deflection are known. Methods for calculating the deflection are given in Chap. 3. These stresses can be considered to be made up of the following components:

Ring compression stress:
$$\sigma_c = \frac{P_v D}{2t} \tag{4.10}$$

and bending stresses:

$$\sigma_b = D_f E \frac{\Delta y}{D} \frac{t}{D} \tag{4.11}$$

where P_v = vertical soil pressure
D = pipe outside diameter
t = pipe wall thickness
E = Young's modulus
Δy = vertical deflection
D_f = shape factor

The shape factor D_f is a function of pipe stiffness, as indicated by Table 4.3. Generally, the lower the stiffness, the higher the D_f factor. Other parameters such as pipe zone soil stiffness and compaction techniques have an influence on this factor, but the values listed in Table 4.3 are recommended design values for proper installations.

TABLE 4.3 Pipe Stiffness

$F/\Delta y$, lb/in^2	D_f
5	15
10	8
20	6
100	4
200	3.5

Total circumferential stress can be obtained by the use of the following:

$$\sigma_T = \sigma_p + \sigma_c + \sigma_b$$

where σ_T = total stress
σ_p = stress due to internal pressure (static and surge)
σ_c = ring compression stress
σ_b = stress due to ring deflection (bending)

This total stress may or may not be necessary to consider in the design (see the next subsection on combined loading).

Combined loading

A method of analysis which considers effects due to external loads and internal pressure acting simultaneously is called a *combined loading analysis*.

Rigid pipes. For rigid pressure pipe such as cast iron or asbestos cement, the combined loading analysis is accomplished in terms of strength. The following procedure was originally investigated and suggested by Prof. W. J. Schlick of Iowa State University. It has since been verified by others.

Schlick showed that if the bursting strength and the three-edge bearing strength of a pipe are known, the relationship between the internal pressures and external loads, which will cause failure, may be computed by means of the following equation:

$$w = W\sqrt{\frac{P - p}{P}} \tag{4.12}$$

where w = three-edge bearing load at failure under combined internal and external loading, lb/ft
W = three-edge bearing strength of pipe with no internal pressure, lb/ft

P = burst strength of pipe with no external load, lb/in^2
p = internal pressure at failure under combined internal and external loading, lb/in^2

Schlick's research was carried out on cast iron pipe and was later shown to apply to asbestos-cement pipe. Neither of these piping materials is currently manufactured in the United States. However, these materials are available in other countries.

An example of the Schlick method of combined loading design for a rigid pipe is as follows: Suppose a 24-in asbestos-cement water pipe has a three-edge bearing strength of 9000 lb/ft and a bursting strength of 500 lb/in^2. Figure 4.5 shows graphs of Eq. (4.12) for various strengths of asbestos-cement pipes. The curve for this particular pipe is labeled 50. If this pipe were subjected in service to a 200 lb/in^2 pressure (including an allowance for surge) times a safety factor, this graph shows the pipe, in service, would have a three-edge bearing strength of 7000 lb/ft; for an internal service pressure of 400 lb/in^2, the three-edge bearing strength would be 4000 lb/ft; and so on. The three-edge bearing strength must be multiplied by an appropriate load factor to obtain the resulting supporting strength of the pipe when actually installed.

Flexible pipes. For most flexible pipes such as steel, ductile iron, and thermal plastic, a combined loading analysis is not necessary. For these materials, the pipe is designed as if external loading and internal pressure were acting independently. Usually, pressure design is the controlling factor. That is, a pipe thickness or strength is chosen on the basis of internal pressure, and then an engineering analysis is made to ensure the chosen pipe will withstand the external loads.

An exception to the above statement is fiberglass-reinforced thermal-setting resin plastic (FRP) pipe. This particular type of pipe is designed on the basis of strain. The total combined strain must be controlled to prevent environmental stress cracking. A recommended design procedure is given in Appendix A of AWWA C950. The total combined strain in this case is the bending strain plus the strain due to internal pressure. Some FRP pipe manufacturers recommend all components of strain be added together to get the total maximum strain. The following is a list of some loadings or deformations that produce strain.

1. Internal pressure
2. Ring deflection
3. Longitudinal bending
4. Thermal expansion/contraction

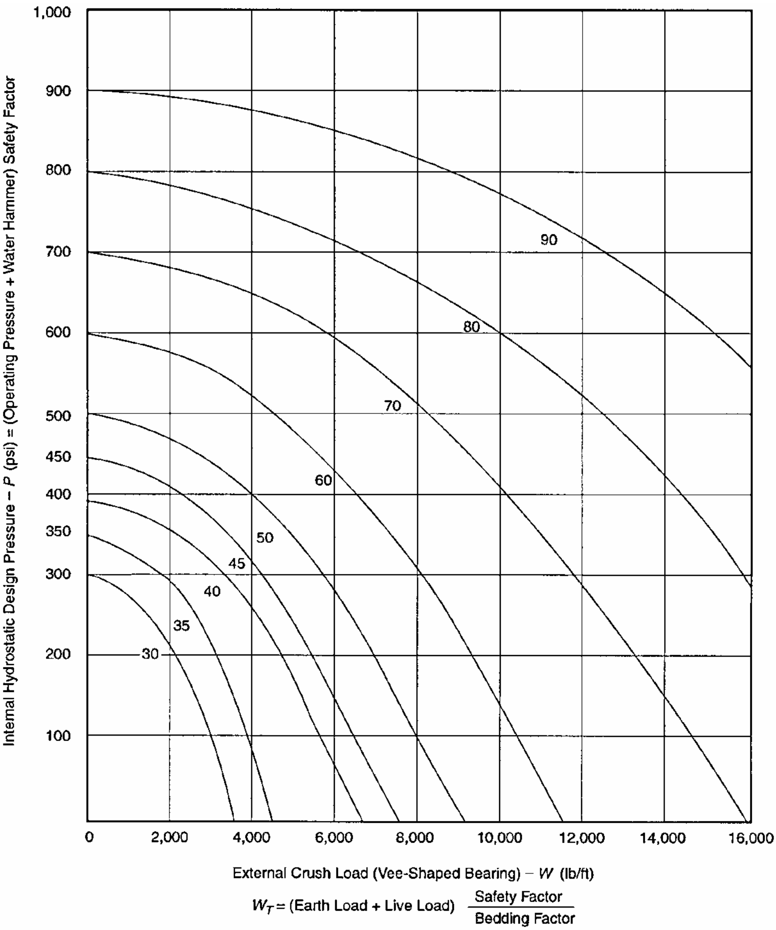

Figure 4.5 Combined loading curves for 24-in asbestos-cement pressure pipe. (*Reprinted from ANSI/AWWA C403-98,*[2] *by permission. Copyright © 1998, American Water Works Association.*)

5. Shear loadings
6. Poisson's effects

Longitudinal stresses

Pressure pipes, as well as gravity flow pipes, are subject to various soil loadings and nonuniform bedding conditions that result in longitudinal bending or beam action. This subject was discussed in Chap. 2.

Pressure pipes may also have longitudinal stresses induced by pressure and temperature which should be given proper consideration by the engineer responsible for installation design.

Poisson's effect. Engineers who deal with the mechanics of materials know that applied stresses in one direction produce stress and/or strains in a perpendicular direction. This is sometimes called the *Poisson effect.* A pipe with internal pressure p has a circumferential stress σ_p. The associated longitudinal stress σ_v, is given by the following equation:

$$\sigma_v = \nu\sigma_p$$

where σ_v = longitudinal stress
v = Poisson's ratio for pipe material
σ_p = circumferential stress

The above equation is based on the assumption that the pipe is restrained longitudinally. This assumption is valid for pipes with rigid joints or for pipes with extra-long lengths even if joined with slip joints such as rubber ring joints. Studies have shown that soil-pipe friction can cause complete restraint in approximately 100 ft. For shorter lengths with slip joints, since the restraint will not be complete, the longitudinal stress will be less than that predicted by the above equation. For reference, some values of Poisson's ratio ν and Young's modulus E are listed in Table 4.4.

Temperature effects. Expansion or contraction due to temperature increase or decrease can induce longitudinal stress in the pipe wall. As with the Poisson stresses discussed above, these stresses are based on longitudinal restraint. The longitudinal stress due to temperature is given by the equation

$$\sigma_T = -\alpha\,(\Delta T)\,E$$

TABLE 4.4 Material Properties

Material	Modulus, lb/in^2	Poisson's ratio
Steel	30×10^6	0.30
Ductile iron	24×10^6	0.28
Copper	16×10^6	0.30
Aluminum	10.5×10^6	0.33
PVC	4×10^6	0.45
Asbestos-cement	3.4×10^6	0.30
Concrete	$57{,}000\,(f_c')^{1/2}$†	0.30

†Where f_c = 28-day compressive strength.

where σ_T = longitudinal stress due to temperature
α = linear coefficient of expansion
ΔT = temperature change
E = Young's modulus for pipe material

An example of a situation that would cause such a stress follows: Consider a welded steel line which is installed and welded during hot summer days and later carries water at 35°F. The resulting ΔT will be substantial, as will the resulting stress. Additional information on temperature-induced stresses in welded steel pipe can be found in AWWA M11, *Steel Pipe Manual,* and in other AWWA standards on welded steel pipe.

Pipe thrust. Longitudinal stresses due to pipe thrust will be present when a piping system is self-restraining with welded, cemented, or locked-joint joining systems. For example, at a valve when the valve is closed, the thrust force is equal to pressure P times area A. The same force is present at a 90° bend.

$$\text{Thrust} = \text{pressure} \times \text{area}$$

$$PA = P\pi r^2$$

The stress due to this thrust is given by

$$\sigma_{\text{th}} = \frac{PA}{2\pi rt} = \frac{P\pi r^2}{2\pi rt} = \frac{Pr}{2t}$$

where σ_{th} = longitudinal stress due to thrust
T = thrust force = $P\pi r^2$
P = internal pressure plus surge pressure
r = average radius of pipe
t = thickness of pipe wall

Stress risers. The pipe system designer should always be aware of stress risers which will amplify the stresses. Stress risers occur around imperfections such as cracks, notches, and ring grooves. They are also present near changes in diameters such as in the bell area. Designs that overlook stress risers can and have led to piping system failure. In a welded bell and spigot type of joint, the longitudinal tensile stresses are not passed across the joint without inducing high bending moments and resulting bending stresses. These bending stresses have been shown to be as high as 7 times the total longitudinal stress in a straight section. For this example, the maximum longitudinal stress is given by

$$(\sigma_L)_{\max} = \beta\,(\sigma_{Lb} + \sigma_{L\nu} + \sigma_{LT} + \sigma_{\text{th}})$$

where $(\sigma_L)_{\max}$ = maximum longitudinal stress
β = stress riser
σ_{Lb} = stress due to longitudinal beam action
$\sigma_{L\nu}$ = longitudinal stresses due to Poisson's effect
σ_{LT} = longitudinal stresses due to temperature
σ_{th} = longitudinal stresses due to thrust

Design Bases

Each piping material has criteria for design such as a limiting stress and/or a limiting strain. Also, each product may be limited as to specific application in terms of fluids it may carry or in terms of temperature. Usually these limiting conditions are translated to codes, standards, and specifications. Such specifications will deal with specific acceptable applications, permissible soil load or depth of cover, internal pressure, safety factors, methods of installation, life, and, in some cases, ring deflection. The limiting parameters for a given product when considered together form the basis for design.

Rigid pipes

The use of pressure pipe constructed wholly from rigid material is rapidly becoming history. Cast iron pipe has been replaced with ductile iron, which is considered to be flexible. Asbestos-cement pressure pipe is still in production in some countries, but is rapidly losing out in the marketplace. Concrete pressure pipe, which is really steel pipe with a concrete liner and a concrete or cement grout coating, is usually considered to be rigid.

Asbestos cement. Design information for asbestos-cement pressure pipe can be found in AWWA C401 and in AWWA C403. A combined load analysis using the Schlick formula is required. This method is discussed under the combined loading section of this chapter. Equation (4.12) is repeated here.

$$w = W\sqrt{\frac{P - p}{P}} \tag{4.12}$$

or

$$p = P\left[1-\left(\frac{w}{W}\right)^2\right] \tag{4.13}$$

It is generally considered desirable to use the thick-walled formula for ratios of diameter to thickness exceeding 10. Equations (4.1) and (4.2) are the thick-walled formula and the thin-walled formula for hoop stress σ_t. Parameters W and P are determined experimentally. With these values, one can determine combinations of internal pressures p and external crush loads w that are necessary to cause failure. In addition, the design pressure will require an appropriate safety factor. Normally, if surges are present, the maximum design (operating) pressure is one-fourth of the pressure to cause failure. If surges are not present, the operating design pressure is four-tenths the failure pressure.

The design crush load is equal to the expected earth load plus live load times the safety factor (usually 2.5) and divided by a bedding factor (see Chap. 3 for bedding factors).

$$W = \frac{(\text{earth load} + \text{live load})\,(\text{safety factor})}{\text{bedding factor}}$$

Design curves are given in AWWA C401 and AWWA C403 (see Fig. 4.5 for an example). The designer enters the graph by locating the appropriate design pressure on the vertical axis and the appropriate external crush load on the horizontal axis. The intersection of these grid lines locates the appropriate pipe curve. If the intersection is between curves, choose the next-higher curve and the associated strength pipe.

Reinforced concrete. Reinforced-concrete pressure pipe is of four basic types:

1. Reinforced-steel cylinder type (AWWA C300)
2. Prestressed-steel cylinder type (AWWA C301)
3. Reinforced noncylinder type (AWWA C302)
4. Bar-wrapped, steel cylinder type (AWWA C303)

For rigid pipes discussed up to this point, the performance limits have been described in terms of rupture of the pipe wall due to either internal or external loads, or some combination thereof, being greater than the strength of the pipe. Performance limits for reinforced-concrete pipe are described in terms of design conditions, such as zero compression stress and so forth. Generally, the design of reinforced-concrete pressure pipe requires the consideration of two design cases:

1. A combination of working pressure and transient pressure and external loads
2. A combination of working pressure and external load (earth plus live load)

Reinforced-steel cylinder pipe is designed on a maximum combined stress basis. The procedure is to calculate stresses in the steel cylinder and steel reinforcement produced by both the external loads and internal pressure. The combined stress at the crown and invert must be equal to or less than an allowable tensile stress for the reinforcing steel and steel cylinder. See AWWA C304-92 and AWWA M9 for details of current recommended design procedures.

Many engineers are more familiar with the simplified design procedures as found in pre-1997 versions of AWWA C300 and pre-1992 versions of AWWA C301. In these standards, prestressed concrete pipe was designed for combinations of internal and external loads by the following cubic equation:

$$w = W_o \sqrt[3]{\frac{P_o - p}{P_o}} \tag{4.14}$$

where P_o = internal pressure which overcomes all compression in concrete core, when no external load is acting, lb/in^2

W_o = 90 percent of three-edge bearing load which causes incipient cracking in core when no internal pressure is acting, lb/ft

p = maximum design pressure in combination with external loads (not to exceed $0.8P_o$ for lined cylinder pipe)

w = maximum external load in combination with design pressure

The value of W_o can be determined by test, and the value of P_o can be either determined by test or calculated. With these parameters known, w and p can be calculated using Eq. (4.14) in a manner that is similar to the use of the Schlick formula for asbestos-cement pipe. Further information concerning the combined loading analysis using the cubic parabola Eq. (4.14) is available in these previous standards.

Pretensioned concrete cylinder pipe is considered by many to be a rigid pipe. Truly, it does not meet the definition of a flexible pipe (must be able to deflect 2 percent without structural distress). The limiting design deflection for pretensioned concrete cylinder pipe ranges from 0.25 to 1.0 percent. AWWA Manual M9 indicates that this type of pipe is semirigid. However, the recommended design procedure found in AWWA C303 and AWWA C304 is based on flexible pipe criteria. The recommended procedure is to limit stresses in steel reinforcement and the steel cylinder to 18,000 lb/in^2 or 50 percent of the minimum yield, whichever is less. The stiffness of the pipe must be sufficient to limit the ring deflection to not more than $D^2/4000$, where D is the nominal inside diameter of the pipe in inches.

Flexible pipes

Thermoplastic. All plastics are, at some stage, soft and pliable and can be shaped into desired forms, usually by the application of heat, pressure, or both. Some can be cast. Thermoplastics soften repeatedly when heated and harden when cooled. At high enough temperatures, they may melt; and at low enough temperatures, they may become brittle. A few familiar examples of thermoplastics used for pipe are polyvinyl chloride (PVC), polyethylene (PE), acrylonitrile butadiene styrene (ABS), polybutylene (PB), and styrene rubber (SR).

No matter what type of thermoplastic pressure pipe, there is common terminology. A detailed review of some of the terms will be made. The design engineer should become familiar with these terms as they are somewhat unique to the plastic pressure pipe industry.

Plastic pressure pipe terminology

Stress regression

Cell classification

Quick-burst strength

Hydrostatic design basis

Hydrostatic design stress

Service factor

Safety factor

Pressure rating

Pressure class

SDR

DR

PVC compounds. The original method for classifying PVC compounds was by types and grades, e.g., for PVC:

1. Type I, grade 1: Normal impact, very high chemical resistance, and highest requirements for mechanical material strength. Type I, grade 1 compounds are by far the predominant material used today for pipe. Other types and grades of compounds are as follows:
2. Type I, grade 2: Essentially the same properties as grade 1, but possesses lower requirements for chemical resistance. Grade 1 has about 5 percent higher hoop stress based on 50-year strength.
3. Type II, grade 1: High impact strength, but sacrifices chemical resistance and tensile strength.
4. Type III, grade 1: Medium impact strength, low chemical resistance.

While this terminology still persists, the current definition of PVC compounds is given in the most current edition of ASTM D 1784, the standard specification for "rigid poly(vinyl chloride) (PVC) compounds and chlorinated poly(vinyl chloride) (CPVC) compounds." This specification defines the physical characteristics of the compound with a five digit cell-class numbering system and a letter suffix describing chemical resistance.

The old type-and-grade compound system is now expressed in cell classification as follows:

Type I, grade 1: 12454B

Type I, grade 2: 12454C

Type II, grade 1: 14333D

Type III, grade 1: 13233

Type IV, grade 1: 23447B

The following is a brief review of what this numbering matrix plus a letter, that is, 12454B, defines.

First number: Material identification (PVC homo polymer)

Second number: Impact strength (izod minimum) (0.65 ft lb/in)

Third number: Tensile strength (7000 lb/in^2 minimum)

Fourth number: Modulus of elasticity (in tension 400,000 lb/in^2 minimum)

Fifth number: Deflection temperature under load (158°F minimum)

Letter: Chemical resistance as defined in Table 2 of ASTM D 1784.

As indicated, the PVC compound most commonly used for water (pressure) pipe application is

Old designation: type I, grade 1

Current designation: 12454B

In late 1980, ASTM approved yet another standard for identifying PVC compounds. ASTM D 3915 utilizes a similar cell-class system as ASTM D 1784, but has deleted the letter suffix and substituted a hydrostatic design basis cell. To date, this system has not been adopted in any PVC pipe standards.

Hydrostatic design basis. ASTM D 2837 establishes the "standard method for obtaining hydrostatic-design basis for thermoplastic pipe materials." The procedure for establishing a hydrostatic design basis is as follows:

1. Classify PVC pipe compound per ASTM D 1784 cell classification, that is, 12454B.
2. Conduct long-term static pressure tests on pipe.
3. Submit data to the hydrostatic design committee of PPI for analysis.
4. Determine the long-term hydrostatic strength (LTHS). [LTHS is the extrapolated hoop stress that will produce failure in 100,000 h (11.4 years).]
5. Determine the hydrostatic design basis (HDB) by categorizing the LTHS per ASTM D 2837, which also involves projections to 50 years.

The pressure test data, when presented on a log-log plot, form a straight line. It is called a *stress regression curve* (see Fig. 4.6 for stress regression curve for PVC). This "declining" curve does not represent a loss of strength with time. It does show that the higher the stress, the shorter the life; conversely the lower the stress, the longer the life. The line relates the life of the pipe to the level of stress in the pipe wall due to internal pressure. It is a series of test data points. For example, for a given stress or pressure, failure will occur

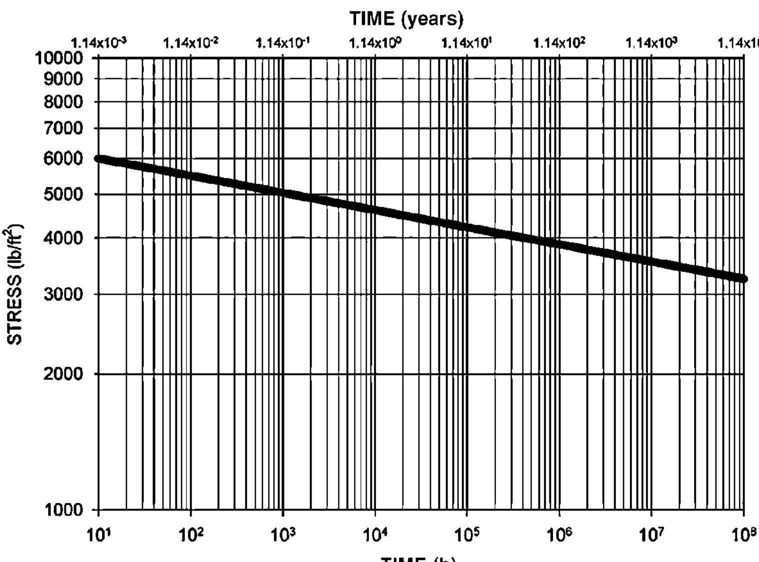

Figure 4.6 Stress regression line for PVC pressure pipe.

in a given time. To establish the regression line, tests must be conducted such that individual failures occur from 10 to 10,000 h (1.14 years). The line is for static pressure only and is temperature-controlled at 73.4°F.

For PVC pipe, long-term static pressure tests have been carried out over more than 200,000 h (22.8 years) that confirm the validity of establishing long-term hydrostatic strength on the basis of log-log straight-line extrapolations.

Hydrostatic design stress. The *hydrostatic design stress* (HDS) is defined in ASTM D 2241 as follows: "The estimated maximum tensile stress in the wall of the pipe in the circumferential orientation due to the internal hydrostatic water pressure that can be applied continuously with a high degree of certainty that failure will not occur."

The ASTM specifications for PVC, PE, and ABS pipe indicate the hydrostatic design basis and hydrostatic design stress for these materials. A comparison of one type-and-grade designation of each material reveals the following:

	HDB	HDS
PVC 1120*	4000	2000
PE 3406	1260	630
ABS 1316	3200	1600

*Equivalent to PVC cell classification 12454B per ASTM D 1784.

The higher HDB and HDS for PVC 1120 partially explains its wide acceptance for plastic water pressure pipe. A complete listing for these values for PVC, PE, and ABS is given in Table 4.5.

Pressure-rated pipe. For the purpose of reviewing the plastic pressure pipe design procedure, PVC pipe and ASTM D 2241, *Standard Specification for Poly (Vinyl Chloride)(PVC) Plastic Pipe (SDR-PR),* will be considered. A similar procedure exists for other thermoplastic materials.

Throughout existing PVC standards and specifications for PVC pipe, one still finds the older type-and-grade designation. For example, the most common designation for pressure pipe is PVC 1120. It can be defined as follows:

PVC: polyvinyl chloride.

First number (1) represents type of compound, in this case, type I.

Second number (1) represents the compound grade, in this instance, grade 1.

TABLE 4.5 Selected ASTM Specifications for PVC, PE, and ABS Pipe

Material type	Hydrostatic design basis, lb/in^2	Hydrostatic design stress, lb/in^2
	PVC ASTM D 2241	
PVC 1120	4000	2000
PVC 1220	4000	2000
PVC 2120	4000	2000
PVC 2216	3200	1600
PVC 2112	2500	1250
PVC 2110	2000	1000
	Polyethylene ASTM D 2239	
PE 2306	1260	630
PE 3306	1260	630
PE 3406	1260	630
PE 2305	1000	500
PE 1404	800	400
	ABS ASTM D 1527	
ABS 1208	1600	800
ABS 1210	2000	1000
ABS 1316	3200	1600
ABS 2112	2500	1250

Third and fourth numbers (20) represent the hydrostatic design stress, in this case 2000 lb/in^2 divided by 100, and decimals that result are dropped.

The design basis for PVC pressure pipe meeting ASTM D 2241 is a balance of forces (Fig. 4.7). The pressure P times the mean diameter $D - t$ equals the stress σ times twice the wall thickness t; or it can be expressed as follows:

$$P\,(D - t) = \sigma \times 2t$$

or

$$\sigma = \frac{P\,(D - t)}{2t} \tag{4.15}$$

where P = internal pressure, lb/in^2, and σ = tensile strength, lb/in^2.

The hydrostatic design stress HDS, or σ in the equation, is the hydrostatic design basis (HDB) times a service factor. HDB for PVC is 4000 lb/in^2 for water-pipe compounds. The service factor is defined in the appendix of ASTM D 2241 and recommended by the Plastic Pipe Institute as equal to 0.5. (The inverse of the service factor is the safety factor, in this case 2.) Thus, the long-term hydrostatic design stress

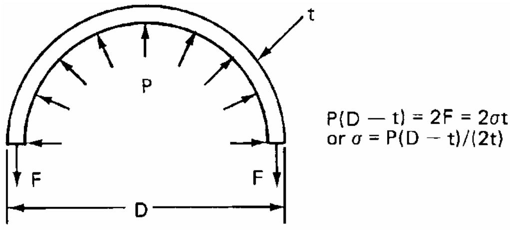

Figure 4.7 Stress due to internal pressure.

for PVC 1120 pressure-rated pipe meeting ASTM D 2241 is 2000 lb/in^2 (HDB × 0.5, or HDB/2).

Equation (4.15) can be rearranged algebraically to reveal the term SDR (standard dimension ratio) or

$$\frac{D}{t} = \frac{\text{average outside diameter}}{\text{minimum wall thickness}}$$

This term is widely used in the thermoplastic pipe industry. Equation (4.15) can therefore be rearranged as follows:

$$2\sigma = P\,\frac{D - t}{t} \qquad \text{but} \qquad \frac{D}{t} = \text{SDR}$$

Therefore,

$$2\sigma = P\,(\text{SDR} - 1)$$

The term *standard dimension ratio* refers to a preferred series of numbers. Also note that the pressure rating of a given SDR is the same no matter what the size; that is, 2-in and 12-in SDR 26 have the same pressure rating.

In review, the four basic ideas that are important to the designer of thermoplastic pressure pipe are as follows:

1. The hydrostatic design basis for a given PVC pipe extrusion compound is established through long-term hydrostatic pressure testing for pipe extruded from that compound.
2. The hydrostatic design stress is the stress in the pipe wall at which plastic pipe will perform indefinitely.
3. The service factor (0.5) times (or the safety factor, 2 to 1, divided into) the hydrostatic design basis equals the hydrostatic design stress.
4. Plastic pipe does not lose strength with time.

AWWA standards. The first AWWA standard approved for plastic pipe was AWWA C900 in 1975. AWWA C900 is the AWWA standard for polyvinyl chloride pressure pipe, 4-in through 12-in for water. This standard contains three pressure classes.

Class 100, DR 25

Class 150, DR 18

Class 200, DR 14

The term *DR* means the same as the standard dimension ratio, i.e.,

$$\text{DR} = \frac{\text{outside diameter}}{\text{minimum wall thickness}} = \frac{D}{t}$$

However, the values do not fall in the referenced ASTM preferred series. The design basis for AWWA C900 differs from ASTM in two areas:

1. It has a higher safety factor.
2. It includes a surge allowance.

The design basis equation in C900 can be expressed in the following way:

$$2.5\,(\text{PC} + \text{PS}) = \frac{2t}{D - t}\,(\text{HDB}) \tag{4.16}$$

where 2.5 = safety factor
PC = pressure class: 100, 150, 200 lb/in^2
PS = surge allowance, lb/in^2, for instantaneous stoppage of flow of 2 ft/s
t = minimum wall thickness, in
D = outside diameter, in
HDB = hydrostatic design basis = 4000 lb/in^2

The actual surge allowances in AWWA C900 PVC pipe that result from stoppage of flow of 2 ft/s are as follows:

Class 100, DR 25	30 lb/in^2
Class 150, DR 18	35 lb/in^2
Class 200, DR 14	40 lb/in^2

Another design parameter included in AWWA and not in ASTM is the effect of sustained elevated temperatures on pressure and/or design stress. For sustained temperature of the pipe wall above 73°F, the design stress should be reduced. This reduction is not necessary for

TABLE 4.6 Temperature Coefficients

Maximum continuous service temperature, °F	Percentage of allowable pressure class or design stress at 73°F
73	100
80	88
90	75
100	62
110	50
120	40
130	30
140	22

short-term excursions of elevated temperatures but is for continuous service at a higher temperature. The recommended percentages of allowable pressure class for various elevated temperatures are shown in Table 4.6.

A review of AWWA C900 and AWWA C905 for PVC water pipe indicates approval of the following:

Compounds	12544A or 12544B (formerly 1120)
Size range	4 through 12 in (AWWA C900); 14 through 36 in (AWWA C905)
Pressure classes	100, 150, and 200 lb/in^2 (AWWA C900); 100, 125, 160, 165, 200, and 235 lb/in^2 (AWWA C905)
DR	25, 18, and 14 (AWWA C900); 41, 32.5, 26, 21, and 18 (AWWA C905)

In 1980, AWWA published a manual, AWWA M23. This manual was a follow-up on the standard AWWA C900 and covers the design and installation of PVC pipe meeting this standard. This manual provides a very thorough presentation on the design and installation of PVC pipes. In 1994, AWWA published AWWA C605, a standard for underground installation of PVC pressure pipe and fillings. This contains some information found in AWWA M23.

AWWA C901 is the AWWA standard for polyethylene pressure pipe, tubing, and fittings, $^1/_2$-in through 3-in for water. This standard is primarily for PE water service piping. AWWA C901 can be summarized as follows:

Compounds	2306, 2406, 3406, 3408
Size range	$^1/_2$ through 3 in
Diameters	ID base, OD base, tubing
Pressure classes	80, 100, 125, 150, 160, and 200 lb/in^2
DR	17.0, 15.0, 13.5, 11.5, 11.0, 9.3, 9.0, 7.3, 7.0, and 5.3

Note that AWWA C901 provides for a wide selection of compounds and pressure classes. The safety factor is 2, and there is no routine test for each piece of pipe.

AWWA C902 is the AWWA standard for polybutylene (PB) pressure pipe, tubing, and fittings, $\frac{1}{2}$- through 3-in for water. This standard is also primarily intended for service water piping. AWWA C902 can be summarized as follows:

Compounds	Type II, grade 1, class B; Type II, grade 1, class C; HDB = 2000 lb/in^2; PB 2110
Size range	$\frac{1}{2}$ through 3 in
Diameters	ID base, OD base, tubing
Pressure classes	125, 160, and 200 lb/in^2
DR	17.0, 15.0, 13.5, 11.5, 11.0, and 9.0

Again, a wide selection is available. The safety factor is also 2, and no routine test is required for each piece of pipe.

Cyclic life of plastics

Cyclic fatigue of plastic pipe. Cyclic surging is a regularly occurring pressure fluctuation produced by action of such equipment as reciprocating pumps, undamped pressure control valves or interacting pressure regulating valves, oscillating demand, or other cyclic effects. Cyclic surges may cause fatigue damage and should be designed out of the system.

A transient surge is often referred to as water hammer. Any action in a piping system that results in a change in velocity of the system is a potential cause of a water hammer surge. A partial listing of some typical causes of water hammer is given below.

Cyclical pressures. Water hammer surges in a water system normally occur on a rather infrequent basis, are transient in nature, and are not cyclic in character although they may be repetitive. Transient surges are discussed in a previous section ("Surge Pressure"). However, if a system is operating out of control, cyclical pressures can occur, and may be somewhat continuous. It is this type of condition that may require additional design considerations for plastic pipe. Research work has shown the following for plastic pipe:

1. Plastic pressure pipe has three independent modes of failure or three independent strengths (life funds).
   a. Failure occurs because the internal pressure has exceeded the pipe short-time strength. Strength due to this mode of failure is called the *quick-burst strength.* A failure due to a water hammer pressure wave is this type of failure.

b. Failure due to a long-term sustained high internal pressure can only take place if the internal operating pressure is much higher than the design pressure. This type of failure is time-based. The strength (stress/life) for this mode of failure is also life (time) based and is determined from the pipe's stress regression curve.

c. Fatigue failure can take place if the water system experiences continuous cyclic pressures. The strength of plastics is independent of the number of cycles experienced by the plastic. This is no different from fatigue in metals. That is, if a specimen is cycled to, say, 80 percent of it fatigue life, taken off test, and then tested for strength, the strength will not be diminished.

2. Thus, these strengths (life funds) are separate and independent of one another.
3. The cyclic pressure life may be a critical parameter if the water system is operating "out of control" and the amplitude and frequency of the cyclic pressures are high and continuous.

Previous cyclic theory for PVC pipe as found in the First Edition of this book. Table 4.7 shows some cyclical pressure research work done on 6-in, 160 lb/in^2, pressure-rated PVC pipe. This table may lead one to believe that the cycles to failure is a function of peak stress only. However, it is fairly well known that cyclic life is a function of average

TABLE 4.7 Cast Iron 6-in-OD, PVC Pressure Pipe

Sample	Outside diameter, in	Min. wall, in	Max. pressure, lb/in^2	Max. stress, lb/in^2	Cycles at failure
1	6.910	0.448	660	4,760	7,163
2	6.909	0.444	480	3,495	40,798
3	6.909	0.443	760	5,546	2,851
4	6.908	0.448	650	4,686	2,851
5	6.913	0.442	485	3,550	27,383
6	6.911	0.436	600	4,455	10,105
7	6.910	0.440	340	2,500	78,403
8	6.904	0.452	340	2,427	121,768
9	6.910	0.452	340	2,429	91,475
10	6.910	0.443	200	1,460	3,018,907
11	6.910	0.443	235	1,715	983,200
12	6.910	0.444	440	3,204	35,633
13	6.908	0.443	340	2,481	119,971
14	6.910	0.447	200	1,446	3,647,182
15	6.910	0.449	200	1,439	2,563,538
16	6.910	0.442	400	2,927	63,616
17	6.907	0.455	600	4,254	3,587
18	6.906	0.450	680	4,878	2,936

stress and stress amplitude. Therefore, cycles to failure is a function of two variables, not just one. Two independent variables are required to determine the dependent variable of cycles to failure. Other variables may be defined in terms of two independent variables. For example,

$$\text{Peak stress} = \text{average stress} + \text{stress amplitude}$$

or

$$\sigma_{\text{max}} = \overline{\sigma} + \sigma_{\text{amp}}$$

and

$$\sigma_{\text{min}} = \overline{\sigma} - \sigma_{\text{amp}}$$

Data in Table 4.7 have been plotted, published, and misused because the table is incomplete. It implies that cycles to failure is a function of one variable only (peak stress). The two graphs in Figs. 4.8 and 4.9 were plotted using linear regression analysis of the data. While the plots represent the data, to conclude that cycles to failure is only a function of peak stress is incorrect. These two curves have been published and misused as follows:

The cyclical data (see Fig. 4.8) for PVC pipe may be represented by a straight line when plotted on log-log axes. The equation of the line is

$$C = (5.05 \times 10^{21})\, S^{-4.906} \tag{4.17}$$

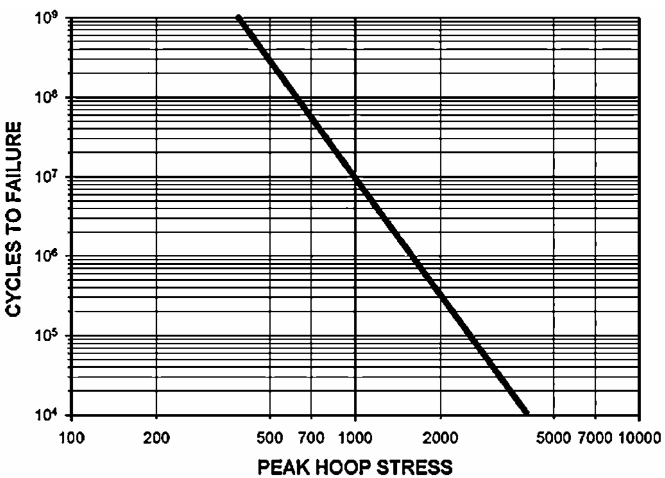

Figure 4.8 Fatigue curve from Vinson and found in the 1991 Uni-Bell *Handbook of PVC Pipe.*

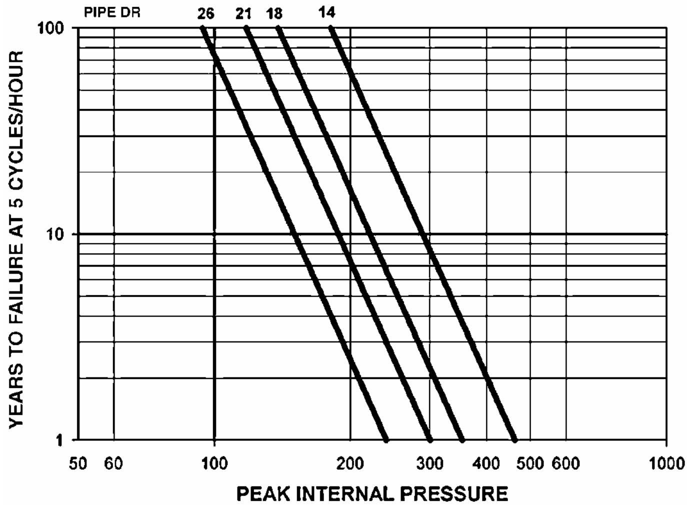

Figure 4.9 Fatigue curves as found in the 1991 Uni-Bell *Handbook of PVC pipe*—data from Vinson.

where S = peak hoop stress, lb/in², and C = number of cycles to failure associated with the peak stress.

One can then determine the peak cyclic hoop stress allowed by modifying the previous equation as follows:

$$S' = \left(\frac{5.05 \times 10^{21}}{C'}\right)^{0.204} \tag{4.18}$$

where S' = allowable design peak hoop stress, lb/in², for anticipated cycles and C' = anticipated number of cycles in life system.

To select the appropriate PVC pipe for a new installation, the following steps can be taken:

1. Determine the years of service required and anticipated cyclic rate.
2. Determine the number of cycles in the life of the system.
3. Use Eq. (4.18) to determine allowable peak stress.

As an alternate, design curves such as those in Fig. 4.9 can be generated from the data.

$$DR = \frac{2S'}{P} + 1 \tag{4.19}$$

where P = peak internal pressure (hydrostatic + surge) , lb/in^2
S' = required design peak hoop stress, lb/in^2
DR = dimension ratio

Corrected theory for cyclic life of PVC pipe. In 1999, the Uni-Bell PVC Pipe Association commissioned a study into the cyclic life of PVC pipes. Ten pipe samples were qualified by USU for long-term cyclic testing. For qualification, the samples met the following tests: (1) acetone immersion, (2) dimensions, (3) quick-burst, and (4) flattening as specified in AWWA C900 (see Figs. 4.10 and 4.11). Ten 6-in-diameter AWWA C900 DR 18 PVC pipes were placed on test (Figs. 4.12 and 4.13). The internal pressure was cycled from 185 to 235 lb/in^2. The hoop stresses were as follows:

$$\text{Peak stress} = \sigma_{\text{max}} = 2000 \text{ lb/in}^2$$

$$\text{Min. stress} = \sigma_{\text{min}} = 1574 \text{ lb/in}^2$$

$$\text{Average stress} = \bar{\sigma} = \frac{\sigma_{\text{max}} + \sigma_{\text{min}}}{2} = 1787 \text{ lb/in}^2$$

$$\text{Stress amplitude} = \sigma_{\text{amp}} = \frac{\sigma_{\text{max}} - \sigma_{\text{min}}}{2} = 213 \text{ lb/in}^2$$

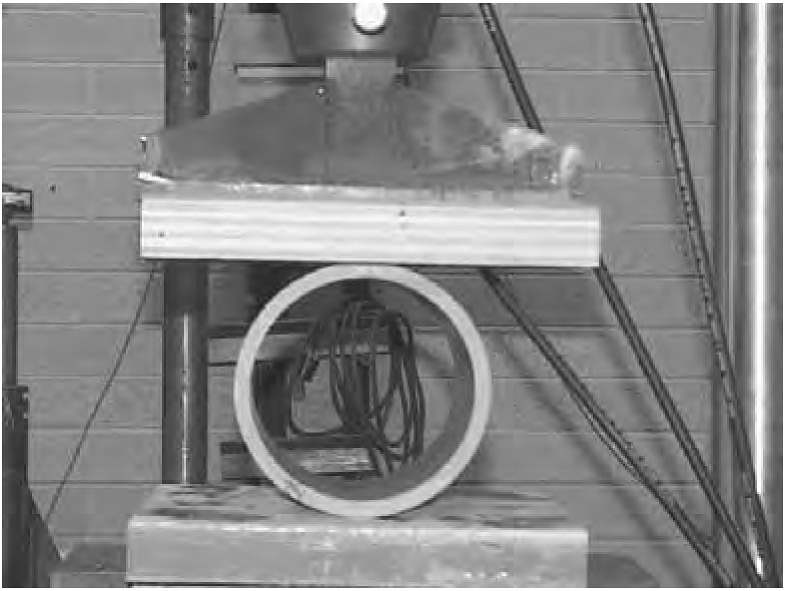

Figure 4.10 Prequalification flattening test (before flattening).

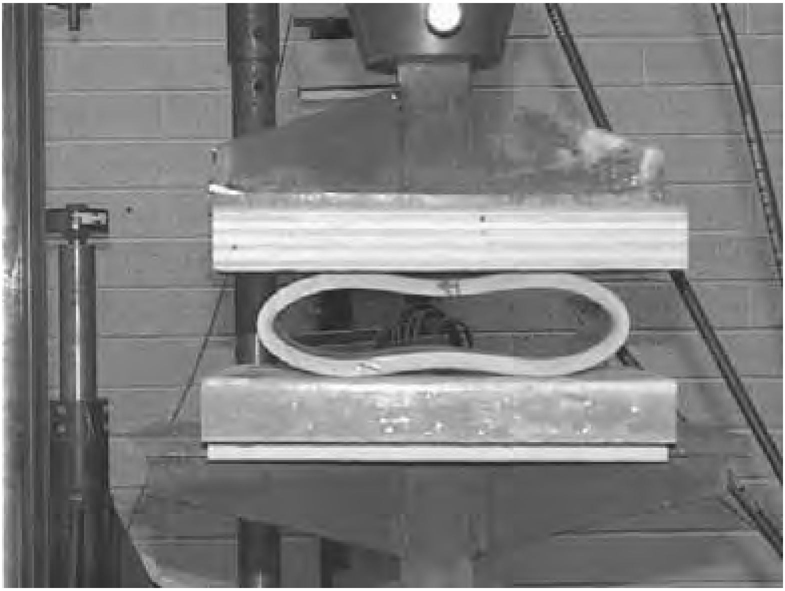

Figure 4.11 Prequalification flattening test (after flattening).

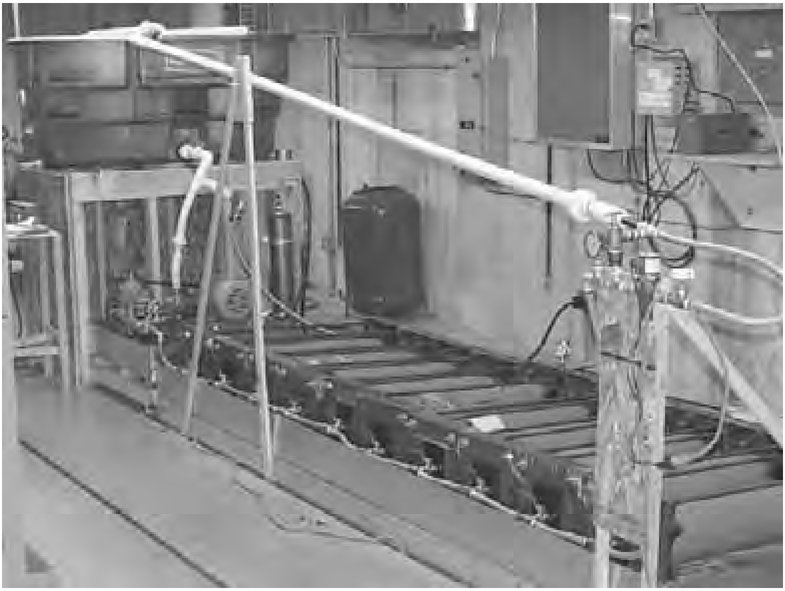

Figure 4.12 Cyclic pressure test setup.

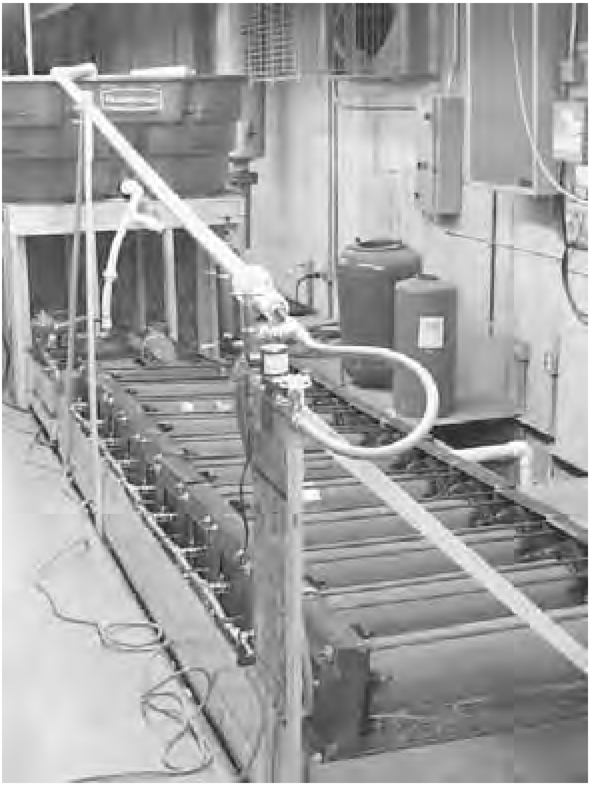

Figure 4.13 Cyclic pressure test setup.

The test temperature was controlled at 73±3°F. Cyclic rate was 18 cycles/min, and the anticipated cycles to failure was less than 0.5 million cycles (cyclic test time was approximately 20 days to failure). The estimated time to failure was determined by existing theory as found in the Uni-Bell *Handbook of PVC Pipe*. According to this theory, failure should have occurred at 322,000 cycles. The test was continued past the 322,000 cycle anticipated failure point to 3.5 million cycles. At this point the test was terminated (see Fig. 4.14).

In fatigue failures, it is well known that the dependent variable "number of cycles to failure" is a function of two independent variables. Temperature is usually eliminated as a variable by testing at a fixed constant temperature. Typically the two independent variables are average stress and stress amplitude. Other variables can be defined, but there are typically two independent variables. Suppose the imposed internal pressure is cyclic. This will induce a

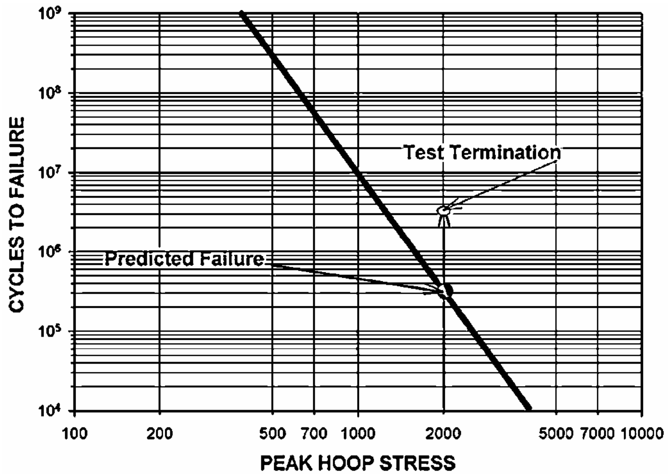

Figure 4.14 Predicted failure for 10 pipes on cyclic test.

cyclic hoop stress in the wall of the pipe. The hoop stress can be considered as being made up of two parts, the steady-state part σ_{av} and the variable part σ_{amp}.

In fatigue failures, stress amplitude is the more important variable of the two independent variables. However, average stress cannot be ignored. It is obvious that at a very high average stress a material will not be able to tolerate a large stress amplitude.

$$\text{Stress amplitude} = \sigma_{amp} = \frac{\sigma_{max} - \sigma_{min}}{2}$$

$$\text{Average stress} = \bar{\sigma} = \frac{\sigma_{max} + \sigma_{min}}{2}$$

$$\text{Stress range} = \Delta\sigma = \sigma_{max} - \sigma_{min} \qquad \text{Stress ratio} = \frac{\sigma_{max}}{\sigma_{min}}$$

$$\text{Min. stress} = \sigma_{min} \qquad \text{Peak stress} = \sigma_{max}$$

Researchers studying the cyclic failure of plastics have plotted cycles to failure as a function of stress range or stress amplitude. For this study three data sets were analyzed (Bowman, Marshall, and Vinson). The Vinson data used to produce the peak stress curves in Figs. 4.8 and 4.9 were analyzed on the basis of stress amplitude. These data along with data from two other researchers are shown in Fig. 4.15. The two sets of data produced by Bowman and Marshall have good agreement.

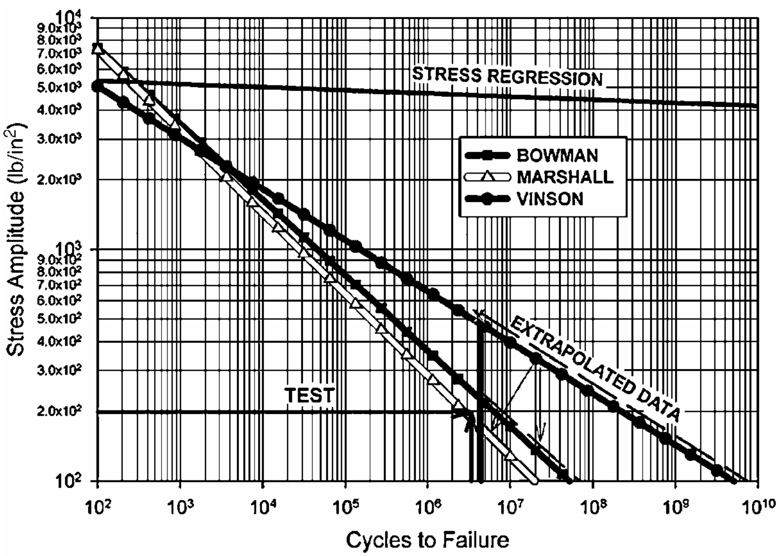

Figure 4.15 Cycles to failure on a stress amplitude basis for PVC pipes.

Both of these sets were produced in England by testing PVC pipe manufactured in England. The Vinson data do not agree with the other two sets. This author has concluded that the PVC manufactured in the United States and tested by Vinson is different from the PVC manufactured in England and tested by Bowman and Marshall. Marshall has now tested both products and has come to the same conclusion.

For the cyclic tests described above, the stress amplitude was 213 lb/in^2. The Vinson line in Fig. 4.15 is from the same data as the line in Fig. 4.14. The curve in Fig. 4.14 predicts failure based on peak pressure and predicts failure at 322,000 cycles. The curve in Fig. 4.15 predicts failure on a stress amplitude basis and predicts failure at 2×10^8 cycles. These two predictions are vastly different, and both are wrong.

As stated previously, the number of cycles to failure is a function of two variables, not just one. The failure surface is three-dimensional. Such a surface can be plotted if sufficient data are available. In such a plot the x axis and y axis are average stress and stress amplitude, and the z axis is cycles to failure.

A computer-based regression analysis was run on the Vinson data. This procedure uses an interpolation method to fill in where data are missing. Such a procedure is not precise but will give failure predictions that are more precise than those of the methods currently in use for PVC. The resulting data were used to plot a three-dimensional plot

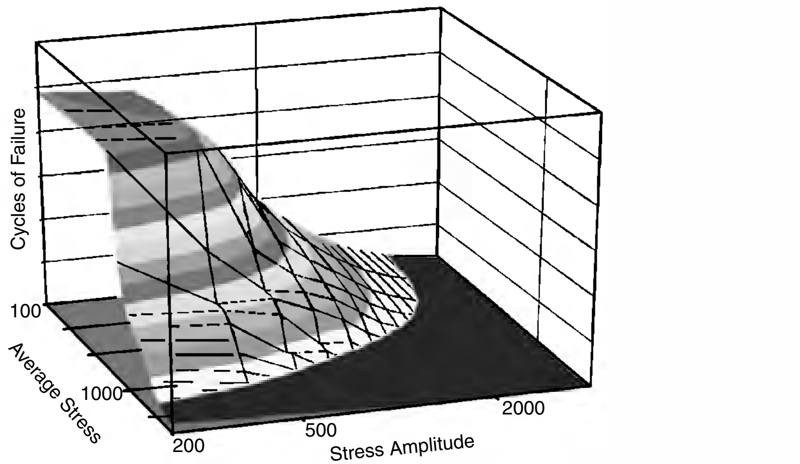

Figure 4.16 Three-dimensional failure surface from regression analysis of cyclic fatigue data of PVC pipe.

of the failure surface. An illustration of such a surface is given in Fig. 4.16. Again, it should be understood that this surface is approximate only, and more test data are required to refine the data used to plot the surface. A two-dimensional projection of the surface is given in Fig. 4.17. A constant color band represents a certain number of cycles to failure. This is a log-log plot and represents a series of curves. Each curve represents a certain number of cycles to failure.

A series of curves of this shape could be represented as shown in Fig. 4.18. Such curves represent equations of exponential decay—a phenomenon that is associated with most natural systems. If the equations of the curves in Fig. 4.18 are plotted on semilog axes, they plot as straight lines. This can be seen in Fig. 4.19.

The purpose of the above analysis is to prove that the cyclic failure curves for PVC plot as straight lines on semilog axes, if those axes are as follows: Linear axis is average stress, and log axis is stress amplitude. If the stress amplitude approaches zero, failure should occur when the average stress reaches the tensile strength for PVC, which is about 7000 lb/in^2. Thus, all lines should go through the point (7000, 0). The log of 0 is undefined, therefore 10 lb/in^2 was selected as the minimum for stress amplitude. The log of 10 is unity.

Since one point (7000, 10) is known for all failure curves, and since the curves are straight lines on semilog axes, only one other point is needed to generate each curve. This point can be obtained from existing test data. This process was used to obtain the curves in Fig. 4.20.

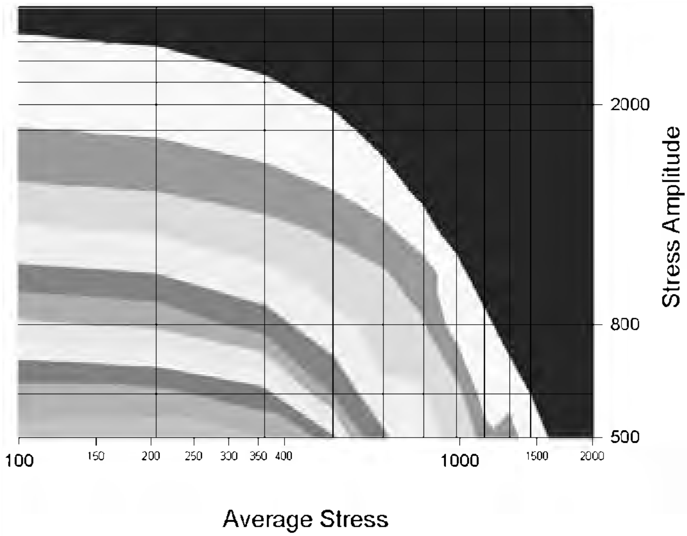

Figure 4.17 Two-dimensional projection of the three-dimensional failure surface.

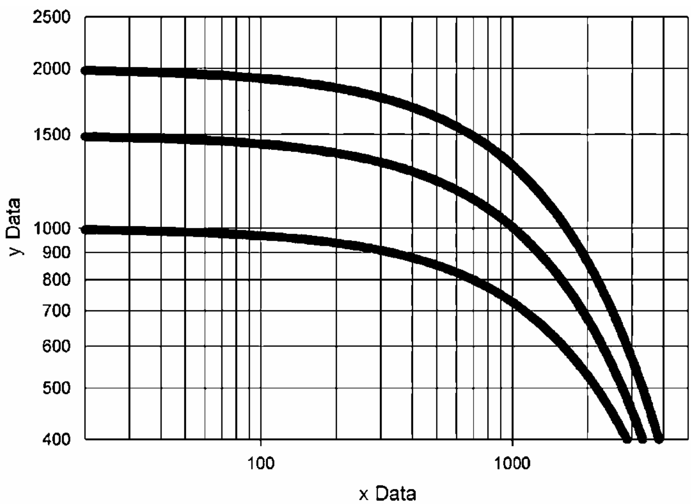

Figure 4.18 Typical exponential decay curves plotted on log-log axes.

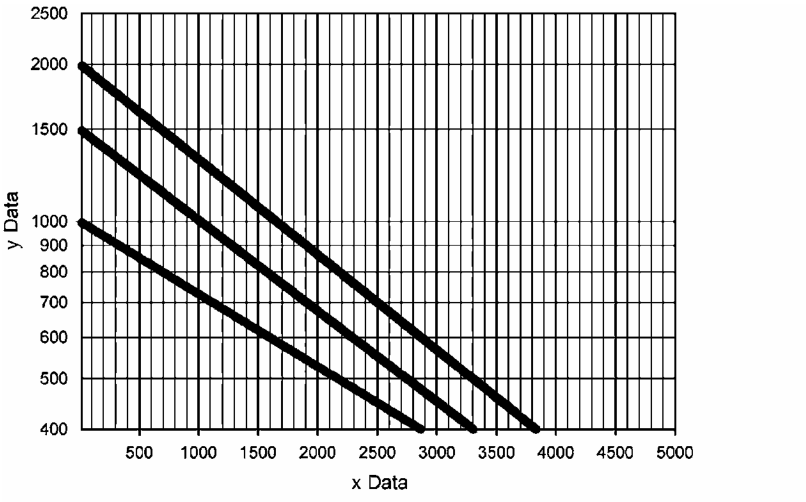

Figure 4.19 Curves in Fig. 4.18 plotted on semilog axes.

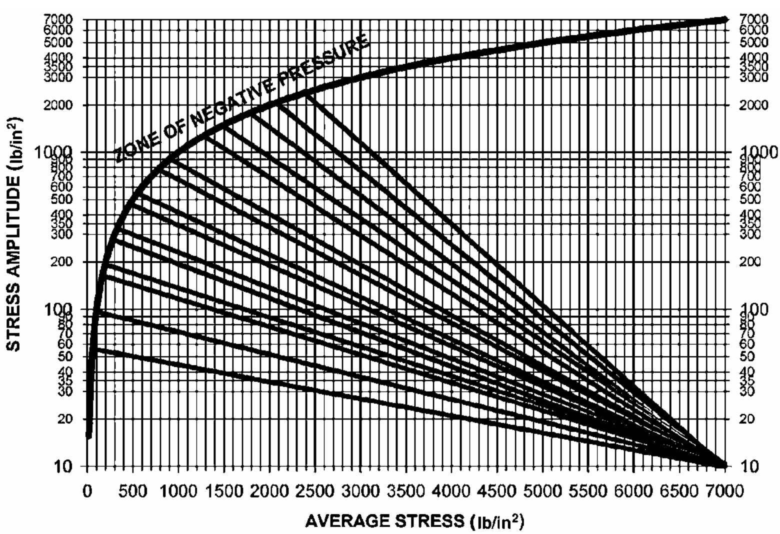

Figure 4.20 Cyclic failure curves for PVC pipe showing all curves converge at the tensile strength.

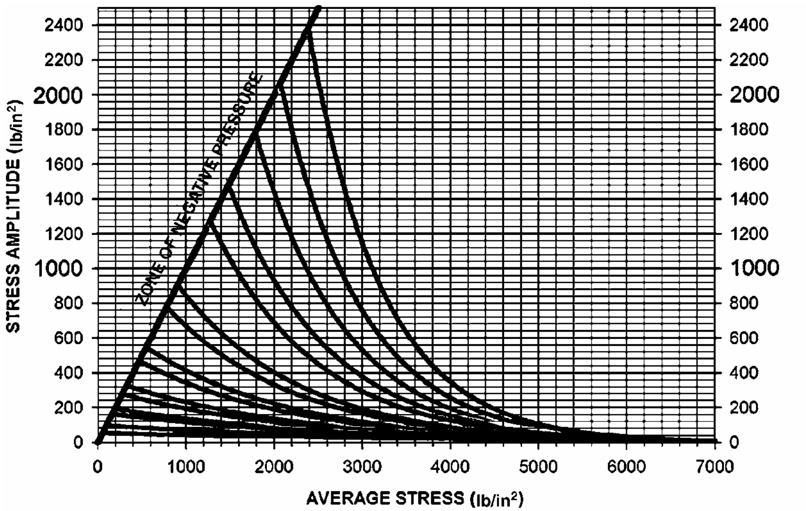

Figure 4.21 Cyclic failure curves on linear axes, for PVC pipe, showing the exponential decay nature of the curves.

If the stress amplitude is greater than the average stress, the total stress can be negative. Since a negative pressure is not an acceptable design condition, the curves were begun for the case of equal average stress and stress amplitude. When the curves in Fig. 4.20 are plotted on linear axes, the result is Fig. 4.21. It is evident from this plot that the curves are exponential decay-type curves. The ranges of stress (on the axes) of Figs. 4.20 and 4.21 are outside admissible values. If the maximum plotted stress in Fig. 4.20 is limited to more acceptable values, the result is Fig. 4.22.

The small circle on the crossed lines of Fig. 4.22 is the failure prediction point of the cyclic tests. For review, the test parameters are repeated here:

Stress amplitude = 213 lb/in^2

Average stress = 1787 lb/in^2

Uni-Bell (Vinson) predicted cycles to failure = 322,000 cycles (bases on peak stress). This is ultraconservative.

Predicted failure based on stress amplitude = 2×10^8 cycles. This is nonconservative.

Three-dimensional theory based on both amplitude and average stress gives slightly over 1×10^7 cycles.

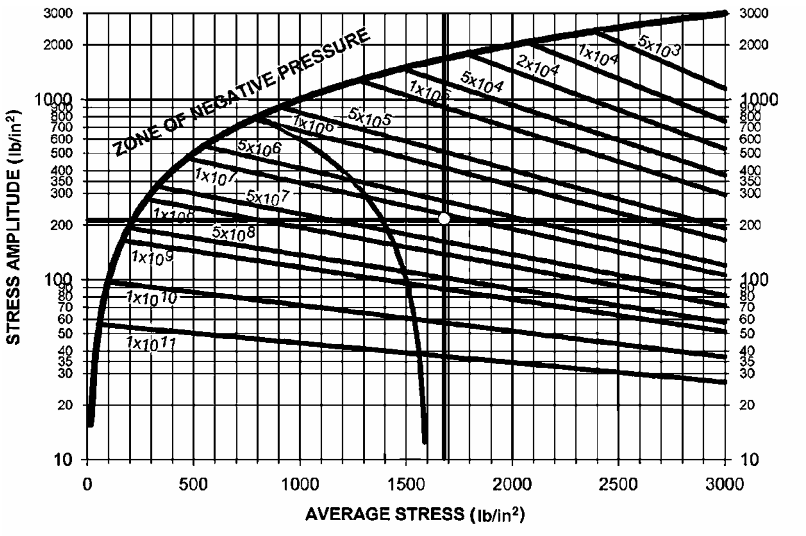

Figure 4.22 Cycles to failure for PVC pipe. The zone between the two curved lines is the design zone for AWWA C900 pipe.

Thus, the (peak stress) failure theory for PVC pipe as given in the Uni-Bell handbook is ultraconservative. For the case analyzed, this theory predicted failure cycles 30 times lower than those of the correct theory. The stress amplitude theory is also incorrect and will be ultra nonconservative for low-stress amplitudes. The correct theory uses both average stress and stress amplitude to predict cycles to failure.

Ductile iron. The design approach for ductile iron pressure pipe is given in AWWA C150. Various thickness classes are available. The required thickness is determined by considering stress due to internal pressure, ring deflection, and earth loads separately and independently.

Calculations are made for the thicknesses required to resist the bending stress and the deflection due to trench load. The larger of the two is selected as the thickness required to resist trench load. Calculations are then made for the thickness required to resist the hoop stress of internal pressure. The larger of these is selected as the net design thickness. To this net thickness is added a service allowance and a casting tolerance to obtain the total calculated thickness. The standard thickness and the thickness class for specifying and ordering are selected from a table of standard class thicknesses. The reverse of the above procedure is used to determine the rated working pressure and maximum depth of cover for pipe of given thickness class.

Trench load P_v. Trench load is expressed as vertical pressure, in pounds per square inch, and is equal to the sum of earth load P_e and truck load P_t.

Earth load P_e. Earth load is computed as the weight of the unit prism of soil with a height equal to the distance from the top of the pipe to the ground surface (prism load). The unit weight of backfill soil is taken to be 120 lb/ft^3. If the designer anticipates additional loads due to frost, the design load should be increased accordingly.

Truck load P_t. The truck loads are computed using the surface load factors for a single AASHTO H-20 truck on unpaved road or flexible pavement, with 16,000-lb wheel load and 1.5 impact factor.

The stress of the pipe invert produced by the total external loading is limited to 48,000 lb/in^2. This stress is the sum of the bending stress and the wall thrust stress. Wall stresses due to external loads are a function of this type of installation. Various installation types are considered in AWWA C150 with associated tables for stresses as a function of depth of cover.

The ring deflection is limited to 3 percent. This is a design condition independent of wall stress. Most ductile iron water pipes have a cement mortar lining. The 3 percent limitation is to protect that lining from cracking or spalling.

The wall stress due to internal pressure must be equal to or less than 21,000 lb/in^2. The yield stress in tension for ductile iron is approximately 42,000 lb/in^2. Thus, a design stress of 21,000 is based on a safety factor of 2.0.

The above procedure is not based on a combined loading analysis, and a combined loading criterion is not recommended. Each performance criterion is evaluated separately, and the controlling parameter dictates the design thickness.

The following is a summary of the design bases for ductile iron pipe:

Soil loading

Prism load + truck load (H-20 × impact)

Deflection

(A) Iowa formula (3 percent limit)

Stress due to soil loading

(B) Calculate stress at invert (limit 48,000 lb/in^2)

Stress due to internal pressure

(C) S (limit 21,000 lb/in^2) = PD/2t (P = working pressure + surge allowance)

Design procedure

1. Calculate the required thicknesses in steps (A), (B), and (C) above.
2. Subtract service allowance (corrosion) of 0.08 in from thickness found in (A), and compare with thickness found in (B) and (C) (largest value controls).
3. Add service allowance (0.08 in) for minimum thickness.
4. Add casting allowance for total thickness.

The net effect of the above procedure is to include a service allowance for stress considerations but not for deflection. The rationale for not including it for deflection is that the deflection limit is based not on the ductile iron, but on the lining.

Steel pipe. There are many types of steel pipe and many applications. AWWA M11 (steel pipe design and installation) adequately covers the design and installation procedures. A brief review is included here.

Steel pipe is, for the most part, designed for internal pressure and installed in such a manner that other design considerations, or limits, are met. The basic design procedure is as follows:

1. Design for pressure.
2. Calculate stiffness.
3. Design the soil system based on pipe stiffness, depth of cover, and performance limits.

Pressure design. Pressure design is based on the thin-walled pressure formula as follows:

$$S = \frac{PD}{2t} \qquad \text{or} \qquad t = \frac{PD}{2S}$$

where S = safe working stress (usually 50 percent of yield)
P = working pressure plus calculated surge
t = steel thickness

Determine stiffness. If the pipe is not cement-coated or lined, the stiffness is easily calculated.

$$\text{Stiffness} = EI = E\left(\frac{t^3}{12}\right)$$

where t = thickness determined from pressure design and E is usually 30×10^6 lb/in^2. For cement-lined and/or coated-steel pipe, the stiffness will be available from the manufacturer or can be determined experimentally. For pipes that are lined after installation, only the steel should be considered in any stiffness calculation.

Soil system design. The known parameters at this point in the design will be

1. Pipe performance limits, usually 2 percent deflection
2. Depth of cover
3. Pipe stiffness

The parameters to be determined are pipe zone soil type and soil density in pipe zone—embedment techniques, and so forth.

Recommended procedures. Loads may be calculated by Marston's Iowa formula for flexible pipe or by the prism load method. See Chaps. 2 and 3 for details.

Deflection is determined by using Spangler's Iowa formula, Watkins's soil strain method, or empirical data. Manufacturers' recommendations should be given serious consideration in this regard as many have developed tables for deflection from actual test data. Also, other standards such as AWWA C200 and AWWA C206 provide useful and pertinent information regarding installation design.

Buckling. Many steel pipelines are extremely flexible and may be subject to buckling or collapse from external pressure or internal vacuum. The engineer should consider buckling in the design and take appropriate action to eliminate it. Vacuum relief values may be necessary. Also, a stiffer pipe may be required (see the section "Wall Buckling" in Chap. 3).

Temperature and longitudinal stresses. Welded steel lines are subject to high-temperature-induced and other longitudinal stresses. Expansion joints and/or closure welds will reduce these stresses and may be required. AWWA M11 and AWWA C206 make specific recommendations concerning expansion joint and closure welds.

Fiber-reinforced plastic. Reinforced thermosetting resin pipes are widely used in the industrial market, but have gained very little acceptance in the U.S. public works market. Aside from the reinforcing aspect, such as fiberglass, the primary difference in these materials lies in the fact that thermosetting resins cannot be melted and re-formed whereas thermoplastic resin can. Members of the thermosetting plastic family include epoxy, polyester, and phenolic resins.

ASTM D 2996 is the standard specification for filament-wound reinforced thermosetting resin pipe. ASTM D 2997 is a standard specification for centrifugally cast reinforced thermosetting resin pipe. Within these standards, there are pipe designation codes and definitions.

ASTM D 2310 is the standard classification for machine-made reinforced thermosetting resin (RTR) pipe. This standard contains a complete definition of the various class and types of RTR pipes. It includes the following:

Manufacturing process:

- Type 1: Filament wound
- Type 2: Centrifugally cast
- Type 3: Pressure-laminated

Resin used:

- Grade 1: Glass-fiber-reinforced—epoxy
- Grade 2: Glass-fiber-reinforced—polyester
- Grade 3: Glass-fiber-reinforced—phenolic
- Grade 4: Asbestos-reinforced—polyester
- Grade 5: Asbestos-reinforced—epoxy
- Grade 6: Asbestos-reinforced—phenolic

Liner classification:

- Class A: No liner
- Class B: Polyester resin—nonreinforced
- Class C: Epoxy resin—nonreinforced
- Class D: Phenolic resin—nonreinforced
- Class E: Polyester resin—reinforced
- Class F: Epoxy resin—reinforced
- Class G: Phenolic resin—reinforced
- Class H: Thermoplastic resin

ASTM D 2992 is the standard method for obtaining hydrostatic design basis for reinforced thermosetting resin pipe and fittings. There are two procedures:

1. Procedure A: cyclic strength. This procedure is based on pipe failure at a minimum of 150×10^6 cycles at 25 cycles/min, 11.4 years.
2. Procedure B: static strength. This procedure is based on pipe failure at a minimum 100,000 h (11.4 years) of static pressure.

It is important to note that ASTM does not specify a service factor for RTR pipe. Therefore, it is up to the design engineer to determine the hydrostatic design basis to be used for a particular pipe. The product designation code, the manufacturer's product data, and ASTM standards make it easy to determine what safety factor is being employed at the recommended working pressure.

The hydrostatic design bases are listed in the applicable ASTM specifications. In the case of ASTM D 2996 for filament-wound RTR pipe, the following hydrostatic design base categories are listed:

Cyclic test method		Static test method	
Designation	Hoop stress, lb/in^2	Designation	Hoop stress, lb/in^2
A	2,500	Q	5,000
B	3,150	R	6,300
C	4,000	S	8,000
D	5,000	T	10,000
E	6,300	U	12,500
F	8,000	W	16,000
G	10,000	X	20,000
H	12,000	Y	25,000
		Z	31,500

Equation (4.3) can be utilized to calculate pressure ratings for RTR pipe.

An AWWA standard for glass-fiber-reinforced thermosetting resin pressure pipe, AWWA C950, was first approved in 1981. It incorporates information from the ASTM standards discussed above.

AWWA C950 can be summarized as follows:

Manufacturing processes:
- Type I filament-wound
- Type II centrifugally cast

Resins: Epoxy and polyester for RTRP and RPMP construction

Liners: none, thermoplastic, reinforced thermoset, nonreinforced thermoset

Size range: 1 to 144 in

Diameters: inside diameters, outside diameters (IPS), outside diameter (CI), metric dimensions

Pressure classes: 50, 100, 150, 200, 250, and over 250 lb/in^2

Hydro safety factors—service and distribution pipe:
- 2-to-1 (including surge)
- Transmission pipe 1.4-to-1 (including surge)

Strains induced by combined loading in buried pressurized flexible pipe

Introduction. It is well known that flexible pipe deflects under normal installation and when pressurized, it rerounds, which reduces the bending strains. Studies of the combined strain behavior of flexible pipe have been reported in the literature, and a summary is presented here.

Also, results are compared to the AWWA (ANSI/AWWA C950-81) standard. The comparison shows that there exists a discrepancy in the region where Spangler's curve and Molin's curve cross. Note that the discussion on combined loading found in AWWA C950-81 has been omitted from AWWA C950-95, which is the current version at the writing of this book.

Tests. A test program was run at Utah State University to determine the rerounding behavior when a buried flexible pipe is pressurized. The test design permitted the efficient study of many variables simultaneously. Variables for this program were haunch type, pipe stiffness, soil compaction, and initial pipe deflection as controlled by overburden pressure.

The pipe and measuring device. In the 6-in-diameter pipe, a single linear variable differential transformer (LVDT) was mounted on a shaft that could be rotated. The LVDT and shaft were enclosed in a rubber bladder that was reinforced with a rubberized canvas covering on the outside of the rubber bladder. The entire mechanism was then placed inside the pipe. It was, therefore, possible to start the shaft and trace out the profile of the pipe. The LVDT readings were digitized via a data acquisition system and passed to a computer where they were analyzed for cross-sectional shape and bending strain. Bending strains were determined by comparing the initial shape profile with the loaded profile. The pipe and assembly were buried in a soil load cell, and the vertical load was applied by hydraulic cylinders. Water was pumped through the hose to the bladder to pressurize the pipe.

Test procedure. Before each test, the soil moisture content was brought to an acceptable range (7 to 10 percent). Soil was then compacted in layers, and the soil density was determined for each layer.

Initially, when the pipe was placed in the cell with no overburden, the pipe was pressurized to 25 lb/in^2. Then a set (four) of pipe profiles was taken. The pressure in the pipe was maintained until the cell was loaded with soil, the loading plate was placed on the soil, and the hydraulic loading cylinders were placed. Before any hydraulic pressure was applied to the cylinders, the 25 lb/in^2 pressure was removed from the pipe and another set of profiles was taken.

The process of loading the cell was accomplished in four steps. For each test, the desired surface load was converted to the appropriate pressure required by the hydraulic cylinders to produce that load. This pressure was then divided into approximately four equal steps. After the pressure reached the value at each step, the readings from the profilometer were monitored and that pressure was maintained until the profilometer reading quit changing for approximately 1 min. This process took up to 5 min depending on the step size and relative density of the soil.

When the appropriate soil load was achieved and the profilometer readings had stabilized, another set of profiles was taken. At this point, internal pressure was applied to the pipe, using pressurized water. The internal pressure was added in 25 lb/in^2 increments from 0 to 125 lb/in^2. After each increment, a set of profiles was taken after the profilometer had stabilized and a constant internal pressure was achieved. At the completion of the test, the surface and internal loads were removed, and the cell was unloaded.

The majority of the tests were run using silty sand. The optimum moisture content for this soil was 10 percent. All the poor haunch tests were run using this soil. To obtain a poor haunch, special care was taken not to compact the soil near the pipe from the base of the pipe to approximately one-third of the distance to the pipe spring line.

Finite element modeling of rerounding. The ability for the FEA code to handle unloading and reloading of soil was added. This allows for a soil element to be in either tension or compression and to respond correctly when the load is reversed. This characteristic is needed to model soil as it is unloaded when the internal pressure begins to pull the pipe away from the soil. The FEA model was successful for tests where the soil density was at least 90 percent Proctor density. There was some difficulty in modeling rerounding for a poor haunch condition in loose soils. Figure 4.23 is a graphical comparison of bending strain as predicted by FEA with test data. There is reasonable agreement. The bending strains shown are for the pipe's outside surface. Figure 4.24 shows FEA data only. It clearly shows the change in both bending and thrust strains as the internal pressure is changed from 0 to 120 lb/in^2.

Residual bending strain data. The data are tabulated in Tables 4.8 and 4.9 and plotted in Figs. 4.25 to 4.29 for rerounding coefficient $R = \varepsilon_P/\varepsilon_I$, where ε_P is the bending strain at a given pressure and ε_I is the initial bending strain. As expected, the general trend is that R decreases as pressure increases. Note that the strains given in Tables 4.8 and 4.9 do not necessarily occur at the same circumferential location on the pipe as pressure increases. As the pipe rerounded, it could change shape slightly, causing the maximum strain to shift location. Thus, the rerounding coefficient is computed by using the ratio of the maximum measured strain at any given pressure to the maximum initial bending strain.

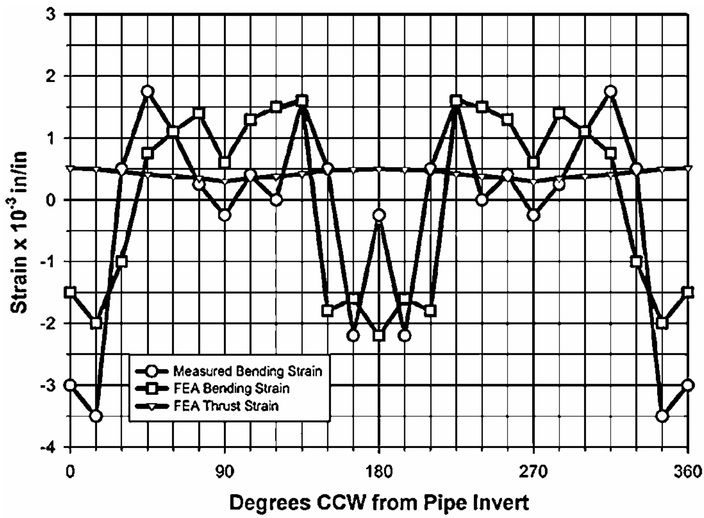

Figure 4.23 Rerounding data for pipe buried 20 ft deep in silty-sand soil compacted to 80 percent of Proctor density. Pipe stiffness = 36 lb/in^2. Internal pressure is 100 lb/in^2.

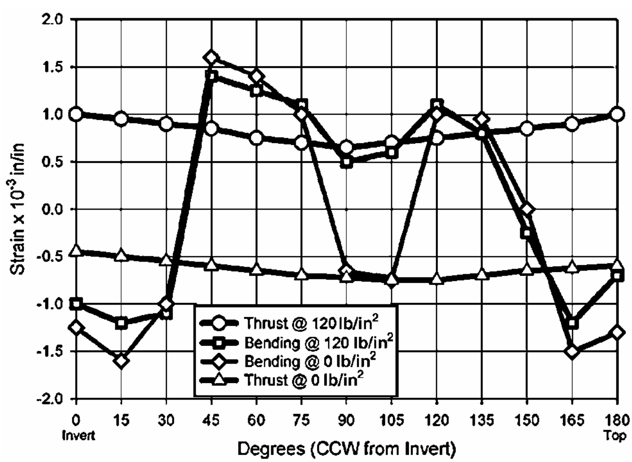

Figure 4.24 FEA rerounding data for pipe buried 20 ft deep in silty-sand soil compacted to 80 percent of Proctor density. Pipe stiffness = 36 lb/in^2.

TABLE 4.8 Poor Haunch

Test no.	Proctor density, percent	Pipe stiffness, lb/in^2	Cover, ft	Initial deflection, percent	Internal pressure, lb/in^2					
					0	25	50	75	100	125
					Strain					
PH1	90	13	10.00	2.90	4,533	3,373	3,776	3,312	2,058	1,649
PH2	85	92	10.00	7.90	11,094	14,601	10,131	8,074	8,222	7,318
PH3	80	92	10.00	10.20	9,916	10,356	9,883	8,500	8,456	6,759
PH4	80	5	3.00	3.00	3,839	3,376	2,355	1,929	1,367	1,239
PH5	80	13	3.00	4.00	6,425	5,559	5,604	5,201	4,769	4,052
PH6	80	35	6.50	7.70	12,331	11,068	11,083	8,330	7,303	6,493
PH7	80	92	5.58	5.38	8,103	8,246	6,977	7,423	6,697	6,759
PH8	80	35	6.50	7.70	11,028	9,732	6,405	8,438	8,486	7,299
PH9	80	35	6.50	6.50	10,381	9,529	9,228	8,727	6,960	6,360
PH10	80	92	5.50	8.70	17,776	16,777	12,988	12,157	9,946	9,255
PH11	85	92	6.50	5.20	11,716	11,597	10,925	8,915	7,749	7,533
					Rerounding coefficient $R = \varepsilon_P/\varepsilon_I$					
PH1	90	13	10.00	2.90	1.00	0.74	0.83	0.73	0.45	0.36
PH2	85	92	10.00	7.90	1.00	1.32	0.91	0.73	0.74	0.66
PH3	80	13	10.00	10.00	1.00	1.04	1.00	0.86	0.85	0.68
PH4	80	5	3.00	3.80	1.00	0.88	0.61	0.50	0.36	0.32
PH5	80	13	3.00	4.00	1.00	0.87	0.67	0.81	0.74	0.63
PH6	80	35	6.50	7.70	1.00	0.90	0.50	0.68	0.59	0.53
PH7	80	92	5.50	5.30	1.00	1.02	0.85	0.92	0.83	0.83
PH8	80	35	6.50	7.70	1.00	0.88	0.58	0.77	0.76	0.66
PH9	80	35	6.50	6.50	1.00	0.92	0.89	0.84	0.67	0.61
PH10	80	92	5.50	5.70	1.00	0.94	0.73	0.68	0.55	0.52
PH11	85	92	6.50	5.20	1.00	0.99	0.93	0.76	0.66	0.64

TABLE 4.9 Complete Haunch

Test no.	Proctor density, percent	Pipe stiffness, lb/in^2	Cover, ft	Initial deflection, percent	Internal pressure, lb/in^2					
					0	25	50	75	100	125
					Strain					
CH1	80	5	3.00	1.60	1,700	1,700	1,800	1,200	1,000	—
CH2	85	13	6.50	4.50	4,954	5,300	4,669	4,526	3,691	3,326
CH3	85	13	6.50	4.90	5,377	4,672	4,095	3,956	3,557	3,453
CH4	85	13	6.50	4.40	3,651	3,247	3,469	3,587	3,359	4,664
CH5	85	92	6.50	3.20	4,807	4,363	3,921	333	2,589	2,348
CH6	85	92	10.00	7.60	2,763	6,222	4,333	2,923	—	—
CH7	95	13	10.00	1.90	2,288	1,947	1,897	1,789	1,488	1,426
CH8	95	92	10.00	2.40	5,037	4,769	4,805	4,516	4,206	3,634
					Rerounding coefficient $R = \varepsilon_P/\varepsilon_I$					
CH1	80	5	3.00	1.60	1.00	1.00	1.06	0.71	0.59	0.36
CH2	85	13	6.50	4.50	1.00	1.07	0.94	0.91	0.75	0.67
CH3	85	13	6.50	4.50	1.00	0.87	0.76	0.74	0.65	0.64
CH4	85	13	6.50	4.40	1.00	0.89	0.95	0.98	0.92	—
CH5	85	92	6.50	3.28	1.00	0.51	0.82	0.69	0.54	0.49
CH6	85	92	10.00	7.60	1.00	2.25	1.57	1.05	—	—
CH7	95	13	10.00	1.50	1.00	0.85	0.83	0.78	0.65	0.62
CH8	95	92	10.00	2.40	1.00	0.95	0.95	0.90	0.84	0.72

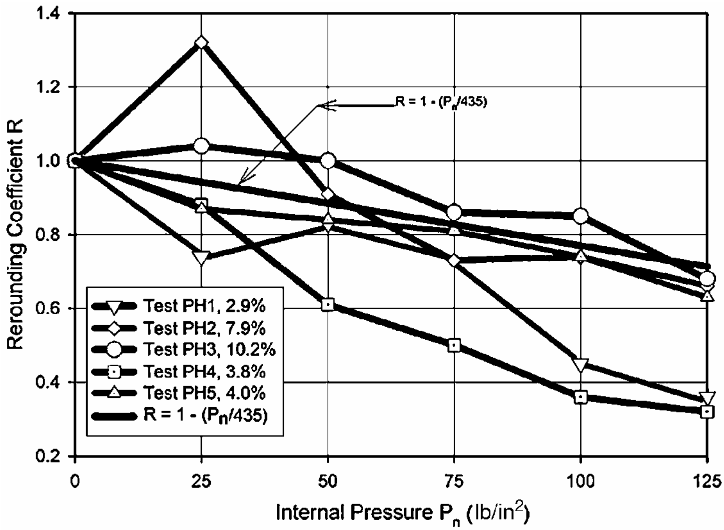

Figure 4.25 Rerounding coefficient from test data—poor haunch condition.

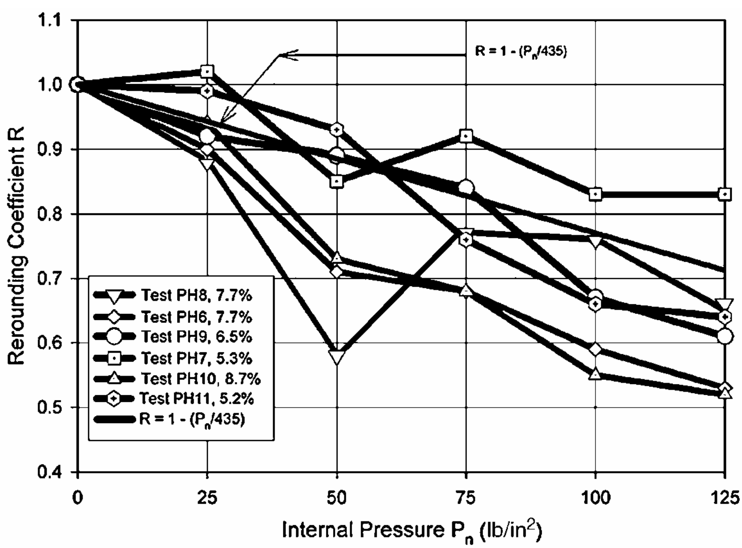

Figure 4.26 Rerounding coefficient from test data—poor haunch condition.

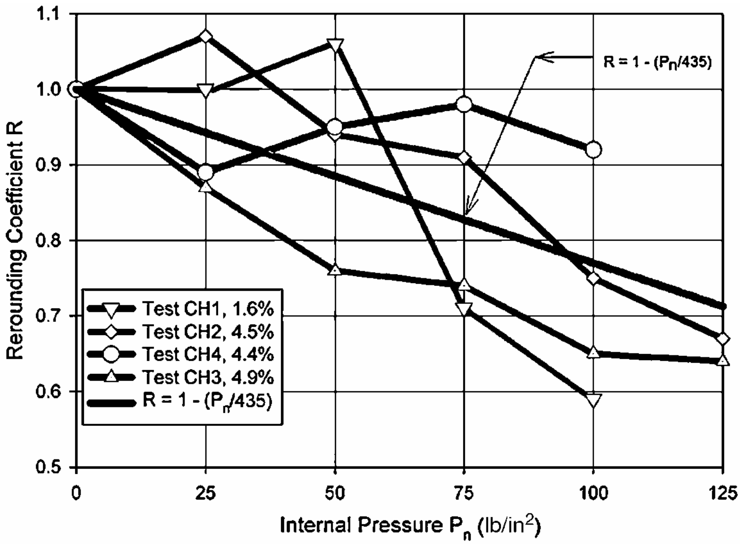

Figure 4.27 Rerounding coefficient from test data—poor haunch condition.

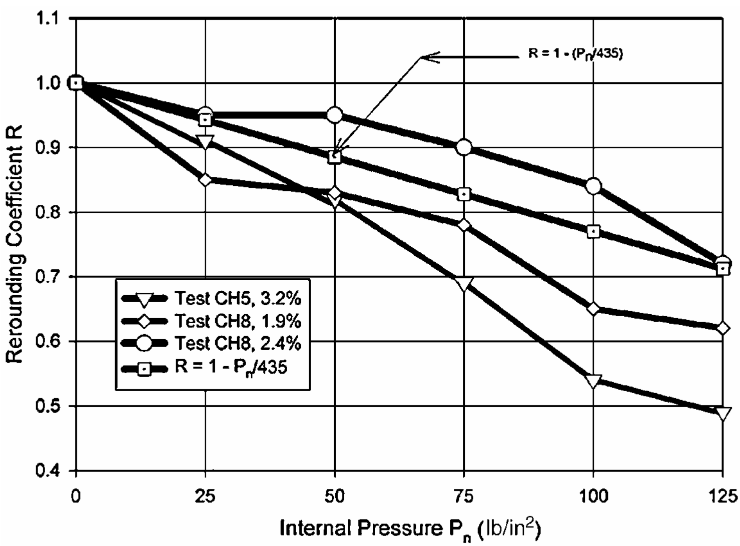

Figure 4.28 Rerounding coefficient from test data—complete haunch condition.

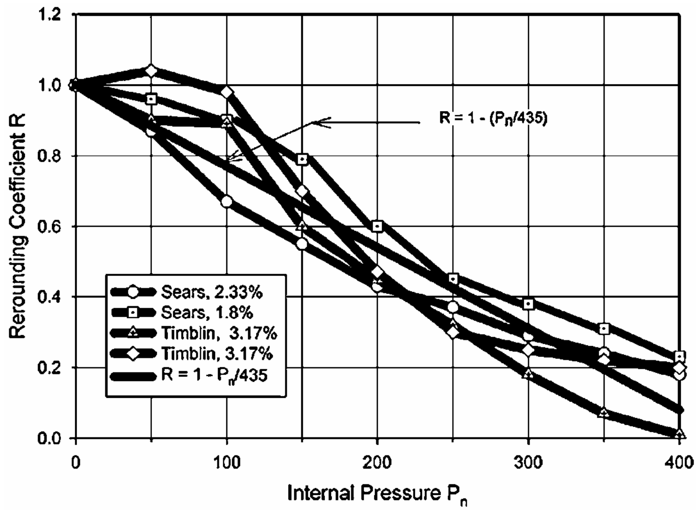

Figure 4.29 Rerounding coefficient from test data on both ductile iron and FRP pipes.

Other data. A review of literature shows that data from rerounding tests conducted on full-scale installations[7,8,19] correlate well with test data obtained from the Utah State University experiments. Table 4.10 data from these references are plotted in Fig. 4.29.

For the Cole and Timblin data,[8] the rerounding coefficients were computed by backing out the calculated pressure strain from the total measured strain plotted in Fig. 4.29.[8] For the Sears data,[19] the rerounding coefficient was computed by using deflection data and differential bending stress data given in Table 4.9,[19] both giving similar results. These coefficients are shown in Table 4.10. For the Carlstrom data[7] the rerounding coefficients were taken from his picture 12.[7]

Observations. Observations from the data tables and the rerounding plots are as follows:

1. Poor and complete haunches permit about the same rerounding to slightly more for the poor haunch type, as shown in Tables 4.8 and 4.9. Note that initial bending strain will be less for complete haunch since it will have a more elliptical shape and a lower D_f factor for use in the bending strain equation.

$$\varepsilon_b = D_f\left(\frac{\Delta y}{D}\right)\left(\frac{t}{D}\right) \tag{4.20}$$

TABLE 4.10 Rerounding Coefficient

Ref.	Δ/D	D	Pipe stiffness, lb/in^2	Pipe mat.	Backfill	Cover depth, ft	Pressure, lb/in^2: 50	100	200	300	400	Remarks
							Rerounding coefficient R					
8	3.17	48	30.5	FRP	Loose dry sand	12.8	1.04	0.98	0.47	0.25		
							0.90	0.89	0.45	0.16		
19	2.0	36	247.0	Ductile iron	Native soil 90% Proctor	8.0	0.87	0.67	0.44	0.29	0.18	1961
							0.96	0.90	0.60	0.38	0.23	1963
7	2.2	35+	97.3	FRP	Native soil	6.6	$R = 0.43$ @ 350 lb/in^2 (initial)					
						11.5	$R = 0.39$ @ 350 lb/in^2 (2 weeks)					

2. The maximum residual bending strains occur when the starting deflections are highest, as shown in Tables 4.8 and 4.9.
3. Rerounding is generally insensitive to soil type, compaction, or pipe stiffness, as shown by all data sets.
4. Rerounding increases steadily, as an approximately linear function of internal pressure, as shown by all data sets. The rerounding factor R may be conservatively approximated as

$$R = 1 - \frac{P_n}{435} \tag{4.21}$$

where P_n = internal pressure, lb/in² ($0 < P_n < 435$).

5. The rerounding coefficients reduce somewhat with time, as seen from the Carlstrom data.[7]

Discussion. A combined loading analysis is outlined in Appendix A of AWWA C950-81. Two methods are given for calculating the combined stresses and strains. One method has been attributed to Spangler and the other to Molin. Both equations are to be used, and the lowest value is the resulting combined stress and/or strain. This lowest value must not exceed the long-term bending strength of the product reduced by a design factor. The method permits the rerounding of a deflected pipe due to internal pressure to be considered when computing the total combined strain in the pipe. The combined strain is taken as the lesser value computed using Eqs. (4.22) and (4.23) by Molin and Spangler.

$$\varepsilon = \frac{PD}{2tE} + 6\left(\frac{t}{D}\right)\left(\frac{\Delta y}{D}\right) \tag{4.22}$$

$$\varepsilon = \frac{PD}{2tE} + \frac{3K_bWDt}{3K_xPD^3 + Et^3} \tag{4.23}$$

Figure 4.30 shows a typical plot of the AWWA C950-81 combined strains versus internal pressure. Research indicates that this procedure is conservative. The dashed line is typical pipe behavior as observed in all data sets from actual tests. The correlation between test data and the AWWA C950 method is generally acceptable. However, at low to intermediate pressure, particularly in the region where the Spangler and Molin curves cross, there is some discrepancy.

Also shown on Fig. 4.30 (dashed line) is typical pipe behavior as observed in all data sets. There is generally good correlation between

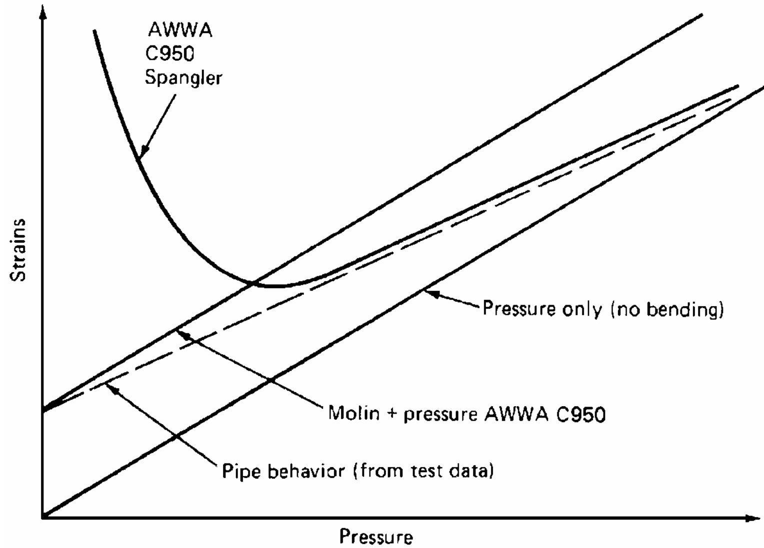

Figure 4.30 Typical plot for combined strains.

the AWWA C950-81 method and the observed pipe behavior except at the lower pressures and particularly in the region where the Spangler and Molin curves intersect.

Conclusions

1. Rerounding is influenced mostly by internal pressure and possibly to some extent by time.
2. It has been shown that rerounding is generally insensitive to soil density, burial depth, pipe stiffness, and pipe material.
3. Maximum combined strains occur when starting deflections are highest.
4. Rerounding generally increases linearly with increasing internal pressure and may be represented by the rerounding factor R computed as follows:

$$R = 1 - \frac{P_n}{435} \tag{4.24}$$

It was found that rerounding is primarily a function of pressure, and a rerounding relationship is proposed which accounts for the reduction of bending strain as pressure increases. It was also found that the highest allowable deflection for a pipe determines the calculated behavior since the residual bending strain for an initial highly deflected pipe is more than the residual strain for a low initial deflected pipe.

Recommendation. Combined strain should be calculated as follows:

$$\varepsilon_C = \frac{PD}{2tE} + RD_f\left(\frac{t}{D}\right)\left(\frac{\Delta y}{D}\right) \tag{4.25}$$

where ε_C = combined strain
D_f = shape factor, from 3 to 8 (3 for uniform compaction and a pipe stiffness greater than 40 lb/in^2, 6 for poor haunch or nonuniform compaction, 8 for nonuniform compaction and pipe stiffness less than 15 lb/in^2)
R = rerounding factor = $1 - P_n/435$
P = internal pressure
t = wall thickness
E = Young's modulus
D = pipe diameter
Δy = vertical pipe deflection
P_n = internal pressure, lb/in^2 ($0 < P_n < 435$)

Thrust restraint

Unbalanced hydrostatic and hydrodynamic forces in piping systems are called *thrust* forces. In the range of pressures and fluid velocities found in waterworks or wastewater piping, the hydrodynamic thrust forces are generally insignificant in relation to the hydrostatic thrust forces and are usually ignored. Simply stated, thrust forces occur at any point in the piping system where the direction or cross-sectional area of the waterway changes. Thus, there will be thrust forces at bends, reducers, offsets, tees, wyes, dead ends, and valves.

Balancing thrust forces in underground pipelines is usually accomplished with bearing or gravity thrust blocks, restrained joint systems, or combinations of these methods. The internal hydrostatic pressure acts perpendicularly on any plane with a force equal to the pressure P times the area A of the plane. All components of these forces, acting radially within a pipe, are balanced by circumferential tension in the wall of the pipe. Axial components acting on a plane perpendicular to the pipe through a straight section of the pipe are balanced internally by the force acting on each side of the plane. Consider, however, the case of a bend, as shown in Fig. 4.31.

The forces PA acting axially along each leg of the bend are not balanced. The vector sum of these forces is shown as T. This is the thrust

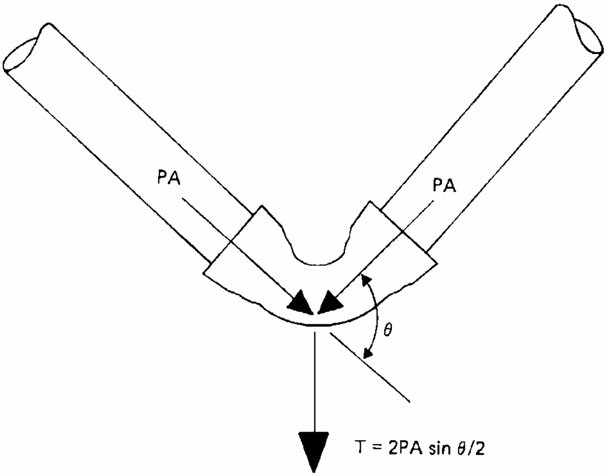

Figure 4.31 Thrust force. (*Reprinted from Thrust Restraint Design for Ductile Iron Pipe, by permission of the Ductile Iron Pipe Research Association.*)

force. To prevent separation of the joints, a reaction equal to and in the opposite direction of T must be established.

Figure 4.32 depicts the net thrust force at various other configurations. In each case, the expression for T can be derived by the vector addition of the axial forces.

Thrust blocks. For buried pipelines, thrust restraint is achieved by transferring the thrust force to the soil structure outside the pipe. The objective of the design is to distribute the thrust forces to the soil structure in such a manner that joint separation will not occur in unrestrained joints.

Figure 4.33 shows standard types of thrust blocking commonly used in pressurized water systems.

Table 4.11 displays the thrust which may develop at fittings and appurtenances for each 100 lb/in^2 of internal pressure. These are approximate values. Thrusts from greater or lesser pressures may be proportioned accordingly. The largest thrust may result from the test pressure, which is usually higher than the operating pressure.

One method for sizing thrust blocks uses assumed soil bearing values. Table 4.12 gives approximate allowable bearing loads for various types of soil. These allowable bearing loads are estimates only, for horizontal thrusts, and for pipe buried 2 ft deep or deeper. When doubt exists, safe bearing loads should be established by soil bearing tests.

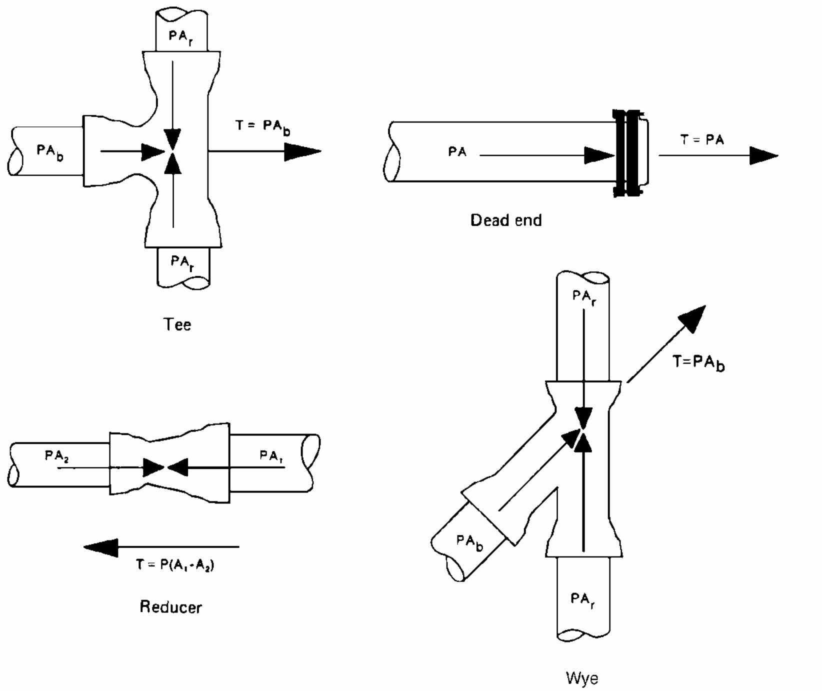

Figure 4.32 Thrust forces. (*Reprinted from Thrust Restraint Design for Ductile Iron Pipe, by permission of the Ductile Iron Pipe Research Association.*)

The design calculation of a thrust block is illustrated in the next example.

Example Problem 4.2 Required is thrust block at 10-in 90° elbow. Maximum test pressure is 200 lb/in^2. Soil type is sand and gravel with clay.

- Calculate thrust. From Table 4.11, thrust on 10-in 90° elbow is 13,680 lb per 100 lb/in^2 operating pressure. Total thrust = 2(13,680) = 27,360 lb.
- Calculate thrust block size. From Table 4.12, safe bearing load for sand and gravel with clay is 2000 lb/ft^2; total thrust support area = 27,360/2000 = 13.68 ft^2.
- Select type of thrust block. From Fig. 4.33, select type 3.

Restrained joints. An alternate method of thrust restraint uses restrained joints. Various mechanical locking-type joints are available to provide longitudinal restraint. Of course, a welded steel joint is considered to be rigid and provides maximum longitudinal restraint.

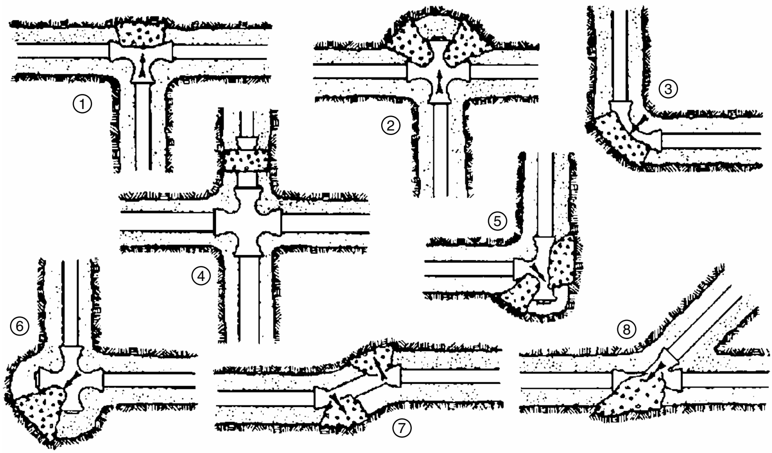

If thrusts, due to high pressure, are expected, anchor valves as below. At vertical bends, anchor to resist outward thrusts.

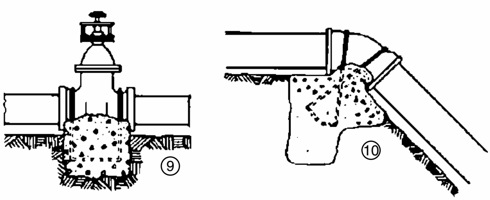

1. Through line connection, tee
2. Through line connection, cross used as tee
3. Direction change, elbow
4. Change line size, reducer
5. Direction change, tee used as elbow
6. Direction change, cross used as elbow
7. Direction change
8. Through line connection, wye
9. Valve anchor
10. Direction change vertical, bend anchor

Figure 4.33 Types of thrust blocking. (*Reprinted from Handbook of PVC Pipe,*[21] *by permission of the Uni-Bell PVC Pipe Association.*)

Restrained joint systems are subjected to the same thrust forces, but these forces are resisted or distributed over the restrained pipe length. The necessary length of restrained pipe interacting with the soil may be determined by the design engineer. Referring to Fig. 4.34, the restrained length on each side of the joint is L. The frictional resistance and bearing resistance are given by F_s and R_b, respectively. Summation of forces results in the following:

$$PA \sin \frac{\theta}{2} = F_s L \cos \frac{\theta}{2} + \frac{1}{2} R_b L \cos \frac{\theta}{2}$$

or

$$L = \frac{PA \tan (\theta/2)}{F_s + R_b/2}$$

TABLE 4.11 Thrust Developed per 100 lb/in² Pressure

Pipe size, in	Fitting 90° elbow, lbf	Fitting 45° elbow, lbf	Valve tees dead ends, lbf
4	2,560	1,390	1,810
6	5,290	2,860	3,740
8	9,100	4,920	6,430
10	13,680	7,410	9,680
12	19,350	10,470	13,690
14	26,010	14,090	18,390
16	33,640	18,230	23,780
18	42,250	22,890	29,860
20	51,840	28,090	36,640
24	73,950	40,070	52,280
30	113,770	61,640	80,420
36	162,970	88,310	115,210

TABLE 4.12 Estimated Bearing Load

Soil type	lb/ft²
Muck, peat, etc.	0
Soft clay	500
Sand	1000
Sand and gravel	1500
Sand and gravel with clay	2000
Sand and gravel cemented with clay	4000
Hard pan	5000

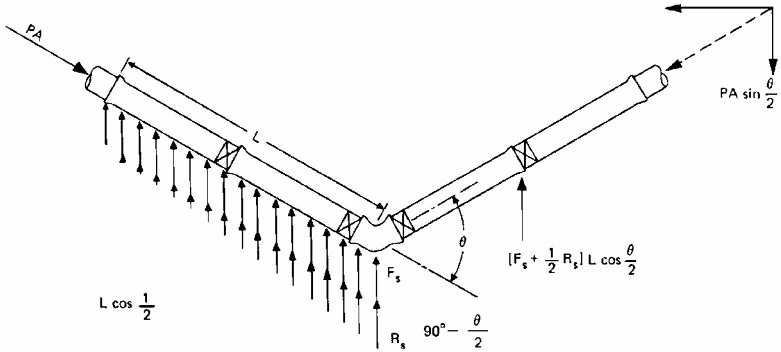

Figure 4.34 Free-body diagram for pipe with restrained joints. (*Reprinted from Thrust Restraint Design for Ductile Iron Pipe, by permission of the Ductile Iron Pipe Research Association.*)

where P = internal pressure
A = cross-sectional area of pipe
F_s = frictional force
F_b = bearing force

For a cohesionless soil, the friction force F_s may be calculated as follows:

$$F_s = W \tan \gamma$$

where $W = 2W_e + W_p$
$\gamma = f_\phi \phi$
W_e = total soil load
W_p = weight of pipe plus water
f_ϕ = friction factor between pipe and soil
ϕ = internal friction angle of soil

The above method will generally produce conservative results. If cohesion is present, cohesive forces will also be involved, which will make results even more conservative. However, since cohesive forces are time-dependent, it is recommended that they be neglected.

Safety factors

Design of pressure pipe is based upon certain performance limits such as long-term hydrostatic burst pressure and/or crush load acting either independently or simultaneously. The allowable total stress or strain is equal to the failure stress or strain reduced by a safety factor. For example,

$$\sigma_A = \frac{\sigma_f}{\text{SF}} \qquad \text{or} \qquad \varepsilon_A = \frac{\varepsilon}{\text{SF}}$$

where σ_A = allowable stress
σ_f = failure stress
ε_A = allowable strain
ε_f = failure strain
SF = safety factor

The total working stress/strain must be equal to or less than the allowable stress/strain. If a combined loading analysis is not required, stresses due to internal pressure and external loads are evaluated separately, and the safety factor is applied to the largest value. For combined loading, the safety factor is applied to the combined stress.

For nonlinear failure theories such as the Schlick formula, safety factors must be applied to both internal pressure and external load. These two factors need not be equal.

For plastic pipe, the design is based on life rather than a failure stress. As previously discussed in this chapter, a hydrostatic design basis (stress) is established on the basis of a life of 100,000 h. The design stress is the hydrostatic design basis reduced by a factor of safety. A factor of safety of 2.0 will give, essentially, infinite life since the stress regression curve is linear on a log-log plot (see Fig. 4.6).

Standards for each pipe product may list recommended safety factors. Also, manufacturers often recommend certain safety factors for their products. The bases for the calculations of these are often quite different. The design engineer should be aware of these differences when comparing products and should always have the option of requiring a safety factor that is different from the recommended value. The need for safety factors arises mainly from uncertainties. These uncertainties are due to causes ranging from the pipe manufacturer to the pipe installation conditions. The greater the uncertainty, the higher the safety factor should be. The engineer should be very cautious in utilizing safety factors that are lower than those recommended by national standards or by the manufacturer.

References

1. ASTM. 1976. *Standard Method of Test for Time-to-Failure of Plastic Pipe under Long-Term Hydrostatic Pressure*, ASTM D 1598. Philadelphia.
2. American Water Works Association. AWWA Standards M11, M9, M23, C150, C200, C206, C300, C301, C303, C400, C401, C402, C403, C900, C901, and C950. Denver, Colo.
3. Andrews, James S. 1970. Water Hammer Generated during Pipeline Filling. Master's thesis. Fort Collins: Colorado State University.
4. Bair, D. A. 1984. Analysis of Strain vs. Internal Pressure of Buried FRP Pipe from Tests and Finite Element Modeling. Master of science thesis. Logan: Utah State University.
5. Bishop, R. R. 1983. *Course Notebook.* Logan: Utah State University.
6. Bowman, J. A. 1990. The Fatigue Response of Polyvinyl Chloride and Polyethylene Pipe Systems. *Buried Plastic Pipe Technology, ASTM STP 1093.* Eds. George S. Buczala and Michael J. Cassady. Philadelphia: American Society for Testing and Materials.
7. Carlstrom, B. I. 1981. Structural Design of Underground GRP Pipe. Paper presented at the International Conference of Underground Plastic Pipe, New Orleans. March.
8. Cole, B. W., and L. O. Timblin, Jr. 1981. Strain Calculations for FRP Pressure Pipe. Paper presented at the International Conference on Underground Plastic Pipe, New Orleans. March.
9. Devine, Miles. 1980. *Course Notebook.* Logan: Utah State University.
10. Ductile Iron Pipe Research Association. 1984. *Thrust Restraint Design for Ductile Iron Pipe.* Birmingham, Ala.
11. Hucks, Robert T. 1972. Design of PVC Water Distribution Pipe. *Civil Engineering ASCE* 42(6):70–73.

12. Jeppson, Roland W., Gordon H. Flammer, and Gary Z. Watters. 1972. Experimental Study of Water Hammer in Buried PVC and Permastran Pipes. PRWG0113-1. March. Logan: Utah Water Research Laboratory/College of Engineering, Utah State University.
13. Jeppson, Roland W., Gordon H. Flammer, and Gary Z. Watters. 1972. Experimental Study of Water Hammer in Buried PVC and Permastran Pipes. April. Logan: Utah Water Research Laboratory/College of Engineering, Utah State University.
14. Kerr, S. Logan. May 1985. Water Hammer—A Problem in Engineering Design. *Consulting Engineer.*
15. Lamé, G. 1852. Leçons sur la théorie delasticité. Paris: Gauthier-Villars.
16. Marshall, G. P., S. Brogden, and M. A. Shepherd. 1998. Evaluation of the Surge and Fatigue Resistance of PVC and PE Pipeline Materials for Use in the U.K. Water Industry. Water, U.K.
17. Moser, A. P. 1983. *Course Notebook.* Logan: Utah State University.
18. Moser, A. P., John Clark, and D. P. Bair. 1985. Strains Induced by Combined Loading in Buried Pressurized Fiberglass Pipe. In *Proceedings ASCE International Conference on Advances in Underground Pipeline Engineering.* Madison, Wis.: American Society of Civil Engineers.
19. Sears, Edward C. 1964. Ductile Iron Pipe. *AWWA Journal,* January, p. 12, Table II.
20. Streeter, Victor L. 1958. *Fluid Mechanics,* 2d ed. New York: McGraw-Hill, pp. 175–187.
21. Uni-Bell PVC Pipe Association. 1991. *Handbook of PVC Pipe.* 3d ed. Dallas.
22. Vinson, H. W. 1981. Response of PVC Pipe to Large, Repetitive Pressure Surges. In *Proceedings of the International Conference on Underground Plastic Pipe.* New York: American Society of Civil Engineers.
23. Walker, Robert P. 1983. *Course Notebook.* Logan: Utah State University.
24. Watters, G. Z. 1971. The Behavior of PVC Pipe under the Action of Water Hammer Pressure Waves. PRWG-93. Logan: Utah Water Research Laboratory, Utah State University.

Chapter

5

Rigid Pipe Products

Chapter 5 deals with various generic rigid pipe products. For each product, selected standards and material properties are listed. The standards are from standard organizations such as the American Water Works Association (AWWA) and American Society for Testing and Materials (ASTM). Actual design examples for the various products are given in this chapter.

Asbestos-Cement Pipe

Asbestos-cement (AC) pipes are available for both gravity and pressure applications (see Tables 5.1 and 5.2). Because of the health risks associated with the handling of asbestos, AC pipe production in the United States has come to a complete halt. It is still produced in some countries and is available in some parts of the United States. This product has some flexibility, especially for lower classes (thinner walls). However, it is generally considered to be a rigid pipe product; therefore, the rigid pipe design method should be used for AC pipe installations.

Asbestos-cement pipes are manufactured from asbestos, cement, silica, and water. The pipe-making machine places this mixture on a polished steel mandrel, and it is pressure-steam-treated (autoclaved) to achieve curing with less than 1 percent uncombined calcium hydroxide (free lime). AC pipes which have less than 1 percent free lime are designated as type 2. Type 2 AC pipes are generally resistant to all levels of soluble sulfates, but will be attacked by acids with a pH level of 5.0 or less. Type 1 pipes have more than 1 percent free lime and are generally not resistant to either soluble sulfates or acids.

Asbestos-cement pipes are joined via rubber-gasketed couplings. The pipe has a hard and fairly smooth internal surface. A Hazen-

TABLE 5.1 Properties and Design Constants

Modulus of elasticity	3.0×10^6 lb/in^2
Tensile strength	3000–4000 lb/in^2
Shear strength	4000 lb/in^2 across pipe axis
Modulus of rupture (MR)	5000–6000 lb/in^2 (bending strength in crush)
Compressive strength	7000 lb/in^2
Thermal conductivity	$K = 5.5$ (Btu·in)/(h·°F·ft^2), 4 when perfectly dry
Thermal coefficient of expansion	4–5 $\times 10^{-6}$ in/(in/°F)
Specific heat	0.27 Btu/(lb·°F) @ 212°F
Moisture coefficient of expansion	1.5–2.0 $\times 10^{-5}$ in/(in/% moisture change) (moisture content is 6 to 7% for normal atmospheric conditions and 15 to 20% for fully saturated conditions)
Hazen-Williams coefficient	$C = 140$
Manning's coefficient	$n = 0.010$

TABLE 5.2 Applicable National Standards

AWWA C400	Asbestos-cement distribution pipe, 4 in through 16 in
AWWA C401	Standard practice for the selection of asbestos-cement distribution pipe
AWWA C402	Standard for asbestos-cement transmission pipe 18 in through 42 in
AWWA C403	Standard practice for the selection of asbestos-cement transmission and feeder main pipe, sizes 18 in through 42 in
AWWA C603	Standard for installation of asbestos-cement water pipe
ASTM C 296	Asbestos-cement pressure pipe
ASTM C 428	Asbestos-cement nonpressure sewer pipe
ASTM C 460	Standard definitions of terms relating to asbestos-cement and related products
ASTM C 500	Standard methods of testing asbestos-cement pipe
ASTM C 663	Asbestos-cement transmission pipes
ASTM D 1869	Specification for rubber rings for asbestos-cement water pipe
Federal Specification SS-P-351c	Specification for pipe, asbestos-cement for under-water pressure
Bureau of Yards and Docks, Navdocks, DM-5	U.S. Navy *Civil Engineering Design Manual* (includes asbestos-cement pressure pipe)
Canadian Standards Association	
CSA B127.1	Components for use in AC drain, waste, and vent (DWV) systems
CSA B122.2	Components for use in AC building sewer systems
CSA B127.11	Recommended practice for the installation of AC DWV pipe and fittings

Williams coefficient of 140 and a Manning coefficient of 0.010 should be used for long-term design. AC pipe can be tapped for water service. Also, various fittings are available for connections. Field cutting for repairs and/or installation is possible. Appropriate safety precautions should be followed to protect workers from airborne asbestos dust. Manufacturer's safety procedures should be followed.

The asbestos-cement-silica composite achieves a remarkably high tensile strength of up to 4000 lb/in². This high strength is directly attributable to the asbestos fiber reinforcement. AC pipe is durable and has been operating in pipelines for more than 45 years. AC pipes are not as prone to impact damage as some rigid pipes; nevertheless, care should be taken in handling. When excavating to make connections to or in repairing AC pipes, care must be taken to prevent the backhoe bucket from damaging the line. For water systems, AC pipes are available for both transmission and distribution systems. They are also available for various specialty applications.

Example 5.1—Gravity storm sewer A 36-in-diameter storm sewer line is to be installed. It passes through a small hill which requires a trench 20 ft deep. Native material, a silty sand with clay, will be used for final backfill. The trench width at the top of the pipe is not to exceed 7 ft. Calculate the minimum strength of asbestos-cement pipe for both B and C bedding. Also, what strength will be required for a possible "worst case" if the trench width exceeds the transition width and only C bedding is achieved? Groundwater is 10 ft below the surface. (See Chap. 2 for design criteria.)

1. Determine the earth load (ditch condition)

$$\frac{H}{B_d} = \frac{20}{7} = 2.86 \qquad (\text{from Fig. 2.2, } C_d = 1.9)$$

$$K\mu = 0.150 \qquad \text{clayey sand}$$

$$W_d = C_d \gamma B_d^2 = 1.9\ (120\ \text{lb/ft}^3)\ (7)^2 = 11{,}172\ \text{lb/ft}$$

where γ = unit weight of soil (assume 120 lb/ft³) and B_d = trench width at the top of the pipe.

2. Determine the earth load (if transition width exceeded)

$$\frac{H}{B_c} = \frac{20}{3} = 6.67 \qquad \left(\text{from Fig. 2.6, } \frac{B_d}{B_c} = 2.65\right)$$

Assume $r_{sd}p = 0.75$. Then

$$B_d\ (\text{transition}) = \frac{B_d}{B_c}\, B_c = 2.65\ (3) = 7.95\ \text{ft} \approx 8.0$$

$$W_d\ (\text{transition}) = C_d \gamma B_d^2 = 1.9\ (120)\ (8)^2 = 14{,}592\ \text{lb/ft}$$

3. Determine the class of pipe required for B bedding, with 7-ft trench width,

$$\text{Load factor (LF) for B bedding} = 1.9 \qquad (\text{see Table 3.2})$$

$$\text{Safety factor} = 1.5$$

$$\text{Required strength} = (\text{design load})\left(\frac{\text{safety factor}}{\text{load factor}}\right)$$

$$= W_d\left(\frac{\text{SF}}{\text{LF}}\right) = 11{,}172\,\frac{1.5}{1.9} = 8200 \text{ lb/ft}$$

Contact the manufacturer to see if this strength or higher is available.

4. Determine the strength of pipe required for C bedding, with 7-ft trench width,

$$\text{Load factor (LF) for C bedding} = 1.5 \qquad \text{(see Table 3.2)}$$

$$\text{Safety factor} = 1.5$$

$$\text{Required strength} = W_d\,\frac{\text{SF}}{\text{LF}} = 11{,}172\,\frac{1.5}{1.5}$$

$$= 11{,}172 \text{ lb/ft}$$

Again, contact the manufacturer for the availability of this strength. Although this is a nonpressure application, a pressure pipe with the required crush strength may be used.

5. Determine the strength of pipe required if the transition width is reached or exceeded, with class C bedding. From item 2 above,

$$\text{Load } W_d = 14{,}592 \text{ lb/ft}$$

$$\text{Required strength} = W_d\left(\frac{\text{SF}}{\text{LF}}\right) = 14{,}592\,\frac{1.5}{1.5} = 14{,}592 \text{ lb/ft}$$

This strength or higher may *not* be available from the manufacturer.

Asbestos-cement pressure pipes are designed using a combined loading theory (Schlick formula) as discussed in Chap. 4. Equations (4.12) and (4.13) are repeated here for convenience as Eqs. (5.1) and (5.2), respectively.

$$w = W\sqrt{1 - \frac{p}{P}} \tag{5.1}$$

$$p = P\left[1 - \left(\frac{w}{W}\right)^2\right] \tag{5.2}$$

Maximum bending stress in a pipe subjected to three-edge loading can be calculated as follows:

$$\sigma = \frac{M\,(t/2)}{I} = \frac{M\,(t/2)}{bt^3/12} = \frac{(M/b)\,(t/2)}{t^3/12} \tag{5.3}$$

$$M = 0.318F\left(r_i + \frac{t}{2}\right)\dagger \tag{5.4}$$

where M = moment
F = load
I = moment of inertia of wall
r_i = internal radius
b = length of specimen thickness
t = wall thickness

Equation (5.3) can be written as follows:

$$\sigma = \frac{6\,(0.318)\,(F/b)\,(r_i + t/2)}{t^2} \tag{5.5}$$

For external loading only, at failure, the stress σ is the strength, sometimes called the *modulus of rupture* (MR). The three-edge bearing load to cause failure (three-edge bearing strength W) is F/b lb/ft. Thus,

$$\text{MR} = \sigma = \frac{6\,(0.318)\,(W\text{ lb/ft})\,(1\text{ ft/12 in})\,[(d_i + t)/2]}{t^2}$$

or

$$\text{MR} = \frac{0.0295W\,(D + t)}{t^2} \tag{5.6}$$

The hoop stress σ_h in a cylinder may be calculated as follows:

$$\sigma_h = \frac{PD}{2t} \tag{5.7}$$

Knowledge of σ_h, MR, and t will allow calculation of w and p through the use of Eqs. (5.1) or (5.2) and (5.6) and (5.7). By solving Eq. (5.7) for P and Eq. (5.6) for W, one may substitute into Eqs. (5.1) and (5.2) to obtain

$$w = \frac{\text{MR}t^2}{0.0795\,(D + t)}\sqrt{\frac{\sigma 2t/D - p}{\sigma 2t/D}} \tag{5.8}$$

and

†This is the maximum moment in a closed ring loaded with diametrically opposite concentrated loads. See a text on the mechanics of materials for details.

TABLE 5.3 Asbestos-Cement Pressure Pipe Design Summary*

Design case	Internal load design	External load design
Case I (live load is zero)	p = (operating pressure) × 4.0 SF = 4.0	w = (transition load) × 2.5 SF = 2.5
Case II (surge pressure is zero)	p = (operating pressure) × 2.5 SF = 2.5	w = (earth + live load) × 2.5 SF = 2.5
Case III (transmission designed for specific surge pressure)	p = (operating pressure + surge pressure) × 2.5 SF = 2.5	w = (earth + live load) × 2.5 SF = 2.5

*See AWWA C401.

$$p = \frac{\sigma 2t}{D}\left\{1 - \left[\frac{0.0795w\,(D + t)}{\mathrm{MR}t^2}\right]^2\right\} \tag{5.9}$$

respectively.

Equations (5.8) and (5.9) express the external and internal loads for a pipe of given thickness, modulus of rupture, and tensile strength which will cause failure when applied simultaneously. It is difficult to solve these equations explicitly. The general procedure is to construct a graphical solution for standard pipe classifications and standard installation and operating conditions (see AWWA C402). In addition, the design process will require the application of an appropriate factor of safety.

Thickness design of asbestos-cement class pressure pipe is outlined in AWWA C401 (see Fig. 5.1). Two cases of design are considered. The design methods are summarized in Table 5.3. Note that the safety factors recommended are different. Asbestos-cement pipe designed by considering case I will generally exceed the capability of pipe designed by case II.

The nature of transmission systems has been recognized by AWWA. AWWA C402 and AWWA C403 cover a wide range of pipe classifications suited to provide exactly the right pipe for the design conditions encountered (see Fig. 5.2). In cases where operating and installation conditions are controlled and the magnitudes of potential surge pressures are known, lower safety factors may be justified. Figure 5.3 also summarizes such a design procedure for asbestos-cement transmission pipe, case III.

Example 5.2—Distribution line A 12-in-diameter distribution line will operate at a working pressure of 100 lb/in^2. Average depth of cover will be 5.0 ft under a paved roadway. The native soil is sand. Using standard AWWA design procedures, what class of asbestos-cement should be used if the pipe is laid in a flat-bottom trench with tamped backfill? Assume the trench width is 3.0 ft, and the bedding factor is 1.3.

Case I:

Hydrostatic: $P = \text{class} \times \text{SF} \qquad \text{SF} = 4.0$

Crush load: $W = \left[\dfrac{\text{earth load (transition)}}{\text{bedding factor}} \right] \text{SF} \qquad \text{SF} = 2.5$

Case II:

Hydrostatic: $P = \text{class} \times \text{SF} \qquad \text{SF} = 2.5$

Crush load: $W = \left(\dfrac{\text{earth load} + \text{live load} + \text{impact}}{\text{bedding factor}} \right) \text{SF} \qquad \text{SF} = 2.5$

In both case I and case II use combined loading.

$$w = W \sqrt{\frac{P - p}{P}}$$

Figure 5.1 Outline of design procedure for asbestos-cement class pressure pipe (6 to 16 in).

Hydrostatic design:

$P = (\text{operating pressure} + \text{surge pressure})\ \text{SF} \qquad \text{SF} = 2.0$

Crush design:

$$W = \left[\frac{\text{earth load (transition)} + \text{live load (H-20)}}{\text{bedding factor}} \right] \text{SF} \qquad \text{SF} = 1.5$$

$$w = W \sqrt{\frac{P - p}{P}}$$

Figure 5.2 Outline of asbestos-cement transmission pipe design procedure (18 to 36 in).

1. Determine the earth load.

$$\frac{H}{B_d} = \frac{5.0}{3.0} = 1.67 \qquad \text{(from Fig. 2.2, } C_d = 1.3)$$

$$K\mu = 0.165 \qquad \text{sand}$$

$$W_d = 1.3\,(120)\,(3.0)^2 = 1404 \text{ lb/ft}$$

2. Determine load at the transition width.*

*13.74 is the outer diameter (OD) which can be obtained from manufacturers' specifications.

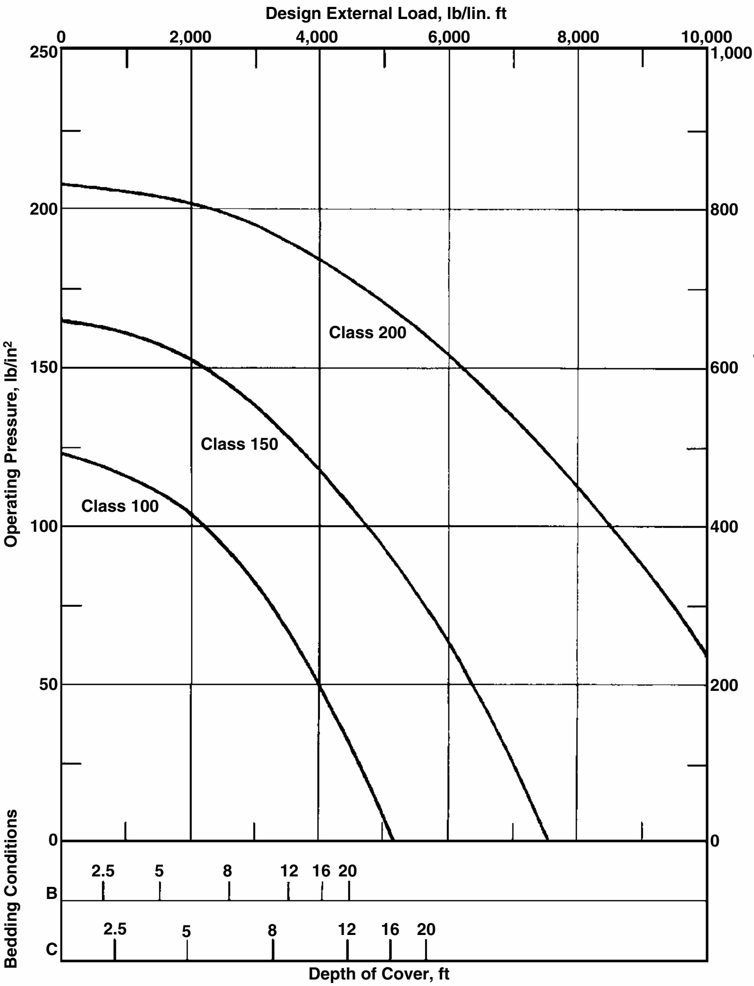

Figure 5.3 Class pipe design curve for 12-in-diameter asbestos-cement pipe (see AWWA C401 for other diameters). (*Reprinted, by permission, from ANSI/AWWA C401-83,*[12] *American Water Works Association, 1986.*)

$$\frac{H}{B_c} = \frac{5.0}{13.74/12} = 4.37$$

(from Fig. 2.6 with $r_{sd}P = 0.5$ and $K\mu = 0.165$, $B_d/B_c = 2.22$)

$$B_d \text{ (transition)} = \left(\frac{13.74}{12}\right)(2.22) = 2.54 \text{ ft}$$

$$\frac{H}{B_d} = \frac{5.0}{2.54} = 1.97 \qquad \text{(from Fig. 2.2, } C_d = 1.4\text{)}$$

$$K\mu = 0.165$$

$$\text{Load } W_d = 1.4\,(120)\,(2.54)^2 = 1084 \text{ lb/ft}$$

(not 1404, as determined previously). Alternatively the load can be obtained by using Fig. 2.5 for projecting conduits.

$$\frac{H}{B_c} = 4.37 \qquad \text{(from Fig. 2.5, } C_c = 7.0\text{)}$$

$$W_c = C_c \gamma B_c^{\,2} = 7.0\,(120)\left(\frac{13.74}{12}\right)^2 = 1111 \text{ lb/ft}$$

The 1111 lb/ft is essentially the same as 1084 lb/ft as previously calculated. The error is due to graphical interpolations for C_d and C_c.

3. Determine the live load.

$$W_L = 340 \text{ lb} \qquad \text{(from Fig. 2.21)}$$

4. Determine the total load.

$$W_T = W_c + W_L = 1111 + 340 = 1451$$

5. Determine the internal pressure requirement.
   Case I (live load is zero):

$$p = (100)\,(4.0) = 400 \text{ lb/in}^2$$

$$w = \frac{1111\,(2.5)}{1.3} = 2136 \text{ lb/ft}$$

Case II (surge is zero):

$$p = (100)\,(2.5) = 250 \text{ lb/in}^2$$

$$w = \frac{1451\,(2.5)}{1.3} = 2790 \text{ lb/ft}$$

By use of the Schlick formula, we can now determine the P and W or wall thickness of the pipe which is required. For AC pipe, the performance criteria P and W may be solved by trial and error as follows (class 100, $P = 490$ lb/in^2, $W = 5200$ lb/ft). See Fig. 5.3.

Case I:

$$w = W\sqrt{\frac{P - p}{P}} = 5200\sqrt{\frac{490 - 400}{490}} = 2228 \text{ lb/ft}$$

Since 2228 $\geq$ 2136, class 100 is acceptable.

Case II:

$$w = 5200\sqrt{\frac{490 - 250}{490}} = 3639 \text{ lb/ft} > 2780 \text{ lb/ft}$$

Class 100 is acceptable.

Figure 14E of AWWA C401 (see Fig. 5.3) is a solution to $r_{sd}p = 0.70$, $K\mu = 0.192$, and $\gamma = 120$ lb/ft^3. Class 100 pipe would therefore perform for any conditions which are below the lowest design curve. The class designations are based on case I with a class C bedding, excavated coupling holes, and 5.0 ft of cover.

Example 5.3—Transmission pipe design A 24-in-diameter transmission line will deliver water at 7000 gal/m and 5.0 ft/s from a reservoir to a treatment plant 10 mi away. The pipe will be buried 5.0 ft deep in a 4.0-ft-wide trench in sand carefully compacted or bedded with a coarse, granular material up to the spring line. Surge devices and valve operating equipment will keep surge pressures to a maximum of 50 lb/in^2. The system will operate at a maximum pressure of 150 lb/in^2. Determine the appropriate asbestos-cement transmission pipe. (See AWWA C402.)

1. Determine the earth load.

$$\frac{H}{B_d} = \frac{5.0}{4.0} = 1.25 \qquad \text{(from Fig. 2.2, } C_d = 1.1\text{)}$$

$$K\mu = 0.165 \qquad \text{sand}$$

$$W_d = 1.1\,(120)\,(4.0)^2 = 2112 \text{ lb/ft}$$

The load at the transition width is

$$\frac{H}{B_c} = \frac{5.0}{26.4/12} = 2.27 \qquad \text{(from Fig. 2.6, } B_d/B_c = 1.8\text{)}$$

$$r_{sd}p = 0.5$$

$$B_d = 1.8 \frac{26.4}{12} = 3.96 \text{ ft}$$

That is, the 4.0-ft trench width just exceeds the transition width, and the load calculated for a 4.0-ft-wide trench is just slightly conservative.

$$\frac{H}{B_c} = \frac{5.0}{2.2} = 2.27 \qquad (\text{from Fig. 2.5, } C_c = 3.4)$$

$$r_{sd}p = 0.5$$

$$W_c = 3.4\,(120)\,(2.2)^2 = 1974 \text{ lb/ft}$$

$$W_d \approx W_c \qquad \text{at transition width}$$

2. Determine the live load.

$$W_L = 340 \qquad (\text{from Fig. 2.21})$$

3. Determine the total load.

$$2112 + 340 = 2452 \text{ lb/ft}$$

4. The combined loading is

$$p = (150 + 50)\,(2.0) = 400 \text{ lb/in}^2$$

$$w = \left(\frac{2112 + 340}{1.9}\right)(1.5) = 1936 \text{ lb/ft}$$

Try T50, $P = 500$ lb/in², and $W = 8100$ lb/ft:

$$w = W\sqrt{\frac{P - p}{P}} = 9100\sqrt{\frac{500 - 400}{500}} = 4070 \text{ lb/ft}$$

Since 4070 lb/ft > 1936 lb/ft, T50 is acceptable. Alternately the pipe could be chosen from the selection curves of Fig. 5.4 (see AWWA C403-95).

Clay Pipe

Vitrified clay pipe is manufactured from clays and shales which are chemically inert. In the manufacturing process, various clays and shales are pulverized, screened, and placed in storage bins. Blended materials are carried to the pugmill and mixed and moistened with water for a proper mix consistency for extrusion. The mix is then forced through a die into a vacuum chamber where trapped air is

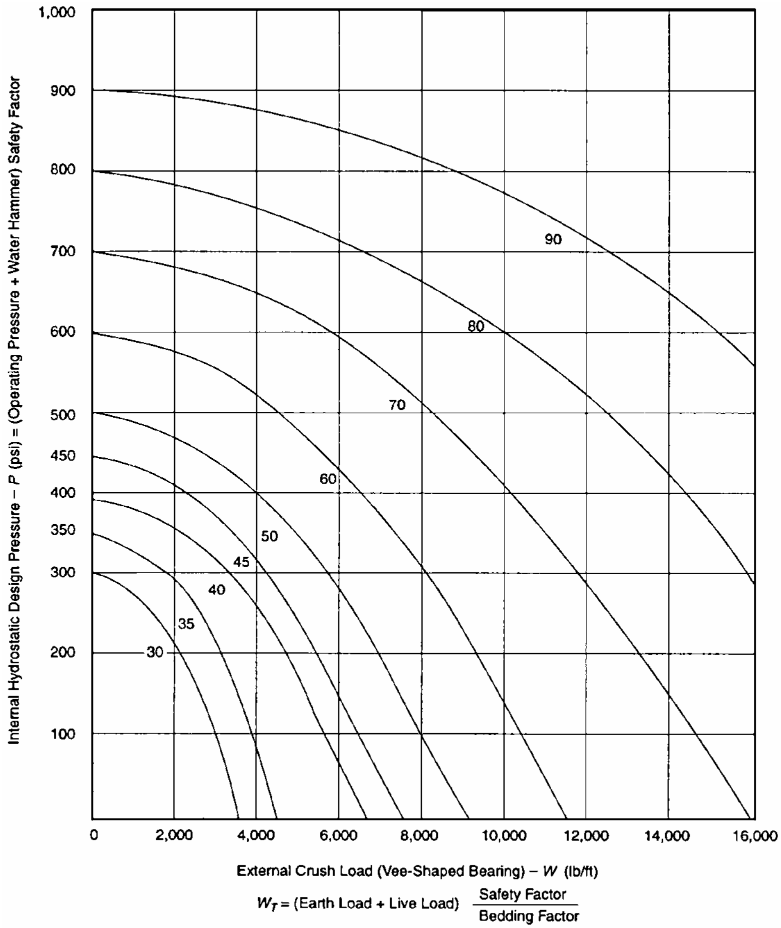

Figure 5.4 Combined loading curves for 24-in transmission pipe. (*Reprinted, by permission, from ANSI/AWWA C401,*[12] *American Water Works Association, 1986.*)

removed. This mixture is then machine-extruded in the form of pipe. This fresh extruded pipe contains about 18 percent water and is called *greenware.* Greenware is placed in drying rooms to reduce the moisture content to about 3 percent. The pipe is then taken to the kilns and preheated to approximately 400°F to drive off the remaining moisture. The pipe travels slowly through the kiln, reaching a temperature near 2000°F where vitrification takes place.

During vitrification the clay fuses into a very hard, chemically sta-

TABLE 5.4 Standards for Clay Pipe

ASTM C 700	Clay pipe, vitrified, extra-strength, standard strength, and perforated
ASTM C 425	Compression joints for vitrified clay pipe and fittings
ASTM C 301	Clay pipe, vitrified (test methods)
ASTM C 12	Installing vitrified clay pipe lines
ASTM C 828	Low-pressure air test of vitrified clay pipe lines
Canadian Standards Association	
CSA A60.1	Vitrified clay pipe
CSA A60.2	Methods of testing vitrified clay pipe
CSA A60.3	Vitrified clay pipe

TABLE 5.5 ASTM C 700 Clay Pipe Minimum Crushing Strengths (Three-Edge Bearing Strength)

Nominal size, in	Extra strength, lb/ft	Nominal size, in	Extra strength, lb/ft
3	2000	21	3850
4	2000	24	4400
6	2000	27	4700
8	2200	30	5000
10	2400	33	5500
12	2600	36	6000
15	2900	39	6600
18	3300	42	7000

ble compound. Vitrified clay is very corrosion- and abrasion-resistant. Because of its inherent low strength, vitrified clay pipe is used for non-pressure applications only. It is brittle and subject to impact damage; therefore, special care in handling is a requirement.

Newer designs do not have extruded clay bells. Instead, a bell is formed by helically winding continuous glass filaments and a thermosetting resin to form a bell on a plain pipe end. A groove is molded into the bell for a rubber gasket.

Clay pipe is generally available in sizes ranging from 4- to 36-in diameter. However, it may be available in some locations in diameters up to 42 in. The strength is determined by the three-edge bearing test, varies with diameter, and ranges from 2000 to 7000 lb/ft (Tables 5.4 and 5.5).

Example 5.4 A 15-in-diameter sanitary sewer line is to be installed 14 ft deep. Native material, which is sand, will be used for final backfill. If the trench width is 3.0 ft, what pipe and bedding classes should be selected? (*Note:* This example was previously given as Example 3.1.)

1. Determine the earth load.

$$\frac{H}{B_d} = \frac{14}{3} = 4.67 \qquad \text{(from Fig. 2.2, } C_d = 2.4\text{)}$$

TABLE 5.6 Required Strength for Various Bedding Classes

Bedding class	LF	Three-edge, lb/ft	Required strength, lb/ft
B	1.9	2046	Extra strength (2900)
C	1.5	2592	Extra strength (2900)
D	1.1	3535	This strength is not available

$$K\mu = 0.165 \qquad \text{sand}$$

$$W_d = C_d \gamma B_d^{\,2} = 2.4\,(120)\,(3.0)^2 = 2592 \text{ lb/ft}$$

2. Determine the live load.

$$W_L = 150 \text{ lb/ft} \qquad \text{(from Fig. 2.21)}$$

Note: $150 \ll 2592$ (live load may be neglected).

3. Select the bedding and the load factor.

Class D	LF = 1.1
Class C (from Table 5.6)	LF = 1.5
Class B	LF = 1.9

4. Select the pipe strength (safety factor = 1.5).

$$\text{Three-edge strength} = \frac{W_d\,(\text{SF})}{\text{LF}} = \frac{2592\,(1.5)}{\text{LF}}$$

Concrete Pipe

Concrete pipe products are made by several processes. Included are nonreinforced products in sizes ranging from 4- to 36-in diameter and various reinforced products in sizes 12- through 144-in diameter (see Tables 5.7, 5.8, and 5.9).

The nonpressure types are described in ASTM C 14 for nonreinforced and in ASTM C 76 for the reinforced type, and in CSA A257 for both types.

Concrete pressure pipe includes various types of wall construction. Some are designed and manufactured for specific service applications, and other types are constructed to be suitable for a broad range of applications.

Prestressed concrete cylinder pipe

Prestressed concrete cylinder pipe has two types of construction: embedded cylinder and lined cylinder (Figs. 5.5 and 5.6). In both types, manufacturing begins with a welded steel cylinder to which joint rings are attached at each end. This steel cylinder is then hydrostatically tested.

TABLE 5.7 ASTM C 14 Nonreinforced Concrete Pipe

	Minimum strength in three-edge bearing, lb/ft		
Pipe diameter, in	Class 1	Class 2	Class 3
4	1500	2000	2400
6	1500	2000	2400
8	1500	2000	2400
10	1600	2000	2400
12	1800	2250	2600
15	2000	2600	2900
18	2200	3000	3300
21	2400	3300	3850
24	2600	3600	4400
27	2800	3950	4600
30	3000	4300	4750
33	3150	4400	4875
36	3300	4500	5000

TABLE 5.8 ASTM C 76 Reinforced Concrete Pipe *D* Load (lb/ft × ft diam.) Required

Class	Size range, in diameter	0.01-in crack	Ultimate
I	60–144	800	1200
II	12–144	1000	1500
III	12–144	1350	2000
IV	12–144	2000	3000
V	12–144	3000	3750

TABLE 5.9 AWWA and ASTM Standards for Concrete Pipe

AWWA C300	Standard for reinforced concrete pressure pipe, steel cylinder type for water and other liquids
AWWA C301	Standard for prestressed concrete pressure pipe, steel cylinder type for water and other liquids
AWWA C302	Standard for reinforced concrete pressure pipe, noncylinder type for water and other liquids
AWWA C303	Standard for reinforced concrete pressure pipe, steel cylinder type, pretensioned for water and other liquids
AWWA C603	Standard for installation of asbestos-cement pressure pipe
AWWA Manual 9	Concrete pressure pipe, manual of water supply practices
ASTM C 118	Concrete pipe for irrigation or drainage
ASTM C 14	Concrete sewer, storm drain, and culvert pipe
ASTM C 505	Nonreinforced concrete irrigation pipe with rubber-gasket joints
ASTM C 985	Nonreinforced concrete specified strength culvert, storm drain, and sewer pipe
ASTM C 654	Porous concrete pipe
ASTM C 506	Reinforced concrete arch culvert, storm drain, and sewer pipe
ASTM C 76	Reinforced concrete culvert, storm drain, and sewer pipe
ASTM C 655	Reinforced concrete *D* load culvert, storm drain, and sewer pipe
ASTM C 507	Reinforced concrete elliptical culvert, storm drain, and sewer pipe
ASTM C 361	Reinforced concrete low-pressure pipe
ASTM C 924	Low-pressure air test of concrete pipe sewer lines

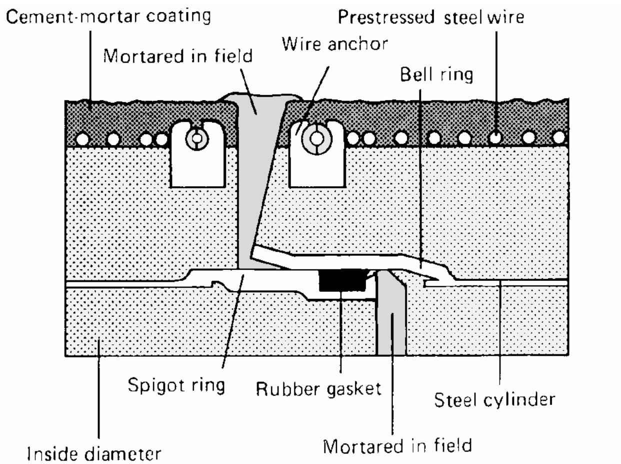

Figure 5.5 Wall cross section of embedded cylinder pipe. (*Reprinted from Bulletin No. 200 by permission of the United Concrete Pipe Corporation.*)

A concrete core is either cast (embedded cylinder) or spun (lined cylinder) in the steel cylinder. After curing, the cylinder is helically wrapped with hard-drawn wire under high-tensile stress. The lead angle is controlled to produce a specific compression stress in the concrete core. After wrapping, the pipe is coated with a cement slurry and a dense mortar or concrete coating.

Embedded-cylinder pipe is commonly available in 24- through 144-in diameter. Lined-cylinder pipe is manufactured in diameters of 16 through 60 in. Prestressed concrete cylinder pipe is designed using a combined loading analysis. This method was discussed in Chap. 4 (see also AWWA C301).

Reinforced concrete cylinder pipe

This pipe is similar to the embedded-cylinder pipe in manufacture. However, no prestressed wire is applied, and instead one or more reinforcing cages and the steel cylinder are positioned between vertical forms and the concrete is cast (Fig. 5.7). Steam or water is used to cure the concrete. This pipe is available in diameters of 24 through 144 in. Design is based on either the strength method or the working stress method. In either case, the pipe is to be designed to withstand internal pressure and external load, each acting separately or in combination (see AWWA C300, Appendix A).

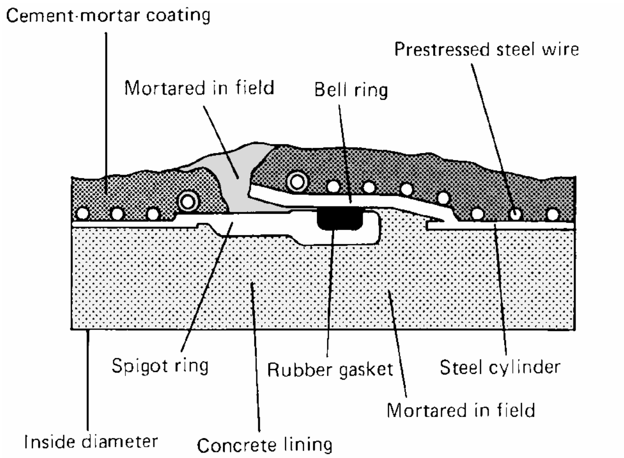

Figure 5.6 Wall cross section of lined cylinder pipe. (*Reprinted from Bulletin No. 200 by permission of the United Concrete Pipe Corporation.*)

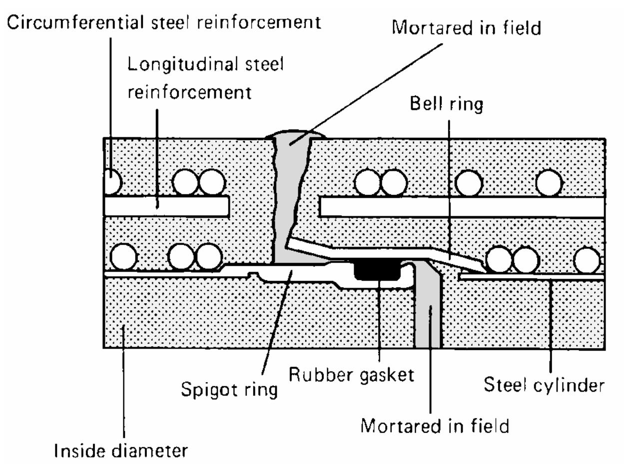

Figure 5.7 Wall cross section of reinforced concrete cylinder pipe. (*Reprinted from Bulletin No. 200 by permission of the United Concrete Pipe Corporation.*)

Reinforced concrete noncylinder pipe

This type of concrete pipe is manufactured by positioning one or more steel cages in proper radial location(s) (Fig. 5.8). The cages are placed between two vertical forms, and the concrete is cast. Alternately, the cages are attached to an outer form, the entire assembly is rotated, and the concrete is cast centrifugally. AWWA C302 outlines a design procedure for internal pressure and external loads acting simultaneously. Reinforced noncylinder pipe is available in diameters of 12 through 144 in.

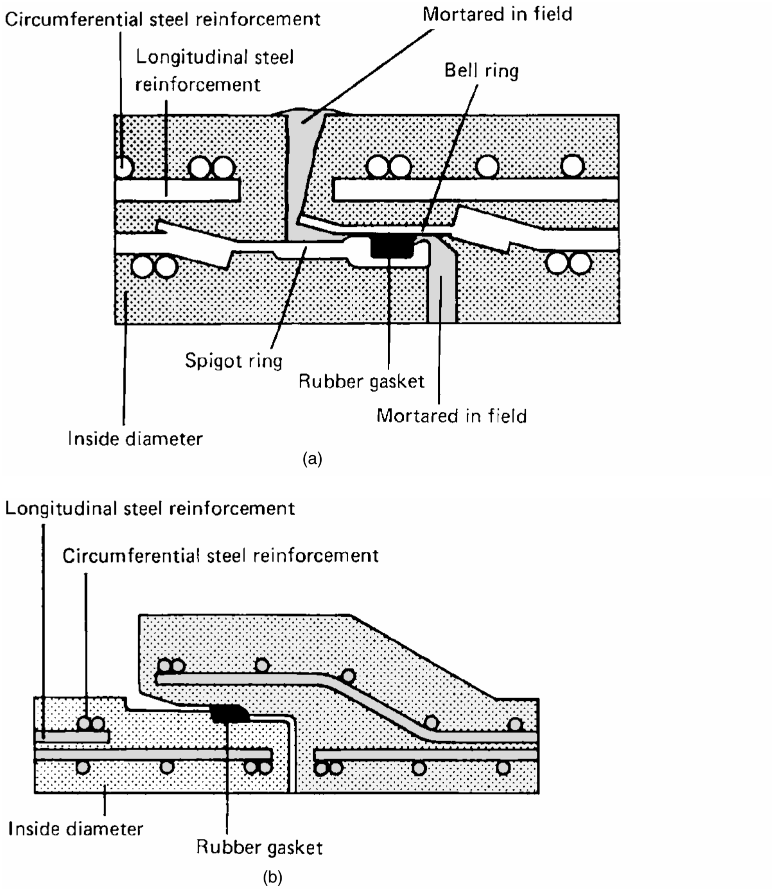

Figure 5.8 Wall cross section of reinforced concrete noncylinder pipe (*a*) with steel join rings and (*b*) with concrete bell and spigot. (*Reprinted from Bulletin No. 200 by permission of the United Concrete Pipe Corporation.*)

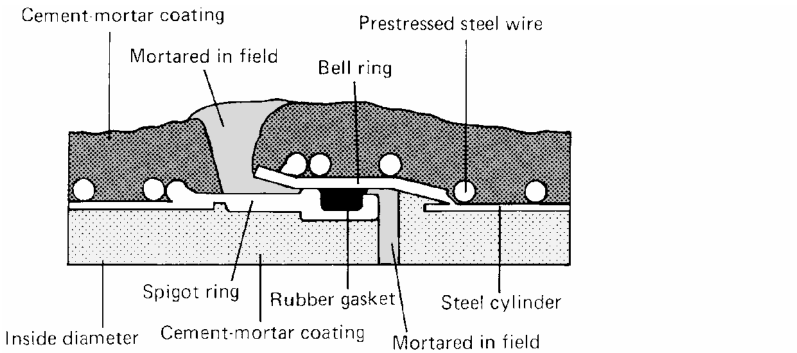

Figure 5.9 Wall cross section of pretensioned shot-cote concrete cylinder pipe. (*Reprinted from Bulletin No. 200 by permission of the United Concrete Pipe Corporation.*)

Pretensioned concrete cylinder pipe

In the manufacture of pretensioned concrete cylinder pipe, one starts with steel cylinders made from steel coils and spirally welded or made from steel sheet and welded longitudinally. End rings are welded to the steel cylinder, and then it is hydrostatically tested to 75 percent of yield strength of the steel. A cement mortar lining is applied centrifugally. After curing, the cement mortar-lined steel cylinder is pretensioned by helically winding steel rod under a small tension to the outside of the steel cylinder. The pitch of the winding is controlled by specific design requirements. A cement-mortar coating is then applied to the exterior surface of the rod-wrapped cylinder, and the completed pipe is cured (Fig. 5.9). This pipe is normally available in diameters of 10 through 42 in. The design of this pipe is based on an analysis of both internal pressure and external loads acting separately but not in combination. This design method is usually used for flexible pipe, which pretensioned concrete is not. The pipe must be installed in such a manner that the deflection is less than $D_2/4000$ (see AWWA C303, Appendix A).

AWWA Design of Reinforced Concrete Pressure Pipe

The following is an abbreviated design procedure for concrete pressure pipes as given in AWWA M9. Additional details are found in the following AWWA standards:

Standards for the reinforced types:

- AWWA C300
- AWWA C302
- AWWA C303

Standards for prestressed concrete pressure pipe:

- AWWA C301
- AWWA C304

Design procedure

There are two basic steps in designing reinforced concrete pressure pipe.

1. Design the wall to resist the internal hydrostatic pressure acting alone.
2. Determine the effect of external loads.
   a. For AWWA C300– and AWWA C302–type pipes, use rigid pipe concepts and a combined load analysis. In this analysis the wall stresses, due to the internal pressure, are considered to be acting simultaneously with the stresses produced by external loads.
   b. AWWA C303–type pipe is designed for external loads to control both stresses and deflections. A combined loading analysis is not required.

Design procedure for rigid pipe (AWWA C300 and C302 types)

The rigid pipe design procedure involves the following steps:

1. Calculate the total circumferential steel area required to resist internal pressure only, using the hoop tension equation for working pressure and working pressure plus surge pressure.

2. For the selected wall thickness of AWWA C302–type pipe, calculate the circumferential tensile stress in the concrete of the pipe wall resulting from working pressure plus surge pressure. The concrete strength or the wall thickness must be increased if the tensile stress exceeds the allowable.

3. Calculate the pipe weight and water weight.

4. Calculate the external earth load on the pipe.

5. Calculate the external live load, if any, on the pipe. External dead loads and live loads must be computed in accordance with recognized and accepted theories, such as those presented in Chap. 2 of this book.

6. Calculate moments and thrusts for each load on the pipe, including internal pressure. Values at the invert and at the side are required. For normal loading conditions, the crown values do not control the design.

The coefficients for moments and thrusts must be from recognized and accepted theories, such as those presented by Paris (1921) and Olander (1950). The bedding angle used in design must be compatible with the installation criteria specified by the purchaser.

7. Calculate the required circumferential steel area for the invert and the side for each of the three combinations of loads shown below. Combined load design means the pipe is designed to resist the flexural and axial stresses from each of the following conditions:

- Condition 1: a combination of working pressure, dead loads (earth, pipe, and water), and live loads
- Condition 2: a combination of dead loads (earth, pipe, and water) and live loads with zero internal pressure
- Condition 3: a combination of working pressure, surge pressure, and dead loads (earth, pipe, and water)

8. Select the controlling maximum steel area for the invert (inner) and the side (outer). The total steel area must be equal to or greater than the steel area required for the hydrostatic design. Increase the inner area, outer area, or both sides to meet the required total.

9. Select appropriate bars or fabric to meet the design circumferential steel areas and spacing. For AWWA C300 type of pipe, ensure that the area of rod reinforcement is at least 40 percent of the total circumferential steel area. Check concrete cover over steel.

10. If AWWA C302 type of pipe is to be installed on supports or in any other condition that would create longitudinal bending, the required beam strength is provided by adjusting either the laying length or the wall thickness, or both, so the concrete flexural tensile stress does not exceed 4.5 lb/in^2. In the determination of the flexural tensile stress, the section modulus of the pipe is calculated about the centroidal axis of the transverse section with no allowance for longitudinal steel reinforcement.

Design procedure for AWWA C303 type of pipe

The pipe design procedure for AWWA C303 type of pipe involves the following steps:

1. Select a steel cylinder thickness equal to or greater than the AWWA C303 minimum. Calculate the total circumferential steel area required to resist internal pressure, using the hoop tension for working pressure and for working pressure plus surge pressure.

2. Calculate the cylinder steel area, and place the remaining required steel area in the bar by selecting a bar diameter and bar spacing within the following limits, established in AWWA C303:
   - The area of bar reinforcement shall not exceed 60 percent of the total area of circumferential reinforcement.
   - The area of bar reinforcement shall not be less than 0.23 in^2/lin ft.
   - The center-to-center bar spacing shall not exceed 2 in.

- The area of bar reinforcement in square inches per linear foot of pipe wall shall be numerically equal to at least 1 percent of the inside diameter of the pipe, in inches.
- The design clear space between bars shall not be less than the diameter of the bar used.
- The bar diameter shall not be less than $^{7}/_{32}$ in.

3. Calculate the total external load on the pipe. External loads must be computed in accordance with recognized and accepted theories, such as those presented in Chap. 2.

4. Determine if the total external load is less than either the maximum allowable external load for minimum designs or the maximum allowable external load for the actual design. If either condition is met, then the selected pipe design meets the project requirements.

The maximum allowable external load W for a given semirigid (bar-wrapped) pipe design is the load producing the limiting pipe deflection $D^2/4000$, where D is the inside diameter of the pipe in inches. Experimental and field observations have shown Spangler's Iowa deflection equation for flexible pipe may be applied to semirigid design. The formula for deflection is

$$\Delta x = \frac{D_l k \,(W/12)\, r^3}{EI + 0.061E'r^3} \tag{5.10}$$

where Δx = horizontal deflection of pipe, in
D_l = deflection lag factor
k = bedding constant
W = total external dead plus live load, lb/lin ft of pipe length
r = mean radius of pipe wall, in inches, calculated as 0.5 $(D + t)$, where D is the inside diameter of the pipe, in inches, and t is the pipe wall thickness, in inches
EI = pipe wall stiffness, in inch-pounds, where for AWWA C303 type of pipe E is the modulus of elasticity of cement mortar, taken as 4,000,000 lb/in^2 and I is 25 percent of the transverse moment of inertia of the composite wall section of the pipe, in^4/in of pipe length
E' = modulus of soil reaction, lb/in^2

By replacing the deflectionΔx with the $D^2/4000$ allowable for AWWA C303 type of pipe, setting $D_l = 1.0$, and solving for the allowable external load in pounds per linear foot, the equation becomes

$$W = \frac{D^2\,(EI + 0.061E'r^3)}{333kr^3} \tag{5.11}$$

5. If required, provide additional external load capacity by increasing the effective moment of inertia of the longitudinal pipe section or by improving the bedding material or compaction requirements. The effective moment of inertia may be increased by increasing the area or diameter of the bar reinforcement or by increasing the coating thickness to a maximum of 1.25 in.

Example 5.5 A 15-in-diameter sanitary sewer line is to be installed 14 ft deep in native sand. The trench width at the top of the pipe is to be 3.0 ft. For class B, class C, and class D bedding, select the required strength for nonreinforced concrete pipe and the required strength for a reinforced concrete pipe.

From Example 5.4,

$$W_d = 2592 \text{ lb/ft}$$

Nonreinforced:

$$\text{Strength } W \text{ (3-edge)} = W_d \frac{\text{SF}}{\text{LF}} = 2952 \ \frac{\text{SF}}{\text{LF}}$$

where SF = safety factor = 1.5 and LF = load factor for particular bedding class (see Example 5.4).

Reinforced: Reinforced concrete pipe is designed using the *D* load. The *D* load is the required three-edge strength divided by the pipe diameter.

$$\text{Strength } W \text{ (}D\text{ load)} = \frac{W_d/D}{\text{LF}} \text{ SF} = \frac{2592/D}{\text{LF}} \text{ SF} = \frac{2592}{D} \ \frac{\text{SF}}{\text{LF}}$$

For this material, the strength for each class is based on a 0.01-in crack, not failure. Actual failure load (ultimate) will be approximately 1.5 times the load which causes a 0.01-in crack. Therefore, a safety factor of 1.0 is recommended based on *D* load or 1.5 based on ultimate load.

Note: The values in Table 5.10 were calculated, and the required classes were selected, from Tables 5.7 and 5.8. Also note that a high enough strength for nonreinforced concrete is not available to withstand loads imposed if bedding is only class D.

Example 5.6—Transmission pipe A 24-in-diameter transmission line will deliver water at 7000 gal/m and 5.0 ft/s from a reservoir to a treatment plant 10 mi away. The pipe will be buried 5.0 ft deep in a 4.0-ft-wide trench in sand carefully compacted or bedded with a coarse granular material up to the spring line. Surge and valve control equipment will allow maximum surge pressures of 50 lb/in^2. The system will operate at maximum pressure of 150 lb/in^2. Determine the appropriate prestressed concrete transmission pipe (see Example 5.3).

TABLE 5.10 Required Strength Based on SF = 1.5 and Ultimate

Bedding class	LF	Three-edge, lb/ft	*D* load, (lb/ft)/ft	Nonreinforced	Reinforced
B	1.9	2046	1637	Choose class 1 (2600)	Choose class III (2000)
C	1.5	2592	2074	Choose class 2 (2600)	Choose class IV (3000)
D	1.1	4025	3220	Not available	Choose class V (3750)

Prestressed concrete pipe may be designed by the cubic parabola method, as discussed in Chap. 4. Equation (4.14) is as follows:

$$W = W_o \sqrt[3]{\frac{P_o - p}{P_o}} \tag{4.14}$$

For lined cylinder:

$$p = 0.8P_o \qquad \text{(see AWWA C301)}$$

For embedded cylinder:

$$p = P_o \qquad \text{(see AWWA C301)}$$

From Example 5.3,

$$W_d = 2112 \text{ lb/ft}$$

The required strength is

$$W = \frac{W_d}{\text{LF}} = \frac{2112}{1.9} = 1111 \text{ lb/ft} \qquad p = 150 \text{ lb/in}^2$$

Therefore,

$$P_o = \frac{150}{0.8} = 187.5 \text{ lb/in}^2 \text{ for lined pipe}$$

$$\text{Total load } W = W_d + W_L = 2452 \qquad \text{(see Example 5.3)}$$

Lined-cylinder pipe

For lined-cylinder pipe,

$$p = 0.8P_o$$

$$P_o = 187.5 \text{ lb/in}^2$$

$$W = W_o \sqrt[3]{\frac{P_o - p}{P_o}}$$

$$W_o = \frac{W}{[\,(P_o - P)\,/P_o]^{1/3}} = \frac{1111}{[\,(P_o - 0.8P_o)\,/P_o]^{1/3}}$$

$$= 1900 \text{ lb/ft}$$

The pipe must be designed or selected for 187.5 lb/in² internal pressure and an external load of 1900 lb/ft, each acting independently. The rated strength as determined by the manufacturer includes a safety factor of 1.2. Thus, the transient capacity is considered to be 1.2 times the design capacity for lined-cylinder pipe.

$$1.2 \times P_o = 1.2 \times 187.5 = 225 \text{ lb/in}^2$$

$$1.2 \times W_o = 1.2 \times 1900 = 2280 \text{ lb/in}^2$$

Case I (no surge):

$$\text{Max. load} = 2280 \sqrt[3]{\frac{225 - 150}{225}} = 1581 \text{ lb/ft}$$

$$\text{Safe live load} = 1581 - 1111 = 470 \text{ lb/ft}$$

Case II (no live load):

$$1111 = 2280 \sqrt[3]{\frac{225 - p}{225}}$$

or

$$p = 225 \left[1 - \left(\frac{1111}{2280}\right)^3\right] = 199 \text{ lb/in}^2$$

$$\text{Safe surge pressure} = 199 - 150 = 49 \text{ lb/in}^2$$

Embedded-cylinder pipe

Try

$$W_o = 1900 \text{ lb/ft}$$

$$P_o = 190 \text{ lb/in}^2$$

$$W = W_o \sqrt[3]{\frac{P_o - p}{P_o}} = 1900 \sqrt[3]{\frac{190 - 150}{190}} = 1130 \text{ lb/ft}$$

$$1130 > 1111$$

Thus, try is okay. For embedded-cylinder pipe, the transient capacity is 1.4 times the design capacity.

$$1.4 \times W_o = 1.4 \times 1900 = 2660 \text{ lb/ft}$$

$$1.4 \times P_o = 1.4 \times 190 = 266 \text{ lb/in}^2$$

Case I (no surge):

$$\text{Max. load} = 2660 \sqrt[3]{\frac{266 - 150}{266}} = 2017 \text{ lb/ft}$$

$$\text{Safe live load} = 2017 - 1111 = 906 \text{ lb/ft}$$

Case II (no live load):

$$P = 266 \left[1 - \left(\frac{1111}{2660} \right)^3 \right] = 247 \text{ lb/in}^2$$

$$\text{Safe surge pressure} = 247 - 150 = 97 \text{ lb/in}^2$$

These excess capacities are for transient conditions only. The pipe should not be expected to perform with a sustained soil load of 2017 lb/ft or with a sustained internal pressure of 247 lb/in².

Problem 5.1 For the above example (embedded cylinder), try the following combinations of W_o and P_o. For the cases that satisfy design requirements, find the safe live load and safe surge pressure.

W_o	P_o
1800	200
2000	185
1800	190

Indirect Methods

Traditionally the Marston-Spangler indirect theories have been used for designing concrete pipe. In 1983, the indirect design procedures were included in a new section of the American Association of State Highway and Transportation Officials (AASHTO) *Standard*

TABLE 5.11 Traditional Bedding Factors

Bedding class	Positive projecting embankment B_{fe}	Bedding factor B_f narrow trench B_{ft}
B	2.5–2.9	1.9
C	1.7–2.3	1.5
D	1.1–1.3	1.1

Specification for Highway Bridges (1.4). Section 17, Soil-Reinforced Concrete Structure Interaction Systems, presents a summarized version of the indirect design procedure with certain graphical design aids which are taken from the *ACPA Concrete Pipe Design Manual.* Some of that information is summarized here. The reader is referred to the *ACPA Concrete Pipe Design Manual* for more detailed information.

Bedding factors B_f are defined as the ratio of total field load to equivalent three-edge bearing load that causes the same bending moment at the invert of the pipe. See Table 5.11.

The strength of the pipe is determined by defining an equivalent three-edge bearing load that produces certain performance limits in the pipe. Thus, in the indirect design procedure,

$$\text{Design } W_{\text{3-edge}} = \frac{W_{\text{Earth}} + W_{\text{Live}} + W_{\text{Water}}}{B_f} \tag{5.12}$$

Three-Edge Bearing Design Criteria

The performance criterion for three-edge bearing strength $W_{\text{3-edge}}$ requires pipe to reach test strengths relative to two design limits:

- Service load condition
- Ultimate strength

For reinforced concrete pipe, traditional design practice uses the $W_{\text{3-edge}}$ load to produce a 0.01-in-maximum crack width, defined in ASTM C 497 as the design load. Thus, in this practice the required $W_{\text{3-edge}}$ load at 0.01-inch crack is given by Eq. (5.12). It is convenient to express three-edge bearing strength requirements in terms of the D load. The D load is defined as the $W_{\text{3-edge}}$ load per foot of inside diameter D_i, with units of pounds per foot per foot:

$$W_{D\text{ load}} = \frac{W_{\text{3-edge}}}{D_i} \tag{5.13}$$

Thus, the required three-edge bearing service load is defined in terms of the D load to produce a 0.01-in crack. The D load required for a particular pipe soil installation is determined as

$$(W_{D\text{ load}})_{0.01} = \frac{W_e + W_L + W_w}{B_f D_i} \tag{5.14}$$

The 0.01-in crack criterion is not applicable to nonreinforced concrete pipe. These pipes are at the $W_{3\text{-edge}}$ strength limit when the first crack occurs. Although nonreinforced pipe may still be able to perform after cracking starts in field installations, a safety factor from 1.25 to 1.5 is normally provided against flexural cracking at the service load. Thus, the required ultimate D load strength for nonreinforced concrete pipe is

$$(W_{D\text{ load}})_{\text{ult}} = \frac{1.5\,(W_e + W_L + W_w)}{B_f D_i} \tag{5.15}$$

Note: W_L (live load) is frequently neglected when the height of earth fill above the pipe is more than 8 ft or the outside pipe diameter, whichever is greater. *Note:* W_w (hydrostatic load) is frequently neglected, especially for small-diameter pipe.

The required ultimate $W_{3\text{-edge}}$ strength for reinforced concrete pipe is given by Eq. (5.15), except for the use of a reduced strength factor for pipe strength classes higher than class 4. For typical pipe strength classes up to class 4, the ultimate strength design limit is 1.5 times the required service load $W_{3\text{-edge}}$ strength. This strength factor is 1.25 for class 5 pipe strength and is linearly interpolated between 1.5 and 1.25 for any strength classes between 4 and 5. An ultimate strength design limit is also defined for reinforced concrete pipe designed by the indirect design procedure. Such a design limit is included in ASTM specifications for reinforced concrete pipe.

Design requirements for nonreinforced pipe with specified $W_{3\text{-edge}}$ strength requirements are given in ASTM C 985. Design $W_{3\text{-edge}}$ strengths for nonreinforced concrete pipe having various standard diameters and wall thicknesses are given in ASTM C 14. The D load definition of three-edge bearing strength is not used in this standard.

Design requirements for reinforced pipe with specified D load strength requirements and special reinforcement designs are given in ASTM C 655. Design $W_{3\text{-edge}}$ strengths for reinforced concrete pipe having various standard diameters, wall thicknesses, concrete strengths, and reinforcement requirements for standard strength classes are given in ASTM C 76, C 506, and C 507.

Specifying agencies sometimes require $W_{3\text{-edge}}$ tests for proof of design. More frequently, they may require $W_{3\text{-edge}}$ tests for proof of quality assurance. A distinction should be made between the ultimate strength design limit to be used in developing the basic pipe design and the requirements for $W_{3\text{-edge}}$ testing of pipe for quality assurance. The pipe reinforcement designs given in ASTM C 76 are based on strength factors of 1.5 to 1.25 over the required service load $(W_{D\,\text{load}})_{0.01}$, but this standard does not require that quality control $W_{3\text{-edge}}$ tests be taken to ultimate. The same applies to ASTM C 506 and C 507.

The required $W_{3\text{-edge}}$ strengths in these indirect designs are obtained from the loads and bedding factors calculated using the Marston-Spangler soil-structure interaction analyses for earth loads. In summary, under the indirect design procedure, the required pipe will have a $W_{3\text{-edge}}$ service and strength as determined from actual three-edge bearing tests, from empirical evaluations of former tests (as given in ASTM standards), or from design procedures derived from reinforced concrete theory and evaluations of appropriate tests.

The Direct Method

The American Concrete Pipe Association (ACPA) recommends a design practice for pipe-soil installations based on a direct design of the pipe for its installed conditions. New standardized installation types are given that differ significantly from those originally developed by Marston and Spangler. The four new standard installations and a direct design procedure are found in a 1993 American Society of Civil Engineers standard entitled *ASCE Standard Practice for Direct Design of Buried Concrete Pipe in Standard Installations (SIDD).*

The four standard installation types are as follows:

Type 1 requires select granular soils in bottom haunch and outside bedding zones with high levels of compaction.

Type 2 permits coarse or fine granular soils with some silts, including some native soils in the haunch and outside bedding zones. Compaction requirements remain high for native soils and are reduced for select granular soils.

Type 3 permits coarse or fine granular soils with some silts or silty clay in haunch zones. Compaction requirements vary with soil type and are reduced for select granular soils to levels where testing is optional. Compaction requirements are high for nonplastic soils with clay particles.

Type 4 has no requirements for embedment soils in haunch and bedding zones, unless clays are used in the haunch zone. Silty clay requires limited compaction with testing being optional. Plastic clays are not recommended.

SIDD design assumes the same design may be used for embankment, trench, and subtrench installations of the same type. The following reasons are given in the *Concrete Pipe and Technology Handbook:*

1. "This assumption precludes the need to specify a maximum allowable trench width for any installation. It is often difficult to control the actual trench width in the field and impossible to restore the specified in-situ trench width after an over-width trench has been constructed."
2. "With a narrow trench, access for compacting the embedment soil in the haunch region usually is too limited for assurance that the specified minimum compaction level will be achieved for many types of placed soils (except in Type 4 installations which do not require haunch zone compaction). Thus, higher quality trench installations require sufficient trench width for access to properly compact soils in the haunch zone below the pipe, and narrow trench installations should be limited to Type 2 or Type 3 installations with 'self-compacting' types of granular embedment soils (i.e., crushed stone or pea gravel), or to Type 4 installations."
3. "Although the vertical earth load on a pipe in a narrow trench typically is lower than the earth load on a similar embankment pipe, the lateral load on the trench pipe typically is also lower than the lateral load on the pipe in a comparable embankment. Since the difference between vertical and lateral loads in a given installation is the primary influence on design requirements, the comparative design requirements for pipe in the two installations are not as favorable to the trench condition, as the comparative magnitudes of vertical earth load."
4. "It is conservative to use the embankment installation criteria for trench installations."

The four standard installations are defined by the types and densities of the bedding and embedment soils required for each installation type. The soil zones that define the locations of soil types and densities specified in the ASCE SIDD Practice are shown in Fig. 5.10 for the embankments and in Fig. 5.11 for trenches. The soil types and densities that are required, or permitted, in the various zones are given in Table 5.12 for embankments and in Table 5.13 for trenches. Note that several alternative combinations of soil types and compaction densities are sometimes permitted for the various zones in each installation type. See Table 3.1 for a description of the soils that are included in each of the standard soil classifications.

The following general descriptions of each installation type provide a summary of the major characteristics of the ASCE standard instal-

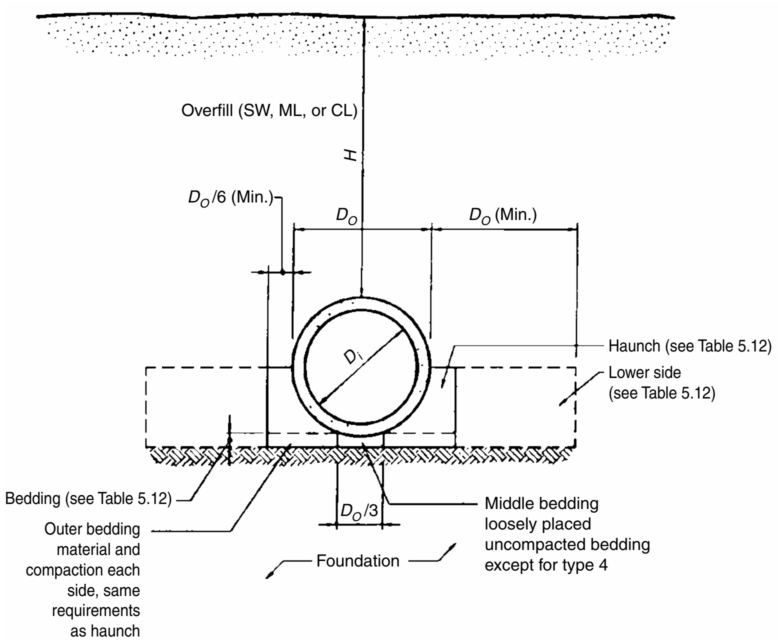

Figure 5.10 Standard embankment installations.

lations. (See ASCE Standard Practice for Concrete Pipe Design, Chapter 8 of *ACPA Concrete Pipe Technology Handbook,* for details.)

Type 1 is considered the highest-quality standard installation.

Type 2 is the highest-quality standard installation where certain native soils are permitted to be used with proper compaction in the haunch and bedding zones.

Type 3 permits the use of soils in the haunch and bedding zones having less stringent compaction requirements, justifying less stringent inspection requirements with granular soils and some native soils.

Type 4 is intended for installations where the most cost-effective design approach is to specify minimal requirements for embedment soil type and density, together with a pipe having sufficient strength to safely resist the increased structural effects that result from using low-quality embedment soils. Thus, type 4 has no requirements for control of compaction and type of placed soil used in the bedding and haunch zones; except if silty clay soils are used in the haunch zone, or below this zone, they must be compacted to at least 85 percent of standard Proctor density, and plastic clays should not be used in this zone.

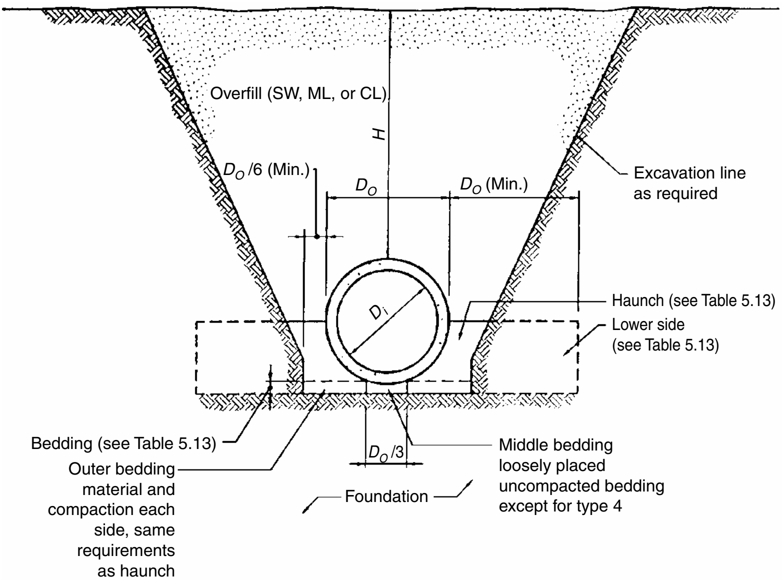

Figure 5.11 Standard trench installations.

The SIDD method may be applied by the use of hand calculations. However, the method is much easier and more efficient if the SIDD computer program and computer-aided calculations are used. A complete discussion of SIDD is outside the scope of this book, but can be found in *Concrete Pipe Technology Handbook*.

Design Strengths for Concrete Pipes

Design $W_{3\text{-edge}}$ strengths for reinforced concrete pipe having various standard diameters, wall thicknesses, concrete strengths, and reinforcement requirements for standard strength classes are given in ASTM C 76, C 506, and C 507. Design requirements for reinforced pipe with specified D load strength requirements and special reinforcement designs are given in ASTM C 655. The pipe reinforcement designs given in ASTM C 76 are based on strength factors of 1.5 to 1.25 over the required service load $D_{.01}$, but this standard does not require that quality control $W_{3\text{-edge}}$ tests be taken to ultimate. The same applies to ASTM C 506 and C 507.

In summary, under the indirect procedure, pipe designs for wall thickness, reinforcement, and concrete strength to provide specific required $W_{3\text{-edge}}$ service and strength performance have been obtained

TABLE 5.12 Standard Embankment Installation Soils and Minimum Compaction Requirements

Installation type	Bedding thickness	Haunch and outer bedding	Lower side
Type 1	$D_o/24$ minimum, not less than 3 in (75 mm). If rock foundation, use $D_o/12$ minimum, not less than 6 in (150 mm).	95% SW	90% SW, 95% ML, or 100% CL
Type 2	$D_o/24$ minimum, not less than 3 in (75 mm). If rock foundation, use $D_o/12$ minimum, not less than 6 in (150 mm).	90% SW or 95% ML	85% SW, 90% ML, or 95% CL
Type 3	$D_o/24$ minimum, not less than 3 in (75 mm). If rock foundation, use $D_o/12$ minimum, not less than 6 in (150 mm).	85% SW, 90% ML, or 95% CL	85% SW, 90% ML, or 95% CL
Type 4	No bedding required, except if rock foundation, use $D_o/12$ minimum, not less than 6 in (150 mm).	No compaction required, except if CL, use 85% CL	No compaction required, except if CL, use 85% CL

NOTES:

1. Compaction and soil symbols (that is, 95% SW) refer to SW soil material with a minimum standard Proctor compaction of 95 percent.
2. Soil in the outer bedding, haunch, and lower side zones, except within $D_o/3$ from the pipe spring line, shall be compacted to at least the same compaction as the majority of soil in the overfill zone.
3. Subtrenches
   a. A subtrench is defined as a trench with its top below finished grade by more than $0.1H$ or, for roadways, its top at an elevation lower than 1 ft (0.3 m) below the bottom of the pavement base material.
   b. The minimum width of a subtrench shall be $1.33D_o$ or wider if required for adequate space to attain the specified compaction in the haunch and bedding zones.
   c. For subtrenches with walls of natural soil, any portion of the lower side zone in the subtrench wall shall be at least as firm as an equivalent soil placed to the compaction requirements specified for the lower side zone and as firm as the majority of soil in the overfill zone, or shall be removed and replaced with soil compacted to the specified level.

from actual three-edge bearing tests, from empirical evaluations of former tests (as given in ASTM standards), or from design procedures derived from reinforced concrete theory and evaluations of appropriate tests. The required $W_{3\text{-edge}}$ strengths in these indirect designs are obtained from the loads and bedding factors calculated using the Marston-Spangler soil-structure interaction analyses for earth loads.

The Marston-Spangler indirect method has been the most prevalent procedure for designing buried concrete pipe. However, the direct design procedures are becoming more accepted and, in many instances, preferred. Direct design procedures usually require more design infor-

TABLE 5.13 Standard Trench Installation Soils and Minimum Compaction Requirements

Installation type	Bedding thickness	Haunch and outer bedding	Lower side
Type 1	$D_o/24$ minimum, not less than 3 in (75 mm). If rock foundation, use $D_o/12$ minimum, not less than 6 in (150 mm).	95% SW	90% SW, 95% ML, 100% CL, or natural soils of equal firmness
Type 2	$D_o/24$ minimum, not less than 3 in (75 mm). If rock foundation, use $D_o/12$ minimum, not less than 6 in (150 mm).	90% SW or 95% ML	85% SW, 90% ML, 95% CL, or natural soils of equal firmness
Type 3	$D_o/24$ minimum, not less than 3 in (75 mm). If rock foundation, use $D_o/12$ minimum, not less than 6 in (150 mm).	85% SW, 90% ML, or 95% CL	85% SW, 90% ML, 95% CL, or natural soils of equal firmness
Type 4	No bedding required, except if rock foundation, use $D_o/12$ minimum, not less than 6 in (150 mm).	No compaction required, except in CL, use 85% CL	85% SW, 90% ML, 95% CL, or natural soils of equal firmness

NOTES:
1. Compaction and soil symbols (that is, 95% SW) refer to SW soil material with a minimum standard Proctor compaction of 95 percent.
2. The trench top elevation shall be no lower than $0.1H$ below finished grade or, for roadways, no lower than an elevation of 1 ft (0.3 m) below the bottom of the pavement base material.
3. Soil in bedding and haunch zones shall be compacted to at least the same compaction as specified for the majority of soil in the backfill zone.
4. The trench width shall be wider than shown if required for adequate space to attain the specified compaction in the haunch and bedding zones.
5. For trench walls that are within 10° of vertical, the compaction or firmness of the soil in the trench walls and lower side zone need not be considered.
6. For trench walls with greater than 10° slopes that consist of embankment, the lower side shall be compacted to at least the same compaction as specified for the soil in the backfill zone.

mation than does the indirect method. For example, direct design usually considers the distribution and variation of earth pressure around the pipe circumference. Two assumptions for earth pressure distribution have been presented in the technical literature, and they are identified by the principal characteristics of the assumptions about pressure variation. These are termed *uniform* (uniform distributed vertical and horizontal components of pressure) and *radial* (pressures act normal to the pipe surface and vary as a trigonometric function). These assumed pressure variations are often referred to by the names of the individuals who proposed them: uniform, Paris[34]; radial, Olander.[32]

Soil-Pipe Interaction Design and Analysis (SPIDA)

Another computer program that has been developed for the design and analysis of buried concrete pipe is named SPIDA. The SPIDA program is owned and made available by the American Concrete Pipe Association. SPIDA was developed as a fundamental analysis tool for determining the earth loads and pressure distribution on a buried concrete pipe having a wide variety of embedment soils, backfill, and natural soils around and over the pipe.

The program has versatile capability for soil-structure interaction analysis and design of buried concrete pipe installations. Its more significant capabilities and limitations are as follows:

1. The program is capable of analysis and design of circumferential structural effects in a buried circular concrete pipe.
2. It is limited to circular pipe with constant wall thickness.
3. It assumes installations are symmetric about a vertical plane.
4. It is capable of analyzing both trench and embankment installations; sloping trench walls are approximated with the use of steps in the finite element mesh.
5. It is capable of providing pipe designs with the following reinforcement cage arrangements:
   - Nonreinforced pipe
   - Single circular
   - Double circular
   - Single elliptical
   - Combination of circular plus elliptical
   - Combination of circular plus Mat at invert, or Mats at invert and crown, or Mats at invert, crown, and spring line
6. Surface loads may include AASHTO HS-series and interstate trucks, Cooper E-series railroad, user-specified concentrated and uniformly distributed surcharge.
7. Fluid effects may include specified unit weight of fluid in full pipe and internal pressure [up to maximum head of 50 ft (21.7 lb/in^2)].
8. The program is capable of providing pipe designs at intermediate levels of backfill height in a single computer run.

Pipe system designers interested in using SPIDA should contact the American Concrete Pipe Association.

References

1. American Association of State Highway and Transportation Officials (AASHTO). T-99, Standard Methods of Test For the Moisture-Density Relations of Soils and Soil-Aggregate Mixtures Using 5.5-lb (2.49-kg) Rammer and 12-in. (304.8-mm) Drop. Washington.
2. AASHTO. T-180, Standard Method of Test Moisture-Density Relations of Soils and Soil-Aggregate Mixtures Using 10-lb (4.54-kg) Rammer and 18-in. (457-mm) Drop. Washington.
3. AASHTO. 1992. Standard Specifications for Highway Bridges. Washington.
4. AASHTO. M 145, The Classification of Soils and Soil-Aggregate Mixtures for Highway Construction Purposes, Standard Specifications for Transportation Materials and Methods of Sampling and Testing, Part 1. Washington.
5. American Concrete Institute (ACI). 1989. Building Code Requirements for Reinforced Concrete, ACI 318, and ACI 318R Commentary. Detroit.
6. American Concrete Pipe Association (ACPA). 1994. *Concrete Pipe Technology Handbook*. Vienna, Va.
7. American Railway Engineering Association (AREA). 1972. *Manual for Railway Engineering*. Washington.
8. American Society for Testing and Materials. ASTM Standards C 14, C 39, C 76, C 497, C 506, C 507, C 655, C 985, D 698, D 1557, D 2487. Philadelphia.
9. American Society of Civil Engineers (ASCE). 1969. Manual of Practice No. 37, *Design and Construction of Sanitary and Storm Sewers* (also Water Pollution Control Federal Manual of Practice No. 9, *Design and Construction of Sanitary and Storm Sewers*). New York.
10. ASCE. 1993. Standard Practice for Direct Design of Buried Precast Concrete Pipe Using Standard Installations (SIDD) with Appendix A—Manufacturing Specification, and Commentary. New York.
11. ASCE. 1982. *Gravity Sanitary Sewer Design and Construction*. ASCE Manuals and Reports on Engineering Practice, No. 60 (see also Water Pollution Control Federal Manual of Practice No. FD-5). New York.
12. American Water Works Association. AWWA Standard M11, M9, M23, C150, C200, C206, C300, C301, C302, C303, C304, C400, C401, C402, C403, C900, C901, C905, and C950. Denver.
13. Concrete Pipe Division of U.S. Pipe and Foundry Company. *Bulletin 200*. Birmingham, Ala.
14. Federal Aviation Authority (FAA). Aircraft Pavement Design and Evaluation. AC 150/5320-6C.
15. FAA. Aircraft Data. AC 150/5325-5C.
16. Federal Highway Administration (FHWA). 1992. PIPECAR Version 2.0, *User Manual*. FHWA-IP-89-019. U.S. Department of Transportation (available from McTrans Center, 512 Weil Hall, Gainesville, Fla.).
17. Heger, F. J. 1988. New Installation Designs for Buried Concrete Pipe. In *Pipeline Infrastructure—Proceedings of the Concrete,* pp. 117–135. New York: American Society of Civil Engineers.
18. Heger, F. J., and T. J. McGrath. January-February 1983. Radial Tension Strength of Pipe and Other Curved Flexural Members. Detroit: American Concrete Institute.
19. Heger, F. J., and T. J. McGrath. March-April 1984. Crack Width Control in Design of Reinforced Concrete Pipe and Box Sections. Detroit: American Concrete Institute.
20. Hild, J. W. 1975. Compacted Fill. In *Foundation Engineering Handbook*. Eds. H. F. Winterkorn and H. Y. Fang. New York: Van Nostrand Reinhold.
21. Janbu, N. 1963. Soil Compressibility as Determined by Odometer and Triaxial Tests. In *Proceedings of European Conference on Soil Mechanics and Foundation Engineering,* pp. 19–25. Wiesbaden, Germany: Soil Mechanics Foundation.
22. Katona, M. G., J. B. Forrest, F. J. Odello, and J. R. Allgood. 1976. CANDE—A Modern Approach for the Structural Design and Analysis of Buried Culverts. Report FHWA-RD-77-5. U.S. Department of Transportation.
23. Katona, M. G., P. D. Vittes, C. H. Lee, and H. T. Ho. 1981. CANDE-1980: Box Culverts and Soil Models. Springfield, Va.: National Technical Information Service.

24. Konder, R. L., and J. S. Zelasko. 1963. A Hyperbolic Stress-Strain Formulation of Sands. In *Proceedings of the Second Pan American Conference on Soil Mechanics and Foundation Engineering.* 1:209.
25. Krizek, R. J., R. A. Parmelee, N. J. Kay, and H. A. Elnaggar. 1971. Structural Analysis and Design of Buried Culverts. National Cooperative Highway Research Program Report 116. Washington: National Research Council.
26. Kulhawy, F. H., J. M. Duncan, and H. B. Seed. 1969. Finite Element Analysis of Stresses and Movements in Embankments during Construction. Report TE-69-4. Berkeley: Office of Research Services, University of California.
27. Marston, A. 1930. The Theory of External Loads on Closed Conduits in the Light of the Latest Experiments. *Bulletin 96.* Ames: Iowa Engineering Experiment Station.
28. Marston, A., and A. O. Anderson. 1913. The Theory of Loads on Pipes in Ditches and Tests of Cement and Clay Drain Tile and Sewer Pipe. *Bulletin 31.* Ames: Iowa State College.
29. Marston, A., W. J. Schlick, and H. F. Clemmer. 1917. The Supporting Strength of Sewer Pipe in Ditches and Methods of Testing Sewer Pipe in Laboratories to Determine Their Ordinary Supporting Strength. *Bulletin 47.* Ames: Iowa State College.
30. Moser, A. P. 1990. *Buried Pipe Design,* 1st ed. New York: McGraw-Hill.
31. Nyby, D. W. 1981. Finite Element Analysis of Soil Sheet Pipe Interaction. Ph.D. dissertation. Logan: Department of Civil and Environmental Engineering, Utah State University.
32. Olander, H. C. October 1950. *Stress Analysis of Concrete Pipe.* Engineering Monograph No. 6. U.S. Department of the Interior, Bureau of Reclamation.
33. Ozawa, Y., and J. M. Duncan. 1973. ISBILD: A Computer Program for Analysis of Static Stresses and Movements in Embankments. Report No. TE-73-4. Berkeley: Office of Research Services, University of California.
34. Paris, J. M. November 10, 1921. Stress Coefficients for Large Horizontal Pipes. *Engineering News Record* 87(19).
35. Piping Systems Institute. 1980. *Course Notebook.* Logan: Utah State University.
36. Portland Cement Association. 1944. Vertical Pressure on Culverts under Wheel Loads on Concrete Pavement Slabs. Skokie, Ill.
37. Schlick, W. J., and J. W. Johnson. 1926. Concrete Cradles for Large Pipe Conduits. *Bulletin 80.* Ames: Iowa State College.
38. Schlick, W. J. 1932. Loads on Pipe in Wide Ditches. *Bulletin 108.* Ames: Iowa State College.
39. Schlick, W. J. 1920. Supporting Strength of Drain Tile and Sewer Pipe under Different Pipe-Laying Conditions. *Bulletin 57.* Ames: Iowa State College.
40. Selig, E. T. 1988. Soil Parameters for Design of Buried Pipelines. In *Pipeline Infrastructure—Proceedings of the Conference,* pp. 99–116. New York: American Society of Civil Engineers.
41. Smith, W. W. May 1978. Stresses in Rigid Pipe. *ASCE Transportation Engineering Journal* 104(TE3).
42. Spangler, M. G. 1950. Field Measurements of the Settlement Ratios of Various Highway Culverts. *Bulletin 170.* Ames: Iowa State College.
43. Spangler, M. G. 1933. The Supporting Strength of Rigid Pipe Culverts. *Bulletin 112.* Ames: Iowa State College.
44. Spangler, M. G., and R. L. Handy. 1982. *Soil Engineering,* 4th ed. New York: Harper & Row.
45. Spangler, M. G., and W. J. Schlick. 1953. Negative Projecting Conduits. *Report 14.* Ames: Iowa State College.
46. The Asphalt Institute. March 1978. *Soils Manual for the Design of Asphalt Pavement Structures.* Manual Series No. 10 (MS-10). College Park, Md.
47. Timoshenko, S., and D. H. Young. 1962. *Elements of Strength of Materials,* 4th ed., pp. 111, 139. Princeton, N.J.: Van Nostrand Company.
48. Timoshenko, S. P. 1968. *Strength of Materials: Part II—Advanced Theory and Problems.* Princeton, N.J.: Van Nostrand Company.
49. Watkins, R. K., and M. G. Spangler. 1958. Some Characteristics of the Modulus of Passive Resistance of Soil: A Study in Similitude. In *Highway Research Board Proceedings* 37:576–583.

50. Wilson, E. 1971. Solid SAP: A Static Analysis Program for Three-Dimensional Solid Structures. SESM Report 71-19. Berkeley: Structural Engineering Laboratory, University of California.
51. Wong, K. S., and J. M. Duncan. 1974. Hyperbolic Stress-Strain Parameters for Nonlinear Finite Element Analysis of Stresses and Movements in Soil Masses. Report TE-74-3. Berkeley: Office of Research Services, University of California.
52. Zienkiewitcz, O. C. 1977. *The Finite Element Method,* 3d ed. New York: McGraw-Hill.

Chapter

6

Steel and Ductile Iron Flexible Pipe Products

Steel Pipe

Steel pipe is used in many diverse applications. It is available in various sizes, shapes, and wall configurations. For pressure application, the cross section is circular. However, for gravity flow, steel pipes can have cross sections which are vertical elongated ellipses, arch-shaped for low head room, called *long-span arched sections,* and other shapes.

For the most part, steel pipes used for gravity applications have a corrugated wall. The corrugated shape produces a larger moment of inertia which results in a larger pipe stiffness. Such pipes are usually galvanized for corrosion protection, but are also available as aluminized steel. Common coatings and linings available include bitumen-type materials, Portland cement–type materials, and polymers. In certain applications, the lining may be applied after installation. The linings and coatings are usually ignored in strength and stiffness calculations.

Corrugated steel pipes

Introduction. The use of corrugated steel pipes as buried conduits has increased phenomenally since they first appeared on the market about 100 years ago. Both producers and consumers have conducted innumerable tests and continual observation since that time. No purpose could be served here by reviewing the findings. More important are the design techniques that have evolved from these tests and observations.

At first, corrugated metal pipe design tables showed up with only the metal thicknesses (gages) available in each diameter. However, a preferred gage was designated which would produce a reasonably stiff pipe for handling and installation.

Later, fill height tables were developed on the basis of favorable experience on actual installations and then were extended as pipes were placed under higher fills. Limits were imposed when trouble developed. These tables were sometimes shown in manufacturers' literature and were often reproduced in highway design standards. This procedure was sometimes reversed when an agency examined its experience on a large number of installations made under controlled conditions.

Development of the art in this fashion was appropriate for the relatively low fills used in highway construction, and the conservative performance limits that evolved were of little consequence from an economic standpoint. However, as pipe applicability expanded and as depth of cover increased, greater attention was focused on significant bases for design. At least three emerged:

1. Excessive ring deflection or flattening of the pipe
2. The strength of longitudinal and helical seams
3. Ring compression stress in large pipes (wall crushing or elastic buckling of the pipe wall)

Champions of each of the design criteria could cite examples and propose installation procedures which tended to limit the investigation to one basis and obviate the others. With the advent of modern highway design and construction methods, larger culverts and higher fills demanded more rigorous design procedures in order to provide safe, economical installations. With a considerable amount of cooperation, effort, and compromise, design factors and other considerations have been established. Design factors should be verified and modified if necessary. Maximum allowable limits of performance should be reviewed.

Various simplified theories have been proposed for the design of buried, corrugated steel pipes. Each may be valid, but only within limitations. One theory is based on ring deflection Δ/D. (See Fig. 6.1.)

The external soil load on a buried pipe generally causes the cross section (or ring) to deflect such that the vertical diameter decreases and the horizontal diameter increases. According to the ring deflection theory, to design the pipe, some maximum allowable ring deflection is specified, then the actual ring deflection is predicted by one of several available equations. The vertical deflection Δy is usually more predictable and more meaningful than the horizontal deflection Δx. However, Δy and Δx are approximately the same for steel pipe (although opposite in sign) with Δy usually the larger.

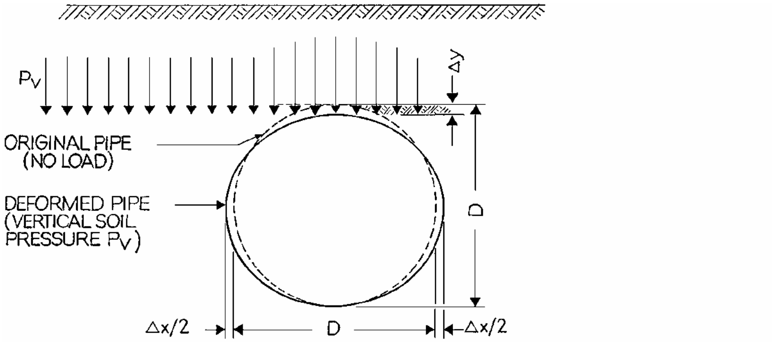

Figure 6.1 Ring deflection of buried flexible pipe.

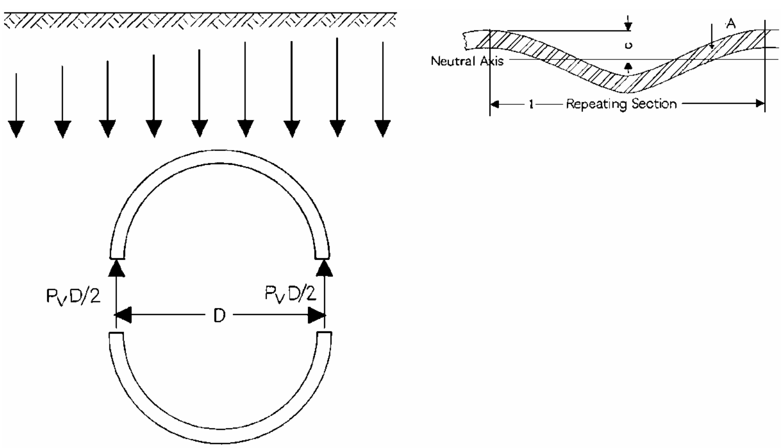

Figure 6.2 Ring compression of buried flexible pipe. A = area of wall cross section per unit length of pipe = area/l; I = moment of inertia about neutral axis per unit length of pipe; E = modulus of elasticity of pipe material; c = distance to most remote fiber from neutral axis; l = unit length of pipe.

Other design theories are based on the compressive ring stress in the pipe wall. The ultimate (or maximum allowable) compressive stress f_c is specified, then the computed compressive stress S is determined from the formula $S = P_v(D/2A)$. (See Fig. 6.2.)

The vertical soil pressure P_v is usually defined as the soil pressure at the level of the top of the pipe if no pipe were in place. This implies that the ring cross section compresses precisely as much as the soil. Actually the pipe in place may cause pressure concentration or pressure relief (if the soil is more or less compressible than the ring cross section) which could possibly be taken into account by a stress concentration factor.

The *ring compression method* specifies that the ring compression thrust $P_vD/2$ must be less than the allowable thrust, which is the allowable strength of longitudinal seam per unit length of pipe. This method assumes that the vertical soil pressure on the pipe is P_v and that the soil completely supports the ring radially.

A modification of the ring compression concept includes wall crushing and wall buckling in addition to seam strength as performance limits. The computed stress is $S = P_v(D/2A)$ (see Fig. 6.2), and the ultimate stress f_c is the crushing strength of the wall (yield point stress), the buckling strength of the wall, or the seam strength. Again, it must be assumed that the soil is precisely as compressible as the ring cross section. Actually soil is not precisely as compressible as the ring cross section, and so the soil pressure on the ring is not exactly P_v. But another problem arises also. Which wall strength, crushing or buckling, actually controls performance and so limits design? At one extreme, if the soil could resist all ring deflection, crushing would control and f_c would be the yield point stress. At the other extreme, if the soil were fluid, (i.e., could resist no ring deflection), buckling might control. Of course, soil is somewhere between the two extremes and is compressible.

Still other theories are based on a predicted stress S in the pipe wall as calculated by classical formulas such as

$$S = \frac{P}{A} + \frac{Mc}{I}$$

where P = ring compression thrust, that is, $P = P_vD/2$
A = area of wall cross section
M = moment on the wall

$$= EI\left(\frac{I}{R_i} - \frac{I}{R_o}\right)$$

I = moment of inertia of wall
c = distance to most remote fiber

To use this formula, the curvature R_i of the deformed pipe ring must be known. The precision of R_i is doubtful. Moreover, the pipe wall is not crushed just because the stress S reaches the yield point. Stress S is the stress in the most remote fiber only, and it may already be at the yield point due to cold-forming. See Fig. 6.3.

The design limit is performance limit divided by a safety factor. The *performance limit* is excessive distortion of the soil-pipe system so that either the pipe or the soil cannot perform adequately its designed func-

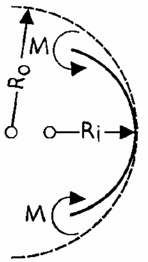

$$d\theta = \frac{M}{EI} = \frac{1}{R_i} - \frac{1}{R_o}$$

$$M = EI\left(\frac{1}{R_i} - \frac{1}{R_o}\right)$$

Figure 6.3 Relationship of moment to change in radius of curvature of pipe ring.

tion. Performance limits do not include a yield point stress in the most remote fiber, or necessarily a specific ring deflection.

The performance limit of a buried corrugated steel pipe ring is deformation of the ring beyond which the system can no longer perform the purpose for which it was designed. If an unacceptable hump or dip or crack develops in the soil surface above the pipe, the performance limit is exceeded. If the flow characteristics of the pipe are reduced below designed values because of ring deformation, the performance limit is exceeded. The final definition of performance limit must be left up to the design engineer.

For most installations, the definition of the performance limit is incipient ring failure, as shown in Fig. 6.4. Incipient ring failure is defined as some deformation of the ring beyond which the ring would continue to deform (to collapse) if loads on it were not relieved by the arching action of the soil. This is an arbitrary performance limit. It does not mean collapse. The proposed strength envelopes shown in Fig. 6.4 become a design chart for this performance limit. The strength envelope for dense soil exceeds the yield point for steel because part of the vertical soil pressure is supported by the soil in arching action. An additional safety factor is "built in" because the ring does not collapse even though it is deformed to incipient ring failure.

The performance limit for buried corrugated steel pipes is not a single phenomenon, but the interaction of a number of phenomena. For example, the performance limit is not simply crushing of the wall, buckling of the wall, shearing of the longitudinal seam, or ring deflection. Each of these influences the others, and all are interrelated to varying degrees under varying circumstances. As might be anticipated, the crushing strength of the wall is less if the ring deflection is large. This is due to flexural stresses. A longitudinal seam in one panel causes a stress concentration in the wall of the adjacent panel and triggers wall crushing. Of course, as wall crushing develops, wall buckling is initiated and buckling near seams causes seam failure—truly an interaction phenomenon.

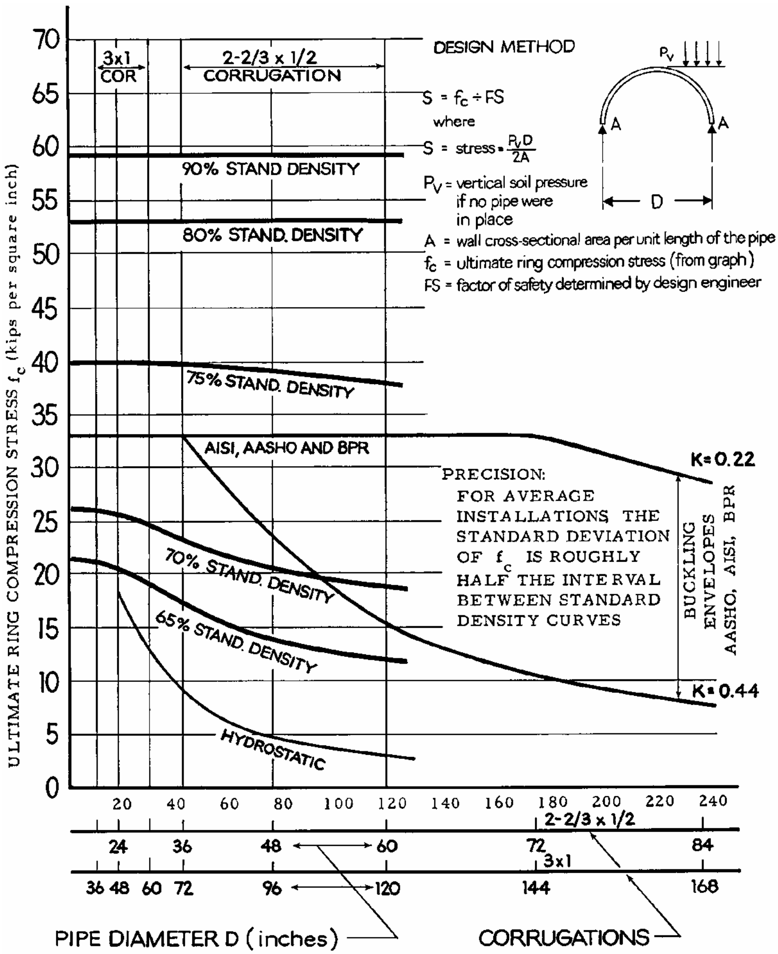

Figure 6.4 Ultimate ring compression stress as a function of diameter and corrugations for various values of soil density in percent of standard as determined by AASHTO method T-99.

In every case, the performance limit is a ring deformation observable inside the pipe. The probable deviation in observing performance limits may be as much as 10 percent of vertical soil pressure, especially near the critical void ratio. The following are some deformations identified as performance limits in these tests.

Wall crushing. When the pipe is buried in densely compacted soil (denser than the critical void ratio), wall crushing is often the first

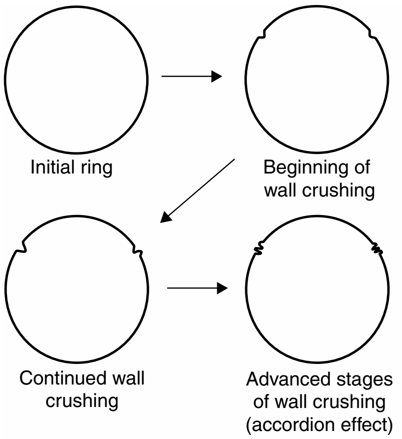

Figure 6.5 Diagrammatic sketch of the mechanism of wall crushing.

indication that the performance limit has been reached. Slight dimpling of the corrugations is the first visual indication of distress. Dimpling is not a performance limit, but dimpling portends the location of general wall crushing. This crushing usually occurs between 10 and 2 o'clock in the ring. Deep corrugations dimple as soon as or sooner than shallow corrugations, but general wall crushing shows up at equal or slightly higher pressures. In general, wall crushing develops as shown in Fig. 6.5. It starts with a dimpling of the corrugations and progresses into an accordion effect.

The crushing strength of the wall is the yield point stress times the wall cross-sectional area per unit length of pipe. The yield point stress of the steel involved in this experiment varied between 35 and 45 kips/in^2. This variation was not significant because the influence is partially masked by other variables, such as seam strength and ring deflection. There is little doubt that crushing strength would be directly proportional to the yield point stress if seams were 100 percent efficient and ring deflection were constrained to zero. Also, for a given gage of steel, the cross-sectional area increases as the corrugation height is increased.

In Utah State University tests, it was shown that ring flexibility $(D/r)^2$ influences crushing strength in loose soil. This is seen in Fig. 6.4 where the curves drop off to the right as the ring flexibility increases.

Reversal of curvature. As the load increases, a section of the ring may tend to flatten and then reverse curvature (Fig. 6.6). There are two general types of reversal of curvature. In the case of very loose soil (density less than the critical void ratio), as the soil is compressed downward, the pipe tends to form an ellipse, but in so doing high flexural stresses

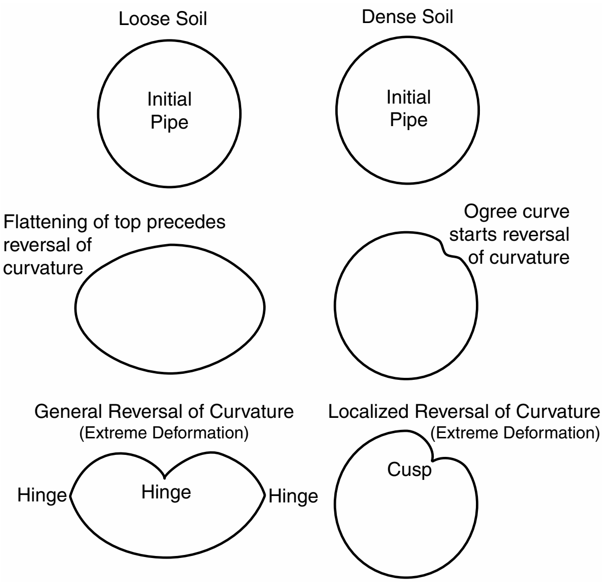

Figure 6.6 Comparison of the types of reversal of curvature observed in dense and loose soil.

develop at the sides. These stresses combined with some ring compression cause plastic hinges. If this deformation is carried to the extreme, the top of the pipe comes down in a reversal of curvature, and ultimately a third plastic hinge forms in the top center. The other type of reversal occurs in dense soil and may be referred to as localized buckling. This is not confined to top center. It usually forms between 10 and 2 o'clock, but not necessarily so. Occasionally the reversal occurs in the bottom between 5 and 7 o'clock. None has been seen in the sides between about 2 and 5 o'clock or between almost 7 and 10 o'clock. The performance limit for deep corrugations tends to be plastic hinges at the sides rather than reversed curvature. For shallow corrugation, plastic hinges at the sides form only if the soil is very compressible; otherwise, the performance limit is reversal of curvature. The difference is insignificant in light of uncertainties in soil placement, density, or boundaries.

Seam separation. There is no question about identifying seam separation; the question usually relates to what triggers seam separation. In the case of the helical lockseam, when a reversal of curvature commences, and more especially as it develops into a cusp, the seam tends to open. This is a simple tension separation. See Fig. 6.7. Apparently

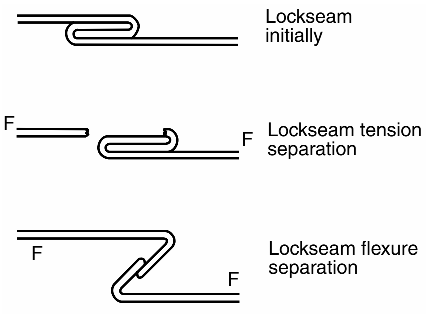

Figure 6.7 Diagrammatic sketch of seam separation of lockseam joint.

cold working of the metal in processing the seam weakens it enough that the separation occurs in the metal adjacent to the seam due to a combination of tensions and unfolding of the seam. If the reversal proceeds faster on one side of the lockseam, one side of the seam may lift with respect to the other and so open the seam by unfolding it. This usually happens in the bottom of the pipe and is due to nonuniform bedding conditions. See Fig. 6.7.

In all cases, it is important to note that dimpling of the crests of the corrugations is not a performance limit. Neither is slipping of riveted or lockseam joints. These should be accepted as stress relievers. It is highly significant that the *extreme deformations* referred to above are not typical of field installations, but can be observed in a test cell.

Each design theory is based on an entirely different performance limit based on entirely different phenomena. For example, ring deflection is based on compression of the soil and flexibility of the pipe ring. Conversely, the ring compression theory is based on soil pressure and either the strength of the wall (crushing or buckling) or the strength of the seam, and soil compression and ring flexibility are not usually included. A buried pipe can begin to register distress of one type which then triggers a response and complete failure in another category.

Under soil loading the pipe tends to form an ellipse, but in doing so, flexural stresses develop. These stresses combined with some ring compression cause what appears to be wall crushing, which may be described better as a plastic hinge (see Fig. 6.8). If this deformation is carried to the extreme, the top of the pipe comes down in an inversion, and ultimately a third plastic hinge forms in the top center.

The other type of reversal occurs in dense soil and may better be referred to as localized buckling. This is not confined to top center. It usually forms between 10 and 2 o'clock, but not always. Occasionally, the reversal occurs in the bottom half between 5 and 7 o'clock. None has been seen in the sides between about 2 and 5 o'clock or between about 7 and 10 o'clock.

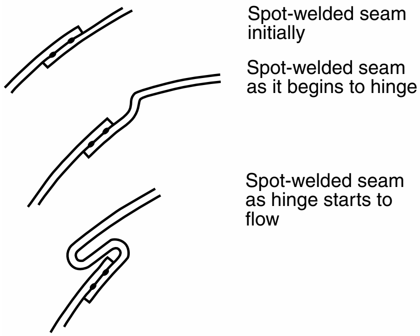

Figure 6.8 Diagrammatic sketch of welded seam showing typical formation of hinge followed by plastic flow.

The most important factors influencing the above-described performance limits are the pipe wall crushing strength and the soil compression. Of lesser influence are the ring flexibility and the longitudinal seam strength. Other factors such as soil friction angle are insignificant or unknown.

The most significant results of the Utah State University (USU) tests are shown in Fig. 6.4. The ordinate is the apparent ring compression strength f_c. It is defined as the apparent ring compression stress at the performance limit, i.e.,

$$f_c = \frac{PD}{2A} \qquad \text{at performance limit} \tag{6.1}$$

where P = apparent vertical soil pressure, i.e., calculated pressure at level of top of pipe if no pipe were in place

D = nominal diameter of pipe

A = cross-sectional area of pipe wall per unit length of pipe

Performance limit is ring deformation beyond which the soil-pipe system does not perform adequately. To design the pipe ring, one can employ the well-known, universal design criterion stress < strength, i.e.,

$$\frac{PD}{2A} = \frac{f_c}{N} \tag{6.2}$$

where $P = D_L + L_L$ = apparent vertical soil pressure (i.e., calculated pressure at level of top of pipe if no pipe were in place) that compromises dead load D_L and live load L_L

$D_L = \gamma H$ = or unit weight of soil γ times the height of fill H over top of pipe

L_L = vertical soil pressure at level of top of pipe due to surface loads

f_c = apparent ring compression strength that can be simply picked off the plots (Fig. 6.4)

N = safety factor

The ordinate in Fig. 6.4 is labeled *ultimate* ring compression stress. The abscissa is ring flexibility $(D/r)^2$. More correctly this should be $(D/r)^2/E$, where D is the diameter, r is the centroidal radius of gyration of the longitudinal pipe wall cross section, and E is the modulus of elasticity of the pipe material. However, in these tests the only material used in the pipes is steel for which $E = 29 \times 10^6$ lb/in^2, so E is a constant and is not included in the variable $(D/r)^2$. Within the precision of these tests, the radius of gyration r is constant for a given corrugation configuration (i.e., it is essentially independent of the gage of steel); so the abscissa can be displayed as a pipe diameter D for each given corrugation configuration.

In dense soil, the ring flexibility does not have a significant effect on the ultimate ring compression stress. This is so because the ring deflection is so small that any stress in the ring is pure compression (not flexure). The performance limit is wall crushing and is independent of ring flexibility. However, the factor of safety against reversal of curvature is greater if the depth of corrugation is increased.

It is noteworthy that the strength envelopes dip down to the right with increasing ring flexibility. This is due to the increased sensitivity of the very flexible ring to nonuniform soil density. If the soil could be placed particle by particle, the strength envelopes would not dip down so much (especially in well-compacted soil). However, present soil placement techniques result in nonhomogeneous soil that causes pressure spots and precipitates wall buckling in the very flexible rings. This is shown as the ring buckling zone.

Compression of the soil has a major effect on performance limits. Compression is determined by the average vertical soil pressure P_v and the soil modulus E'. Soil modulus E' is increased by increasing the soil density. From the tests, the greater the soil density (greater E'), the greater the ultimate ring compression stress f_c in the pipe wall. Quantitative results are shown in Fig. 6.4. The difference between the values of f_c in dense and loose soil is roughly a 3:1 ratio. Why should the strength of the pipe be greater in dense soil if the pipe is exactly the same? Even though the value f_c is called an ultimate *ring* compression stress, it actually is a measure of strength of the *soil-pipe system*—not just the pipe. The contribution of the soil as a supportive structure increases the system strength if the soil is dense and relatively rigid. On the other hand, if the soil is loose and highly compressible, it will develop a pressure concentration on the pipe as the soil compresses down under vertical pressure. Moreover, soil compression causes ring deflection which further weakens the system by adding flexural stress into the conduit wall and by increasing the wall thrust by increasing the horizontal diameter. If the pipe compresses down exactly as much as the soil, then the vertical pressure on the pipe is the same as the vertical pressure P_v in the soil. If the soil is dense, then soil compression is small and the cross-sectional area of the pipe may be reduced more than the cross-sectional area of the soil. So the pipe will relieve itself of vertical soil pressure. This is tantamount to arching action inasmuch as the soil is forced to bridge or arch over the pipe. Of major significance is the critical void ratio of the soil. If a soil is compacted such that it is denser than the critical void ratio, then the pressure concentrations on these corrugated steel pipes are only about 20 to 40 percent of the pressure concentrations if the soil is looser than the critical void ratio.

Particularly noteworthy is the great difference in the general slope of the load-deflection plots for pipes buried in loose soil in contradistinction to pipes buried in dense soil. The horizontal deflection data are about the same as the vertical deflection data; however, it has been found that vertical deflection data can be measured with greater precision and, for most analyses, are considerably more meaningful.

Some plots of general results are indicated in Fig. 6.4, which shows the ultimate ring compression stress as a function of the ring flexibility. Because the material is steel with a constant modulus, the ring flexibility can be reduced to $(D/r)^2$; or because the radius of gyration is essentially constant for any depth of corrugation, this reduces to just pipe diameter D for specific corrugation configurations.

It must be understood, of course, that this presentation applies only for a given yield point stress. In this case, about 35 to 40 kips/in^2. If the yield point were twice as high, all the allowable stress lines would go up roughly twice as high. This is not precise, however, because ring flexibility, soil compressibility, and ring deflection, as well as yield point of the material, influence the allowable stress lines. The test data indicate that the longitudinal seams do influence the ultimate ring compression stress lines, but that this influence is much less significant than the soil compression and pipe wall crushing strength.

Conclusions

1. A performance limit of a buried corrugated steel pipe is best defined as that maximum deformation beyond which either the pipe or the soil cannot perform its design function. Unless limited by some other factor, the maximum deformation is defined as that

deflection of the pipe ring beyond which the ring could develop no additional resistance even though the external soil pressures were increased.

2. The most important factors in predicting performance limits of buried corrugated steel pipes are soil compression and pipe wall crushing strength. Soil compression is determined by the vertical soil pressure and soil modulus, which is dependent upon soil density. The relationship of these factors to the performance limit is presented in Fig. 6.4, which becomes the basis for design.

3. The results presented are conservative (especially at excessive deformations). If a collapse failure cannot occur at a safety factor of 1.0, there seems to be little justification for a safety factor of 4.0. A factor of 2.0 should be adequate for most controlled installations. Where no control is exercised, the design engineer must use her or his judgment.

4. Longitudinal seams are generally adequate.

Example 6.1 Suppose that a 48-in-diameter $2\frac{2}{3}$- by $\frac{1}{2}$-in corrugated steel pipe is to be installed under 120 ft of soil embankment. The soil about the pipe is to be compacted to 90 percent modified density (found to have a unit weight of about 120 lb/ft^3). Determine the pipe wall thickness (gage) if the performance limit is defined as incipient ring failure (Fig. 6.4). Suppose that H-20 loading will pass over the surface. If control of the installation is dubious, a safety factor of $N = 2$ will be assumed.

The apparent vertical soil pressure on the pipe ring is

$$P = D_L + L_L = 14.4 \text{ kips/ft}^2$$

where $D_L = \gamma H = 120 \text{ lb/ft}^3 \times 120 \text{ ft}$
L_L = negligible

The apparent ring compression stress is

$$\frac{PD}{2A} = \frac{(14.4 \text{ kips/ft}^2)\,(4.0 \text{ ft})}{2A} = \frac{28.8 \text{ kips/ft}}{A}$$

where A = area per unit length

The apparent ring compression strength (based on 40 ksi yield point) is

$$f_c = 60 \text{ kips/in}^2$$

which is the ordinate to the strength envelope shown in Fig. 6.4 corresponding to soil density of 90 percent and a pipe diameter of 4.0 ft in a $2\frac{2}{3}$- by $\frac{1}{2}$-in corrugation. (Where the yield point is something other than 40 ksi, the apparent ring compression strength f_c is modified proportionally.) Equating stress to strength divided by safety factor yields

$$\frac{PD}{2A} = \frac{f_c}{N}$$

or

$$\frac{28.8 \text{ kips/ft}}{A} = \frac{60 \text{ kips/in}^2}{2}$$

Solving for the area yields $A = 0.96$ in^2/ft. One should use 12-gage steel that has an area of 1.356 in^2/ft.

A check on ring deflection would predict a ring deflection of less than 3 percent at a soil density of 90 percent.

The ring flexibility factor (handling factor) is adequate.

Three-dimensional FEA modeling of a corrugated steel pipe arch. Finite element modeling of a corrugated structure presents special problems that must be addressed if a solution is to be meaningful. If the structure is to be used as an underground shelter, it must be designed to withstand very large longitudinal forces. These forces are developed from large dynamic pressure loads acting on the shelter's concrete end walls, which in turn transmit a longitudinal load to the side of the corrugated arch.

The modulus of elasticity and shear modulus of steel are a material property that is usually considered to be independent of geometry. In the case of corrugated pipe, the corrugations behave somewhat as springs and allow structural deformation in addition to material elasticity. The combined structural and material deformation may be determined such that an equivalent modulus of elasticity and shear modulus can be defined. The use of equivalent properties allows the structural analysis to be completed by assuming orthotropic plate conditions. The equivalent properties determined here represent analytical approximations that depend upon hypothetical boundary and loading conditions. The purpose of these approximations is to assist in the simplification of design.

Two separate finite element analysis (FEA) models were created for determining the extensional elastic modulus and shear modulus of corrugated plates. These models were created using the pre-processing graphics capabilities of CAEDS finite element software. Then nodes and elements were transported to NASTRAN for computer analysis.

Each computer model was run multiple times to provide results for various material thicknesses of a 6×2 corrugation. The same basic geometry was used for each of the different thicknesses. Uncoated material thicknesses were used for all analyses.

The extensional elastic modulus of the corrugated plate was determined by applying increasing forces to one end of a finite element corrugation model one wavelength in length and 1 in wide. Load-deflection curves were then constructed from the FEA results. The equivalent extensional elastic modulus of the corrugation may be calculated from the slope of the load-deflection curve in the linear region

$$E = \sigma/\varepsilon = \frac{\text{force/area}}{\text{elongation/length}}$$

A condition of plane strain as opposed to plane stress was assumed to represent the corrugated structure. Consequently, the plane strain elastic modulus was considered to be $E/(1 - \nu^2)$, where E is the plane stress modulus of elasticity.

An equivalent Poisson's ratio was found for the corrugated geometry by determining the change in width of the small representative strip and dividing it by the original width to find ε_2 and by the original length to determine ε_1. Poisson's ratios were then calculated from the equation

$$\nu_{12} = \frac{\varepsilon_2}{\varepsilon_1}$$

Poisson's ratio ν_{21} was then determined by the relation between the orthotropic elastic moduli in the 1 and 2 directions:

$$\nu_{21}E_1 = \nu_{12}E_2$$

Material nonlinearities occur when the steel corrugation reaches its yield strength (33 ksi). At that point, the displacements are no longer directly proportional to the applied forces. This point is interpolated from the load-displacement curves where the curve is no longer linear. The force at which this occurs divided by the cross-sectional area of the corrugated plate is equal to the elastic limit.

A nonlinear finite element analysis was used to determine the corrugation elastic limit. To accomplish this, NASTRAN applied a fraction of the total static load to the geometry, formed a new stiffness matrix using the deformed geometry and changing material properties, and then applied the remaining force in the same iterative manner. When equivalent orthotropic elements are used in a corrugated arch structural analysis, the elastic limit may be used as a criterion of failure in the case of stresses caused by longitudinal loading.

A square corrugated plate 6 in on a side was used for the 6×2 corrugation. These models were attached to ground at each corner by very soft springs, and then a 100-lb shearing force was applied to each edge around the perimeter.

Forces were distributed evenly across the straightedge and proportionate to the lineal distance between nodes on the corrugated edges of the model. Iterations on spring strength showed the springs must have a minimum strength to provide model stability.

Shear modulus was calculated from the displacements output by NASTRAN for the given geometry and material thickness. The displacements divided by the length of the sides determined the angular deformation γ of the square element. The 100-lb force was divided by the area of the side to determine the shearing stress τ.

$$F = \frac{\tau}{\gamma}$$

The shear and extensional elastic moduli and Poisson's ratios determined may be used to formulate equivalent orthotropic elements for use in large FEA models of corrugated structures. The elastic limit may be used as one criterion of failure in corrugated arch structures subject to end loading.

The NASTRAN finite element analysis program was used to complete a three-dimensional analytical model of the arch. The extensional modulus, shearing modulus, and Poisson's ratio were used to create equivalent orthotropic plate elements that would approximate the actual corrugated plate, use far fewer elements and computer time, and allow for easier failure analysis of the structure.

An arch support structure was analyzed using finite element modeling. Rather than model the corrugated geometry in detail, equivalent orthotropic plate elements were derived from the material properties obtained from smaller analytical models of the actual corrugated geometry. The analysis included a simulation of structural restraints, load distributions, soil interaction assumptions, material properties, and other parameters. The application of the model results is obviously dependent upon the proper characterization of the model parameters.

Quarter symmetry may be utilized to reduce the number of finite elements and thus the computer runtime for the model. This was possible since loading on either end was assumed equal, and the loads were applied symmetrically at the faces. Appropriate boundary conditions were used to constrain the deflecting elements from violating boundaries of symmetry.

The three-dimensional finite element model with model parameters, as defined, using equivalent properties works well. These equivalent material properties (see Tables 6.1 and 6.2) were determined by assuming orthotropic plate conditions. The combined structural and material deformation may be determined such that an equivalent modulus of elasticity and shear modulus can be defined. The equivalent properties determined here represent analytical approximations that may be used to assist in the simplification of design.

TABLE 6.1 6 × 2 Shear Modulus and Poisson's Ratio

Thickness, in	Shear modulus G, lb/in^2	ν_{12}	ν_{21}
0.1345	120,682	8.47E-04	0.273
0.1644	174,828	1.26E-03	0.274
0.1838	211,916	1.58E-03	0.274
0.2145	277,500	2.15E-03	0.274
0.2451	348,123	2.80E-03	0.275
0.2758	423,364	3.54E-03	0.275
0.1875	219,326	1.64E-03	0.274
0.2500	359,892	2.91E-03	0.274
0.3125	512,500	4.53E-03	0.274
0.3750	676,142	6.49E-03	0.274

TABLE 6.2 6 × 2 Extensional Modulus and Elastic Limit

Thickness, in	Extensional modulus E, lb/in^2	Elastic limit, lb/in^2
0.1345	89,818	1004
0.1644	133,523	1204
0.1838	167,406	1518
0.2145	227,184	1608
0.2451	295,729	1854
0.2758	372,941	1946
0.1875	174,018	1520
0.2500	308,021	1848
0.3125	480,000	2211
0.3750	686,695	2636

Tests on spiral ribbed steel pipe

Introduction. Tests were conducted on a ribbed steel pipe (approximately 29.4-in inside diameter). The pipe has a rib profile wall with a smooth bore. It is a helical pipe with an interlocking helical joint. The tests were conducted at Utah State University in the small soil load cell (see Figs. 6.9 and 6.10).

The soil used for the tests was a silty sand. It was selected because of the wide range of possible densities, which makes it ideal for pipe testing. The soil gradation curve and the Proctor density curve for this soil are given in Figs. 6.11 and 6.12, respectively.

Pipe material properties are as follows:

The Steel Sheet

Gauge	Thickness	Modulus, lb/in^2	Yield, lb/in^2		Tensile strength, lb/in^2	
			Minimum	Actual	Minimum	Actual
16	0.064 in	29.5×10^6	33,000	40,800–44,000	45,000	51,100–53,500

Figure 6.9 Placement of ribbed steel pipe in test cell.

Sectional properties of the pipe are as follows:

Area per length: $A = 0.364\ \text{in}^2/\text{ft}$

Moment of inertia: $I = 2.390\ \text{in}^4/\text{ft} \times 10^{-3}$

Radius of gyration: $r = 0.281\ \text{in}$

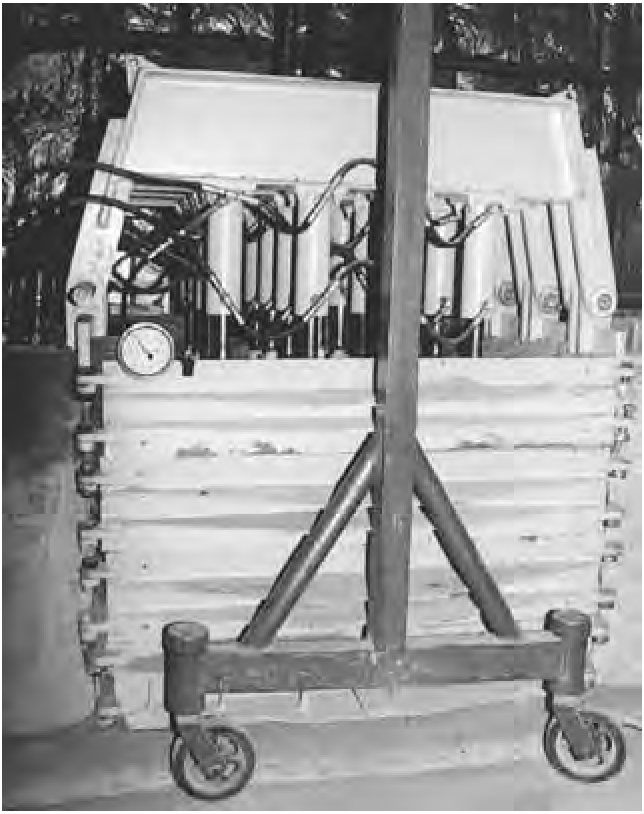

Figure 6.10 Test cell in operation—pistons of cylinders extended.

Description of pipes tested. The pipe is ribbed and is formed by helical winding. The closed rib is 1 in tall and is spaced on 10.25-in centers. The lockseam is spaced midway between the ribs.

Three tests were conducted by installing the test pipe in the small soil load cell. The test data are reported in terms of height of cover. Height of cover is calculated from measured vertical soil pressure using a soil unit weight of 120 lb/ft³ as follows:

$$\text{Height of cover (ft)} = \frac{\text{vertical soil pressure (lb/ft}^2\text{)}}{120\ \text{lb/ft}^3}$$

In each test vertical loading was increased until plastic hinging was observed. At that point, the load was held constant. The pipe did not

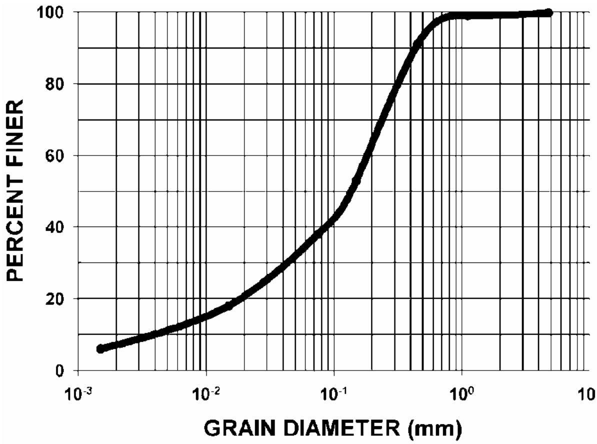

Figure 6.11 Gradation curve and classification for the silty-sand soil used in the tests. Atterberg limits: liquid limit, NA; plastic limit, NA. Soil classification: SM. Specific gravity: 2.72.

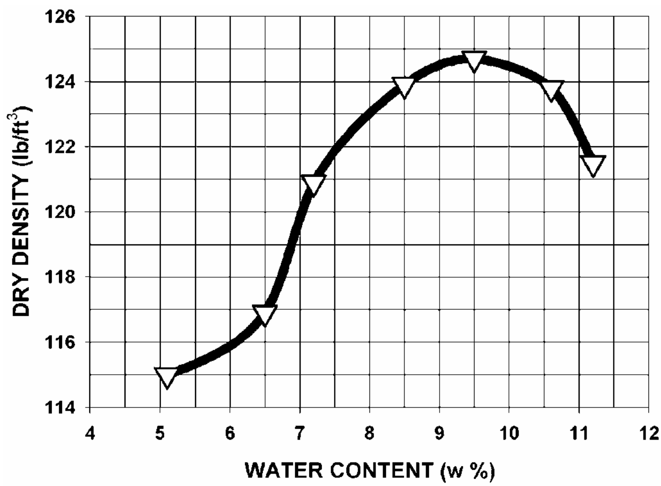

Figure 6.12 Compaction (standard Proctor) curve for silty-sand soil used in tests. Maximum dry density: 124.7 lb/ft^3. Optimum moisture: 9.5 percent.

Figure 6.13 Inside the pipe at 35 ft of cover.

collapse or continue to deflect under that load. An increase in load was required for the deflection to continue. Therefore, even after plastic hinging, the pipe-soil system is still under stable equilibrium.

Test 1. The test pipe was installed in silty-sand soil compacted to 76 percent standard Proctor density. This type of installation would be considered a poor installation and would normally not be recommended. At about 35 ft of cover, the top began to flatten, and signs of localized buckling began to appear at the sides of the pipe (see Fig. 6.13). As the load was increased, the localized buckling became more pronounced, and at about 40 ft of cover, plastic hinges began to form. (See Fig. 6.14.) The results of this test are shown in the graph of Fig. 6.15.

Test 2. This pipe was installed in silty-sand soil compacted to 84 percent standard Proctor density. This type of installation would be considered good and is typically what is achieved in normal practice. At about 50 ft of cover, the top began to flatten, and the seams started to show some signs of distress. As the load was increased, localized buckling started at the sides of the pipe. As the load increased further, this buckling became more pronounced, and at 68 ft of cover, plastic hinges began to form. The results of this test are shown in Fig. 6.16.

Test 3. The test pipe was installed in silty-sand soil compacted to 95 percent standard Proctor density. This type of installation would be considered excellent and would normally be the very best installation

Figure 6.14 Inside the pipe after completion of test (40 ft of cover).

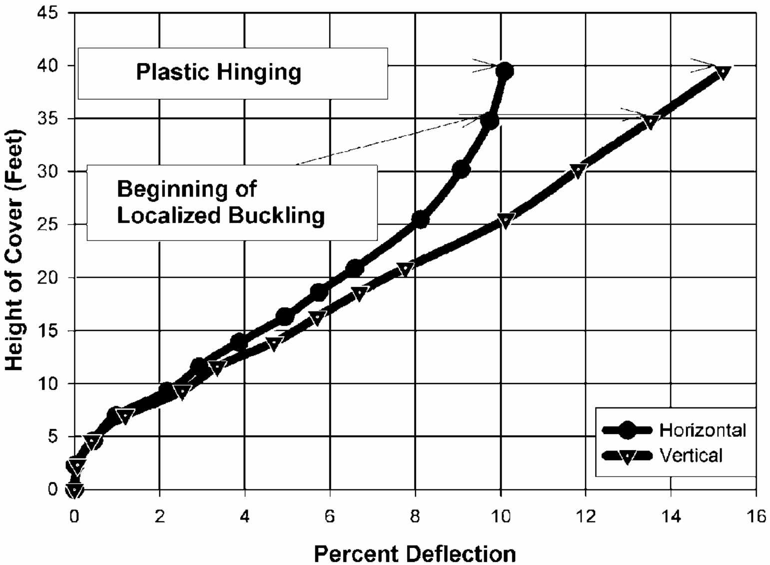

Figure 6.15 Test 1, silty-sand soil at 76 percent standard Proctor density.

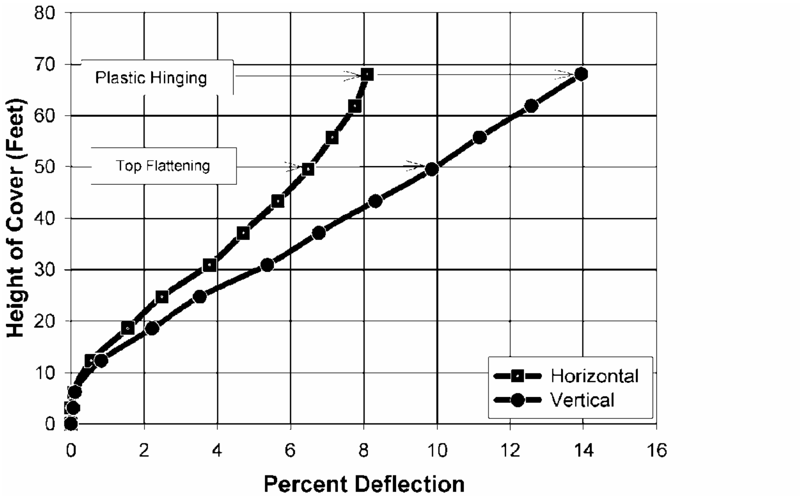

Figure 6.16 Test 2, silty-sand soil at 84 percent standard Proctor density.

that could be expected. At about 86 ft of cover, slight local buckling began at the sides of the pipe. At about 100 ft of cover, the top began to flatten and started to show signs of localized buckling. At 105 ft of cover, small local buckles were visible at some seams. At 110 ft of cover, plastic hinges were definite at the sides of the pipe. Some bulging also occurred at the bottom of the pipe. (See Fig. 6.17.) The results of this test are shown in Fig. 6.18.

Overall results. The vertical deflections of the three tests are shown in Fig. 6.19. This graph shows the importance of soil density in the performance of buried pipes. The response to soil pressure was excellent. The resulting deflections were reasonable and about what would be expected. No seams opened or failed during the tests, even at extreme heights of cover. Because the rib height is properly designed, the rib acts as an integral part of the pipe wall. This allows the rib to stiffen the wall and resist buckling.

Tests on low-stiffness ribbed steel pipe

Introduction. Tests were performed on a ribbed steel pipe which has been designed for use in the small-diameter drainage pipe market. The pipe is a smooth bore, helically ribbed pipe with essentially closed ribs. Pipes tested are 18-, 24-, and 30-in diameters. A total of 10 tests were

Figure 6.17 Inside pipe at completion of test 3. The cover height is 110 ft.

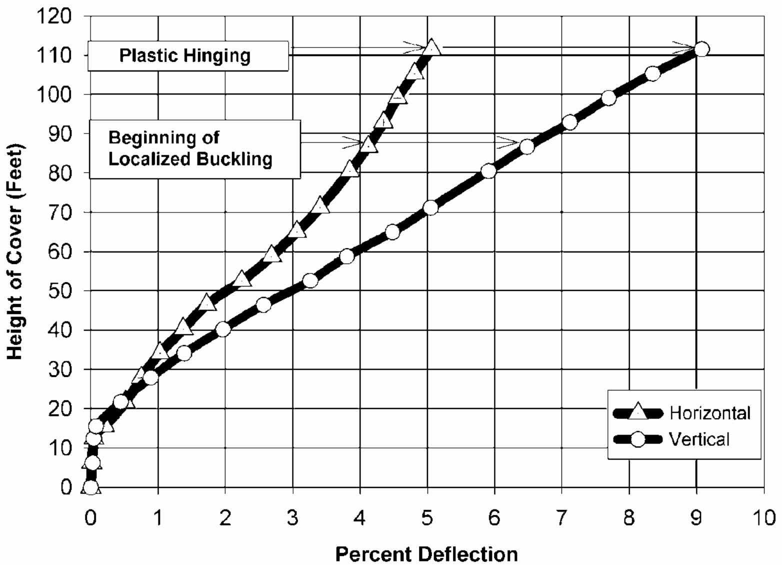

Figure 6.18 Test 3, silty-sand soil at 95 percent standard Proctor density.

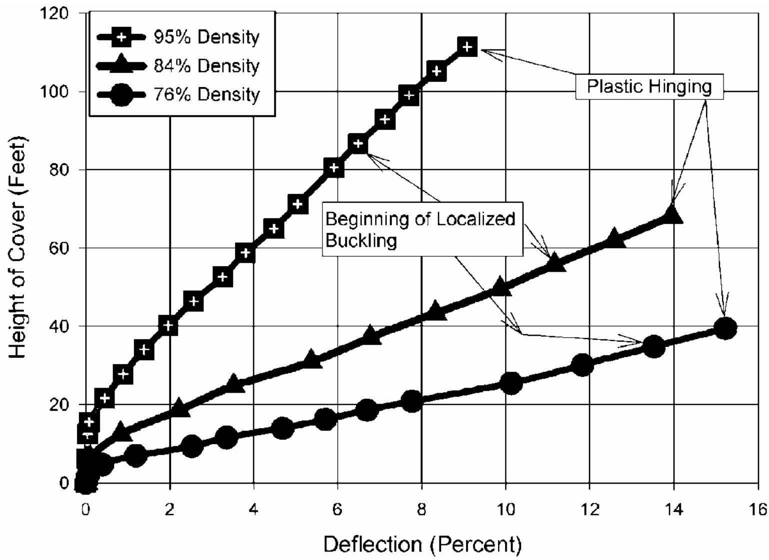

Figure 6.19 Vertical deflection for the three tests in silty-sand soil at various densities.

conducted. The tests were run at Utah State University in the small soil load cell (see Figs. 6.20 and 6.21). The pipe properties are as follows:

The Steel Sheet

Gage	Measured thickness, in	Modulus, lb/in^2	Yield, lb/in^2		Tensile strength, lb/in^2	
			Minimum	Actual	Minimum	Actual
26	0.023	29.5×10^6	33,000	48,700	45,000	56,100

Description of pipes tested

1. The pipe is ribbed and is formed by helical winding with a lock-seam.
2. The closed rib is 0.375 in tall for the 18- and 24-in pipes and 0.50 in tall for the 30-in pipe. Three ribs are spaced over 5.43 in.

Sectional properties of the pipe are as follows:

	30-in pipe	18- and 24-in pipes
Area per length	$A = 0.230$ in^2/ft	$A = 0.200$ in^2/ft
Moment of inertia	$I = 0.550$ in^4/ft $\times 10^{-3}$	$I = 0.261$ in^4/ft $\times 10^{-3}$
Radius of gyration	$r = 0.169$ in	$r = 0.125$ in

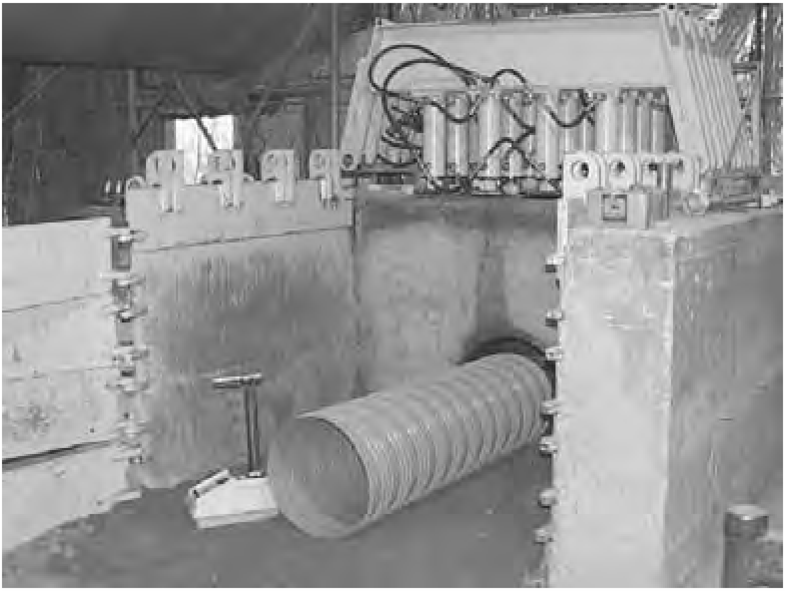

Figure 6.20 An 18-in ribbed pipe is being installed in small soil load cell at Utah State University.

Figure 6.21 An 18-in ribbed pipe is being installed in small soil load cell at Utah State University.

The soil used for the tests was a silty sand. It was selected because of the wide range of possible densities, which makes it ideal for pipe testing. The soil gradation curve and the Proctor density curve for this soil are given in Figs. 6.11 and 6.12, respectively.

Test results

Live load tests. The purpose of these tests was to simulate a loaded truck passing over the pipe. The standard AASHTO H-20 load represents a 16,000-lb load on a single dual-wheel assembly and distributed over a 10-in × 20-in area, as shown in Fig. 6.22.

For low cover heights over the pipe, this test is very severe. These test pipes were buried in silty-sand soil compacted to 90 percent standard Proctor density. From the level of the top of the pipe to the upper-soil surface, the soil was compacted to achieve as high a density as possible to provide a compacted bearing surface for the 10-in × 20-in plate.

The 18-in-diameter live load test. This test was conducted with only 1 ft of cover over the pipe to simulate a minimum cover application. The load was first applied to the surface of the soil, but directly to the side of the pipe. This simulates an approaching truck. At 16,000 lb the 10-in × 20-in plate penetrated the soil about 2 in. The pipe reaction was a small inversion at the side of the pipe, as seen in Fig. 6.23. This inversion is a precursor to the buckling seen in Fig. 6.24.

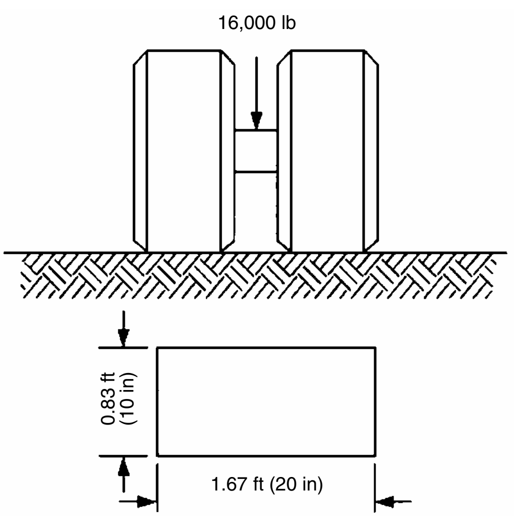

Figure 6.22 H-20 live load schematic.

Figure 6.23 Small inversion in sidewall due to 16,000-lb live load adjacent to pipe. Pipe installed with 1 ft of cover.

Figure 6.24 Buckling due to 14,000-lb live load over one-half of pipe.

The loading plate was then positioned on the soil surface, just off the centerline of the pipe, so the load is over one-half of the pipe. This is the most critical position for a live load. The load was increased toward the required 16,000 lb. At 14,000 lb, a soil failure wedge formed, the plate began to penetrate the soil, and the pipe could not support the resulting load. At this load, there was a catastrophic failure (buckling) of the pipe (see Fig. 6.24). It is evident from the figure that the pipe does not have enough longitudinal stiffness to transfer the load longitudinally along the pipe.

The 24-in-diameter live load test. This test was also conducted with only 1 ft of cover over the pipe to simulate a minimum cover application. The load was first applied to the surface of the soil, but directly to the side of the pipe. For this test, the loading plate was increased to 10 in × 40 in—twice the area of the previous 18-in pipe. The decision was made in view of the poor performance observed in that test and because similar-sized plates had been used in the evaluation of other types of pipe. In general, the larger plate is justified because the longitudinal distribution of pressure through the soil in this test is more severe than in the case of an actual pavement. Also, penetration into the soil does not occur in a typical application. The loading plate penetrated the soil about 1 in. The pipe showed no adverse reaction. This pipe was more flexible than intended (see footnote to Table 6.3).

The loading plate was then positioned on the soil surface just off the centerline of the pipe so the load is over one-half of the pipe. Again, this is the most critical position for a live load. The load was increased toward the required 16,000 lb. A soil failure wedge formed at 16,000 lb, the plate began to penetrate the soil, and the pipe could not support the resulting load. At this load, there was a catastrophic failure (buckling) of the pipe (see Figs. 6.25 and 6.26).

30-in-diameter live load test. This test was also conducted with only 1 ft of cover over the pipe to simulate a minimum cover application. The load was first applied to the surface of the soil but directly to

TABLE 6.3 Summary of Soil Cell Results

Diameter, in	30	24*	18
Rib depth, in	1/2	3/8	3/8
Wall thickness, intended, in	0.022	0.028	0.022
Wall thickness, measured, in	0.023	0.023	0.023
Fill height performance limit test at 95 percent minimum density, ft	52	27	64
Fill height performance limit test at 90 percent minimum density, ft	30	24	30

*According to the manufacturer, the steel sheet used for the 24-in pipe was thinner than intended (0.023 in instead of 0.028 in); hence, the pipe was more flexible than would be permitted in practice.

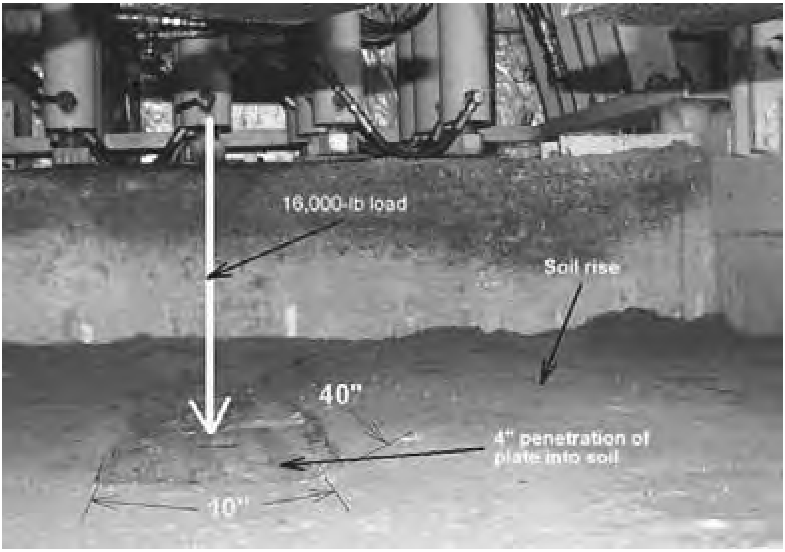

Figure 6.25 Photograph showing soil surface, plate penetration, and resulting soil rise due to buckling of the pipe.

Figure 6.26 Buckled 24-in pipe resulting from a 16,000-lb live load.

the side of the pipe. Again, because of the catastrophic failure of the 18-in pipe, the 16,000 lb was distributed over a 10-in × 40-in area—twice the area of the 18-in test. The loading plate penetrated the soil about 1 in. The pipe showed no adverse reaction.

The loading plate was then positioned on the soil surface just off the centerline of the pipe (the most critical position for a live load), so the load is over one-half of the pipe. The load was increased toward the required 16,000 lb. At 16,000 lb, the plate penetrated the soil about 4 in and otherwise was in equilibrium (see Fig. 6.27). The load was held for several minutes, and there was no adverse reaction of the pipe (see Fig. 6.28). This pipe, when properly installed with cover heights of 1 ft or greater, will withstand an H-20 loading.

The load was gradually increased to determine what load would cause failure. At 18,853 lb, a soil failure wedge formed, the plate began to penetrate the soil, and the pipe could not support the resulting load. At this load, there was a catastrophic failure (buckling) of the pipe (see Figs. 6.29 and 6.30).

Rerun of the 18-in-diameter live load test. Based on the experience with the previous tests, this test was run with 2 ft of cover instead of the 1 ft used for the other tests. Also, because of the 2 ft of cover, the

Figure 6.27 Application of 16,000 lb.

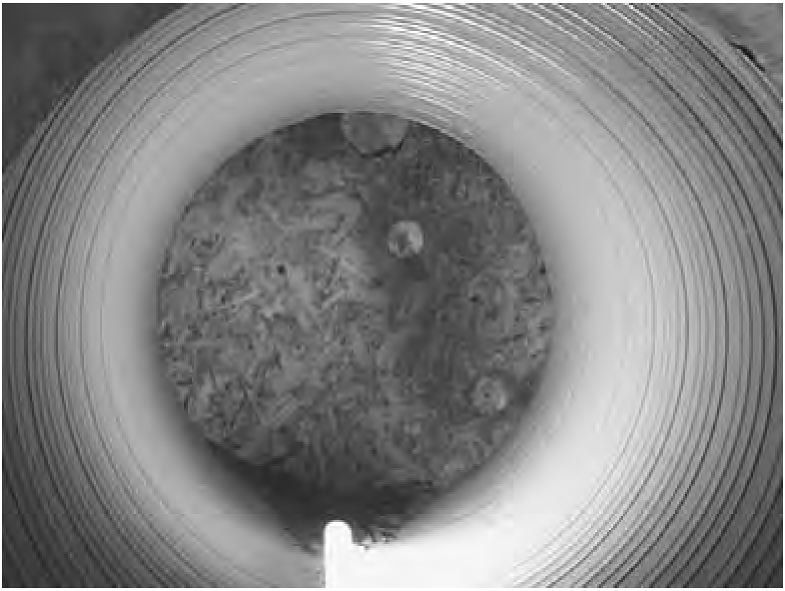

Figure 6.28 A 30-in pipe showing no negative reaction to a 16,000-lb live load.

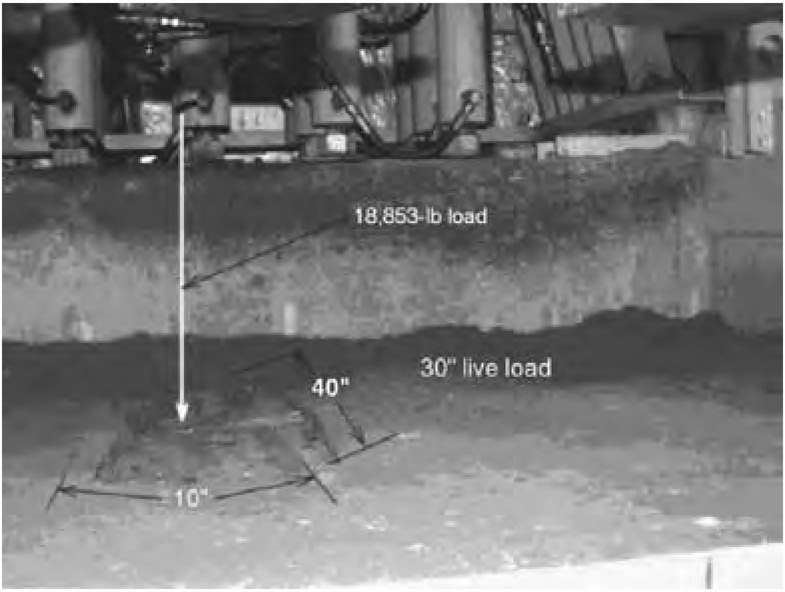

Figure 6.29 Application of an 18,853-lb load.

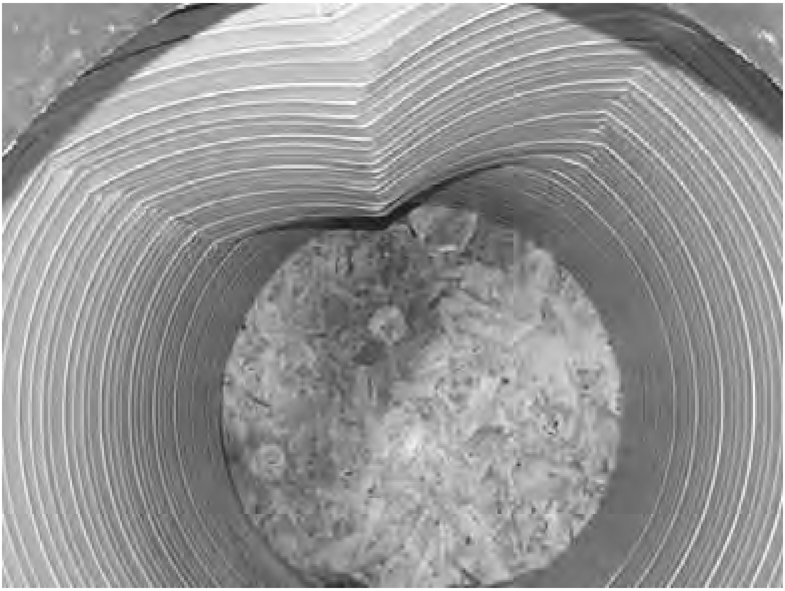

Figure 6.30 A 30-in pipe with buckled wall due to an 18,853-lb live load.

10-in $\times$ 20-in plate was used to distribute the load. The load was first applied to the surface of the soil, but directly to the side of the pipe. At 16,000 lb, the 10-in $\times$ 20-in plate penetrated the soil about 3 in. The pipe had no adverse reaction to the load.

The loading plate was then positioned on the soil surface just off the centerline of the pipe (the most critical position for a live load), so the load is over one-half of the pipe. The load was increased toward the required 16,000 lb. At 16,000 lb, the plate penetrated the soil about 4 in and otherwise was in equilibrium. The load was held for several minutes, and there was no adverse reaction of the pipe (see Figs. 6.31 and 6.32). This pipe, when properly installed with 2 ft of cover, will withstand an H-20 loading.

Load-deflection tests. Six load-deflection tests were run on test pipes buried in the small soil cell. There were three diameters (18-in, 24-in, and 30-in) and two soil densities (90 and 95 percent standard Proctor). In each test, vertical loading was increased until plastic hinging or wall crushing was observed.

Height of cover. The tests were conducted by installing the test pipe in the small soil load cell. The test data are reported in terms of height

Figure 6.31 Photograph showing 16,000-lb load being applied to a 10-in × 20-in plate over one-half of the pipe.

Figure 6.32 A 24-in pipe, with 2 ft of cover, showing no adverse reaction to a 16,000-lb live load.

of cover. Height of cover is calculated from measured vertical soil pressure by using a soil unit weight of 120 lb/ft^3 as follows:

$$\text{Height of cover (ft)} = \frac{\text{vertical soil pressure (lb/ft}^2\text{)}}{120 \text{ lb/ft}^3}$$

Load-deflection test 1. The 18-in test pipe was installed in silty-sand soil compacted to 95 percent standard Proctor density. This type of installation is considered excellent and is difficult to achieve in field conditions. At about 64 ft of cover and 5.7 percent deflection, the top of the pipe began to buckle (see Fig. 6.33). A buckling failure is a stiffness failure and takes place because of low ring stiffness. As the load was increased the buckling became more pronounced, and at 75 ft of cover the test was terminated. The results of this test are shown in Fig. 6.34.

Load-deflection test 2. This 18-in test pipe was installed in silty-sand soil compacted to 90 percent standard Proctor density. This type of installation would be considered very good and is typically the best that is achieved in normal practice. At about 30 ft of cover and 8 percent deflection, the top began to buckle, and the seams started to show some signs of distress (see Fig. 6.35). As the load was increased,

Figure 6.33 Steel-ribbed pipe (18-in diameter) at 75 ft of cover in silty-sand soil at 95 percent density.

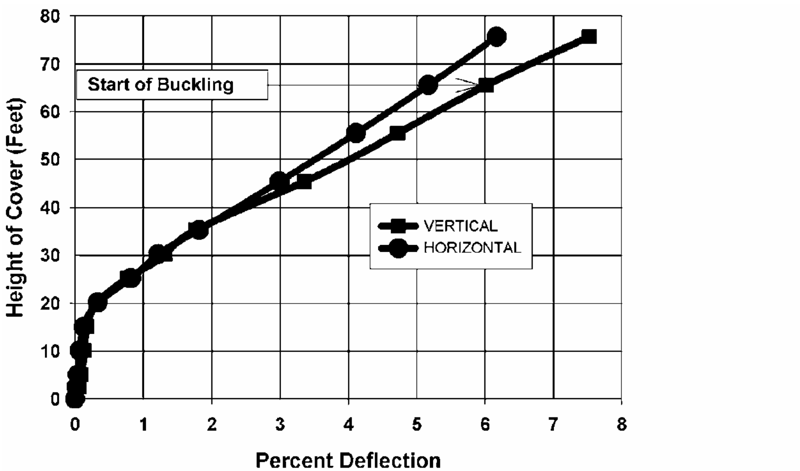

Figure 6.34 Load-deflection curves for 18-in ribbed steel pipe, silty-sand soil compacted to 95 percent standard Proctor density.

buckling became more pronounced. The test was stopped at 35 ft of cover. The results of this test are shown in Fig. 6.36.

Load-deflection test 3. This test pipe had 24-in diameter and was installed in silty-sand soil compacted to 95 percent standard Proctor density. Again, this type of installation would be considered excellent and is difficult to achieve in actual field conditions. At about 27 ft of cover and 3.5 percent deflection, the sidewalls began to crush (see Fig. 6.37). A wall-crushing failure is a strength failure and takes place because the wall area is inadequate to support the ring compression stress induced by the soil load. As the load was increased, wall crushing became more pronounced. The test was stopped at about 45 ft of cover. The results of this test are shown in Fig. 6.38. (See footnote to Table 6.3.)

Load-deflection test 4. This 24-in test pipe was installed in silty-sand soil compacted to 91 percent standard Proctor density. This type of installation would be considered very good and is typically the best that is achieved in normal practice. At about 24 ft of cover and 4 percent deflection, the sidewalls began to crush (see Fig. 6.39). As the load was increased, wall crushing became more pronounced. The test was stopped at 50 ft of cover. The results of this test are shown in Fig. 6.40. (See footnote to Table 6.3.)

Load-deflection test 5. This test pipe had 30-in diameter and was installed in silty-sand soil compacted to 97 percent standard Proctor density. Again, this type of installation would be considered excellent and is difficult to achieve in actual field conditions. At about 52

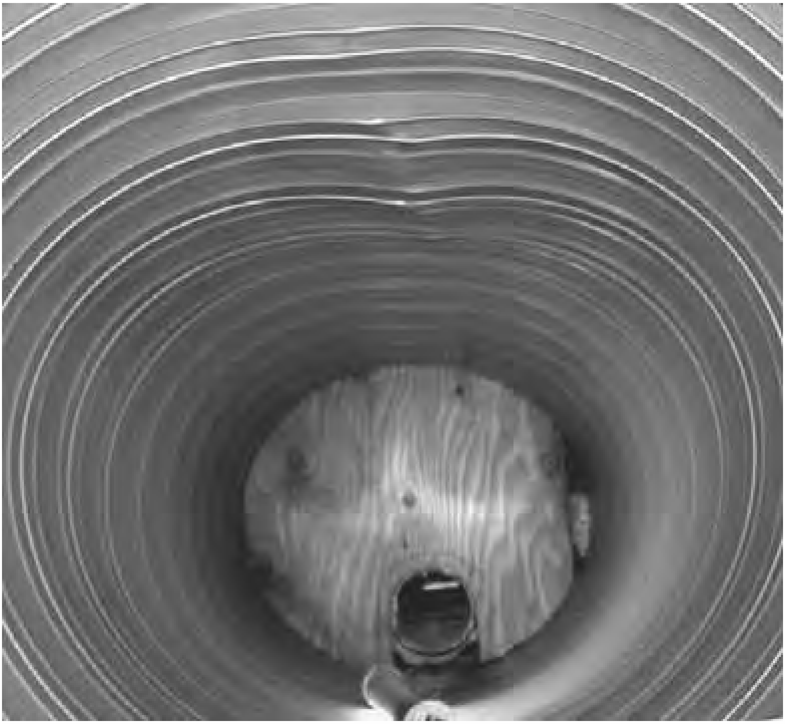

Figure 6.35 Steel-ribbed pipe (18-in diameter) at 30 ft of cover in silty-sand soil at 90 percent density.

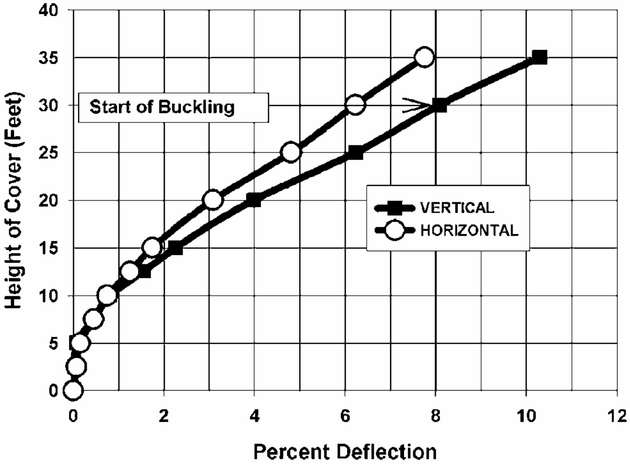

Figure 6.36 Load-deflection curves for 18-in ribbed steel pipe, silty-sand soil compacted to 90 percent standard Proctor density.

Figure 6.37 Steel-ribbed pipe (24-in diameter) at 43 ft of cover in silty-sand soil at 95 percent density.

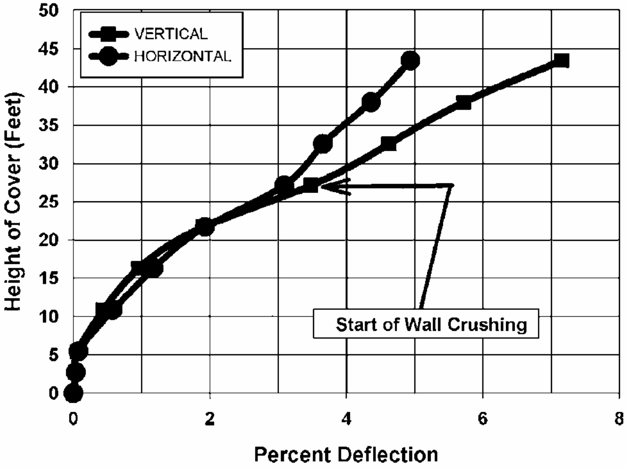

Figure 6.38 Load deflection curves for 24-in ribbed steel pipe, silty-sand soil compacted to 95 percent standard Proctor density.

Figure 6.39 Steel-ribbed pipe (24-in diameter) at 49 ft of cover in silty-sand soil at 91 percent density.

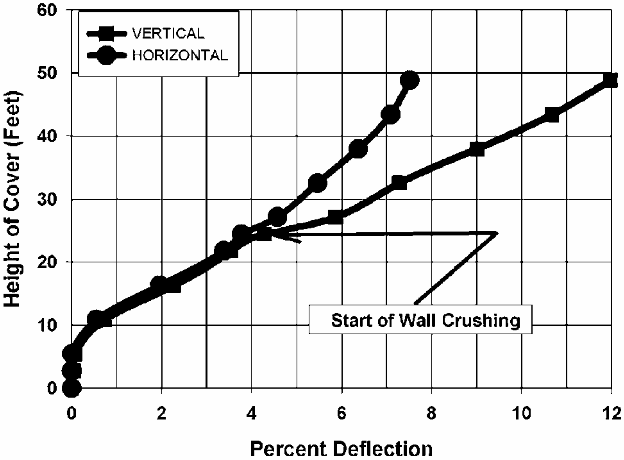

Figure 6.40 Load-deflection curves for 24-in ribbed steel pipe, silty-sand soil compacted to 91 percent standard Proctor density.

Figure 6.41 Steel-ribbed pipe (30-in diameter) at 60 ft of cover in silty-sand soil at 97 percent density.

ft of cover and 3 percent deflection, the sidewalls began to crush (see Fig. 6.41). Again, a wall-crushing failure is a strength failure and takes place because the wall area is inadequate to support the ring compression stress induced by the soil load. As the load was increased, wall crushing became more pronounced. The test was stopped at about 65 ft of cover. The results of this test are shown in Fig. 6.42.

Load-deflection test 6. This 30-in test pipe was installed in silty-sand soil compacted to 90 percent standard Proctor density. This type of installation would be considered very good and is typically the best that is achieved in normal practice. At about 30 ft of cover and 3.4 percent deflection, the sidewalls began to crush. As the load was increased, wall crushing became more pronounced, and simultaneously wall buckling took place (see Fig. 6.43). It is interesting to note that in this test, the stiffness and the strength performance limits occur almost simultaneously. The test was stopped at about 47 ft of cover. The results of this test are shown in Fig. 6.44.

Comparison of results. The vertical deflections of the six tests are shown in Fig. 6.45. This graph shows the importance of soil density in

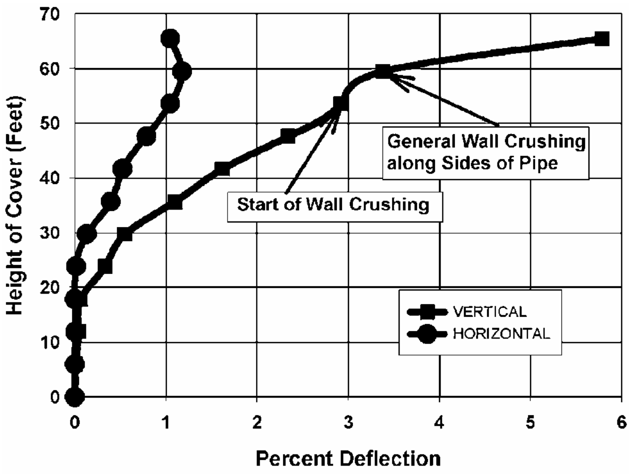

Figure 6.42 Load-deflection curves for 30-in ribbed steel pipe, silty-sand soil compacted to 97 percent standard Proctor density.

Figure 6.43 Steel-ribbed pipe (30-in diameter) at 42 ft of cover in silty-sand soil at 90 percent density.

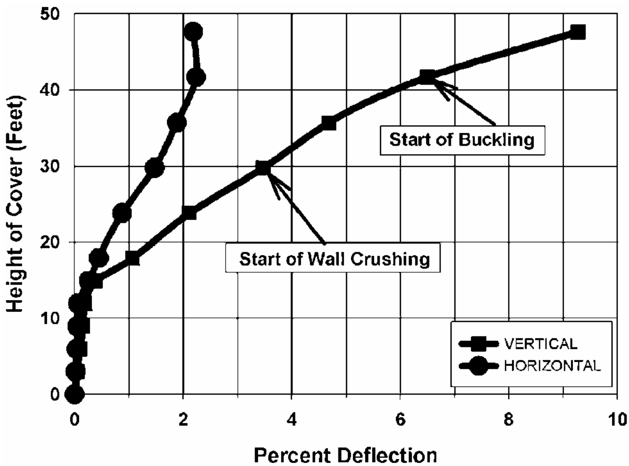

Figure 6.44 Load-deflection curves for 30-in ribbed steel pipe, silty-sand soil compacted to 90 percent standard Proctor density.

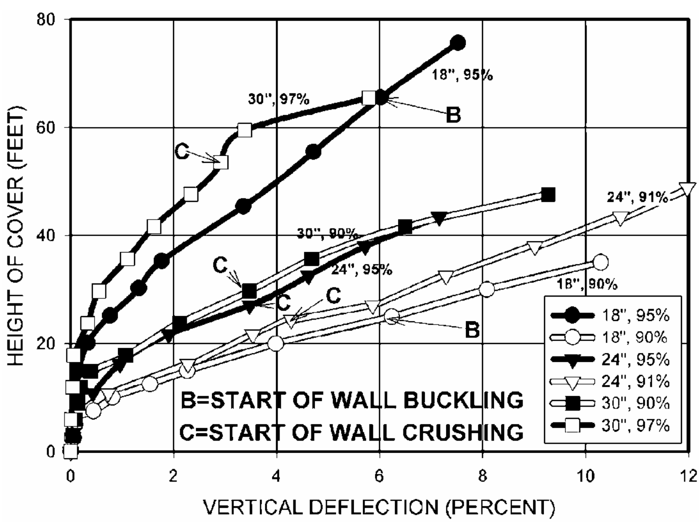

Figure 6.45 Vertical deflections for the six load deflection tests. Start of wall buckling and crushing are noted by B and C, respectively.

the performance of buried pipes. It is interesting to note that for the 24- and the 30-in tests, wall crushing starts at deflections in the range of 3.5 to 4.0 percent. For the 18-in tests, wall buckling occurred first and took place at about 6.0 percent deflection.

Overall performance. The pipe performed well for a pipe of that level of stiffness and wall area. The resulting deflections were reasonable and about what would be expected. The seam integrity was good. No seams opened or failed during the tests, even at extreme heights of cover.

Live load tests. In tests with simulated H-20 live load, the pipe did not perform well in tests with a minimum cover (before loading) of 1 ft. However, tests showed the pipe would perform well with a cover of 2 ft. The actual minimum cover at which the pipe will perform well is between 1 and 2 ft. Additional tests would be required to determine the actual critical minimum cover. Results show the performance of the pipe could be enhanced if the ring stiffness and the local longitudinal stiffness were increased.

Load deflection tests. The 18- and 30-in pipes demonstrated a capacity for a height of cover (before wall crushing or severe deformation) of 52 to 64 ft in soil at 95 percent of standard Proctor density, and 30 ft in soil at 90 percent standard density. The 24-in-diameter test pipes were thinner than intended and, therefore, more flexible than would be permitted in practice. The performance limits for the 24-in pipes tested ranged from 24 to 27 ft of cover.

AISI Handbook

Design information for corrugated steel products is available in the *Handbook of Steel Drainage and Highway Construction Products,* which is published by the American Iron and Steel Institute (AISI). Also, many manufacturers publish design information for their products. Such information should be secured and considered by the designer. For corrugated steel pipes with circular sections, standard analysis and design procedures which have been discussed in this book apply and may be used by the design engineer. See Table 6.4.

Example 6.2—Corrugated steel A 48-in-diameter (3 in by 1 in) corrugated steel pipe is to be placed in an embankment with 60 ft of soil cover. The soil in the pipe zone is to be coarse sand with some fines and is to be compacted to 90 percent Proctor density.

What thickness is required so that the pipe deflection does not exceed 5 percent?

TABLE 6.4 Sectional Properties of Corrugated Steel Sheets

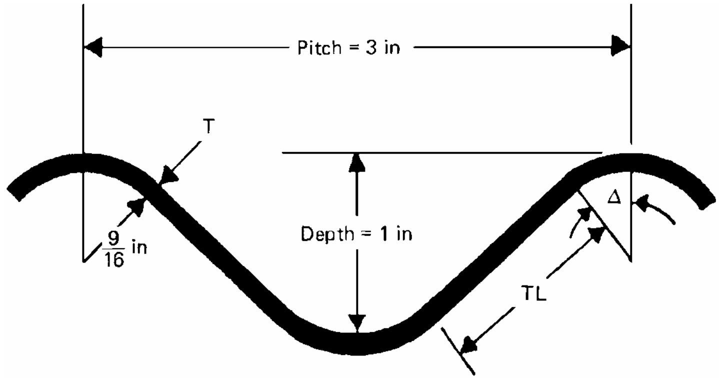

Specified thickness, in	Uncoated thickness I, in	Area of section A, in^2/ft	Tangent length TL, in	Tangent angle Δ, deg	Moment of inertia† I, in^4/ft	Section modulus† S, in^3/ft	Radius of gyration r, in	Developed width‡ factor
0.040*	0.0359	0.534	0.963	44.19	0.0618	0.1194	0.3403	1.239
0.052	0.0478	0.711	0.951	44.39	0.0827	0.1578	0.3410	1.240
0.064	0.0598	0.890	0.938	44.60	0.1039	0.1961	0.3417	1.240
0.079	0.0747	1.113	0.922	44.87	0.1306	0.2431	0.3427	1.241
0.109	0.1046	1.560	0.889	45.42	0.1855	0.3358	0.3448	1.243
0.138	0.1345	2.008	0.855	46.02	0.2421	0.4269	0.3472	1.244
0.168	0.1644	2.458	0.819	46.65	0.3010	0.5170	0.3499	1.246

*Thickness not commonly available. Information only.
†Per foot of projection about the neutral axis. To obtain A, I, or S per inch of width, divide by 12.
‡Developed width factor measures the increase in profile length due to corrugating. Dimensions are subject to manufacturing tolerances.

Use Spangler's equation.

$$\frac{\Delta y}{D} = \frac{0.1\ \gamma H}{EI/r^3 + 0.061E'}$$

$$H = 60 \text{ ft} \qquad D = 48 \text{ in}$$

Let

$$\gamma = 120 \text{ lb/ft}^3$$

$$E = 30 \times 10^6 \text{ lb/in}^2$$

$$E' = 1000 \text{ lb/in} \qquad \text{(from Table 3.4)}$$

Solve for EI/r^3.

$$\frac{EI}{r^3} = \frac{0.1\ \gamma H}{\Delta y/D} - 0.061\ E'$$

$$= \frac{(0.1)\,(120)\,(60)\,(1/144)}{0.05} - 0.061\ (1000)$$

$$= 100 - 61 = 39$$

or

$$I = \frac{39r^3}{E} = \frac{39\ (24)^3}{30 \times 10^6}$$

$$= 0.018 \text{ in}^4\text{/in}$$

$$= 0.22 \text{ in}^4\text{/ft}$$

From Table 6.4, the uncoated thickness should be 0.1345 in.

Now assume the yield stress σ_y for the steel is 33,000 lb/in². What wall area is required for ring compression design with a safety factor of 2?

$$\text{Design compression stress } f_c = \frac{\sigma_y}{2} = 16{,}500 \text{ lb/in}^2$$

$$\text{Vertical soil pressure } P_v = (120)\,(60) = 7200 \text{ lb/ft}^2$$

or

$$P_v = \frac{7200}{144} = 50 \text{ lb/in}^2$$

$$f_c = \frac{PDL}{2A} = \frac{PD}{2A/L}$$

Solve for A/L.

$$\frac{A}{L} = \frac{PD}{2f_c} = \frac{(50)(48)}{2\,(16{,}500)} = 0.073 \text{ in}^2/\text{in}$$

$$= (0.073 \text{ in}^2/\text{in})\,(12 \text{ in/ft}) = 0.88 \text{ in}^2/\text{ft}$$

From Table 6.4, the uncoated thickness is 0.0598 in. Thus, the deflection design controls, and the thickness found in the beginning of the example is the required thickness.

Steel pressure pipes are used in many varied and diverse applications in industrial, agricultural, and municipal markets. The discussion here will be limited to steel pipe used primarily in the municipal water market (see Table 6.5). However, principles used are applicable to all steel pressure pipe.

AWWA M11, *Steel Pipe—A Guide for Design and Installation*

This manual gives procedures for determining the required thickness for steel pressure pipe. The internal pressure used in design should be that to which the pipe may be subjected during its lifetime. The thickness selected should be that which satisfies the most severe requirement. The minimum thickness of a cylinder should be selected to limit

TABLE 6.5 Selected Standards for Steel Pressure Pipes in Water Service

AWWA C200	Steel water pipe 6 in and larger
AWWA C203	Coal-tar protective coatings and linings for steel water pipelines—enamel and tape applied hot
AWWA C205	Cement-mortar protective lining and coating for steel water pipe—4 in and larger—shop-applied
AWWA C206	Field welding of steel water pipe
AWWA C207	Steel pipe flanges for waterworks service—sizes 4 through 144 in
AWWA C208	Dimensions for fabricated steel water pipe fittings
AWWA C209	Cold-applied tape coatings for special sections, connections, and fittings for steel water pipelines
AWWA C210	Coal-tar epoxy coating system for the interior and exterior of steel water pipe
AWWA C213	Fusion-bonded epoxy coating for the interior and exterior of steel water pipelines
AWWA C214	Tape coating systems for the exterior of steel water pipelines
AWWA C602	Cement-mortar lining of water pipelines in place—4 in (100 mm) and larger
AWWA M11	Steel pipe design and installation

the circumferential tension stress to a certain level. The maximum pressure in the pipe must be used in the design calculations. Surge or water hammer pressures and pressures created by the pumping operations must also be considered.

With pressure determined, the wall thickness is found by using Eq. (4.2):

$$t = \frac{P_i D}{2\sigma_{\max}}$$

where t = minimum specified wall thickness, in
P_i = internal pressure, lb/in^2
D = outside diameter of pipe steel cylinder (not including coatings), in
$\sigma_{\max}$ = allowable stress, lb/in^2

For steel pipe, a design stress equal to 50 percent of the specified minimum yield strength is often accepted for steel water pipe. This design (working) stress is determined with relation to the steel's yield strength rather than its ultimate strength. For some applications, other safety factors may apply. For example, the Bureau of Reclamation in its design criteria for penstocks has adopted a safety factor of 3 based on the ultimate tensile strength or a safety factor 1.33 based on the minimum yield strength.

Table 6.6 is reprinted from AWWA M11. It lists grades of steel referenced in AWWA C200, *Standard for Steel Water Pipe 6 Inches and Larger,* and gives design stresses to be used as a basis for working pressure. Also given are the yield stresses and the ultimate stresses for the various grades of steel.

The designer can easily calculate working pressure, via Eq. (4.2), corresponding to 50 percent of the specified minimum yield strength for several types of steel commonly used. A required thickness may not be available from a manufacturer. It is, therefore, recommended that the pipe manufacturers be consulted before final selection of diameter and wall thicknesses.

For transient pressures, the hoop stress may be allowed to rise, within limits, above 50 percent of yield for transient loads. When ultimate tensile strength is considered, a safety factor well over 2 is realized. The stress of transitory surge pressures together with static pressure may be taken at 75 percent of the yield point stress, but should not exceed the mill test pressure. The designer should, however, never overlook the effect of water hammer or surge pressures in design.

Internal pressure, external pressure, special physical loading, type of lining and coating, and other practical requirements govern wall

TABLE 6.6 Grades of Steel Used in AWWA C200

Specifications for fabricated pipe		Design stress 50% of yield point, lb/in^2	Minimum yield point, lb/in^2	Minimum ultimate tensile strength, lb/in^2
ASTM A 36		18,000	36,000	58,000
ASTM A 283	GR C	15,000	30,000	55,000
	GR D	16,500	33,000	60,000
ASTM A 570	GR 30	15,000	30,000	49,000
	GR 33	16,500	33,000	52,000
	GR 36	18,000	36,000	53,000
	GR 40	20,000	40,000	55,000
	GR 45	22,500	45,000	60,000
	GR 50	25,000	50,000	65,000
ASTM A 572	GR 42	21,000	42,000	60,000
	GR 50	25,000	50,000	65,000
	GR 60	30,000	60,000	75,000
Specifications for manufactured pipe		**Design stress 50% of yield point, lb/in^2**	**Minimum yield point, lb/in^2**	**Minimum ultimate tensile strength, lb/in^2**
ASTM A 53, A 135, and A 139	GR A	15,000	30,000	48,000
	GR B	17,500	35,000	60,000
ASTM A 139	GR C	21,000	42,000	60,000
	GR D	23,000	46,000	60,000
	GR E	26,000	52,000	66,000

thickness. Good practice with regard to internal pressure is to use a working tensile stress of 50 percent of the yield point stress under the influence of maximum design pressure. Select linings, coatings, and cathodic protection, as necessary, to provide the required level of corrosion protection.

The wall thickness selected must resist external loadings imposed on the pipe. Such loadings may take the form of outside pressure, either atmospheric or hydrostatic, both of which are uniform and act radially as collapsing forces. Buried pipe must be designed to resist earth pressure in the trench or fill condition. These considerations are discussed in Chaps. 2 and 3.

For external pressure or internal vacuum, buckling should be considered. The following formula from Chap. 3 applies:

$$P_{cr} = \frac{E}{4\,(1 - \nu^2)} \left(\frac{t}{R}\right)^3 \tag{3.14}$$

where R = radius to neutral axis of shell (for thin pipes, difference between inside diameter, outside diameter, and neutral-axis diameter is negligible), in

t = wall thickness, in
P_{cr} = collapsing pressure, lb/in^2
E = modulus of elasticity (30,000,000 for steel)
ν = Poisson's ratio (usually taken as 0.30 for steel)

Substituting the above values of E and ν gives

$$P_c = 528 \times 10^6 \left(\frac{t}{R}\right)^3 \tag{6.3}$$

For convenience to the reader, the more exact approach to buckling is repeated here from Chap. 3 as follows:

$$q_a = \left(\frac{1}{\mathrm{FS}}\right)\left(32\, R w B' E' \frac{EI}{D^3}\right)^{1/2}$$

where q_a = allowable buckling pressure, lb/in^2
FS = design factor
$= \begin{cases} 2.5 & \text{for } (h/D) \geq 2 \\ 3.0 & \text{for } (h/D) < 2 \end{cases}$
h = height of ground surface above top of pipe, in
D = diameter of pipe, in
R_w = water buoyancy factor
$= 1 - (0.33 h_w/h) \qquad 0 \leq h_w \leq h$
h_w = height of water surface above top of pipe, in
B' = empirical coefficient of elastic support (dimensionless)

Coefficient B' was given by Luscher in 1966. The equation is as follows:

$$B' = \frac{4\,(h^2 + Dh)}{(1 + \nu)\,[\,(2h + D)^2 + D^2\,(1 - 2\nu)\,]}$$

The B' has some dependence on Poisson's ratio for the soil. However, this effect is small, as is shown in Fig. 3.22. The above equation simplifies when the value for Poisson's ratio is taken as $^1/_2$. This equation is conservative and should be used for the calculation of B'.

$$B' = \frac{4\,(h^2 + Dh)}{1.5\,(2h + D)^2}$$

Minimum plate or sheet thicknesses for handling are based on two formulas adopted by many specifying agencies:

$$t = \frac{D}{288} \qquad \text{pipe sizes up to 54-in ID} \tag{6.4}$$

$$t = \frac{D + 20}{400} \qquad \text{pipe sizes greater than 54-in ID} \qquad (6.5)$$

In no case shall the shell thickness be less than 14 gage (0.0747 in).

Example 6.3—A 108-in transmission A 108-in-diameter water transmission line is to be installed. Steel has been selected as the piping material. The joint is to be a bell-and-spigot type of joint welded both inside and out as shown:

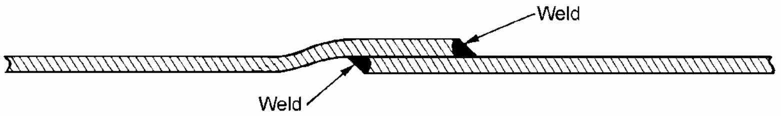

The wall thickness is to be 0.5 in. Because of the large diameter, the pipe will be very flexible and will be braced with internal bracing (stills) when manufactured. These stills will remain in the pipe sections until the pipes have been installed and pipe zone soil has been placed and compacted to the specified density. The stills will be removed after backfilling is complete. The pipeline will then be lined with a Portland cement type of mortar before the line is placed in service.

Design parameters:

Wall thickness	0.5 in
Yield stress	36,000 lb/in^2
Ultimate strength	60,000 lb/in^2
Modulus	29×10^6 lb/in^2
Poisson's ratio	0.3
Thermal coefficient of expansion	6.5×10^{-6} (1/°F)
Ductile-brittle transition temperature	70°F
Surge pressure allowance	40 lb/in^2
Cover depth	6 ft
Pipe zone soil	Crushed stone
Pipe zone density	90 percent standard Proctor
Water temperature	34°F

Evaluate the proposed steel pipe for this application. Are there any special precautions which should be taken or special construction methods which should be followed?

1. Check pipe stiffness PS and evaluate possible ring deflection.

$$\text{PS} = \frac{F}{\Delta y} = 6.7\,\frac{EI}{r^3}$$

$$= \frac{6.7\,(29 \times 10^6)\,(0.5)^3}{(12)\,(54)^3}$$

$$= 12.85 \text{ lb/in}^2$$

This pipe is quite flexible. However, the pipe is going to be held in the undeflected state until pipe zone soil is compacted and the overburden is placed. The resulting deflection after the stills are removed will be quite low.

2. Check the pressure design. First, find the hoop stress for design pressure plus surge.

$$\sigma_h = \frac{PD}{2t} = \frac{(120 + 40)\,(108)}{2\,(0.5)} = 17{,}280 \text{ lb/in}^2$$

Second, find the hoop stress for design pressure only.

$$\sigma_h = \frac{PD}{2t} = \frac{(120)\,(108)}{2\,(0.5)} = 12{,}960 \text{ lb/in}^2$$

The yield stress is 36,000 lb/in^2. The safety factor is greater than 2; therefore, pressure design is all right.

3. Consider longitudinal stresses. AWWA C206 indicates that temperature considerations should be made in design. AWWA C206 and AWWA M11 suggest the use of either closure welds or expansion joints to alleviate stresses due to temperature change.

Longitudinal stresses will also be produced by the Poisson effect. Temperature stresses and Poisson stresses, along with bending stresses due to nonparallel loading in the bell-spigot connection, may be large enough to cause failure.

Assume the pipe is placed and tack-welded during the day. It is July and August, and the pipe temperature during tack welding is between 80 and 130°F. The tack welds hold firm, and the welding process is completed by a welding crew who are following behind the pipe-laying crew. No closure welds or expansion joints are being used. After the line is completed, it is put in service with water at 120 lb/in^2 and 34°F. (See Chap. 4, the steel pipe longitudinal stresses section.)

First, find the longitudinal stress due to the Poisson effect.

$$\sigma_p = \nu\sigma_h \qquad \text{but} \qquad \sigma_h = 12{,}960 \text{ lb/in}^2$$

$$\sigma_p = (0.3)\,(12{,}960) = 3888 \text{ lb/in}^2$$

Second, find the longitudinal stress due to temperature change.

$$\sigma_T = E\alpha\,(\Delta T)$$

$$= (29 \times 10^6)\,(6.5 \times 10^{-6})\,(\Delta T)$$

$$= (188.5)\,(\Delta T)$$

Assume $\Delta T = 70°F$. Then

$$\sigma_T = 13{,}195 \text{ lb/in}^2$$

Third, what is the total longitudinal stress?

$$\sigma_L = \sigma \text{ (Poisson)} + \sigma \text{ (temperature)}$$

$$= 3888 + 13{,}195 = 17{,}083 \text{ lb/in}^2$$

Fourth, the nonparallel loading in the bell and spigot will produce a bending moment and will effectively magnify the stress found above. What is that magnification factor?

$$\text{Bending stress} = \sigma_B = \frac{MC}{I}$$

where M = moment = $\sigma_L A t = \sigma_L\,(bt)\,(t)$
t = thickness
A = area = bt

$$C = \frac{t}{2}$$

$$I = \frac{bt^3}{12}$$

Therefore,

$$\sigma_B = \frac{(\sigma_L)\,(bt)\,(t)\,(t/2)}{bt^3/12}$$

$$= 6\sigma_L$$

Then, the bending stress is 6 times the longitudinal stress. However, the maximum stress is the sum of the bending stress and the longitudinal stress.

$$\sigma_{\max} = \sigma_B + \sigma_L = 7\sigma_L$$

The magnification factor is 7. Therefore, $\sigma_{\max} = (7)(17{,}083) = 119{,}581$ lb/in².

The pipe will fail before this stress is reached. In fact, it did. This pipeline was actually designed and constructed as described in this example. The designer failed to consider longitudinal stresses and did not allow for closure or expansion joints. There were three separate failures caused by longitudinal stresses. Each time a repair was made, the line was returned to service. After the third failure, a general repair was ordered. Every other joint was cut to relieve the built-in stresses. As the joints were cut, there were snap-back openings of as much as 1 in. The temperature of the pipe during the repair was 55°F, which is 21° higher than the service temperature, so there will still be some stress at 34°F. Had the steel been more ductile, it might have been able to relieve itself by simply stretching. For the steel selected, the ductile-brittle transition temperature was 70°F. Therefore, the steel behaved in a brittle manner and failed.

Ductile Iron Pipe

Ductile iron pipe has essentially replaced gray cast iron pipe. Ductile iron (DI) is, as its name implies, more ductile than gray cast iron, but still retains somewhat brittle properties. It is very popular among public works people who repair and maintain water systems. Many perceive this pipe to be able to withstand abuse during handling and repair operations.

The corrosion rate for ductile iron is essentially the same as for gray cast iron. However, since the wall is usually thinner, corrosion is more critical. Design procedures call for a corrosion allowance called a *service factor*. When pipe is installed in highly corrosive soil, steps should be taken to protect it. Ductile iron pipe usually has a cement-mortar lining. This lining improves the hydraulic efficiency and also provides some corrosion protection. Other linings and coatings are available. See Table 6.7.

Example 6.4—A 30-in DI pipe Calculate the thickness for 30-in ductile iron (DI) pipe laid on a flat-bottom trench with backfill tamped to the centerline of the pipe, laying condition type 2 (Fig. 6.46), under 10 ft of cover for a working pressure of 200 lb/in^2. (See ductile iron section in Chap. 4 for design procedure for pressure pipe. Also see AWWA C150. Certain tables from AWWA C150 have been reproduced here for the reader's convenience. This example is taken from AWWA C150.)

1. Design for trench load. First, earth load (Table 6.8) P_e = 8.3 lb/in^2 may be obtained from Fig. 2.19. Truck load (Table 6.8) P_t = 0.7 lb/in^2, and trench load $P_v = P_e + P_t = 9.0$ lb/in^2.

Second, select Table 6.13 for diameter-thickness ratios for laying condition type 2. Third, entering the P_v of 9.0 lb/in^2 in Table 6.13, we see that the

TABLE 6.7 Selected Standards for Ductile Iron Pipe

AWWA C104	Cement mortar lining for ductile iron
AWWA C105	Polyethylene encasement for ductile iron
AWWA C110	Ductile iron and gray iron fittings
AWWA C111	Rubber-gasket joints for ductile iron
AWWA C115	Flanged ductile iron
AWWA C150	Thickness design of ductile iron pipe
AWWA C151	Ductile iron pipe in metal- and sand-lined molds
AWWA C600	Installation of ductile iron water mains and their appurtenances
ASTM E 8	Materials properties test
ASTM A 539	Physical properties

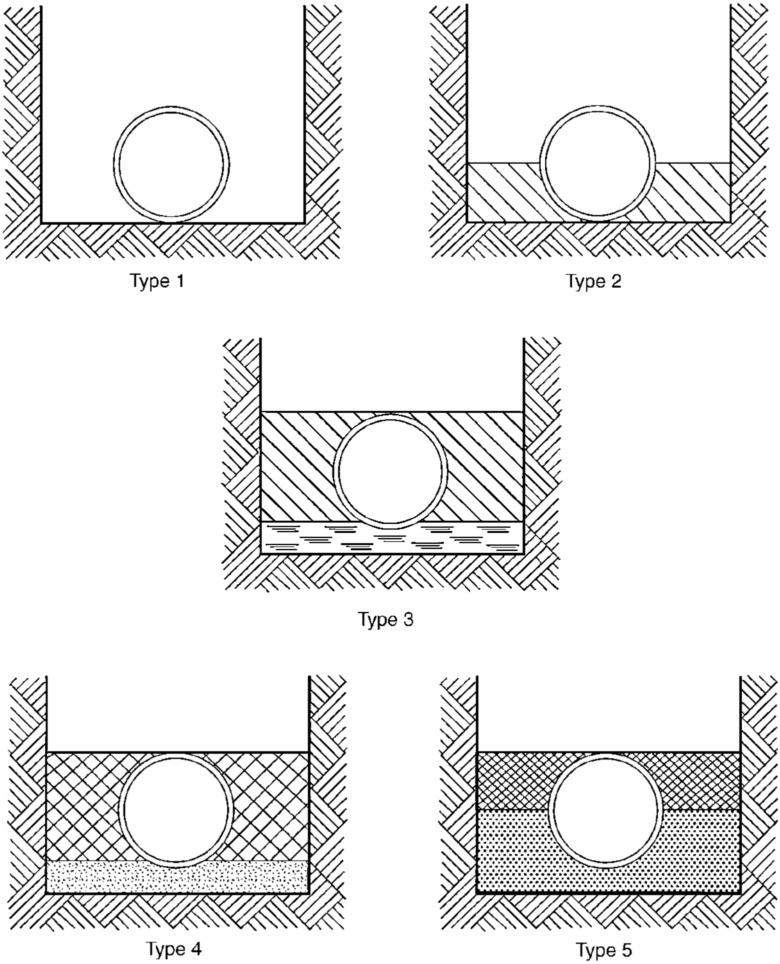

Figure 6.46 Standard pipe-laying conditions. (*Reprinted, by permission, from ANSI/AWWA C-150/A21.50-96, American Water Works Association, 1996.*)

bending stress design requires a D/t of 128. From Table 6.12, diameter D of 30-in-OD pipe is 32.00 in. Net thickness t for bending stress is

$$t = \frac{D}{D/t} = \frac{32.0}{128} = 0.25 \text{ in}$$

Fourth, also from Table 6.13, the deflection design requires D/t_1 of 108. Minimum thickness t_1 for deflection design is

TABLE 6.8 Earth Loads P_e, Truck Loads P_t, and Trench Loads P_v, lb/in^2

Depth of cover, ft	P_e	18-in pipe P_t	18-in pipe P_v	20-in pipe P_t	20-in pipe P_v	24-in pipe P_t	24-in pipe P_v	30-in pipe P_t	30-in pipe P_v	36-in pipe P_t	36-in pipe P_v
2.5	2.1	7.8	9.9	7.5	9.6	7.1	9.2	6.7	8.8	6.2	8.3
3	2.5	5.9	8.4	5.7	8.2	5.4	7.9	5.2	7.7	4.9	7.4
4	3.3	3.9	7.2	3.9	7.2	3.6	6.9	3.5	6.8	3.4	6.7
5	4.2	2.6	6.8	2.6	6.8	2.4	6.6	2.4	6.6	2.3	6.5
6	5.0	1.9	6.9	1.9	6.9	1.7	6.7	1.7	6.7	1.7	6.7
7	5.8	1.4	7.2	1.4	7.2	1.3	7.1	1.3	7.1	1.3	7.1
8	6.7	1.2	7.9	1.1	7.8	1.1	7.8	1.1	7.8	1.1	7.8
9	7.5	1.0	8.5	0.9	8.4	0.9	8.4	0.9	8.4	0.8	8.3
10	8.3	0.8	9.1	0.7	9.0	0.7	9.0	0.7	9.0	0.7	9.0
12	10.0	0.5	10.5	0.5	10.5	0.5	10.5	0.5	10.5	0.5	10.5
14	11.7	0.4	12.1	0.4	12.1	0.4	12.1	0.4	12.1	0.4	12.1
16	13.3	0.3	13.6	0.3	13.6	0.3	13.6	0.3	13.6	0.3	13.6
20	16.7	0.2	16.9	0.2	16.9	0.2	16.9	0.2	16.9	0.2	16.9
24	20.0	0.1	20.1	0.1	20.1	0.1	20.1	0.1	20.1	0.1	20.1
28	23.3	0.1	23.4	0.1	23.4	0.1	23.4	0.1	23.4	0.1	23.4
32	26.7	0.1	26.8	0.1	26.8	0.1	26.8	0.1	26.8	0.1	26.8

TABLE 6.8 Earth Loads P_e, Truck Loads P_t, and Trench Loads P_v, lb/in^2 (*Continued*)

Depth of		42-in pipe		48-in pipe		54-in pipe		60-in pipe		64-in pipe	
cover, ft	P_e	P_t	P_v	P_t	P_v	P_t	P_v	P_t	P_v	P_t	P_v
2.5	2.1	5.8	7.9	5.4	7.5	5.0	7.1	4.8	6.9	4.5	6.6
3	2.5	4.6	7.1	4.4	6.9	4.1	6.6	3.9	6.4	3.8	6.3
4	3.3	3.3	6.6	3.1	6.4	3.0	6.3	2.9	6.2	2.8	6.1
5	4.2	2.3	6.5	2.2	6.4	2.1	6.3	2.1	6.3	2.1	6.3
6	5.0	1.7	6.7	1.6	6.6	1.6	6.6	1.6	6.6	1.5	6.5
7	5.8	1.3	7.1	1.2	7.0	1.2	7.0	1.2	7.0	1.2	7.0
8	6.7	1.0	7.7	1.0	7.7	1.0	7.7	1.0	7.7	1.0	7.7
9	7.5	0.8	8.3	0.8	8.3	0.8	8.3	0.8	8.3	0.8	8.3
10	8.3	0.7	9.0	0.7	9.0	0.7	9.0	0.7	9.0	0.7	9.0
12	10.0	0.5	10.5	0.5	10.5	0.5	10.5	0.5	10.5	0.5	10.5
14	11.7	0.4	12.1	0.4	12.1	0.4	12.1	0.4	12.1	0.4	12.1
16	13.3	0.3	13.6	0.3	13.6	0.3	13.6	0.3	13.6	0.3	13.6
20	16.7	0.2	16.9	0.2	16.9	0.2	16.9	0.2	16.9	0.2	16.9
24	20.0	0.1	20.1	0.1	20.1	0.1	20.1	0.1	20.1	0.1	20.1
28	23.3	0.1	23.4	0.1	23.4	0.1	23.4	0.1	23.4	0.1	23.4
32	26.7	0.1	26.8	0.1	26.8	0.1	26.8	0.1	26.8	0.1	26.8

SOURCE: Table 1 from AWWA C150.

$$t_1 = \frac{D}{D/t_1} = \frac{32.0}{108} = 0.30 \text{ in}$$

Minimum thickness	0.30 in
Less service allowance	−0.08 in
Net thickness t for deflection control	0.22 in

Fifth, the larger net thickness is 0.25 in, obtained by the design for bending stress.

2. Design for internal pressure:

$$P_i = 2.0 \text{ (working pressure + 100 lb/in}^2 \text{ surge allowance)}$$

If anticipated surge pressures are greater than 100 lb/in^2, which results from instantaneous stoppage of a column of water moving at 2 ft/s, then the actual anticipated pressures must be used.

$$P_i = 2.0\ (200 + 100) = 600 \text{ lb/in}^2$$

$$t = \frac{P_i D}{2S} = \frac{600\ (32.00)}{2\ (42{,}000)} = 0.23 \text{ in}$$

Net thickness t for internal pressure is 0.23 in.

3. Select net thickness and add allowances. The larger of the thicknesses is given by the design for trench load, step 1, and 0.25 in is selected.

Net thickness	= 0.25 in
Service allowance	= 0.08 in
Minimum thickness	= 0.33 in
Casting tolerance	= 0.07 in
Total calculated thickness	= 0.40 in

4. Select the standard thickness and class. The total calculated thickness of 0.40 in is nearest to 0.39, class 50, in Table 6.12. Therefore, class 50 is selected.

Testing of ductile iron pipe

A significant result of research and testing of buried flexible pipes is the identification of performance limits. Traditionally, design is a two-step process: (1) the conceiving of a device or system and (2) the predicting of performance of this system to determine whether it will accomplish the purpose for which it was conceived. Any inability to

TABLE 6.9 Design Values for Standard Laying Conditions

Laying condition*	Description	E'	Bedding angle, deg	K_b	K_s
Type 1†	Flat-bottom trench.‡ Loose backfill.	150	30	0.235	0.108
Type 2	Flat-bottom trench. Backfill lightly consolidated to centerline of pipe.	300	45	0.210	0.105
Type 3	Pipe bedded in 4-in-minimum loose soil.§ Backfill lightly consolidated to top of pipe.	400	60	0.189	0.103
Type 4	Pipe bedded in sand, gravel, or crushed stone to depth of one-eighth pipe diameter, 4 in minimum. Backfill compacted to top of pipe (approximately 80 percent standard Proctor, AASHTO T-99)	500	90	0.16	0.096
Type 5	Pipe bedded to its centerline in compacted granular material, 4 in minimum under pipe. Compacted granular or select§ material to top of pipe (approximately 90 percent standard Proctor, AASHTO T-99)	700	150	0.128	0.085

*See Fig. 6.1.

†For pipe 30 in and larger, consideration should be given to the use of laying conditions other than type 1.

‡Flat bottom is defined as "undisturbed earth."

§Loose soil or select material is defined as "native soil excavated from the trench, free of rocks, foreign material, and frozen earth."

¶AASHTO T-99, *Standard Method of Test for the Moisture Density Relations of Soils Using a 5.5-lb (2.5-kg) Rammer and a 12-in (305-mm) Drop*. Available from the American Association of State Highway and Transportation Officials, 444 N. Capital St. NW, Washington, DC 20001.

SOURCE: Table 2 from AWWA C150.

TABLE 6.10 Allowances for Casting Tolerance

Size, in	Casting allowance, in
3–8	0.05
10–12	0.06
14–42	0.07
48	0.08
54	0.09

SOURCE: Table 3 from AWWA C150.

achieve this objective is called failure. Most designers visualize failure as a sudden, calamitous, or catastrophic deformation such as a break or a collapse. In the case of a buried pipe, failure could be the rupture of a pipe due to internal pressure, but it could also be the deformation of a pipe due to external soil pressure. However, only under a rare combination of extenuating circumstances does a buried pipe ever collapse. So failure needs to be defined. The problem is to identify the performance limits. Just how much ring deflection is tol-

TABLE 6.11 Reduction Factors *R* for Truck Load Calculations

	Depth of cover, ft			
	<4	4–7	>7–10	>10
Size, in	Reduction factor			
3–12	1.00	1	1.00	1.00
14	0.92	1.00	1.00	1.00
16	0.88	0.95	1.00	1.00
18	0.85	0.90	1.00	1.00
20	0.83	0.90	0.95	1.00
24–30	0.81	0.85	0.95	1.00
36–64	0.80	0.85	0.90	1.00

SOURCE: Table 4 from AWWA C150.

erable? Just how much cracking of the mortar lining may be permitted? And so on. Design of buried pipes should be based on performance limits that have been identified in actual tests. This includes the identification of pertinent fundamental variables. It includes the interrelationship of these variables as determined from the actual tests (see Fig. 6.47).

From experience, the following parameters are found to be most pertinent:

1. The D/t ratio or ring flexibility where D = mean diameter of the ring and t = wall thickness (pipe or bell).
2. A measure of soil compressibility E' or ρ, where E' = soil stiffness—the most important soil property—and ρ = density of soil (percent of standard)—the single most important determinant of E'.
3. The $PD/(2A)$ or ring compression stress where P = apparent vertical soil pressure on the pipe (unit weight of soil times height plus the effect of surface loads at the level of the top of the ring), D = diameter, and A = cross-sectional area of the pipe wall per unit length of pipe.
4. Ring deflection $\Delta y/D$, where Δy = vertical decrease in pipe diameter and D = diameter.
5. Performance limit.

From the testing program it was concluded that the following three performance limits are pertinent for ductile iron pipe.

1. Spalling or unbonding of the cement lining—observable by eye
2. Cracking of the ductile iron in the bell—observable by eye
3. Loss of compression in the gasket in the joint—measurable by gage

TABLE 6.12 Nominal Thicknesses for Standard Pressure Classes of Ductile Iron Pipe

Size, in	Outside diameter, in	Pressure class 150	200	250	300	350
		Nominal thickness, in				
3	3.96	—	—	—	—	0.25*
4	4.80	—	—	—	—	0.25*
6	6.90	—	—	—	—	0.25*
8	9.05	—	—	—	—	0.25*
10	11.10	—	—	—	—	0.26
12	13.20	—	—	—	—	0.28
14	15.30	—	—	0.28	0.30	0.31
16	17.40	—	—	0.30	0.32	0.34
18	19.50	—	—	0.31	0.34	0.36
20	21.60	—	—	0.33	0.36	0.38
24	25.80	—	0.33	0.37	0.40	0.43
30	32.00	0.34	0.38	0.42	0.45	0.49
36	38.30	0.38	0.42	0.47	0.51	0.56
42	44.50	0.41	0.47	0.52	0.57	0.63
48	50.80	0.46	0.52	0.58	0.64	0.70
54	57.56	0.51	0.58	0.65	0.72	0.79
60	61.61	0.54	0.61	0.68	0.76	0.83
64	65.67	0.56	0.64	0.72	0.80	0.87

NOTE: To convert inches (in) to millimeters (mm), multiply by 25.4.

*Calculated thicknesses for these sizes and pressure ratings are less than those shown above. (See Table 6.11 for actual calculated thicknesses.) Presently these are the lowest nominal thicknesses available in these sizes.

Pressure classes are defined as the rated water working pressure of the pipe in pounds per square inch (psi or lb/in^2). The thicknesses shown are adequate for the rated water working pressure plus a surge allowance of 100 lb/in^2 (689 kPa). Calculations are based on a minimum yield strength in tension of 42,000 lb/in^2 (289,590 kPa) and 2.0 safety factor times the sum of working pressure and 100 lb/in^2 (689 kPa) surge allowance.

Thickness can be calculated for rated water working pressure and surges other than the above by use of the formula shown in Section 4.1.2 of AWWA C150.

Ductile iron pipe is available for water working pressures greater than 350 lb/in^2 (2413 kPa).

Pipe is available with thicknesses greater than pressure class 350. See Table 6.13.

Lowest nominal thicknesses shown in Table 15.1 of ANSI/AWWA C115/A21.15 for threaded flanged pipe are still required.

Lowest nominal thicknesses shown in ANSI/AWWA C606 for pipe with grooved and shouldered joints are still required.

SOURCE: Table 5 from AWWA C150.

Of the three, spalling or unbonding of the cement-mortar lining is the first performance limit to occur as a result of external soil pressure. The second performance limit is bell cracking, and the third, which seems to be most remote, is loss of compression in the gasket. It is noteworthy that the two most pertinent parameters in all three performance limits are the ring deflection $\Delta y/D$ and the D/t ratio.

TABLE 6.13 Diameter-Thickness Ratios for Laying Condition Type 2*

Trench load P_v, lb/in^2			Trench load P_v, lb/in^2		
Bending-stress design	Deflection design	D/t or D/t_1†	Bending-stress design	Deflection design	D/t or D/t_1†
6.29	6.18	170	9.70	7.94	120
6.34	6.19	169	9.79	8.01	119
6.39	6.21	168	9.89	8.08	118
6.44	6.23	167	9.99	8.16	117
6.50	6.25	166	10.09	8.23	116
6.55	6.26	165	10.19	8.31	115
6.60	6.28	164	10.29	8.40	114
6.66	6.30	163	10.40	8.48	113
6.71	6.32	162	10.51	8.57	112
6.77	6.34	161	10.62	8.66	111
6.82	6.37	160	10.73	8.76	110
6.88	6.39	159	10.84	8.86	109
6.94	6.41	158	10.96	8.96	108
6.99	6.43	157	11.08	9.07	107
7.05	6.46	156	11.21	9.18	106
7.11	6.48	155	11.33	9.29	105
7.17	6.50	154	11.46	9.41	104
7.23	6.53	153	11.59	9.54	103
7.29	6.56	152	11.73	9.67	102
7.35	6.58	151	11.87	9.80	101
7.42	6.61	150	12.01	9.94	100
7.48	6.64	149	12.16	10.09	99
7.54	6.67	148	12.31	10.24	98
7.61	6.70	147	12.46	10.40	97
7.67	6.73	146	12.62	10.56	96
7.74	6.76	145	12.79	10.73	95
7.80	6.79	144	12.96	10.91	94
7.87	6.83	143	13.13	11.10	93
7.94	6.86	142	13.31	11.29	92
8.01	6.89	141	13.49	11.50	91
8.08	6.93	140	13.68	11.71	90
8.15	6.97	139	13.88	11.94	89
8.22	7.01	138	14.08	12.17	88
8.29	7.05	137	14.30	12.42	87
8.37	7.09	136	14.51	12.67	86
8.44	7.13	135	14.74	12.94	85
8.52	7.17	134	14.97	13.22	84
8.59	7.22	133	15.21	13.52	83
8.67	7.26	132	15.46	13.83	82
8.75	7.31	131	15.72	14.16	81
8.83	7.36	130	15.99	14.50	80
8.91	7.41	129	16.28	14.86	79
8.99	7.46	128	16.57	15.24	78
9.07	7.51	127	16.87	15.64	77
9.16	7.57	126	17.19	16.06	76
9.25	7.63	125	17.52	16.51	75
9.33	7.69	124	17.86	16.98	74
9.42	7.75	123	18.22	17.48	73
9.51	7.81	122	18.59	18.00	72
9.60	7.87	121	18.98	18.56	71

NOTE: See p. 346 for footnotes.

TABLE 6.13 Diameter-Thickness Ratios for Laying Condition Type 2* (*Continued*)

Trench load P_v, lb/in^2			Trench load P_v, lb/in^2		
Bending-stress design	Deflection design	D/t or D/t_1†	Bending-stress design	Deflection design	D/t or D/t_1†
19.39	19.14	70	33.84	44.09	50
19.82	19.77	69	35.08	46.56	49
20.27	20.43	68	36.41	49.26	48
20.73	21.13	67	37.83	52.19	47
21.23	21.87	66	39.34	55.40	46
21.74	22.67	65	40.96	58.89	45
22.28	23.51	64	42.70	62.73	44
22.85	24.41	63	44.57	66.93	43
23.45	25.37	62	46.57	71.56	42
24.07	26.39	61	48.73	76.66	41
24.74	27.49	60	51.06	82.29	40
25.43	28.66	59	53.57	88.54	39
26.17	29.91	58	56.30	95.48	38
26.95	31.26	57	59.25	103.21	37
27.77	32.71	56	62.46	111.85	36
28.64	34.26	55	65.96	121.54	35
29.56	35.93	54	69.79	132.44	34
30.53	37.74	53	73.98	144.74	33
31.57	39.69	52	78.57	158.68	32
32.67	41.80	51	83.64	174.54	31

NOTE: To convert pounds per square inch (lb/in^2) to kilopascals (kPa), multiply by 6.895.
*E' = 300 lb/in^2; K_b = 0.210; K_x = 0.105.
†The D/t or D/t_1 for the tabulated P_v nearest to the calculated P_v is selected; when the calculated P_v is halfway between two tabulated values, the smaller of D/t or D/t_1 should be used.
SOURCE: Table 8 from AWWA C150.

Consequently, the same general rationale applies to all three performance limits. Any one of these three performance limits can be predicted in terms of $\Delta y/D$ and D/t. All three performance limits are discussed in the following paragraphs. However, only the cracking and spalling of the lining are considered in detail.

Because of academic emphasis on the stress theory of failure, there has been great interest in the maximum stress in the ring. Maximum stress can be calculated by adding the ring compression stress

$$\sigma_c = \frac{PD}{2A}$$

to the flexural stress

$$\sigma_f = \frac{t\,(3\Delta y/D)}{D\,(1 - 2\Delta y/D)}$$

(*Text continues on p. 357.*)

TABLE 6.14 Thickness for Earth Load plus Truck Load

		Laying condition									
		Type 1		Type 2		Type 3		Type 4		Type 5	
Size, in	Depth of cover,* ft	Total calculated thickness,† in	Use pressure class	Total calculated thickness,† in	Use pressure class	Total calculated thickness,† in	Use pressure class	Total calculated thickness,† in	Use pressure class	Total calculated thickness,† in	Use pressure class
10	2.5	—	—	0.25	350	0.23	350	0.20	350	0.18	350
	3	0.26	350	0.24	350	0.22	350	0.19	350	0.18	350
	4	0.25	350	0.22	350	0.21	350	0.19	350	0.17	350
	5	0.24	350	0.22	350	0.20	350	0.18	350	0.17	350
	6	0.24	350	0.22	350	0.20	350	0.18	350	0.17	350
	7	0.24	350	0.22	350	0.20	350	0.19	350	0.17	350
	8	0.25	350	0.22	350	0.21	350	0.19	350	0.17	350
	9	0.25	350	0.23	350	0.21	350	0.19	350	0.17	350
	10	0.26	350	0.23	350	0.21	350	0.19	350	0.17	350
	12	—	—	0.24	350	0.22	350	0.20	350	0.18	350
	14	—	—	0.26	350	0.23	350	0.20	350	0.18	350
	16	—	—	—	—	0.24	350	0.21	350	0.18	350
	20	—	—	—	—	—	—	0.22	350	0.19	350
	24	—	—	—	—	—	—	0.24	350	0.19	350
	28	—	—	—	—	—	—	0.26	350	0.20	350
	32	—	—	—	—	—	—	—	—	0.21	350
12	2.5	—	—	0.27	350	0.25	350	0.21	350	0.19	350
	3	0.28	350	0.25	350	0.23	350	0.20	350	0.18	350
	4	0.26	350	0.24	350	0.22	350	0.19	350	0.18	350
	5	0.26	350	0.23	350	0.21	350	0.19	350	0.18	350
	6	0.26	350	0.23	350	0.21	350	0.19	350	0.18	350
	7	0.26	350	0.23	350	0.21	350	0.19	350	0.18	350
	8	0.27	350	0.24	350	0.22	350	0.20	350	0.18	350
	9	0.27	350	0.24	350	0.22	350	0.20	350	0.18	350
	10	0.28	350	0.25	350	0.23	350	0.20	350	0.18	350

NOTE: See p. 354 for footnotes.

TABLE 6.14 Thickness for Earth Load plus Truck Load (*Continued*)

		Laying condition									
		Type 1		Type 2		Type 3		Type 4		Type 5	
Size, in	Depth of cover,* ft	Total calculated thickness,† in	Use pressure class	Total calculated thickness,† in	Use pressure class	Total calculated thickness,† in	Use pressure class	Total calculated thickness,† in	Use pressure class	Total calculated thickness,† in	Use pressure class
	12	—	—	0.26	350	0.24	350	0.21	350	0.18	350
	14	—	—	0.28	350	0.25	350	0.21	350	0.19	350
	16	—	—	—	—	0.26	350	0.22	350	0.19	350
	20	—	—	—	—	—	—	0.24	350	0.20	350
	24	—	—	—	—	—	—	0.26	350	0.20	350
	28	—	—	—	—	—	—	0.28	350	0.21	350
	32	—	—	—	—	—	—	—	—	0.23	350
14	2.50	‡	‡	0.29	300	0.26	250	0.23	250	0.20	250
	3			0.28	250	0.25	250	0.22	250	0.20	250
	4			0.26	250	0.24	250	0.21	250	0.19	250
	5			0.25	250	0.23	250	0.21	250	0.19	250
	6			0.25	250	0.23	250	0.21	250	0.19	250
	7			0.26	250	0.24	250	0.21	250	0.19	250
	8			0.26	250	0.24	250	0.21	250	0.19	250
	9			0.27	250	0.24	250	0.22	250	0.19	250
	10			0.28	250	0.25	250	0.22	250	0.20	250
	12			0.29	300	0.26	250	0.23	250	0.20	250
	14			0.31	350	0.28	250	0.23	250	0.20	250
	16			—	—	0.29	300	0.24	250	0.21	250
	20			—	—	—	—	0.26	250	0.21	250
	24			—	—	—	—	0.29	300	0.22	250
	28			—	—	—	—	—	—	0.25	250
	32			—	—	—	—	—	—	0.27	250
16	2.50	‡	‡	0.31	300	0.27	250	0.23	250	0.21	250
	3			0.29	250	0.26	250	0.23	250	0.20	250

	4			0.27	250	0.25	250	0.22	250	0.20	250
	5			0.27	250	0.24	250	0.22	250	0.20	250
	6			0.27	250	0.24	250	0.22	250	0.20	250
	7			0.27	250	0.25	250	0.22	250	0.20	250
	8			0.28	250	0.25	250	0.22	250	0.20	250
	9			0.28	250	0.26	250	0.22	250	0.20	250
	10			0.29	250	0.26	250	0.23	250	0.20	250
	12			0.31	300	0.28	250	0.24	250	0.21	250
	14			0.33	350	0.29	250	0.24	250	0.21	250
	16			—	—	0.31	300	0.25	250	0.21	250
	20			—	—	0.34	350	0.28	250	0.22	250
	24			—	—	—	—	0.30	250	0.24	250
	28			—	—			0.34	350	0.27	250
	32			—	—			—	—	0.29	250
18	2.50	‡	‡	0.32	300	0.28	250	0.24	250	0.21	250
	3			0.30	250	0.27	250	0.23	250	0.21	250
	4			0.28	250	0.26	250	0.23	250	0.20	250
	5			0.28	250	0.25	250	0.22	250	0.20	250
	6			0.28	250	0.25	250	0.22	250	0.20	250
	7			0.28	250	0.26	250	0.23	250	0.20	250
	8			0.29	250	0.26	250	0.23	250	0.20	250
	9			0.30	250	0.27	250	0.23	250	0.21	250
	10			0.31	250	0.28	250	0.24	250	0.21	250
	12			0.33	300	0.29	250	0.24	250	0.21	250
	14			0.35	350	0.31	250	0.25	250	0.22	250
	16			—	—	0.33	300	0.26	250	0.22	250
	20			—	—	—	—	0.29	250	0.23	250
	24			—	—	—	—	0.32	300	0.26	250
	28			—	—	—	—	0.36	350	0.29	250
	32			—	—	—	—	—	—	0.32	300
20	2.50	‡	‡	0.33	250	0.29	250	0.25	250	0.21	250
	3			0.31	250	0.28	250	0.24	250	0.21	250
	4			0.30	250	0.27	250	0.23	250	0.21	250
	5			0.29	250	0.26	250	0.23	250	0.20	250

TABLE 6.14 Thickness for Earth Load plus Truck Load (*Continued*)

		Laying condition									
		Type 1		Type 2		Type 3		Type 4		Type 5	
Size, in	Depth of cover,* ft	Total calculated thickness,† in	Use pressure class	Total calculated thickness,† in	Use pressure class	Total calculated thickness,† in	Use pressure class	Total calculated thickness,† in	Use pressure class	Total calculated thickness,† in	Use pressure class
	6			0.29	250	0.26	250	0.23	250	0.20	250
	7			0.30	250	0.27	250	0.23	250	0.21	250
	8			0.30	250	0.27	250	0.24	250	0.21	250
	9			0.31	250	0.28	250	0.24	250	0.21	250
	10			0.32	250	0.29	250	0.24	250	0.21	250
	12			0.35	300	0.31	250	0.25	250	0.22	250
	14			0.37	350	0.33	250	0.26	250	0.22	250
	16			—	—	0.35	300	0.28	250	0.23	250
	20			—	—	—	—	0.32	250	0.24	250
	24			—	—	—	—	0.35	300	0.28	250
	28			—	—	—	—	0.38	350	0.32	250
	32			—	—	—	—	—	—	0.35	300
24	2.50	‡	‡	0.36	250	0.32	200	0.26	200	0.22	200
	3			0.33	200	0.30	200	0.25	200	0.22	200
	4			0.32	200	0.29	200	0.25	200	0.21	200
	5			0.31	200	0.28	200	0.24	200	0.21	200
	6			0.31	200	0.28	200	0.24	200	0.21	200
	7			0.32	200	0.29	200	0.25	200	0.22	200
	8			0.33	200	0.30	200	0.25	200	0.22	200
	9			0.35	250	0.30	200	0.26	200	0.22	200
	10			0.36	250	0.31	200	0.26	200	0.22	200
	12			0.39	300	0.33	200	0.27	200	0.23	200
	14			0.41	350	0.36	250	0.29	200	0.24	200

	16			—	—	0.38	300	0.31	200	0.24	200
	20			—	—	—	—	0.36	250	0.26	200
	24			—	—	—	—	0.40	300	0.32	200
	28			—	—	—	—	0.43	350	0.37	250
	32			—	—	—	—	—	—	0.40	300
30	2.50	‡	‡	0.40	250	0.34	150	0.29	150	0.24	150
	3			0.37	200	0.33	150	0.28	150	0.23	150
	4			0.36	200	0.32	150	0.27	150	0.23	150
	5			0.35	200	0.31	150	0.26	150	0.23	150
	6			0.35	200	0.31	150	0.27	150	0.23	150
	7			0.36	200	0.32	150	0.27	150	0.23	150
	8			0.37	200	0.33	150	0.27	150	0.23	150
	9			0.39	250	0.34	150	0.28	150	0.24	150
	10			0.41	250	0.35	200	0.29	150	0.24	150
	12			0.44	300	0.38	200	0.30	150	0.25	150
	14			0.48	350	0.41	250	0.33	150	0.26	150
	16			—	—	0.44	300	0.37	200	0.26	150
	20			—	—	—	—	0.43	300	0.29	150
	24			—	—			0.48	350	0.38	200
	28			—	—			—	—	0.44	300
	32							—		0.48	350
36	2.50	‡	‡	0.43	250	0.37	150	0.31	150	0.25	150
	3			0.41	200	0.36	150	0.30	150	0.25	150
	4			0.39	200	0.34	150	0.29	150	0.24	150
	5			0.39	200	0.34	150	0.29	150	0.24	150
	6			0.39	200	0.34	150	0.29	150	0.24	150
	7			0.40	200	0.35	150	0.29	150	0.24	150
	8			0.42	200	0.36	150	0.30	150	0.25	150
	9			0.44	250	0.38	150	0.31	150	0.25	150
	10			0.46	250	0.39	200	0.31	150	0.26	150
	12			0.50	300	0.42	200	0.33	150	0.27	150
	14			0.54	350	0.46	250	0.38	150	0.28	150
	16			—	—	0.50	300	0.43	250	0.29	150
	20			—	—	—	—	0.51	300	0.33	150
	24			—	—	—	—	0.56	350	0.44	250

TABLE 6.14 Thickness for Earth Load plus Truck Load (*Continued*)

		Laying condition									
		Type 1		Type 2		Type 3		Type 4		Type 5	
Size, in	Depth of cover,* ft	Total calculated thickness,† in	Use pressure class	Total calculated thickness,† in	Use pressure class	Total calculated thickness,† in	Use pressure class	Total calculated thickness,† in	Use pressure class	Total calculated thickness,† in	Use pressure class
	28			—	—	—	—	—	—	0.51	300
	32			—	—	—	—	—	—	0.56	350
42	2.50	‡	‡	0.47	200	0.40	150	0.32	150	0.27	150
	3			0.44	200	0.38	150	0.31	150	0.26	150
	4			0.42	200	0.37	150	0.30	150	0.25	150
	5			0.43	200	0.37	150	0.31	150	0.26	150
	6			0.43	200	0.37	150	0.31	150	0.26	150
	7			0.44	200	0.38	150	0.31	150	0.26	150
	8			0.46	200	0.40	150	0.32	150	0.26	150
	9			0.48	250	0.41	150	0.33	150	0.27	150
	10			0.50	250	0.43	200	0.34	150	0.27	150
	12			0.55	300	0.47	200	0.36	150	0.28	150
	14			0.60	350	0.52	250	0.43	200	0.30	150
	16			—	—	0.57	300	0.49	250	0.31	150
	20			—	—	—	—	0.57	300	0.38	150
	24			—	—	—	—	—	—	0.50	250
	28			—	—	—	—			0.58	350
	32			—	—	—	—	—		0.63	350
48	2.50	‡	‡	0.50	200	0.44	150	0.35	150	0.29	150
	3			0.48	200	0.42	150	0.34	150	0.28	150
	4			0.46	150	0.41	150	0.33	150	0.28	150
	5			0.47	200	0.41	150	0.34	150	0.28	150
	6			0.48	200	0.41	150	0.34	150	0.28	150
	7			0.49	200	0.43	150	0.35	150	0.28	150

	8			0.51	200	0.44	150	0.35	150	0.29	150
	9			0.54	250	0.46	150	0.37	150	0.29	150
	10			0.56	250	0.48	200	0.38	150	0.30	150
	12			0.62	300	0.54	250	0.40	150	0.31	150
	14			0.67	350	0.60	300	0.49	200	0.33	150
	16			—	—	0.65	350	0.56	250	0.34	150
	20			—	—	—	—	0.66	350	0.43	150
	24			—	—			—	—	0.57	250
	28			—	—	—	—	—	—	0.66	350
54	2.50	‡	‡	0.54	200	0.47	150	0.38	150	0.31	150
	3			0.53	200	0.46	150	0.37	150	0.30	150
	4			0.51	150	0.44	150	0.36	150	0.30	150
	5			0.52	200	0.45	150	0.37	150	0.30	150
	6			0.53	200	0.46	150	0.37	150	0.30	150
	7			0.54	200	0.47	150	0.38	150	0.31	150
	8			0.57	200	0.49	150	0.39	150	0.32	150
	9			0.60	250	0.51	150	0.40	150	0.32	150
	10			0.63	250	0.53	200	0.41	150	0.33	150
	12			0.69	300	0.61	250	0.44	150	0.34	150
	14			0.75	350	0.68	300	0.55	200	0.36	150
	16			—	—	0.73	350	0.63	250	0.37	150
	20			—	—	—	—	0.74	350	0.48	150
	24			—	—			—	—	0.64	250
	28			—	—			—		0.74	350
60	2.50	‡	‡	0.56	200	0.48	150	0.39	150	0.32	150
	3			0.54	150	0.47	150	0.38	150	0.31	150
	4			0.53	150	0.46	150	0.38	150	0.31	150
	5			0.54	150	0.47	150	0.38	150	0.31	150
	6			0.55	200	0.48	150	0.39	150	0.31	150
	7			0.57	200	0.49	150	0.39	150	0.32	150
	8			0.59	200	0.51	150	0.40	150	0.33	150
	9			0.63	250	0.53	150	0.42	150	0.33	150
	10			0.67	250	0.55	200	0.43	150	0.34	150
	12			0.74	300	0.65	250	0.46	150	0.35	150

TABLE 6.14 Thickness for Earth Load plus Truck Load (*Continued*)

		Laying condition									
		Type 1		Type 2		Type 3		Type 4		Type 5	
Size, in	Depth of cover,* ft	Total calculated thickness,† in	Use pressure class	Total calculated thickness,† in	Use pressure class	Total calculated thickness,† in	Use pressure class	Total calculated thickness,† in	Use pressure class	Total calculated thickness,† in	Use pressure class
	14			0.79	350	0.72	300	0.58	200	0.37	150
	16			—	—	0.78	350	0.67	250	0.38	150
	20			—	—	—	—	0.79	350	0.51	150
	24			—	—			—	—	0.68	250
	28			—	—	—	—	—	—	0.79	350
64	2.50	‡	‡	0.58	200	0.50	150	0.40	150	0.32	150
	3			0.56	150	0.49	150	0.39	150	0.32	150
	4			0.55	150	0.48	150	0.39	150	0.32	150
	5			0.56	150	0.48	150	0.39	150	0.32	150
	6			0.57	200	0.49	150	0.40	150	0.32	150
	7			0.59	200	0.51	150	0.41	150	0.33	150
	8			0.62	200	0.53	150	0.42	150	0.33	150
	9			0.67	250	0.55	150	0.43	150	0.34	150
	10			0.70	250	0.58	200	0.45	150	0.35	150
	12			0.78	300	0.68	250	0.48	150	0.37	150
	14			0.84	350	0.76	300	0.61	200	0.38	150
	16			—	—	0.82	350	0.70	250	0.40	150
	20			—	—	—	—	0.83	350	0.54	150
	24			—	—			—	—	0.72	250
	28			—	—			—		0.83	350

NOTE: To convert inches (in) to millimeters (mm), multiply by 25.4; to convert feet (ft) to meters (m), multiply by 0.3048.
*Pipe may be available for depths of cover greater than those shown in the table.
†Total calculated thickness includes service allowance and casting tolerance added to net thickness.
‡For pipe 14 in (356 mm) and larger, consideration should be given to laying conditions other than type 1.
SOURCE: Table 12 from AWWA C150.

TABLE 6.15 Thickness for Internal Pressure

	Rated water working pressure, lb/in^2									
	150		200		250		300		350	
Pipe size, in	Total calculated thickness,* in	Use pressure class	Total calculated thickness,* in	Use pressure class	Total calculated thickness,* in	Use pressure class	Total calculated thickness,* in	Use pressure class	Total calculated thickness,* in	Use pressure class
3	0.15	350	0.16	350	0.16	350	0.17	350	0.17	350
4	0.16	350	0.16	350	0.17	350	0.18	350	0.18	350
6	0.17	350	0.18	350	0.19	350	0.20	350	0.20	350
8	0.18	350	0.19	350	0.21	350	0.22	350	0.23	350
10	0.21	350	0.22	350	0.23	350	0.25	350	0.26	350
12	0.22	350	0.23	350	0.25	350	0.27	350	0.28	350
14	0.24	250	0.26	250	0.28	250	0.30	300	0.31	350
16	0.25	250	0.27	250	0.30	250	0.32	300	0.34	350
18	0.27	250	0.29	250	0.31	250	0.34	300	0.36	350
20	0.28	250	0.30	250	0.33	250	0.36	300	0.38	350
24	0.30	200	0.33	200	0.37	250	0.40	300	0.43	350
30	0.34	150	0.38	200	0.42	250	0.45	300	0.49	350
36	0.38	150	0.42	200	0.47	250	0.51	300	0.56	350
42	0.41	150	0.47	200	0.52	250	0.57	300	0.63	350
48	0.46	150	0.52	200	0.58	250	0.64	300	0.70	350
54	0.51	150	0.58	200	0.65	250	0.72	300	0.79	350
60	0.54	150	0.61	200	0.68	250	0.76	300	0.83	350
64	0.56	150	0.64	200	0.72	250	0.80	300	0.87	350

NOTES:

1. To convert inches (in) to millimeters (mm), multiply by 25.4; to convert pounds per square inch (lb/in^2) to kilopascals (kPa), multiply by 6.895.

2. The thicknesses shown are adequate for the rated working pressure plus a surge allowance of 100 lb/in^2 (689 kPa). Calculations are based on a minimum yield strength in tension of 42,000 lb/in^2 (289,590 kPa) and a 2.0 safety factor times the sum of working pressure and 100 lb/in^2 (689 kPa) surge allowance.

*Total calculated thickness includes service allowance and casting tolerance added to net thickness.

SOURCE: Table 13 from AWWA C150.

TABLE 6.16 Rated Working Pressure and Maximum Depth of Cover

			Laying condition				
			Type 1 trench	Type 2 trench	Type 3 trench	Type 4 trench	Type 5 trench
Size, in	Pressure class,* lb/in^2	Nominal thickness, in	Maximum depth of cover, ft†				
3	350	0.25	78	88	99	100‡	100‡
4	350	0.25	53	61	69	85	100‡
6	350	0.25	26	31	37	47	65
8	350	0.25	16	20	25	34	50
10	350	0.26	11§	15	19	28	45
12	350	0.28	10§	15	19	28	44
14	250	0.28	¶	11§	15	23	36
	300	0.30	¶	13	17	26	42
	350	0.31	¶	14	19	27	44
16	250	0.30	¶	11§	15	24	34
	300	0.32	¶	13	17	26	39
	350	0.34	¶	15	20	28	44
18	250	0.31	¶	10§	14	22	31
	300	0.34	¶	13	17	26	36
	350	0.36	¶	15	19	28	41
20	250	0.33	¶	10	14	22	30
	300	0.36	¶	13	17	26	35
	350	0.38	¶	15	19	28	38
24	200	0.33	¶	8§	12	17	25
	250	0.37	¶	11	15	20	29
	300	0.40	¶	13	17	24	32
	350	0.43	¶	15	19	28	37
30	150	0.34	¶	—	9	14	22
	200	0.38	¶	8§	12	16	24
	250	0.42	¶	11	15	19	27
	300	0.45	¶	12	16	21	29
	350	0.49	¶	15	19	25	33
36	150	0.38	¶	—	9	14	21
	200	0.42	¶	8§	12	15	23
	250	0.47	¶	10	14	18	25
	300	0.51	¶	12	16	20	28
	350	0.56	¶	15	19	24	32
42	150	0.41	¶	—	9	13	20
	200	0.47	¶	8	12	15	22
	250	0.52	¶	10	14	17	25
	300	0.57	¶	12	16	20	27
	350	0.63	¶	15	19	23	32
48	150	0.46	¶	—	9	13	20
	200	0.52	¶	8	11	15	22
	250	0.58	¶	10	13	17	24
	300	0.64	¶	12	15	19	27
	350	0.70	¶	15	18	22	30
54	150	0.51	¶	—	9	13	20
	200	0.58	¶	8	11	14	22
	250	0.65	¶	10	13	16	24
	300	0.72	¶	13	15	19	27
	350	0.79	¶	15	18	22	30

NOTE: See p. 357 for footnotes.

TABLE 6.16 Rated Working Pressure and Maximum Depth of Cover (*Continued*)

Size, in	Pressure class,* lb/in^2	Nominal thickness, in	Laying condition: Type 1 trench	Type 2 trench	Type 3 trench	Type 4 trench	Type 5 trench
			Maximum depth of cover, ft†				
60	150	0.54	¶	5§	9	13	20
	200	0.61	¶	8	11	14	22
	250	0.68	¶	10	13	16	24
	300	0.76	¶	13	15	19	26
	350	0.83	¶	15	18	22	30
64	150	0.56	¶	5§	9	13	20
	200	0.64	¶	8	11	14	21
	250	0.72	¶	10	13	16	24
	300	0.80	¶	12	15	19	26
	350	0.87	¶	15	17	21	29

NOTE: To convert inches (in) to millimeters (mm), multiply by 25.4; to convert feet (ft) to meters (m), multiply by 0.3048; and to convert pounds per square inch (lb/in^2) to kilopascals (kPa), multiply by 6.895.

*Ductile iron pipe is adequate for the rated working pressure indicated for each nominal size plus a surge allowance of 100 lb/in^2 (689 kPa). Calculations are based on a 2.0 safety factor times the sum of working pressure and 100 lb/in^2 (689 kPa) surge allowance. Ductile iron pipe for working pressures higher than 350 lb/in^2 (2413 kPa) is available.

†An allowance for a single H-20 truck with 1.5 impact factor is included for all depths of cover.

‡Calculated maximum depth of cover exceeds 100 ft (30.5 m).

§Minimum allowable depth of cover is 3 ft (0.9 m).

¶For pipe 14 in (356 mm) and larger, consideration should be given to the use of laying conditions other than type 1.

SOURCE: Table 14 from AWWA C150.

However, for ductile iron pipe, flexural stress is not an adequate indicator of performance and need not be used in the design of the ring to resist external loads. Due to soil-structure interaction, i.e., the lateral support of soil at the sides in combination with the arching action of the soil over the pipe, failure does not occur even though the yield point may have been reached in the outer fibers of the pipe wall. The first observable sign of distress is cracking of the cement mortar which is followed by spalling of the cement mortar lining. The performance limit is not due to stress in the wall, but rather is due to deformation.

Performance limit 1—spalling or unbonding of cement lining. The cause of cracking and spalling of cement linings in ductile iron pipes is determined by wall strain—not just ring deflection. In the design of cement-lined pipe, an arbitrary value of $\Delta y/D = 2$ percent maximum is often specified to prevent damage to the cement lining.

Because cracking and spalling of the mortar lining are the best indicators of distress (performance limit) and because cracking and spalling are caused primarily by change in radius of curvature of the

TABLE 6.17 Special Thickness Classes of Ductile Iron Pipe

Size, in	Outside diameter, in	Thickness class* 50	51	52	53	54	55	56
		Thickness, in						
3	3.96	—	0.25	0.28	0.31	0.34	0.37	0.40
4	4.80	—	0.26	0.29	0.32	0.35	0.38	0.41
6	6.90	0.25	0.28	0.31	0.34	0.37	0.40	0.43
8	9.05	0.27	0.30	0.33	0.36	0.39	0.42	0.45
10	11.10	0.29	0.32	0.35	0.38	0.41	0.44	0.47
12	13.20	0.31	0.34	0.37	0.40	0.43	0.46	0.49
14	15.30	0.33	0.36	0.39	0.42	0.45	0.48	0.51
16	17.40	0.34	0.37	0.40	0.43	0.46	0.49	0.52
18	19.50	0.35	0.38	0.41	0.44	0.47	0.50	0.53
20	21.60	0.36	0.39	0.42	0.45	0.48	0.51	0.54
24	25.80	0.38	0.41	0.44	0.47	0.50	0.53	0.56
30	32.00	0.39	0.43	0.47	0.51	0.55	0.59	0.63
36	38.30	0.43	0.48	0.53	0.58	0.63	0.68	0.73
42	44.50	0.47	0.53	0.59	0.65	0.71	0.77	0.83
48	50.80	0.51	0.58	0.65	0.72	0.79	0.86	0.93
54	57.56	0.57	0.65	0.73	0.81	0.89	0.97	1.05

NOTE: To convert inches (in) to millimeters (mm), multiply by 25.4.
*These special thickness classes were designated standard thickness classes in the 1986 edition of this standard.
SOURCE: Table 15 from AWWA C150.

ring and by wall thickness t, it is necessary to relate these variables. A theoretical equation for doing this is as follows:

$$\varepsilon = \frac{t}{D}\left(\frac{3\Delta y/D}{1 - 2\Delta y/D}\right) \tag{3.19}$$

where ε = maximum tangential strain in pipe ring
t = wall thickness
D = diameter
$\Delta y/D$ = vertical ring deflection

It is assumed that the ring remains essentially elliptical during deflection. As long as the D/t ratio is constant, according to Eq. (3.19), the flexural strain is a function only of ring deflection $\Delta y/D$ in an elliptical ring. The flexural strain in Eq. (3.19) increases as wall thickness increases. Actually, hydrostatic ring compression will affect strain also, but usually to a lesser extent. Therefore, the prediction of mortar cracking by ring deflection is somewhat imprecise. Clearly it is more precise to predict mortar cracking in terms of surface strain. However, as demonstrated in the above equation, strain cannot be predicted unless the assumptions of ellipticity are made; and under those assumptions, ring deflection is just as good a fundamental variable as surface strain.

Figure 6.47 Reynold Watkins at the USU test cell.

If the performance limit for design is spalling of the mortar lining, the best parameters for design are D/t and either the single variable $\Delta y/D$ or the two variables ρ and P, where ρ is soil density and P is vertical soil pressure (ρ and P determine $\Delta y/D$). Secondary criteria include type of bell, bedding, etc. Precision does not justify the inclusion of secondary criteria.

Figure 6.48 shows measured strain as a function of vertical ring deflection for tests 4 through 12 on buried ductile iron pipe. Up to 3 percent deflection, the probable deviation is under ±13 percent, which may not be too bad considering the great variability of soil

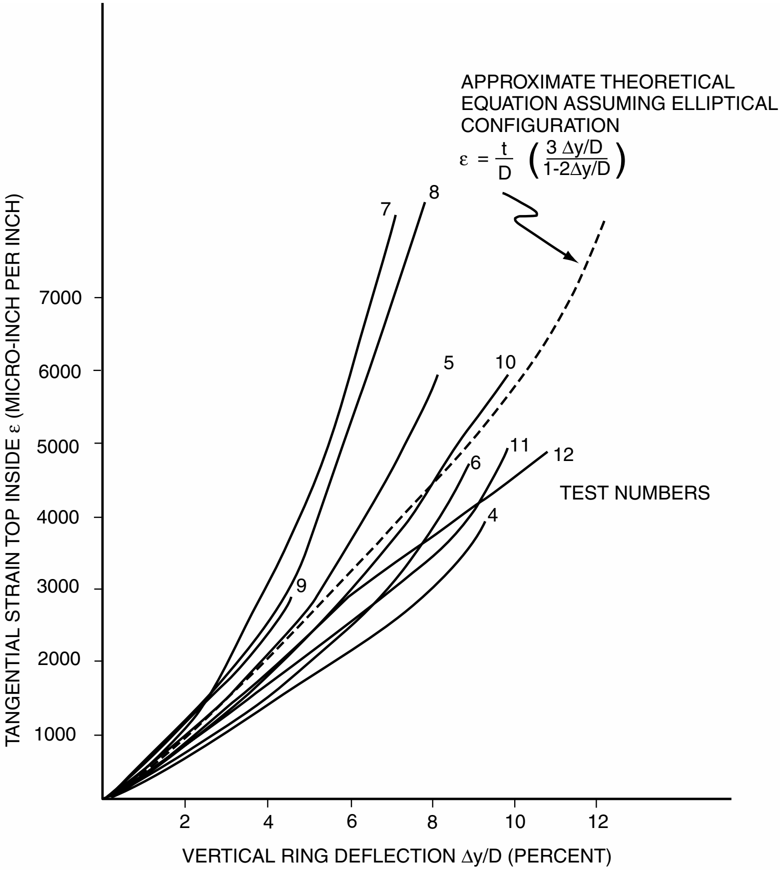

Figure 6.48 Strain in pipe wall as a function of percent of vertical deflection.

placement. It is also interesting to note that the plots fall randomly on both sides of the theoretical equation, suggesting that greater precision requires generally better soil control. No single variable is causing the deviation. The assumption of elliptical configuration is as good as can be achieved under typical techniques for soil placement.

Performance limit 2—bell cracking. Cracking of the bell, although a rare phenomenon, was found to be basically a function of ring deflection and the *D*/*t* ratio. Here again, design would be the same except for the strength envelope which is based on a different performance limit.

Performance limit 3—loss of compression in the gasket. Differential transverse movement between the bell and spigot can cause high compression of the gasket on one side of the joint with a consequent loss of compression on the other side. Similar loss of compression of the gasket can be caused at opposite sides of the joint if either bell or spigot is not circular (some ring deflection). Because the bell has a ring stiffness greater than that of the spigot, when loaded, the bell tends to remain more nearly circular and the spigot tends to deform out of round. The deflection of a spigot can be calculated for a concentrated diametral load. However, soil loading is different. If the ring is semiflexible (as is typical of ductile iron pipes), then the deflection of the ring due to soil pressure is approximately elliptical. If this assumption is adequate, then the loss of compression in the gasket is a function of ring deflection $\Delta y/D$ and the dimensions t and D. As a result, the design method involves the same parameters $\Delta y/D$ and D/t as do cracking and spalling of the mortar lining. The only difference would be the performance limit. Of course, a hard spot such as a rock outcrop under the spigot would cause a nonelliptical deformation which could result in loss of compression in the gasket. There is really no way of predicting or controlling such an occurrence except by care and control in the installation of the pipe and placement of the soil.

Instrumentation. On one 24-in and two 36-in tests, the primary objective was to determine the action of the spigot in relation to the bell under external load. The secondary objective was to record pipe deflections for determining the structural performance of the pipe wall. These three tests were instrumented much more extensively than the remainder of the tests. Two instruments especially designed and constructed were used to trace the inside profile of the bell and spigot during loading. One of these instruments was mounted at each joint. To determine the offset condition at the throat, eight dial indicators were mounted in tapped holes at 45° points around the circumference at the position directly opposite the throat. Horizontal and vertical deflections were taken with dial indicators at the midspan of the pipe. The bell and spigot of each pipe was carefully measured with inside micrometers and dial indicator thickness micrometers before and after the tests.

The primary objective of the remainder of the tests was to determine a structural performance limit of the pipe wall with secondary observation of the action of the cement lining during loading. Instrumentation of these tests consisted of strain gages placed inside and outside of the pipe wall at the midspan and vertical and horizontal deflection readings at the bell and spigot of both joints and midspan. Joint deflections and pull-out were measured for all tests. Measurement of the joints before and after the tests was also performed.

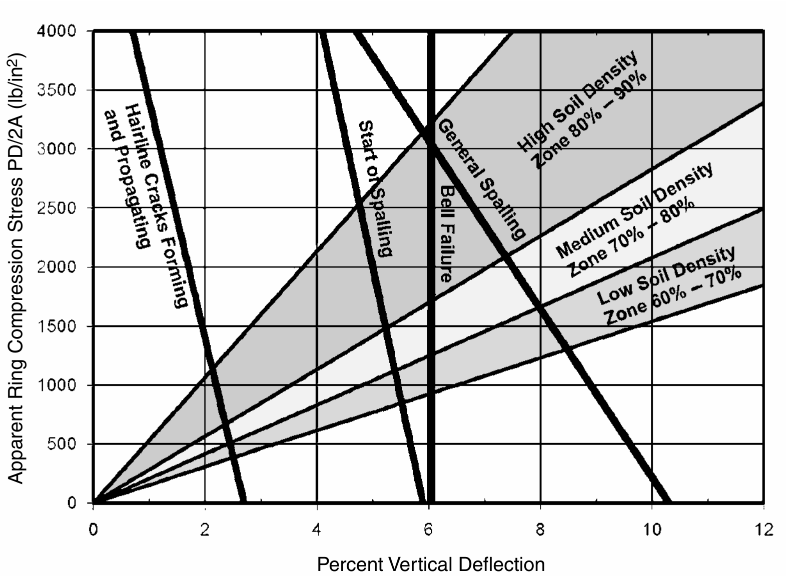

Figure 6.49 Ring compression stress versus ring deflection for buried ductile iron pipe.

Test results. Figure 6.49 shows apparent ring compression stress versus percent of vertical ring deflection at the midspan for the various tests. The lower zone is for loose soil tests, the center zone for tests in medium-dense soil, and the upper zone is for dense soil tests.

Figure 6.48 shows strain data for the various tests plotted as a function of percent of deflection. The dashed line in the figure is the plot of the theoretical equation

$$\varepsilon = \frac{t}{D}\left(\frac{3\Delta y/D}{1 - 2\Delta y/D}\right)$$

It is interesting to note how closely this equation follows the data. This equation can be derived by assuming the pipe deflects as an ellipse. In other words, this shows that strain in the pipe wall can be determined to a fair degree of accuracy from pipe geometry and deflection data. However, it is obvious that other variables such as soil placement also influence strain.

Tests 4 through 10 were performed on pipes which were cement-lined. Tests 4 and 10 were in loose soil, and tests 5 through 9 were in medium to dense soil. The cement lining performed similarly in both loose soil and dense soil.

Prior to loading, each pipe was examined with a strong light, and all existing cracks were marked. After each increment of load, the lining was reexamined and any new cracks or old crack changes noted. All pipe tested had cracked linings prior to installation. These cracks were mainly confined to the spigot area. In some cases the lining was unbonded in the spigot areas prior to installation.

As load is applied, the pipe deflects. Its vertical diameter decreases significantly in the midspan of the pipe and usually to a lesser degree at the joints. During this loading, the first significant change in the cement lining is a crackling noise. In conjunction with this noise, small hairline cracks appear in the tension areas and existing cracks tend to lengthen. These cracks are generally parallel to the pipe axis and extend only a short distance (in the range of 1 to 3 ft) down the pipe and stop. As deflection proceeds, new cracks open parallel to the existing cracks. These first cracks were approximately the same in appearance as those cracks which occurred prior to installation. These first cracks should not be considered a performance limit of the cement lining since the lining was not in danger of falling out or being washed out.

The second significant occurrence, which happened in every case, was a spalling or flaking of the cement lining in the vicinity of the bell. During this occurrence, pieces of cement lining fell out. The failure was in the compression areas of the pipe bell (horizontal centerline). This spalling is defined as the performance limit for the pipe tested. Figure 6.50 shows the performance limit (critical ring compression stress which will cause spalling at the bell) as a function of average soil density.

Spalling at Bell (Horizontal Centerline)

Test no.	Percent deflection at bell ($100 \times \Delta y$/barrel OD)
4	4.03
5	3.62
6	3.24
7	3.38
8	5.5
9	3.54
10	4.46

NOTE: Since the bell is much stiffer than the midspan of the pipe, the bell deflection usually occurs at a much lower rate.

During the deflection immediately preceding and following the spalling of the cement lining in the vicinity of the bell, an audible tearing or unbonding occurred in four tests. Although present in the other three tests, it appeared to have occurred very gradually, and the exter-

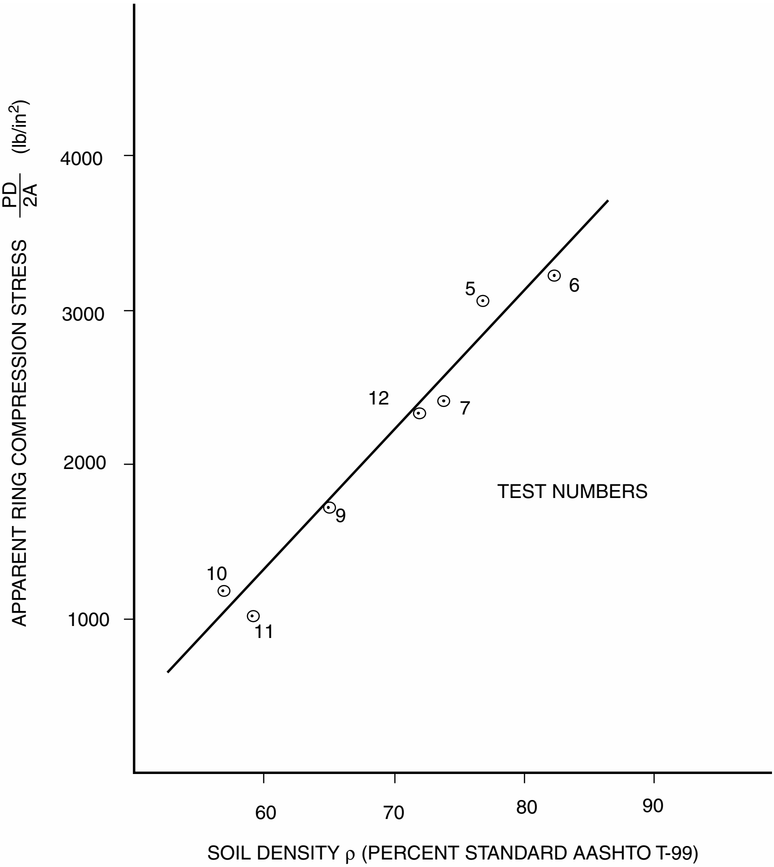

Figure 6.50 Performance limits for spalling at the bell.

nal load at which it first started could not be determined. The load and deflections at which this unbonding occurs are inconsistent and are seemingly related to initial defects or unbonding which occurs during the curing and/or handling of the cement-lined pipe prior to installation.

In four of the seven tests on 36-in cement-lined pipe, the performance of the lining was climaxed by a general spalling in the compression areas along one of the horizontal centerlines. The cement lining of the remaining three test pipes was stress-relieved by cracks in other areas, and general compression spalling did not occur.

As previously mentioned, there is a good possibility that the cement lining in large-diameter pipes will be cracked due to handling or other problems prior to installation. If these cracks remain small and unbonding does not take place, the lining will continue to perform its intended function—the prevention of tuberculation. A phenomenon called *autogenous healing* takes place in Portland cement exposed to water. This phenomenon in combination with swelling due to water absorption will tend to close cracks. Therefore, it is more reasonable to define performance limit as spalling of the lining or general unbonding, whichever occurs first. Ring deflection, per se, ceases to be a performance limit.

During a test in 85 percent Proctor density soil, the performance limit of the 36-in pipe was reached at a vertical soil pressure of 18,000 lb/ft^2 when the bell on the full-length test piece suddenly cracked. Upon visual examination, the crack was found to be completely through the bell wall, extending approximately 15 in back from the face of the bell. On two other tests similar failures occurred. These were installed in soil of 75 and 67 percent average Proctor density, respectively. It appears that a bell deflection of 6 percent is the lower limit for bell failure. This corresponds to a deflection at the midspan of the barrel of approximately 10 percent. Photomicrographs made from specimens taken from these bells all indicate the material to be a pearlite matrix with nodular graphite. Tensile tests made from samples also indicated a pearlitic structure.

Methods of design

The stress theory of design allows a structure to be designed analytically by setting the performance limit of the structure at a stress level less than the yield point strength of a simple tensile specimen. Analytical equations for determining the stress level can be used for most structures, thus eliminating costly experimental work in the design stages. So long as the structure and the load are fairly simple and dependable, a reliable structure can be designed by the so-called stress theory of design.

It is well known, however, that some structures can fail before the yield point stress has been reached (elastic buckling) while other structures continue to perform their function long after the yield point of the outer fibers has been reached (plastic design of structures, see *AISC Manual of Steel Construction*). Therefore, the design methods for many types of structures have been formulated by the more reasonable approach of relating the variables or parameters governing the performance of the structure through experimentation and then limiting the parameters to conservative values.

In the case of an internally pressurized pipe, the performance limit can be the bursting of the pipe wall or leakage of the joint. If bursting is the performance limit, the pertinent variables can be related using the stress theory of design. The pertinent variables are

P_i = internal pressure, lb/in^2

D = pipe diameter, in

A = pipe wall cross-sectional area per unit length (in^2/in) = thickness t

The allowable hoop tension stress is

$$\sigma_t = \frac{P_i D}{2A} = \frac{S_t}{N}$$

where S_t = strength of pipe wall in tension, lb/in^2, and N = safety factor.

For design purposes, σ_t is limited to values below the bursting strength of the pipe by some safety factor N. If the bursting strength is not known, a conservative performance limit to choose is the yield point (strength) of the pipe material.

In the case of a pipe externally loaded, the important variables are

1. EI/D^3 = ring stiffness, lb/in^2. Since E is a constant (24,000,000 lb/in^2) for ductile iron, in this case ring stiffness can be reduced to D/A or D/t, where t is the wall thickness.
2. E' or ρ = a measure of soil stiffness, where E' = soil stiffness and ρ = density of soil (% compaction).
3. P = apparent vertical soil pressure (unit weight of soil, times height of cover plus effect of surface loads at level of top of pipe).
4. $\Delta y/D$ = ring deflection, where Δy = vertical decrease in diameter and D = diameter.
5. Performance limit.

Ring stiffness, soil density, and vertical soil pressure are *independent* variables which are set by specification, etc., for each installation. The performance limit and $\Delta y/D$ are *dependent* variables depending upon various combinations of ring stiffness, soil density, and vertical soil pressure.

Ring stiffness and vertical soil pressure can be combined in the convenient parameter $PD/(2A)$. This parameter is very useful in the stress theory of design for external hydrostatic pressure and is widely used in the design of corrugated culvert pipe under external soil pressure. Therefore, it is easily understood and simplifies design calculations. This form will be used to relate the independent variables. For design, the value of $PD/(2A)$ should be limited to a value well below the performance limit; $PD/(2A)$ has been related to soil density, performance limit, and $\Delta y/D$ through the tests. This relationship is shown in Fig. 6.49.

$$\text{Ring compression stress } \sigma_c = \frac{PD}{2A} = \frac{S_c}{N}$$

where P = calculated or apparent vertical soil pressure at level of top of pipe
= height of cover times unit weight of soil plus effect of surface loads
D = diameter of pipe
A = wall cross-sectional area per unit length of pipe
= wall thickness t for cylindrical pipe
S_c = compression strength of pipe wall
N = safety factor

For design purposes, σ_c must be limited to the ultimate compression strength of the pipe wall and must be reduced by some factor of safety N. This ultimate compression strength is simply the ring compression stress $PD/(2A)$ at performance limit as determined by actual tests. Two examples of design follow.

Example 6.5 A 36-in ductile iron pipe is to be used to function with an internal pressure of 200 lb/in^2 working pressure with a 100 lb/in^2 surge pressure allowance and is to be buried under 30 ft of cover. What is the required thickness for the internal pressure, and what should be the method of installation, i.e., compaction of surrounding soil?

1. Calculate the required thickness.

$$\frac{S_t}{N} = \frac{P_i D}{2A} = \frac{P_i D}{2t\ (1\ \text{in})}$$

$$t = \frac{P_i DN}{2S_t}$$

where P_i = 200 + 100 = 300 lb/in^2
D = 38.30 in
N = 2.5
S_t = 42,000 lb/in^2

$$t = \frac{300\ (38.30)\ (2.5)}{2\ (42{,}000)} = 0.34\ \text{in}$$

2. What is the soil density or percent of compaction required for this pipe to withstand 30 ft of cover without spalling of the cement lining?

$$P = 30\ \text{ft} \times 120\ \text{lb/ft}^3 = 3600\ \text{lb/ft}^2$$

$$D = \frac{38.30 \text{ in}}{12 \text{ in/ft}} = 3.2 \text{ ft}$$

$$A = 0.34 \text{ in} \times 12 \text{ in/ft} = 4.08 \text{ in}^2/\text{ft}$$

$$\frac{PD}{2A} = \frac{3600 \text{ lb/ft}^2 \text{ (3.2 ft)}}{2 \text{ (4.08 in}^2/\text{ft)}} = 1412 \text{ lb/in}^2$$

Entering Fig. 6.49 at $PD/(2A)=1412$ lb/in^2, we can see that if the density of the soil is between 80 and 90 percent standard Proctor density, the deflection can be kept between 2.5 and 4.5 percent. A safety factor against cement-lining spalling can be calculated as follows. At $PD/(2A) = 1412$ lb/in^2, the cement lining would spall at about 5.2 percent. Therefore, the safety factor is between 1.2 and 2.1. A 90 percent Proctor should be specified. A 90 percent Proctor density can be obtained with a moderate amount of work on ordinary soils by placing the soil in 1-ft lifts and passing over it with a rammer-type compactor.

Example 6.6 A 36-in ductile iron pipe is to be designed for an internal pressure of 200 lb/in^2 working pressure and 100 lb/in^2 surge pressure. It is to be installed under 5 ft of cover under a roadway. Calculate the required thickness for internal pressure, and recommend an installation procedure.

1. This is identical to Example 6.5. The required thickness is 0.34 in.
2.

$$\begin{aligned} P &= 5 \text{ ft} \times 120 \text{ lb/ft}^3 + \text{(live load)} \\ &= 600 + 340 = 940 \text{ lb/ft}^2 \end{aligned}$$

$$\frac{PD}{2A} = \frac{940 \text{ lb/ft}^2 \text{ (32 ft)}}{2 \text{ (4.08 in}^2/\text{ft)}} = 369 \text{ lb/in}^2$$

See Fig. 6.49.

If it is installed in loose soil (60 to 70 percent standard Proctor density), the deflection is 1.8 to 2.5 percent. Therefore, the safety factor against cement-lining spalling is about 2.3 to 3.1.

Note: Tamping is not required in this installation unless it is required to protect the roadway pavement from damage.

Prequalification Testing of Pipes Used in Underground Heating Distribution Systems

Introduction

For large institutions with multiple buildings, often there is a central heating plant. The pipes used to carry the hot fluid to the buildings and to return the condensate to the plant are insulated and are frequently actually two concentric pipes (a casing pipe and a carrier pipe) with insulation in the annulus between them. Such pipe must be tested to demonstrate that the pipe system meets the criteria specified by the Federal Agency Pre-Qualification Procedures for Underground Heat Distribution Systems. The testing program is carried out in accordance with a set test protocol. Test equipment to meet the protocol was designed and constructed by the Buried Structures Laboratory at Utah State University.

The test apparatus is described in the test protocol; however, photographs and diagrams are included here to give the reader some visual perception of the actual test setup. Sample results of some tests are also given. See Figs. 6.51 to 6.66.

Test protocol

System classification. The thermal pipe and the condensate pipe must be described and qualified for use in the specific site conditions such as follows:

Groundwater conditions: Class B—bad. The water table is expected to be occasionally above the bottom of the system, and surface water is expected to accumulate and remain for short periods (or not at all) in the soil surrounding the system, or the water table is expected never to be above the bottom of the system, but surface water is expected to accumulate and remain for long periods in the soil surrounding the system.

Soil corrosiveness: corrosive—all the soil resistivities.

Soil pH: Soil pH down to 4.5 for the hot pipe and 2.0 for the condensate pipe. Both systems can be used in soil up to pH 12.

Soil stability: Both systems can be used in all soils where thrust blocks are required, by direct bearing against undisturbed or satisfactorily tamped soil; where friction block can be used; where unstable soil can be replaced by ballast of sufficient size and weight to resist thrust; or where tie rods or piling can be used.

Operating temperature: Continuous operating temperatures of 200 to 450°F for hot pipe and 100 to 250°F condensate return piping.

Test procedures for the hot pipe. The purpose of the tests specified in this section is to demonstrate that the hot pipe system meets the criteria specified by the Federal Agency Pre-Qualification Procedures for Underground Heat Distribution Systems. The following tests will be performed:

1. Resistance to groundwater infiltration

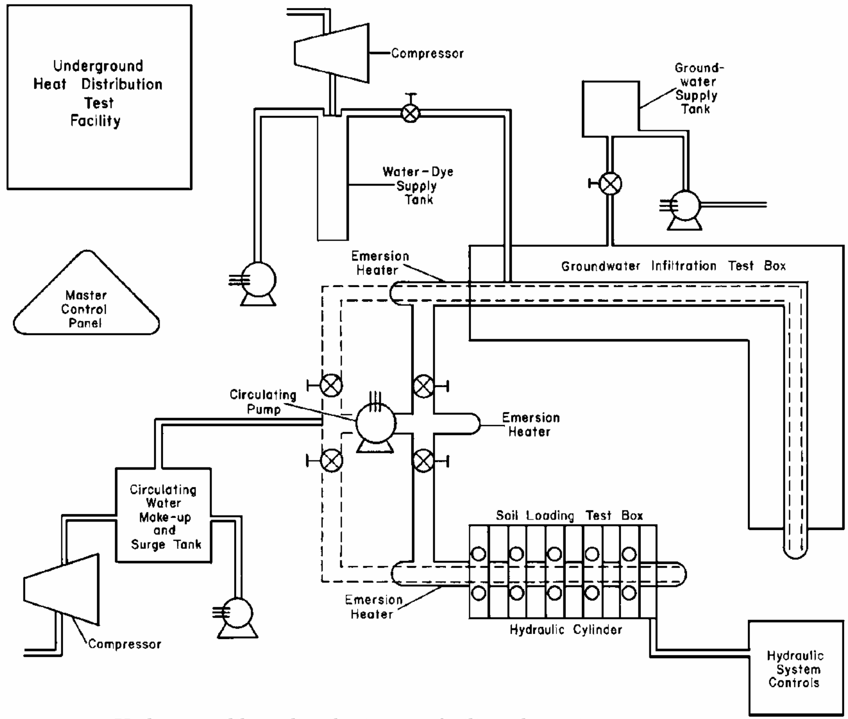

Figure 6.51 Underground heat distribution test facility schematic.

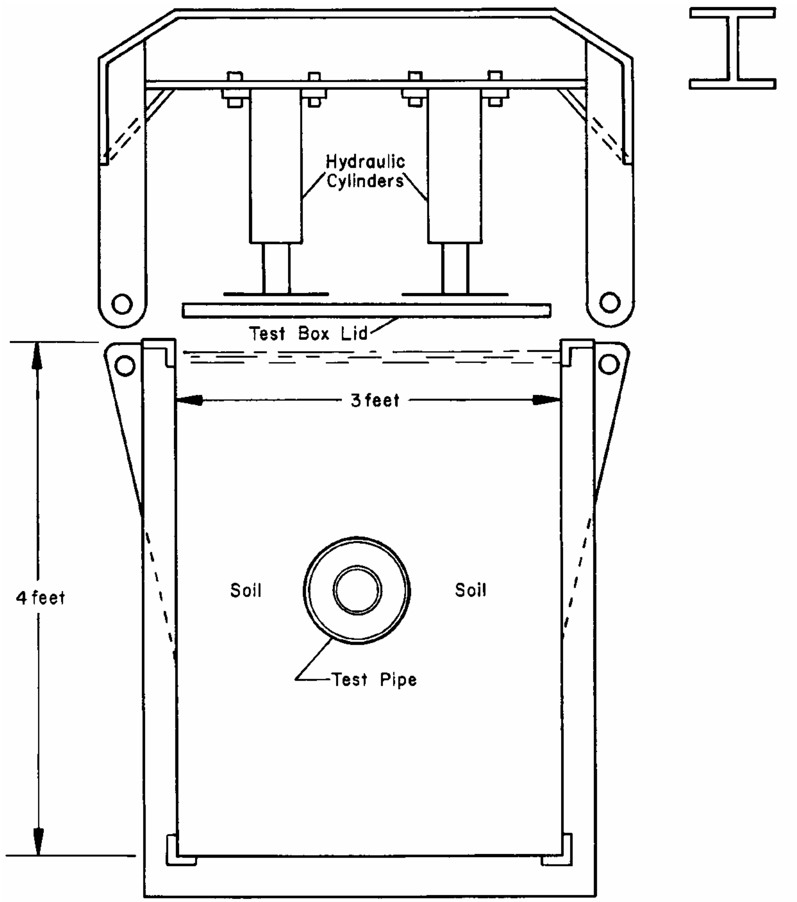

Figure 6.52 Cross-sectional view of the soil loading test cell.

a. Apparatus is a test box or tank 3 ft wide and 4 ft deep with a cover that can be bolted in place to make the tank pressure tight up to 10 lb/in^{2}gage. The foundation is capable of supporting 600 lb/ft^2. The tank has a drain fill plug at its lowest point and a vent at its highest point. Manhole terminals are centrally located on the two end plates. This tank, its appurtenances, and all other apparatus needed are shown in Figs. 6.51 to 6.54.

b. Two electric water heaters, 500 W each, a watthour meter, and a circulation pump.

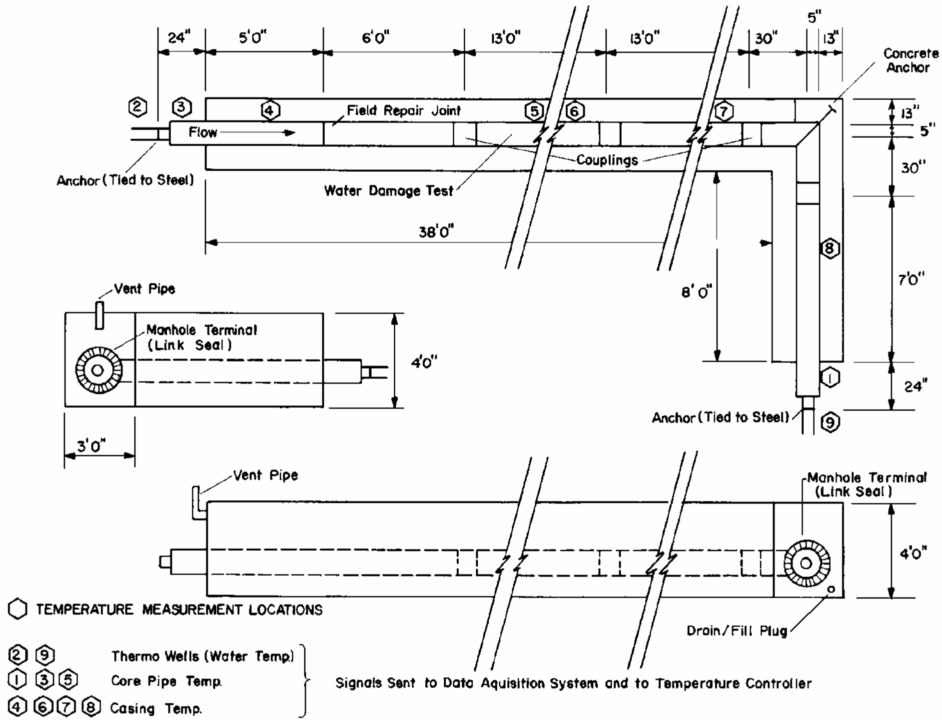

Figure 6.53 Test layout for water damage, water infiltration, and joint leakage tests. This schematic shows the test pipe layout including placement of the following: (1) couplings; (2) field repair joint; (3) concrete anchor on elbow; (4) anchor of pipe protrusion to the test cell; (5) the fitting where dyed water was inserted under pressure for the water damage test; (6) manhole terminals (link seals); and (7) thermocouples for temperature measurement and control.

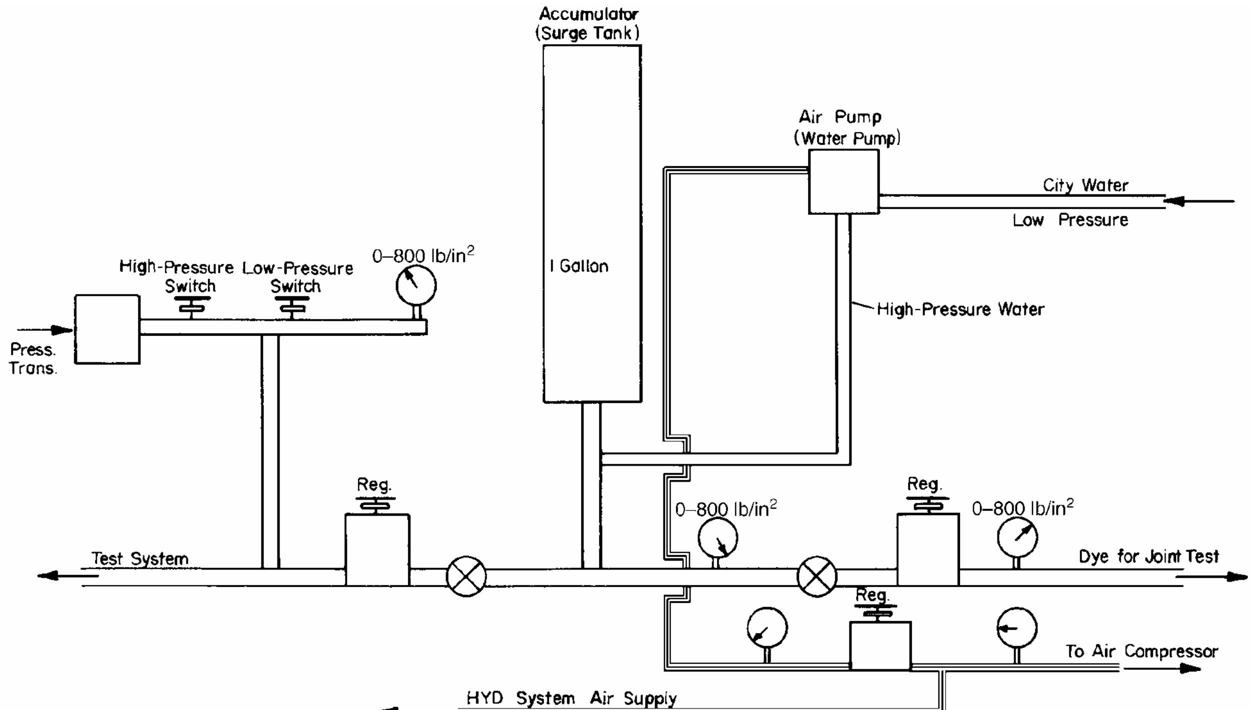

Figure 6.54 Schematic of pressure controls.

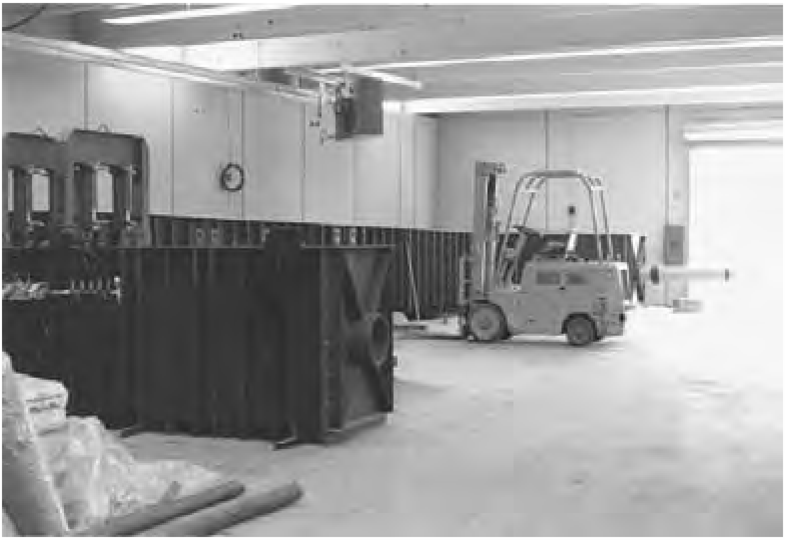

Figure 6.55 Test facility under construction. Foreground: soil load cell; center to rear: water infiltration test cell.

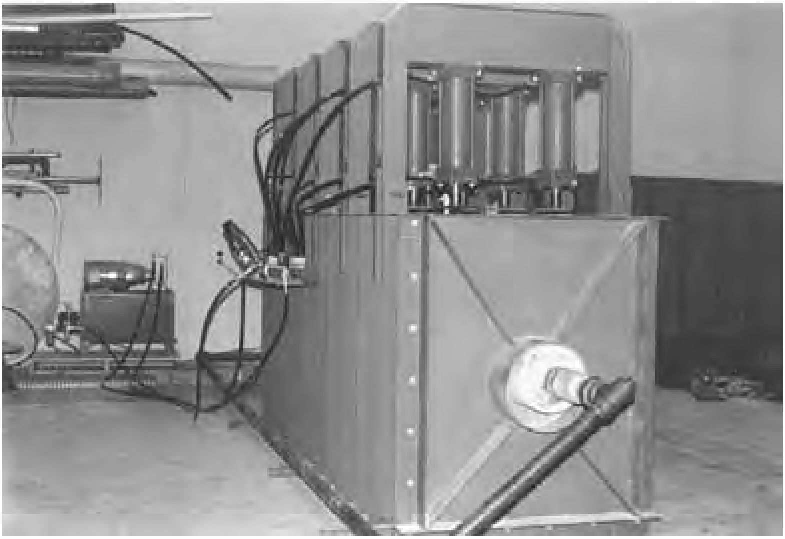

Figure 6.56 Soil load cell used in structural damage test with test pipe in place and return line connected. Note the hydraulic pump in the background and the hydraulic controls.

Figure 6.57 Soil load cell showing the insulation used on return piping.

- *c.* A 200 lb/in^{2}gage water pressure pump and a 500 lb/in^{2}gage water pump.
- *d.* A 0 to 500°F thermometer input temperature recorder.
- *e.* A temperature controller capable of handling the electric heater load and controlling a temperature of 450°F ± 3 percent.
- *f.* A surge tank (1-gal capacity). The static pressure capacity must be at least 500 lb/in^{2}gage equipped with suitable pressure gage.
- *g.* Thermocouples shall be mounted as shown on the drawing.

2. *Procedure:* A 4-in system consisting of 500 ft of test pipe with at least three 13-ft sections, one 90° ell, one anchor at the ell, and one short section with a field joint installed in the tank in a gravel soil. (The field joint used in this test is the same joint that will be used on the casing of a 20-ft length of pipe.) Each joint is misaligned with its mate by 1.5°, with at least two of the misalignments in the horizontal plane. The installation shall be made in strict accord with installation guidelines except for these misalignments.

   The power input to the heater will be measured and the heat loss from heaters to outside ambient calibrated so that the net electrical energy input to the test sections can be accurately measured.

   The pipe system shall have a 5 percent slope, with the lower exit being the low point of the system. After the installation is completed, the tank cover is bolted in place. A water source is attached to the drain/fill, and a 5-gal surge tank is attached to the vent with a tee fitting. The surge tank shall have a water sight glass and a 0 to

Figure 6.58 System control center with the following features: (1) temperature controller, (2) temperature fail-safe circuits, (3) pressure controls, (4) pressure fail-safe circuits, (5) dual control timer (concealed in photo), (6) flowmeter readout, (7) power meter with digitized output for data system, (8) associated warning lights for system operation. Safety controls were necessary because the system was operated at 500 lb/in^2 and 450°F. An electronically operated pressure relief valve was controlled by the fail-safe circuits. In addition, a manual pressure relief valve was incorporated into the system.

15 lb/in^{2}gage static pressure gage. The other tee line shall contain a shutoff valve on the side open to the atmosphere. With the vent shutoff valve open, water is admitted into the tank through the drain/fill until the tank is full and water spills from the open vent. The vent valve is then closed and filling continues until the pressure reaches 9 lb/in^{2}gage (the surge tank should be about two-thirds full as observed in the sight glass). Tank pressure shall be

Figure 6.59 Looking down on the heating section located between the two test cells. Note the following: (1) Tops of two 5000-W immersion-type heaters (center right of photo). A third heater is concealed from view. (2) Motor that runs the circulation pump (center left of photo). (3) Insulation applied to external piping to conserve energy.

maintained for 48 h, and water up to 450°F shall be circulated through the carrier pipe to 24 h and drained. The hot water system shall be disconnected, and pipe ends shall remain open for the remaining 24 h. The lower end of the carrier pipe shall be monitored for water leakage during the next 24 h. At the end of the 48 h, the pressure is relieved by opening the vent valve, and the water is drained from the tank through the vent drain/fill fitting.

a. Results: At no time during the test period shall water be observed coming from the low end of the open pipe to indicate water has entered the insulation through the pipe or end seals.

Figure 6.60 High-temperature pipe installed in the test cell. Note the following: (1) joints misaligned by 1.5°, (2) thermocouple wire running along pipe, (3) fitting and hose for water damage test.

Figure 6.61 Elbow with steel anchor plate before concrete thrust block was cast in corner.

Figure 6.62 Test cell filled with soil.

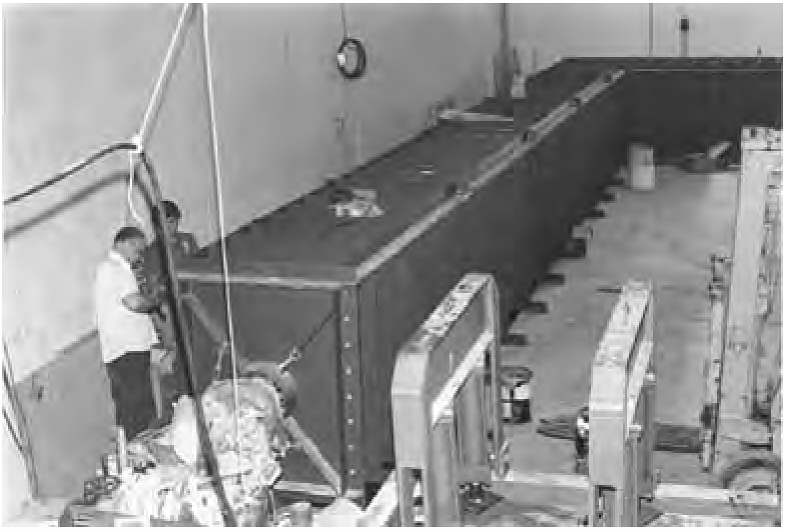

Figure 6.63 Adjusting water pressure in cell to simulate a 20-ft head of groundwater (9 lb/in^2). Note the link seal around the pipe where it penetrates the tank.

Figure 6.64 Elbow and thrust restraint for condensate pipe.

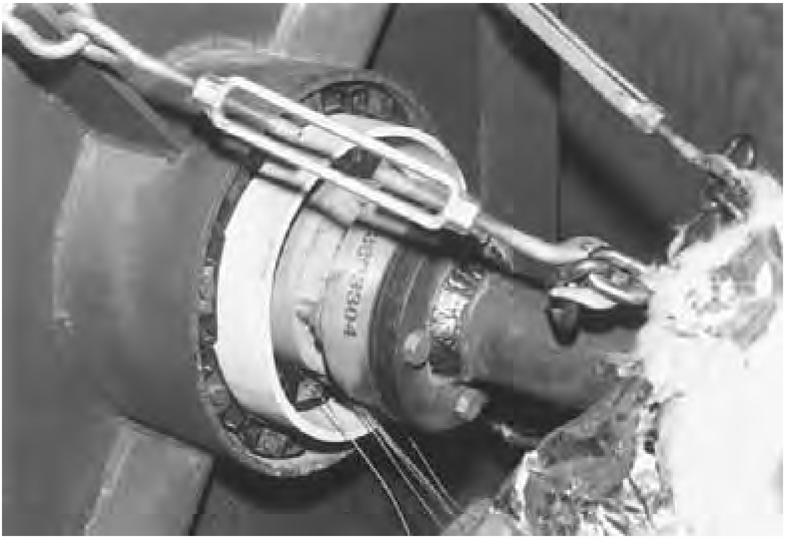

Figure 6.65 External connection and thrust restraint.

Figure 6.66 Condensate pipe in test cell.

3. Resistance to water damage
   a. *Apparatus:* The same system configuration used for the groundwater infiltration test shall be used for the water damage testing, except no pressure will be applied to simulate groundwater. A "zero" groundwater pressure will produce a more critical test situation for water damage. After the 48-h groundwater infiltration test has been inspected and approved, a system similar to the system used in the groundwater infiltration tests, except for the 0.25-in NPT female fitting, shall be set in the outer casing of one of the sections and firmly epoxied and mechanically anchored. The system will be connected externally with the heater, pump, and valving system. The 0.25-in water line shall be connected to the 150 lb/in^{2}gage water system. Thermocouples shall be set, as shown on the drawing, to record the surface temperature of the conduit and water temperature entering and leaving the carrier pipe.

   b. *Procedure:* Circulation is begun, and the heater is turned on. After 24 h the heater is turned off for 24 h. This cycle is repeated for 14 days. The cycle is continued, except that 150 lb/in^{2}gage water-dye solution is introduced into the 0.25-in pipe and “leaked” into the insulation cavity between the core and casing. This test is continued for 14 days or until water is flowing from the casing relief valve or end seal. At the conclusion of the test, the leak is stopped. The tank is drained, the pipe water system is drained, and each section is examined for migration of leaking water.
   c. *Results:* The spread of the “leak” at which the dyed water is introduced shall be confined to one section of pipe. It shall be understood that water leakage through the casing or end seals does not constitute a failure.
4. Resistance to mechanical or structural damage (balance loading test)
   a. *Apparatus:* A 3-ft-wide by 4-ft-deep by 11-ft-long steel tank is equipped with vertically sliding panels in the end plates.
   b. *Procedures:* A steady and constant vertical load of 200 lb/ft^2 is applied to a 13-ft length of buried conduit system for 14 days. A 13-ft conduit system with a field joint in the center of the length (the field joint is the same as will be used in the casing of a 20-ft length of pipe), pipe anchor, pipe supports, and a 4-in carrier pipe and end seals will be anchored at one end of the tank with carrier pipe lengths protruding from the sliding panels. This system is installed on at least 12 in of firmly tamped soil over 6 in of sand. Soil surrounds the conduit and comes to within 4 in of the tank top. The soil used in this test is a fine blow sand and has been selected because of the relative ease with which it can be handled and because it can be used to simulate clay soil. A steel plate lid is placed on top of the soil. The lid dimensions are 10 ft 10 in by 2 ft 10 in (allowing a 1-in clearance on all sides between the lid and the tank perimeter). Hydraulic jacks are used to apply a steady loading to the steel plate lid of 2000 lb/ft^2. This load is maintained for 14 days. During the 14-day loading period, ambient and water up to 450°F, 500 lb/in^2 are alternately circulated through the carrier pipe at 24-h intervals. The vertical positions of the two end pipes are recorded every 8 h during the 14 days.
   c. *Results:* The differential deflection shall not have been sufficient to allow conduit or system to be damaged or deformed enough to impair functioning of the system. The conduit envelope shall not rupture or deform. The pipe supports shall not be crushed, cracked, or abraded. Pipe anchors shall not fail.
5. Resistance to mechanical or structural damage (unbalanced loading)
   a. *Apparatus:* The test tank, conduit section, and jacking appara-

tus used in the loading test, a steel plate 3 ft by 2 ft 10 in and a source of 500 lb/in^{2}gage water.

b. Procedures: With one end of the protruding carrier pipe capped, introduce 500 lb/in^{2}gage dyed water into the other protruding end. Place the 3-ft by 2-ft 10-in steel plate at one end of the tank over the buried conduit system. Apply a steady load of 2000 lb/ft^2 to the plate for 5 min. After removing the load and draining the carrier pipe, uncover the conduit system. Disassemble the conduit and insulation at the field joint, and inspect the joint area for water leaks. Inspect the entire system for mechanical or structural damage.

c. Results: No water leakage from the carrier pipe to the surrounding insulation shall occur. Casing and insulation integrity must be maintained.

6. Joint leakage test

a. Apparatus: Same as used in water damage test.

b. Procedure: The joint leakage test is performed simultaneously with the water damage test. Each joint is misaligned with its mate by 1.5°, with at least two of the misalignments in the horizontal plane. As with the water damage test, water up to 450°F is circulated in the system for 24 h, at which time the heater is turned off for 24 h. This cycling is continued for 14 days. At the conclusion of this period, the tank is drained and the outer casing is removed.

c. Results: With the exception of field joints connecting the one section with the 0.24-in female fitting, no other joints shall have allowed any of the circulating water to leak into the surrounding insulation.

7. Expansion/contraction test

a. Apparatus: Same as used in the joint leakage test.

b. Procedure: The expansion/contraction test is performed simultaneously with the joint leakage tests. Each joint is misaligned with its mate by 1.5°, with at least two misalignments in the horizontal plane. As with the other tests, water up to 450°F is circulated in the system for 24 h, at which time the heaters are turned off for 24 h. This cycling is continued for 14 days. With anchors at the ends and at the elbow, the carrier pipe will expand and contract at the joints. There is sufficient space between each carrier pipe and on the machined surface of the ends to allow an uneven distribution of the expansion/contraction. A schematic of the test setup is shown in Fig. 6.53.

c. Results: With the expansion/contraction caused by the cycling above, the system shall have performed satisfactorily without any damage to the joint or leakage into the insulation.

Test procedures for condensate return piping

1. *Purpose:* To demonstrate that the condensate return piping meets the criteria specified by the Federal Agency Pre-Qualification Procedures for Underground Heat Distribution Systems. The carrier pipe shall meet MIL-P-28584 with one exception: The joint to be supplied and tested in this protocol is a rubber ring joint not covered by MIL-P-28584. For that reason only, the following tests shall be performed.
2. Joint leakage test and expansion/contraction test
   a. Apparatus: Same as used for joint leakage tests for the high-temperature pipe.
   b. Procedure: A 3-in system consisting of 40 ft of insulated test pipe and a 90° ell installed in the tank in gravel soil. Each joint is misaligned with its mate by 1.5°, with at least two misalignments in the horizontal plane. The installation shall be made in strict accord with installation guidelines, except for misalignments.

      Water shall be alternately passed through the carrier condensate pipe at a temperature of 65°F (±5°) for a minimum of 2 min and 300°F (±5°) for a minimum of 3 min. Time intervals at each temperature level shall begin when the temperature of the water reaches the required range. The test shall continue until a minimum of 100 cycles shall be completed.

   c. Results: No joints shall have allowed any of the circulating water to have leaked into the surrounding insulation or soil.
3. Resistance of groundwater infiltration
   a. Apparatus: The same apparatus as used for the groundwater infiltration and water damage tests for high-temperature pipe.
   b. Procedure: A 3-in system consisting of 40 ft of test pipe with at least two 20-ft sections, a 90° ell, and one anchor at the ell installed in the tank in a gravel soil. Each joint is misaligned with its mate by 1½° with at least two of the misalignments in the horizontal plane. The installation shall be made in strict accord with installation guidelines, except for the misalignments.

      The pipe system shall have a 5 percent slope with the lower exit being the low point of the system. After the installation is completed, the tank cover is bolted in place. A water source is attached to the drain/fill, and a 5-gal surge tank is attached to the vent with a tee fitting. The surge tank shall have a water sight glass and a 0 to 15 lb/in^{2}gage static pressure gage. The other tee line shall contain a shutoff valve on the side open to the atmosphere. With the vent shutoff valve open, water is admitted into the tank through the drain/fill until the tank is full and water spills from the open vent. The vent valve is then closed, and filling continues until the pressure reaches 9 lb/in^{2}gage (the surge tank should be about two-thirds full as observed in the sight glass). Tank pressure shall be maintained for 48 h and water up to 300°F shall be circulated through the carrier pipe for 24 h and drained. The hot water system shall be disconnected, and pipe ends shall remain open for the remaining 24 h. The lower end of the carrier pipe shall be monitored for water leakage during the next 24 h. At the end of the 48 h, the pressure is relieved by opening the vent valve, and the water is drained from the tank through the vent drain/fill fitting.

c. Results: At no time shall water leaks be allowed at the end seals or shall water be observed coming from the low end of the open carrier pipe.

References

1. American Association of Civil Engineers and Water Pollution Control Federation. 1982. Gravity Sanitary Sewer: Design and Construction.
2. American Iron and Steel Institute. 1971. *Handbook of Steel Drainage and Highway Construction Products.* New York: Donnelley.
3. Armco Drainage and Metal Products, Inc. 1955. *Handbook of Drainage and Construction Products.* Middletown, Ohio.
4. American Water Works Association. AWWA Standards M11, M9, M23, C150, C200, C206, C300, C301, C303, C400, C401, C402, C403, C900, C901, C905, and C950. Denver.
5. Bishop, R. R. 1983. *Course Notebook.* Logan: Utah State University.
6. Boscardin, M. D., E. T. Selig, R. S. Lin, and G. R. Yang. January 1990. Hyperbolic Parameters for Compacted Soils. *ASCE Journal of Geotechnical Engineering* 116(1).
7. Burns, J. Q., and R. M. Richard. 1964. Attenuation of Stresses for Buried Cylinders. In *Proceeding of the Symposium on Soil Structure Interaction,* pp. 378–392. Tucson: University of Arizona.
8. Concrete Pipe Division of U.S. Pipe and Foundary Company. *Bulletin No. 200.* Birmingham, Ala.
9. Devine, Miles. 1980. *Course Notebook.* Logan: Utah State University.
10. Ductile Iron Pipe Research Association. 1984. *Thrust Restraint Design for Ductile Iron Pipe.* Birmingham, Ala.
11. Duncan, J. M., P. Byrne, K. S. Wong, and P. Mabry. 1980. *Strength, Stress-Strain and Bulk Modulus Parameters for Finite Element Analyses of Stresses and Movements in Soil Masses*. Department of Civil Engineering Report UCB/GT/80-0. University of California, Berkeley.
12. Dunn, I. S., L. R. Anderson, and F. W. Kiefer. 1980. *Fundamentals of Geotechnical Analysis.* New York: Wiley.
13. Federal Aviation Authority (FAA). Aircraft Pavement Design and Evaluation. AC 150/5320-6C.
14. Federal Aviation Authority (FAA). Aircraft Data. AC 150/5325-5C.
15. Howard, Amster K. 1977. Modulus of Soil Reaction (E') Values for Buried Flexible Pipe. *Journal of the Geotechnical Engineering Division, ASCE* 103(GT). Proceedings Paper 127000.
16. Janbu, N. 1963. Soil Compressibility as Determined by Odometer and Triaxial Tests. In *Proceedings of European Conference on Soil Mechanics and Foundation Engineering,* pp. 19–25. Wissbaden, Germany: Soil Mechanics Foundation.
17. Katona, M. G., J. B. Forrest, F. J. Odello, and J. R. Allgood. 1976. CANDE—A Modern Approach for the Structural Design and Analysis of Buried Culverts. Report FHWA-RD-77-5. U.S. Department of Transportation.

18. Katona, M. G., P. D. Vittes, C. H. Lee, and H. T. Ho. 1981. CANDE-1980: Box Culverts and Soil Models. Springfield, Va.: National Technical Information Service.
19. Konder, R. L., and J. S. Zelasko. 1963. A Hyperbolic Stress-Strain Formulation of Sands. In *Proceedings of the Second Pan American Conference on Soil Mechanics and Foundation Engineering.* 1:209.
20. Krizek, R. J., R. A. Parmelee, N. J. Kay, and H. A. Elnaggar. 1971. Structural Analysis and Design of Buried Culverts. National Cooperative Highway Research Program Report 116. Washington: National Research Council.
21. Kulhawy, F. H., J. M. Duncan, and H. B. Seed. 1969. Finite Element Analysis of Stresses and Movements in Embankments during Construction. Report TE-69-4. Berkeley: Office of Research Services, University of California.
22. Marston, A. 1930. The Theory of External Loads on Closed Conduits in the Light of the Latest Experiments. *Bulletin 96.* Ames: Iowa Engineering Experiment Station.
23. Moser, A. P. 1990. *Buried Pipe Design,* 1st ed. New York: McGraw-Hill.
24. Moser, A. P. 1983. *Course Notebook.* Logan: Utah State University.
25. Nyby, D. W. 1981. Finite Element Analysis of Soil Sheet Pipe Interaction. Ph.D. dissertation. Logan: Department of Civil and Environmental Engineering, Utah State University.
26. Ozawa, Y., and J. M. Duncan. 1973. ISBILD: A Computer Program for Analysis of Static Stresses and Movements in Embankments. Report No. TE-73-4. Berkeley: Office of Research Services, University of California.
27. Paris, J. M. November 10, 1921. Stress Coefficients for Large Horizontal Pipes. *Engineering News Record* 87(19).
28. Piping Systems Institute. 1980. *Course Notebook.* Logan: Utah State University.
29. Spangler, M. G. 1950. Field Measurements of the Settlement Ratios of Various Highway Culverts. *Bulletin 170.* Ames: Iowa State College.
30. Spangler, M. G. 1933. The Supporting Strength of Rigid Pipe Culverts. *Bulletin 112.* Ames: Iowa State College.
31. Spangler, M. G., and R. L. Handy. 1982. *Soil Engineering,* 4th ed. New York: Harper & Row.
32. Spangler, M. G., and W. J. Schlick. 1953. Negative Projecting Conduits. *Report 14.* Ames: Iowa State College.
33. Steel Plate Fabricators Association, Inc. 1970. *Welded Steel Water Pipe Manual*. Des Plaines, Ill. p. 24.
34. The Asphalt Institute. March 1978. *Soils Manual for the Design of Asphalt Pavement Structures.* Manual Series No. 10 (MS-10). College Park, Md.
35. Timoshenko, S. P. 1961. *Theory of Elastic Stability,* 2d ed. New York: McGraw-Hill.
36. Timoshenko, S. 1956. *Strength of Materials,* Part 11, 3d ed. New York: D. Van Nostrand.
37. Watkins, R. K., and M. G. Spangler. 1958. Some Characteristics of the Modulus of Passive Resistance of Soil: A Study in Similitude. In *Highway Research Board Proceedings* 37:576-583.
38. Wong, K. S., and J. M. Duncan. 1974. Hyperbolic Stress-Strain Parameters for Nonlinear Finite Element Analysis of Stresses and Movements in Soil Masses. Report TE-74-3. Berkeley: Office of Research Services, University of California.
39. Zienkiewitcz, O. C. 1977. *The Finite Element Method,* 3d ed. New York: McGraw-Hill.

Chapter

7

Plastic Flexible Pipe Products

Thermoplastic Pipe Materials

There are several types of thermoplastics that are used in the manufacture of pipe. A brief discussion of thermoplastics and design bases is contained in Chap. 4. There are four principal thermoplastics used to make pipe: polyvinyl chloride (PVC), acrylonitrile-butadiene-styrene (ABS), polyethylene (PE), and polybutylene (PB). Pipes made from other thermoplastics command an extremely small market and are primarily used for specialty applications, such as styrene rubber (SR) and cellulose-acetate-butyrate (CAB).

Polyvinyl chloride

PVC pipe is available for both pressure and gravity applications (Fig. 7.1). For gravity sewer applications, it is available in both solid-wall and profile-wall varieties. Size ranges are as follows:

PVC pressure pipe: $^1/_2$ to 36 in

PVC solid-wall gravity pipe: 2 to 27 in

PVC profile-wall sewer pipe: 4 to 48 in

The above listed sizes are generally available. However, sizes outside the listed ranges may be available on special order from the manufacturer.

Figure 7.1 PVC's high strength-to-weight ratio is a real advantage. (*Reprinted by courtesy of Uni-Bell PVC Pipe Association.*)

Polyvinyl chloride is manufactured from ethylene and chlorine. Ethylene is extracted from natural gas or crude oil, usually from natural gas. It is also possible to use coal; however, that process is much more expensive. Chlorine is manufactured via electrolysis from saltwater. Vinyl chloride monomer is produced by oxychlorination (a reaction of ethylene with chlorine). The vinyl chloride monomer (VCM) is polymerized to make polyvinyl chloride resin. PVC resin is a white, powdery substance having the consistency of table sugar.

This PVC resin is the basic "building block" for PVC pipe. To optimize processibility and performance properties, the pipe manufacturer takes PVC resin and compounds it with lubricants, stabilizers, fillers, and pigments. After the mixing takes place at an elevated temperature, the mixture is allowed to cool to ambient temperature. This PVC compound is fed to a PVC pipe extruder (Fig. 7.2). The extruders are usually of multiscrew design. The PVC compound is worked under

Figure 7.2 PVC pipe extrusion plant. (*Reprinted by courtesy of Uni-Bell PVC Pipe Association.*)

high pressure (via extruder screws) and at a controlled elevated temperature so that it is converted to a viscous plastic. A die at the end of the extruder barrel forms the hot viscous plastic into a cylindrical shape. Outside-diameter tolerances are maintained by forcing the hot material through a sizing sleeve. After passing through the extruder head and sizing sleeve, the hot pipe is cooled from approximately 400°F as it passes through a spray tank and water bath. The wall thickness and internal diameter dimensions are controlled by balancing the pipe puller speed with the extruder speed. The process is continuous. A cutoff saw which moves with the extruded pipe cuts the pipe in appropriate lengths. The pipe ends are chamfered, and the pipe proceeds to a rack where it is positioned for belling (Fig. 7.3).

As explained in Chap. 4, thermoplastics can be heated and reshaped. The pipe belling operation takes advantage of this important property. One end of the pipe is heated and placed in a belling machine where the bell is formed along with a groove for a rubber ring, if required. The bell end is then cooled and will maintain its new shape.

The resulting PVC pipe is extremely durable. It is completely inert to water and to chemicals commonly encountered in sewage and soil environments. The surfaces of the pipe are very smooth and resist any buildup of deposited minerals and other solids. It is totally corrosion-resistant. It is not attacked by hydrogen sulfide or the resulting sulfu-

Figure 7.3 PVC pipe belling operation. (*Reprinted by courtesy of Uni-Bell PVC Pipe Association.*)

ric acid. PVC pipe is not subject to biological degradation. Abrasive resistance is excellent, and no special care for cleaning is needed compared to other pipe products. Dimensional control is excellent, and the resulting joints are extremely tight. The use of PVC sewer pipe has all but eliminated infiltration and exfiltration and the accompanying tree-root problems.

PVC pipe was first produced and installed on a very limited basis in Germany in the mid-1930s. PVC pipe began to have wide acceptance in the 1960s. Today it commands a large share of the world market, including the market in the United States. It is by far the most widely used plastic pipe. About 90 percent of all plastic pressure-water pipe is PVC, and almost 100 percent of plastic sewer pipe is PVC. (Both of these percentages are based on weights shipped.) See Tables 7.1 and 7.2.

PVC gravity sewer pipe. PVC sewer pipe is a flexible pipe, and design methods presented in Chap. 3 for flexible pipe are appropriate. Specifically, Table 3.9 was developed for any PVC pipe with a pipe stiffness $F/\Delta y = 46$ lb/in^2 and diameter of 4 through 18 in.

$$\text{Pipe stiffness PS} = \frac{F}{\Delta y} = \frac{6.7EI}{r^3} = 0.559\,E\,\frac{t^3}{r^3}$$

TABLE 7.1 Typical PVC Pipe Design Properties

Hydrostatic design basis (HDB)	4000 lb/in^2
Hydrostatic design stress (HDS)	1600 to 2000 lb/in^2
Elastic modulus (pressure formulation)	400,000 lb/in^2
Elastic modulus (sewer formulation)	400,000 to 550,000 lb/in^2
Tensile stress	7000 lb/in^2
Hazen-Williams coefficient C	150
Manning's coefficient n	0.009

TABLE 7.2 Standards for PVC Pipe

AWWA C605	Standard for Underground Installation of Polyvinyl Chloride (PVC) Pressure Pipe and Fittings for Water
AWWA C900	Polyvinyl Chloride (PVC) Pressure Pipe, 4 in through 12 in for Water
AWWA C905	Polyvinyl Chloride (PVC) Water Transmission Pipe (Nominal Diameters 14 to 36 in)
AWWA C950	Polyvinyl Chloride (PVC) Water Transmission Pipe, 14 in through 36 in
ASTM D 2672	Bell-end Poly(vinyl Chloride) (PVC) Pipe
ASTM F 800	Corrugated Poly (vinyl Chloride) Tubing and Compatible Fittings
ASTM D 3915	Poly(vinyl Chloride) (PVC) and Related Plastic Pipe and Fitting Compounds
ASTM F 679	Poly(vinyl Chloride) (PVC) Large-Diameter Plastic Gravity Sewer Pipe and Fittings
ASTM F 789	Standard Specification for Type PS-46 Poly(vinyl Chloride) (PVC) Plastic Gravity-Flow Sewer Pipe and Fittings
ASTM F 794	Poly(vinyl Chloride) (PVC) Large Diameter Ribbed Gravity Sewer Pipe and Fittings Based on Controlled Inside Diameter
ASTM D 2665	Poly(vinyl Chloride) (PVC) Plastic Drain, Waste, and Vent Pipe and Fittings
ASTM D 2466	Poly(vinyl Chloride) (PVC) Plastic Pipe Fittings, Schedule 40
ASTM D 1785	Poly(vinyl Chloride) (PVC) Plastic Pipe, Schedules 40, 80, and 120
ASTM D 2241	Poly(vinyl Chloride) (PVC) Plastic Pipe (SDR-PR)
ASTM D 2740	Poly(vinyl Chloride) (PVC) Plastic Tubing
ASTM D 2729	Poly(vinyl Chloride) (PVC) Sewer Pipe and Fittings
ASTM F 599	Poly(vinylidene Chloride) (PVDC) Plastic-Lined Ferrous-Metal Pipe and Fittings
ASTM F 656	Primers for Use in Solvent Cement Joints of Poly(vinyl Chloride) (PVC) Plastic Pipe and Fittings
ASTM F 512	Smooth-Wall Poly(vinyl Chloride) (PVC) Conduit and Fittings for Underground Installation
ASTM D 3036	Socket-Type Poly(vinyl Chloride) (PVC) Plastic Line Couplings
ASTM D 2467	Socket-Type Poly(vinyl Chloride) (PVC) Plastic Pipe Fittings, Schedule 80
ASTM D 3138	Solvent Cements for Transition Joints Between Acrylonitrile-Butadiene-Styrene (ABS) Poly(vinyl Chloride) (PVC) Nonpressure Piping Components
ASTM D 2564	Solvent Cements for Poly(vinyl Chloride) (PVC) Plastic Pipe and Fittings
ASTM F 758	Smooth-Wall Poly(vinyl Chloride) (PVC) Plastic Underdrain Systems for Highway, Airport, and Similar Drainage
ASTM F 409	Thermoplastic Accessible and Replaceable Plastic Tube and Tubular Fittings

TABLE 7.2 Standards for PVC Pipe (*Continued*)

ASTM D 2464	Threaded Poly(vinyl Chloride) (PVC) Plastic Pipe Fittings, Schedule 80
ASTM F 789	Type PS-46 Poly(vinyl Chloride) (PVC) Plastic Gravity-Flow Sewer Pipe and Fittings
ASTM D 3034	Type PSM Poly(vinyl Chloride) (PVC) Sewer Pipe and Fittings
ASTM D 2855	Making Solvent Cemented Joints with Poly(Vinyl Chloride) (PVC) Pipe and Fittings
Canadian Standards Association	
CSA B137.0	Definitions, General Requirements, and Methods of Testing for Thermoplastic Pressure Piping
CSA B137.3	Rigid Poly(vinyl Chloride) (PVC) Pipe for Pressure Applications
CSA B181.2	PVC Drain Waste and Vent Pipe and Pipe Fittings
CSA B181.12	Recommended Practice for the Installation of PVC Drain Waste and Vent Pipe and Pipe Fittings
CSA B182.1	Plastic Drain and Sewer Pipe and Pipe Fittings
CSA B182.2	Large-Diameter, Type PSM PVC Sewer Pipe and Fittings
CSA B182.3	Large-Diameter, Type IPS PVC Sewer Pipe and Fittings
CSA B182.4	Large-Diameter, Ribbed PVC Sewer Pipe and Fittings

where

$$r = \text{mean radius} = r_o - \frac{t}{2} = \frac{D_o}{2} - \frac{t}{2} = \frac{D_o - t}{2}$$

Thus

$$\text{PS} = \frac{F}{\Delta y} = \frac{4.47E}{(\text{DR} - 1)^3}$$

where DR = dimension ratio = D_o/t.

For PVC pipes (solid-wall or profile-wall) with diameters larger than 18 in, the manufacturer's recommendations should be obtained and followed. Alternately, Table 3.9 may be used.

Most solid-wall PVC sewer pipes have DR = 35 and a minimum pipe stiffness of 46 lb/in^2. PVC gravity sewer pipe with pipe stiffnesses in the range of 10 lb/in^2 has been tested and performed adequately when properly installed with a soil density in the pipe zone of at least 85 percent of standard Proctor density. For any pipe with very low pipe stiffness, extreme care must be taken in preparing and compacting the soil envelope around the pipe. Pipes with less than 10 lb/in^2 pipe stiffness should be used only if a qualified soils engineer is responsible for the direction and surveillance of the installation.

Example 7.1—A 12-in gravity sewer pipe A 12-in-diameter gravity sewer pipe is to be installed in a very deep cut (30 ft). The soil is clay and has been determined to be corrosive, and the sewage is septic. Select an appropriate piping material, and design the pipe soil embedment system. The trench width at the top of the pipe may be as much as 4 ft.

1. Calculate the soil load (see Chap. 2). The rigid pipe load is

$$W_d = C_d \gamma B_d^2 = 3.3\,(120)\,(4)^2$$

$$= 6336 \text{ lb/ft} \qquad \text{(see Fig. 2.2 for } C_d\text{)}$$

The flexible pipe load is

$$\text{Prism load} = \gamma H = 120\,(30) = 3600 \text{ lb/ft}^2$$

or

$$W = \frac{\gamma H}{B_c} = \frac{\gamma H}{D} = \frac{3600}{1} = 3600 \text{ lb/ft}$$

2. Select the piping material. A check will reveal that extra-strength clay is not strong enough to withstand the 6336 lb/ft soil load. Also, the highest-strength concrete pipe (class 3) is not strong enough. These corrosive conditions would have eliminated concrete and will usually eliminate iron or steel pipe. Use SDR 35 ASTM D 3034 PVC pipe.

3. Design the pipe soil embedment system. For SDR 35 PVC, Table 3.9 may be used for design. The pipe should be installed in a manner such that resulting deflection is less than 7.5 percent. Table 3.9 indicates that class I, class II, or class III soil may be used if compaction is at least 85 percent (see Chap. 3 for definitions of soil classes). Specify class II soil to be used for bedding, haunching, and initial backfill (Fig. 7.4). Pipe zone soil, to the level of the top of the pipe, must be compacted to at least 85 percent of standard Proctor density. It is evident from Table 3.9 that the 7.5 percent design deflection will be exceeded if only 80 percent of standard Proctor density is achieved. Also note that class I soil could have been used without compaction since its natural placement density will be sufficient.

4. The alternate design approach (Spangler's formula), Eq. (3.5), is

$$\Delta x = \frac{D_L K W_c r^3}{EI + 0.061E'r^3} \tag{3.5}$$

$$\Delta x = \Delta y$$

Assume that

$$K = 0.1 \qquad \text{(see Chap. 3 for bedding factors)}$$

$$\frac{W_c}{D} = \gamma H = \text{prism load}$$

$$D_L = 1.0 \qquad \text{when prism load is used}$$

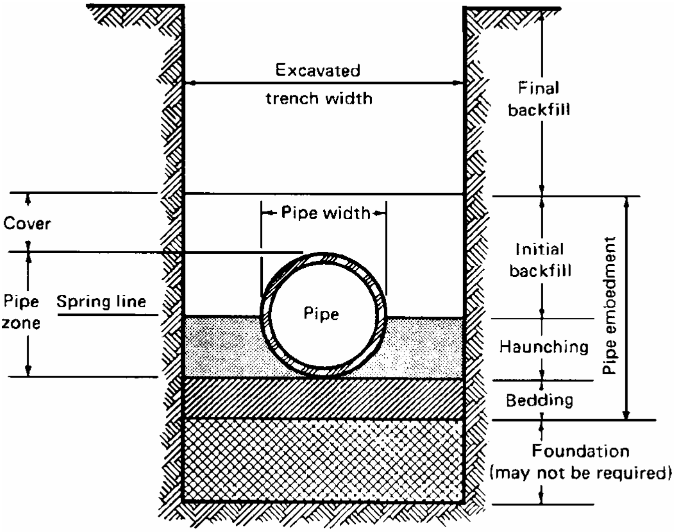

Figure 7.4 Trench cross-section showing terminology. (*Reprinted by courtesy of Uni-Bell PVC Pipe Association.*)

Therefore,

$$\Delta y = \frac{0.1\,(D\gamma H)\,r^3}{EI + 0.061E'r^3}$$

or

$$\frac{\Delta y}{D} = \frac{0.1\gamma H}{EI/r^3 + 0.061E'} \tag{7.1}$$

$$\text{Pipe stiffness PS} = \frac{F}{\Delta y} = \frac{6.7EI}{r^3}$$

or

$$\frac{EI}{r^3} = \frac{\text{PS}}{6.7}$$

Equation (7.1) becomes

$$\frac{\Delta y}{D} = \frac{0.1\gamma H}{\text{PS}/6.7 + 0.061E'}$$

or

$$\frac{\Delta y}{D} = \frac{0.67\gamma H}{\text{PS} + 0.41E'} \tag{7.2}$$

Usually PS and E' are expressed in units of pounds per square inch. If γ is in pounds per cubic foot and H is in feet, γH is in pounds per square foot. This must be divided by 144 to convert to pounds per square inch. Assuming $\gamma = 120$ lb/ft³, Eq. (7.2) becomes

$$\frac{\Delta y}{D} = \frac{0.67\,(120H/144)}{\mathrm{PS} + 0.41E'}$$

$$\frac{\Delta y}{D} = \frac{0.56H}{\mathrm{PS} + 0.41E'} \tag{7.3}$$

In the above equation, H is feet of cover. The pipe stiffness PS and soil modulus E' are to be expressed in pounds per square inch. This equation can be solved for E' as follows:

$$E' = \frac{0.56H/(\Delta y/D) - \mathrm{PS}}{0.41} = \frac{1.37H}{\Delta y/D} - \frac{\mathrm{PS}}{0.41} \tag{7.4}$$

For this example,

$$H = 30 \text{ ft}$$

$$\frac{\Delta y}{D} = 0.075 \text{ (or 7.5 percent)}$$

$$\mathrm{PS} = 46 \text{ lb/in}^2$$

Thus,

$$\text{Required } E' = \frac{1.37\,(30)}{0.075} - \frac{46}{0.41} = 434 \text{ lb/in}^2$$

Data in Table 3.9 indicate a soil density of 85 percent is required for finer-grain soils with little or no plasticity. Coarse-grain soils may be used with little compactive effort required. The two design approaches produce results which agree fairly well. Obviously the use of empirical data from Table 3.9 is the easier method.

Example 7.2—A 10-in gravity sewer pipe A 10-in gravity sewer pipe is to be installed 16 ft deep. The native soil is silty clay, and the water table is 10 ft below the surface. Select a PVC pipe, and specify the proper installation design if the long-term deflection is not to exceed 7.5 percent.

solution Select an ASTM D 3034, SDR 35, 10-in sewer pipe. This choice allows the use of Table 3.5 in determining the required embedment soil and soil density. Because of the water table, the trench condition will be wet, and the required densities in the pipe zone may not be achievable with native soil. Required compaction must be achieved before high soil loads are imposed and the well points removed. Otherwise, the soil will densify with the rising water, which may cause excess deflection. However, sufficient backfill must be placed over the pipe (about 3 ft) to prevent flotation of the pipe.

Design I. Use a select clean sand or gravel backfill material (class II; Table 3.9) for bedding, haunching, and initial backfill compacted to 85 percent standard Proctor density. From Table 3.9, long-term deflection will be about 3 percent (see Chap. 3 for additional discussion on the use of Table 3.9).

Design II. Use a select silty-sandy gravel backfill material (class III; Table 3.9) for bedding, haunching, and initial backfill compacted to 85 percent standard Proctor density. From Table 3.9, long-term deflection will be 3.5 percent.

Note: These deflections are substantially lower than the allowed 7.5 percent long-term deflection. However, because of the wet condition and the relatively deep cover soil, density in the pipe zone must not be less than the density at the critical void ratio. This density is often around 90 percent of Proctor density. For added safety, 90 percent density is recommended. Also design I is preferred to design II because in wet trench conditions, the compaction of class III backfill is more difficult.

Example 7.3—A 27-in gravity sewer pipe A 27-in SDR = 35, PS = 46, PVC sewer pipe is to be installed 15 ft deep. The soil is clay, except in most areas there is some basalt rock which must be blasted. What type of soil embedment system will be required for this installation?

1. Pipe must not be laid directly on hardpan, bedrock, or any sharp stones with dimensions larger than $1^1/_2$ in and preferably no stones larger than $^3/_4$ in.
2. Excavate at least 6 in below grade, and prepare a firm uniform bedding of crushed, well-graded stone.
3. Select haunching and initial backfill material: Consider class I, class II, class III, or class IV materials as listed in Table 3.9. A Proctor density of 80 percent is sufficient for either class II or class III soils. Class IV soils are often overlooked as pipe embedment materials, but could be used if the trench is not wet and the soil is compacted to 85 percent Proctor density. Of course, class I soil will also meet design requirements ($\Delta y/D \leq 7.5$ percent).
4. Spangler's method could also be used, but it is not required.
5. Pipe should not be placed directly on sharp rock outcroppings. Also, large sharp blasted basalt rock should not be placed directly against the pipe. (A select imported material is recommended.)

Example 7.4—A 48-in ribbed PVC pipe A 48-in ribbed PVC pipe is to be installed 20 ft deep. The native soil is fine sand with traces of silt and clay. The pipe stiffness of the ribbed pipe is 10 lb/in^2. For a special design the owner has requested that this pipe be installed such that the maximum vertical deflection does not exceed 3 percent. Also, to keep costs down, he would like to use the native material for bedding, haunching, and initial backfill. Are these design requirements possible?

solution Use Spangler's formula. From Eq. (7.4)

$$\text{Required } E' = \frac{0.56H/(\Delta y/D) - \text{PS}}{0.41} = \frac{1.37H}{\Delta y/D} - \frac{\text{PS}}{0.41}$$

where $H = 20$ ft

$$\frac{\Delta y}{D} = 0.03$$

$$\text{PS} = 10 \text{ lb/in}^2$$

So

$$\text{Required } E' = 886$$

From Table 3.9, the required density is 95 percent. This is possible to achieve, but will be difficult to obtain. The owner should be asked to either relax his 3 percent deflection limit or allow a coarser material to be used in the pipe zone. Costs associated with compaction may exceed the cost of a select material. For a 5 percent deflection limit,

$$E' = \frac{0.56\ (20)/0.05 - 10}{0.41} = 522 \text{ lb/in}^2$$

For a 7.5 percent deflection limit,

$$E' = \frac{0.56\ (20)/0.075 - 10}{0.41} = 340 \text{ lb/in}^2$$

The latter can easily be achieved with the native sand used in the pipe zone.

Long-term stress relaxation and strain limit testing of PVC pipes

In the early 1970s, a concern was voiced for an appropriate material property design limit for PVC pipe used in gravity applications. One proposal was to impose a strain limit, derived from constant stress testing, on buried gravity flow pipes subjected to constant strain. To shed light on this subject, laboratory tests of pipe ring samples exposed to various constant strains and temperatures have been underway since January 1977 on filled and unfilled PVC compound formulations. Samples of PVC pipe were placed on long-term test under various levels of constant strain. The objectives of the tests were to determine stress relaxation characteristics and constant-strain failure data. These test results were used to draw conclusions concerning the applicability of a material strain limit for constant-strain design conditions.

The first issue of ASTM D 3034 contained material requirements for a single PVC cell class of 12454B as described in ASTM D 1784. The second issue published in 1973 contained a 13364B cell class as a second option. This option increased the material's modulus of elasticity from 400,000 to over 500,000 lb/in^2 through the introduction of higher amounts of calcium carbonate. These higher-modulus materials are often called filled compounds. The filled compounds exhibit slightly less tensile strength and tensile elongation, but do not compromise any of the finished product requirements of ASTM D 3040. Sewer pipes of both compounds have found wide use since 1974.

Two fundamental questions which arose in the early 1970s are, What particular PVC compounds are suitable as sewer pipe? and What material property limits should be used for structural design purposes? At least partial answers to these questions have been published in the literature over the years. An initial proposal by Chambers and Heger in 1975 was to limit strain to 50 percent of an assumed ultimate strain of only 1 percent. This suggestion was shown by research to be too conservative and was never followed (see Refs. 25, 35, and 38).

Tests to help fully answer questions concerning strain limits were established in 1975 and 1977 at Utah State University. An early reporting of the results of these tests was published by Moser[39] and Bishop.[11] Another report of the data was published by Moser, Shupe, and Bishop.[43] At this writing the tests are still underway, and data through 1999 are included here.

Stress relaxation tests. Researchers have shown that buried pipe and soil systems stabilize to an equilibrium condition which typifies a fixed deflection or fixed strain condition (see Moser[37]). Therefore, data from constant-deformation tests (fixed strain tests) can be used in predicting the performance of PVC pipe.

Stress relaxation tests were performed on ring sections cut from PVC pipe (see Figs. 7.5 to 7.10). These test specimens were each diametrically deformed to a specified deflection. The load necessary to hold each deformation constant has been measured at various time intervals. Each specimen was maintained at one of three temperatures: ambient (70°F), 40°F, and 0°F. The ambient temperature was held to ±5°F. A refrigerator was used to maintain the 40°F temperature and was found to fluctuate between 38 and 41°F. The 0°F specimens were placed in a freezer, and the temperature varied between −5 and 0°F. The purpose of the lower-temperature test was to slow down the stress relaxation which would amplify any tendency toward brittle

Figure 7.5 Stress relaxation specimens in the refrigerator at 40°F.

fracture. (For dimensions of the test specimen, see Table 7.3.) Two PVC compounds were tested: filled and unfilled. The filled compound contained 30 parts calcium carbonate by weight and is designated as ASTM cell class 12364B, and the unfilled compound is designated as ASTM cell class 12454B.

Some of the pipe ring test specimens were notched prior to deflection to produce stress and strain intensifiers which would amplify any tendency for brittle fracture. The notches were placed along the length in four places corresponding to the locations of the highest tensile stresses—12 and 6 o'clock positions on the inside surface and the 3 and 9 o'clock positions on the outside surface. These longitudinal notches were cut to a depth of 0.012 ± 0.006 in. In all, there are 91 specimens being tested in the study which started January 1977 (see Table 7.4 for details).

Figure 7.6 Stress relaxation specimens (ring and tensile) in the freezer at 0°F.

Figure 7.11 shows one of the stress relaxation curves plotted on linear axes. This figure clearly shows the time interval since 1990. As has been reported previously, stress relaxation curves for PVC pipe compounds follow an inverse exponential function. As such, the curves plot as straight lines on log-log axes.

Figures 7.12 through 7.17 show stress relaxation data that plot as straight lines on log-log axes. As of August 1999, after more than 22 years, none of the test specimens had failed. The data are similar for pipes manufactured from both filled and unfilled PVC compounds when tested at the same temperature. The slopes of the stress relaxation lines show that the relaxation rate is less for lower temperatures in both the filled and unfilled PVC pipe compounds. Thus, lower-temperature testing may be representative of longer-duration constant-strain conditions at higher temperatures. Calcium carbon-

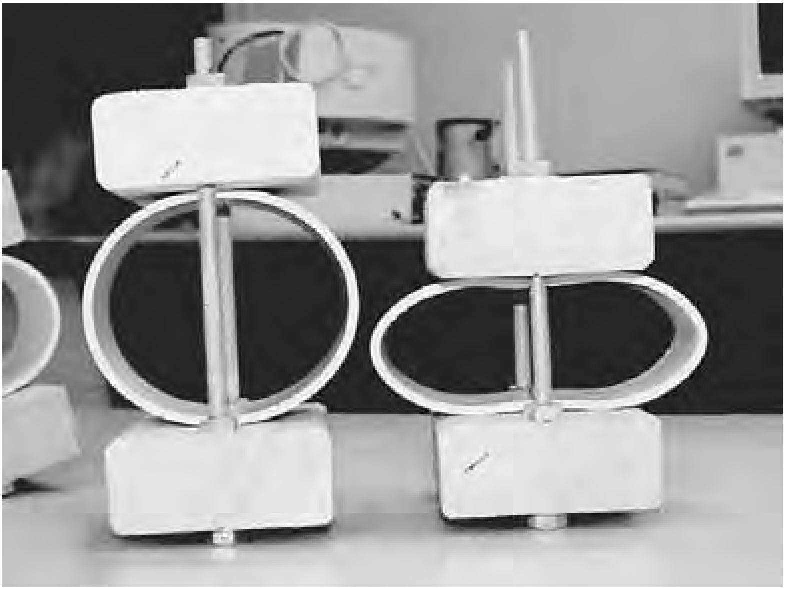

Figure 7.7 Pipe ring specimens held in constant deformation.

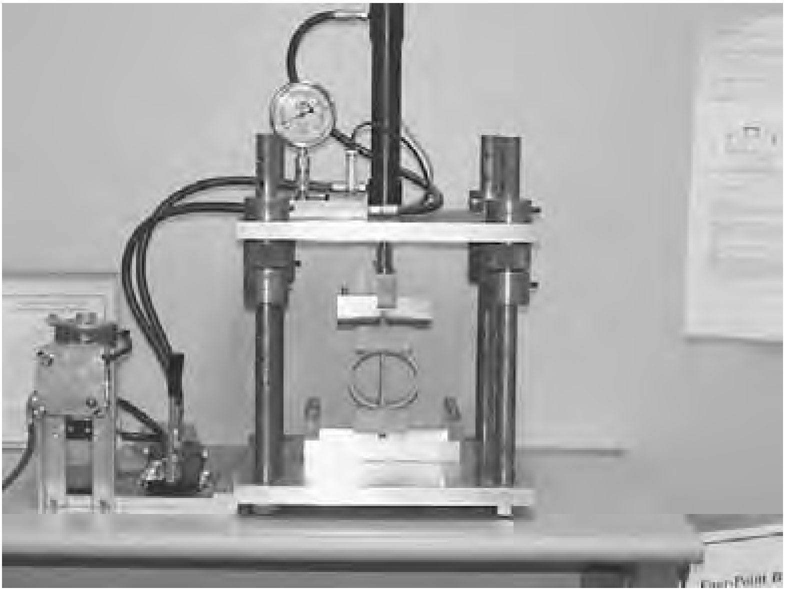

Figure 7.8 Pipe ring undergoing stress relaxation testing.

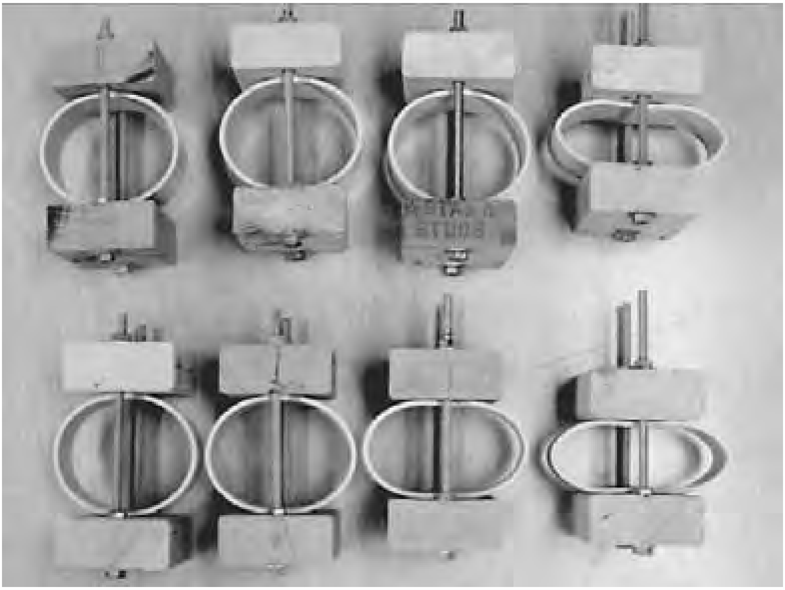

Figure 7.9 Pipe rings at various constant deflections.

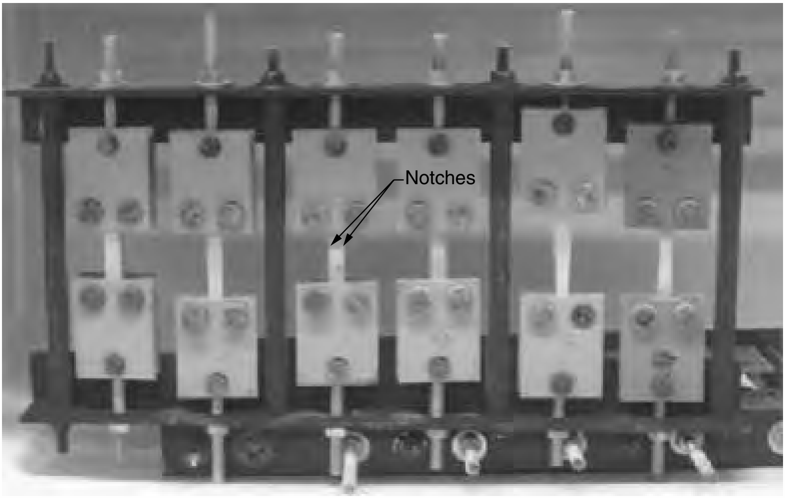

Figure 7.10 Uniaxial tensile stress relaxation specimens.

TABLE 7.3 Pipe Ring Properties Used In Stress Relaxation Tests
(Pipe rings were cut from 4-in-diameter PVC pipe)

Material PVC	Wall thickness, in	Length, in	Average flexure modulus, lb/in^2	Average pipe stiffness, lb/in^2
Filled	0.132 ± 0.05	2.0	540,000	87
Unfilled	0.153 ± 0.04	2.0	470,000	117

TABLE 7.4 Grouping of the 91 Pipe Specimens in the Stress Relaxation Tests

Groups	Sets	Deflections of number of specimens, percent					
		1	2	3	4	5	6
Group 1: Specimens were filled and unnotched	Set 1, ambient	5	10	15	25	50	
	Set 2, 40°F	5	10	15	25	50	
	Set 3, 0°F	5	10	15	25	50	
Group 2: Specimens were filled and unnotched	Set 1, ambient	5	10	15	25	50	
	Set 2, 40°F	5	10	15	25	50	
	Set 3, 0°F	5	10	15	25	50	
Group 3: Specimens were filled and notched	Set 1, ambient	5	10	15	25	40	
	Set 2, 40°F	5	10	15	25	35	
	Set 3, 0°F	5	10	15	25	35	
Group 4: Specimens were filled and notched	Set 1, ambient	5	10	15	25	40	35
	Set 2, 40°F	5	10	15	25	40	
	Set 3, 0°F	5	10	15	25	40	
Group 5: Specimens were unfilled and unnotched	Set 1, ambient	5	10	15	25	50	
	Set 2, 40°F	5	10	15	25	50	
	Set 3, 0°F	5	10	15	25	50	
Group 6: Specimens were unfilled and notched	Set 1, ambient	5	10	15	25	50	
	Set 2, 40°F	5	10	15	25	50	
	Set 3, 0°F	5	10	15	25	50	

ate additions, up to 30 parts by hundredweight evaluated in this study, do not cause brittle failure to occur with time. The difference in the stress relaxation curves for filled and unfilled PVC is that greater force was required to deflect the unfilled specimens. The unfilled PVC specimens had thicker pipe walls which gave them a pipe stiffness higher than those of the filled PVC pipe specimens. Had the same wall thickness been used for both the filled and unfilled specimens, the filled specimens would have been stiffer due to a higher elastic modulus.

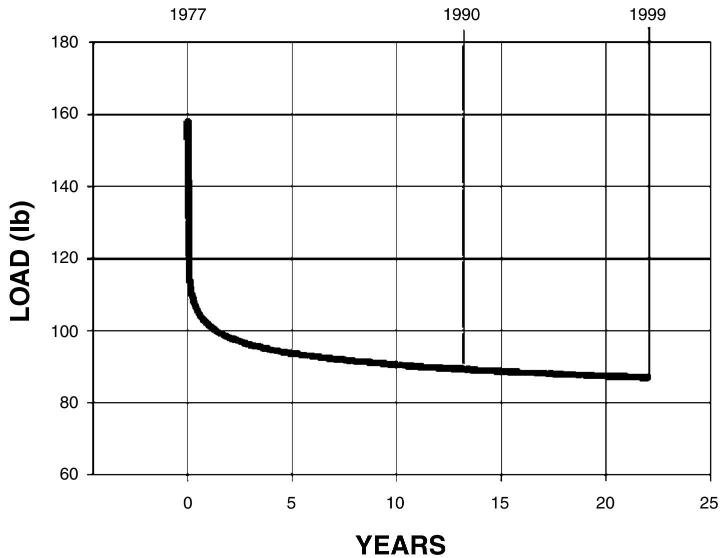

Figure 7.11 Typical stress relaxation curve plotted on linear axes.

In comparing the stress relaxation curves for the notched and unnotched specimens, within the filled and unfilled groups, respectively, no significant difference could be observed. The increased strain at the base of the notches had no apparent effect on the stress relaxation characteristics of either filled or unfilled PVC. Therefore, it was concluded that PVC is not notch-sensitive when it is deformed diametrically in a constant-deflection test.

It is interesting to note that the relaxation that has taken place in the 22-year period is small. The total stress relaxation associated with the 5 percent initial deflection is small for the ambient temperature and is negligible for the 40 and 0°F temperatures. A slightly higher relaxation rate occurs with higher initial deflections. This is evident because the slope of the relaxation line is steeper for specimens which have the greatest imposed deflection or initial load.

Bending strain versus ring deflection. For the convenience of the reader, the following from Chap. 3 is repeated here: Ring deflection produces bending in the pipe wall which in turn leads to bending strains. The bending strains can be calculated by using the following equation. The equation requires ring deflection $\Delta y/D$ and the dimension ratio D/t. The equation is based on the pipe's deforming into an elliptical

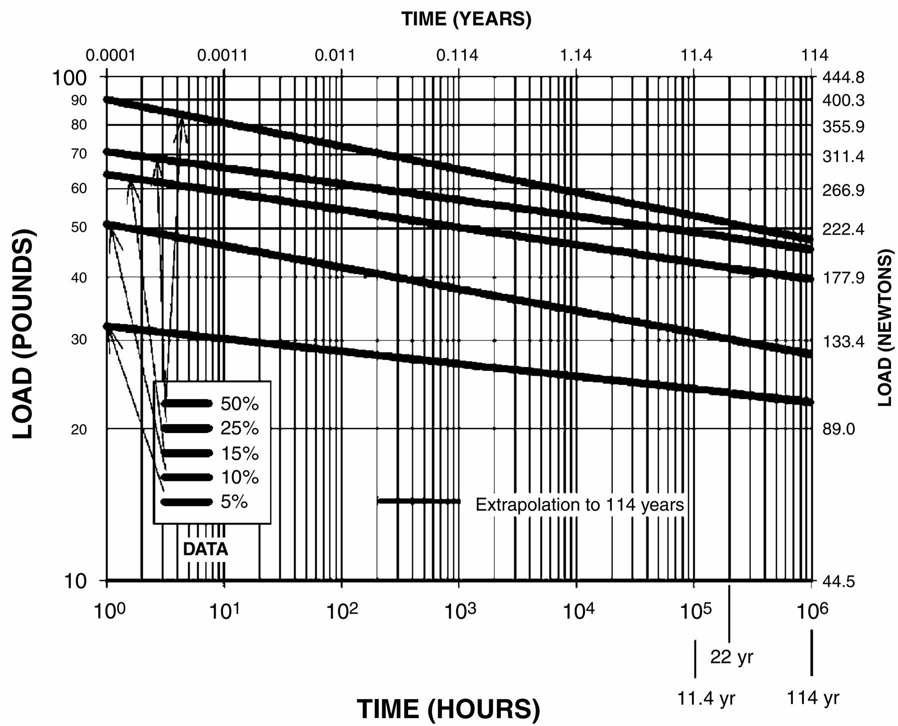

Figure 7.12 Relaxation curves for filled, unnotched PVC pipe rings at specified deflections and a temperature of 40°F.

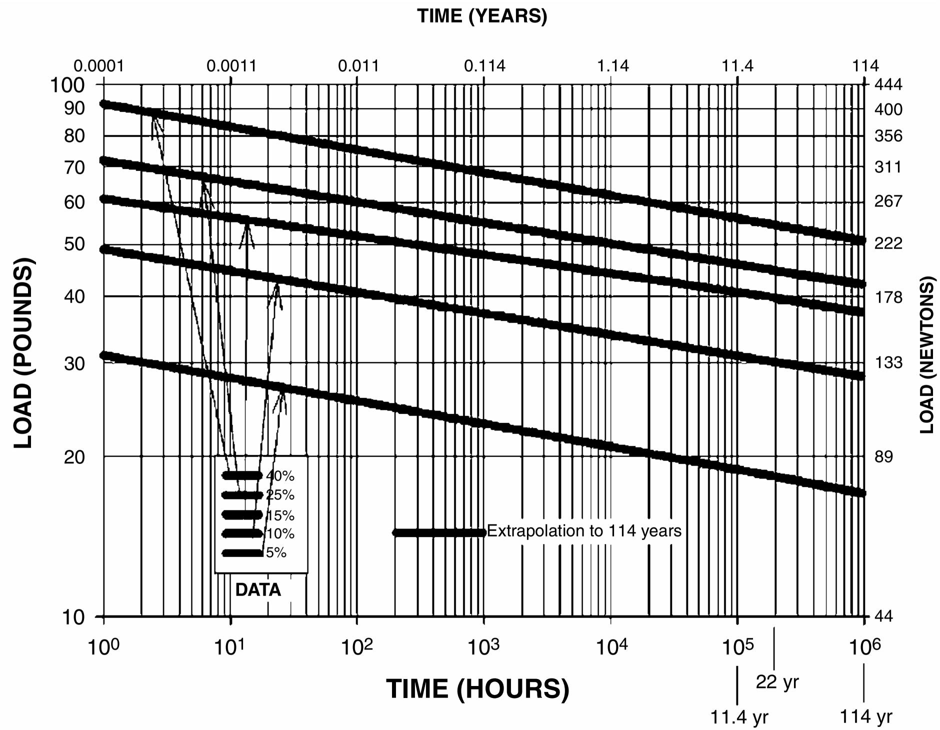

Figure 7.13 Relaxation curves for filled, notched PVC pipe rings at specified deflections and a temperature of 40°F.

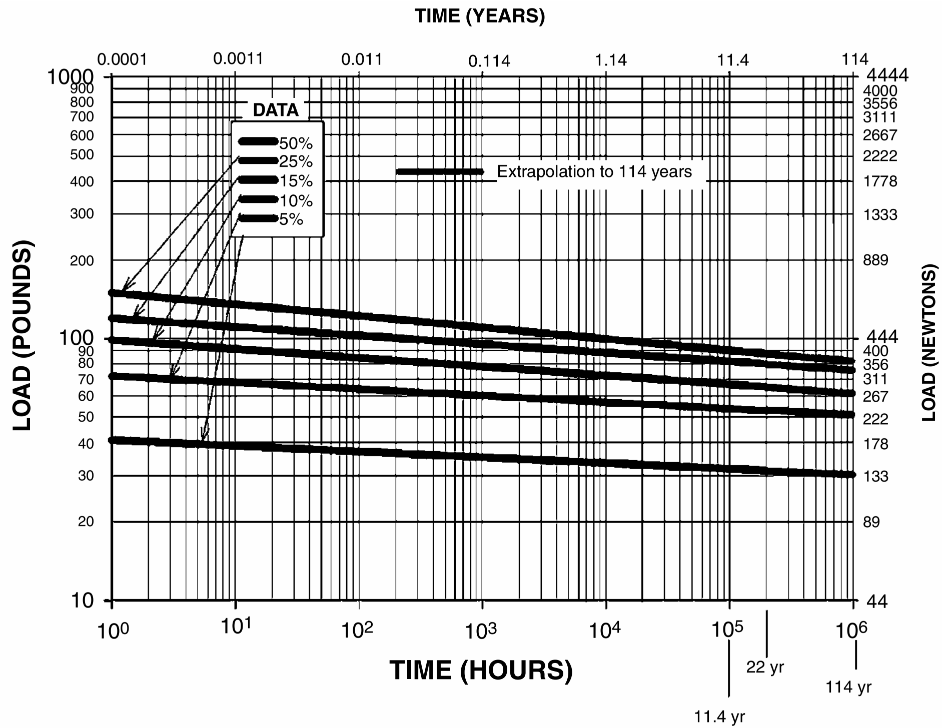

Figure 7.14 Relaxation curves for unfilled, unnotched PVC pipe rings at specified deflections and a temperature of 40°F.

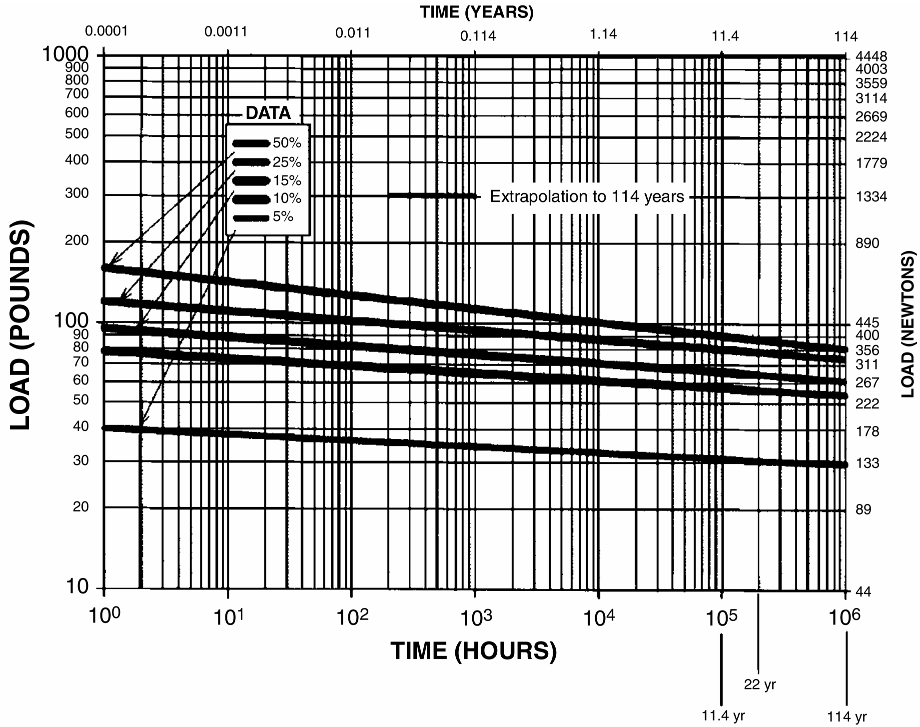

Figure 7.15 Relaxation curves for unfilled, notched PVC pipe rings at specified deflections and a temperature of 40°F.

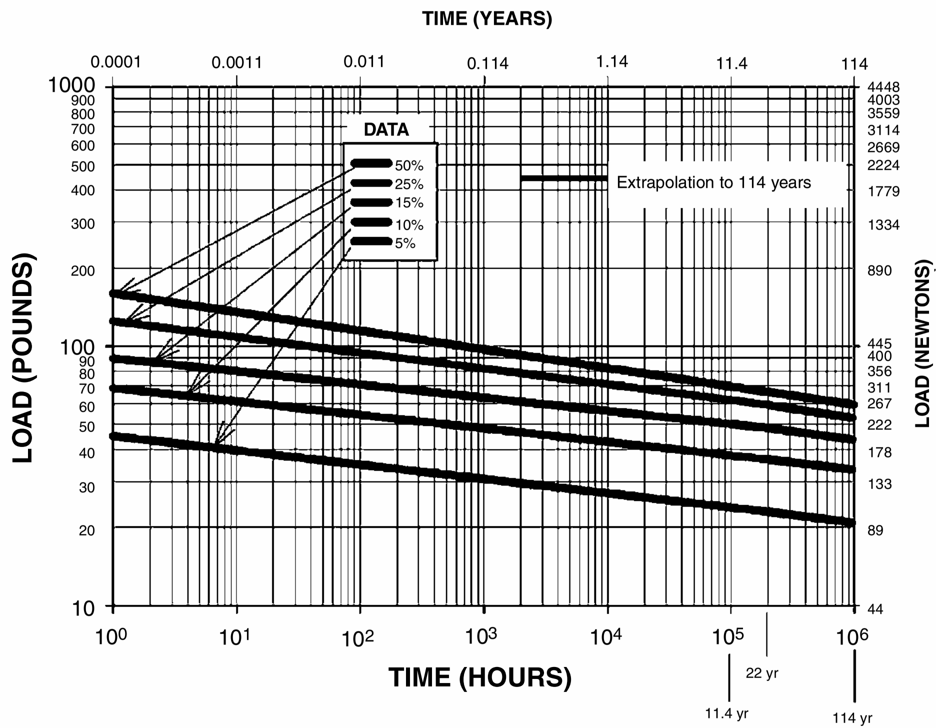

Figure 7.16 Relaxation curves for unfilled, unnotched PVC pipe rings at specified deflections and a temperature of 70°F.

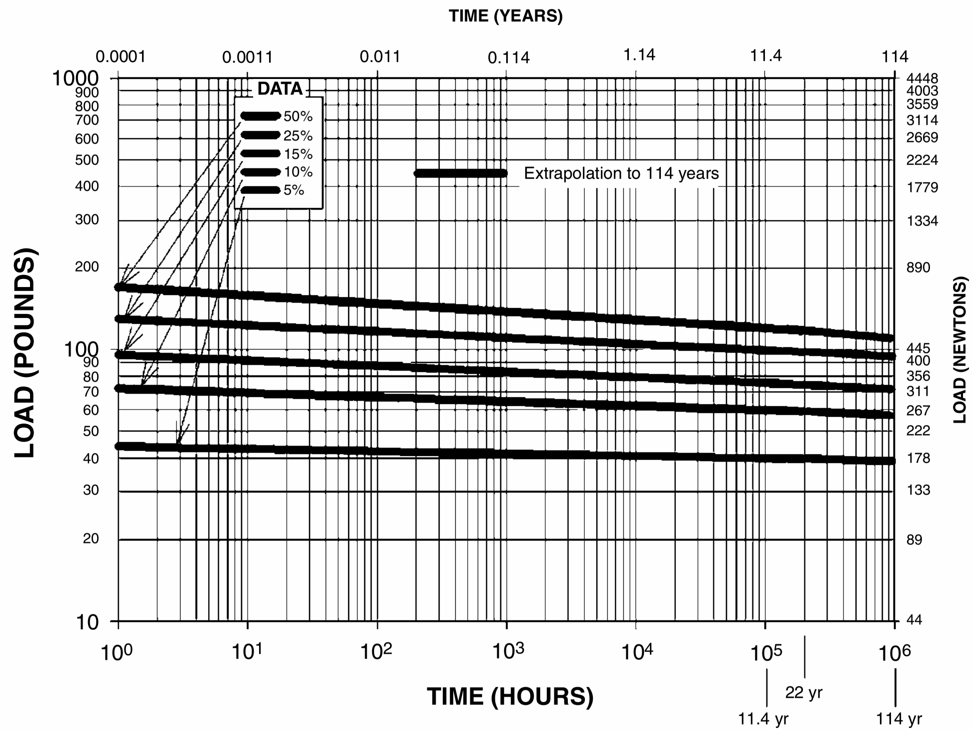

Figure 7.17 Relaxation curves for unfilled, unnotched PVC pipe rings at specified deflections and a temperature of 0°F.

shape. The assumption of an elliptical shape has been shown to be a very close approximation for PVC pipe.

$$\varepsilon = \pm \left(\frac{t}{D}\right)\left(\frac{3\,\dfrac{\Delta y}{D}}{1 - 2\,\dfrac{\Delta y}{D}}\right)$$

where ε = maximum strain in pipe wall due to ring bending (can be assumed to occur at crown or invert of pipe)
t = pipe wall thickness
D = pipe diameter
Δy = vertical decrease in diameter

For example, if $t = 0.132$, $d = 4$, and the ring deflection is 10 percent, the bending strain is calculated as follows:

$$\varepsilon = \pm \frac{0.132}{4}\left(\frac{3\,(0.10)}{1 - 2\,(0.10)}\right) = 0.0124 \quad \text{or} \quad 1.24 \text{ percent strain}$$

The following simplified equation for calculating maximum strain due to ring deflection has been proposed. This equation predicts strains that are too high for low ring deflections. The two equations predict the same bending strain when the deflection $\Delta y/D$ is 0.25, which is a 25 percent deflection.

$$\varepsilon = 6\left(\frac{t}{D}\right)\left(\frac{\Delta y}{D}\right)$$

Stiffness data for the stress relaxation specimens are given in Table 7.5. Stiffness measurements conducted at the end of the 13-year and 22-year test periods are incremental stiffnesses. Each specimen was deflected an additional 5 percent from its preset value. The stiffnesses were then calculated by dividing the incremental load per length by the 5 percent incremental deflection. These long-term values are the instantaneous stiffnesses and are the stiffnesses that resist any additional deflection. These data show that pipe stiffnesses and the modulus for PVC pipe do not decrease with time.

Uniaxial constant-strain tests. The specimens used for these tests were taken from filled and unfilled DR 35 PVC pipe. Strips of PVC were obtained from the pipe in either the horizontal or the circumferential direction. The circumferential strips were straightened in an oven set at 180°F. Dog-bone type of specimens were machined from these strips. Each specimen was pulled to a predetermined strain. Some specimens were notched. The notches (in the two parallel sides of the specimen) were 0.024 ± 0.006 in deep. Notching the samples intensifies the strain.

TABLE 7.5 Pipe Stiffness of Constant-Strain Ring Samples

Sample			Pipe stiffness					
			5 percent			25 percent		
Filled	Notched	Temperature*	Initial†	13 years‡	22 years‡	Initial†	13 years‡	22 years‡
Yes	No	0	71	69	70	39	63	64
Yes	Yes	40	76	74	74	38	65	62
Yes	Yes	0	75	69	70	41	63	63
No	No	40	101	89	90	60	91	90
No	No	0	102	91	92	65	110	109
No	Yes	40	101	96	98	63	87	89

*Constant temperature during 22-year test. Sample conditioned to 73°F for stiffness testing.
†Pipe stiffness determined by secant method after being held at the specified deflection for 1 h.
‡The 13- and 22-year stiffnesses are determined by applying an additional 5 percent deflection increment to the specified deflection.

The intensified strain in combination with the maintained lower temperature accelerates brittle fracture if it is going to occur.

These specimens were strained in a range of 1.0 to 95 percent. The specimens were then placed in the freezer at 0°F (see Fig. 7.10). The samples have now been on test for almost 22 years. No failures have occurred, even in the notched specimens. The tests show that, under a constant-strain condition, if the initial strain can be achieved, failure will not occur (see Table 7.6).

As has been discussed, the initial bending stress in a pipe where the deflection is constant will relax in the course of time. Consequently, a critical stress limit for structural design cannot easily be defined. Instead we have to consider strain as a geometric parameter that is constant with time. The strain can also easily be defined and measured as a constant geometric quantity. Some have asked the question, Is there a critical strain limit which must not be exceeded if long-term failure is to be prevented?

Additional investigations have been undertaken in recent years where PVC pipes have been kept constantly deflected for long periods of time (see Janson). In spite of very high strain values, it has not been possible to simulate any pipe failure. For all the test pipes subjected to stress relaxation, some with extremely large deflections and strains, no failures or cracking has occurred in any PVC samples. This may be regarded as somewhat strange because the initial bending stresses are extremely high in many cases and would have caused immediate pipe failures had the stress been constant and the material free to creep, as is the case for pipes subjected to constant internal hydrostatic pressure.

A hypothesis has been developed that it is just the stress relaxation procedure that contributes to the fact that no failure occurs. Consequently, the hypothesis implies that if no failure occurs immediately, then it will never occur; and this is independent of the magnitude of the bending strain. Obviously, this hypothesis is valid only for well-processed pipes made of high-quality resins. This means, in particular, that pipes and fittings have to be manufactured of high-molecular-weight resins. In the case of PE, the actual MFR values meet the requirements according to current international standards, and for PVC all studies have been performed on resins with K values exceeding 65. However, even for high-quality pipes, the hypothesis is not valid if the pipe material properties change with time from the original values. This may occur when the chemical stabilization system is no longer intact. For PE pipes, the material must not become crystalline with time.

Janson reported on tests by Hoechst on small-diameter HDPE pipes (without carbon black). Hoechst applied a constant tensile stress/strain equally distributed through the pipe wall by expanding the pipe samples using internal steel circular, applying constant ten-

TABLE 7.6 Uniaxial Constant-Strain Failure Data—Unfilled Specimens Taken from the Circumferential Direction of Pipe

Specimen number	Notched	Filled	Cross-sectional area, in^2	Strain level, percent	Starting time (1978)	Failure time	Temperature, °F
3	No	No	0.0531	48	March 26	No failure	0
4	No	No	0.0526	50	March 26	No failure	0
7	Yes	No	0.0530	1.0	March 27	No failure	0
8	Yes	No	0.0525	1.5	March 27	No failure	0
13	No	Yes	0.0560	90	March 30	No failure	0
14	No	Yes	0.0564	95	March 30	No failure	0
17	Yes	Yes	0.0554	1.5	March 30	No failure	0
18	Yes	Yes	0.0561	2.0	March 30	No failure	0

sile strains from 2 to 15 percent. Some samples have now been on test for 40 years in *room temperature* without failure. He reported failures in samples at elevated temperatures (40 to 80°C). This does not contradict the hypothesis discussed above. On the contrary, it supports the requirement that the chemical stabilization system be intact for the hypothesis to be valid. Thus, the reported failures indicated that the chemical aging of the material is dependent on the temperature and also that the degradation rate will increase with increased strain.

Aging. Studies of both PVC and PE pipes that have been installed for 13 years and 8 years, respectively, show that the consequence of the physical aging of the polymer material is that the short-term E modulus does not decline after long-term loading. In both studies, sections of pipe were removed and held in the deflected state, and an incremental load was applied, increasing the deflection. The calculated modulus did not decrease, but, in fact, increased. Since the ring stiffness is a linear function of the E modulus, it also means that after a long loading time, the ring stiffness will retain or improve its short-term value for each future new impulse of loading. This fact is of great importance to an adequate understanding of the deflection process undergone by buried thermoplastic gravity pipes.

Conclusions based on test data

1. Stress relaxation in filled and unfilled PVC can be approximated by a straight line on log-log paper, and the relaxation rate is temperature-dependent. The rate of relaxation decreased with a decrease in temperature.
2. Filled or unfilled PVC does not appear to be notch-sensitive when loaded under constant deformation.
3. Buried PVC pipes maintain the same capacity to resist additional deflection increments as when initially installed; i.e., the modulus does not decrease with time.
4. PVC pipes manufactured from compounds of cell classes 13364B and 12454B do not lose stiffness with time.
5. Apparent or creep modulus is an inappropriate property to predict long-term deflection of buried PVC gravity sewer pipe. Pipes continue to respond to additional deflection increments by resisting movement at the same stiffness as newly made pipe.

Frozen-in stresses

Stresses caused during pipe manufacture occur in all thermoplastic pipes. These stresses have their origin in the cooling phase of the man-

Figure 7.18 Control of frozen-in stresses in PVC pipe samples.

ufacturing process. The cooling of the extruded pipe normally takes place externally in a water bath, inducing stresses in the pipe wall. During cooling, the external surface layer cools first and contracts while the still warm inner surface layer of the pipe compresses plastically. Later, as the inside layer subsequently cools, it attempts to contract as a consequence of the thermal contraction, but is prevented from doing so by the outer cool surface layer which has already become solid and assumed its form. The outcome is tensile stresses on the inside and compressive stress on the outside. The net result is a frozen-in bending stress in the pipe wall. The greater the material thickness and/or the greater the cooling rate, the more severe the bending stresses. If a pipe sample is cut in the axial direction along its entire length, the pipe will open, leaving an angular gap. See Fig. 7.18.

The solution to the problem of an angular gap in a circular ring was given by Timoshenko in his book *Theory of Elasticity.* This can be found on pp. 71 to 80. The assumption he makes is that the ring is circular and subjected to pure bending. If the pipe is circular and if it is uniformly cooled around its circumference during manufacture, these conditions will be met.

The frozen-in stresses can be determined by measuring the angular gap that opens immediately after the longitudinal cut is made. This measured gap is then used in the Timoshenko solution as follows:

$$\sigma = \frac{-\alpha E}{4}\left(\frac{2D_o^{\,2}}{D_o^2 - D_i^2}\ln\frac{D_i}{D_o + 1}\right)$$

where σ = maximum stress
α = angular gap, rad
E = modulus of pipe material
D_o = outside diameter of pipe
D_i = inside diameter of pipe
ln = natural log function

The calculation may require the introduction of the time-dependent value of E. This means that E must be related to the interval of time occurring between cutting and measuring. It is recommended that the measurement be accomplished within 3 min of cutting so that the published short-term modulus can be used.

Because of the Poisson effect, axial frozen-in stresses also exist. These may be observed by sawing out a thin rod in the longitudinal direction of the pipe which then acquires a bend. The frozen-in stress in the axial direction is recognized as an inward bending of the pipe walls at the end of a cutoff pipe. Because of the three-dimensional state of stress, the length of the sample will have some effect on the resulting gaps and bending. To avoid this length effect, the sample length chosen should be at least equal to the diameter of the pipe.

Example 7.5 Suppose that a 24-in-long, 18-in-diameter, AWWA C900 DR 18 PVC pipe sample is tested for frozen-in stresses. Further suppose that when the sample is cut longitudinally, a 5° gap opens. What is the magnitude of the frozen-in stress?

$$\alpha = \text{angular gap} = 5\left(\frac{2\pi}{360}\right) = 0.087 \text{ rad}$$

$$E = \text{modulus} = 400{,}000 \text{ lb/in}^2$$

$$D_o = 18 \text{ in (assumed)}$$

$$t = \text{thickness} = \frac{D_o}{\text{DR}} = \frac{18}{18} = 1 \text{ in}$$

$$D_i = D_o - 2t = 18 - 2 = 16 \text{ in}$$

Using Timoshenko's equation, we have

$$\sigma = \frac{-\alpha E}{4}\left(\frac{2D_o^2}{D_o^2 - D_i^2}\ln\frac{D_i}{D_o} + 1\right)$$

$$= \frac{-0.087\,(400{,}000)}{4}\left(\frac{2\,(18)^2}{18^2 - 16^2}\ln\frac{16}{18} + 1\right) = 1065 \text{ lb/in}^2$$

As has been discussed earlier, a bending stress caused by a constant strain will decrease in the course of time due to relaxation. Such a stress alone will not give rise to any failure. However, large frozen-in stresses, in combination with tensile stresses caused by constant internal hydrostatic pressure, will give rise to stresses that are not usually fully evaluated. This is acceptable because thermoplastic pipes have been pressure-rated by testing with the frozen-in stresses in the pipe wall. This means the published test results were obtained having the influence of the frozen-in stresses. Nevertheless, these stresses should not be greater than about one-fourth the hydrostatic design basis.

If the frozen-in stress is very large, the end of the pipe will be bent inward. This could cause a problem, particularly for PE pipes that are to be joined by butt welding. Problems arise because of the unpredictable multiaxial stresses in the finished weld joint.

PVC pressure pipe

PVC pressure pipes are considered to be flexible pipes, and methods presented in Chap. 3 for calculating ring deflection apply. However, most pressure pipes are installed with about 4 ft of cover. Thus the resulting vertical soil pressure is relatively small, and consequently ring deflection is usually not a major concern. Only for the lower pressure classes (larger dimension ratios) where the pipe wall is relatively thin and the resulting pipe stiffnesses $F/\Delta y$ are relatively low is it necessary to consider ring deflection (Table 7.7). As before, pipe stiffness is calculated as follows:

$$\mathrm{PS} = \frac{F}{\Delta y} = \frac{4.47E}{(\mathrm{DR} - 1)^3}$$

The procedure for hydrostatic design is given in Chap. 4. Equation (4.15) is repeated here as Eq. (7.5) for convenience:

$$P\,(D - t) = \sigma \times 2t \tag{7.5}$$

where P = total internal pressure (static plus surge)
D = outside pipe diameter

TABLE 7.7 Selected Dimension Ratios (OD/*t*) and Resulting Pipe Stiffness (*F*/Δ*y*) for PVC Pipes

OD/*t* DR or SDR	Minimum *E* = 400,000 lb/in^2	Minimum *E* = 500,000 lb/in^2
42	26	32
41	28	35
35	46	57
33.5	52	65
32.5	57	71
28	91	114
26	115	144
25	129	161
21	234	292
18	364	455
17	437	546
14	815	1019
13.5	916	1145

t = wall thickness
σ = hydrostatic design stress

This equation can be rewritten as follows:

$$2\sigma = P\,(\mathrm{DR} - 1) \tag{7.6}$$

where

$$\mathrm{DR} = \frac{D}{t}$$

Equation (7.6) may be solved for DR in terms of the hydrostatic design stress and pressure.

$$\mathrm{DR} = \frac{2\sigma}{P} + 1 \tag{7.7}$$

Example 7.6—A 10-in PVC pressure pipe A 10-in PVC pipe is to be used for a transmission pipe in a rural water system. The static pressure will not exceed 150 lb/in^2. The pipe will be buried in a sandy clay soil with depths between 4 and 5 ft. Select the dimension ratio (DR = OD/t), and design the installation so that the vertical deflection does not exceed 5 percent.

solution

1. The working pressure is 150 lb/in^2—no surge pressure needs to be added unless the engineer is aware of surge conditions.
2. Assume the material is PVC 12454B with a hydrostatic design basis (HDB) of 4000 lb/in^2. A safety factor of 2 is required, resulting in a hydrostatic design stress of 2000 lb/in^2 (see Chap. 4).
3. Use Eq. (7.7) to determine the dimension ratio.

$$\mathrm{DR} = \frac{\mathrm{OD}}{t} = \frac{2\sigma}{P} + 1$$

$$= \frac{2\,(2000)}{150} + 1 = 27.7$$

Choose the next-thicker wall from Table 7.7. Use

$$\mathrm{DR} = 26 \qquad \frac{F}{\Delta y} = 115 \text{ lb/in}^2$$

4. Determine required pipe zone material to limit deflection to 5 percent. Data in Table 3.9 indicate that even for loose soil with 5 ft of cover, the maximum deflection will not exceed the 5 percent limit imposed. This table is for pipe with a stiffness of 46 lb/in^2. For the pipe in this example, the stiffness is 115 lb/in^2, so it will deflect less. Therefore, no compaction

effort is required except for the purpose of limiting surface settlement. The soil placed around the pipe should be free of large stones or frozen lumps.

Example 7.7—A 10-in PVC pressure pipe Resolve Example 7.6 for an internal pressure of 100 lb/in^2 instead of 150 lb/in^2.

1. Total pressure is 100 lb/in^2 static plus zero surge pressure, so $p = 100$ lb/in^2.
2. Again, PVC 12454B with a hydrostatic design stress of 2000 lb/in^2 is selected.
3. Use Eq. (7.2) to determine the dimension ratio.

$$\text{DR} = \frac{\text{OD}}{t} = \frac{2\sigma}{P} + 1$$

$$= \frac{2\,(2000)}{100} + 1 = 41$$

Therefore, select a PVC pipe where

$$\text{DR} = \frac{\text{OD}}{t} = 41$$

From Table 7.7,

$$\text{Pipe stiffness} = \frac{F}{\Delta y} = 28 \text{ lb/in}^2$$

4. Select pipe zone material and required compaction. Vertical ring deflection is to be less than 5 percent per Example 7.6. Use Spangler's equation to determine the required E' [see Eq. (7.4)].

$$E' = \frac{0.56\,H/(\Delta y/D) - \text{PS}}{0.41}$$

For this example,

$$H = \text{height of cover} = 5 \text{ ft}$$

$$\frac{\Delta y}{D} = \frac{\text{vertical deflection}}{\text{diameter}} = 0.05$$

$$\text{PS} = \frac{F}{\Delta y} = 28 \text{ lb/in}^2$$

Thus,

$$E' = \frac{0.56\,(5)/0.05 - 28}{0.41} = 68 \text{ lb/in}^2$$

Data in Table 3.9 indicate that a dumped or slightly compacted soil will meet the design criteria. Only uncompacted clays may not meet the specified conditions.

Examples 7.6 and 7.7 indicate that for PVC pressure pipes in medium soil cover, the design of the pipe embedment system is not critical. The primary embedment objective is to protect the pipe from large objects, such as stones, frozen lumps, and objects which could cause impact damage or penetrate the pipe wall.

Example 7.8—DR 41 PVC pipe The DR 41 PVC pipeline operating at 100 lb/in^2 selected in Example 7.7 is to cross a roadway with only 3 ft of cover. Are there special design considerations for this road crossing if a maximum of 2 percent deflection is allowed to protect the road surface?

1. Determine the total load.

$$\text{Total load } W_T = \text{prism load} + \text{live load}$$

(See Fig. 2.19 for H-20 highway loading.) From the graph, $W_T = 950 \text{ lb/ft}^2$.

2. Use Spangler's equation to calculate the required soil modulus E' [see Eq. (7.4)].

$$E' = \frac{0.56\, H/(\Delta y/D) - \text{PS}}{0.41}$$

In the above equation, H represents the height of cover. For this example, the total load is due to not just soil load, but also live load. An effective height H can be calculated as follows:

$$H = \frac{W_T}{120} = \frac{950 \text{ lb/ft}^2}{120 \text{ lb/ft}^3} = 7.9 \text{ ft}$$

Use

$$H = 8 \text{ ft} \qquad \frac{\Delta y}{D} = 0.02$$

From the previous example,

$$\text{PS} = \frac{F}{\Delta y} = 28$$

Thus

$$E' = \frac{0.56\,(8.0)/0.02 - 28}{0.41} = 478 \text{ lb/in}^2$$

Table 3.4 indicates that a granular material compacted to at least 85 percent standard Proctor density is required. A coarse-grained material with slight compaction will also meet the E' requirement. Experience has shown that for such installations, little or no movement can be tolerated, or else the road surface will break up. Therefore, a coarse granular material with high compaction is recommended.

Example 7.9a—A 12-in PVC pressure pipe A 12-in PVC distribution line is to be installed 5 ft deep. The line is to operate at pressures up to 200 lb/in². Select the proper dimension ratio, and comment on the backfill requirements.

1. Calculate the design stress. Distribution line AWWA C900 applies.

$$\text{HDB} = 4000 \text{ lb/in}^2$$

$$\text{AWWA safety factor} = 2.5$$

$$\text{Hydrostatic design stress} = \frac{\text{HDB}}{\text{SF}} = \frac{4000}{2.5} = 1600 \text{ lb/in}^2$$

2. Determine the design pressure.

$$P = \text{static pressure} + \text{surge pressure}$$

AWWA C-900 recommends a 40 lb/in² surge pressure for class 200 pipe. Thus,

$$P = 200 + 40 = 240 \text{ lb/in}^2$$

3. Calculate the dimension ratio. Use Eq. (7.2).

$$\text{DR} = \frac{2\sigma}{P} + 1$$

$$= \frac{2\,(1600)}{240} + 1 = 14.33$$

Choose DR = 14, which has a slightly thicker wall than required.

4. Comment on the backfill requirements. Table 7.7 indicates that DR 14 PVC pipe has a pipe stiffness of 815 lb/in². This pipe will not require special compaction or a select soil type when placed with only 5 ft of cover. Compaction may be necessary to prevent road or surface settlement and to provide soil friction and soil weight, to prevent the pipe from floating in saturated soils. Design and construction for thrust restraint will be required at fittings such as elbows and tees (see Chap. 4 for details).

Example 7.9b—Pressure surge design A water main in a municipal water system with temperatures below 70°F operates with a maximum sustained pressure of 85 lb/in². Design engineers predict the maximum instantaneous surge velocity input to be 2 ft/s. For a 12-in-diameter pipe, what dimension ratio and corresponding pressure class are required?

1. Try DR = 18. From AWWA C900, average dimensions are

$$\text{OD} = 13.200 \text{ in}$$

$$\text{Wall thickness } t = 0.733 \text{ in}$$

$$\text{ID} = \text{OD} - 2t = 11.734 \text{ in}$$

2. Calculate the wave speed [see Chap. 4 and Eq. (4.8)].

$$a = \frac{4822}{\sqrt{1 + (K/E)\,(\text{ID}/t)}}$$

$$= \frac{4822}{\sqrt{1 + (313{,}000/400{,}000)\,(11.734/0.733)}} = 1311 \text{ ft/s}$$

3. Calculate the surge pressure P_s.

$$P_s = \left(\frac{a}{g}\right)(V)\,(0.43) = \left(\frac{1311}{32.2}\right)(2)\,(0.43) = 35 \text{ lb/in}^2$$

4. Total pressure equals working pressure plus surge pressure.

$$P = 85 + 35 = 120 \text{ lb/in}^2$$

5. Calculate the DR, using Eq. (7.2).

$$\text{DR} = \frac{2\sigma}{P} + 1 \qquad \text{where} \qquad \sigma = \frac{\text{HDB}}{\text{SF}} = \frac{4000}{2.5} = 1600 \text{ lb/in}^2$$

$$= \frac{2\,(1600)}{120} + 1 = 27.7$$

Select the next available DR which is lower. Use DR = 25 which is AWWA C900 pressure class 100.

6. Check the design with actual dimensions. Use the equation in step 2 to recalculate the wave velocity.

$$\text{ID} = 12.144 \text{ in}$$

$$t = 0.528 \text{ in}$$

$$\text{Wave speed } a = 1106 \text{ ft/s}$$

Use the equation in step 3 to recalculate surge pressure.

$$P_s = \left(\frac{1106}{32.2}\right)(2)\,(0.43) = 29.5 \text{ lb/in}^2$$

Actual surge pressure is lower than that used in the design calculations. Therefore, the design is okay.

Example 7.10—A 6-in PVC force main An existing 6-in sewer force main is to be replaced with a 6-in PVC pressure pipe. The line is known to operate with an average pressure of 140 lb/in^2, a minimum pressure of 100 lb/in^2, and cyclic pressure peaks of 180 lb/in^2. The average number of cycles in a 24-h period is 200. The design life of the system is to be a minimum of 100 years. Determine the required dimension ratio.

1. Determine the number of cycles in the 100-year life of the system.

$$C = \text{cycles during life} = (200 \text{ cycles/day})\,(365 \text{ days/yr})\,(100 \text{ yr})$$

$$= 7.3 \times 10^6 \text{ cycles}$$

2. Determine the pressure amplitude.

$$P_{\text{amp}} = \pm \frac{P_{\max} - P_{\min}}{2} = \pm \frac{180 - 100}{2} = \pm 40 \text{ lb/in}^2$$

3. Solution is the trial-and-error type. Select a DR for the PVC pipe. Try DR 18. Use Eq. (4.19) to solve for stresses in terms of pressures.

$$S = \frac{\text{DR} - 1}{2} P$$

Calculate the average stress.

$$S = \frac{\text{DR} - 1}{2} P = \frac{17}{2} (140) = 1190 \text{ lb/in}^2$$

Calculate the stress amplitude.

$$S = \frac{\text{DR} - 1}{2} P = \frac{17}{2} (40) = 340 \text{ lb/in}^2$$

4. Use the graph in Fig. 4.22 to determine the number of cycles to failure.

$$\left(\frac{\text{Ordinate} = 340}{\text{Abscissa} = 1190} \right) (\text{cycles to failure}) = 5 \times 10^6 = 68.5 \text{ yr}$$

This is less than the desired 100 years. Select DR = 14 which is AWWA class 200. It is left to the reader to show that the life of DR 14 under these cyclic conditions is more than 400 yr.

Example 7.11. During the past several years, a city in the southwestern part of the United States has experienced numerous breaks in DR-18 AWWA C900 PVC pipe installed in its water system. The majority of these breaks have occurred in specific areas (not randomly). The distribution of breaks would lead one to conclude that, for these specific areas, either system operation is at fault or faulty pipe was installed.

Is the pipe faulty? Samples of failed pipe were subjected to acetone immersion testing per ASTM D 2152. If a sample or samples fail this test, additional tests such as burst tests and/or impact tests may be considered. Extrusion quality tests (acetone immersion) were conducted on samples (see Table 7.8). Three or four specimens were prepared from each pipe sample. The specimens were tested per ASTM D 2152. No flaking or wall separation was noted on any of the test samples. These tests show that the extrusion quality for the pipe in question is good. A sample of this pipe was subjected to the heat reversion test according to ASTM F 1057. This sample passed this test without any wall separation, distortion, or blistering—again indicating good-quality pipe.

Heat reversion technique (as taken from ASTM F 1057). This practice is applicable to distinguish between properly and improperly extruded PVC plastic pipe. It can be used to (1) reveal incomplete exsiccation of a compound before or during extrusion,* (2) determine the presence of stress in the pipe wall produced by the extrusion process,† (3) determine whether infused areas are present, and (4) reveal contamination. The conclusion is that there is no indication of faulty pipe.

An investigation reveals the following system information:

- There have been 19 failures over a 2-year period. This is not a high number considering that there is more than 100 mi of PVC in the system.
- The system is complex, with many changes in elevation and numerous pressure-reducing valves (PRVs), some of which are redundant. Also, there are deep wells, pumping stations, and reservoirs. Parts of the system are operating out of control in terms of cyclic pressures. Operating pressures range from about 70 to 180 lb/in^2 with occasional spikes to 190 lb/in^2. However, most of the system is operating in the 70 to 130 lb/in^2 range. A pressure range of 50 lb/in^2 is common in the areas where failures are occurring. The cyclic rate is about 3 cycles/min.
- In many places in the system, water temperatures were found to be above 73.4°F. It was determined that in some of the failure zones the pipe wall temperatures were as high as 96°F.

---

*Residual moisture in the compound vaporizes at extrusion temperatures and is normally evacuated as it forms vapor. Pockets of moisture trapped in the pipe wall result from incomplete exsiccation of the compound, and may reduce the physical properties of the pipe.

†Minor residual stress in the pipe wall will not impair field performance and handleability. High residual stress has no proven effect on performance, but may impair handleability during installation.

No statement is made about either the precision or bias of Practice F 1057 for estimating the quality of PVC pipe, since the results merely state whether there is conformance to the criteria for acceptability suggested by the interpretation.

This test is not required by any standards for PVC pipe whereas the acetone immersion test is required by both AWWA C900 and ASTM D 2241.

TABLE 7.8 Extrusion Quality Tests on PVC Pipe Samples

Sample identification number	Description	Manufacturer	Other	Results
1		A	VHH G21D	Passed
2	12-in white	A	Possible megalug	Passed
3	12-in white	B	Bell & Spigot	Passed
4	8-in white	A	M15C4	Passed
5	12-in blue	C		Passed
6	8-in white	A		Passed
7	12-in blue	C	No crack	Passed
8	12-in white	B	VHH G21D	Passed
9	12-in blue	C	No crack	Passed
10	12-in white	B		Passed
11	12-in white	B		Passed
12	12-in white	B		Passed
33	8-in blue	C		Passed
SH	8-in blue	C		Passed
HV I	12-in blue	C		Passed
HV II	12-in blue	C		Passed
Special sample*	12-in blue		From yard	Passed

*This sample was heat reversion tested.

- Examination of failures and failed samples revealed the following: No sample exhibited a failure due to long-term sustained pressure. In such a failure, there is some ductile deformation associated with the failure. The failure is usually catastrophic in nature (does not start with a short crack that later propagates).
- Inspection of actual breaks shows that all were breaks that took place with virtually no ductile yielding. The inspected breaks were all brittle, which is typical for fatigue failures and failures produced by impact or induced by high stress intensity. An example of high-stress-intensity crack propagation is a failure induced by tapping when the pipe is under pressure. In this case, the crack moves very rapidly and does so with little deformation. One of the samples inspected had failed due to tapping. The failure was brittle in appearance and very similar to other failures. All the samples inspected exhibited a brittle-type failure typical of a fatigue break. Failures due to fatigue will usually start with short crack and will later propagate because of the high stress intensity associated with the crack. If the short crack exists for a time before it propagates, there will be erosion on the pipe wall due to leaking water under pressure. Many of the samples exhibited erosion, which is a definite indication of fatigue failure.

The preliminary conclusion is that the pipe probably failed because of fatigue. Will calculations concerning temperature and fatigue support this conclusion? Or did the pipe fail because of high temperature only?

Check design. The design basis for AWWA C900 pipe includes a safety factor of 2.5 and an allowance for occasional surges. The design basis equation in C900 can be expressed in the following way:

$$2.5\ (\mathrm{PC} + P_s) = \frac{2t}{D - t}\ (\mathrm{HDB}) \tag{7.8}$$

where 2.5 = safety factor
PC = pressure class (100, 150, or 200 lb/in^2)
P_s = surge allowance, lb/in^2, for instantaneous stoppage of flow of 2 ft/s
t = minimum wall thickness, in
D = outside diameter, in
HDB = hydrostatic design basis = 4000 lb/in^2

The actual surge allowances, in AWWA C900, are the increases in pressure that result from stoppage of flow of 2 ft/s and are as follows:

Class 100, DR 25	30 lb/in^2
Class 150, DR 18	35 lb/in^2
Class 200, DR 14	40 lb/in^2

Another design parameter included in AWWA C900 is the effect of sustained elevated temperatures on pressure and/or design stress. For sustained temperature of the pipe wall above 73°F, the design stress should be reduced. This reduction is not necessary for short-term excursions of elevated temperatures, but is necessary for continuous service at a higher temperature. The recommended percentages of allowable pressure class for various elevated temperatures are as shown [Table 4.6 is repeated for the reader's convenience (see Table 7.9)].

Derating a PVC pipe due to operating temperature. Temperatures were determined to be as high as 96°F. For calculation purposes, use 100°F. For a class 150 pipe operating at 100°F, the pipe should be derated to 62 percent of its class. Thus, the 150 lb/in^2 pipe will be effectively a 93 lb/in^2 pipe, which would then be like a DR 29 pipe operating at a temperature of 73°F or below. Therefore, a DR 18 PVC pipe operating at 100°F can be analyzed as if it were a DR 29 PVC pipe operating at normal water temperatures (equal to or less than 73.4°F).

Safety factors: The design equation is

$$P_t = P_w + P_s = \frac{2}{\mathrm{DR} - 1} \times \frac{\mathrm{HDB}}{F} \tag{7.9}$$

Solve for the factor of safety F:

TABLE 7.9 Temperature Derating Factors

Maximum continuous* service temperature, °F	Percentage of allowable pressure class or design stress at 73°F
73	100
80	88
90	75
100	62
110	50
120	40
130	30
140	22

*Note from *Uni-Bell Handbook:* The derating factors assume sustained elevated service temperatures. When the contents of a buried PVC pressure pipe are only intermittently and temporarily raised above the service temperature shown, a further reduction may not be needed.

$$F = \frac{2}{P_w + P_s} \times \frac{\text{HDB}}{\text{DR} - 1} \tag{7.10}$$

where P_w = working pressure (average steady state pressure at a given location in system)

P_s = surge pressure (occasional pressure wave due to starting and stopping of pumps and closure and opening of valves, sometimes called water hammer)

$P_t = P_s + P_w$ = total pressure

DR = dimension ratio = thickness divided by outside diameter

HDB = 4000 lb/in^2 for AWWA C900, 4200 lb/in^2 for ASTM D 2241

F = factor of safety

The AWWA C900 standard is more conservative than the ASTM D 2241 standard, for the following three reasons:

1. The AWWA standard recommends that the surge pressure be included before applying the factor of safety. The ASTM standard does not directly address surge pressure.
2. The AWWA standard uses a factor of safety of 2.5 whereas the ASTM standard uses a factor of safety of 2.0.
3. The AWWA standard uses an HDB of 4000 lb/in^2 whereas the ASTM standard uses an HDB of 4200 lb/in^2.

The safety factor values listed in Table 7.10 were calculated using Eq. (7.10) and temperature derating factors as given in Table 4.6 and Table 7.9 and in AWWA C900. The tables show factor of safety as a function of both temperature and pressure. They are based on a system that has

TABLE 7.10 Safety Factors for AWWA C900 DR 18 PVC Pipe

		Temperature, °F					
Working pressure	Working plus surge	73.4	80	85	90	95	100
75	110	4.28	3.76	3.49	3.21	2.93	2.65
80	115	4.09	3.60	3.34	3.07	2.80	2.54
85	120	3.92	3.45	3.20	2.94	2.69	2.43
90	125	3.76	3.31	3.07	2.82	2.58	2.33
95	130	3.62	3.19	2.95	2.71	2.48	2.24
100	135	3.49	3.07	2.84	2.61	2.39	2.16
110	145	3.25	2.86	2.65	2.43	2.22	2.01
120	155	3.04	2.67	2.47	2.28	2.08	1.88
130	165	2.85	2.51	2.32	2.14	1.95	1.77
140	175	2.69	2.37	2.19	2.02	1.84	1.67
150	185	2.54	2.24	2.07	1.91	1.74	1.58
165	200	2.35	2.07	1.92	1.76	1.61	1.46

occasional surge pressures but without continuous cyclic pressures.

The shaded areas in Table 7.10 are those combinations of pressure and temperature that lead to factors of safety less than recommended by the standards (that is, 2.5 for AWWA C900). However, this does not mean that the pipe will not perform as expected. If a factor of safety is approaching 1.0, it means that particular pipe is expected to perform under those conditions for 11.4 years only. No pipes should be replaced unless there is a pattern of continual breaks, and then only if a cost analysis shows that replacement is more economical than repair. In such an analysis, actual costs as well as public inconvenience and public goodwill must be considered.

At 200 lb/in², the safety factor of a derated pipe (operating at 100°F) is 1.46. This means that the effective stress is

$$\sigma = \frac{4000}{1.46} = 2640 \text{ lb/in}^2$$

Failure due to long-term sustained pressure. According to the stress regression line (Fig. 4.6), the pipe will never fail by stress regression. Thus, it is virtually impossible for the pipe in this system to be failing due to long-term sustained pressure. Even when one derates the pipe because it is operating at 100°F, the pipe will not fail due to the sustained operating pressures of the system. Derating the DR 18 pipe to 62 percent of its strength is equivalent to analyzing the pipe as though it were a DR 29 pipe (see Table 7.11). A DR 18 pipe operating at 185 lb/in² has an internal hoop stress of 1573 lb/in². By derating this pipe to a DR 29, the effective hoop stress is 2590 lb/in². According to the stress regression line for PVC pipe, this pipe will not fail due to sustained pressure. No sample exhibited a failure due to long-term sustained pressure. In such

TABLE 7.11 Cyclic Life Data

	DR 18					DR 29 (derated DR 18 at 100°F)			
Average pressure, lb/in^2	100	130	150	185	210	100	130	150	185
Peak stress, lb/in^2	850	1105	1275	1573	1785	1400	1820	2100	2590
Pressure amplitude	25	25	25	25	25	25	25	25	25
Stress amplitude	213	213	213	213	213	350	350	350	350
No. cycles to failure	1.00E+08	5.00E+07	4.00E+07	2.00E+07	1.00E+07	4.00E+06	1.50E+06	6.00E+05	2.00E+05
For 50-yr life									
Cycles per year	2,000,000	1,000,000	800,000	400,000	200,000	80,000	30,000	12,000	4000
Cycles per day	5479.5	2739.7	2191.8	1095.9	547.9	219.2	82.2	32.9	11.0
Cycles per hour	228.3	114.2	91.3	45.7	22.8	9.1	3.4	1.4	0.5
Cycles per minute	3.81	1.90	1.52	0.76	0.38	0.152	0.057	0.023	0.008
Life (in years) @ 3 cycles/min	63.4	31.7	25.4	12.7	6.3	2.5	1.0	0.4	0.1

a failure, there is some ductile deformation associated with the failure. The failure is usually catastrophic in nature (does not start with short crack that later propagates).

The conclusion is that the pipes did not fail due to sustained pressure.

An obvious conclusion that follows is that the failures are not due to temperature only. A further proof of this is as follows: If the failures were due to temperature only, then they would be somewhat randomly located wherever the temperature was elevated. Areas with the highest temperatures should have the most failures. This pattern was not evident.

Cyclic pressure analysis. Design standards make the tacit assumption that the water system will not be operating in such a manner that the pipe will be subjected to more than 1 million pressure surges in the design life of the system. In certain areas in this water system, the pressures are cycling at 2 to 4 cycles/min. For 3 cycles/min, the pipe will be subjected to more than 1.5 million cycles in just 1 year.

The cycles to failure in Table 7.11 were determined from Fig. 4.22, which is the cyclic failure graph given in Chap. 4. Consider an average pressure of 150 lb/in^2 and a stress amplitude of 25 lb/in^2. This is for the case of pressure varying from 125 to 175 lb/in^2 and is typical for our system. According to Table 7.11, DR 18 will have the ability to take this abuse for 25.4 years, which is less than the typical design life. For the derated pipe operating in the same manner, the predicted life is only 0.4 year ($\approx$5 months). The data are very clear: Without the cyclic pressures that are being experienced in this system, the pipe would not be failing.

The overall conclusion is that the primary cause of failure in this system is that the system is operating with continuous cycling of pressures. That is, the system is subjected to a high cyclic loading rate along with peak pressures high enough to cause premature failure. Temperature is an aggravating cause and allows the cyclic fatigue to take place in a shorter time.

The follow-on conclusion is that if the pressure fluctuations can be brought under control, the breaks due to fatigue will stop. It is well known that the life of PVC pipes due to sustained pressure and the life of PVC pipes due to cyclic loading are independent.

Cyclical pressures and surges. In a water distribution system, surge conditions normally occur on a rather infrequent basis. However, a system that is operating such that frequent and/or continuous cyclical pressure surges occur, will need to be brought under control. Surge is the occasional pressure rise brought on by the stopping of flow, often called water hammer. In the water system, there were occasional spikes that were seen in the pressure charts. AWWA warns of the necessity of controlling these occasional water hammer spikes. (See page 12 of AWWA C900.) Surge, as allowed for in AWWA C900, and continuous cyclic pressures found in our system are two totally different things.

Cyclic pressures can and will cause fatigue failures. These are not even addressed in AWWA C900 because they should not be present in a water system. If such conditions are not corrected, additional design considerations are required. Research work has shown that

1. Plastic pipe possesses two life funds—static and dynamic (or hydrostatic and cyclic).
2. These funds are separate and independent of each other.
3. The cyclic pressure life fund is a critical parameter if the number of surges is very large or if the magnitude of surges is high.

To select the appropriate PVC pipe for a new installation, the following steps can be taken:

1. Determine the years of service required.
2. Determine the average pressure and the pressure amplitude anticipated in your system.
3. Calculate the average hoop stress* and the stress amplitude for the class of pipe.
4. Use the graph in Fig. 4.22 to determine the number of cycles that will cause failure.
5. Based on these data and the cyclic rate, the expected system lifetime can be calculated.
6. If the calculated life is not sufficient, return to step 3 and use a higher class of pipe. Or better yet, control the cyclic stresses and/or rate to acceptable levels.

Evaluation of PVC pipe performance

AWWA Research Foundation. In 1994 Utah State University completed a study which was sponsored by the AWWA Research Foundation (AWWARF). Some water utilities reported pipe failures of installed polyvinyl chloride pipe. These reported failures ranged from joint leakage to catastrophic failures during tapping under pressure. In addition,

*Hoop stress is the tensile stress in the wall of the pipe in the circumferential direction due to internal hydrostatic pressure.

there were reported long-term failures which some have attributed to aging of the PVC material. Other concerns that were expressed dealt with chemical permeation, variability of PVC composition between manufacturers, and variability between runs of PVC pipe from the same manufacturer. The extent and seriousness of the reported failures and the bases for these concerns at the time were unknown. Also, comprehensive information on the extent to which installation techniques and tapping procedures have influenced performance was lacking.

The objectives of this study were (1) to perform a comprehensive evaluation of the use and performance characteristics (including performance limits) of PVC water pipe, (2) to conduct the necessary research and analysis to resolve problems and concerns identified by the first objective, and (3) to report results of analyses along with appropriate conclusions and recommendations.

Procedure. The technical approach for this study was as follows: (1) A questionnaire was developed and used to survey utilities and engineering firms. (2) The research team compiled the data from the questionnaire and analyzed the results. (3) Follow-up telephone survey questionnaires were developed to resurvey selected utilities who reported tapping and long-term problems with PVC pipe. (4) Utilities were resurveyed for additional tapping information, and some were resurveyed for more data on long-term problems. (5) Failure analysis studies were conducted that involved (*a*) the analysis of collected data, (*b*) the collection of pipe samples, (*c*) the running of tests for product quality, and (*d*) the analysis of test data. (6) All the above were conducted under standards of quality assurance and quality control. There were 162 water utilities and 29 engineering firms who contributed valuable time in collecting and submitting information. In addition, 79 of these utilities participated in a more detailed follow-up survey on long-term performance and tapping of PVC pipe. Seventeen utilities contributed by collecting representative PVC pipe samples and shipping the samples at their expense to Utah State University for testing.

Quality assurance. Two areas must be considered when a questionnaire is used to gather information: questionnaire design and sampling bias.

The principles which were used to design the questionnaire ensured that the information obtained via the questionnaire would provide data from which meaningful conclusions could be drawn. Each research team member determined areas to be covered by the questionnaire and evaluated every question. Overall and specific areas of information content of the questionnaire were thoroughly considered. Questions were designed to be answered with a minimum of effort. Research team areas of expertise included geotechnical engineering (soils), structures, engineering mechanics, materials, science, and hydraulics and fluid mechanics. This varied technical background of the team members provided multiple insights into the problems and ensured clarity of individual questions and linkages between questions. A possible bias was due to nonresponse. The response rate was 71 percent, which is very good for this type of survey. Based on the above, it was concluded that this bias was kept to a minimum. Responses from engineering firms provided data from a different perspective than that received from utilities. Engineering firms are further removed from the day-to-day operation and the associated problems. However, agreement of utility data and data from engineering firms was quite good in most areas.

The 162 utilities surveyed were made up of 125 PVC users and 37 nonusers. The nonusers of PVC reported 0 mi of PVC in their systems. There were some utilities that have PVC in their systems, but no longer allowed it to be installed. These utilities were classified as users since they reported their experience with PVC. Forty-one utilities reported 1 to 10 mi of PVC, 38 reported 10 to 50 mi of PVC, and 46 reported over 50 mi of PVC in their systems. The utilities were fairly well distributed in each user group. These data are shown graphically in Fig. 7.19.

Data on PVC pipe given in the tables and figures are classified as follows: Data labeled PVC are inclusive of all data reported in the survey on PVC pipe, data identified as AWWA are inclusive of data reported on AWWA C900/C905 pipe only, and data labeled ASTM are for ASTM D 2241 PVC pipe only.

Pressure surges. Pressure fluctuations and pressure surges are known to influence pipe performance, so each utility was asked to report on pressure variations in its system during a typical day's oper-

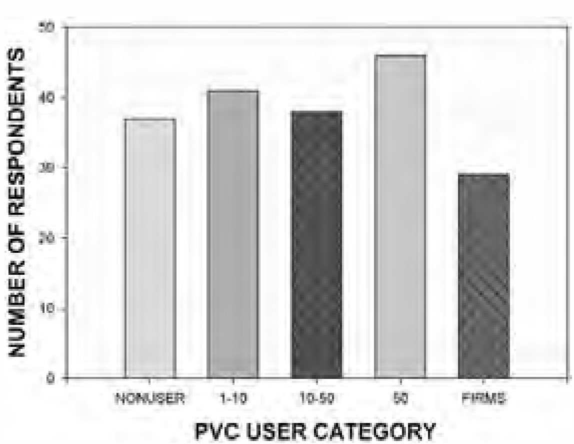

Figure 7.19 Number of respondents in each PVC user category (based on miles of installed PVC pipe) and number of responses from firms.

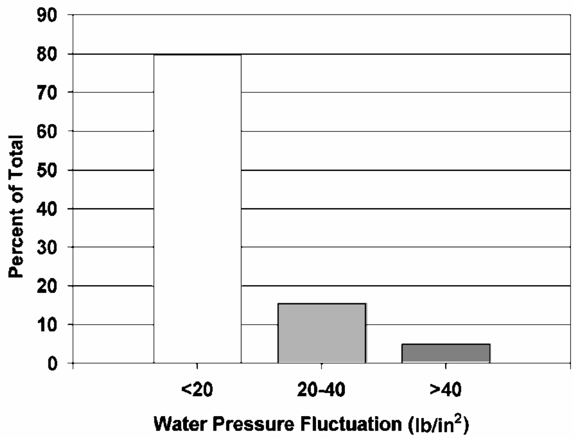

Figure 7.20 Percent of respondents reporting a pressure fluctuation in each range.

ation. Figure 7.20 shows the percentage of utilities reporting water pressure variations in each of three pressure ranges.

Tapping. Each utility was asked to respond to the following question regarding pressure tapping of various pipe products. "Based on experience in your water system, are problems associated with pressure tapping for each listed product considered to be major, minor, or no problem?" Figure 7.21 gives tallies of responses. In the figures, AWWA refers to AWWA C900/C905 PVC pipe, ASTM refers to ASTM D 2241 PVC pipe, D.I. refers to ductile iron pipe, ST refers to steel pipe, and R.C. refers to reinforced-concrete pipe.

Tapping of PVC pipe. In the utility survey, utilities were asked for tapping information on PVC only. Figure 7.22 gives data on how taps were made. About 80 percent of all taps are made with saddles, and more than 60 percent of taps are made with pipe under system operating pressure—sometimes called *hot tapping.* A tally of responses regarding the type of training provided for those making taps is given in Fig. 7.23. They indicated most of the training on tapping techniques for their technicians was informal-type training.

Utilities were asked, "How many PVC pipe failures do you experience per year that are caused by direct pressure tapping?" The answers to this question were linked to other questions dealing with tapping; the results of this analysis are given in Fig. 7.24. The listed restrictions are constraints placed on the query of the database as explained below. Restriction V, for example, produced data from those utilities that

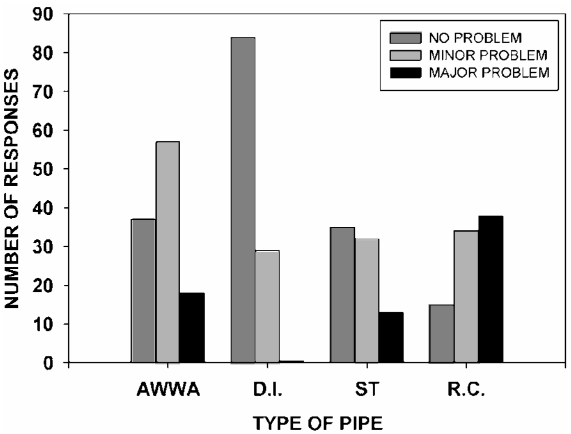

Figure 7.21 Tally showing whether respondents consider pressure tapping to be a major problem, a minor problem, or no problem for various pipe types.

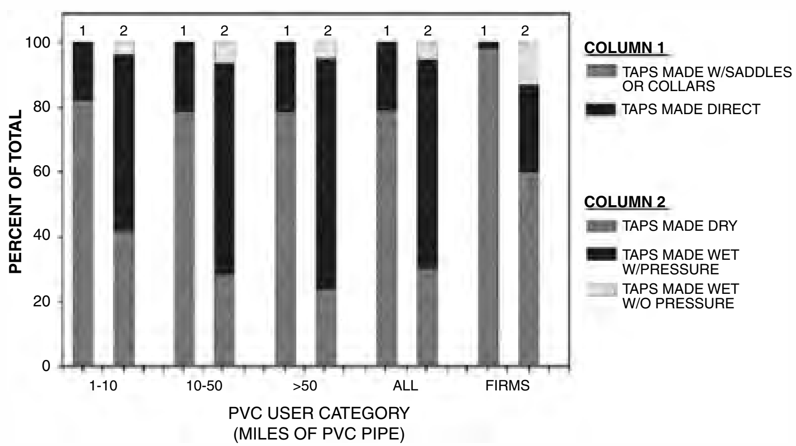

Figure 7.22 Average responses concerning taps made on AWWA C900/C905 PVC pipe for each PVC user group and engineering firms.

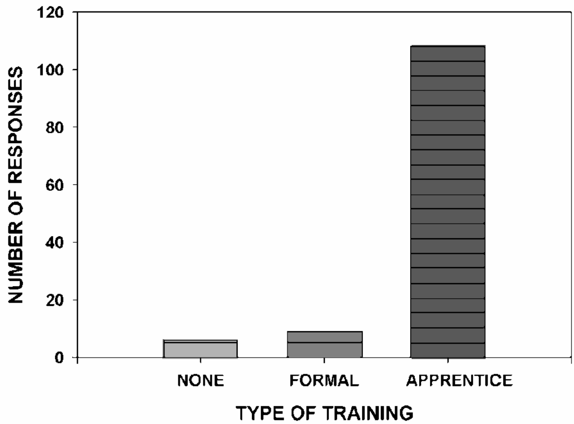

Figure 7.23 Tally showing the type of training provided to technicians making direct pressure taps.

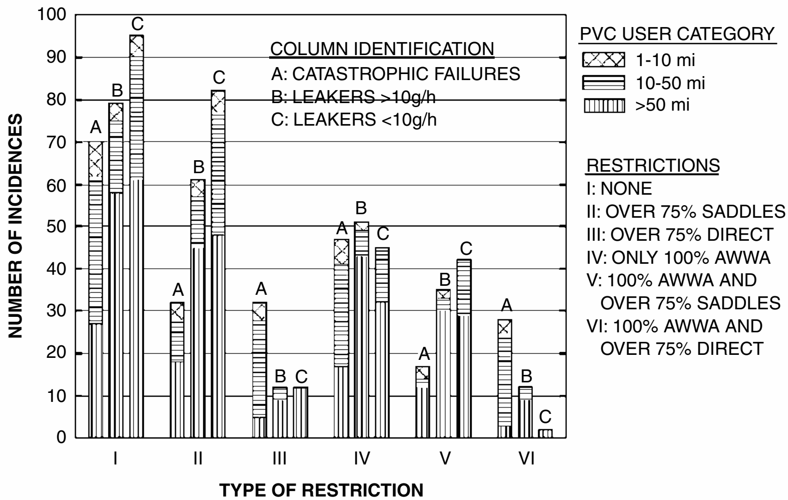

Figure 7.24 Stacked bar graph showing reported tapping problems.

reported that all PVC pipe in their systems was AWWA C900/C905 and more than 75 percent of their taps were done with saddles.

Restriction	Explanation
I: None	No restriction—data are from all respondents.
II: Over 75% saddles	Utilities reporting over 75% of taps are with saddles.
III: Over 75% direct	Utilities reporting over 75% of taps are done directly.
IV: Only 100% AWWA	Utilities reporting all PVC pipe in system is 100% AWWA.
V: 100% AWWA and over 75% saddles	Utilities reporting all PVC pipe in system is 100% AWWA and over 75% of taps are made with saddles.
VI: 100% AWWA and over 75% direct	Utilities reporting all PVC pipe in system is 100% AWWA and over 75% of taps are made directly.

Information obtained in the follow-up telephone resurvey on the number of taps made was combined with data given in Fig. 7.24 to produce a tapping incident rate (incidents per 1000 taps made). Figure 7.25 is a representation of these normalized data. The use of saddles with AWWA C900/C905 pipe does not reduce the number of tapping problem incidents. However, the use of saddles does reduce the rate of catastrophic failures. It is interesting to note that utilities reporting 10 to 50 mi of PVC in their systems report the largest number of cata-

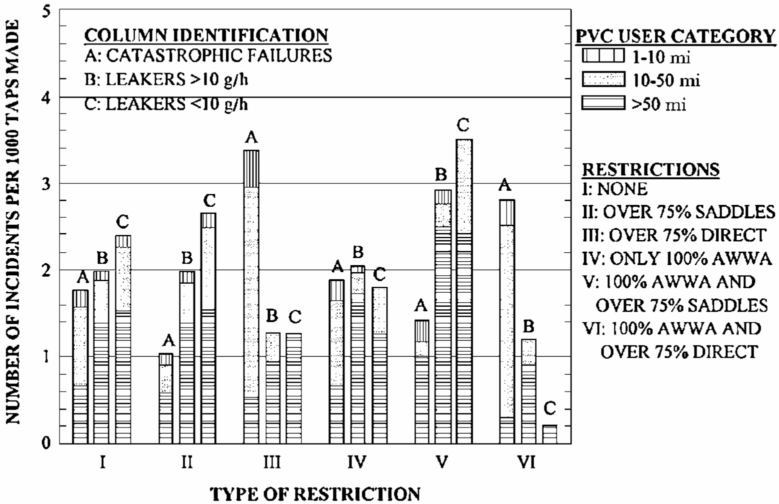

Figure 7.25 Stacked bar graph showing the reported number of tapping problem incidents per 1000 taps made.

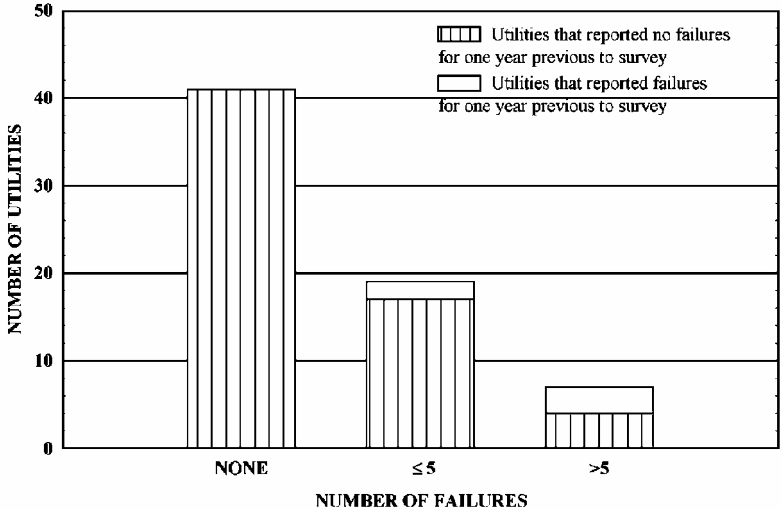

Figure 7.26 Number of utilities reporting catastrophic tapping failures (grouped according to number of reported tapping failures in 5 years).

strophic failure incidents and the largest catastrophic failure rates. No reason for this observation was determined.

Sixty-seven of the 162 utilities surveyed reported tapping problems on the original survey questionnaire. All these 67 were selected for the follow-up resurvey and were solicited for additional tapping information. Figure 7.26 is a grouping of these utilities into three categories based on the number of catastrophic tapping failures reported in the 5-year period preceding the survey as follows:

- None = that group of utilities reporting no failures during the 5-year period
- ≤5 = that group of utilities reporting less than or equal to five failures
- >5 = that group of utilities reporting more than five failures

Twenty-six utilities reported catastrophic tapping failures during the 5-year period. Nineteen of those 26 utilities had on average one failure per year or less. Only seven utilities averaged more than one failure per year. Those utilities represented as none in Fig. 7.26 had no catastrophic failures in the period. Tapping comments from the resurveyed utilities reveal that about 60 percent of those utilities reporting catastrophic tapping failures in the first survey reported they had solved their tapping problems and had not had any failures in the 5

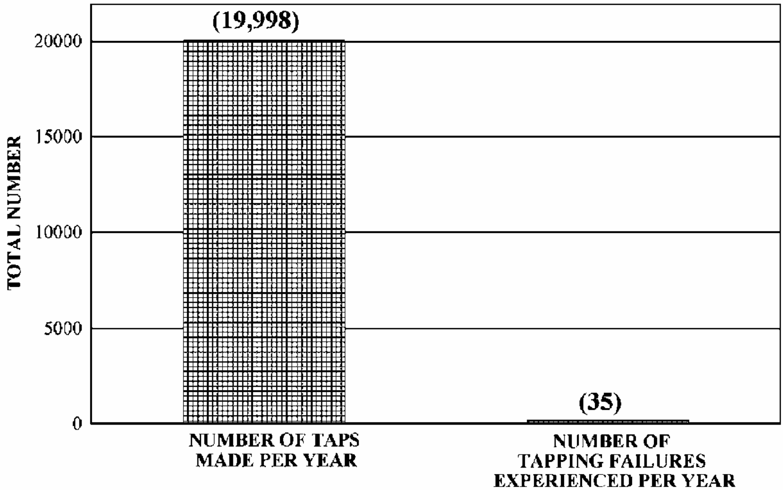

Figure 7.27 Comparison of the total number of taps made per year to the number of catastrophic tapping failures per year.

years preceding the survey. About 80 percent have had no failures in the 2-year period preceding the survey.

Figure 7.27 provides a comparison of the total number of taps made per year to the total number of catastrophic tapping failures experienced per year for the 67 utilities in the follow-up tapping study. In the resurvey, the utilities were asked to estimate the number of catastrophic tapping failures they had experienced in the last 5 years. These numbers were summed and then divided by 5 to obtain the number per year used in Fig. 7.27. This indicates one catastrophic tapping failure for every 571 taps made. This failure rate and Fig. 7.26 may imply that the reported catastrophic failures for the last 5 years are uniformly distributed. However, comments given in Table 7.12 and data given in Fig. 7.26 indicate that they are not uniformly distributed because a large majority of the utilities reported declining failure rates with time. Thus, today's failure rate is probably much less than Fig. 7.27 implies. The three most often cited reasons for tapping failures are as follows: (1) in a hurry, tapping too fast; (2) trying to tap a pipe with residual stresses (i.e., the pipe is bent to conform to a curved trench); (3) using a dull cutter or the wrong saddle or both. Two other interesting statistics were obtained from the tapping data:

- Forty-one percent of the utilities reported 100 percent of the tapping problems. (Fifty-nine percent of the utilities reported no tapping problems.)

TABLE 7.12 Unedited Comments from Follow-up Phone Calls of Utilities Reporting at Least One Catastrophic Tapping Failure during the 5-Year Period Preceding the Survey

- Used the wrong saddle.
- Had problems 3 to 4 years ago, tapped too quickly, and used a drill bit.
- About 1 failure per year prior to 1989, pipes were bent and tapped too fast.
- Had problems 5 to 6 years ago; have used more saddles in recent years and problems are fewer.
- Problems with using the wrong saddle and tapping direct; other problems associated with tapping too fast and overtightening saddle on the main.
- Had a problem in 1985, trying to tap too fast.
- Last problem was in 1985, don't tap hot (*under system pressure*) anymore.
- Had problems in 1989; contractor in a hurry, tapping too fast.
- Had a failure in 1990, trying to tap too fast.
- Had a couple of problems in 1987; manufacturer's representative came out and told the utility the pipe was cooled too fast during extrusion (i.e., bad pipe).
- Had problems in 1990 and 1991; cutter was dull and overheated the pipe, causing the pipe to break; now use sharp bits, no problem.
- Had problems 4 to 5 years ago, poor tapping technique, tapping too fast.
- Since we switched from twist drill to shell cutter, no problem.
- Problems in 1989, believe due to bends in pipe.
- Had problems prior to 1988 when taps were made hot; switched to wet taps (*system pressure removed*) and problem went away.
- We were using the wrong saddle.
- Believe failures were due to poor tapping procedure.
- About 1 failure per year and we don't know what we are doing wrong, if anything.
- Had numerous failures from 1987 to 1990, switched from pressure taps to wet taps and changed specification for filler content, have had no problems in last 2 years.

- Four percent of the utilities reported 70 percent of the catastrophic tapping failures.

The 67 utilities were also asked about training provided for technicians who make the taps. Fifty-nine of the 67 (88 percent) said they had some sort of apprentice training with an experienced individual, and mostly on an informal basis. Five out of the 67 (7 percent) said they contracted all tapping to an outside contractor. Only three of 67 (4 percent) said their training had a formal component which involved some classroom-type instruction.

As stated above, all 67 of the utilities in the original survey that reported any catastrophic tapping failures were included in the resurvey. Thus, the catastrophic tapping failure data given here are representative of the entire 162-utility database. Shown in Fig. 7.28 is the number of catastrophic tapping failures by year. The data in the graph for 1992 are for one-half year only. Tapping failures were definitely decreasing with time.

Length of time for problems to occur. Utilities were asked: "Of all problems experienced in your system with AWWA C900/C905 PVC pipe, estimate the percentage that has occurred within each of the following

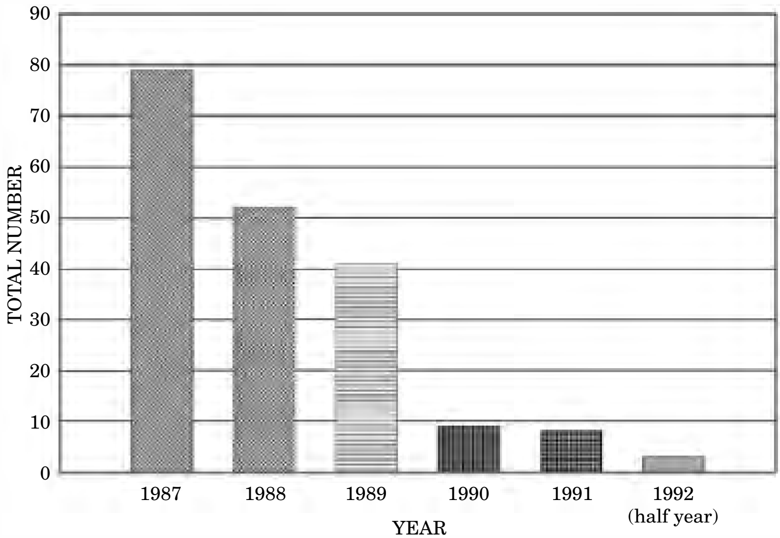

Figure 7.28 Number of reported catastrophic tapping failures by year.

age brackets." Figure 7.29 gives the average responses. About 45 percent of the problems occur in the first year, with lesser percentages in subsequent years.

Exposure to ultraviolet light. Question 25 asked: "Have you experienced any PVC water pipe problems that could be directly related to exposure to ultraviolet light?" About 10 percent indicated they had experienced some problem. Specific comments indicate that most of these problems had not occurred in the recent past. Utilities were generally aware that PVC pipe will sunburn if exposed to direct sunlight for a sufficient time. PVC pipe should be shielded if the exposure to direct sunlight is in excess of 2 years (*Handbook of PVC Pipe,* 1991).

Question 27 asked: "Have you experienced any problems with PVC water pipe being delivered sunburned?" And question 28 asked, "If PVC pipe is delivered with discoloration from sunburn, do you use it?" The results of these questions are presented in Fig. 7.30.

Exposure to aggressive chemicals and problems attributed to a particular manufacturer. Question 30 asked: "Have you experienced any PVC water pipe failures or complaints that could be directly related to exposure to aggressive chemical environment and/or permeation?" Question 31 asked: "Have you experienced defects or deficiencies in PVC water pipe that can be attributed to a particular type of PVC pipe and/or manufacturer?" Responses are given in Fig. 7.31.

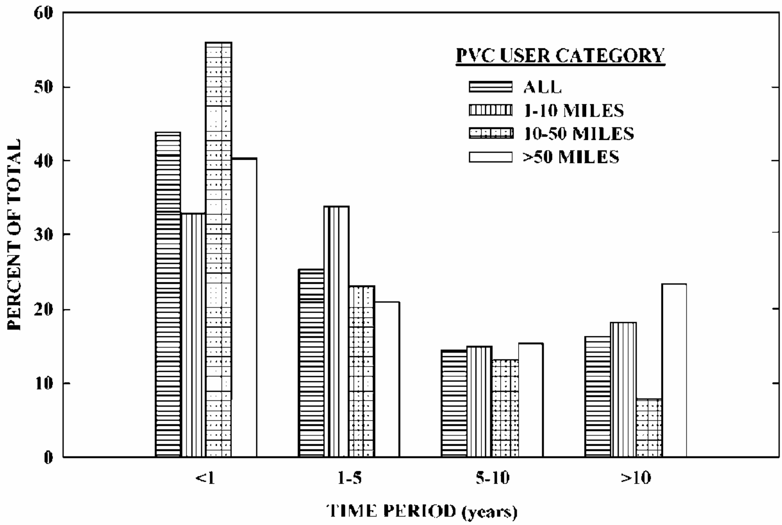

Figure 7.29 When problems were experienced with AWWA C900/C905 PVC pipe.

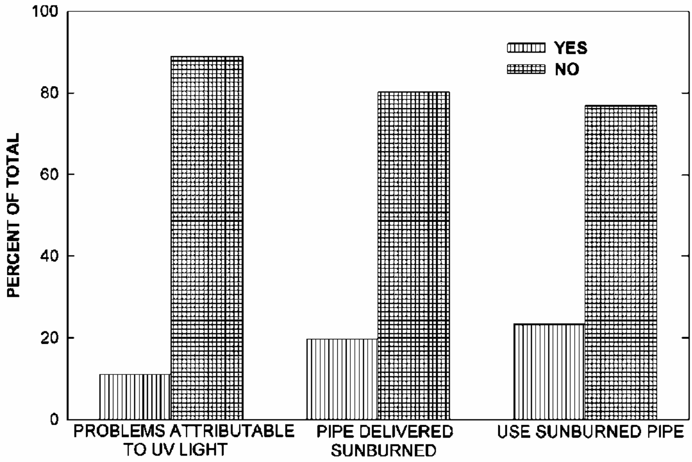

Figure 7.30 Percent negative and percent positive responses to questions 25, 27, and 28.

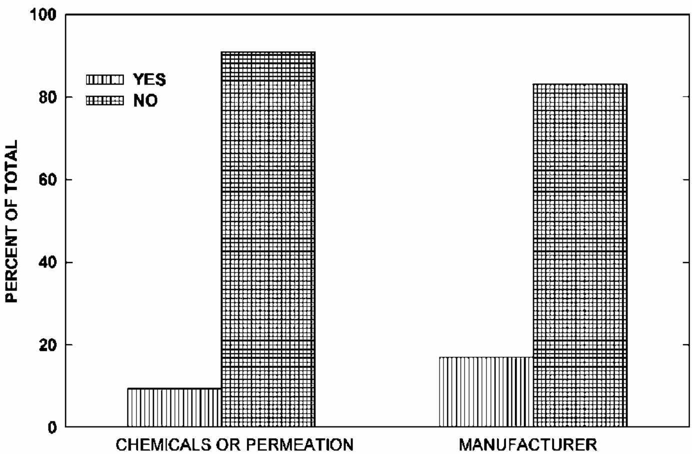

Figure 7.31 Percent negative and percent positive responses to questions 30 and 31.

Eleven of the 162 utilities indicated some problem with permeation. The questionnaire did not ask the respondent to differentiate between permeation of the pipe wall and permeation of the rubber gasket. Subsequent follow-up found that 1 of the 11 had problems with polybutylene, not PVC; 2 of the 11 had only heard of problems in other utilities and had not had personal experience; and 1 utility had problems with low-head irrigation pipe. This left only 7 utilities of the 162 (4 percent) that claimed actual experience with permeation of PVC water pipe. This is a fairly low percentage and is an indication that permeation is not a major problem for PVC pipe. This is consistent with works of others on permeation of PVC. See Thompson and Jenkins[54] and Berens.[9] Also see the Uni-Bell *Handbook of PVC Pipe Design and Construction.*[58]

Problems attributed to aging of PVC. Data were given in Fig. 7.29 on problems as a function of time after installation for AWWA C900/C905 pipe only. Figure 7.32 shows combined data for all PVC pipe. Figure 7.33 compares the data given in Fig. 7.29 for AWWA pipe with those given in Fig. 7.32 for all PVC users. There is little difference in the two sets of data. This may be due to the predominance of AWWA C900/C905 users in the database.

It is evident that the problem rate decreases as a function of time after installation. If the pipe material were degrading as it aged, one would expect just the opposite trend in the data (i.e., the problem rate should increase with time). This is consistent with previous studies on the aging of PVC. Moser and Shupe[42] indicate that they found no

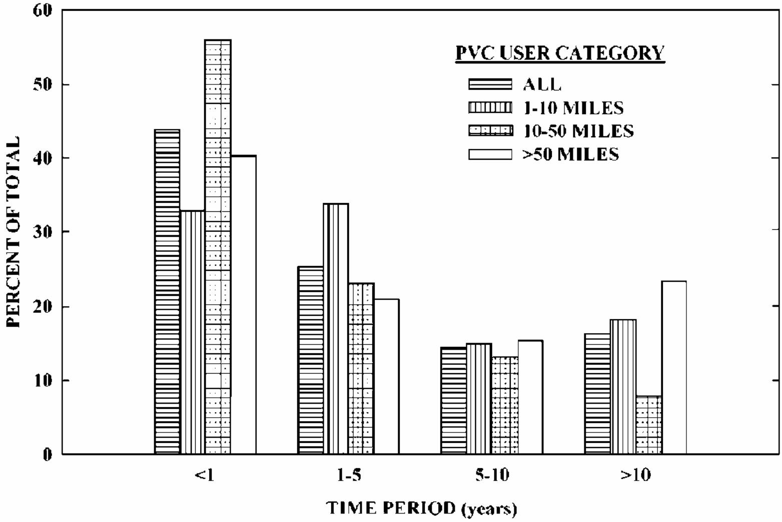

Figure 7.32 When problems occurred for various user groups (includes both AWWA and ASTM pipe).

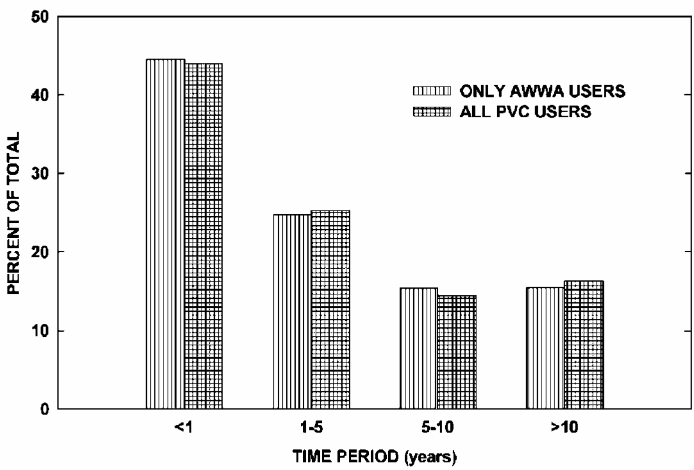

Figure 7.33 Reported problems as function of elapsed time after installation. Figure compares AWWA C900/C905 with all PVC.

degradation in properties in PVC pipe that had been installed for 15 years. This was also reported by Bauer[8] who said, "PVC pipe's ability to perform has not changed over 15 years and all indications suggest it will not change in the foreseeable future."

In the original survey, 22 utilities reported a significant number of problems occurring more than 5 years after installation. These utilities were selected for a detailed follow-up phone survey concerning long-term performance of PVC pipe. *Long-term* as used in this context refers to pipe that has been in service for at least 5 years. Performance items of interest included joint problems, pressure-related problems (breaks), and problems associated with tapping. Real or perceived problems associated with the inability to locate buried PVC pipe and problems resulting from future excavation around the pipe are not considered to be performance-related and were not addressed in the follow-up phone calls.

Of the 22 utilities selected for additional long-term information, 13 utilities, or 59 percent, reported no performance-related long-term problems. The problems reported by these 13 utilities in the original survey were long-term, but were not pipe-related.

This left 9 utilities that did report performance-related problems. One of the 9 was dropped from the analysis, as all the reported problems for that utility occurred within the first to fifth year of service. The 8 remaining utilities provided information about the types of problems they were experiencing, number of problems in the 5-year period, the length of time in service of the pipe, and whether the frequency of the problems was increasing, decreasing, or remaining static. Long-term problems were classified in three broad categories (joint problems, pressure problems, and tapping problems). The joint classification includes all long-term problems that can be directly associated with the joint (for example, joint leakage) that can be attributed to the aging of the pipe. The tapping classification as used here is for tapping problems that are perceived to occur on a more frequent basis as the PVC pipe ages. The pressure classification includes all other long-term problems such as breaks and leaks, other than joints and tapping, that can be attributed to the aging of the PVC pipe. Shown in Fig. 7.34 is a breakdown of the reported problems by type. Three utilities reported having joint problems, three utilities reported having pressure-break problems, and two utilities reported both joint and pressure problems. None of the utilities experienced any tapping problems related to aging.

Figure 7.35 shows the total number of occurrences reported over the 5-year period for each problem type. In the 5-year period, there were more than 3 times as many pressure-related problems as there were joint-related problems reported. The large majority of the data in this figure was supplied by one utility, and for that reason this figure is biased and is not representative of the balance of the utilities surveyed.

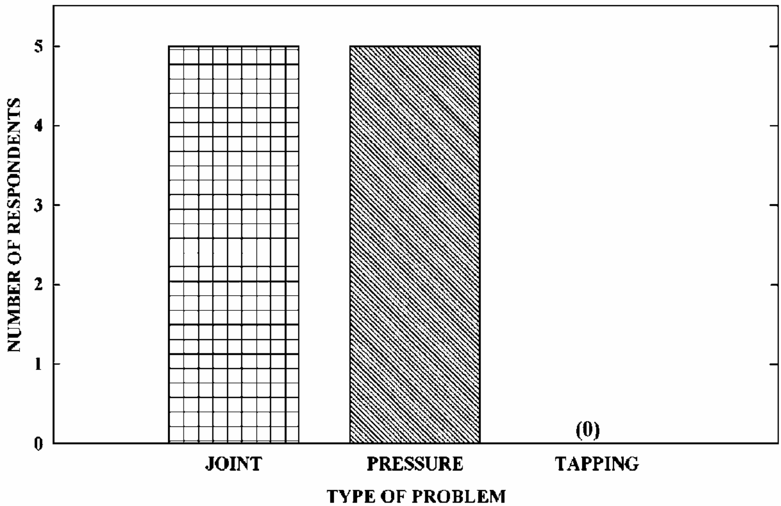

Figure 7.34 Number of respondents reporting various long-term problems.

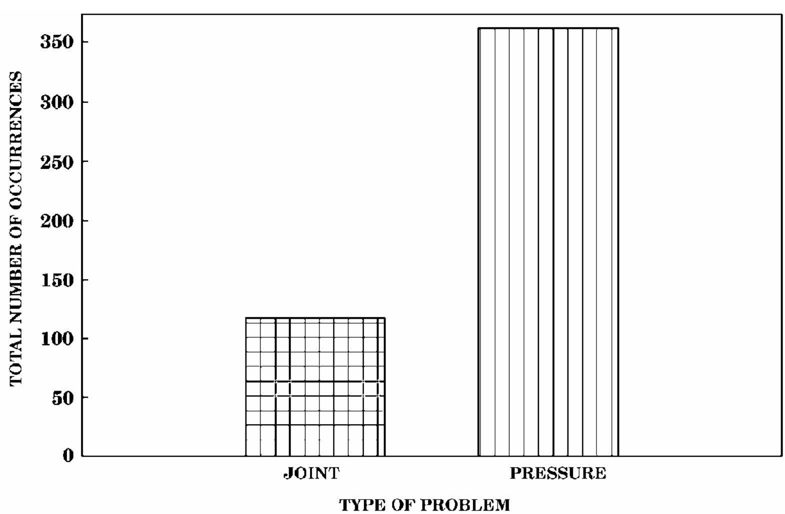

Figure 7.35 Tally of number of reported occurrences of joint and pressure problems over the 5-year period.

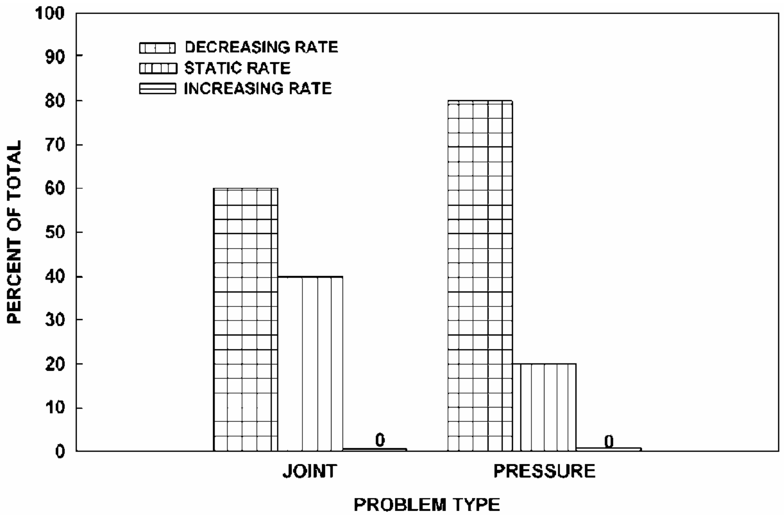

Figure 7.36 Indication of whether long-term problems are increasing, decreasing, or remaining static with respect to time.

The utility manager admitted that his water system was out of control with large repetitive pressure surges (see utility 166 in Table 7.13).

Figure 7.36 provides an indication as to whether the reported problems seem to be increasing, decreasing, or remaining static. The interesting thing to note is that none of the utilities stated that their problems were increasing with time. Table 7.13 gives a summary of reported long-term problems.

Linkage of aging of PVC with specific problems. Utilities were asked about problems with respect to elapsed time after installation. The results of this question for various subgroups were analyzed for any indication that aging may be either a cause or related to certain problems. Figure 7.37 compares the results shown in Fig. 7.29, which was for all AWWA PVC users, to a subgroup who answered yes to question 25 concerning problems with ultraviolet light exposure. The same type of comparison is made in Fig. 7.38 for a subgroup who answered yes to the question "Do you use sunburned pipe?" Figure 7.39 also makes a comparison of data concerning elapsed time for problems to occur with a subgroup who answered yes to question 30 concerning exposure to aggressive chemicals. The data shown in Fig. 7.29 are compared with data from a subgroup who answered yes to question 31, having to do with problems with a particular type of PVC pipe or a particular manufacturer (see Fig. 7.40). There seems to be little or no link between these problems and the

TABLE 7.13 Summary of Reported Long-Term Problems with PVC Pipe

Utility no./ problem type	No. in last 5 years	Average time in service, yr	Is rate increasing or decreasing?	AWWA or ASTM	Pipe size, in	Pipe manu-facturer	Testing samples available	Details
Utility 19								
Joint	5	15–20	Static	AWWA	6	?	No	No correlation between problem and pipe proximity to pumps and valves
Bedding	2–3 per year	15–20	Decreasing	AWWA	6	?	No	Problem with poor bedding not pipe's fault
Utility 26								
Joint	Not sure	5–8	Decreasing	ASTM CL 160	2	?	No	Problems w/glue joints, not rubber ring, usually class 160 pipe; don't use glue joints anymore
Utility 48								
Joint	4	10	Static	AWWA	6, 8	?	No	Not near any pumps or valves; pipe deflected around inlet box
Utility 51								
Pressure	10–15	10	Decreasing	ASTM	2	A	No	Pipe in proximity of pump station; pressure 190–250 lb/in^2; pipe is class 200
Bedding	2	10	Decreasing	ASTM	2	A	No	Problem with digging down and hitting pipe; is brittle and breaks; soil has pH of 6.5, class 200
Utility 103								
Pressure	10	<5	Decreasing	AWWA	80%, 6 20%, 8	?	Yes	Bad soil conditions; pipe had defect
Joint	20	1–5 per year	Decreasing	AWWA	80%, 6 20%, 8	?	Yes	Problem occurs when joint is made between PVC and some other type of pipe

TABLE 7.13 Summary of Reported Long-Term Problems with PVC Pipe (*Continued*)

Utility no./ problem type	No. in last 5 years	Average time in service, yr	Is rate increasing or decreasing?	AWWA or ASTM	Pipe size, in	Pipe manu-facturer	Testing samples available	Details
Utility 151								
Pressure	65	5–6	Decreasing	?	10	?		Pipe laid on Coquinia rock (coral-like) when combined with water hammer rubbed weak spot
Utility 156								
Pressure	<5	8	Static	ASTM	6, 8	?	Call	Problem with ASTM class 200, not C900; thinks due to old-age brittleness
Utility 163								
Pressure	5–8	10–30	Decreasing	ASTM C 1160	6, 8	B	No	Believes problem due to manufacturer and class 160 pipe
Joint	<8	10–30	Decreasing	?	8	?	No	Problems with slip joint; not sure of cause; came and went in 1 year (probably personnel)
Utility 166								
Pressure	250–300	6–18	Decreasing	ASTM C 1200	6, 8	A	Yes	Could be due to changes in pressure; varies from 20–200 lb/in^2
Joint	100	6–18	Decreasing	ASTM C 1200	6, 8	?	Yes	Problem occurs around bell and spigot; lots of surges, system unstable

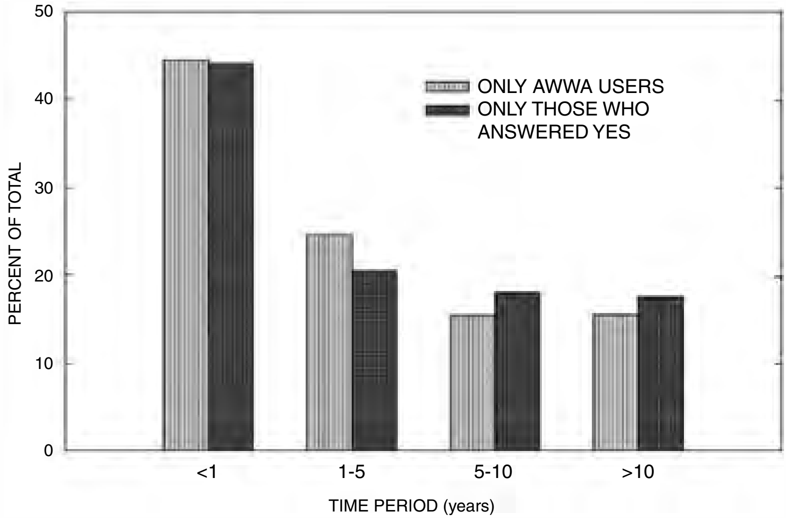

Figure 7.37 When PVC pipe problems occurred—a comparison of those who have experienced problems due to exposure to ultraviolet light with AWWA C900/C905 PVC pipe users.

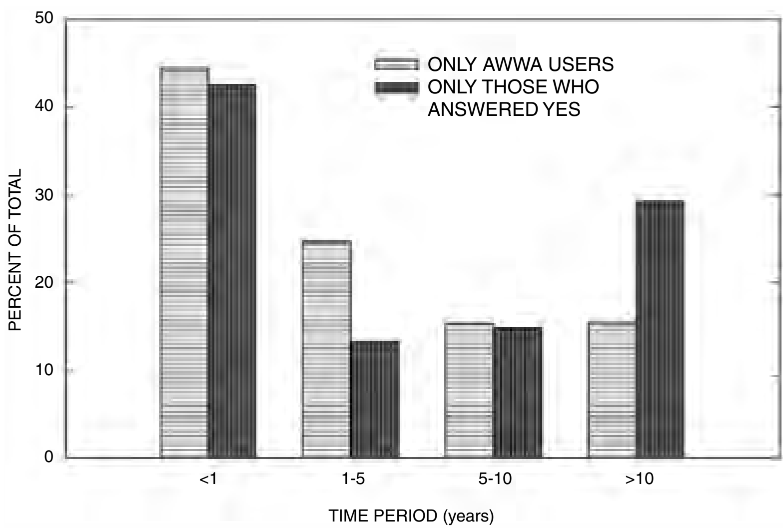

Figure 7.38 When PVC pipe problems occurred—a comparison of those who reported using sunburned pipe with AWWA C900/C905 PVC pipe users.

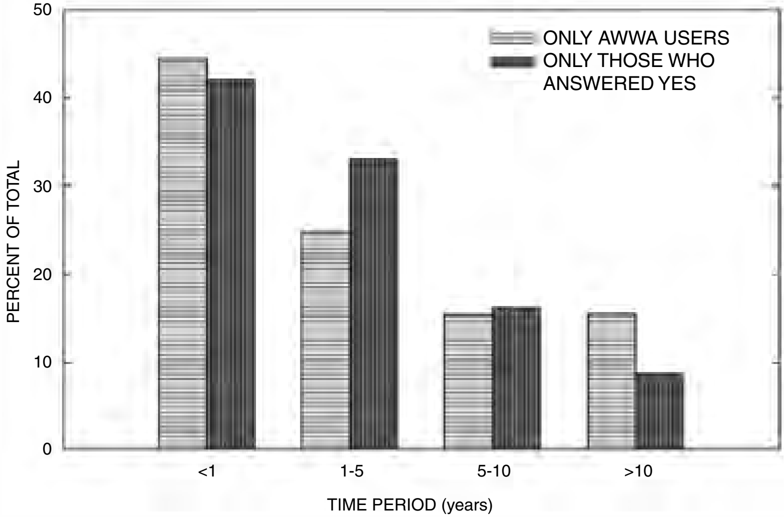

Figure 7.39 Comparison of when pipe problems occurred for AWWA C900/C905 PVC pipe users with those who reported problems with aggressive chemicals.

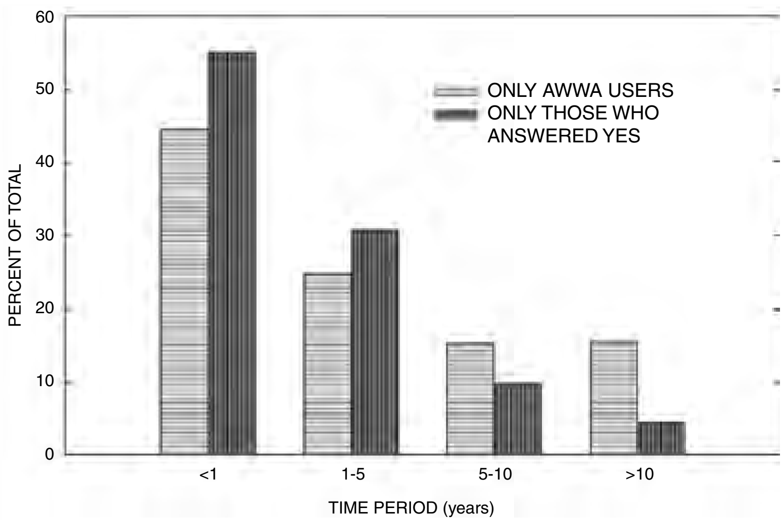

Figure 7.40 Comparison of when pipe problems occurred for AWWA C900/C905 PVC pipe users with those who reported problems with a particular manufacturer.

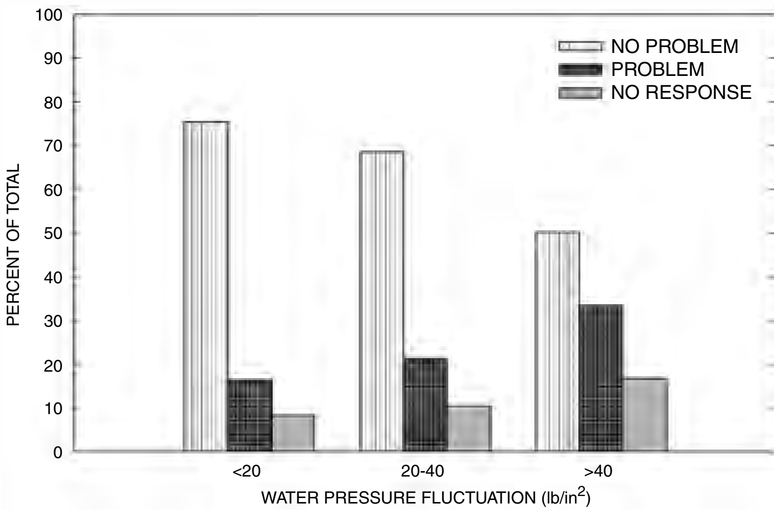

Figure 7.41 A comparison of water pressure fluctuation and whether the respondents consider problems due to water hammer and/or transient pressure to be either a problem or not a problem.

age of the pipe, with one exception—the group who answered yes to the question "Do you use sunburned pipe?" has more problems with pipe older than 10 years. However, the data may not be statistically valid since each subgroup is small. Also, there is no direct link with a particular problem in a specific length of pipe and the age of that length of pipe.

Water hammer. Data from a question concerning water hammer problems were linked with data from the question concerning system pressure variations. Results are given in Fig. 7.41.

Testing of pipe samples supplied by utilities. The extent to which a field sample is useful depends to a large degree upon the documentation provided by the utility supplying the sample. Efforts were made to identify the manufacturer, date of manufacture, etc., on each pipe sample. In some cases, this information could not be determined.

Each of the utilities involved in the follow-up phone survey was asked if it could provide PVC pipe samples for testing. The intention was to obtain as many pipe samples as possible from those utilities reporting long-term problems and those utilities having numerous catastrophic tapping failures. These pipe samples were to be taken from pipes where actual problems had been experienced. Extreme difficulty was experienced in obtaining samples of actual pipe that had experienced problems. For the most part, the utilities indicated that such pipe samples were no longer available, but they would call us if new problems occurred. A genuine reluctance on the part of most utilities to contribute pipe samples for testing was sensed. The reasons for this resistance are unknown, but one reason may be they were not sure of anonymity. Another possibility is that they were concerned with what the results might show. However, two utilities supplied pipe samples for testing. Results of these tests are included in this book.

Selected utilities who had reported problems were then asked to supply samples of PVC pipe they were currently installing. These samples were representative of PVC pipe that was currently being delivered to the utilities and of PVC pipe that was being manufactured. Sixteen utilities from throughout the United States responded with samples. The samples included pipe from 10 separate manufacturers.

Test methods. The pipe samples were subjected to the following three tests to determine basic composition and extrusion quality.

1. A degree of fusion test: The procedures and limitations prescribed in ASTM D 2152 were followed.
2. An impact test: This test procedure is as prescribed in ASTM D 2444 along with the standards described in ASTM D 2241.
3. Filler content test(s): The filler content was determined by one or both of the following test methods. (Cell class information is given in ASTM D 1784.)
   a. A burnout test which consists of weighing a sample of pipe, approximately 1 in square, burning the sample for a sufficient length of time to burn off the resin, and then weighing the residue to obtain the amount of filler.
   b. Specific gravity (density) was determined by weighing samples in air and then determining volume by displacement of a liquid.

Tests on samples of problem pipe. As stated above, only two utilities supplied pipe samples from “problem pipe.” All pipe from utility 70 was manufactured and installed in the 1970 to 1972 time frame and was from a single manufacturer. This utility is one of the largest users of PVC pipe in the United States, with several hundred miles of PVC pipe installed. The utility manager was certain that this was inferior pipe because of continued problems with it over the years. The failure rate was decreasing with time, but simply because the problem pipe was gradually being replaced.

The second utility (utility 166) to supply problem pipe samples indicated some problems, but did not have as long a history for the particular pipe samples in question. The samples provided were also from a single manufacturer, but no date markings were evident on the samples so the date of manufacture is not known.

Table 7.14 summarizes the results of tests performed on pipe samples from these two utilities. The filler content is provided as percent by weight and by parts by weight. The parts-of-filler listing is based on 100 parts of PVC resin. As can be seen, samples provided by utility 70 are of questionable quality. The 2- and 3-in pipe samples have too much filler, and the 4-, 6-, and 8-in samples are of poor fusion quality. It appears that these pipes may have been extruded on a twin-screw machine with low heat on one side of the extruder. Samples from utility 166 that passed the acetone test have little or no filler content and generally appear to be okay.

Tests on new samples of PVC pipe (never installed). PVC pipe samples were received from 16 utilities, representing 10 manufacturers, and in diameters ranging from 2 to 12 in. All samples passed the fusion quality (acetone) test. The filler content can be resolved approximately by determining the density of the sample. This method is not as accurate as a burnout test, but is simpler to run and is much safer from an environmental point of view. In determining filler content from a density test, the possible error is on the order of ±2 percentage points. For example, if the filler content as calculated from the density test is determined to be 5 percent, the actual percentage of filler could range from 3 to 7 percent. Burnout tests were run only where there was some question in results as determined from the density tests or where the filler content, as calculated, appeared to be abnormally high. Filler content for pressure pipe should be under 10 parts by weight, which is about 9 percent by weight. Results from these tests are given in Table 7.15.

A test specimen from each sample of pipe supplied by the utilities was prepared and tested to the energy level specified in ASTM D 2241. While there is no impact strength called out for AWWA C900/C905 pipe, it was decided to impact the samples to the energy level for the specific diameter as listed in ASTM D 2241. The results of these tests are given in Table 7.15. Of the 60 samples impact-tested, all except 4 survived without any indication of structural distress. Many of the PVC pipe samples that were supplied by utilities were sunburned to some degree. The four samples that failed the impact test were severely sunburned and probably failed for that reason.

Conclusions

1. Almost 50 percent of problems that are experienced with PVC pipe occur in the first year after installation.
2. Material-related long-term problems occurring in PVC pipe are few and are decreasing with time. This is an indication that these problems are not a result of aging.

TABLE 7.14 Laboratory Test Results for Pipes with Reported Problems

Utility no.	Acetone tests: Pipe size, in	Acetone tests: Sample ID	Acetone tests: Attack/no attack	Filler content tests: Pipe size, in	Filler content tests: Sample ID	Filler content tests: % by weight	Filler content tests: % by parts
70	2	70-2-1A	No attack	2	70-2-1F	15	18
					70-2-2F	17	20
					70-2-3F	14	16
					70-2-4F	14	15
	3	70-3-1A	No attack	3	70-3-1F	9	10
					70-3-2F	9	9
					70-3-3F	8	9
	4	70-4-1A	Attack	4	70-4-1F	9	10
					70-4-2F	9	11
					70-4-3F	7	8
	6	70-6-1A	Attack	6	70-6-1F	8	9
					70-6-2F	8	9
					70-6-3F	8	9
	8	70-8-1A	Attack	8	70-8-1F	5	5
					70-8-2F	11	12
					70-8-3F	8	9
166	6	166-6-1A	No attack	6	166-6-1F	0	0
	6	166-6-2A	No attack	6	166-6-2F	0	0

TABLE 7.15 Laboratory Test Results on Samples of Pipe Currently Being Installed by Utilities

Utility no.	Pipe diameter, in	Pipe manuf.	Spec./class	Passed acetone test	Filler content percent by weight	Passed impact test
115	4	A	C900/150	Yes	5	Yes
	6	A	C900/?	Yes	2	No
	8	?	C900/150	Yes	2	Yes
	10	A	C900/150	Yes	1	Yes
	12	A	C900/150	Yes	1	Yes
138	2	C	D 2241/200	Yes	1	Yes
	4	B	D 2241/200	Yes	15	Yes
	6	B	C900/150	Yes	6	Yes
	8	B	C900/200	Yes	6	Yes
	10	A	C900/150	Yes	6	Yes
	12	A	C900/150	Yes	7	Yes
6	6	E	C900/150	Yes	2	Yes
	8	E	C900/150	Yes	3	Yes
	12	E	C900/150	Yes	4	Yes
64	6	F	C900/150	Yes	3	Yes
	8	F	C900/150	Yes	3	Yes
	12	F	C900/150	Yes	3	Yes
20	2	G	D 2241/200	Yes	3	Yes
	4	F	C900/200	Yes	5	Yes
	6	E	C900/200	Yes	2	Yes`
	8	B	C900/200	Yes	5	Yes
	12	A	C900/200	Yes	7	Yes
150	4	A	C900/150	Yes	4	No
	6	A	C900/150	Yes	4	No
	8	A	C900/150	Yes	6	Yes
	10	A	C900/150	Yes	6	Yes
	12	A	C900/150	Yes	3	Yes
60	4 (A)	H	C900/150	Yes	3	Yes
	4 (B)	A	C900/150	Yes	4	Yes
	6	A	C900/200	Yes	3	Yes
	8	H	C900/200	Yes	1	Yes
	10	A	C900/150	Yes	5	Yes
	12	H	C900/200	Yes	0	Yes

TABLE 7.15 Laboratory Test Results on Samples of Pipe Currently Being Installed by Utilities (*Continued*)

Utility no.	Pipe diameter, in	Pipe manuf.	Spec./class	Passed acetone test	Filler content percent by weight	Passed impact test
25	6	B	C900/150	Yes	4	Yes
	8	B	C900/150	Yes	3	Yes
	12	B	C900/150	Yes	4	Yes
85	6	E	C900/150	Yes	2	Yes
	8	E	C900/150	Yes	0	Yes
	12	E	C900/150	Yes	3	Yes
70	2	C	D 2241/200	Yes	4	Yes
	3	I	D 2241/200	Yes	3	Yes
	4	C	D 2241/200	Yes	0	Yes
	6	J	D 2241/200	Yes	4	Yes
160	2	A	D 2241/160	Yes	3	Yes
	4	E	C900/150	Yes	2	No
	6	A	C900/150	Yes	5	Yes
	8	A	C900/150	Yes	5	Yes
50	6	F	C900/150	Yes	3	Yes
	8	F	C900/150	Yes	5	Yes
40	6	F	C900/150	Yes	5	Yes
	8 (A)	F	C900/150	Yes	7	Yes
	8 (B)	F	C900/150	Yes	4	Yes
7	2	B	D 2241/200	Yes	1	Yes
	6	B	D 2241/200	Yes	3	Yes
79	6	H	C900/200	Yes	2	Yes
	8	A	C900/200	Yes	2	Yes
151	6	?	D 2241/160	Yes	6	Yes
	8 (A)	D	D 2241/160	Yes	3	Yes
	8 (B)	?	D 2241/160	Yes	4	Yes
	10	F	D 2241/160	Yes	3	Yes

3. An analysis of reported data shows that the chance of any problem's occurring in PVC water pipe is about twice as high for pipe manufactured to the ASTM D 2241 standard as for pipe manufactured to the AWWA C900 standard.
4. Reported experiences with problems associated with exposure to ultraviolet light or aggressive chemicals are low in number.
5. Tapping problems associated with PVC pipe are decreasing with time as utilities gain more experience. Of those utilities reporting catastrophic tapping failures in the 5-year period, only about 27 percent reported having, on average, more than one failure per year. In addition, approximately 80 percent of those utilities reporting catastrophic failures felt they had solved their tapping problems and have not had any failures in the 2-year period just before the survey. It was determined that the majority of pipe tappers learn tapping procedures through an informal apprenticeship program.
6. Some utilities require the use of saddles for tapping of PVC pipe and feel that this requirement reduces tapping problems. However, an analysis of data indicates that utilities requiring the use of saddles reported, on average, about the same number of problems as those using direct tapping.
7. PVC pipe being installed was determined to be of high quality.
8. Some samples of PVC pipe manufactured in the 1970s were of poor quality as determined by the acetone test for extrusion quality. (*Note:* This conclusion is based on results from a small sample of pipe from a single utility and from only one manufacturer. Thus, this conclusion should not be generalized. Also, all other PVC pipe samples were determined to be of high quality.)

Polyethylene (PE) Pipes

Polyethylene used to manufacture pipe is available in several types and grades per ASTM D 1248. Some grades of polyethylene may crack or craze when subjected to certain levels of stress or when in contact with certain chemicals. This degradation is usually accelerated when high stresses and certain chemicals act simultaneously. This phenomenon is known as environmental stress cracking. Certain grades are highly resistant to stress cracking. Type III, class C, category 5, grade P34 polyethylene is a high-density, weather-resistant, stress-crack-resistant material (Table 7.16).

Polyethylene pipes are available in various sizes and wall configurations for varied applications, some of which are listed in Table 7.17. Other sizes for specific applications may be available from a particular manufacturer. See Table 7.18 for polyethylene standards.

TABLE 7.16 Polyethylene Design Properties

Hydrostatic-design basis (HDB)	1250 lb/in^2
Hydrostatic-design stress (HDS)	625 lb/in^2
Elastic modulus	100,000 lb/in^2
Tensile stress (short-time)	3200 lb/in^2
Hazen-Williams coefficient *C*	150
Manning's coefficient *n*	0.009

TABLE 7.17 Polyethylene Pipes

Application	Type	Size range, in
Industrial (includes gas)	Solid wall	$^3/_4$–48
Water (new service)	Solid wall	$^1/_2$–3
Water (insertion)	Solid wall	$^1/_2$–4
Gravity sewer (lining)	Solid wall	4–48
Gravity sewer	Profile (ribbed) wall	18–96

TABLE 7.18 Standards for Polyethylene

ASTM D 3287	Biaxially Oriented Polyethylene (PEO) Plastic Pipe (SDR-PR) Based on Controlled Outside Diameter
ASTM D 3261	Butt Heat Fusion Polyethylene (PE) Plastic Fittings for Polyethylene Plastic Pipe and Tubing
ASTM D 405	Corrugated Polyethylene Tubing and Fittings
ASTM D 3197	Insert-type Polyethylene Fusion Fittings for SDR 11.0 Polyethylene Pipe
ASTM D 2609	Plastic Insert Fittings for Polyethylene Plastic Pipe
ASTM D 2104	Polyethylene Plastic Pipe, Schedule 40
ASTM D 2239	Polyethylene Plastic Pipe (SIDR-PR) Based on Controlled Inside Diameter
ASTM D 3350	Polyethylene Plastics Pipe and Fittings Materials
ASTM F 714	Polyethylene Plastic Pipe (SDR-PR) Based on Outside Diameter
ASTM D 3035	Polyethylene Plastic Pipe (SDR-PR) Based on Controlled Outside Diameter
ASTM D 2447	Polyethylene Plastic Pipe, Schedules 40 and 80, Based on Outside Diameter
ASTM D 2737	Polyethylene Plastic Tubing
ASTM F 771	Polyethylene Thermoplastic High-Pressure Irrigation Pipeline Systems
ASTM D 2683	Socket-Type Polyethylene Fittings for Outside Diameter-Controlled Polyethylene Pipe and Tubing
ASTM F 810	Smooth-Wall Polyethylene Pipe for Use in Drainage and Waste Disposal Absorption Fields
ASTM D 1248	Polyethylene Plastics Molding and Extrusion Materials
AWWA C901	Polyethylene Pressure Pipe, Tubing and Fittings, $^1/_2$ in through 3 in, for Water

Many of the larger-diameter gravity sewer polyethylene pipes have pipe stiffness $F/\Delta y$ of 10 lb/in^2 and some even lower than 4 lb/in^2. Extreme care must be taken during installation of these low-stiffness pipes because of the possibility of overdeflection and buckling due to soil load.

Handling factor

Ring stiffness, the pipe's ability to resist ring deflection, is a function of EI/D^3 (see Chap. 3). Some literature promoting polyethylene pipe gives EI/D^2 as the property which is a measure of the pipe's resistance to deflection. This idea has absolutely no theoretical or experimental basis, and if used in the design of a pipe installation could be the direct cause of pipe overdeflection or collapse.

The term EI/D^2, called *handling stiffness,* is sometimes used to rate the ease of handling without damage. The inverse of this factor, $D^2/(EI)$, is called the *flexibility factor* and is used by the corrugated-steel pipe industry to rate handling flexibility. These factors arise from a bending strain consideration as follows:

$$\text{Bending strain} = \frac{Mc}{EI} = \frac{C_1\,(PD)\,(D/2)\,(t/2)}{EI}$$

where
C_1 = a constant
P = pressure
D = diameter
PD = vertical load
$D/2$ = moment arm
$t/2$ = half-wall thickness
I = wall moment of inertia
E = modulus of elasticity

One can easily see that $D^2/(EI)$ is a factor in the above equation. Thus bending strain for a given pressure is directly proportional to this factor. The inverse of this factor is a measure of the particular product's ability to resist bending strain. Of course, ring deflection is not a direct function of $D^2/(EI)$, but is a direct function of $D^3/(EI)$. It matters not what causes the deflection-handling, installation, concentrated loads, or soil pressure—the deflection is still a function of $D^3/(EI)$, not $D^2/(EI)$. Also buckling, whether hydrostatic or due to soil pressure, is a function of $D^3/(EI)$. Thus, $D^2/(EI)$ or EI/D^2 should not be used in design calculations, nor should this factor be used to classify a pipe's stiffness characteristics for deflection control.

Example 7.12—A 150 lb/in^2 polyethylene pipe Calculate the required dimension ratio (DR) for a polyethylene pressure pipe. The maximum working pressure is 150 lb/in^2, no surge is anticipated, and the safety factor is to be 2.5.

solution

1. Calculate the hydrostatic-design stress:

$$\text{HDS} = \frac{\text{HDB}}{\text{safety factor}}$$

$$\text{HDB} = 1250 \text{ lb/in}^2$$

$$\text{HDS} = \frac{1250}{2.5} = 500 \text{ lb/in}^2$$

2. Calculate DR, using Eq. (7.7):

$$\text{DR} = \frac{2\sigma}{P} + 1$$

where

$$\sigma = \text{HDS}$$

$$\text{DR} = \frac{2\,(500)}{150} + 1 = 7.67$$

Select the next-lower available DR:

$$\text{DR} = 7.0$$

Example 7.13—A 6-in pressure sewer pipe It is proposed to use 6-in polyethylene pipe for a pressurized sewer line. The maximum pressure including surge is 50 lb/in^2, and the maximum depth of cover is 20 ft. (*a*) Select the proper wall thickness. (*b*) What requirements will be necessary concerning pipe-zone soil type and compaction? (Use safety factor = 2.0, OD = 6.625, and deflection limit = 5 percent.)

solution For part (*a*),

1. Hydrostatic-design stress equals HDB/safety factor.

$$\text{HDS} = \frac{\text{HDB}}{2.0} = \frac{1250}{2} = 625 \text{ lb/in}^2$$

2. Use Eq. (7.7) to calculate the dimension ratio:

$$\text{DR} = \frac{2}{P} + 1$$

$$= \frac{2\,(625)}{50} + 1 = 26$$

$$= 26 = \frac{\text{OD}}{t}$$

$$\text{Thickness } t = \frac{\text{OD}}{\text{DR}} = \frac{6.625}{26} = 0.25 \text{ in}$$

For part (*b*),

1. Determine pipe stiffness $\dfrac{F}{\Delta y}$:

$$\frac{F}{\Delta y} = \frac{6.7EI}{r^3}$$

where $E = 100{,}000 \text{ lb/in}^2$

$$I = \frac{t^3}{12} = \frac{(0.25)^3}{12}$$

$$r = \text{mean radius} = \frac{\text{OD} - t}{2} = 3.19 \text{ in}$$

So

$$\frac{F}{\Delta y} = \frac{(6.7)\,(100{,}000)\,(0.25/3.19)^3}{12} = 27 \text{ lb/in}^2$$

2. Use Spangler's equation to find required soil modulus E' [see Eq. (7.4)].

$$E' = \frac{0.56\text{H}/\,(\Delta y/D) - \text{PS}}{0.41}$$

where PS = pipe stiffness = $F/\Delta y$, so

$$E' = \frac{0.56\,(20)\,/\,(0.05) - 27}{0.41} = 480 \text{ lb/in}^2$$

Thus, a granular soil compacted to at least 85 percent Proctor density will be required in the pipe zone (see Table 3.4).

Example 7.14—A 96-in storm sewer pipe A 96-in storm sewer pipe is to be installed. The deepest cut will require 14 ft of cover. A profile-wall polyethylene pipe is to be considered. The wall moment of inertia I of this proposed PE pipe equals 0.524 in^4/in. The pipe is to be installed in such a manner that the resulting vertical deflection is less than 5.0 percent. (1) Calculate the pipe stiffness $F/\Delta y$. (2) If selected, how should this particular type of pipe be installed? (3) Comment on the suitability of the proposed pipe for this application.

1. Calculate pipe stiffness.

$$\frac{F}{\Delta y} = \frac{6.7EI}{r^3}$$

where $E = 100{,}000 \text{ lb/in}^2$
$I = 0.524 \text{ in}^4\text{/in}$
$r = 96/2 = 48 \text{ in}$

So

$$\frac{F}{\Delta y} = \frac{(6.7)\,(100{,}000)\,(0.524)}{(48)^3} = 3.17 \text{ lb/in}^2$$

Note: This is a very low value—pipe will be extremely flexible.

2. For the design installation, use Spangler's equation to calculate the required E'.† [See Eq. (7.4).]

$$E' = \frac{0.56H/(\Delta y/D) - \text{PS}}{0.41}$$

$$= \frac{0.56H/0.05 - 3.17}{0.41} = 374 \text{ lb/in}^2$$

It can be determined from Table 3.4 that for $E' = 374 \text{ lb/in}^2$, a granular material compacted to at least 85 percent Proctor density is required. It appears that this particular pipe can be made to work under tightly controlled installation conditions. For pipes with such low stiffnesses, buckling due to soil load is much more likely. This failure mode is discussed in detail in Examples 7.16 and 7.17.

3. Because pipe stiffnesses below 10 lb/in² offer little inherent resistance to deflection, the pipe ring may need to be braced internally while the soil around the pipe is placed and compacted. After the required soil density is obtained, the braces (stills) may be removed. For plastic pipe, bracing may penetrate the pipe wall unless the bracing is carefully designed and positioned. Because of the above concerns, this pipe should be selected only if the above concerns can be addressed. Also, a granular material compacted to at least 85 percent standard Proctor density should be specified for the pipe zone.

†*Note:* This equation is derived directly from Spangler's Iowa formula. The Iowa formula is not accurate for very low pipe stiffnesses. Test data at Utah State University indicate that this equation is nonconservative for a pipe stiffness $F/\Delta y = 10 \text{ lb/in}^2$ and may not be appropriate for $F/\Delta y = 3.17$. A quick examination of the above equation will show that it cannot hold in the limit as pipe stiffness approaches zero since it indicates a 0 lb/in² pipe will perform essentially the same as, say, a 10 lb/in² pipe. Thus, the above equation can be used for pipe stiffness of 10 lb/in² and higher. The error involved is a function of other parameters as well as pipe stiffness. However, the error is within acceptable limits for pipe stiffnesses of 10 lb/in² or greater. Pipes with 3.17 lb/in² pipe stiffness have virtually no inherent strength and stiffness compared with soil. Thus, the pipe in this example should be installed in a well-compacted granular material.

Long-term ductility of polyethylene materials

Introduction. Plastic pipes derive their outstanding performance characteristics from their ability to deform and transfer the earth load to the surrounding soil. The design rationale is based on its ductility—its ability to undergo localized strains and deformations without cracking or structural failure. This is true for all thermoplastics and is especially true for polyethylene.

A principal advantage of thermoplastic piping for buried applications is that it allows for the pipe-soil interaction which stabilizes and strengthens buried pipe; it safely reduces stress concentrations; it facilitates handling and installation; it simplifies product and installation design; and it results in more forgiving and durable installations. Design protocols and construction recommendations for thermoplastic buried piping have been developed on the assumption of ductile behavior. Standards for thermoplastic piping include material and product requirements intended to ensure that the product is made from materials with high strain capacity.

Ductility. Ductile materials are able to tolerate marked deformation before failure. This allows for the redistribution and possible reduction of stresses. Thus, ductile structures can safely shed stress concentrations. Designs using ductile materials can be based on average stress and, therefore, can be greatly simplified. On the other hand, designers using brittle materials must anticipate the maximum strains and stresses and know the points at which they act. By necessity, brittle materials require design procedures that are more complex.

Engineers who design piping systems are well aware of the better performance of ductile iron pipe over the old gray cast iron pipe. Ductile iron pipe is a flexible pipe, and installation demands are less stringent. The better performance characteristics are directly attributable to ductility. Engineers are also aware that more ductile, milder steels have simpler design procedures that usually result in improved field performance when compared to higher-strength, more brittle steels. Ductile structures are more forgiving in regard to stresses that are often not considered by designers. Such stresses include, but are not limited to, those induced by improper handling and installation and those locked in during the manufacturing process.

Ductile—but not always. A designer would like to use a material whose properties are known and do not change with time. Some polyethylene pipes have been reported to have failed in a brittlelike manner at low strain levels. This transformation from a ductile to a brittlelike material is the consequence of the formation and propagation of slowly growing cracks. For these cracks to initiate, the PE material must have a crystalline structure. The more crystalline the structure, the easier it is for the cracks to initiate. The transition from the ductile to the brittlelike state results in not only lower longer-term strain capacity, but also lower longer-term strength and less endurance to cyclic stressing.

For nonpressure pipes, it is possible for cracks to form and grow to such extent as to eventually compromise the infiltration and exfiltration requirements on the pipe and may also destroy the structural integrity of the pipe-soil system. The possibility of the development and continued growth of cracks in a pressure pipe is usually unacceptable, particularly when the pipe is carrying a dangerous material such as natural gas.

PE materials used to manufacture pipes must offer adequately high resistance to crack initiation and propagation. PE polymer materials are partially crystalline and partially amorphous. Density and molecular weight have tremendous influence on the properties of the particular polyethylene. The reader should understand that high molecular weight and high density are not the same thing, nor are they always mutually beneficial. Higher-density polyethylene materials are more crystalline in structure, which results in higher stiffness, tensile strength, and hardness. Increases in these properties are often considered beneficial. However, these benefits are accompanied by decreases in toughness, impact strength at lower temperatures, and long-term crack resistance. One may somewhat compensate for these losses by increasing the molecular weight of the PE. The downside of increasing the molecular weight is a simultaneous increase in the melt viscosity. Manufacturers of pipe are concerned because high melt viscosities mean the ease of processability is diminished, and it becomes more difficult to manufacture pipe. The challenge is to balance density and molecular weight to offer long-term ductility, and resistance to stress cracking, and still be able to process the material into a pipe.

To meet this challenge, resin suppliers have copolymerized ethylene with small amounts of other monomers. Extreme care must be taken by polymer chemists because experience has shown that such copolymers can become more crystalline with time. The rate in the process in moving away from an amorphous structure to a crystalline structure is a function of temperature. This is more of a concern for commercially available PE polymers (compared to simple homopolymers such as PVC) because of the greater diversity in the molecular structure. For PVC, it is possible to fairly precisely link basic polymer characteristics such as density, molecular weight, and melt viscosity with resultant mechanical properties, such as strain capacity and long-term strength.

The percentage of elongation in a tensile test is commonly used as a measure of ductility for metals. However, it is well known that even ductile materials can fail at low strains and in a brittlelike fashion if subjected to a multiaxis stress field and if a small material flaw (crack) is present. With this said, it is still important to understand that the more ductile the pipe material, the more "forgiving" will be the end product. Thus, for materials like PE, it is necessary to have test requirements for ensuring that only materials of adequate long-term strain capacity are used for buried piping, whether it be intended for pressure or nonpressure uses.

Such a test will only determine properties of the material at the time of the test. Therefore, there must also be some assurance that the material will not become more crystalline with time and thus make a transition from ductile to brittle behavior. For PE materials the testing required is by no means a simple matter because ductility can be compromised by slow-acting crack initiation and crack growth.

The ESCR test

In 1959, ASTM standard test method D 1693 was issued. Soon after, an environmental stress crack resistance (ESCR) criterion was added to the ASTM specification for the classifying of PE compositions. Other PE specifications followed based on the ESCR test. The ESCR test is imprecise and is recognized as giving only a rough measure of long-term crack resistance. The bent-strip ESCR test has never been adopted for the defining of minimum crack resistance requirements for the pipe material. Instead, industry adopted the hydrostatic-design basis requirement to ensure adequate strength (which also takes into account the adequacy of long-term crack resistance). HDB-rated resins are required for pressure pipe.

The HDB requirement for PE

PE materials that pass the HDB requirement when manufactured into pipe will perform well. This is true for both pressure and nonpressure applications. However, the HDB requirement excludes materials from nonpressure uses with lower but quite adequate long-term crack resistance.

The procedure by which the HDB method excludes materials of low crack resistance may be described by referring to Fig. 7.42. This figure depicts the characteristic stress-rupture behavior for PE pipe at ambient temperature which results in two zones: an initial zone of gradual regression of rupture strength with increased time to fail (in which the pipes fail by ductile yielding) and a zone of more rapid regression of strength (where failures are small brittlelike slits with no evidence of

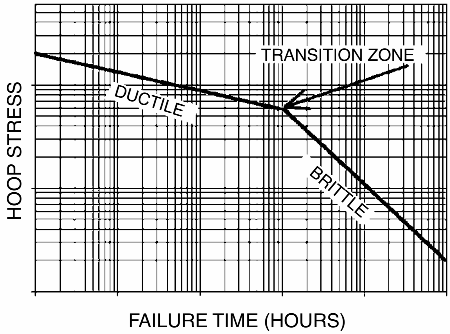

Figure 7.42 Schematic of stress regression for PE pipe.

any yielding). The later this transition occurs, the more resistant the material is to crack initiation and growth. In 1986, a requirement was added to ASTM D 2837. This new requirement stated that no HDB may be awarded to a PE unless it is demonstrated (through a specially devised elevated-temperature test protocol) that the transition from ductile to brittlelike zone in the stress-rupture properties occurs beyond 100,000 h. While this requirement has resulted in very strong assurance of permanence of ductility, it is believed by some to be too demanding to apply in the case of PE materials used in gravity pipe.

The NCTL test

There is an obvious need for a fairly simple and quick test that gives a reliable relative measure of a PE pipe's capacity to safely tolerate sustained straining. Dr. Grace Hsuan of Drexel University has reported on a research program to find such a test. A preliminary evaluation indicates that an ASTM method, the notched constant tensile load (NCTL) test, can fulfill this need. This evaluation also shows that this test can be used on PE materials containing postconsumer (i.e., recycled) resins. The ASTM D 5397 (NCTL) test was developed to evaluate the stress crack resistance (SCR) of medium-density polyethylene geomembranes. The test is performed using notched dumbbell specimens under constant tensile stress in a controlled-temperature surface active solution.

Dr. Hsuan states the following:

> Unfortunately, this test also requires a relatively long testing time to obtain the full NCTL stress rupture characterization curve, typically on the order of a few weeks. Thus it is not well suited for a MQC test. However, an abbreviated version of the test has been developed based on a single point evaluation, hence it is referred to as a SP-NCTL test. Because stress cracking is caused by the slow crack growth mechanism,

the most important part of the ductile-to-brittle curve is the brittle region. A single value of selected stress at any value below the transition stress can be used. This single point test drastically shortens the overall testing time and can be applied as a MQC test.

Dr. Hsuan also reported on the utilization of postconsumer resins (PCRs). The primary concern is the effects on long-term performance of material. This obviously includes the stress crack resistance (SCR). She incorporated into her study the influence of PCR on SCR of virgin PE resins. A single PCR was blended with two virgin resins in fractions of 25, 50, and 75 percent. The two types of virgin resins used were blow molding grade HDPE and PE 3408. The SCR of the blended and virgin materials was evaluated using the SP-NCTL test at 10 percent yield stress. Figures 7.43 and 7.44 show the failure times corresponding to the PCR fraction in the blends. The failure time decreased as the amount of PCR increased in both sets of blends.

As is evident from Dr. Hsuan's research, the SP-NCTL test, which is relatively simple and quick to conduct, can be used to establish the long-term crack resistance of a PE. Additional research still needs to be done to establish a suitable empirical correlation between the SP-NCTL test results and field performance of PE pipe. Also the use of postconsumer resins in the manufacture of PE pipe could lead to long-term crack failures.

Structural performance of buried profile-wall HDPE pipe

HDPE profile-wall pipes. Manufacturing techniques make it possible to provide smooth liners for corrugated or profile-wall polyethylene

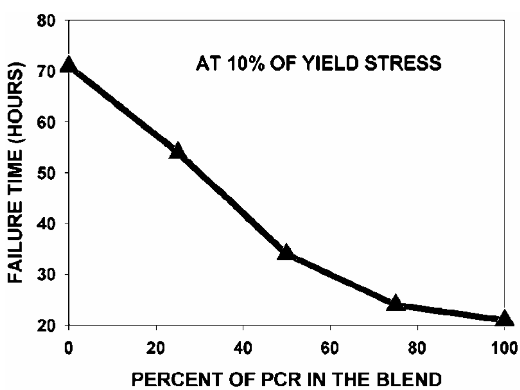

Figure 7.43 Effect of PCR on the blow molding grade of HDPE resin. (*From Hsuan.*[24])

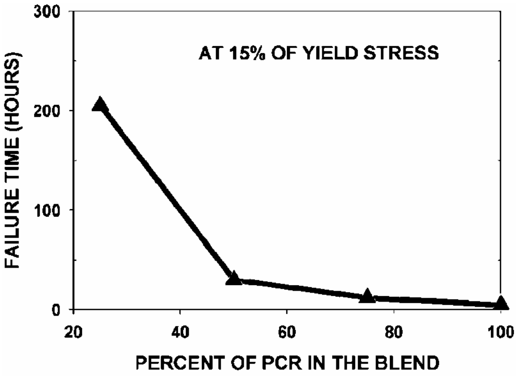

Figure 7.44 Effect of PCR on the HDPE 3408 resin. (*From Hsuan.*[24])

pipes. The ribbed profile wall adds ring stiffness to the pipe to maintain the cross-sectional shape during installation and to support the soil overburden. The plastic wall has a very low frictional resistance for improved flow characteristics. Also, the plastic wall provides most of the longitudinal stiffness of the pipe.

Full-scale testing. Analytical methods for predicting performance of buried pipes use empirical constants to make them work[13,18,22,29,61]—all require experimental investigation to determine the unknown constants. The full-scale testing procedure has been used with great success at various research laboratories such as those at Utah State University, the U.S. Bureau of Reclamation, and Ohio University. Data obtained in this manner can be used directly in the design of pipe-soil systems and in the prediction of overall performance. The possibility of buckling, overdeflection, and wall crushing is evaluated simultaneously by actual tests. No attempt to explain the pipe-soil interaction phenomenon is necessary in the use of this method, and the end results leave nothing to be estimated on the basis of judgment. In the collection of test data, a pipe is installed in a manner similar to that used in practice, and the height of cover is increased until performance levels are exceeded. The use of empirical curves or data eliminates the need to determine the actual soil pressure since the pipe performance as a function of height of cover is determined.

Profile of the pipe wall. Profile-wall pipes are designed and manufactured to minimize the use of material by increasing the section modulus of the pipe wall. The concept of a profile-wall pipe is not new, since corrugated steel pipe is truly a profile-wall pipe and has been available for many years. Some of the newer plastic pipe products are of this type. Many of these products have been shown to perform with the profile section acting as a unit as designed. For adequate safety for any such product, the design should include sufficient plastic between the inner and outer walls and/or between the ribs to carry shear and to ensure that the profile section indeed acts as a unit. Also, the cross-sectional area per unit length and the individual wall component thickness should be sufficient to resist localized buckling.

The most important parameters for flexible pipe analysis and design are (1) load, (2) soil stiffness, (3) pipe stiffness, and (4) profile design.[37] Any design method that does not include a consideration of these parameters is incomplete. For many flexible pipes, vertical deflection is the variable that must be controlled by proper installation design. Deflection is a function of the first three parameters discussed above. Note that controlling vertical deflection may not control localized buckling as a performance limit.

Test results. Tests on profile-wall polyethylene pipes were conducted to provide information on performance. A list of the tests that were performed is given in Table 7.19.

Procedure. High-density polyethylene pipes were tested at Utah State University (USU). The objective of the tests was to determine structural performance characteristics as a function of depth of cover. The observed parameters (dependent variables) were ring deflection and any visual evidence of distress. The independent variables were soil type, soil density (compaction), and the vertical soil load simulating a high soil cover.

The basic soil type was silty sand and is designated as a class III soil by ASTM D 2321. This soil is classified as SM according to the Unified Soil Classification System. The maximum dry density (T-99) is 124.8 lb_m/ft^3 (1997 kg/m^3), and the optimum moisture is 9.5 percent. SM soil is used because it is common, it is of lesser quality than most soils specified as backfill (and so is a worst-case test for most installations), and it can be compacted over a wide range of soil densities.

These tests permitted an investigation of the performance limits of the pipes subjected to external soil pressures. Tests were performed in the USU large soil cell into which the sample pipe is buried and onto which a vertical soil load is applied by means of 50 hydraulic cylinders (see Fig. 7.55).

The large pipe test cell has 10 loading beams with 5 cylinders on each beam for a total of 50 hydraulic cylinders. These cylinders (rams) provide the vertical load on the soil simulating an embankment condition. Figure 7.45 shows a steel-ribbed HDPE pipe being installed in the soil test cell.

TABLE 7.19 Overall Test Results

Test data				Local buckling		General buckling	
Test number	Manu-facturer	Diameter, in	% Proctor density	Cover, m	Deflection, percent	Cover, m	Deflection, percent
X-1	X	48	95	10.4	2.0	21.0	6.0
X-2	X	48	75	6.7	6.5	10.4	9.0
X-3	X	48	85	5.8	3.0	14.0	8.7
X-4*	X	48	85	10.4	5.5	15.8	9.8
X-5	X	60	94	20.0	5.3	32.0	12.2
X-6	X	60	85	16.0	6.5	22.0	11.7
Y-1	Y	48	75	8.5	10.0	10.4	13.1
Y-2	Y	48	85	8.8	5.0	18.0	11.5
Y-3	Y	48	96.5	36.6	3.5	55.0	6.3

*Double-thickness liner.

Figure 7.45 Test pipe being placed in test cell.

Test X-1. A 48-in-diameter pipe with a single-thickness liner was placed in soil compacted to 95 percent of standard Proctor density. At 10.4 m of cover and about 2 percent vertical deflection, a dimpling pattern on the inside wall became noticeable to the eye. This pattern, which is the beginning of localized buckling, started at about the 2 and 10 o'clock positions. The center distance between dimples was about the same as the external rib spacing. This pattern was somewhat checkerboard in appearance and, of course, just the beginning of localized instability of the thin inner wall.

General buckling of the wall at the 3 and 9 o'clock positions began at 21 m of cover. As the load was increased, general buckling became more pronounced. Buckling of a pipe in soil is not like classical buckling. In classical buckling, once the critical load is reached, catastrophic failure is imminent. However, for a buried pipe, it normally takes another increment of load to produce another increment in the buckling phenomenon. Loading was terminated at 30 m of cover. Data for this test are given in Fig. 7.46.

Test X-2. In test X-2, a pipe with a single-thickness liner was installed in soil compacted to 75 percent of standard Proctor density. At 6.7 m of cover and about 6.5 percent vertical deflection, local buckling, as described in test X-1, began to form. At 34 ft of cover, general

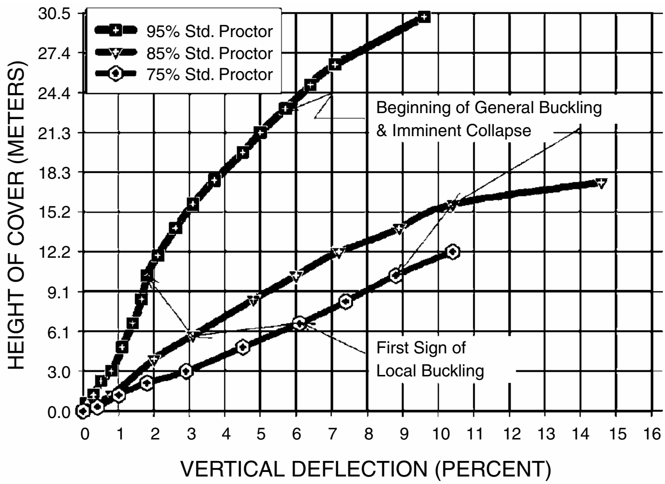

Figure 7.46 Data for tests X-1, X-2, and X-3.

buckling of the wall began at the 3 and 9 o'clock positions. Loading was terminated at 12.2 m of cover as general buckling was extremely pronounced. Data are shown in Fig. 7.52.

Test X-3. In this test, a 48-in-diameter pipe with a single-thickness liner was installed in soil compacted to 85 percent of standard Proctor density. Local buckling began to form at 5.8 m of cover and about 6 percent vertical deflection. At 14 m of cover, general buckling of the wall began at the 3 and 9 o'clock positions. Buckling became more pronounced as cover was increased from 14 m. Loading was terminated at 17.7 m of cover as general buckling was extremely pronounced. Data for this test are given in Fig. 7.46.

Test X-4. In test X-4, the test setup was the same as that of test X-3 except the 48-in-diameter test pipe had a double-thickness liner. The soil was compacted to 85 percent of standard Proctor density. Local buckling, as described in test X-1, began to form at 10.4 m of cover and about 5.5 percent vertical deflection. This buckling became more pronounced as the soil load was increased and moved toward the 3 and 9 o'clock positions. General buckling (hinges in the pipe wall) began to form at the 3 and 9 o'clock positions at 15.8 m of cover. Loading was terminated at 17.7 m of cover as general buckling was pronounced. Figure 7.46 also shows graphically the importance of soil density in controlling the pipe deflection. Figure 7.47 compares data for the pipe with the double-thickness liner to data from the pipe with the single-thickness liner. It is interesting to note that the first visual indication of local buckling

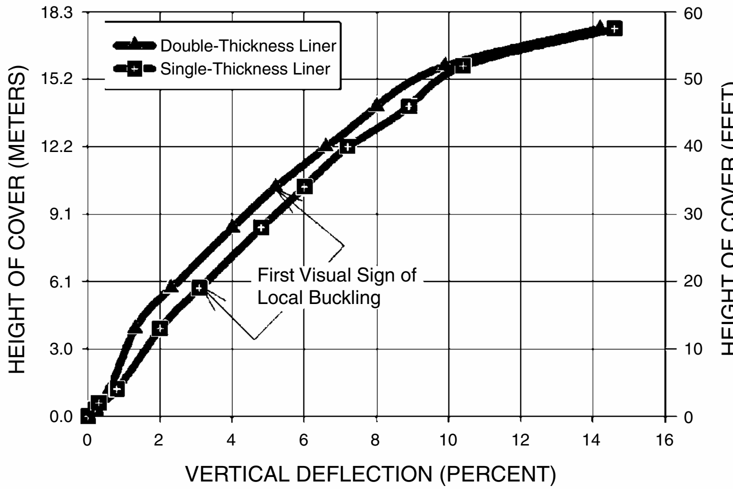

Figure 7.47 Data for test X-4 and a comparison with test X-3.

took place at 10.4 m of cover, but for the single-thickness liner pipe (test X-3) local buckling took place at only 5.8 m of cover.

Test X-5. A 60-in-diameter pipe was placed in soil compacted to 94 percent of standard Proctor density. At 20 m of cover and about 5.3 percent vertical deflection, a dimpling pattern on the inside wall became apparent (see Fig. 7.48). This pattern, which is the beginning of localized buckling, started at about the 2 and 10 o'clock positions. The center distance between dimples was about the same as the external rib spacing. This dimpling became more pronounced as the height of cover was increased and spread toward the crown and the 3 and 9 o'clock positions. The dimpling formed a waffle pattern at 25 m of cover. Such a pattern is typical in classical wall buckling in pressure vessels. This waffling pattern is somewhat checkerboard in appearance and is just the beginning of instability of the pipe wall. Also, a slight flattening was noted at the 8 o'clock position. Figure 7.49 shows the waffling pattern and some localized buckling.

General wall buckling became apparent as the vertical cover approached 32 m. At 34 m of cover, the top of the pipe began to form an inverse curvature which is considered to be general buckling of the pipe wall. The pipe could not maintain the imposed load of 34 m of cover, and the test was terminated. Data for this test are given in Fig. 7.50.

Test X-6. In this test, a 60-in-diameter pipe was installed in soil compacted to 85 percent of standard Proctor density. At 16 m of cover, local

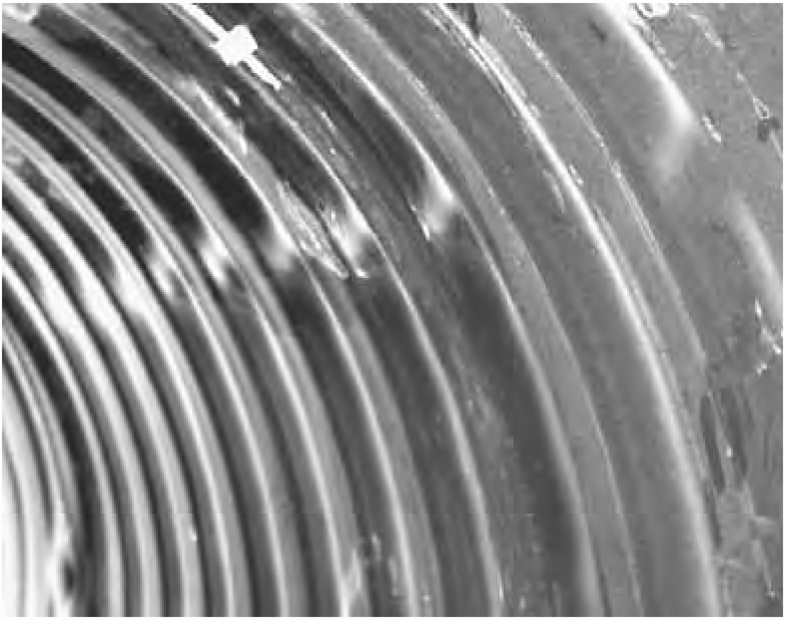

Figure 7.48 Test X-5, inception of dimpling (18 m of cover).

buckling began at about the 3 o'clock position. As the vertical load was increased, this spread to the 2 o'clock position. The buckling formed a waffling pattern at 18 m of cover. The pipe wall began to buckle on the east side of the pipe at 22 m of cover. General wall buckling occurred at the crown of the pipe at 23 m of cover. The pipe could not sustain this load, and the test was terminated (see Fig. 7.51).

Test Y-1. A 48-in-diameter pipe was placed in soil compacted to 75 percent of standard Proctor density. A dimpling pattern on the inside wall became noticeable to the eye at 8.5 m of cover and at about 10 percent vertical deflection. A hinge line in the wall began to form at the 3 and 9 o'clock positions at 10.4 m of cover. This hinge line (crease) is due to high compression stresses produced by a combination of ring compression, ring bending, and localized buckling. As the load was increased from 10.4 m of cover, this hinge became more pronounced (see Fig. 7.52 for data).

Test Y-2. A 48-in-diameter pipe was installed in soil placed at 85 percent of standard Proctor density. At about 5.8 m of cover and about 3 percent vertical deflection, the weld/ribbing began to become pronounced (more visible). Small dimples began to form near the 3 and 9 o'clock positions at about 8.8 m of cover and about 5 percent deflection.

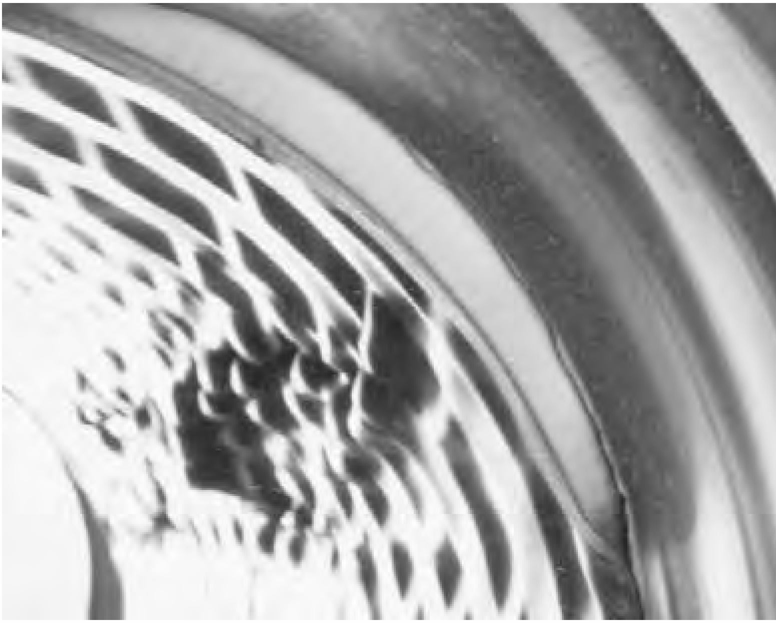

Figure 7.49 Test X-5, waffling pattern and local buckling (25 m of cover).

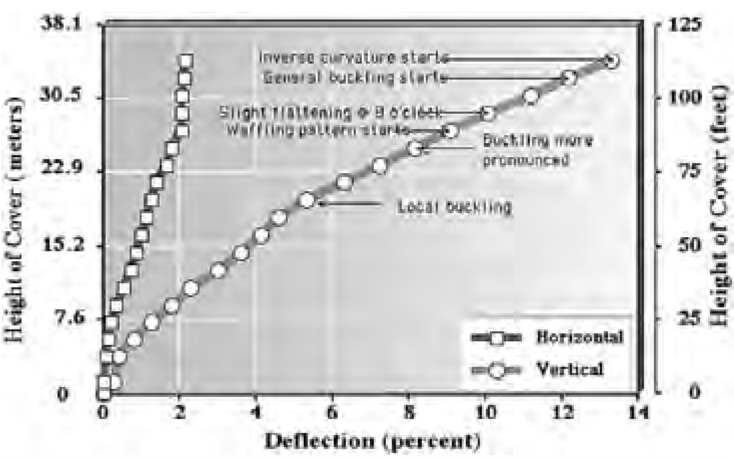

Figure 7.50 Test X-5, 60-in-diameter HDPE pipe tested in silty-sand soil compacted to 94 percent of standard Proctor density.

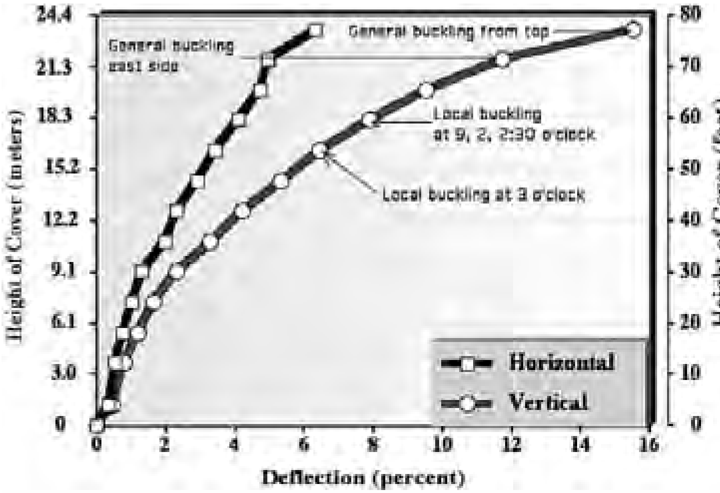

Figure 7.51 Test X-6, 60-in-diameter HDPE pipe tested in silty-sand soil compacted to 85 percent of standard Proctor density.

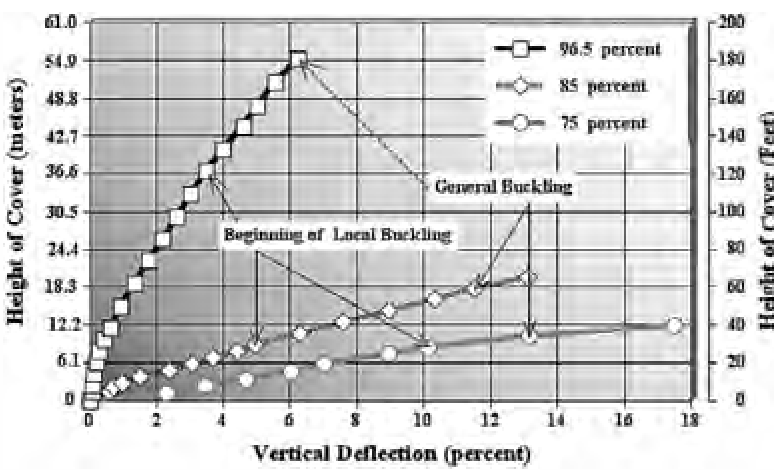

Figure 7.52 Data for tests Y-1, Y-2, and Y-3; vertical pipe deflections for the three soil densities tested.

At 18 m of cover, a hinge (crease) began to form in the wall at the 9 o'clock position (west side). Loading was terminated at 19.8 m of cover. Data for this test are given in Fig. 7.52.

Test Y-3. This 48-in-diameter pipe was placed in soil at 96.5 percent of standard Proctor density. The weld/ribbing became visually noticeable at 18.9 m of cover and about 1.35 percent vertical deflection. A slight dimpling pattern began at 36.6 m of cover. General localized buckling of the wall began at the 3 and 9 o'clock positions at 55 m of cover (see Fig. 7.52). This shows graphically the importance of soil density in controlling the pipe deflection.

Comments on test results. Noteworthy is the high load that can be applied without distress to the pipe ring. Clearly the pipes deflect more (for the same load) in loose soil than in dense soil because loose soil compresses more. From a structural point of view, there are no reasons why high-density polyethylene pipes cannot perform well. The soil should be granular and carefully compacted if the pipe is buried under high soil cover or under heavy surface loads. Granular pipe-zone backfill material at moderate to high densities ensures that the pipes will perform well even at high earth covers.

The load at which localized buckling occurs is primarily due to ring compression stress and is some function of soil density. At this point it is not totally clear what is the exact role of soil density in preventing buckling. It is clear that pipes installed in soils at high densities will support higher loads without buckling. However, in the range of 75 to 85 percent standard Proctor, the effect of soil density is not clear.

General wall buckling in these tests was considered the upper performance limit. The height of cover at which general wall buckling takes place is as low as 10.4 m for lower-density soils. However, the height of cover for generalized wall buckling can be as high as 55 m for well-compacted soils.

The pipe cross sections started out circular and became elliptical as the height of cover increased. None of the test pipes exhibited a so-called squaring or a square shape at any load. For polyethylene, which has a fairly low modulus, ring compression stresses cause circumferential ring shortening. This ring shortening is small for pipes installed with low heights of cover and in low to moderately compacted soils. For high-density soils at high earth covers, this circumferential ring shortening is very significant and is the primary deformation that takes place. This circumferential shortening is extremely beneficial in the performance of the pipe. The decrease in circumference relieves the pipe ring of some of the soil pressure and causes the surrounding granular pipe-zone material to carry a higher percentage of the load. This works on exactly the same principle as the slotted bolthole in corrugated metal pipe. In a very large measure, the pipes in these tests were able to withstand high loads because of substantial circumferential shortening that took place.

HDPE pipes with a steel rib. In another design, a polyethylene profile section is wound helically to form the pipe; then a steel rib is also wound helically, interlocking mechanically with the profile section of the polyethylene. The result is a polyethylene pipe with an external steel rib. In this design, the steel rib is much stiffer than the plastic. Thus, in ring deflection, the steel rib carries most of the load. When buried in soil, polyethylene relaxes with time if the ring configuration is held constant. In good backfill, for a given height of cover, the soil does hold the pipe in a constant cross section; so the polyethylene experiences stress relaxation, and the steel rib carries essentially all the load on the pipe. In addition, the composite pipe (steel and HDPE) is flexible so the soil takes a large share of the vertical load. The statically indeterminate soil-structure interaction is mutually beneficial. The pipe serves as a form for the soil arch, and the soil supports and protects the pipe against vertical loads by arching action of the soil. The steel rib stiffens the pipe and helps to maintain the cross-sectional shape during backfilling. However, for a HDPE pipe with a steel rib, catastrophic failure is possible if the pipe is subjected to a load sufficient to cause either yielding or buckling in the steel rib.

Test C-1. A 1900-mm steel-ribbed HDPE pipe was installed in soil compacted to 87 percent of standard Proctor density. Audible sounds were heard, indicating a slipping of the steel with respect to the plastic at 8.5 m of cover. Yielding of the steel may have been taking place. A slight bulging was noted near the 3 and 9 o'clock positions at about 10.4 m of cover. As the vertical load was increased, this bulging increased. Localized buckling occurred at 15.5 m of cover. At 18 m of cover, general wall buckling was evident, the pipe began to collapse, and the test was terminated. For results, see Fig. 7.53.

Test C-2. A 2000-mm pipe was installed in soil compacted to 86 percent of standard Proctor density. Audible sounds were heard, indicating a slipping of the steel with respect to the plastic at 10.4 m of cover. Yielding of the steel may have been taking place. Local wall buckling was noted, and the joint liner buckled at about 14 m of cover. General buckling occurred at the top of the pipe at 15.8 m of cover. At 17.7 m of cover, the pipe could no longer sustain the load, and the test was terminated (see data in Fig. 7.53).

Test C-3. A 2000-mm pipe was installed in soil compacted to 91 percent of standard Proctor density. Localized buckling began near the 5 and 7 o'clock positions at 12.2 m of cover. At about 14 m of cover, local

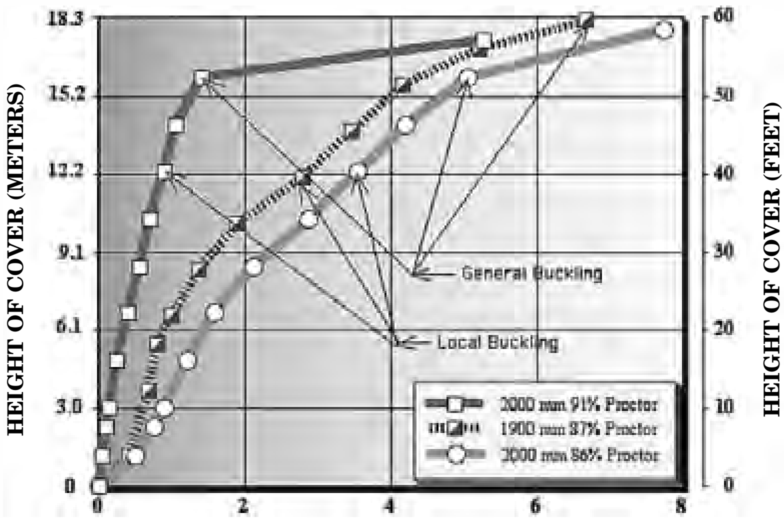

Figure 7.53 Data for tests C-1, C-2, and C-3; vertical deflections and buckling.

wall buckling at the 5 and 7 o'clock positions became more pronounced. This buckling became more prominent as the vertical load was increased. General buckling began near the 2, 3, 9, and 10 o'clock positions at 15.9 m of cover. At 17.4 m of cover, the pipe could no longer sustain the load, and the test was terminated (see data in Fig. 7.53).

The steel-ribbed pipe behaves essentially the same as a low-stiffness corrugated metal pipe. This is because the steel rib is much stiffer than the polyethylene material. The higher-stiffness steel essentially carries all the load. Thus, the behavior of the steel rib is essentially the behavior of the pipe. The load-deflection curves for the steel-ribbed pipes do not resemble curves for other plastic pipe; rather, they resemble curves for low-stiffness corrugated metal pipes. For example, for polyethylene pipes, the horizontal deflection is substantially less than the vertical deflection (see Fig. 7.50). On the other hand, for steel-ribbed pipe, the horizontal and vertical deflections are close to being equal up to the point where the pipes begin to fail (see Fig. 7.54). This is the way a metal pipe behaves. Also, in the tests of plastic pipe, signs of distress at the 5 to 7 o'clock positions do not occur. However, on the steel-ribbed pipe, localized buckling took place on the invert section of the pipe. Tests of corrugated metal pipe installed in highly compacted soil show this same type of behavior. Also, failure is much more catastrophic in the steel-ribbed polyethylene than in either corrugated steel or HDPE (i.e., collapse can progress without an increase in load).

TABLE 7.20 Overall Test Results for Steel-Ribbed HDPE Pipe

Test data				Local buckling		General buckling	
Test number	Manu-facturer	Diameter, in	% Proctor density	Cover, m	Deflection, percent	Cover, m	Deflection, percent
C-1*	C	1900	87	12.0	2.8	18.0	6.7
C-2*	C	2000	86	12.2	3.5	15.8	5.0
C-3*	C	2000	91	12.2	0.9	15.9	1.4

*Steel-ribbed polyethylene pipe.

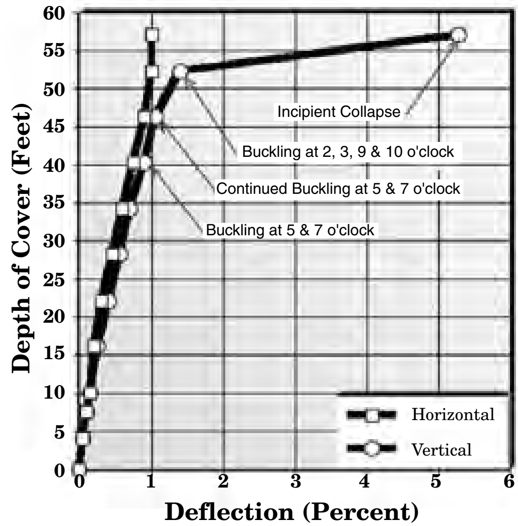

Figure 7.54 Performance of 2000-mm steel-ribbed HDPE pipe tested in silty-sand soil compacted to 91 percent of standard Proctor density shows that horizontal and vertical deflections are almost equal.

The behavior of this pipe shows that pipe stiffness alone will not control localized buckling.

Test results for HDPE profile-wall pipe. Part of the data included in the previous section were published in Transportation Research Record No. 1624, 1998. The data reported here are from a follow-on study. This data are for 42-, 48-, and 60-in-diameter pipes. Profile design parameters have significant influence on the structural performance of a pipe. Stable wall designs will exhibit higher performance limits than less stable designs, in terms of both dimpling of the interior and ultimate failure.

Procedure. During the summer of 1999, tests were performed on profile-wall polyethylene pipes. These tests permitted an investigation of the performance limits of the pipes subjected to external soil pressures. Tests were performed in the USU large soil cell into which the sample pipe is buried and onto which a vertical soil load is applied by means of 50 hydraulic cylinders (see Figs. 7.55 through 7.60 for test cell and testing procedure). The basic soil type was silty sand and is designated as a class III soil by ASTM D 2321. This soil is classified as SM according to the Unified Soil Classification System. See Figs. 6.11 and 6.12 for soil gradation and Proctor data.

Figure 7.55 A 60-in HDPE pipe being placed in the test cell.

Figure 7.55 shows the test pipe being placed in the large soil test cell. Figure 7.56 is a photo of the loading rams used to apply the vertical load simulating a soil embankment. Figure 7.57 shows the embedment soil being compacted to the required density. Figures 7.58 and 7.59 show part of the process used to fill the test cell. Figure 7.60 shows the test cell full with the vertical load being applied.

Test details

Test 1

- Pipe: 60-in diameter. Profile 1, HDPE
- Embedment soil: silty sand
- Compaction: 83% of standard Proctor
- Test date: 6/24/99

Figure 7.56 Photograph showing the 50 hydraulic cylinders used for loading.

Test 2

- Pipe: 60-in diameter. Profile 1, HDPE
- Embedment soil: silty sand
- Compaction: 95% of standard Proctor
- Test date: 7/07/99

Test 3

- Pipe: 60-in diameter. Profile 1, HDPE
- Embedment soil: silty sand
- Compaction: 75% of standard Proctor
- Test date: 7/15/99

Figure 7.57 Soil placement, compaction, and density measurement.

Test 4

- Pipe: 42-in diameter. Profile 1, HDPE
- Embedment soil: silty sand
- Compaction: 83% of standard Proctor
- Test date: 7/30/99

Test 5

- Pipe: 42-in diameter. Profile 1, HDPE
- Embedment soil: silty sand
- Compaction: 95% of standard Proctor
- Test date: 8/09/99

Figure 7.58 Backhoe loading soil in test cell.

Figure 7.59 Soil placement process.

Figure 7.60 Soil cell full, loading beams down, and load being applied to soil surface.

Test 6

- Pipe: 42-in diameter. Profile 1, HDPE
- Embedment soil: silty sand
- Compaction: 75% of standard Proctor
- Test date: 8/15/99

Test 7

- Pipe: 48-in diameter. Profile 2, HDPE
- Embedment soil: silty sand
- Compaction: 77% of standard Proctor
- Test date: 9/14/99

Test 8

- Pipe: 48-in diameter. Profile 2, HDPE
- Embedment soil: silty sand
- Compaction: 95% of standard Proctor
- Test date: 9/22/99

Test 1 results. The pipe was placed in soil compacted to 83 percent of standard Proctor density, and the vertical soil load was increased to 8664 lb/ft^2 (72.2 ft of cover based on a soil weight of 120 lb/ft^3). At a soil pressure equivalent to 52 ft of cover and about 12 percent vertical deflection, a dimpling pattern on the inside wall became noticeable to the eye. This pattern, which is the beginning of localized buckling, started at the 3 o'clock position. The center distance between dimples was about the same as the internal rib spacing. This pattern was somewhat like a wavy checkerboard in appearance and, of course, just the beginning of localized instability of the inner wall. However, this dimpling was small and would in no way impair the structural performance of the pipe.

As the soil load increased, these dimples became slightly more pronounced, but did not cause a performance limit. At a soil pressure equivalent to 58 ft of cover, a flattening was noted at the invert about 1 ft away from the joint. At a soil pressure equivalent to 65 ft of cover, a dimpling pattern was very apparent in the zones around the 3 and 9 o'clock positions. As the load was increased from 65 ft, the dimpling pattern became more pronounced and two cracks formed near the center of the test section and on the horizontal diameter. These small cracks followed the helix joint and were longitudinally about 2 ft apart. Loading was terminated at a soil pressure equivalent to 72 ft of cover. Data for this test are given in Fig. 7.61.

Test 2 results. In test 2, the pipe was installed in soil compacted to 95 percent of standard Proctor density and was loaded to a vertical soil load of 17,167 lb/ft^2 which is equivalent to 143 ft of cover. At a soil pressure equivalent to about 108 ft of cover and about 3.5 percent deflection, small dimples began forming near the 3 and 9 o'clock positions. This dimpling was extremely small and would in no way impair the structural performance of the pipe. As the soil load was increased, these dimples became more pronounced and were concentrated in the 3 and 9 o'clock positions but did not cause a performance limit. The test was terminated at 143 ft of cover. Data for this test are given in Fig. 7.62.

Test 3 results. The pipe was placed in soil compacted to only 75 percent of standard Proctor density. The vertical soil load was increased to 7340 lb/ft^2 (61 feet of cover based on a soil weight of 120 lb/ft^3). At 44 ft of cover and about 13 percent vertical deflection, a slight dimpling pattern began. This pattern started at about the 3 and 9 o'clock positions and spread as the load was increased. The center distance between dimples was about the same as the internal rib spacing. This pattern was somewhat like a wavy checkerboard in appearance and of course just the beginning of localized instability. However, this dimpling was extremely small and in no way would impair the structural performance of the pipe.

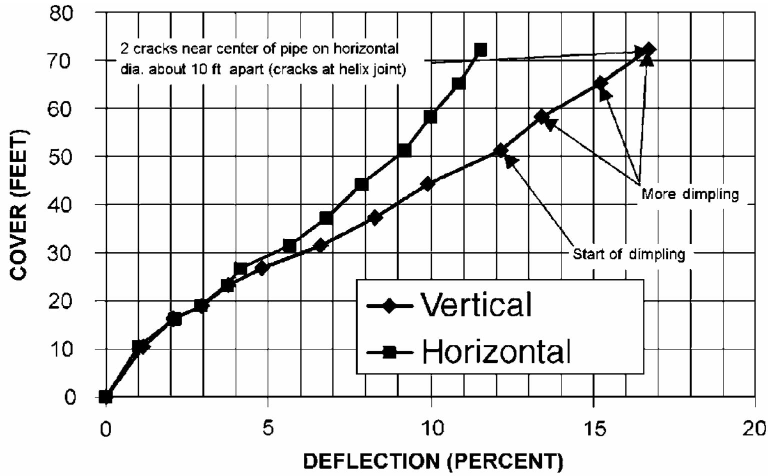

Figure 7.61 Load-deflection curves for 60-in-diameter HDPE pipe. Soil is silty sand compacted to 83 percent of standard Proctor density. Measurements made at center of pipe.

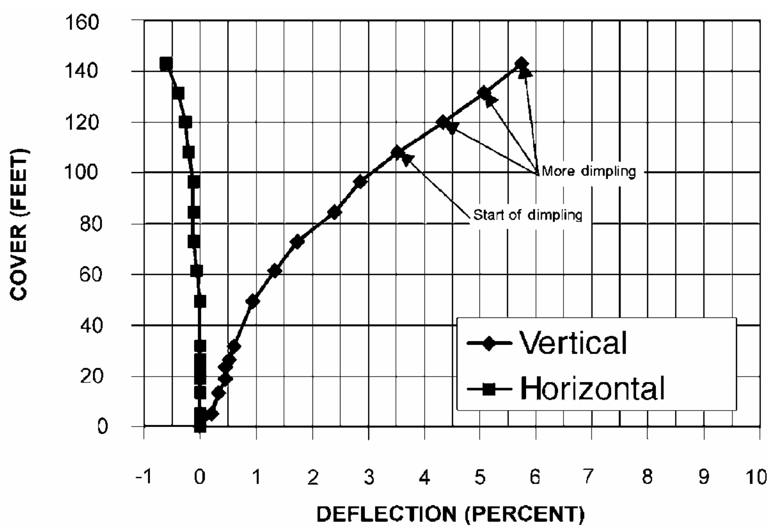

Figure 7.62 Load-deflection curves for 60-in-diameter HDPE pipe. Soil is silty sand compacted to 95 percent of standard Proctor density. Measurements are made at center of pipe.

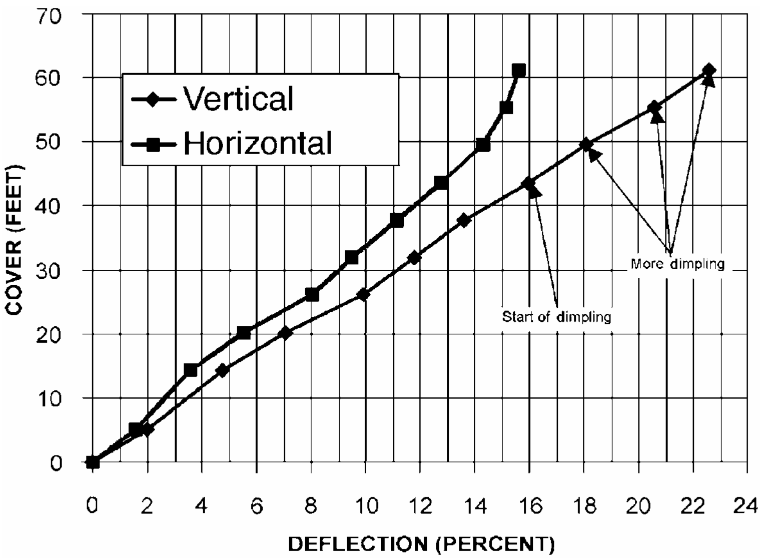

Figure 7.63 Load deflection curves for 60-in-diameter HDPE pipe. Soil is silty sand compacted to 75 percent of standard Proctor density. Measurements are made at center of pipe.

As the soil load increased, these dimples became more pronounced but still were not judged to be a performance limit of the pipe. At 61 ft of cover, the test was terminated. Data for this test are shown in Fig. 7.63.

Figure 7.64 gives the vertical deflection curves for the pipes tested in three soil densities in the height of cover range typically encountered in actual projects. These curves in this height-of-cover range (0 to 40 ft) show graphically the importance of soil density in controlling the pipe deflection in typical installations. This figure also shows approximated vertical deflection curves for intermediate soil densities (dashed lines).

Test 4 results. The pipe was placed in soil compacted to 83 percent of standard Proctor density, and the vertical soil load was increased to 9972 lb/ft^2 (83 ft of cover based on a soil weight of 120 lb/ft^3). At 55 ft of cover and about 12 percent vertical deflection, a dimpling pattern on the inside wall became noticeable to the eye. This pattern started at the 3 and 9 o'clock positions. The center distance between dimples was about the same as the internal rib spacing. This pattern was somewhat like a wavy checkerboard in appearance. However, this dimpling was small and would in no way impair the structural performance of the pipe.

As the soil load increased, these dimples became more pronounced but did not cause a performance limit. At 69 ft of cover, the dimpling pattern

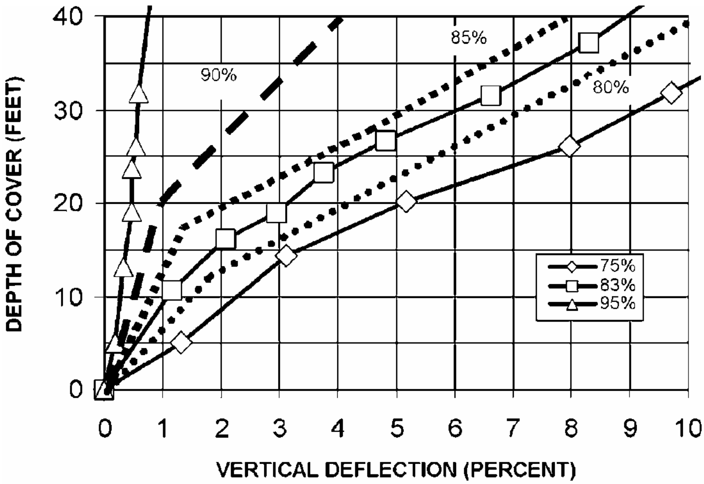

Figure 7.64 Vertical deflection curves for 60-in HDPE pipe at various soil densities. The dashed lines are approximated curves for intermediate densities.

was very apparent in the zones around the 3 and 9 o'clock positions, and hinging began at the 3 and 9 o'clock positions. As the load was increased from 69 ft, the helix seams showed distress. At 76 ft of cover, cracks formed near the center of the test section and on the horizontal diameter. These small cracks followed the helix joint. Loading was terminated at 83 ft of cover. Data for this test are given in Fig. 7.65.

Test 5 results. In test 5, the pipe was installed in soil compacted to 95 percent of standard Proctor density and was loaded to a vertical soil load of 20,196 lb/ft^2, which is equivalent to 168 ft of cover. At about 126 ft of cover and about 6 percent deflection, small dimples began forming near the 3 and 9 o'clock positions. This dimpling was extremely small and would in no way impair the structural performance of the pipe. These dimples became more pronounced as the soil load was increased and were concentrated in the 3 and 9 o'clock positions but did not cause a performance limit.

At about 168 ft of cover, circumferential cracks were noted on the horizontal diameter. These cracks were at the helix weld. At this point, the test was terminated. Data for this test are given in Fig. 7.66.

Test 6 results. The pipe was placed in soil compacted to only 75 percent of standard Proctor density. The vertical soil load was increased incrementally to 8268 lb/ft^2 (about 69 ft of cover based on a soil weight of 120 lb/ft^3). At 48 ft of cover and about 15 percent vertical deflection, a slight dimpling pattern began. This pattern started at about the 3

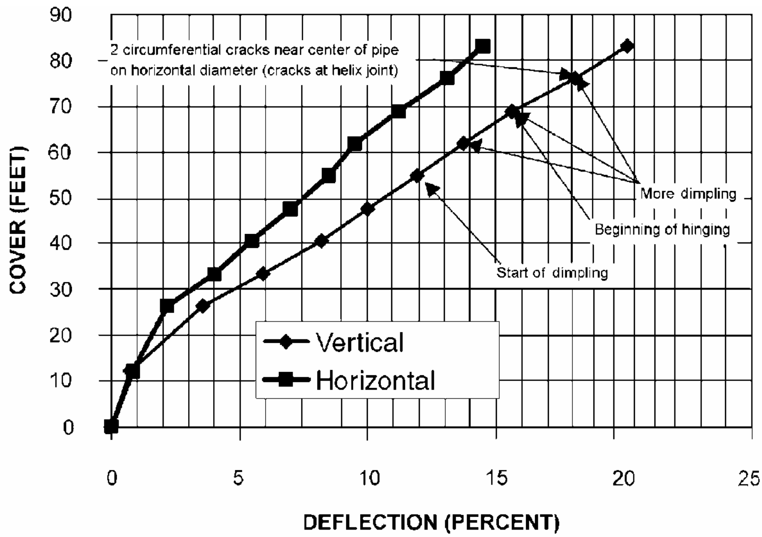

Figure 7.65 Load deflection curves for 42-in-diameter HDPE pipe. Soil is silty sand compacted to 83 percent of standard Proctor density. Measurements are made at center of pipe.

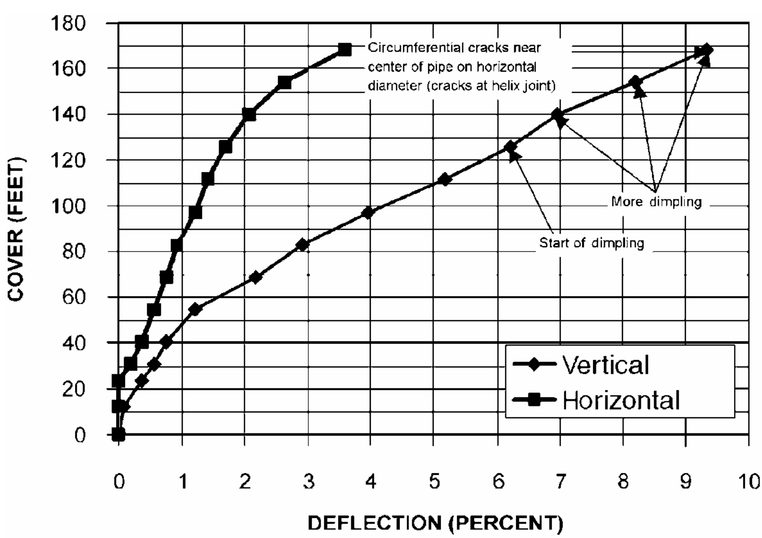

Figure 7.66 Load deflection curves for 42-in-diameter HDPE pipe. Soil is silty sand compacted to 95 percent of standard Proctor density. Measurements are made at center of pipe.

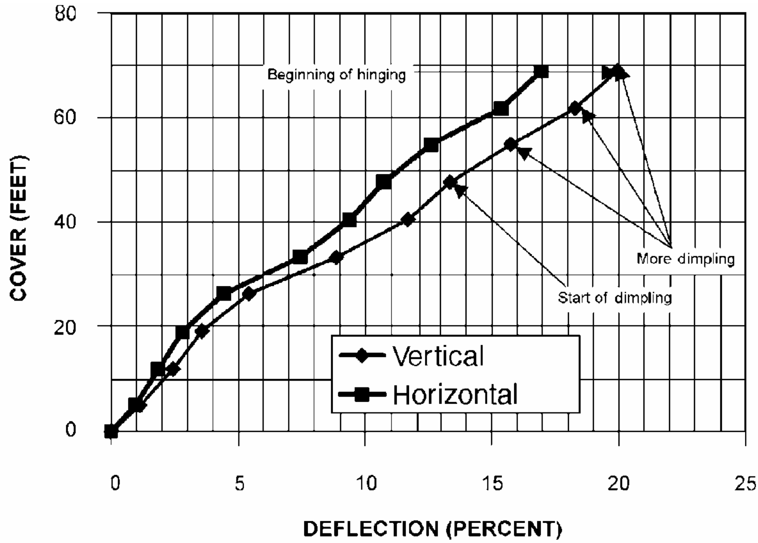

Figure 7.67 Load deflection curves for 42-in-diameter HDPE pipe. Soil is silty sand compacted to 75 percent of standard Proctor density. Measurements are made at center of pipe.

and 9 o'clock positions and spread as the load was increased. The center distance between dimples was about the same as the internal rib spacing. This dimpling was extremely small and in no way would impair the structural performance of the pipe.

As the soil load increased, these dimples became more pronounced, but still were not judged to be a performance limit of the pipe. At 69 ft of cover, wall hinging was noted at the 3 and 9 o'clock positions, and the test was terminated. Data for this test are shown in Fig. 7.67.

Figure 7.68 provides the vertical deflection curves for the pipes tested in three soil densities in the height-of-cover range typically encountered in actual projects. These curves in this cover range (0 to 40 ft) show graphically the importance of soil density in controlling pipe deflection in typical installations. This figure also shows approximated vertical deflection curves for intermediate soil densities (dashed lines).

Test 7 results. The pipe was placed in soil compacted to 77 percent of standard Proctor density, and the vertical soil load was increased to 6918 lb/ft^2 (57.7 ft of cover based on a soil weight of 120 lb/ft^3). A flattening at the 5 o'clock position started at 46 ft of cover (see Fig. 7.69). Excavation after the test showed this to be buckling of the ribs at that position.

At 52 ft of cover and about 18 percent vertical deflection, a dimpling pattern on the inside wall became noticeable to the eye. This pattern,

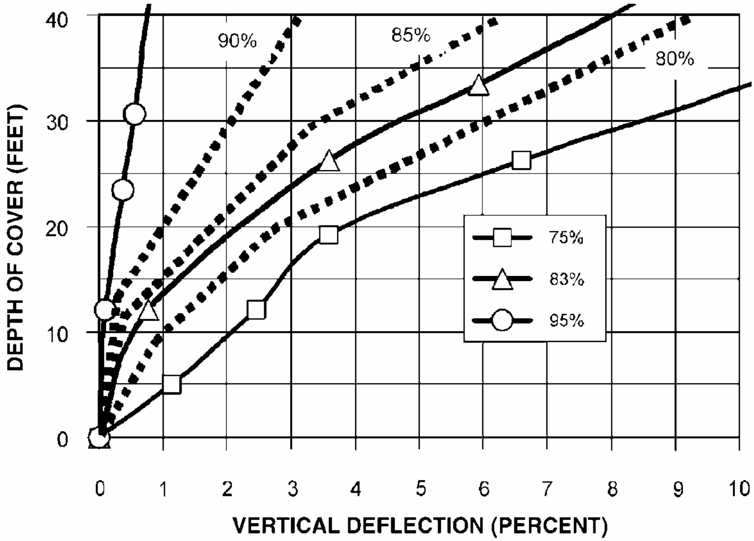

Figure 7.68 Vertical deflection curves for 42-in HDPE pipe at various soil densities. The dashed lines are approximated curves for intermediate densities.

Figure 7.69 Local buckling at 5 o'clock. Density = 77 percent, and load is 46 ft of cover.

which is the beginning of localized buckling, started at the 3 and 9 o'clock positions. The center distance between dimples was about the same as the external rib spacing. This pattern was somewhat like a wavy checkerboard in appearance and, of course, just the beginning of localized instability of the inner wall. Also, the joint began opening at the 3 and 9 o'clock positions.

As the soil load increased, the dimples became more pronounced. At 58 ft of cover, the pipe buckled at the 11 and 1 o'clock positions (see Fig. 7.70), and the joint failed at 3 and 9 o'clock. Buckling of a pipe in soil is not like classical buckling. In a buried pipe it takes another increment of load to produce another increment in the buckling phenomenon. Loading was terminated at 58 ft of cover. Data for this test are given in Fig. 7.71.

Test 8 results. In test 2, the pipe was installed in soil compacted to 95 percent of standard Proctor density and was loaded to a vertical soil load of 18,228 lb/ft^2 which is equivalent to 152 ft of cover.

At 87 ft of cover, flattening started at a location between the 5 and 6 o'clock positions. After excavation of the test pipe, a visual inspection of the external ribs revealed that the flattening was caused by rib buckling.

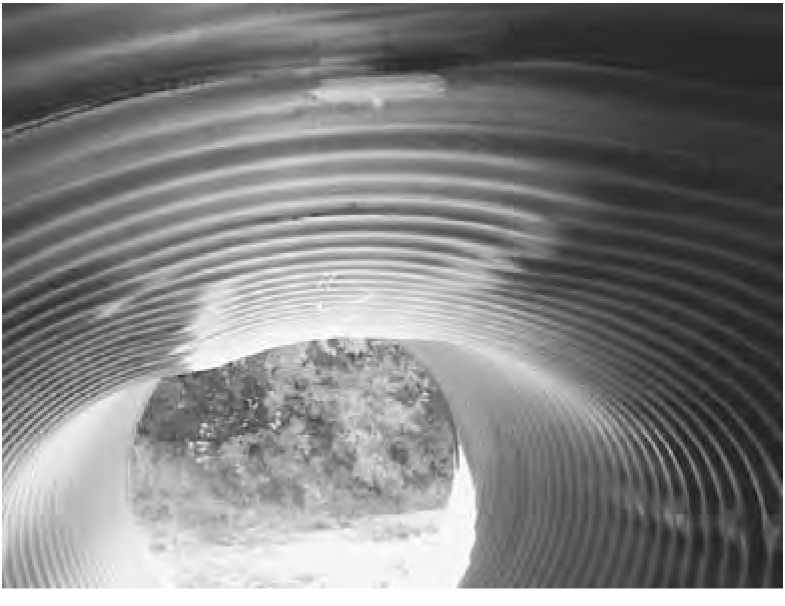

Figure 7.70 General buckling at 11 o'clock. Density = 77 percent, and load is 58 ft of cover.

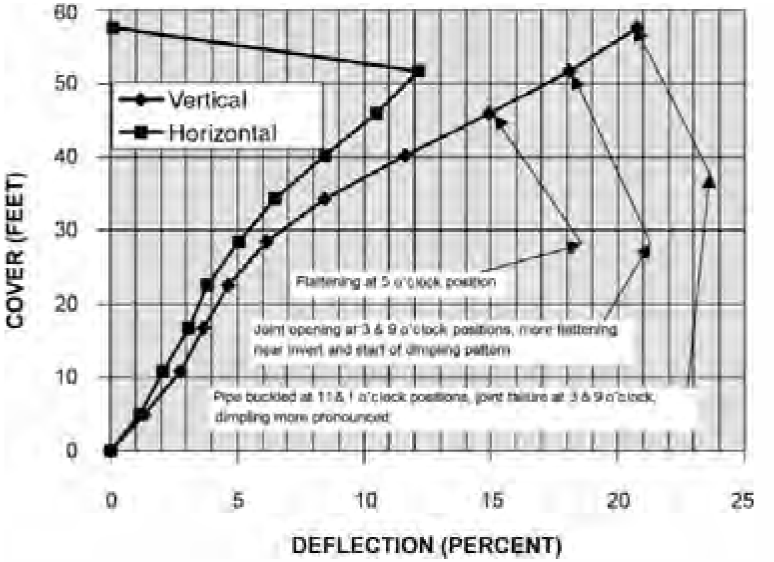

Figure 7.71 Load deflection curves for 48-in-diameter HDPE pipe. Soil is silty sand compacted to 77 percent of standard Proctor density. Measurements are made at center of pipe.

At about 113 ft of cover and about 4.9 percent deflection, dimples began forming near the 3 and 9 o'clock positions. This dimpling was small and would in no way impair the structural performance of the pipe. As the soil load was increased, these dimples became more pronounced and were concentrated in the 3 and 9 o'clock positions. The dimples spread to the 2 and 4 o'clock positions as the cover was increased to 126 ft.

Wall crushing started at the 9:30 and 2:30 o'clock positions at a cover of 139 ft. As the load increased past 139 ft, the crushing and dimpling became more pronounced. The test was terminated at 152 ft of cover. Data for this test are given in Fig. 7.72.

Figure 7.73 gives the vertical deflection curves for the pipes tested in the two soil densities. This shows graphically the importance of soil density in controlling the pipe deflection. This figure also shows approximated vertical deflection curves for intermediate soil densities (solid lines).

Dimpling. The term *dimpling* as used in this book refers to the wavy pattern that occurred in the inner wall of the pipe due to local instability of the wall. This is not general buckling and is not a structural performance limit.

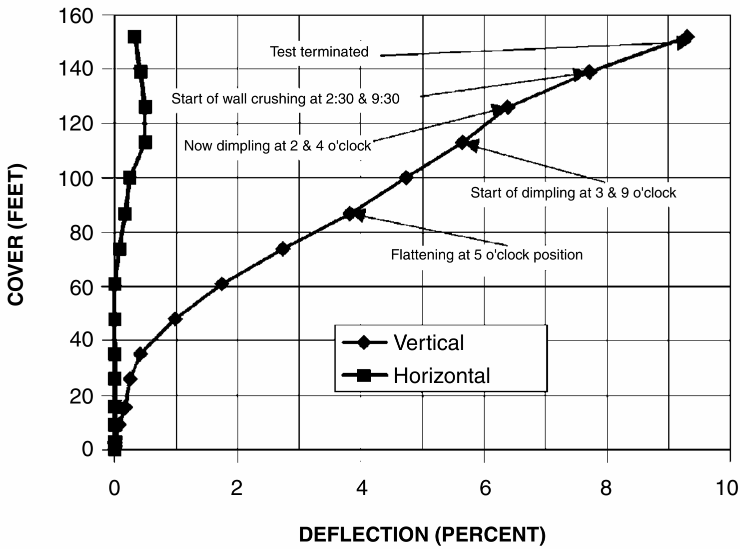

Figure 7.72 Load deflection curves for 48-in-diameter HDPE pipe. Soil is silty sand compacted to 95 percent of standard Proctor density. Measurements are made at center of pipe.

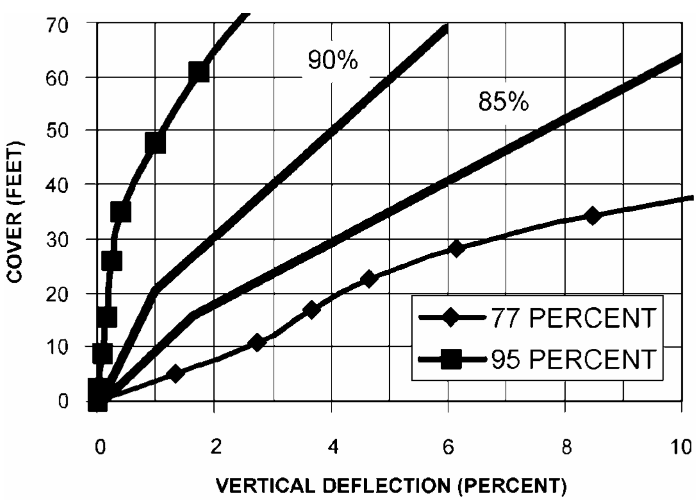

Figure 7.73 Vertical deflection curves for 48-in HDPE pipe at various soil densities. The solid lines are approximated curves for intermediate densities.

Hinging. The term *hinging* is used to describe yielding of the material due to an excessive bending moment in the wall. These hinges usually take place at the 3 and 9 o'clock positions. These plastic hinges, although primarily due to bending, can be influenced by a combination of localized buckling and wall yielding caused by thrust in the wall of the pipe. Hinging is usually considered to be a structural performance limit.

Wall crushing. The term *wall crushing* is used to describe yielding in the wall produced by excessive compressive stresses resulting from thrust in the wall. These large compressive stresses produce local yielding and/or local buckling. Crushing is usually considered to be a structural performance limit (see Figs. 7.74 and 7.75).

Summary and conclusions. The pipe cross section started out circular and became elliptical as the height of cover increased. For the 75 and 77 percent dense soils, this deviation from a circle to an elliptical shape was quite pronounced, and for the 83 percent dense soil the deflected shape was elliptical, but less pronounced. The shape of the pipe in the 95 percent dense soil remained closer to being circular even

Figure 7.74 Wall crushing and dimpling pattern on left side. Density = 95 percent, and load is 152 ft of cover.

Figure 7.75 Wall crushing and dimpling pattern on right side. Density = 95 percent and load is 152 ft of cover.

for extremely high heights of cover. None of the test pipes ever exhibited a so-called squaring or a square shape at any load. This result is just what one would expect. The ratio of ring compression stress to bending stress for the 75 percent dense soil is very low (much less than 1). For the 83 percent dense soil, this ratio is low, but may approach a value of 1. The ratio of ring compression stress to bending stress for the pipe tested in soil compacted to 95 percent of standard Proctor density is much greater than unity.

For polyethylene, which has a fairly low modulus, ring compression stresses cause circumferential ring shortening. This ring shortening is small for pipes installed with low heights of cover and in low to moderately compacted soils. For high-density soils, at high earth covers, this circumferential ring shortening is very significant and is the primary deformation that takes place. This circumferential shortening is extremely beneficial in the performance of the pipe. The decrease in circumference relieves the pipe ring of some of the soil pressure and causes the surrounding granular pipe zone material to carry a higher percentage of the load. This works on exactly the same principle as the slotted bolthole in corrugated metal pipe. In a very large measure, the pipe in test 3 was able to withstand extremely high loads because of the substantial circumferential shortening that took place.

Noteworthy is the high load that can be applied without distress to the pipe ring. Clearly, the pipes deflect more in loose soil than in dense soil because loose soil compresses more. The pipes do not collapse, even in loose soil.

The soil should be granular and carefully compacted if the pipe is buried under high soil cover or under heavy surface loads. Granular pipe-zone backfill material at moderate to high densities ensures that the pipes will perform well at high earth covers.

Incipient dimpling occurred at equivalent depths of cover in the range of 44 to 126 ft (see Table 7.21). For the pipes tested, this incipient dimpling load is primarily a function of soil density. Dimpling is not a structural performance limit.

The load at which a structural performance limit takes place is also a function of the soil density. For a relatively poor installation (75 percent standard Proctor), the performance limit is at 55 ft of cover. For a good installation (83 percent standard Proctor density), hinging or cracking begins at about 70 ft of cover. For an excellent installation (95 percent standard Proctor), the lowest performance limit was 143 ft of cover (see Table 7.22).

Performance limits and preliminary design recommendations for profile-wall HDPE pipes

A performance limit for a pipe is reached when the pipe no longer performs in an acceptable manner. For a polyethylene pipe, overdeflection, wall buckling, and wall crushing are usually considered unacceptable. Deflection is usually controlled by proper installation. Wall buckling can be controlled by controlling strains and by maintaining proper wall thicknesses. Wall crushing is controlled by maintaining an adequate area per unit length. Thus, area per unit length is the most important parameter since wall thickness is directly related to the area.

Pipe stiffness is directly related to the moment of inertia which, in turn, is a function of area, shape, and corrugation height. It is important to meet minimum requirements for pipe stiffness. Increasing the pipe stiffness above the minimum will give some added performance

TABLE 7.21 Dimpling of HDPE Pipes Tested

Test no.	Manufacturer, type	Diameter, in	Percent of Proctor density	Load at start of dimpling, ft of cover	Deflection at start of dimpling, percent
1	Y, type 1	60	75	44	13
2	Y, type 1	60	83	51	12
3	Y, type 1	60	95	108	3.5
4	Y, type 2	42	75	48	13
5	Y, type 2	42	83	55	12
6	Y, type 2	42	95	126	6
7	Z, type 3	48	77	52	18
8	Z, type 3	48	95	113	4.9

TABLE 7.22 Performance Limit for HDPE Pipes Tested

Test no.	Manufacturer, type	Diameter, in	Percent of Proctor density	Load at performance limit	Deflection at performance limit, percent
1	Y, type 1	60	75	Excessive deflection and dimpling at 55 ft of cover	17
2	Y, type 1	60	83	Cracks at 72 ft of cover	17
3	Y, type 1	60	95	Excessive dimpling at 143 ft of cover	5.7
4	Y, type 2	42	75	Excessive deflection at 55 ft of cover, hinging at 69 ft of cover	16, 20
5	Y, type 2	42	83	Hinging at 69 ft of cover, cracks at 76 ft	15.6, 18
6	Y, type 2	42	95	Cracks at 168 ft of cover	9.3
7	Z, type 3	48	77	Excessive deflection and rib buckling at 46 ft	15
8	Z, type 3	48	95	Rib buckling at 87 ft of cover	3.6

benefits. However, a higher pipe stiffness without a sufficient wall area can lead to premature pipe failure. The proper design sequence for a specific installation condition is as follows:

1. Choose area to prevent wall crushing.
2. Choose wall thickness to prevent buckling.
3. Corrugation height will be fairly well defined by the first two items if pitch and shape are predetermined.

Test data were analyzed, and numerous finite element analysis (FEA) runs were made using the computer program PIPE5 for HDPE pipe buried in a silty-sand soil. Various combinations of wall area, wall thickness, and corrugation height were run to determine the minimum wall area for various depths of cover. Because of space limitations in this book, FEA data are not presented. Also, the theoretical basis for much of the following discussion is the field of dimensional analysis, sometimes called *similitude,* which is well documented in engineering texts. The conditions under which one may use results from one system (test setup) to predict the behavior of another similar system are determined by dimensional analysis and the use of dimensionless numbers. One major advantage of such a theory is that a solution that works for one diameter can be immediately extrapolated to other diameters.

Area and thickness. The most important parameters in controlling performance are area per unit length and wall thickness. Corrugation height is a direct function of the area and thickness and can be calculated if the area per unit length, thickness, and shape are known.

It is recommended that all thicknesses, including the thickness of the liner, be as close to equal as possible. The reason for this is that the liner is strained close to the same level as the crown of the corrugation (rib top). This is due to high ring compressive stresses at the spring line. The thinner the wall, the more likely it is that localized buckling will occur. It may be a detriment to make one part of the profile thick and another thin. The one area that will be thicker is where the liner joins the valley of the corrugation. The strains across the cross section are fairly uniform because a major contributor to strain is thrust in the wall which is uniform through the cross section. The above discussion should not be construed to mean that thickness alone will control buckling, since it is well known that controlling the unsupported length of a section is of equal importance.

Corrugation height. If the corrugation height is too large, bending strains become significant; and if one increases corrugation height

TABLE 7.23 Profile Wall Pipe Dimensionless Geometric Parameters to Control

Dimensionless parameters	Possible value for HDPE
t_{min}/r	≥ 0.005
t_{min}/l_{uns}	≥ 0.02
I/r^3	$\geq 4 \times 10^{-5}$
A/r	≥ 0.02
L_p/r	≤ 0.3

A = area per unit length of cross section of profile
r = effective radius of pipe
t_{min} = minimum thickness of any particular section of profile
l_{uns} = unsupported length (or width) of any particular section of profile
I = moment of inertia per unit length of profile section
L_p = length of profile section

while holding the area constant, then thickness has to decrease, which leads to early wall buckling.

Pitch. Geometrically, pitch should be a function of diameter. That is, if a pitch of 4 in works well for a 24-in-diameter pipe, a pitch of 8 in will work well for a 48-in-diameter pipe.

Nondimensional parameters. Test data and finite element data suggest that, for a profile-wall pipe, certain dimensionless parameters be set within limits to ensure satisfactory performance of pipes subjected to earth loadings. Table 7.23 is a list of possible parameters that arise from the data, along with suggested limiting values. These values appear to provide adequate structural stability. The pipes tested generally meet these requirements. However, these studies are still in progress, and these values are provided as guidelines only.

Acrylonitrile-Butadiene-Styrene Pipes

ABS plastic for pipe manufacture is available in several types and grades per ASTM D 1788. The physical properties of the various ABS materials vary quite widely, as is indicated by Table 7.24. Most ABS

TABLE 7.24 ABS Design Properties

Hydrostatic-design basis, lb/in^2	1600–3200
Hydrostatic-design stress, lb/in^2	800–1600
Elastic modulus, lb/in^2	200,000–400,000
Tensile stress, lb/in^2	2500–7000
Hazen-Williams coefficient C	150
Manning's coefficient n	0.009

TABLE 7.25 Selected Standards for ABS Plastic Pipe

ASTM D 1788	Rigid Acrylonitrile-Butadiene-Styrene (ABS) Plastics
ASTM D 2680	Acrylonitrile-Butadiene-Styrene Composite Sewer Piping
ASTM D 2661	Acrylonitrile-Butadiene-Styrene Plastic Drain, Waste and Vent Pipe, and Fittings
ASTM D 628	Acrylonitrile-Butadiene-Styrene Plastic Drain, Waste and Vent Pipe Having a Foam Core
ASTM D 2468	Acrylonitrile-Butadiene-Styrene Plastic Pipe Fittings, Schedule 40
ASTM D 1527	Acrylonitrile-Butadiene-Styrene Plastic Pipe, Schedules 40 and 80
ASTM D 2282	Acrylonitrile-Butadiene-Styrene Plastic Pipe (SDR-PR)
ASTM D 2750	Acrylonitrile-Butadiene-Styrene Plastic Utilities Conduit and Fittings
ASTM D 2751	Acrylonitrile-Butadiene-Styrene Sewer Pipe and Fittings
ASTM D 2469	Socket-type Acrylonitrile-Butadiene-Styrene Plastic Pipe Fittings, Schedule 80
ASTM D 2235	Solvent Cement for Acrylonitrile-Butadiene-Styrene Plastic Pipe and Fittings
ASTM D 3138	Solvent Cements for Transition Joints between Acrylonitrile-Butadiene-Styrene and Poly(vinyl Chloride) (PVC) Nonpressure Piping Components
ASTM D 2465	Threaded Acrylonitrile-Butadiene-Styrene Plastic Pipe Fittings, Schedule 80

pipes, especially pressure pipes, are manufactured from grades with the higher tensile properties.

Solid-wall ABS is used widely for drain, waste, and vent piping. It is also used for smaller-diameter sanitary sewers. It is used to a very limited extent for smaller-diameter pressure piping.

The design methods and procedures are essentially the same as those for PVC pipes with the appropriate elastic modulus for calculating pipe stiffness and the appropriate hydrostatic-design stress for pressure pipe design.

A list of selected ASTM standards for ABS plastic pipes is given in Table 7.25.

Example 7.15—An 8-in ABS pipe An 8-in solid-wall ABS pipe has been selected for a sewer installation. The native soil is clay, and the water table is about 8 ft deep. Most of the line will be installed about 10 ft deep, but one section has depths up to 20 ft. The long-term deflection is not to exceed 5 percent. What pipe-zone soil and soil density should be specified?

solution From ASTM D 2751, SDR = 42 and PS = $F/\Delta y$ = 20 lb/in^2. Use Spangler's equation. See Eq. (7.4) of Example 7.1.

$$\text{Required } E' = \frac{0.56H/(\Delta y/D) - \text{PS}}{0.41}$$

$$H = 20 \text{ ft} \qquad \text{PS} = 20 \text{ lb/in}^2 \qquad \frac{\Delta y}{D} = 0.05$$

$$E' = 498 \text{ lb/in}^2 \approx 500 \text{ lb/in}^2$$

The pipe-zone material should be either a granular material compacted to 90 percent Proctor density or a crushed angular stone. Because of the high water table, the crushed stone should be specified since little or no compaction will be required for an angular stone. See Table 3.4 for E' values for various soils.

Other Thermoplastic Pipes

In addition to the thermoplastic piping materials discussed previously, there are other types of thermoplastic piping materials which are used to a lesser degree. These materials include polybutylene (PB), cellulose acetate butyrate (CAB), and styrene-rubber (SR). A selected list of standards for these materials is given in Tables 7.26, 7.27, and 7.28. The design techniques which are used for thermoplastics such as PVC can also be applied to these thermoplastic materials. The design engineer should obtain necessary design parameters such as the hydrostatic-design stress and pipe stiffness for the particular pipe and material. These parameters may be used in design equations discussed previously.

Example 7.16—Brittle behavior A strain-sensitive plastic sewer pipe has been installed in an area where expansive soils are known to exist. The pipe deflects as a flexible pipe, has a high pipe stiffness, and has a somewhat brittle behavior. A TV inspection made 2 years after installation indicates vertically elongated pipe with many pipe sections showing longitudinal cracks along the 3 and 9 o'clock positions. The pipe was installed with a compacted granular material around the pipe and 10 ft of cover. The expansive soil is to the sides and under the pipe but not over the pipe. The TV photographs indicate the pipe to be vertically elongated in the 3 to 8 percent range. Estimate the horizontal swell pressure exerted by the soil. (Assume $E' = 1000$ lb/in^2.)

solution The actual buried pipe may be used as a transducer to obtain a fair estimate of the in situ horizontal swell pressures. This is accomplished by use of the Iowa formula and the actual deflection behavior of the pipe. In short, this formula may be used by providing pipe properties, soil properties, and pipe deflection and then back-calculating the pressure necessary to produce that deflection. [See Eqs. (7.1) and (7.2).]

$$\text{Soil modulus } E' = 1000 \text{ lb/in}^2$$

$$\text{Pressure} = (\text{deflection ratio})\,(10)\,\frac{\text{pipe stiffness}}{6.7 + 0.061\ (\text{soil modulus})}$$

or

$$P = \left(\frac{\Delta y}{D}\right)(10)\left(\frac{F/\Delta y}{6.7} + 0.061E'\right)$$

TABLE 7.26 Selected Standards for Polybutylene

ASTM F 809	Large-Diameter Polybutylene Plastic Pipe
ASTM F 809M	Large-Diameter Polybutylene Plastic Pipe (Metric)
ASTM F 845	Plastic Insert Fittings for Polybutylene (PB) Tubing
ASTM D 2662	Polybutylene Plastic Pipe (SDR-PR)
ASTM D 3000	Polybutylene Plastic Pipe (SDR-PR) Based on Outside Diameter
ASTM D 2666	Polybutylene Plastic Tubing
AWWA C902	Polybutylene Pressure Pipe, Tubing, and Fitting, $^1/_2$ in through 3 in, for Water

TABLE 7.27 Selected Standards for CAB

ASTM D 2446	Cellulose-Acetate-Butyrate-Plastic Pipe (SDR-PR) and Tubing
ASTM D 1503	Cellulose-Acetate-Butyrate Plastic Pipe, Schedule 40
ASTM D 2560	Solvent, Cements for Cellulose-Acetate-Butyrate Plastic Pipe, Tubing, and Fittings

TABLE 7.28 Selected Standards for Styrene-Rubber (SR) Pipe

ASTM D 3122	Solvent Cements for Styrene-Rubber Plastic Pipe and Fittings
ASTM D 3298	Styrene-Rubber Plastic Drain Pipe, Perforated
ASTM D 2852	Styrene-Rubber Plastic Drain Pipe and Fittings

Table 7.29 indicates probable swell pressures in the range of 23 to 60 lb/in^2 for deflections of 3 to 8 percent.

Thermoset Plastic Pipe

Thermosetting resins give off heat during the curing process (exothermic). Such resins cannot be melted and reformed as thermoplastics can. Epoxy, polyester, and phenolic resins are part of the thermosetting resin family. Pipes made from such resins are usually fiber-reinforced, and the fiber is normally E-type glass. The glass may be continuous strands or rovings placed in a winding process, or it may be chopped and placed in a centrifugal casting process. Glass fabric and glass mats may also be used.

TABLE 7.29 Horizontal Swell Pressures for Various Vertical Deflections

Deflection, percent	Swell pressure, lb/in^2
3	22.8
4	30.4
5	38.0
6	45.5
7	53.1
8	60.7

There are two broad classes of reinforced thermoset pipes: (1) reinforced plastic mortar (RPM) pipe and (2) reinforced thermosetting resin (RTR) pipe. This type has been referred to as fiberglass-reinforced plastic (FRP) pipe. The thermoset resin used in either may be filled or unfilled. The filler in the resin is used as a resin extender and will usually influence the chemical and physical properties.

Reinforced thermoset plastic pipe is available in a wide range of sizes. Because of the high tensile strength of the reinforced plastic, a smooth-wall pipe may have low pipe stiffness, especially in large diameters. To overcome this, some pipes are made stiffer by molding external ribs which run circumferentially and are spaced along the length. The pipe stiffness is determined with the assumption that the pipe wall and wall stiffeners act integrally as a unit. Such pipes are often designed and manufactured for the specific job with different designs along the installation in response to varying conditions. Table 7.30 gives selected standards for reinforced thermosetting resin pipes. (See Chap. 4 for additional information and design criteria.)

Reinforced thermosetting resin pipe

RTR pipes are manufactured from a thermosetting resin and glass fiber reinforcement. The resin may be filled or unfilled. This type of pipe is available in many diameters and for diverse uses for both pressure and nonpressure applications. Liners are available to meet various chemical requirements.

Example 7.17—An 84-in cooling water pipe A fiberglass-reinforced polyester resin material has been selected for the pipe to supply cooling water for a large power plant. Selected design parameters are given in Table 7.31. (See AWWA C950 for design procedures.)

1. Design for deflection.

Earth load $W_e = (5.5)\,(110) = 605 \text{ lb/ft}^2$

Live load $W_L = 300 \text{ lb/ft}^2$

Total load $W = 605 + 300 = 905 \text{ lb/ft}^2 = 6.28 \text{ lb/in}^2$

TABLE 7.30 Selected Standards for Reinforced Thermosetting Resin Pipe

ASTM D 3517	Reinforced Plastic-Mortar Pressure Pipe
ASTM D 3262	Reinforced Plastic-Mortar Sewer Pipe
ASTM D 2992	Standard Method for Obtaining Hydrostatic-Design Basis for Reinforced Thermosetting Resin Pipe and Fittings
ASTM D 2290	Standard Test Method for Apparent Tensile Strength of Ring or Tubular Plastics and Reinforced Plastics by Split-Disk Method
ASTM D 2997	Centrifugally Cast Reinforced Thermosetting Resin Pipe
ASTM D 2996	Filament-Wound Reinforced Thermosetting Resin Pipe
ASTM D 2310	Machine-Made Reinforced Thermosetting Resin Pipe
ASTM D 2517	Reinforced Epoxy Resin Gas Pressure Pipe and Fittings
ASTM D 3840	Reinforced Plastic Mortar Pipe Fittings for Nonpressure Applications
ASTM D 3754	Reinforced Plastic Mortar Sewer and Industrial Pressure Pipe
ASTM D 4160	Reinforced Thermosetting Resin Pipe (RTRP) Fittings for Nonpressure Applications
ASTM D 4163	Reinforced Thermosetting Resin Pressure Pipe (RTRP)
ASTM D 4024	Reinforced Thermosetting Resin (RTR) Flanges
ASTM D 4162	Reinforced Thermosetting Resin Sewer and Industrial Pressure Pipe (RTRP)
ASTM D 4184	Reinforced Thermosetting Resin Sewer Pipe (RTRP)
ASTM D 1694	Threads for Reinforced Thermosetting Resin Pipe
AWWA C950	Glass-Fiber-Reinforced Thermosetting-Resin Pipe

TABLE 7.31 Selected Design Parameters

Pipe inside diameter	84 in
Burial depth	5.5 ft (maximum)
Unit weight (soil)	110 lb/ft^3
Live load	300 lb/ft^2
Internal pressure (maximum)	60 lb/in^2
Internal pressure (minimum)	14.7 lb/in^2 vacuum
Water temperature (maximum)	140°F
Hoop modulus (pipe)	3.5×10^6 lb/in^2
Bending strain basis	0.0054 in/in
Design strain	0.0036 in/in
Backfill soil	Medium sand at 90 percent Proctor density
Soil modulus E'	Use 650 lb/in^2
Deflection limit	3 percent
Hydrostatic-design basis	10,000 lb/in^2

Use Spangler's equation to determine the required pipe stiffness to control ring deflection. For RTR pipe, a limiting deflection is usually set at some value less than 5 percent. For our problem, the deflection limit has been set at 3 percent. Spangler's equation may be expressed as follows (see Example 7.1):

$$\frac{\Delta y}{D} = \frac{0.1\ \gamma H}{\mathrm{PS}/6.7 + 0.061E'}$$

In this case, H may be replaced by the total load, and the above equation will be solved for pipe stiffness (PS).

$$\mathrm{PS} = \left(\frac{0.1W}{\Delta y/D} - 0.061E'\right)(6.7)$$

For $W = 6.28$ lb/in², $\Delta y/D = 0.03$, and $E' = 650$ lb/in², the pipe stiffness PS is found to be negative; therefore, deflection does not control design. This conclusion is based on the assumption that the pipe will be installed properly with a resulting E' equal to 650 lb/in².

2. Assume that the pipe may not be installed per design specifications. What is the minimum soil modulus E' that can be accepted and still meet the 3 percent deflection limit (assume pipe stiffness PS = 10 lb/in²)?

Use Spangler's equation to solve for E'.

$$\begin{aligned} E' &= \left(\frac{0.1W}{\Delta y/D} - \frac{\mathrm{PS}}{6.7}\right)\left(\frac{1}{0.061}\right) \\ &= \left[\frac{(0.1)\,(6.28)}{0.03} - \frac{10}{6.7}\right]\left(\frac{1}{0.061}\right) \\ &= 319\ \mathrm{lb/in^2} \end{aligned}$$

3. Design for buckling (see AWWA C950). The buckling equation given in AWWA C950 is

$$q_a = \frac{[32R_w B'E'\ (EI/D^3)]^{1/2}}{\mathrm{SF}}$$

or

$$q_{\mathrm{cr}} = \left[32R_w B'E'\left(\frac{EI}{D^3}\right)\right]^{1/2}$$

where q_a = allowable buckling pressure
SF = safety factor or design factor, usually taken as 2.5 or greater
R_w = water buoyancy factor; 1.0 for our problem
$= 1 - 0.33h_w/h \qquad 0 \le h_w \le h$
h_w = height of water surface above top of pipe, in

B' = empirical coefficient of elastic support (dimensionless)
$= 4\,(h^2 + Dh)\,/1.5\,(2h + D)^2$ (see "Buckling" in Chap. 3)
$= 0.57$ for our problem
h = burial depth from top of pipe, ft
D = diameter of pipe, ft

$$\text{Applied pressure } q_a = 14.7 \text{ lb/in}^2 \text{ vacuum} + 6.28 \text{ lb/in}^2 \text{ soil pressure}$$

$$= 20.98 \approx 21 \text{ lb/in}^2$$

Use the AWWA equation to solve for EI/D^3.

$$\frac{EI}{D^3} = \frac{q_a{}^2\,(\text{SF})^2}{32R_w B'E'}$$

$$= \frac{(21)^2\,(2.5)^2}{(32)\,(1)\,(0.57)\,(650)} = 0.23 \text{ lb/in}^2$$

$$\text{PS} = 6.7\,\frac{EI}{r^3} = 6.7\left(\frac{EI}{D^3}\right)(8)$$

$$= 53.6\,\frac{EI}{D^3}$$

Therefore, the required pipe stiffness is

$$\text{PS} = (53.6)\,(0.23) = 12.33 \text{ lb/in}^2$$

$$q_{\text{cr}} = [32\,(1.0)\,(0.57)\,(650)\,(0.23)\,]^{1/2} = 52.2 \text{ lb/in}^2$$

The thickness required for a straight-wall pipe may be determined using the above stiffness as follows:

$$\text{PS} = 6.7\,\frac{EI}{r^3} = 53.6\,\frac{EI}{D^3}$$

or

$$I = \frac{(\text{PS})\,(D^3)}{53.6E}$$

but

$$I = \frac{t^3}{12}$$

then

$$t^3 = \frac{12\,(\text{PS})\,(D^3)}{53.6E}$$

or

$$t = 0.61D\,(\text{PS})^{1/3}E^{-1/3}$$

$$= 0.61D\,(\mathrm{PS})^{1/3}\,(3.5 \times 10^6)^{-1/3}$$

$$= 0.78 \text{ in}$$

4. Check the pressure design. Internal pressure including surge is given as 60 lb/in². A quick check on stress due to internal pressure reveals a low value.

$$\sigma = \frac{PD}{2t} = \frac{(60)\,(84)}{2\,(0.78)} = 3231 \text{ lb/in}^2$$

$$3231 \ll 10{,}000$$

Thus, stress due to internal pressure acting alone is not a critical factor.

5. Check strain due to ring deflection. The bending strain caused by the 3 percent design ring deflection is calculated using Eq. (3.20).

$$\varepsilon_b = 6\left(\frac{t}{D}\right)\left(\frac{\Delta y}{D}\right) = 6\left(\frac{0.78}{84}\right)(0.03) = 0.00167$$

The above strain is less than the 0.0036 design strain.

6. Calculate strain due to combined loading. (See Chap. 4 and AWWA C950.) Two equations are given in AWWA C950 for calculating strain due to the simultaneous action of ring bending and internal pressure. The *Molin equation* is to be used for low pressures, and another equation based on Spangler's Iowa formula is to be used for higher pressures. The maximum strain is the lower of the two calculated values. For our problem, the internal pressure is quite small; therefore, the equation attributed to Molin applies.

$$\text{Combined strain } \varepsilon_c = \frac{PD}{2Et} + 6\left(\frac{\Delta y}{D}\right)\left(\frac{t}{D}\right)$$

This equation is just the simple addition of the strain due to internal pressure with the strain due to ring bending—a simple concept of elementary mechanics of materials.

For the problem at hand,

$$\varepsilon_c = \frac{60\,(84)}{2\,(3.5 \times 10^6)\,(0.78)} + 6\,(0.03)\left(\frac{0.78}{84}\right)$$

$$= 0.923 \times 10^{-3} + 1.67 \times 10^{-3} = 2.59 \times 10^{-3} = 0.00259$$

This is less than the design strain of 0.0036. Thus, combined strain is all right.

Example 7.18—An 84-in ribbed pipe A manufacturer has been successfully marketing a fiber-reinforced plastic pipe. The wall thickness for the 84-in-diameter pipe is 1.02 in, and the pipe stiffness PS = 27.34 lb/in². The manufacturer desires to replace this pipe with a ribbed pipe instead of the solid-wall design. The ribbed pipe is to have ribs spaced on 78-in centers, and the wall thickness between ribs is to be 0.6 in. The ribs will be constructed to act in an integral manner with the wall such that the pipe stiffness is equal to 27.34 lb/in^2 as in the solid-wall pipe. Carry out necessary calculations to determine if the ribbed pipe will perform adequately when installed with the same installation conditions as the pipe in Example 7.17.

1. Check the pressure design (see Example 7.17).

$$\sigma = \frac{PD}{2t} = \frac{60\ (84)}{2\ (0.6)} = 4200 \text{ lb/in}^2$$

Since the hydrostatic-design basis = 10,000 lb/in^2, the safety factor is 10,000/4200 = 2.38.

2. Check the bending strain (see Example 7.17). First, find the strain in the wall at a point away from the rib.

$$\varepsilon_b = 6\left(\frac{t}{D}\right)\left(\frac{\Delta y}{D}\right) = 6\left(\frac{0.6}{84}\right)(0.03) = 1.29 \times 10^{-3} \text{ in/in}$$

Second, find the strain in the wall at a point near the rib. Assume the rib thickness from the inside wall to the outside of the rib is 2.10 in; also assume the distance from the inside wall to the centroid of the wall section is $X_c = 0.68$ in.

Since the wall thickness is 0.60 in, the centroid is 0.08 in outside of the wall.

$$\varepsilon_b = 6\left(\frac{t}{D}\right)\left(\frac{\Delta y}{D}\right) = 12\left(\frac{t}{2D}\right)\left(\frac{\Delta y}{D}\right)$$

where $t/2$ may be replaced by 0.68. Thus,

$$\varepsilon_b = 12\left(\frac{0.68}{84}\right)(0.03) = 2.91 \times 10^{-3} \text{ in/in}$$

Wall bending strain is within design limits.

3. Check the combined strain (see Example 7.17). For a near rib

$$\varepsilon_c = \frac{PD}{2Et} + 6\left(\frac{t}{D}\right)\left(\frac{\Delta y}{D}\right)$$

$$= \frac{PD}{2Et} + 12\left(\frac{t}{2D}\right)\left(\frac{\Delta y}{D}\right)$$

where $t/2$ can be replaced by 0.68 in (see Example 7.17). Thus

$$\varepsilon_c = \frac{60\ (84)}{2\ (3.5 \times 10^6)\ (0.6)} + 12\left(\frac{0.68}{84}\right)(0.03)$$

$$= 1.20 \times 10^{-3} + 2.91 \times 10^{-3} = 4.11 \times 10^{-3} \text{ in/in}$$

This strain exceeds the design strain of 3.6×10^{-3}. However, the design strain included a safety factor, and the pressure used included a surge pressure. Also, the effective thickness near the rib is larger than the 0.6 used in the calculation. In any case, the limiting long-term strain of 5.4×10^{-3} in/in has not been exceeded, so the combined strain is all right.

In the wall away from the rib

$$\varepsilon_c = \frac{PD}{2Et} + 6\left(\frac{t}{D}\right)\left(\frac{\Delta y}{D}\right)$$

$$= \frac{60\,(84)}{2\,(3.5 \times 10^6)\,(0.6)} + 6\left(\frac{0.6}{84}\right)(0.03)$$

$$= 1.20 \times 10^{-3} + 1.29 \times 10^{-3} = 2.49 \times 10^{-3}$$

4. Check the buckling. The ribbed pipe in this example has a larger pipe stiffness than that of the solid-wall pipe of Example 7.17. Therefore, general buckling will not occur, and a design check should be made for localized buckling. Texts dealing with advanced mechanics of materials or theory of elasticity usually have solutions for localized buckling of tubes with ring stiffeners. The book *Theory of Elastic Stability,* by Timoshenko and Gere, gives such a solution in graphical form on p. 480 (see Fig. 7.76). These solutions are for tubes subjected to hydrostatic pressure and *not* constrained by soil. The surrounding soil effectively stiffens the pipe. Thus, a pipe in soil will take a larger buckling load than a pipe subjected to hydrostatic pressure. Therefore, the hydrostatic solutions are conservative.

From Fig. 7.76, we can determine the following:

$$\ell = \text{rib spacing} = 78 \text{ in}$$

$$a = \text{pipe radius} = 42 \text{ in}$$

$$\nu = \text{Poisson's ratio} = 0.3$$

$$h = \text{pipe thickness} = 0.6 \text{ in}$$

$$\alpha = \frac{t^2}{12r^2} = \frac{0.6}{12\,(42)^2} = 1.7 \times 10^{-5}$$

$$E = \text{elastic modulus} = 3.x5 \times 10^6 \text{ lb/in}^2$$

$$q_{\text{cr}} = \text{buckling pressure}$$

From the curves, $\psi = 0.9 \times 10^{-4}$ and

$$q_{\text{cr}} = \frac{\psi E h}{\alpha\,(1 - \nu^2)}$$

$$= \frac{(9 \times 10^{-4})\,(3.5 \times 10^6)\,(0.6)}{42\,(1 - 0.9)} = 49.5 \text{ lb/in}^2$$

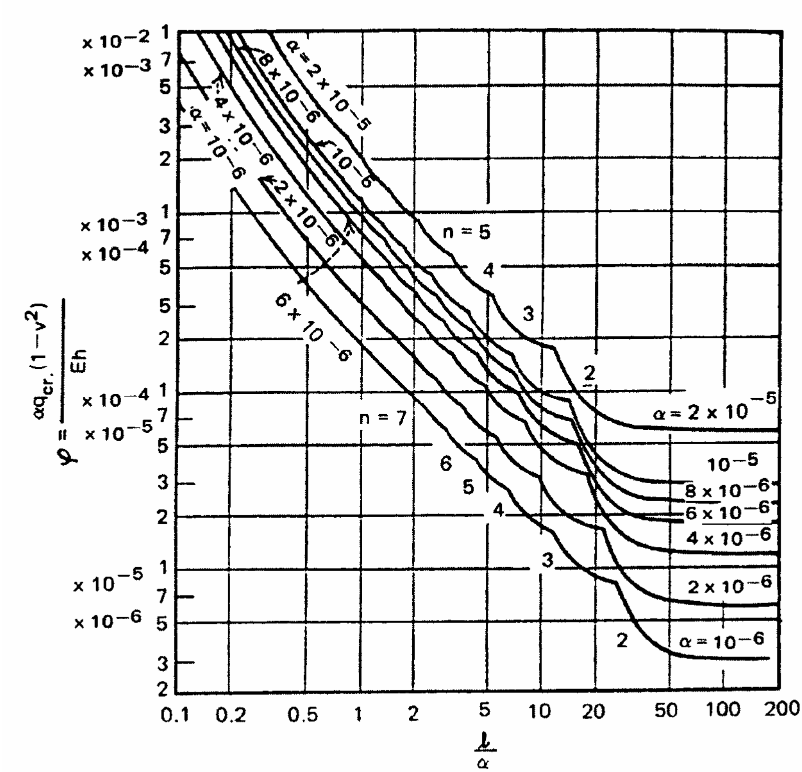

Figure 7.76 Curves for critical buckling pressure q_{cr} for stiffened circular cylinders subjected to a uniform radial pressure. (*Reprinted by permission from Timoshenko and Gere*).[55]

Again, this is the buckling pressure for a pipe subjected to hydrostatic pressure without soil support. The actual buckling pressure will be larger and can be approximated as follows:

The general buckling pressure for a long tube (pipe) subjected to only hydrostatic loading is given by

$$q_{cr} = \frac{3EI}{r^3\,(1-\nu^2)} \qquad \text{see Eq. (3.13)}$$

For the pipe in our example,

$$q_{cr} = \frac{3EI/r^3}{1-\nu^2} = \frac{3\,(4.08)}{0.91} = 13.5\ \text{lb/in}^2$$

Calculate the general buckling pressure for pipe in soil as was accomplished in Example 7.17:

$$q_{cr} = \left[32 R_w B' E' \left(\frac{EI}{D^3} \right) \right]^{1/2}$$

$$= [32\ (1.0)\ (0.52)\ (650)\ (0.51)\ ]^{1/2} = 77.8\ \text{lb/in}^2$$

Note that this pressure is $77.8/13.5 = 5.8$ times greater than that for the pipe with no soil support. Consequently, for localized buckling in soil, in this example, a factor of 3 can be used conservatively. Thus, the localized buckling pressure in soil can be approximated by multiplying the unsupported hydrostatic buckling pressure value by 3.

$$q_{cr} = 49.5\ (3) = 148\ \text{lb/in}^2$$

The applied pressure is 21 lb/in2 (see Example 7.17). Thus, the pipe in this example will not experience localized buckling. Again, general buckling will occur at a lower pressure than localized buckling. In fact, localized buckling will not occur even without soil support.

A note of caution: The above analyses assume a fairly uniform pressure. Nonuniform pressures or high pressure concentration will substantially lower the critical buckling pressures and may lead to localized buckling. Extreme hard spots such as large rocks or other hard debris next to the pipe can cause such pressure concentrations. These can be avoided by proper construction practices. Nonuniform pressures occur when a large-diameter pipe has only a low hydrostatic head. In such a case, the hydrostatic pressure is not uniform around the pipe, and if buckling occurs, it will usually be at the bottom of the pipe. Many examples of this type of failure are known to have occurred in buried tanks. Quantitative analyses for such cases are not precise, and higher safety factors are required.

References

1. American Association of Civil Engineers and Water Pollution Control Federation. 1982. *Gravity Sanitary Sewer: Design and Construction.*
2. ASTM D 1784. 1990. *Standard Specification for Rigid Poly(Vinyl Chloride) (PVC) Compounds and Chlorinated Poly(Vinyl Chloride) (CPVC) Compounds.* Philadelphia.
3. ASTM D 2152. 1980. *Standard Test Method for Degree of Fusion of Extruded Poly(Vinyl Chloride) (PVC) Pipe and Molded Fittings by Acetone Immersion.* Philadelphia.
4. ASTM D 2241. 1989. *Standard Specification for Poly(Vinyl Chloride)(PVC) Plastic Pipe (SDR-PR).* Philadelphia.
5. AWWA C900. 1989. *AWWA Standard for Polyvinyl Chloride (PVC) Pressure Pipe, 4 in. through 12 in. for Water.* Denver.
6. AWWA C905. 1988. *AWWA Standard for Polyvinyl Chloride (PVC) Water Transmission Pipe, Nominal Diameters 14 in. through 36 in.* Denver.
7. AWWA Standards M11, M9, M23, C150, C200, C206, C300, C301, C303, C400, C401, C402, C403, C900, C901, C905, and C950; American Water Works Association, Denver.
8. Bauer, D. E. 1990. 15 Year Old Polyvinyl Chloride (PVC) Sewer Pipe: A Durability and Performance Review. In *Buried Plastic Pipe Technology,* ASTM STP 1093. George S. Buczala and Michael J. Cassady, eds. Philadelphia.

9. Berens, A. R. 1985. Prediction of Organic Chemical Permeation through PVC Pipe. *Journal of AWWA* 77(11):57–65.
10. Bishop, R. R. 1983. *Course Notebook.* Logan: Utah State University.
11. Bishop, R. R. 1981. Time Dependent Performance of Buried PVC Pipe. In *Proceedings of the International Conference on Underground Plastic Pipe,* American Society of Civil Engineering Conference, New York, pp. 202–212.
12. Boscardin, M. D., E. T. Selig, R. S. Lin, and G. R. Yang. January 1990. Hyperbolic Parameters for Compacted Soils. *ASCE Journal of Geotechnical Engineering* 116(1).
13. Burns, J. Q., and R. M. Richard. 1964. Attenuation of Stresses for Buried Cylinders. In *Proceedings of the Symposium on Soil-Structure Interaction.* Tucson: University of Arizona Engineering Research Laboratory.
14. Chambers, R. E., and F. J. Heger. 1975. *Buried Plastic Pipe for Drainage of Transportation Facilities.* Cambridge, Mass.: Simpson Gumpertz and Heger, Inc.
15. Concrete Pipe Division of U.S. Pipe and Foundry Company. (No date.) *Bulletin 200.* Birmingham, Ala.
16. Devine, Miles. 1980. *Course Notebook.* Logan: Utah State University.
17. Ductile Iron Pipe Research Association. 1984. Thrust Restraint Design for Ductile Iron Pipe. Birmingham, Ala.
18. Duncan, J. M., P. Byrne, K. S. Wong, and P. Mabry. 1980. *Strength, Stress-Strain and Bulk Modulus Parameters for Finite Element Analysis of Stress and Movements in Soil Masses.* Report no. UCB/GT/80-0. Berkeley: University of California, Office of Research Services.
19. Dunn, I. S., L. R. Anderson, and F. W. Kiefer. 1980. *Fundamentals of Geotechnical Analysis.* New York: Wiley.
20. Federal Aviation Authority (FAA). Aircraft Pavement Design and Evaluation. AC 150/5320-6C.
21. Federal Aviation Authority (FAA). Aircraft Data. AC 150/5325-5C.
22. Goddard, J. B. 1996. *An Analysis of Flexible Pipe Using the Burns & Richard Solution.* A computer program provided by Advanced Drainage Systems, Inc., Columbus, Ohio.
23. Howard, Amster K. 1977. Modulus of Soil Reaction (E^{TM}) Values for Buried Flexible Pipe. *Journal of the Geotechnical Engineering Division, ASCE* 103(GT). Proceedings Paper 127000.
24. Hsuan, Grace. 1996. Evaluation of Stress Crack Resistance of Polyethylene Pipe Resins via the Notched Constant Tensile Load (NCTL) Test. Paper presented at the Transportation Research Board Annual Meeting, Culverts and Hydraulic Structures A2C06, Washington, D.C. January 10.
25. Janbu, N. 1963. Soil Compressibility as Determined by Odometer and Triaxial Tests. In *Proceedings of European Conference on Soil Mechanics and Foundation Engineering,* pp. 19–25. Wissbaden, Germany: Soil Mechanics Foundation.
26. Janson, L-E. 1981. Plastic Gravity Sewer Pipes Subjected to Constant Strain by Deflection. In *Proceedings of the International Conference on Underground Plastic Pipe,* American Society of Civil Engineering Conference, New York, pp. 104–116.
27. Janson, L-E. 1996. *Plastic Pipes for Water Supply and Sewage Disposal.* Borealis, Stockholm, Sweden.
28. Jensen, Brent M. 1977. Investigation of Stain Limits Proposed for Use in Designing PVC Pipe Subjected to External Pressure. Master's thesis. Logan: Utah State University.
29. Katona, M. G., J. B. Forrest, R. J. Odello, and J. R. Allgood. 1976. *CANDE-A Modern Approach for the Structural Design and Analysis of Buried Culverts.* Report FHWA-RD-77-5. FHWA, U.S. Department of Transportation.
30. Katona, M. G., P. D. Vittes, C. H. Lee, and H. T. Ho. 1981. CANDE-1980: Box Culverts and Soil Models. Springfield, Va.: National Technical Information Service.
31. Konder, R. L., and J. S. Zelasko. A Hyperbolic Stress-Strain Formulation of Sands. In *Proceedings of the Second Pan American Conference on Soil Mechanics and Foundation Engineering.* 1:209.
32. Krizek, R. J., R. A. Parmelee, N. J. Kay, and H. A. Elnaggar. 1971. Structural Analysis and Design of Buried Culverts. National Cooperative Highway Research Program Report 116. Washington: National Research Council.

33. Kulhawy, F. H., J. M. Duncan, and H. B. Seed. 1969. Finite Element Analysis of Stresses and Movements in Embankments during Construction. Report TE-69-4. Berkeley: University of California, Office of Research Services.
34. Kunz, Walter M. 1982. Mechanical Properties of Filled Poly Vinyl-Chloride. Master's thesis. Logan: Utah State University.
35. Marston, A. 1930. The Theory of External Loads on Closed Conduits in the Light of the Latest Experiments. *Bulletin 96.* Ames: Iowa Engineering Experiment Station.
36. Molin, J. 1985. Long Term Deflection of Buried Plastic Sewer Pipes. In *Advances in Underground Pipeline Engineering.* American Society of Civil Engineers, New York, pp. 263–277.
37. Moser, A. P. 1990. *Buried Pipe Design,* 1st ed. New York: McGraw-Hill.
38. Moser, A. P. 1983. *Course Notebook.* Logan: Utah State University.
39. Moser, A. P. 1981. Strain as a Design Basis for PVC Pipes? In *Proceedings of the International Conference on Underground Plastic Pipe,* American Society for Civil Engineering Conference, New York, pp. 89–102.
40. Moser, A. P., John Clark, and D. P. Blair. 1985. Strains Induced by Combined Loading in Buried Pressurized Fiberglass Pipe. In *Proceedings ASCE International Conference on Advances in Underground Pipeline Engineering.* Madison, Wis.: ASCE.
41. Moser, A. P., and K. G. Kellogg. 1994. *Evaluation of Polyvinyl Chloride (PVC) Pipe Performance.* Denver: AWWARF.
42. Moser, A. P., and O. K. Shupe. 1989. *Testing Fifteen Year Old PVC Sewer Pipe.* Logan: Buried Structures Laboratory, Utah State University.
43. Moser, A. P., O. K. Shupe, and R. R. Bishop. 1990. Is PVC Pipe Strain Limited after All These Years? In *Buried Plastic Pipe Technology,* ASTM STP 1093. George S. Buczala and Michael J. Cassady, eds. Philadelphia.
44. Moser, A. P., R. K. Watkins, and O. K. Shupe. 1976. Design and Performance of PVC Pipes Subjected to External Soil Pressure. Logan: Buried Structures Laboratory, Utah State University.
45. Nyby, D. W. 1981. Finite Element Analysis of Soil Sheet Pipe Interaction. Ph.D. dissertation. Logan: Department of Civil and Environmental Engineering, Utah State University.
46. Ozawa, Y., and J. M. Duncan. 1973. ISBILD: A Computer Program for Analysis of Static Stresses and Movements in Embankments. Report no. TE-73-4. Berkeley: Office of Research Services, University of California.
47. Paris, J. M. November 10, 1921. Stress Coefficients for Large Horizontal Pipes. *Engineering News Record* 87(19).
48. Piping Systems Institute. 1980. *Course Notebook.* Logan: Utah State University.
49. Spangler, M. G. 1950. Field Measurements of the Settlement Ratios of Various Highway Culverts. *Bulletin 170.* Iowa State College.
50. Spangler, M. G. 1941. The Structural Design of Flexible Pipe Culverts. *Bulletin 153.* Ames: Iowa Engineering Experiment Station.
51. Spangler, M. G. 1933. The Supporting Strength of Rigid Pipe Culverts. *Bulletin 112.* Iowa State College.
52. Spangler, M. G., and R. L. Handy. 1982. *Soil Engineering,* 4th ed., New York: Harper & Row.
53. Spangler, M. G., and W. J. Schlick. 1953. Negative Projecting Conduits. Report 14. Iowa State College.
54. The Asphalt Institute. March 1978. *Soils Manual for the Design of Asphalt Pavement Structures.* Manual Series no. 10 (MS-10). College Park, Md.
55. Thompson, C., and D. Jenkins. 1987. *Review of Water Industry Plastic Pipe Practices.* Denver, AWWARF.
56. Timoshenko, S. P., and J. M. Gere. 1961. *Theory of Elastic Stability,* 2d ed. New York: McGraw-Hill.
57. Timoshenko, S. 1956. *Strength of Materials, Part 11,* 3d ed. New York: D. Van Nostrand.
58. Uni-Bell PVC Pipe Association. 1982. *Handbook of PVC Pipe Design and Construction.* Dallas.
59. Uni-Bell PVC Pipe Association. 1991. *Handbook of PVC Pipe Design and Construction.* Dallas.

60. Walker, Robert P. 1983. *Course Notebook.* Logan: Utah State University.
61. Watkins, R. K., and M. G. Spangler. 1958. Some Characteristics of the Modulus of Passive Resistance of Soil—A Study in Similitude. In *Highway Research Board Proceedings* 37:576–583.
62. Walsh, Thomas, and Stanley Mruk. 1996. A New Index of Long Term Ductility for Polyethylene Piping Materials. Paper presented at the Transportation Research Board Annual Meeting, Culverts and Hydraulic Structures A2C06, Washington, D.C. January 10.
63. Wong, K. S., and J. M. Duncan. 1974. Hyperbolic Stress-Strain Parameters for Nonlinear Finite Element Analysis of Stresses and Movements in Soil Masses. Report TE-74-3. Berkeley: Office of Research Services, University of California.
64. Zienkiewitcz, O. C. 1977. *The Finite Element Method,* 3d ed., New York: McGraw-Hill.

Chapter 8

Pipe Installation and Trenchless Technology

Introduction

This chapter briefly discusses a number of the more common requirements of installation, omitting precise details that vary in individual installations. Also included are some safety aspects of pipeline construction; however, a general treatise on safety is outside the scope of this text. The use of trenchless methods for installing pipe and rehabilitating pipe is becoming more common, and some information on techniques used is included in this chapter.

The construction of a pipeline depends on many controlling factors, including pipe materials, trench depth, topography, soil conditions, and operating conditions. The properties of the soil being excavated and the soil used as backfill in the pipe zone are particularly important. How the pipe is handled and installed can have huge effects on its external load-carrying capacity and can be a controlling factor in the design of the pipe. How the pipe supports the loads from handling, soil cover, and water must be determined when the pipe installation is designed. If the cover or other external load on the pipe is high, the degree and uniformity of bedding support can have a substantial influence on the required pipe strength.

Transportation

Delivery of the pipe to the job site is usually considered part of the installation process. Requirements for packaging, stowing, restraining pipe during transit, unloading, and handling during the installation process are all important considerations. Transporting by railroads, on water via ships, or by trucks presents complications, but they can be overcome if given the proper consideration in advance of shipping. Most pipes shipped by truck are carried on flatbed trucks and trailers directly to the job site. Often damage is done to the pipe by tie-down equipment that is overly tensioned. One-time handling between shipper and customer will often avoid damage encountered by multiple loadings and unloadings. Whether the pipe is delivered directly to the job site or placed in temporary storage areas, care should be taken to place the pipe so it can be reached for movement to the trench with as little extra handling as possible. Also, every precaution should be taken to prevent damage to the pipe. Pipe ends are particularly vulnerable to damage from impact or point loading that may result from contact with construction equipment, rocks, or other obstacles on the ground.

When nesting a smaller-diameter pipe inside a larger pipe, the nested pipe should be padded to protect both pipes from damage. Loads should be prepared with sufficient stringers so that high concentrated loads are not applied to a single bearing point.

Pipe should, at all times, be handled with equipment designed to prevent damage to either the inside or the outside surface of the pipe. Care should be used in loading and unloading so as not to damage the pipe. Equipment to be used for handling pipe includes nylon straps, wide canvas or padded slings, wide padded forks, and skids designed to prevent damage. Unacceptable items include cables, hooks, narrow forks, unpadded chains, sharp edges on buckets, and metal bars. The placement of pipe along a rough right-of-way could damage the pipe. Necessary support to the pipe should be supplied. The pipe may be laid on sandbags, mounds of sand, wood blocks (padded if necessary), or other suitable supports to protect the pipe. Supports should be about one-quarter length from each end. It is usually not acceptable to allow pipes to roll or fall from the truck to the ground.

Trenching

If the pipe-zone bedding and backfill require densification by compaction, the width of the trench at the bottom of the pipe should be determined by the space required for the proper and effective use of tamping equipment. Where the sides of the trench will afford reasonable side support, the trench width that must be maintained at the top of the pipe, regardless of the depth of excavation, is the narrowest practical width that will allow proper densification of pipe-zone bedding and backfill materials. The space between the pipe and trench wall must be wider than the compaction equipment used in the pipe zone. Minimum width shall be not less than the greater of either the pipe outside diameter plus 16 in or the pipe outside diameter times 1.25, plus 12 in. The effect of the trench width on the performance of the pipe is dependent on the type of pipe and is discussed in Chap. 3. Safety considerations are of the utmost importance. Where possible, sloping the sides of the trench above the top of the pipe to the ground surface may be desirable if costs associated with sheeting and bracing can be reduced. Specially designed equipment may enable the satisfactory installation and embedment of pipe in trenches narrower than specified above.

Depth of trenches in city streets may be governed by existing utilities or other conditions. Where no other requirement is provided, the minimum cover should be generally selected to protect the pipe from transient loads where the climate is mild and should be determined by the depth of the frost line in freezing climates. The profile should be selected to minimize high points where air may be trapped. With favorable ground conditions, excavation can be accomplished in one operation; under more adverse conditions it may require several steps.

The trench bottom should receive careful attention and adequate provisions for maintaining grade. Typically, the trench bottom is excavated to a depth of at least 2 in, and more typically, 4 in below the established grade line. The bottom is brought to grade with material in which all stones and hard lumps have been removed. This bedding material should be firm, stable, and uniform along the pipe. In some soils, this bedding under the invert can be achieved by raking the trench bottom with the backhoe teeth to loosen the soil. The bedding is then brought to grade by the workers in the trench.

If excavation requires blasting, such as in hard rock, the sharp rock in the bottom of the trench may cause damage to the pipe. In such cases, the trench bottom should be excavated 6 in below grade, and a bedding of crushed rock or sand should be used to establish grade.

For unstable foundations, the foundation material should be removed to a sufficient depth. This should be done under the direction of a soils engineer. Excavate to the depth required by the engineer and replace with a foundation of ASTM class IA, class IB, or class II material (see Chap. 2). Use a suitably graded material where conditions may cause migration of fines and loss of pipe support. Place and compact foundation material. Control of unstable trench bottom conditions may be accomplished with the use of appropriate geofabrics.

Place pipe and fittings in the trench with the invert conforming to the required elevations, slopes, and alignment. Provide bell holes in pipe bedding, no larger than necessary, in order to ensure uniform pipe support. Fill all voids under the bell by working in bedding material. Also, excavation for sling removal should be provided to permit removal of the slings without damaging the pipe. In special cases where the pipe is to be installed to a curved alignment, maintain angular *joint deflection* (axial alignment) or pipe bending radius, or both, within acceptable design limits. Minimize localized loadings and differential settlement wherever the pipe crosses other utilities or subsurface structures, or whenever there are special foundations such as concrete-capped piles or sheeting. Provide a cushion of bedding between the pipe and any such point of localized loading. If trench sidewalls slough off during any part of excavating or installing the pipe, remove all sloughed and loose material from the trench.

The primary function of trench boxes, sheeting, and bracing is for safety, to prevent a cave-in of the trench walls or areas adjacent to the trench. In noncohesive soils combined with groundwater, it may be necessary to use steel sheet piling to prevent soil movement. Continuous steel sheet piling can be installed so that it is relatively watertight; and, if necessary, dewatering with trench-bottom sump pumps can be undertaken.

In some soil conditions, it is economical and practical to use a prefabricated unit that is at least as long as one section of pipe. The units are called *laying shields, trench shields,* or *trench boxes.* Such a box is pulled forward as the trenching and pipe laying progress. These movable supports should not be used below the top of the pipe zone unless approved methods are used for maintaining the integrity of embedment material. The shields protect workers from sloughs and cave-ins. They do not support the trench walls. Before moving such a device forward, place and compact embedment soil to sufficient depths to provide necessary support for the pipe. As the shield is advanced forward, the placement and compaction of the embedment soil at the rear of the device should be completed.

The design of the system of supports should be based on sound engineering principles of soil mechanics and the materials to be used, and the design must comply with applicable safety requirements. Normally supports are left in place unless otherwise directed by the engineer. Sheeting driven into or below the pipe zone should be left in place to preclude loss of support of foundation and embedment materials. If sheeting is to be removed, especially heavy sheeting, consideration must be given to the additional soil loads that may be transferred to the pipe. Make sure that the pipe, foundation materials, and embedment materials are not disturbed by support removal. If pulling leaves voids, fill all voids with the same materials and compact to required densities.

When top of sheeting is to be cut off, make the cut 1.5 ft (0.5 m) or more above the crown of the pipe. Leave the rangers, whalers, and braces in place as required to support cutoff sheeting and the trench wall in the vicinity of the pipe zone. Timber sheeting to be left in place is considered a permanent structural member and should be treated against biological degradation (e.g., attack by insects or other biological forms) as necessary, and against decay if above groundwater. A note of caution: Certain preservative and protective compounds may react adversely with some types of rubber ring gaskets and certain thermoplastics, and their use should be avoided in proximity of the pipe. All applicable local, state, and federal laws and regulations should be carefully observed, including those relating to the protection of excavations and the safety of persons working therein.

Dewatering

Groundwater can be a serious hindrance during excavation, pipe laying, and backfilling. If properly planned for in advance of construction, difficulties associated with groundwater can be minimized. Maintain the water level below the pipe bedding and foundation to provide a stable trench bottom. It is important to ensure the groundwater is below the bottom of the cut at all times, to prevent washout from behind sheeting or sloughing of exposed trench walls. Where feasible, the trench should be dewatered until the pipe has been installed with the prescribed bedding and backfill has been placed to a height at least above the groundwater level. For dewatering smaller volumes of water, the trench may be overexcavated and backfilled to grade with crushed stone or gravel to facilitate drainage of water to the point of removal. Dewatering a large amount of groundwater will require the use of a well-point system consisting of a series of perforated pipes driven into the water-bearing strata and connected to a header pipe and pump. Control the running water emanating from drainage of surface or groundwater to avert undermining of the trench bottom or walls, the foundation, or other zones of embedment. Provide dams, cutoffs, or other barriers periodically along the installation to preclude transport of water along the trench bottom. If needed, well-graded materials, along with perforated underdrains, can be used to enhance the transport of running water. The gradation of the drainage materials should be selected to minimize migration of fines from surrounding materials. Backfill all trenches after the pipe is installed to prevent disturbance of pipe and embedment.

Pipe Installation

The pipe trench should be kept free from water that could impair the integrity of bedding and joining operations. While pipe is placed in the trench, slings should be used and the pipe should not be dragged along the bottom of the trench. It should be supported by the sling while preparations are made to make the joint. Pipe should be laid to lines and grades shown on the contract drawings and specifications. The pipe must never be struck with the excavating bucket or other equipment accidently or on purpose to drive the pipe to grade. Such impact loads will damage the pipe wall, interior wall, or coating. Such damage is often not visible on the outer surface but will result in eventual pipe failure.

Pipe is normally assembled in the trench except under the most unusual conditions. Pipe that has O-ring rubber gaskets as seals must be assembled section by section in the trench. Smaller-diameter pipe joined by welding or couplings may be assembled aboveground in practicable lengths for handling and then lowered into the trench by suitable means which allows progressive lowering of the assembled run of pipe. If the method of assembling pipe aboveground prior to lowering it into the trench is used, care must be taken to limit the degree of curvature of the pipe during the lowering operation so as to not exceed the yield strength of the pipe material and/or damage the lining or coating materials on the pipe. Pipe deflection at any joint should be limited to the manufacturer's recommendation during the lowering operation. Work normally should proceed with the bell end of the pipe facing the direction of laying. The bell and spigot should both be thoroughly cleaned and lubricated in accordance with the pipe manufacturer's recommendations before the spigot is inserted in the bell. Following assembly, the pipe joint should be checked to determine that the proper insertion depth has been achieved. Most manufacturers have a mark on the spigot end. This joint should be mated so this mark is just at the bell, not inside the bell. Also, a thin metal feeler gage should be used to ensure that proper gasket placement exists. A gasket that has been rolled out of its groove is called a fish-mouthed gasket, and such a joint will leak.

Making the Joint

For elastomeric seal joints, verify that pipe ends are marked to indicate the insertion stop position, and ensure that pipe is inserted into pipe or fitting bells to this mark. Push the spigot into the bell using methods recommended by the manufacturer, keeping pipe true to line and grade. Protect the end of the pipe during homing, and do not use excessive force that may result in overassembled joints or dislodged gaskets. If the force required for insertion is excessive, the ring is probably rolling from its groove. In such a case, disassemble, clean the joint, and reassemble. Use only lubricant supplied or recommended for use by the pipe manufacturer. Do not exceed manufacturer's recommendations for angular joint deflection (axial alignment).

For solvent cement joints, follow recommendations of both the pipe and solvent cement manufacturers. If full entry is not achieved, disassemble or remove and replace the joint. Allow freshly made joints to set for the recommended time before moving, burying, or otherwise disturbing the pipe. Make sure the joining area is well ventilated.

For heat fusion joints, the process should be in conformance with the recommendations of the pipe manufacturer. Pipe may be joined at ground surface and then lowered into position, provided it is supported and handled in a manner that precludes damage.

Thrust Blocks

(See Chap. 4.)

Pipe-Zone Soil

(See Chaps. 2 and 3.)

Bedding and Backfill

Bedding and backfill should be brought to the specified density around the pipe and to the specified height over the top of the pipe. In-place tests of soil density should be made as required by the engineer. To guard against loss of pipe support from lateral migration of fines from the trench wall into open-graded embedment materials, it is sufficient to follow the minimum embedment width guidelines found in ASTM D 2321. Maximum particle size should be limited to $^3/_4$ in or less. This enhances placement of embedment material for nominal pipe, sizes 8 in and larger. For smaller pipe, a maximum particle size of about 10 percent of the nominal pipe diameter is recommended. All backfill materials should be free of lumps, clods, boulders, frozen matter, and debris. The presence of such material in the embedment may preclude uniform compaction and result in excessive localized loads and deflections.

When coarse and open-graded material is placed adjacent to a finer material, fines may migrate into the coarser material under the action of the hydraulic gradient from groundwater flow. Field experience shows that migration can result in significant loss of pipe support and continuing deflections that may exceed the design limits. Significant hydraulic gradients can arise in the pipeline trench during construction when water levels are being controlled by various well-point methods or after construction when permeable underdrain or embedment materials act as a “French” drain under high groundwater levels. The gradation and relative size of the embedment and adjacent materials must be compatible in order to minimize migration. In general, where significant groundwater flow is anticipated, avoid placing coarse, open-graded materials, such as class IA, above, below, or adjacent to finer materials unless methods are employed to impede migration such as the use of an appropriate stone filter or filter fabric along the boundary of the incompatible materials.

Embedment Density

(See Chap. 3 for details.) Embedment density requirements should be determined by the engineer based on deflection limits established for the pipe, pipe stiffness, and installation quality control, as well as the in situ soil and compactibility characteristics of the embedment materials used. For the design of a particular installation, the project engineer should verify that the density he or she specifies will produce the desired pipe performance.

The engineer should not specify densities higher than required. Achieving soil densities that are much higher than required is a waste of money, and it is usually the taxpayers' money. Specify what is required, and then have good field inspection to ensure that the design assumptions are met. The densification of the backfill envelope must include the haunches under the pipe to control both horizontal and vertical pipe deflections. There are several methods used to achieve a required density. These are listed in Chap. 3.

Safety Procedures for Construction and Related Activities

Introduction

Safety measures have always been important to protect both workers and the public. Safety has gained increasing attention in the United States since the advent of the Occupational Safety and Health Act (OSHA). It is imperative that responsibility for safety be assigned to an authoritative person who has full knowledge of the rules, regulations, and requirements of federal, state, and local agencies. A project can be shut down for what may seem to be even a minor infraction of the safety act. This section is only a brief outline of some safety concerns associated with pipeline construction, and in no way should it be considered official, inclusive, or definitive.

Pipe storage

Keep pipe yards and walkways clean and orderly. Always block pipe to prevent it from rolling or falling. Arrange and block each row of stacked pipe to prevent it from rolling from the pile. Use reasonably permanent material, such as chemically treated wood, for blocking. Store small pipe in racks according to length and size. Store pipes larger than 2 in diameter by stacking them with spacing strips placed between each row. Withdraw pipe from the top rows.

Shoring and bracing

Use proper shoring and bracing to prevent cave-ins while vaults or similar openings are under construction. Proper shoring cannot be reduced to a standard formula. Each job is an individual problem and must be considered under its own conditions. Federal and state or provincial standards list specific recommendations for shoring of excavations. The worker should take the following general precautions:

1. Do not take chances that may lead to injury.
2. Either use tight sheet shoring to guard against the caving in of sandy soil or loose material when the depth of the excavation exceeds 5 ft, or cut back the bank to the proper slope. Keep shoring at or near the bottom of the ditch as it is excavated, and follow with bracing to ensure safety. Trench shields are also acceptable as a protective system. A trench shield does not protect the environment, only the worker.
3. The placement of shores will depend on the type (classification) of soil encountered. Local, state or provincial, and federal laws mandate the distances and sizing of shoring support systems.
4. Extend shoring of any type below the excavation bottom whenever possible, and brace it thoroughly using timbers, wedges, and cleats, or a pipe/screw-jack combination. Place all bracing at right angles to the sheeting or uprights, and rigidly wedge, bolt, or cleat it to prevent movement. Hydraulic units are being used in many types of utility trench construction.
5. Use only full-sized lumber that is assessed to be sound and straight.
6. Install the upper braces or screw jacks first, and remove them last for best protection.
7. Also consider excavation dimensions, soil stability, variable weather and moisture conditions, proximity of other structures, weight and placement of soil and equipment used on the job, and sources of vibration when choosing the type of shoring to use, if any. The decision must rest with the engineer or foreman in charge.
8. Use hydraulic jacks temporarily only, and replace them with properly sized screw jacks or solid bracing.

Hard hats

Workers should always wear hard hats, especially subsurface workers.

Lifting

Personnel should not be required to do heavy lifting that may cause injury; use mechanical lifting devices to raise, lower, or suspend heavy or bulky material to work in trenches, manholes, or vaults.

Safe distance

Keep a safe distance from other workers to avoid striking them with tools.

Ladders

Use ladders where required. Do not jump into an excavation.

Adequate means of trench exit

Provide an adequate means of trench exit, such as a ladder or steps. Locate it so that no more than 25 ft of lateral travel is required. Extend the ladder from the bottom of the excavation to at least 3 ft above the ground surface.

Edge of excavation

Do not place excavated material closer than 2 ft from the edge of an excavation.

Falling tools

Falling tools are a danger to workers in the trench. Keep all tools, working materials, and loose objects orderly and away from the excavation shoulder.

Keep open traffic lanes clear

Keep tools, equipment, and excavated material out of open traffic lanes. Continually remove pebbles and small stones from, or prevent them from lodging on, a hard-surface roadway where tires may pick them up and throw them.

Posting barricades and warning signs

Provide and maintain all necessary barriers, watchmen, and flaggers to protect workers, vehicles, and pedestrians.

1. Place advance warnings, instructional signs, barricades, and delineators well ahead of the construction area to warn motorists and pedestrians of the area and safely take them through or past it. All such protection devices must meet the appropriate federal, state or provincial, or local specifications for size, shape, color, and placement.
2. Protect the work area with barricades, barriers, or planks to provide a safe working space. If necessary, use flaggers to direct and slow down traffic. When used, place trucks or air compressors between the work and the traffic.
3. During periods of reduced visibility, use adequate lighting on all barricades.
4. When no work is in progress, place adequate barriers, barricades, flashing lights, and signs to warn and divert traffic. Use reflecting tape on all barricades.
5. In winter, divert traffic, if necessary, from streets covered with surface ice resulting from a main break until sanding or scarifying restores safe driving conditions.
6. All personnel should wear protective clothing including hard hats and high-visibility traffic vests.

Debris in excavation

If the walls of an excavation contain glass, wire, or other sharp objects, carefully remove them.

Heavy rains or freezing weather

When resuming excavation after heavy rains or freezing weather, inspect all banks for cracks. These may indicate earth movement and the probability of cave-in.

Cave-ins

Frequently inspect the sides and rim of all open excavations to guard against cave-in. Operate earthmoving equipment from a position that will not imperil personnel or property by a cave-in due to vibration, stress, or dead weight.

Overhanging bank

If it is absolutely necessary to work above an overhanging bank, use a safety belt and a lifeline. Have a helper nearby to assist in an emergency.

Other utility lines

To avoid striking electric or telephone conduits, gas lines, or other substructures, locate other utility installations before starting work.

Protective clothing

Require workers to wear adequate eye, ear, and foot protection when using a jackhammer or when exposed to flying particles or falling objects.

Machines

Workers should always be aware of locations of running machines (backhoes, trenching machines, etc.). Workers should keep clear of the sweep path and try never to turn their backs toward the working machine(s).

Work breaks

Take work breaks, rests, etc. at designated locations away from the excavation.

Trenching machines

The following rules apply equally to all mechanical devices used to dig trenches and/or make excavations, including various types of trenchers, backhoes, buckets, scoops, and similar pieces of equipment.

1. Operators should always wear hard hats.
2. Never attempt to oil or grease a mechanism or repair or adjust any moving part of a trenching machine while it is in operation. Only qualified personnel should operate a trenching machine.
3. Guard all moving parts. Before starting the conveyor, make sure that no person is endangered by it.
4. To remove obstructions from the conveyor mechanism or buckets, stop the machines.
5. Be alert for falling material that might roll from the conveyor.
6. When practicable, drop dirt between the excavation and the highway to act as a barrier.
7. Cautiously fill gasoline or diesel tanks. Keep the spout in metallic contact with the machine to prevent static sparks from bridging the gap and igniting the vapors. Do not smoke. Keep proper fire extinguishers available when refueling construction equipment. Use only approved containers when storing flammables on the job site; clearly mark and define storage areas.

8. Use flags by day and flashing lights or flares by night to warn the public of the trenching machine and its operations. Liberally use these precautions on all highway or street work. Plan the warning system before the work is started.

9. Operate the machine vertically to prevent undercutting of the trench walls.

10. When loading or unloading trenching machines or other heavy equipment from truck beds, lowboys, or other conveyances, provide suitable skids and ample blocking to prevent movement of the conveyance.

11. When manually lifting or lowering pipe in an excavation, use two or more rope slings looped under the pipe, and handle from each side of the excavation. To prevent a heavy pipe from pulling workers into the excavation, anchor one end of each rope sling to a massive object such as a truck.

12. When aligning pipe in the excavation either manually or mechanically, keep hands and fingers away from ends of pipe and other substructures that could crush.

13. Govern crane operations by the signals of a qualified worker only.

14. Never try to catch and hold a length of pipe that slips from a crane or hoist sling.

15. Be alert to unsafe excavation sides when measuring, testing, or inspecting pipe in place on an excavation bottom.

16. When cutting sections of pipe, keep feet in the clear and use adequate blocking, chocks, or pipe vices to prevent pipe movement. Wear safety goggles.

17. Keep tools and appliances in good condition for handling, cutting, threading, or treating pipe. Always use the right tool for the job.

18. Do not let tools or materials become stumbling hazards where pipe is being handled.

19. Avoid shortcuts and makeshift methods that may increase the hazards of handling pipe.

Blasting operations

Only authorized and experienced employees may use explosives. These employees must conduct blasts in accordance with nationally recognized good practices. Always heed the following principles for avoiding accidents when using explosives:

1. Train these people properly. Handle explosives carefully and with respect. The fewest possible people should handle explosives to reduce the risk of accident. Choose only those with good judgment to handle explosives.

2. Have the explosive manufacturer's technical representative instruct the field crews in all blasting practices.
3. Rigidly enforce all safety regulations.
4. Do not use a two-way radio near blasting areas, as it might prematurely detonate a charge.
5. Open kegs or cases of explosives only outside and away from the magazine.
6. Use wooden, rubber, or fiber tools to open cases of explosives.
7. Cut the fuse long enough to extend at least 2 ft beyond the collar of the hole to allow time to get safely away. The minimum length of a safety fuse is 36 in.
8. Use a standard cap crimper, making sure that the cap is securely fastened to the fuse.
9. Under wet conditions, thoroughly waterproof the joint between fuse and cap.
10. Always keep the fuse free of kinks.
11. Use sufficient stemming to protect explosives from the end spit of a fuse or flying matchheads.
12. After a blast, permit only an experienced powderman to work in the area until it is definitely proved safe.
13. Burn empty explosives cases in the open to prevent them from being used as fuel.

Storing explosives

Always purchase, possess, store, transport, handle, or use explosives in accordance with local, state or provincial, and federal regulations. A few rules follow:

1. Store explosives only in a magazine that is dry, well ventilated, properly located, substantially constructed, and securely locked. Keep the area within 25 ft of the magazine clean and clear.
2. Prohibit smoking, carrying of matches, open lights, or other fire or flame in or near a magazine or while explosives are being handled.
3. Store only explosives in a magazine; leave all other materials outside.
4. Replace the cover on a partially used package or case of explosives.
5. Store all cases of dynamite so that cartridges lie horizontally.
6. Store blasting caps or electric blasting caps in a box, container, or magazine separate from other explosives.

7. Protect blasting caps or electric blasting caps from the direct rays of the sun.
8. Store fuse or fuse lighters in a cool, dry place away from any flammable liquids.

Working in confined spaces

Underground structures, such as manholes and vaults, may have contaminated air. Workers have died in manholes contaminated by gas from a leaking gas main or by methane from decaying organic matter. Do not enter an underground structure without first ensuring that the air is safe. Follow these precautions:

1. Use proper tools for opening the manhole or vault and handling the cover, to prevent foot and back injuries.
2. Exercise every precaution to protect the work area from traffic hazards. Barricades, signs, high-level warning devices, and lights should meet local and state or provincial regulations to adequately warn traffic.
3. Continually station an attendant at the manhole entrance. Manhole entrants should wear a lifeline and harness.
4. Prohibit smoking in or about a manhole.
5. The attendant should be knowledgeable about safety procedures. He or she should have immediate access to rescue respiratory equipment and should maintain communication with the person inside the confined space. A two-way radio is handy for obtaining emergency help, if needed.
6. Train all employees working in or near confined spaces in proper work procedures, confined space hazards, and rescue procedures.
7. Use approved equipment and methods to verify the absence of harmful or toxic gases in an underground chamber before personnel enter. Do not consider safe any underground or confined structure until it has been demonstrated to be free of harmful gases and to contain sufficient oxygen to sustain life. Use an approved device to determine oxygen deficiency and concentrations of toxic or flammable gases. Periodically calibrate all monitoring or indicating equipment, and maintain records.
8. Provide adequate and continuous ventilation to ensure sufficient fresh air for personnel within a vault or manhole. When a blower is used for this purpose, place the discharge end near the bottom of the manhole to force the air up and out.
9. Prevent surface water or debris from accidentally entering the vault or subsurface during work.

Trenchless Technology

Introduction

In modern U.S. cities, piping services are complex and marvelous. But average city dwellers don't know about buried pipes, could care less, and simply take them for granted. They cannot contemplate the consequences if these services were to be disrupted. Cities can improve only to the extent that city service systems are improved. Improvement is slow because buried pipes are out of sight and, therefore, out of mind to planners and to sources of funding. Without maintenance of the piping systems, cities can only deteriorate. Without well-maintained cities, the quality of human life deteriorates.

Pipeline engineers and city managers are sobered by the present-day reality of deteriorating pipe systems. Leaks in buried (out-of sight) sewer pipes are either overloading treatment plants or are charging the soil and groundwater with contamination. The first thought is to replace the pipes. But many sewers have served so long that they are overgrown with streets and buildings. Excavation and replacement become an unattractive remedy.

Among the alternatives to replacement by excavation are trenchless technologies. Small-diameter gas lines are being jetted into place. Large-diameter traffic tubes and tunnels are being bored into place and lined. Moles and directional drilling are evolving with remarkable success.

Might something be done to rehabilitate existing pipelines? In fact, many sewer lines could handle increased sewage loads (1) if groundwater infiltration were eliminated by stopping leaks and (2) if flow rates could be increased by smooth-lining the pipes. Plastic pipe inserts are successful and attractive. They can be inverted, folded, or swaged; then inserted, inflated, and heated to thermoset the plastic. Leakage is stopped. Plastic inserts provide resistance to corrosion and to abrasion of sediment flushed along the pipe. Plastic inserts even contribute significantly to the structural integrity of the conduit.

But plastic has lower strength and lower stiffness than do most of the older, traditional materials. So how do flexible plastic pipes hold up under external water pressure? If leaks are stopped by inserting a plastic liner into a deteriorated sewer pipe (casing), groundwater no longer drains into the sewer pipe and the water table rises. Still the casing leaks, so external water pressure must be resisted by the liner. The conditions exist for buckling of the liner if external pressure is increased. A typical scenario for failure is the following.

The empty liner floats up, leaving a gap on the bottom where the external pressure (head h) is greatest. The liner is flattened a bit on the bottom because the perimeter shrinks under pressure. Consequently, the radius of curvature is increased. Both the increased radius of curvature and the loss of support, at the point where pressure is greatest, are the conditions for buckling of the liner. If pressure is increased, the liner will buckle. Because of plastic creep over the long term, the perimeter shrinks even more over time and the conditions for buckling worsen. What is the time to failure? What is the decrease in failure pressure in 50 years—or 100 years?

Tests at Utah State University (USU) have given some answers to these questions. Failure was defined as the maximum pressure when the liner is just on the verge of buckling. Buckling is the reversal of curvature. It is the result of instability and might be initiated by a slight glitch (holiday) in the material of the liner, by a slight deviation of the shape, or over a period of time.

Data from the report "Long Term External Hydrostatic Pressure Testing of Encased Insitupipes" show that long-term failure pressure is about one-half the short-term (quick-load) failure pressure. The ratio $^1/_2$ of long-term to short-term failure pressures applied to all Insitupipes tested with approximately the same D/t ratio. With ample safety factor, long-term design can be based on the half-ratio rule of thumb.

Except for an allowance for long-term plastic creep, the structural performance and performance limits of plastic pipes are based on the same generic properties required of all flexible pipes, including metals, composites, etc. Of course, pipe performance must not exceed performance limits. We refer to performance limits rather than failure because failure implies rupture or complete collapse. Performance limits usually fall short of failure. Performance limit is usually defined as excessive deformation of the pipe. Deformation includes rupture, buckling, ring deflection, puncturing, denting, etc.

Design of pipe liners

For a pipe liner in a casing, internal pressure is usually of no concern. Even if the liner inflates, it is confined by the casing as an innertube in a tire. External pressure on the liner causes ring compression stress of $a = P(\mathrm{OD})/(2t)$, where P is the external pressure, OD is the outside diameter, and t is the wall thickness. The ring compression stress must be less than the yield strength of the pipe wall. If steel has a yield strength 8 times as great as that of PVC, then the PVC pipe liner wall must be 8 times as thick as the equivalent steel pipe liner wall. This can be demonstrated by a section of pipe placed in shaped blocks and loaded to crushing of the pipe wall.

Buckling of the pipe liner wall is more complicated. It depends upon both the yield strength of the pipe wall and the pipe stiffness. But pipe stiffness depends upon wall thickness, modulus of elasticity *E,* shape, and degree of confinement by the casing. Because there are so many interactions, wall buckling of the liner is best found by experience, either from tests or from performances and failures in service.

Bases for evaluation of liners

Structural evaluation of liners must include wall strength to resist ring compression and pipe stiffness to resist buckling. Both rigid liners (such as mortar liners) and flexible liners (such as plastics) must meet the same requirements. Both must be designed for long-term service. Long-term service includes deterioration, corrosion, abrasion, and creep in the case of plastic liners. Long-term service for creep means long-term, persistent pressure. Design by ring compression is based on long-term strength. If pressure is only instantaneous, ring compression design is based on short-term strength. Short-term external pressure may be caused by a sudden vacuum inside the liner. It should be emphasized that testing is important in order to evaluate the performance and performance limits of liners.

Liners in broken casings

The question arises, Do liners reestablish any of the original strength of broken casings? Often the soil backfill retains the casing which continues to perform as a conduit. Of course, if horizontal soil support were lost, the pipe would collapse. Collapse could occur if sidefill soil were fine enough to be washed into the pipe through the cracks, leaving voids on the sides of the casing. But what if the ring deflection of the casing were to increase, say, due to increased surface loads or due to partial loss of horizontal side support? The results of tests performed at Utah State University show that for a typical Insitupipe installation in prebroken pipes, the vertical soil load at any given pipe deflection is roughly 1.5 times greater for the casing with the Insituform lining than for the casing with no lining. This is a significant increase in strength in the event that ring deflection increases. If there is no increase in ring deflection, at least the margin of safety is increased by roughly one-half.

Design specifications for plastic inserts should be based on proven performance—a track record. In general, design specifications are either procedural or performance. Procedural specifications spell out the details of manufacture and installation. Performance specifications describe the required performance. “Turnkey” projects are typical of performance specifications. Details on how to do it are left to the engineer and manufacturer. After the project is completed, the owner only has to turn the key and operate it with assurance of adequate performance for the design life of the project. Many products, such as home appliances, are sold on the basis of performance specifications—with a guarantee that performance will be satisfactory over the life of the product.

In buried flexible pipe design, procedural specifications have been the traditional basis for design. Pipe materials, shape, strength, modulus, seams, etc., are all spelled out. Soil type, placement, compaction, and zones of backfill soil are all carefully specified. Even the installation procedure is described in detail.

In reinforced-concrete pipe design, from experience, pipe design is so complex and specialized that pipeline engineers favor performance specifications, leaving the burden of pipe manufacture to the specialists. Besides the complexities of forming and casting the pipes, design details include a multitude of variables such as reinforcing steel—size, strength, smooth or deformed, spacing, directions, bonding, shear-steel, cages, longitudinal steel, etc. Likewise, the concrete is a function of many variables such as strength, aggregate size and distribution, water/cement ratio, type of cement, admixtures, and length of pipe sections. Consequently, engineers who specify reinforced concrete pipe, write performance specifications based on the D load strength of the pipe. The D load strength is essentially a parallel-plate load to failure. A section of pipe is compressed between the two heads of a testing machine. The D load is the load per unit length of pipe at failure. Failure is defined either as the load at the opening of a 0.01-in crack in the wall of the pipe, or the maximum load that the pipe section can take. The pipe engineer must then relate D load strength to anticipated loads: internal pressure, external pressure (soil, water table, and pressure due to live loads), and soil bedding conditions. The pipe is specified by performance, i.e., the minimum D load. The D load is ensured by testing a statistically representative number of the pipe sections.

The design of plastic inserts for rehabilitation of deteriorated pipes, like that of reinforced concrete pipes, is specialized and complex. Specialists are emerging with technology based on testing and on experience with in-service performance. They are identifying the most important performance limits, such as resistance to persistent external hydrostatic pressure for a period of 50 years. Long-term testing is essential because plastics creep. Long-term performance cannot simply be related to strength regression test data. As the plastic insert creeps, it changes shape with consequent increase in stress. Stress does not remain constant as reported by strength regression data. Long-term performance tests are essential.

Whenever performance specifications are in conflict with procedural specifications, performance usually prevails over procedure. Courts usually construe for (i.e., weigh more heavily) performance specifications and construe against procedural specifications.

Legal liability for performance

As products and installation methods become more complex and more specialized, legal obligations of the manufacturer are tightened. The traditional *caveat emptor* (let the buyer beware) approach is yielding to doctrines such as strict liability. According to *caveat emptor,* once the product is sold, the contract is executed, ownership is transferred, and the previous owner has no further liability. This doctrine began to change when guarantees and warrantees became part of the sales contract. Statutes of limitation (time limit for filing a lawsuit) were adjusted in common law to accommodate warrantees. Further changes are occurring as a doctrine of strict liability takes shape. Strict liability holds that the statute of limitations for filing a lawsuit against any previous owner, or anyone involved in manufacture, handling, marketing, dealership, repair, modification, installation, etc., of a product, begins at the time of injury—not the time of sale. The manufacturer has continuing liability and legal exposure. The legal exposure may be mitigated by modification or abuse of the product, or by reasonable anticipated wear or deterioration.

Testing of Insituform Pipes

Introduction

Insitupipes in broken buried rigid pipes stop leaks. But to what extent does the liner contribute to the structural strength and shape of the broken pipes? The cracked rigid pipe will take some additional load without collapse. The Insitupipe liner itself has structural strength and has significant pipe stiffness. What is the strength of the composite ring, i.e., of the cross section, of buried, broken, lined pipe? Because theoretical analyses are extremely complex and because of the many assumptions needed for solution, full-scale physical tests were undertaken. Two full-scale tests were performed in the large soil cell at Utah State University.

Procedure

The experiment comprised two tests, each with two parallel test sections, in the USU large soil cell shown in Fig. 8.1. In each test, the two parallel test sections were 30-in pipes placed in the soil cell separated by a spacing of 7.5 ft center to center. The test sections were 20 to 25 ft long. The height of soil cover over the tops of the test sections was 3 ft. The bedding was firm and uniformly compacted soil. The pipe-zone

Figure 8.1 The testing of Insituform pipe in the USU large test cell.

backfill soil was silty sand placed in layers and compacted to a uniform density. A vertical soil load was applied by 50 hydraulic cylinders attached to 10 beams, as shown in the photograph. Vertical diameters of the test sections were measured after each increment of load.

Each of the two parallel pipe sections in the first test was made up of 4-ft lengths of unreinforced concrete pipes, 30-in inside diameter. These were class 3 pipes with a minimum specified three-edge bearing strength of 3000 lbs/lin ft. The joints were tongue-and-groove. No gaskets or sealants were used at the joints. Each test section comprised five of these 4-ft-long pipe sections for a laid length of 20 ft. Both of the test sections in the first test were broken. An unbroken pipe 4 ft long was placed on each end of each of the parallel test sections to serve as a transition. Access pipes were placed in tandem with each of the transition pipes to provide for entrance of personnel. After backfill was placed, one of the test sections was lined with Insituform pipe. See Fig. 8.2. The 10 broken sections of concrete pipe were cracked in a three-edge-bearing device. The average ultimate load was 3806.4 lb/lin ft of pipe. The standard deviation was 398.04 lb/lin ft of pipe. Before loading in the three-edge-bearing device, each pipe section was banded with steel bands and stuffed with three 14-in-diameter paper sonotubes to serve as mandrels for holding the circular pipe cross section during transportation and installation in the soil cell. Figure 8.3 is a photograph of broken rigid pipes.

Figure 8.2 Test sections of pipe in place showing the process of inserting the Insituform pipe. The pipes visible are access pipes.

Figure 8.3 Broken rigid pipe after breaking in three-edge-bearing device. Broken pipes have paper sonotubes inside and are steel-banded on the outside to hold broken segments together.

The two test pipes in the second test were Insitupipes that had been inverted and cured in paper sonotubes of 30-in ID. One of the Insitupipes was made from a standard resin with modulus of elasticity of 300 to 400 kips/in^2. Its thickness was about 21 mm. The other was a formulation of resin with a modulus of elasticity of about 500 to 600 kips/in^2. Its thickness was about 16.5 mm.

For each test, two parallel test pipe sections were placed in the cell on a level soil bedding. A 12-in uncompacted lift of backfill soil was located on each side of both test sections and was hand-shoveled into place under the haunches. Shoveling or shovel-slicing of soil under the haunches is a typical procedure on the job. Backfill soil was then brought up in 1-ft lifts to 3 ft above the tops of the test pipe sections. The surface was leveled and covered with steel plates onto which the hydraulic cylinders would bear for loading the cell.

For the first test, each of the soil lifts was dropped into place from a conveyor and leveled, but was not mechanically compacted. Moisture content was kept on the dry side of optimum so that the soil density was as uniform as possible under the weight of the soil itself. The average soil density was 75.7 percent AASHTO.

For the second test, each of the 1-ft lifts of backfill soil was leveled and then compacted by one pass of a vibroplate compactor. The average soil density was 83.4 percent AASHTO T-99.

Figure 8.4 Equipment for inverting the Insitutube.

Figure 8.5 Process of inverting the Insitutube.

Test 1

This test comprised two parallel 20-ft-long test sections of 30-in-ID rigid pipes that had been previously cracked by a vertical line load in a three-edge-bearing test device. The cracks occurred approximately at 3, 6, 9, and 12 o'clock. The pipes were so oriented in the soil cell that the top cracks in all five pipes in each test section were at the top and were in line. One of the two test sections was lined with a 21-mm-thick Insitupipe. The objective of the first test was to provide a direct comparison between the structural performance of two buried broken rigid pipes under increasing vertical soil pressures, one test section lined and the other unlined (see Figs. 8.4 and 8.5 for process). Structural support is tantamount to an increase in safety factor or a margin of safety against further deformation or collapse. Collapse of broken rigid pipes can occur if cracks in the pipes allow leaks large enough for in-migration of soil particles from around the pipe, thus leaving an empty vault in the soil at the sides and over the pipe. A soil vault is the prime condition for collapse of a broken rigid pipe. With no side support, the broken pipe collapses when the soil vault collapses. The test also provided data for comparing the load-deflection diagram with the load-deflection relationship predicted by theory.

With the two test sections positioned in the soil cell, the sonotube mandrels were removed. Access pipes were then located in line with the test sections for entrance of personnel. The first backfill soil lift was placed on the bedding, shoveled under the haunches, and leveled. A second lift was then placed and leveled. With two lifts of soil backfill to support the broken rigid pipes, the steel bands holding the pipes together were cut and removed. The backfill was placed in 1-ft lifts, but was not compacted. The soil lifts were continued on up to 3 ft above the tops of the test sections. Soil embankments were then shaped up at the ends of the cell. Loading beams were lowered and pinned into place. A preliminary vertical soil pressure of 1450 lb/ft^2 was applied with a corresponding pipe deflection less than one percent. This configuration was established as the configuration of the broken rigid pipes for Insituforming. Pipe deflections during loading were based on this initial pipe deflection as zero and on this vertical diameter of the broken rigid pipes. Insides of pipes were cleaned, and an Insitutube was placed and inverted in one test pipe. For the Insitupipe with wall thickness of $t = 21$ mm, the dimension ratio DR was in the range of 36 to 38. The Insitutube was inverted at the recommended pressure head using a polyester resin and standard cure.

Vertical loads were applied in increments equivalent to about 6 ft of soil cover at a unit weight of 120 lb/ft^3. After each increment of load, the vertical ring deflections were measured at various locations. All other pertinent observations were recorded. This procedure continued until a soil load of 8700 lb/ft^2 was reached, which is equivalent to 72.5 ft of soil cover at unit weight 120 lb/ft^3. Measurements and observations were recorded, and the test was terminated.

Results of test 1

Pertinent observations from test 1 follow:

1. The Insitupipe contributes significant strength to the pipe-soil system. The strength contribution is the result of two phenomena, the reinforcement phenomenon and the stiffener phenomenon, as explained in the next paragraphs.

2. As the soil load increased above $P = 2200$ lb/ft^2, the unlined test section began to deflect. The lined test section did not begin to deflect until the soil load was 2900 lb/ft^2. This increase in strength is the reinforcement phenomenon. The Insitupipe serves as reinforcement. As cracks inside the rigid pipe widen at 6 and 12 o'clock, the Insitupipe holds the cracks together.

3. Above a soil pressure of 2900 lb/ft^2, the load-deflection curves were approximately linear up to about 10 percent deflection, but the slope of the curve for the lined pipe is 1.5 times as steep as that of the unlined curve. This is the stiffener phenomenon. This increase in strength is the contribution of pipe stiffness by the Insitupipe.

4. The safety factor due to the reinforcement phenomenon is 1.4. The safety factor due to the stiffener phenomenon is 1.5. The two are not cumulative, but clearly the safety factor is not less than 1.5, even if bond is not achieved. In this test, the soil load was increased. Therefore, the pipe deflection increased. In practice, the pipe deflection does not increase—it has already occurred, probably at the time the rigid pipe broke. Therefore, the increased strength contributed by the Insitupipe is available as a margin of safety of at least 1.5.

5. It is noteworthy that neither of the two test sections collapsed completely, even though both were deformed beyond what most engineers would accept as performance limits.

6. As the pipe deflection increases in the broken rigid pipe sections, the cracks widen and the potential for leakage increases. If the leakage allows for in-migration of soil particles into the pipe, in time an empty soil vault will develop around and over the pipe. The pipe loses its sidefill soil support. When the soil vault becomes large, it collapses and soil falling on the broken pipe collapses the pipe. The photographs of Figs. 8.6 and 8.8 show the potential for leakage and in-migration of soil particles into the unlined section. No such leakage potential occurred in the lined section. See Figs. 8.7 and 8.9.

7. At the highest vertical soil pressure of P = 8700 lb/ft^2, a discontinuous, longitudinal hair crack was observed inside the pipe in the

Figure 8.6 The inside of the broken rigid pipe test section after loading to a vertical soil pressure of 5040 lb/ft^2 (equivalent burial depth of 42 ft).

Figure 8.7 The inside of the lined broken rigid pipe test section. The vertical soil pressure is 5040 lb/ft^2 (equivalent burial depth of 42 ft).

Figure 8.8 The inside of the broken rigid pipe test section after loading to a vertical soil pressure of 8700 lb/ft^2.

Figure 8.9 The inside of the lined broken rigid pipe test section. The vertical soil pressure is 8700 lb/ft^2.

crown of the Insitupipe. This was not a leak, but is indicative of the high tensile stress in the Insitupipe due to increasing deflection of the rigid pipe. The probability of such a crack in practice is low because the broken rigid pipe does not continue to deflect.

Test 2

The purpose of the second test was to provide a comparison between two 30-in-OD buried Insitupipes—one of standard resin formulation, with a 21-mm wall thickness, DR = 36 to 38; and the other of a new resin formulation with a 16.5-mm wall thickness, DR = 46 to 48. The two test sections were located in parallel in the soil cell, and so, for comparison, were subjected to the same backfill soil conditions and the same vertical soil pressures. This test provided a quantitative comparison of the load-carrying capacity of each Insitupipe and provided load-deflection diagrams of each for comparison.

The Insitupipes for this test were formed inside paper sonotubes. Soil was placed to at least 1 ft over the two sonotubes into which Insitupipes were formed. This soil cover provided a uniform insulation and heat-transfer medium during curing and cooling of the two 30-ft sections of Insitupipe.

The two parallel test sections of the Insitupipe were placed in the test cell. Access pipes were located in tandem at the other end of each test section. Backfill was placed in 1-ft lifts. Each soil lift was compacted by one pass of a vibroplate compactor. Compaction was continued in lifts on up to 3 ft above the tops of the test sections. The average soil density was 83.4 percent AASHTO T-99. Vertical soil pressure was applied in increments of 50 lb/ft^2 in the hydraulic cylinders. Measurements and observations were the same as those in the first test.

Results of test 2

Data for standard Insitupipes and Insitupipes with additive A are as follows:

Data	Standard Insitupipe	Type 2 Insitupipe
OD = outside diameter, in	30	30
t = wall thickness, mm	21	16.5
DR = dimension ratio	37	47
E = modulus of elasticity, kips/in^2	350	550

1. The ratio of pipe stiffnesses for the type 2 Insitupipe and the standard Insitupipe is $R = 0.75$. Despite the greater modulus of elasticity E for the type 2 Insitupipe, its lesser wall thickness prevails and the pipe stiffness is only three-fourths as great as that of the standard Insitupipe.
2. The standard pipe deflected slightly less than the type 2 pipe.
3. No distress was observed in either of the test pipe sections. Even at vertical soil pressure of 7300 lb/ft^2, both pipes would perform adequately in service.

Trenchless Technology Methods

Trenchless technology methods include all methods of installing or renewing underground utility systems with minimum disruption of the surface or subsurface. The demand for installing new underground utility systems in congested areas with existing utility lines has increased the necessity for innovative systems to go underneath in-place facilities. Environmental concerns, social (indirect) costs, new safety regulations, difficult underground conditions (existence of natural or artificial obstructions, high water table, etc.), and new developments in equipment have increased the demand for trenchless technology.

New installation methods

Soil information needed for tunneling and trenchless construction may be different from what is needed for design. The project designers usually use the Unified Soil Classification System (USCS). For trenchless technology construction, additional information is required. The trenchless technology contractor is concerned with the behavior of the soil during excavation and removal. The terms commonly used in the trenchless technology industry are running ground, flowing ground, raveling ground, squeezing ground, and swelling ground. Some trenchless contractors are more familiar with such terms as wet running sand, wet stable sand, dry sand, dry clay, wet clay, soil with small gravel, soil with large gravel, cobbles, boulders, hard pan, soft or hard rock, and fill and mixed face conditions.

The successful completion of a trenchless construction project requires a clear understanding of underground conditions and the selection and utilization of equipment used for the specific conditions of the project. The trenchless contractor must navigate through soil without seeing the excavation face and conduit installation process. Trenchless construction requires appropriate planning for expected underground conditions. Once the trenchless excavation has started, it might be too late to make any changes in equipment and method without extra costs and delays.

Contractors involved with construction of underground utility systems should familiarize themselves with compatibility of these methods and characteristics of underground conditions for a specific project. The subsurface conditions will be important in the selection of the proper trenchless equipment and method.

No one trenchless construction method (TCM) is best suited for all conditions. It is important that all the project participants, including the owner, installer, designer, contractor, and regulatory agencies involved with TCMs, be familiar with the capabilities of the available methods, as some methods provide more flexibility than others. Due to the increasingly critical nature of installations of utility systems in congested areas, the need for monitoring and control systems has increased. In many situations, it has become necessary that the systems be installed with a high degree of precision. However, conditions may vary from project to project. Therefore, the methods permitted should be based on an evaluation of the specific project. Methods considered acceptable in stable clay may not be suitable in wet sand, and the required precision for a sanitary gravity sewer line is not necessary, in most cases, for pressure systems or cables.

Quality contract by developing partnering and cooperating attitudes among all parties involved and total quality management in trenchless projects is extremely important. Total quality management involves owners, designers, contractors, and all other parties in the construction sharing risks and providing a quality design and quality construction.

At critical locations which involve public health and safety, it becomes the designer's and the regulatory agency's responsibility to limit proposed methods to only those compatible for the conditions. This should be accomplished with adequate and complete specifications prepared with an understanding of the operating principles of available methods.

Renewal methods

The basic trenchless pipeline renewal methods can be categorized into the following types: (1) cured-in-place pipe (CIPP), (2) slip-lining, (3) in-line replacement, (4) close-fit pipe, and (5) point-source repair.

Cured-in-place pipe. CIPP is a liquid thermoset resin-saturated material inserted into the existing pipeline by hydrostatic or air inversion or by mechanically pulling with a winch and cable. The material is heat-cured in place. Insituform introduced CIPP in the United Kingdom in 1971 and entered the U.S. market in 1977. In 1989, the InLiner USA process was introduced in Houston, Texas. Other CIPP systems have since been introduced into the market.

The primary components of the CIPP are a flexible fabric tube and a thermosetting resin system. For typical CIPP applications, the resin is the primary structural component of the system. These resins generally fall into one of the following generic groups: (1) unsaturated polyester, (2) vinyl ester, and (3) epoxy. Each resin has distinct chemical resistance and structural properties. All have excellent chemical resistance to domestic sewage.

Polyester resins were originally selected for the first CIPP installations due to their chemical resistance to municipal sewage and their economic feasibility. Unsaturated polyester resins have remained the most widely used systems for the CIPP processes for more than two decades.

Pressure pipeline and industrial applications typically use vinyl ester and epoxy resin systems where their special corrosion and/or solvent resistance and higher-temperature performances are needed and higher cost is justified. In drinking water pipelines, epoxy resins are required.

The primary function of the fabric tube is to carry and support the resin until it is in place in the existing pipe and is cured. This requires that the fabric tube withstand installation stresses with a controlled amount of stretch, but with enough flexibility to dimple at side connections and expand to fit against existing pipeline irregularities. The fabric tube material can be woven or nonwoven, with the most common material being nonwoven. These fabrics provide some reinforcement to the plastic after it has set.

The primary differences between the various CIPP systems are in the composition and structure of the tube, method of resin impregnation (at the project site by hand or by vacuum, or at the factory), installation procedure, and curing processes. There are two primary approaches to installing the flexible tube—inverting in place and winching in place. Specific variations of installation procedures and materials are employed by different manufacturers. See Figs. 8.10 to 8.14.

Slip-lining. Slip-lining is one of the earliest forms of trenchless pipeline rehabilitation. A new pipe of smaller diameter is inserted by pulling or pushing into a deteriorated host pipe, and the annulus space between the existing pipe and new pipe is usually grouted. In spite of

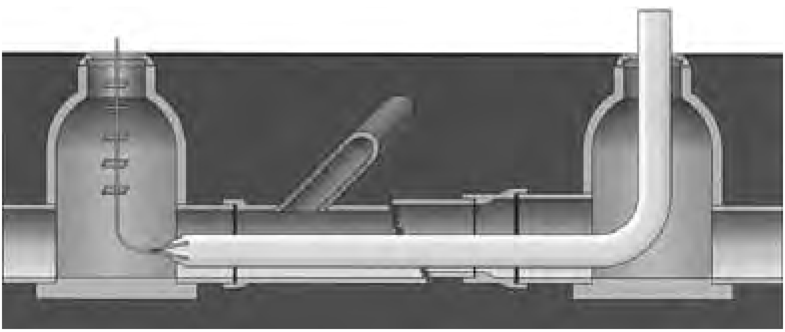

Figure 8.10 Diagram of liner pipe being pulled in a prepared host pipe. (*Courtesy of Ultraliner.*)

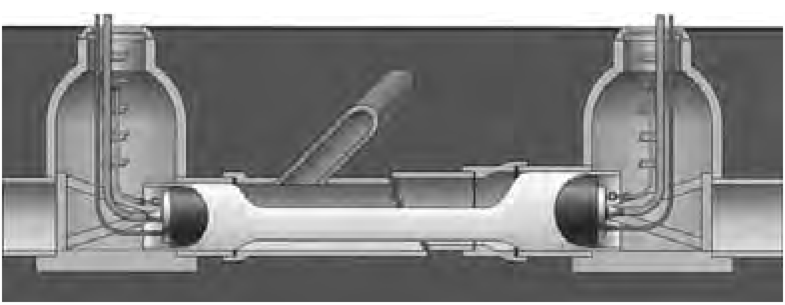

Figure 8.11 Diagram of plugged liner pipe to be expanded with steam pressure. (*Courtesy of Ultraliner.*)

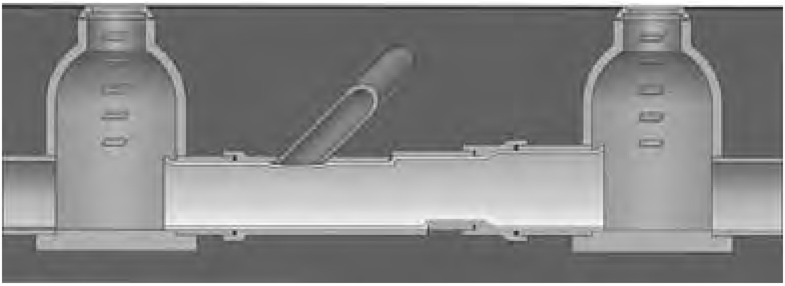

Figure 8.12 Diagram of liner pipe after expansion. The liner forms a permanent, tight-fitting new pipe. (*Courtesy of Ultraliner.*)

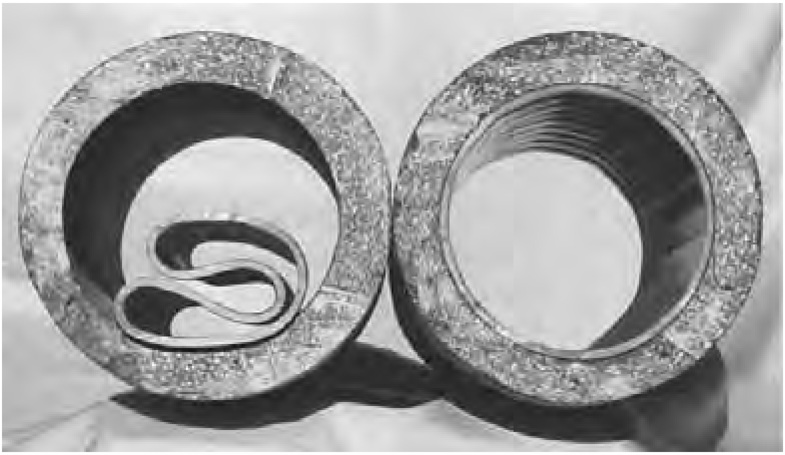

Figure 8.13 Portrayal of the folded pipe as inserted and how it appears after expansion. (*Courtesy of Ultraliner.*)

a decrease in cross-sectional area, often there is an increase in hydraulic capacity due to the smoothness of new pipe. This system is used where the host pipe does not have excessive joint settlements, severe misalignments, large deformations, or similar defects. The new pipe can form a continuous, watertight pipe within the existing pipe after installation. The service connections are then reconnected to the new pipe. The new pipe has the same grade as the existing pipe. Dependent on the type of loading on the new pipe, grouting may be required. Slip-lining can be categorized into three types—continuous, segmental, and spiral-wound. Each method is discussed below.

The continuous slip-lining method involves accessing the deteriorated pipe at strategic points and inserting HDPE pipe joined into a

Figure 8.14 A 24-in-diameter pipe after relining. (*Courtesy of Ultraliner.*)

continuous tube through the existing pipe structure. This technique has been used to renew gravity sewers, sanitary force-mains, water mains, outfall lines, gas mains, highway and drainage culverts, and other pipeline structures. The technique has been used to restore pipe as small as 1 in (25.4 mm), and the maximum pipe diameter is limited by the availability of factory-made pipes. An installation shaft long enough to handle the bending radius of HDPE pipe and the depth of the existing pipe is required. Existing flow may need to be plugged or bypassed during the installation process. More than 30 years of field experience shows that this is a proven cost-effective means that gives a new structure minimum disruption of service, surface traffic, or property damage that would be caused otherwise by extensive excavation.

The segmental slip-lining method involves the use of individual sections of pipe (usually 20 ft or less) that incorporate a low profile joint (for smaller diameters) or a flush gasket-sealed joint (for larger diameters). Segments of the new pipe are assembled at entry points and pushed inside the host pipe. After the new pipe is positioned in place, the annular space can be grouted. This is a very simple method and can be carried out by a general pipe contractor. Another advantage of this method is that installation can be carried out without plugging or bypassing existing flow. In fact, existing flow helps the insertion process by floating the new pipe and lowering the frictional resistance. The laterals are usually reconnected by excavation from outside. A number of plastic pipe products, such as GRP, PVC, PP, and PE, which include short-length sections with a variety of proprietary smooth joints (both inside and outside) have been specially developed for slip-lining sewers. Dependent on how the new pipe is pushed inside the existing pipe, an installation shaft, 3 to 6 ft (1 or 2 m) more than the length of the pipe section, is required. This method is applicable for diameters more than 12 in (300 mm) with typical diameters of 24 in (600 mm) and larger.

The spiral-wound slip-lining method uses a PVC-ribbed profile section with interlocking edges. A pipe is formed in situ by spirally inserting the profile section into the existing pipe. The edges of the profile lock as it is inserted. This method can be used for either structural or nonstructural purposes, depending on the grouting requirements.

In-line replacement. This method of pipeline renewal is relatively expensive since the existing pipe is removed and a completely new pipe is installed. In-line replacement should be considered when pipelines no longer have sufficient capacity or have failed structurally. This trenchless method is broken into two categories: pipe bursting and pipe removal.

Pipe bursting was originally developed for the gas industry, but the method has found application in the replacement of water lines and gravity sewers, especially where upsizing is necessary. Pipe bursting is a technique for breaking out the existing pipe by use of radial forces from inside the existing pipe. The fragments are forced outward into the soil, and a new pipe is pulled into the bore formed by the bursting device. The deteriorated host pipe (made of friable materials such as clay, concrete, and cement asbestos) is broken outward by means of an expansion tool, and the new pipe is either towed behind the bursting machine or jacked into place using conventional pipe jacking techniques. This method requires the reconstruction of laterals by excavation from the surface.

Pipe removal. Pipe removal without trenching has been made possible with the development of microtunneling machines with the capability of crushing rocks and stones. Pipe removal equipment is modified remote-controlled microtunneling systems with crushing capacities. This method can be used to upsize an existing pipe. However, this technique has had little use in the United States because of the high costs of equipment associated with this method of pipe removal. A patented pipe removal system using directional drilling equipment to replace and upsize an existing pipe has been employed with success. This system removes the existing clay, PVC, asbestos-cement, or nonreinforced-concrete pipe and simultaneously replaces it with a new pipe of equal or greater diameter. The removal process is accomplished by back-reaming using a regular directional drilling machine. The directional drilling machine is equipped with a cutterhead having spirally placed carbide-tipped teeth that grind and pulverize the existing pipe into pieces. The pipe particles and excess materials, resulting from upsizing, are carried with drilling fluid to manholes or receiving pits and are retrieved with a vacuum truck or slurry pump for disposal. The new pipe (PVC or HDPE) is attached behind the mandrel and follows the cutterhead as it progresses. Thus the destruction of the existing pipe, cutting the soil to the required size, and the installation of the new pipe are a simultaneous process. Another advantage of this system is that the primary equipment is a directional drilling system that can also be used in other trenchless technology projects. In recent years an auger boring method has been used to remove an existing pipe and install a new pipe.

Close-fit pipe. This type of trenchless pipeline renewal uses coiled, deformed, new pipe before it is installed; then it is expanded to its original size and shaped after placement to give a close fit to the existing pipe. Most lining pipe is first deformed in the manufacturing plant, shipped to the job site, then inserted and finally re-formed by heat and pressure or naturally. Compared with CIPP, and assuming other project factors to be the same, close-fit technology does not require a long curing process and therefore requires less time to complete a project. This method can be used for both structural and nonstructural purposes.

The modified cross-section method uses a jointless extruded PVC or HDPE pipe folded or deformed to reduce the cross-sectional area. The folded pipe is mechanically pulled into the existing pipeline, then formed to the shape of the existing pipeline by using heat, pressure, and in some cases a mechanized rounding device.

The drawdown method slip-lines a HDPE solid-wall pipe into an existing pipeline after joints are butt-fused and the HDPE pipe is swaged down in the diameter. Diameter reduction depends on historic memory that depends on the deforming temperature. Compressing the pipe temporarily crushes the chain structure, allowing the pipe to be reduced in diameter and later reverted to its original size without affecting performance. Pipes 3 to 24 in (76 to 600 mm) in diameter can be installed utilizing this method. After long, continuous lengths of the tube are pulled into the existing pipe, pressure is applied to the inside of the new pipe to speed up the reversion process. The pipe in its reverted form usually fits closely to the existing pipe wall, and no annular space remains.

The roll-down system is similar to drawdown except that the new pipe diameter is reduced for insertion by running the new pipe through a cold-rolling machine. This rearranges the long-chain structure of the plastic pipe to produce a smaller-diameter pipe with thicker walls and minimal elongation.

Point-source repair. Point-source repairs are considered when local defects are found in a structurally sound pipeline. This method of pipeline rehabilitation covers a broad range of techniques such as robotics repairs, grouting, link-sleeve, shotcrete, coatings, spray-on linings, and CIPP.

Coatings are fixed to the interior wall of the existing pipe by adhesion; or for robotics repairs, the defect is filled with epoxy. Systems are available for remote-controlled resin injection to seal localized defects between 4 and 30 in (100 and 760 mm) in diameter.

The new spot repair devices are used to address four basic problems. The first purpose involves maintaining the loose and separated pieces of unreinforced existing pipe aligned to ensure the load-bearing equivalent of a masonry arch. The second purpose is to provide added structural capacity or support to assist the damaged pipes to sustain structural loads. The third purpose provides a seal against infiltration and exfiltration. Finally, the fourth purpose is to replace missing pipe sections.

In robotic repair, robots are used to structurally repair isolated defect areas in pipelines. First, robots are used to grind the defect area, exposing a clean and smooth surface. Then these grooved areas are injected with epoxy-based resins which bond to surrounding host pipe, creating a structural and a permanent barrier impervious to interior or exterior chemicals or objects. Robotic point repair is used either as stand-alone or as a precursor to other renewal methods. As a stand-alone, robotic point repair is used to repair radial, longitudinal, and spider cracks. The process also lends itself to repairing broken joints, slip joints, open joints, protruding service connections, recessed service connections, roots, and other foreign objects that are usually found in collection pipeline systems.

The robotics process uses the epoxy resin as the final structural fix. The epoxy bonds to the pipe medium and permanently seals the wall from further infiltration of outside material (soil and/or water). Also, due to the epoxy hardness and structural adhesion, a repair to the pipe wall stops the occurrence of further cracking with respect to the location repaired.

Robotic repairs are carried out by an operator manipulating the robotics functions by remote control with the aid of a closed-circuit television. As a first step, the robot is positioned at the defect area and is surveyed for the best starting position. Chemical grouting is carried out if any infiltration of water is present. The operator then begins to grind out the crack(s). This accomplishes two goals. First, the crack is cleared of all foreign material and stopped from further progression due to the groove cut. Second, the groove created gives a larger surface area to inject the epoxy resin. The second step is to fill the void area with the epoxy. This is carefully accomplished, making sure that the groove is fully filled and flush with the pipe wall.

Grouting, like slip-lining, is one of the oldest methods of pipeline renewal. In recent years, there have been new advances in products and equipment for many grouting applications. Chemical grouting is normally used for pipe joints in sewer lines and manholes to seal active leaks or to curtail leaks using joint testing equipment. Sometimes, slight circumferential cracks, small holes, slightly cracked pipe joints, and other minor areas of structural damage can be successfully sealed using chemical grouts. In most applications, however, chemical grouting is used in structurally sound pipelines.

Several types of chemical grouts are currently available. Each type is for a specific application and requires a specific method and equipment. Some grouts are best suited to repair pipe joints, while others are designed to provide an impervious barrier to groundwater leakage on the exterior of the pipe joint or manhole structure. In both cases, the use of chemical grout is to fill large open voids.

By design, chemical grouts have minimal compressive strength, and where large voids and loss of structural support may exist, a grout repair must be supplemented by other structural methods. Chemical grouting will, however, curtail the loss of soil and backfill material through leaking pipe joints and manholes, prolonging the life of sewer line and preventing the formation of larger void areas caused by continued leakage. All chemical grouts are applied under pressure after appropriate cleaning and testing of the joint or the location where grout is going to be applied.

In the spray-on lining method, a thin mortar lining or a resin coating is sprayed onto pipes. This is a well-established technique. Spray-on lining systems use either epoxy resins or cement mortar to form a continuous lining within the host pipe. These systems result in improved corrosion resistance and hydraulic characteristics, but, except for shotcrete and gunite, have little value to enhance the structural integrity of the pipe.

For worker-entry pipes of diameters of 36 to 142 in (900 to 3600 mm), structural reinforced sprayed mortars (shotcrete or gunite) are effective and widely used for renewing pressure pipes and gravity sewers. Acid-resistant mortars have been used in industry as linings in tanks or as mortar bricks. Development of mechanical in-line application methods (centrifugal and mandrel) has established mortar lining as a successful and viable rehabilitation technique for sewer lines, manholes, and other structures. Specialty concretes containing sulfate-resistant additives such as potassium silicate and calcium aluminate have shown greater resistance than typical concrete to acidic attack on sewer pipes and manhole structures. As with any other trenchless pipeline renewal, the pipeline must be thoroughly cleaned and dried before a renewal method can be applied. If the lining is carried by machine or carts and applied manually with a trowel, the application distance is limited by the length of hose available and the distance between valves, bends, tees, etc.

For non-worker-entry pipes of diameters of 4 to 36 in (100 to 900 mm), the lining is sprayed directly onto pipe walls using a remote-controlled traveling sprayer. The lining materials include concrete sealers, coal tar epoxy, epoxy, polyester, silicone, urethane, vinyl ester, and polyurethane. These linings are intended to form an acid-resistant layer that protects the host pipe from corrosion.

The link sleeve method of pipeline renewal uses a sleeve to correct localized structural damage. Spot repairs can be conducted with this method on pipe diameters ranging from 6 to 110 in. For diameters of 6 to 24 in, a stainless steel sleeve wrapped in polyethylene foam is used. This sleeve and an inflatable sewer plug are placed over the damaged area. With the aid of a TV camera, the plug is inflated until the sleeve lock is in place. The plug is then deflated, and a visual inspection takes place.

There are different proprietary techniques for this method. Before the operation, the pipe must be thoroughly cleaned and inspected by TV to identify all the obstructions such as displaced joints, crushed pipes, and protruding service laterals. The operation then continues according to instructions from the system manufacturer and type of application.

The application of point CIPP is for pipelines that are structurally sound, but may contain isolated pipe lengths that have structurally failed. The materials used in point CIPP repair are the same as those in regular CIPP methods with more than two decades of proven performance. Point CIPP installation involves pulling the resin-saturated fabric liner and an inflation hose through the existing sewer line. The alignment of the liner is closely monitored by a closed-circuit TV camera positioned in the sewer line. Once the liner is aligned in the proper position, the inner hose is inflated via a combination of air and water pressure, causing the liner to regain its original circular shape. Hot water is introduced and recirculated within the CIPP. The hot water accelerates the curing of the fabric liner in a tight fit against the existing sewer line wall. Table 8.1 presents a summary of pipeline renewal methods. It should be noted that during the last 5 years the capabilities of these technologies have increased and that design engineers and potential users of these methods need to keep abreast of innovations. Factors to be considered for each method include design methodology, applicable size range, type of material (indicative of chemical resistance), types and degree of disruption (degree of excava-

TABLE 8.1 Comparison of Different Trenchless Pipeline Renewal Methods (Najafi, 1994)

Method	Diameter range, mm (in)	Maximum installation, m (ft)	Liner material	Applications
CIPP				
Inverted in place	100–2700 (4–108)	900 (3000)	Thermoset resin/fabric composite	Gravity and pressure pipelines
Winched in place	100–1400 (4–54)	150 (500)	Thermoset resin/fabric composite	Gravity and pressure pipelines
Slip-lining				
Segmental	300–4000 (12–158)	1700 (5600)	PE, PP, PVC, GRP	Gravity and pressure pipelines
Continuous	100–1600 (4–63)	300 (1000)	PE, PP, PE/EPDM, PVC	Gravity and pressure pipelines
Spiral-wound	100–2500 (4–100)	300 (1000)	PE, PVC, PP, PVDF	Gravity pipelines only
In-line replacement				
Pipe bursting	100–800 (4–32)	100 (300)	PE, PP, PVC, GRP	Gravity and pressure pipelines
Pipe removal	Up to 900 (36)	100 (300)	PE, PP, PVC, GRP	Gravity and pressure pipelines
Close-fit pipe				
Modified cross section	100–400 (4–15)	210 (700)	HDPE, PVC	Gravity and pressure pipelines
Drawdown	62–600 (3–24)	300 (1000)	HDPE, MDPE	Gravity and pressure pipelines
Roll-down	62–600 (3–24)	300 (1000)	HDPE, MDPE	Gravity and pressure pipelines
Point-source repair				
Robotic repairs	200–760 (8–30)	N/A	Epoxy resins/cement mortar	Gravity
Grouting	N/A	N/A	Chemical grouting	Any
Link sleeve	100–600 (4–24)	N/A	Special sleeves	Any
Point CIPP	100–600 (4–24)	15 (50)	Fiberglass/polyester, etc.	Gravity
Spray-on lining	76–4500 (3–180)	150 (500)	Epoxy resins/cement mortar	Gravity and pressure pipelines
Manhole rehabilitation	Any	N/A	Spray-on lining, profile PVC, CIPP, cast-in-place	Sewer manholes

tion required), method of installation, total footage installed (or number of installations), time required for installation, and whether or not bypass pumping is required (especially for large-diameter pipes).

Trenchless construction methods (TCMs)

Directional or horizontal directional drilling methods. Directional or horizontal directional drilling (HDD) methods involve steerable tunneling systems for both small- and large-diameter lines. In most cases, it is a two-stage process. The first stage consists of drilling a small-diameter pilot hole along the desired centerline of a proposed line. The second stage consists of enlarging the pilot hole to the desired diameter to accommodate the utility line and pulling the utility line through the enlarged hole. These methods are so termed because of their unique ability to track the location of the drill bit and steer it during the drilling process. The result is a greater degree of precision in placing the utilities.

Basically all directional methods consist of a drilling unit to form the borehole and a survey system to locate the drill head. The drilling process is accomplished either by mechanical cutting using a drill bit or by fluid cutting with high-pressure jets. There are a variety of survey systems which have been patented by different manufacturers. The choice of a particular system will largely depend on the type of job, the site conditions and accessibility, operator skill, finances available, etc.

Major advantages. The major advantage is the speed of installation combined with the environmental effect. This facilitates the construction permit process, saving a lot of time and expense. Long and complicated crossings can be quickly and economically accomplished with a great degree of accuracy since it is possible to monitor and control the drilling operation. Another advantage is that sufficient depth can be achieved to avoid other utilities. In the case of river crossings, the effect of buoyancy and danger of riverbed erosion and possible damage from river traffic are eliminated. Another advantage is that access and reception pits are usually not required for this method.

Major limitations. It is an extremely specialized operation for which special equipment and a very high degree of operator skill are required. The costs of the equipment and the operation are high; hence the bore length should be sufficient in order for it to be economically feasible. Although it has been done, this type of boring can be difficult for small slopes and may not be suitable for gravity pipeline applications. Also, the type of pipe installed by this method is limited to that being able to withstand sufficient axial tensile force even at the joints.

Hence, mainly steel or high-density polyethylene (HDPE) pipe is being installed by this method.

Mini directional drilling method. The mini directional drilling method is used specifically for the installation of small-diameter lines that need to be installed at a reasonable depth and up to 600 ft (180 in) in length. The process involves the creation of a small-diameter borehole by either mechanical cutting or fluid jetting and then pulling back the utility through the borehole. A slurry is used to stabilize the walls of the borehole in unstable sods and reduce the frictional drag on the cable or pipeline being installed.

The mini directional drilling method has the ability to locate the position of the drill head and steer it in the required direction. The survey systems used for locating the drill head vary with the manufacturer, but they all serve the same purpose of locating the drill head position so that corrections can be made as the boring progresses.

There are a number of manufacturers of mini directional drilling equipment, and significant variations exist in the drilling equipment and survey systems manufactured by them. The mini directional drilling equipment presently being manufactured in the United States falls under one of the following categories: controlled fluid jetting method or the fluid-assisted mechanical cutting method.

Controlled fluid jetting method. The controlled fluid jetting technique uses high water pressure to create small-diameter boreholes. The soil is cut by small-diameter high pressure jets of water or liquefied clay (bentonite). The jets cut the soil in advance of the boring tool, impregnating and lining the borehole wall with clay. The clay lining maintains borehole stability in inherently unstable soils such as fine sand. Also, the clay lining makes the tunnel wall smooth and slippery, greatly reducing frictional drag on the new conduit, cable, or pipe as it is installed.

This method has the capability of monitoring the path and remotely steering the boring tool in the soil. By remotely changing or biasing the direction of the cutting jets at its nose, the boring tool changes directions as it is thrust through the soil. This capability combined with the electronic tool detection system makes it possible to align boreholes up to 600 ft (180 in) long, depending on the soil conditions. The electronic detection system can measure the tunnel position within 1 in (25 mm) at normal utility placement depths. If the tool begins to deviate from the desired path, it can be steered to the design path or pulled back to create a new course. Also, in case of an obstacle, the same principle of backing up to create a new course around the obstacle is applied.

Major advantages. One of the major advantages is that the method does not damage existing utilities. In case of obstacles being encountered, the drill head can be guided around the obstacle. The system does not require any bore pits, and only one person is required to operate the equipment. Since the method uses a continuous length of coiled pipe, there are no rods or pipes of fixed length that require connection and disconnection during the boring and pullback operations. This makes the installation faster. The method is capable of installing lines up to 16 ft (5 m) in depth from the ground surface. Minimal site preparation is required because the system is easy to set up.

Major limitations. Continuous straightening and rewinding of the coil limit the life of the pipe material mainly due to metal fatigue. Hence the coil has to be replaced every 6 months or after 200 operations. Another disadvantage is that the system is capable of installing only small-diameter lines at present. Due to its weight and size, the unit cannot be moved through garden gates to the backyard of houses, as other units can. Hence, it cannot be used in congested places and is mostly used at the curbside.

Fluid-assisted mechanical cutting. The directionally controlled fluid-assisted mechanical cutting method is used for the installation of small-diameter lines. The system uses a mechanical cutting drill bit to cut the soil while the steering is accomplished by using a slanted nosepiece. This equipment is being manufactured by a wide variety of firms under various trade names. These systems use a medium-pressure, low-volume drilling fluid to assist in the drilling process. The method uses the principle of tracking the tool from the ground surface to monitor the accuracy and progress of the bore.

Major advantages. The major advantage of this method is its steering capability. In case obstacles are encountered, the drill head can be guided around the obstacle. The system does not require bore pits, and only three workers are required to conduct the operation. The method is capable of installing lines up to 30 ft (9 m), and with enhancements to 50 ft (15 m) in depth from the ground surface. Minimal site preparation is required because the system is easy to set up.

Major limitations. This method cannot be used to install lines for depths greater than 50 ft (15 m) as the range of the electromagnetic receiver is limited. Since the cutting head consists of a drill bit, the system can cut through existing utilities unless one is very careful. Hence, locating all existing and nondestructively exposed utilities before starting the operation is very important.

Slurry methods. Slurry methods involve the use of a drilling fluid such as water or bentonite slurry to aid in the drilling process and spoil removal. Generally these methods do not have an ability to track the location of the drill bit and to steer in a specified direction. The drill bit takes the path of least resistance and is often deflected from its design path in the case of obstructions. The slurry methods can be classified into two broad categories: slurry boring and water jetting.

Slurry boring. The slurry boring method utilizes drill bits and drill tubing for cutting the earth face. A drilling fluid is used (1) to facilitate the drilling process by keeping the bit cool and clean and (2) aid in spoil removal. This method is distinguished from the water jetting method by the principle of creating the borehole. While the water jetting method uses the force of water to erode the borehole, the soil is mechanically cut in this process by drill bits. The created borehole is stabilized by the slurry by controlling the rate of flow and the pressure.

The slurry boring technique is popular primarily in the sections of the country where the original development took place. It is banned by several state highway departments, counties, and municipalities largely due to misunderstanding and its association with water jetting. These agencies normally cite the jetting action as the reason. While it is possible for jetting to occur if the procedures are abused, an experienced operator would not permit jetting.

Major advantages. The process is quick and easy to set up and has the unique flexibility of being able to set up in a pit or operated from above the ground. Since the pilot hole is installed first, the alignment can be confirmed prior to reaming of the final bore. Since the pilot hole is small in diameter, it can be installed quickly; and if it is out of tolerance, it can be pulled out and reinstalled. Since the boring process is independent of the pipe insertion process, virtually all types of pipes can be installed by this method.

Major limitations. The use of drilling fluid increases the risk of a jetting action's occurrence which may result in overexcavation of the borehole. Hence, special care must be exercised by the operator to make sure that the borehole face is cut through the mechanical action of the drill bit. While the borehole is being drilled and reamed, it is uncased. Many state highway department specifications prohibit the use of any method that results in an uncased borehole at any time.

Water jetting. The water jetting method utilizes the liquification of soil principle to create a borehole. Water pressure and flow rates create a jetting action which places the soil in a quick (liquid) condition; i.e., the soil behaves as a liquid and is washed out. This principle is used as a horizontal boring method to create a borehole.

This method was being used extensively to get water lines under roadways until it was banned by most owners due to the problems associated with it. It is convenient because normally a source of water is readily available. The water jetting method uses water pressure to perform all the cutting action. It uses the flow of water to wash the cuttings out of the borehole. During the boring process, the water jet follows the path of least resistance, and hence there is no way to control the direction of the borehole. There is no way to control the amount of excavation, and overexcavation is inevitable. Hence, over time, surface settlements will occur and cause the same problems that one was attempting to avoid by performing a bore. Due to these reasons, this method has been banned by almost all owners for many years as a horizontal boring technique. However, it is still utilized by owners of water systems with their own crews in isolated situations.

Major advantages. The water jetting method is a very simple operation which requires no special skills and equipment. Therefore, capital expenditure is minimum.

Major limitations. There is no way to control the amount of overexcavation; hence, the method may result in large-scale settlements due to overexcavation during the jetting process. This method has been banned by almost all owners because of this reason.

Pipe ramming method. The basic procedure consists of ramming a steel pipe through the soil by using a device, generally air-powered, attached to the end of the pipe. In this method, the tool does not create a borehole; rather, it acts as a hammer to drive the pipe through the soil. The pipe can be used for water, sewer, electric, gas, or any other utility, and it can be installed under roads, highways, railroads, rivers, etc.

Major advantages. The pipe ramming method is an effective method for installing medium- to large-diameter pipes. The versatile pit sizes, varying lengths of pipe that can be installed, and ability to handle almost all types of soil conditions make this method a practical and economical technique for installing pipes. This method does not require any thrust reaction structure as the ramming action is due to impulses induced in the pipe by the percussion tool. The pipe ramming method is also multifunctional. A single size of pipe ramming tool and the air compressor can be used to install a wide variety of pipe lengths and sizes. Ramming can also be used for vertical pile driving, angular ramming, or pipe replacement.

Major limitations. The major disadvantage of the pipe ramming method is the minimal amount of control over line and grade.

Therefore, the initial setup is of major importance. Also, in the case of obstructions, like boulders or cobbles, especially with small-diameter pipe, the pipe may be deflected. Therefore, sufficient information on the existing soil conditions must be available to determine the proper size of casing to be used.

Auger horizontal earth boring. The auger horizontal earth boring (HEB) is a trenchless excavation technique used extensively throughout every segment of the United States, primarily for road crossings. This method utilizes a process of simultaneously jacking casing though the earth while removing the spoil inside the encasement by means of a rotating flight auger. The auger is a flighted tube which transfers spoil back to the machine and has couplings at each end that transmit torque to the cutting head from the power source located in the bore pit. The casing supports the soil around it as spoil is being removed. The auger HEB method is traditionally classified into two types: track type and cradle type.

Major advantages. The major advantage of auger boring is that the casing is installed as the borehole excavation takes place. Hence, there is no uncased borehole which substantially reduces the probability of a cave-in that could result in surface subsidence. Also, this method can be used in a wide variety of soil types, which makes it a very versatile method.

Major limitations. The auger horizontal earth boring method requires different-size cutting heads and auger sizes for each casing diameter, which calls for a substantial investment in terms of equipment. This method also calls for a substantial investment in terms of the bore pit construction and the initial setup. In case of soils containing large boulders, this method cannot be used advantageously because the size of boulders and other obstacles that this method can handle is limited to one-third the nominal casing diameter.

Compaction method. The compaction method forms the borehole by compressing the earth that immediately surrounds the compacting device. Therefore, the soil is displaced rather than removed. The method is restricted to relatively small-diameter lines in compressible soil conditions. These methods are classified as expansive installation techniques since the earth surrounding the borehole is displaced by the expanding effect. Spoil is not removed, but is compacted and is left in place during the installation process. The compaction method is divided into three subclassifications: push rod method, rotary method, and percussion method.

Push rod method. A rod pusher is a machine that pushes or pulls a solid rod or pipe through the earth to produce a borehole by displacing the soil without rotation or impact. The principle associated with the push rod method is one of the simplest principles. The method literally involves forcing a compaction bit through the earth by using a series of rods connected to a power source. The resulting borehole is of the diameter of the rod thrust through the soil. In case the required borehole size is larger than the rod diameter, the borehole created is used as a pilot hole to pull back a reamer of the required diameter, using the rods.

The power source for pushing the rods through the earth varies from the crude method of using the bucket of a backhoe to hydraulic machines. The use of a backhoe bucket for pushing the pipe is the least accurate of all methods. Although the backhoe has been successfully used on many occasions, it is not recommended for most projects.

There are several manufacturers of commercial rod-pushing machines. The most popular principle of operation consists of a large hydraulic cylinder, a reaction plate, and a rod-gripping device. If the operation requires reaming, then the reaction plate must be designed and installed to resist forces in both directions. The general practice is the construction of a T slot for the borehole. The reaction plate is placed in the branches of the T, and the body of the T houses the cylinder and the rod-gripping device and provides operator working room. The hydraulic cylinder can be powered by the hydraulic manifold system of a backhoe, trencher, etc., or a separate hydraulic power unit.

The push rods are usually 4 ft (1.2 in) in length and 1.375 in (35 mm) to 1.75 in (45 mm) in diameter. Normally, these rods are solid and are thrust through the ground without rotation. The method involves the construction of a bore pit and a receiving pit. As described above, the bore pit is usually T-shaped. The machine is then placed in the bore pit and is connected to the power source. The compaction bit is then placed on the push rod, and the rod is attached to the machine. Final line and grade adjustments are made, and the pushing cycle is begun. The pushing cycle consists of several independent pushes per rod length. The pushes are a function of the cylinder stroke length. The cylinder stroke length varies from machine to machine. It is normally about 9 in (225 mm) in length. The degree of accuracy achieved with this method depends to a great extent on the initial setup and the soil conditions.

Rotary method. The rotary method combines the advantages of a rotating drill rod and the compaction effect developed from utilizing a compaction bit. The power source varies from optional adapter kits that can be attached to a backhoe, trencher, horizontal earth boring unit, etc. These are similar to those used for auger boring except that they use solid drill stems rather than augers and a cutting head.

This method is limited to smaller bores up to 6 in (150 mm) in diameter. For larger bores, the pilot hole can be enlarged to 12 in (300 mm) by back-reaming. This, however, depends greatly on the soil characteristics. Since the expansion of the borehole creates extra volume by compressing the soil around it, one must be careful during this operation to not cause damage due to heaving.

The basic procedure involved in the method is a function of the bore length and the equipment selected for the operation. However, the principle used in this method is that the compactor bit is thrust through the ground by a power source which also has the capability of developing torque in the drill stem. For short bore lengths where accuracy is not very critical, a wide variety of boring units are available. However, for longer bore lengths and higher accuracy, a track-type boring unit is used. The track-type boring unit is set up in a bore pit and utilizes a rigid, solid drill stem.

An appropriate boring pit and receiving pit are required in this method. If the power source is a backhoe or a trencher, the optional adapter kit is attached to it, and then the flexible drill rods are attached. In this case, the bore pit consists of only a bore slot. However, if a track machine is being used, then the same degree of care must be exercised as described for the track-type auger boring machine. It is again emphasized that the accuracy of installation in this case will depend to a great extent on the initial setup of the system.

Percussion method. The percussion or the impact moling method, as it is sometimes called, utilizes an underground piercing tool that is self-propelled by a pneumatic or a hydraulic power source. The diameter and length of the tool vary by manufacturer, but they are all streamlined into a bullet or missile shape. Compressed air or hydraulic fluid, transmitted to the tool through flexible hoses, imparts energy at a blow frequency of 400 to 600 strokes per minute to a reciprocating piston located inside the nose of the tool. This action results in the tool propelling itself through the ground. These tools are effective in most ground conditions, from loose sand to firm clay.

The soil around the tool applies friction to the body holding it in place when the piston returns on its backstroke. Thus, friction is necessary for the proper operation of the tool. Without this friction, for example, in very wet unstable soils, the tool will vibrate, but will not move forward. Percussion tools vary in diameter from 1.75 in (45 mm) to 7 in (175 mm). While all the tools claim a relatively high degree of accuracy, some of the later-developed small-diameter units seem to be more accurate. This has been credited to a properly designed diameter-to-length ratio and weight distribution.

Percussion tools typically travel at a rate of 3 in (75 mm) per minute to approximately 4 ft (1.2 m) per minute, with travel speed being a function of soil conditions and not a function of tool size. Even though the larger tools are more powerful, their speeds are not much different from those of the smaller sizes because they must displace larger volumes of soil. Most of the percussion tools have a reversal capability. This enhances their capability drastically. In case of obstacles or when the tool has swayed away from the desired course, the unit can be backed out of the borehole. Before the development of this feature, the unit would have been lost or required open excavation, resulting in doing what was being avoided in the first place and defeating the purpose of boring. Since this method is for small-diameter bores only, abandonment does not cause any serious problems.

The typical procedures for the percussion method require the use of boring and receiving pits. The bore pit size varies significantly and depends on the depth of the bore and the size of percussion tool selected. For stable ground conditions where a high degree of accuracy is not required, the percussion tool is placed in the bore pit and collared into the embankment by one person. However, when a high degree of accuracy is desired, a launching platform is used. The platform provides support for the tool so that it is aligned as required. A sighting device is used to ensure alignment. Some manufacturers provide adjustable bearing stands so that vertical adjustments can be readily made. After proper alignment has been obtained, the tool is collared into the embankment, the power is applied, and the operation is begun. The operation is monitored until the tool exits in the receiving pit. The tool is then removed, and the cable is attached to the air hose and pulled back through the borehole. When rigid pipe is to be installed, the tool and the air hose are removed and the pipe is pushed through the open borehole.

In most soil conditions, the compaction effect is sufficient to develop a borehole with sufficient stand-up time to perform the necessary pipe insertion. However, overall performance and accuracy of the unit are functions of the type of ground and soil conditions. The factors that need to be taken into consideration are soil type and degree of homogeneity, the degree of soil compactness, soil moisture content and its ability to be deformed and displaced, the critical depth (the minimum depth from point of entry through the line of travel below the surface), the contour of the ground above the line of travel, and the presence of obstructions.

The effectiveness of soil displacement depends on soil properties and characteristics such as compressibility, grain size, and gradation. The presence of a high water table may affect soil compressibility. Generally, compressible soils such as unconsolidated soft silt or clay, mixed-grain, or well-graded soil with a high void ratio are most favorable for soil displacement methods. Poorly graded or dense soils are difficult to pierce.

Special situations can be accommodated with modifications to impact tools. Larger sizes permit harder bores to be completed (rocky conditions). Pulling accessories help the softer bores (silt, sand) to be completed. Shale has always been manageable by piercing tools. Underwater projects are possible by pulling pipe to eliminate water infiltration into the tool body. Large-diameter rocks are the only major stopping points.

Characteristics

1. *Type of pipe installed.* Since the boring process is independent of the pipe insertion process, any type of pipe or cable can be installed in the borehole by these methods. These methods are extremely popular for installation of electric, telephone, or cable TV cables. These methods are also extensively used for the installation of gas pipe, sprinkler irrigation systems, and service lines for water systems.

2. *Pipe size range.* The size of pipe that can be installed by this method is restricted by the size of the borehole that can be bored by this method. These methods are designed to accommodate small-diameter pipes and cables. These are typically limited to 6 in (150 mm) or less. In very favorable soil conditions, boreholes as large as 12 in (300 mm) in diameter have been successfully obtained by these methods.

3. *Bore span.* Even though 200-ft (60-m) bores have been successfully made with these methods without using any sensing or guiding systems, the span length should be limited to 60 ft (18 m) with 40 ft (12 m) being the optimum. The limiting factor controlling the bore span is accuracy, not the ability of the tool to move through the ground. Since the bore size is small, it becomes difficult to control it as the span increases. Without a sensing and guiding system, it becomes very difficult to locate the bore head.

However, with the development of sensing and guidance systems, the ability of these methods has been enhanced substantially. With the use of electronic sensing devices, it is possible to know the location and alignment of the bore head; and with guidance systems, it is possible to maneuver the tool in the desired direction. This has substantially reduced the risk of obtaining a nonusable borehole.

4. *Disturbance to the ground.* The two major problems that can result from the use of these methods in terms of ground disturbance are ground settlement and heaving. Since the compaction method compresses the soil around it and does not remove spoil, it creates extra volume, and heaving is anticipated in such cases. However, when percussion tools are used in loose cohesionless soils, the vibrations due to the percussion tool consolidate the soil to a point where the volume loss due to consolidation may exceed the amount of expansion. This may result in ground settlement. Hence, the compressibility of the soil

is an important factor which should be considered for settlement purposes. A rule of thumb in the industry is that the depth of cover should be 1 ft (0.3 m) for each 1 in (25 mm) of bore diameter. Some manufacturers consider this conservative; but it is reliable, especially when the specific soil characteristics are not known.

5. *Area requirements.* The compaction methods require the use of a bore pit. The bore pit size depends on the method selected, the depth of the bore, and the size of the tool. Bore pit sizes vary from as small as 6 in (150 mm) wide, 36 in (900 mm) long, and 18 in (450 mm) deep to as large as 10 ft (3 m) wide, 30 ft (9 m) long, and 15 ft (4.5 m) deep.

These methods require a minimum surface area because of minimum equipment requirements. In most cases, the equipment required outside the pit is either an air compressor or a hydraulic power source.

6. *Operative skiff requirements.* The operation is very basic, and the procedures and principles are very simple. Hence, no special operator skill is required. In case of obstacles being encountered or other problems, the borehole is abandoned. Since these methods are for small-diameter bores only, abandonment does not cause any serious problems.

7. *Accuracy.* When no sensing and guiding conditions are utilized, the accuracy of installation will depend on the initial setup, ground conditions, length of the drive, and experience of the operator. However, once the operation has started, there is no method to control or change the direction of the drive unless sensing and guiding devices are used. This method is generally not used for installing lines that require a very high degree of accuracy such as gravity sewer lines. A tolerance of 1 percent of the borehole length is normally acceptable for this method. However, for cables and other lines which do not require a very high degree of accuracy, it is accepted where it exits. When sensing and guiding systems are used, a tolerance within a 1-ft (300-mm) radius of the desired point is acceptable.

8. *Recommended ground conditions.* Since the method compresses the soil around the borehole to create extra volume, moderately soft to medium hard compressible soils are best suited for this method. Dense and hard soils are the worst soils for this method.

Major advantages. Compaction is a rapid, economic, and effective method of installing small-diameter lines. This method can install any type of utility line since the installation process is independent of the boring process. The stability of the soil around the borehole is increased since the soil around the borehole is compacted. The increase in soil density decreases permeability, which decreases the possibility of borehole collapse until the desired line is installed. The capital investment in equipment is minimum, and several pieces of equipment such as the air compressor and hydraulic power source are multifunctional.

Major limitations. Compaction methods are limited in their useful drive length by their reliability. The present systems are basically unintelligent, unguided tools that tend to bury themselves, surface in the middle of the road, or damage existing utility lines. The use of sensing and guidance systems on the compaction tools is still rare because this has been recently developed and is not very popular. However, the field test results appear positive.

Pipe jacking and utility tunneling. Pipe jacking (PJ) and utility tunneling (UT) are trenchless construction methods which require workers inside the jacking pipe or tunnel. The tunnel is generally started from an entry pit. The excavation can be done manually or by using machines. However, it is accomplished with workers inside the pipe or tunnel. The excavation method varies from the very basic process of workers digging the face with pick and shovel to the use of highly sophisticated tunnel boring machines (TBMs). Since the method requires personnel working inside the tunnel, the method is limited to personnel-entry-size tunnels. Hence, the minimum tunnel diameter recommended by this method is 42-in (1075-mm) outside diameter. Even though it is theoretically possible for a person to enter a 36-in-diameter (900-mm) tunnel, it is very difficult and impractical for the person to work in such tight quarters.

Irrespective of the method, the excavation is generally accomplished inside an articulated shield which is designed to provide a safe working environment for the people working inside and to allow the bore to remain open for the pipe to be jacked in place or the tunnel lining to be constructed. The shield is guidable to some extent with individually controlled hydraulic jacks.

Pipe jacking. Pipe jacking is differentiated from horizontal earth boring (HEB) in the sense that pipe jacking requires workers inside the pipe. Although it is possible to install pipes up to 60 in using the HEB method, it should be classified as HEB if the excavation is done by a cutting head and the spoil is removed by augers or by any means which does not require workers inside the pipe.

The process involves a simple, cyclic procedure of utilizing the thrust power of hydraulic jacks to force the pipe forward. In unstable conditions, the face is excavated simultaneously with the jacking operation to minimize the amount of overexcavation and the risk of face collapse. In stable ground conditions, excavation may precede the jacking process if necessary. The spoil is removed through the inside of the pipe to the jacking pit. After a section of pipe has been installed, the rams are retracted and another joint is placed into position so that the thrust operation can be started again.

The first step in any pipe jacking operation is site selection and equipment selection per the site requirements. A pipe jacking project should be planned properly for a smooth operation. The site must provide space for storage and handling of pipes, hoisting equipment for the pipe, spoil storage and handling facility, etc. If adequate space is available, a big jacking pit is preferred so that longer pipe segments can be jacked, and so the total project duration is reduced.

The jacking pit size is a function of the pipe diameter, length of pipe segment, shield dimensions, jack size, thrust wall design, pressure rings, and guiderail system. The space available at the site governs the selection of all the above components. The operator should be located near the face so that she or he can readily see what is going on and can take necessary action to control any situation that might develop.

The spoil is commonly removed by small carts. These carts are either battery-powered or powered by a winch cable. The spoil can also be removed by using small-diameter augers or by using a conveyer belt system.

Packing material is placed between the pipe joints to provide cushioning and flexibility. The most commonly used and the only industry-wide packing material is 0.5- to 0.75-in (12- to 19-mm) plywood.

Utility tunneling. Utility tunnels are differentiated from the major tunneling industry by virtue of the tunnel's typical sizes and use. These tunnels are used primarily as conduits for utilities rather than as passages for pedestrian and/or vehicular traffic. While methods of excavation for pipe jacking and utility tunneling are similar, the difference is in the lining. In the pipe jacking technique, pipe is the lining, whereas in the utility tunneling technique, either tunnel liner plates or rib and lagging become the lining. The linings for utility tunnels are considered to be temporary structures providing support until the utility is installed, and the annular void between the utility and tunnel lining is filled with an adequate filler material.

In this case, too, the excavation takes place inside a specially designed tunneling shield. The excavation can be either manual or mechanical. Manual excavation is done by craftsmen utilizing either pneumatic tools or simply by picks and shovels. Mechanical excavation can be done either by using a full-face cutting head similar to those used in the auger horizontal earth boring method or by a hydraulic backhoe mounted inside the shield. In either technique, the operator is located near the face so that he or she can readily see what is going on and can take necessary action to counter any situation that might develop. In cohesive soil conditions and in some instances where the shield cannot be removed due to lack of a relieving pit, steel liner plates can be installed without the use of a shield. Experienced and properly trained tunnel operators are required when a shield is not used.

Major advantages. Pipe jacking and utility tunneling can be accomplished through almost all types of soils. A high degree of accuracy can be obtained with a minimum amount of skilled labor. The operator, located at the excavation face, can see what is taking place and take immediate corrective action for changing subsurface conditions. The face can be readily inspected personally or by using a video camera. When unforeseen obstacles are encountered, they can be identified and removed. Many options are available for handling the sod conditions.

In utility tunneling, only a small jacking force sufficient to drive only the shield has to be developed. Also, large sections of prefabricated pipe do not have to be handled or stored.

Major limitations. Pipe jacking and utility tunneling are specialized operations. They require a lot of coordination. While these operations can be conducted on a radius, it is recommended that all direction changes be made at the shafts. The pipe and liners used for the operation should be strong enough to resist the jacking forces. Hence, not all types of pipes and liner systems can be used for this operation.

The liner systems are classified as temporary structures. Therefore, a carrier pipe or utility must be inserted through the tunnel liner, and the void between the carrier pipe and the tunnel liner filled to provide adequate support.

Microtunneling

One definition, used in Europe, of *microtunneling* (MT) is that microtunneling is a pipe jacking operation for lines that are less than or equal to 36 in (900 mm) and, therefore, require non-worker-entry tunneling machines (see Fig. 8.15). However, in North America the term *microtunneling* is used for remote-controlled pipe jacking operations, even for larger diameters and worker-entry pipes (see Figs. 8.16 and 8.17). MT machines are laser-guided and remotely controlled, and they have the capability to install pipelines on precise line and grade. The MT method is used to install pipe within a tolerance of 1 in (25.4 mm) with respect to both the horizontal and vertical alignments. This method can be used to install pipes in virtually any type of ground conditions up to 45 m (150 ft) below the ground surface and usually up to 225 m (750 ft) in length from the drive shaft to the reception shaft, without intermediate jacking stations (Iseley and Najafi[16]).

In 1984, North America witnessed the first, difficult but successful, microtunneling trial for a sewer installation project in Florida. Since then, this advanced new technology has been slowly making its way

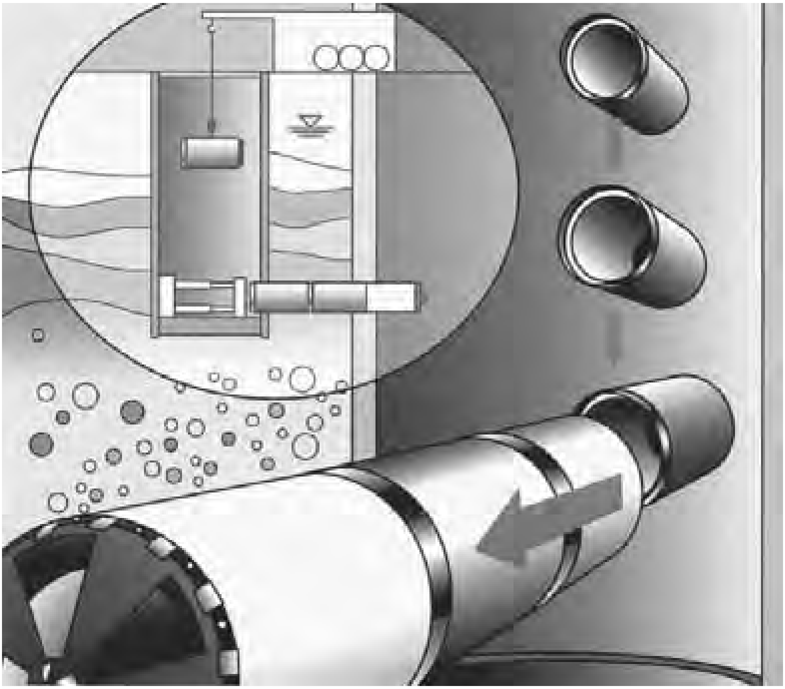

Figure 8.15 Diagram of how pipe is installed by jacking with a boring machine. (*Courtesy of Meyer-Polycrete.*)

across the continent and gradually has received wider and wider acceptance in the United States. In 1995 Akkerman Inc. of Brownsdale, Minnesota, manufactured the first microtunneling system completely designed and built in the United States.

Najafi and Iseley[26] reported a field testing at Louisiana Tech University in Ruston, where PVC sewer pipe was installed with a microtunnel boring machine (MTBM) in a test bed consisting of clay, silt, sand, and clayey-gravel ground conditions. The PVC sewer pipe used in this research study utilizes a joint system developed by Lamson Vylon Pipe in Cleveland, Ohio. The joint provides a smooth outside-inside transition from one pipe section to another, making the pipe suitable for both slip-lining and microtunneling applications. This connection permits the pipe and joint system to mate up with the MTBM.

The microtunneling method is a remotely controlled pipe jacking process which controls the applied pressure and provides continuous

Figure 8.16 Polycrete pipe is being placed in the jacking pit. Note prepackaged tubes for supplying fluid to boring machine and removing slurry. (*Courtesy of Meyer-Polycrete.*)

support at the excavation face. A laser is typically used to establish the desired line and grade. Gravity sanitary and storm sewer lines are the most common type of underground infrastructure system installed by microtunneling. The pipes most often jacked in these nonpressure applications include PC, RCP, GRP, and VCP. All these pipe materials have a substantial microtunnel installation history in sewer applications. However, MT can be used to install other underground utility systems that require a high degree of installation accuracy. In addition, the newest microtunneling pipe is solid-wall PVC, first installed in the United States in 1997. Microtunneling of pressure pipes was limited prior to 1998. Suitable for this application is DI, RCP, reinforced-concrete cylinder pipe, GRP, and steel pipe.

Steel pipe, although rarely used in sewers without proper coating, is routinely installed by jacking and microtunneling for casings and various other structural applications. New methods of joining steel pipe,

Figure 8.17 Polycrete pipe in jacking pit. (*Courtesy of Meyer-Polycrete.*)

such as a new push-on jointing process offered by Permalok Corporation of St. Louis, and new coating and lining technology will likely broaden the application of steel pipe to include both gravity and pressure systems.

Microtunneling pipe should meet the following general requirements:

1. Strength sufficient to withstand both the installation loads and the in-place, long-term service loads
2. Circular shape with a flush outside surface (including at the joints)
3. Dimensional tolerances on length, straightness, roundness, end squareness, and allowable angular deflection
4. Durability for the service exposure (internal and external corrosion resistance)
5. Joints capable of the specified level of watertight performance and transfer of jacking loads between pipes

TABLE 8.2 Product Standards and Available Dimensions

Material type	Standards: Nonpressure	Standards: Pressure	Range of nominal diameters, in	Range of available lengths, ft
DI	AWWA C150/C151 ASTM A 716, A 746	AWWA C150/CI51	4–24	To 19.5
PC	DIN 54815-1 & 2	N/A	6–102	3–10
PVC	ASTM F 789	N/A	12–18	2–10
RCP	ASTM C 76	ASTM C 361 AWWA C300/C302	12–144	7.5–24
RPM	ASTM D 3262	ASTM D 3517 AWWA C950	18–102	4–20
Steel	ASTM A 139 grade B API 2B	AWWA C200 API 2B	3–144+	2–40
VCP	ASTM C 1208 EN 295-7	N/A	4–48	2–10

6. Strength sufficient to withstand both the installation loads and the in-place, long-term service loads.

The following are seven general types of pipe materials that see the greatest use in microtunneling (listed alphabetically; see Table 8.2):

1. Ductile iron (DI)
2. Glassfiber-reinforced polymer mortar (GRP)
3. Polymer concrete (PC)
4. Polyvinyl chloride (PVC)
5. Reinforced concrete
6. Steel
7. Vitrified clay

The selection criteria for the type of pipe to use include many factors, some of which are listed here:

1. Pipe properties and performance capabilities. Except in pressure applications, the most critical material property is normally compressive strength. While the specific value impacts the wall design (thickness required), the load capacity (strength times minimum cross-sectional area) is generally the governing parameter. The compressive strengths, for the pipes listed, range from approximately 3000 to 50,000 lb/ft^2 (21 to 345 MPa), yet all can be used successfully in microtunneling and jacking.

2. Jacking machine (type and diameter), anticipated jacking loads, and drive lengths.
3. Pipeline operating conditions (pressure—operating, test, transient, and vacuum).
4. External loads (soil loads, surface live loads, and water head).
5. Pipe deformation and rebound (during jacking) for plastic/elastic materials.
6. Pipeline service environment (fluid, temperature, and corrosivity).
7. Pipe inside diameter required.
8. Pipe hydraulic characteristics.
9. Pipe availability, reliability, and durability.
10. Life-cycle cost.

Jacking forces

A pipe installed by microtunneling is subject to large transient axial loads, called jacking forces. These forces are applied during the installation process in order to advance the pipe and microtunnel boring machine (MTBM). The nominal factor of safety for jacking loads is the ratio of the pipe's design jacking strength for an evenly distributed load to the actual applied load at the jacks. This nominal factor of safety may be fully utilized or exceeded because of eccentric loading or end-squareness tolerances. The required safety factor against failure due to jacking is not the same for all pipe materials.

Jacking forces are largest on sections of pipe nearest jacking shafts or just in front of intermediate jacking stations. These forces are rarely distributed evenly around the pipes' end circumference because the squareness and mating of joints and the pipe alignment are seldom perfect. Some eccentricity of the axial load will typically occur in the field. The result is force concentrations in portions of the pipe ends (joints). The maximum jacking stress at any point in the pipe is at least as great as the maximum jacking force recorded at the jack (minus any friction losses along the drive between the jacking shaft and the point in question), divided by the effective minimum cross-sectional area of the pipe wall. The pipe and joints must be able to withstand these stresses without cracking, breaking, or suffering other damage.

As the pipes are jacked through the ground behind the MTBM, the pipe and joint exterior surfaces will experience skin friction from the surrounding soils. The pipes and joints must have sufficient durability and toughness to withstand this phenomenon without significant abrasion, loss of joint seal, damage, or failure. Adequate overcut and lubrication can significantly reduce skin friction.

TABLE 8.3 Tolerances of Pipe Used in Microtunneling

Dimensional characteristic	Tolerances: Range of all products	Tolerances: Desirable limit
End squareness/planeness		
Diameter $\leq$48 in	±0.04–0.25	±0.06
Diameter $\geq$54 in	±0.04–0.25	±0.12
Pipe length, in	±0.08–±0.5	±0.25
Straightness (per 10-ft length), in deviation	0.06–0.5	Within 0.12
Outside diameter, % deviation	0.1–2.0	Within 0.5
Exterior roundness, % deviation	0.1–2.0	Within 0.5

A lubricant is applied in the annular space by injection under pressure from the MTBM and/or through ports in the pipe walls. The lubricant, as well as groundwater and earth loads, can impose external pressure on the pipe. The pipes and joints must not leak, be damaged, or fail from applications of these pressures.

Pipes, in diameters large enough to permit personnel entry, are normally equipped with lubrication ports (fittings) in the wall to permit injection of a lubricant (usually bentonite) during jacking, or to permit the placement of grout after jacking to fill any residual annular space.

When the pipe's dimensional tolerances are controlled within certain limits, jacking is easier and installation performance is increased. The range and desirable tolerances for pipe products used in microtunnelling operations are shown in Table 8.3.

Pipe may perform if tolerances are outside of the desirable limits, but jacking loads will be higher, the possible drive distance will be shortened, and the probability of achieving the desired safety factor will be diminished.

Square, plane pipe ends and straight sections improve the jacking load distribution uniformity on the pipe ends and the load transfer. Deviations in straightness, squareness, and planeness increase uneven loading on the pipe ends and also increase load concentrations. These load concentrations, when severe enough, may cause pipe damage or failure. Poor control of the pipe end geometry results in concentrated loads on the pipe ends and increases the required steering of the MTBM. When steering becomes excessive, typically jacking loads tend to increase significantly.

The pipe's length must be controlled to within tolerance. Some of the microtunneling equipment, particularly the spoil removal transfer system, is made in preset, uniform, discrete lengths and is connected through the pipes during the microtunneling operation.

Variations in the outside diameter increase the jacking loads. This can result in decreased safe jacking drive distances and/or increased need for intermediate jacking stations, and ultimately, in severe cases, pipe failures.

Joints

All microtunneling pipe should have these characteristics:

1. Gasket-sealed joints are needed to facilitate rapid assembly.
2. Flush joints are important (joint OD same as OD of pipe barrel) (see Fig. 8.18).
3. Smooth outer surface is needed to reduce jacking force.
4. Pipe performance should not be significantly degraded by scratches and gouges internally and externally. Unique to microtunneling installation are the exterior pipe friction during the jacking drive and the extensive activity inside the pipes throughout the operation. These events may have an effect.
5. Pipes should tolerate exposure to long-term fluids and/or gases conveyed internally and/or externally to groundwater and soil chemicals and, occasionally, to stray electrical currents and hydrocarbon contamination.
6. High compressive strength is needed.

Major advantages

The method is capable of installing pipes to extremely accurate line and grade tolerances. It has the capability of performing in very difficult ground conditions without expensive dewatering systems and/or compressed air. Lines can be installed at a greater depth without a drastic effect on the cost. The depth factor becomes increasingly important as congestion is increased. Safety is enhanced as workers are not required to enter trenches or tunnels. The finished-product (carrier) pipe can be jacked directly without the need of a separate casing pipe.

Major limitations

The capital cost of microtunneling equipment is high. However, the process uses a closed-face microtunnel boring machine, and it can be used in a wide range of soil conditions. Applicable soil types range from highly unstable to very firm materials. The MTBM will

Figure 8.18 Example of flush-type joint.

have difficulty in soils with boulders with sizes greater than 20 or 30 percent of the machine diameter, and there are problems caused by obstructions, such as old humanmade structures. Traditionally, one of the major disadvantages of microtunneling methods has been the inability to utilize flexible or low-strength pipes such as PVC or PE.

Components of microtunnel boring machine

The MTBM is capable of controlling rotation or roll by means of either a bidirectional drive on the cutter head or the use of fins or grippers. The MTBM cutter head is powered by electric or hydraulic motors. The MTBM is articulated to enable remote steering of the system.

A display showing the position of the shield in relation to a target is available to the operator at an operation console together with other information such as face pressure, roll, pitch, steering attitude, and valve positions. The MTBM has a closed-face system capable of supporting the full excavated area at all times. It has the capability of positively measuring the earth pressure at the face and counterbalancing earth pressure.

Automated spoil transportation. The spoil removal system for microtunneling can be a slurry transportation system (Fig. 8.19) or a small encased screwed auger conveyor system (Fig. 8.20). The automated spoil transportation system should match the excavation rate to the rate of spoil removal, thereby maintaining settlement or heave within tolerances specified in the contract documents. The balancing of groundwater pressures is achieved by the use of either a slurry pressure or compressed air for the auger MTBM system. The system is capable of any adjustment required to maintain face stability for the particular soil condition encountered on the project. The system monitors and continuously balances the groundwater pressure to prevent the loss of slurry and/or groundwater.

In a slurry spoil transportation system, the groundwater pressure is managed by the use of the variable-speed slurry pumps, pressure control valves, and a flowmeter. A slurry bypass unit is included in the system to allow the direction of flow to be changed and isolated, as necessary.

A separation process is provided when using the slurry transportation system. The process is designed to provide adequate separation of the spoil from the slurry so that the clean slurry can be returned to the cutting face for reuse. The type of separation process used is dependent upon the size of the tunnel being constructed, the soil type being excavated, and the space available for erecting the plant.

If an auger spoil transportation system is utilized, the groundwater pressures are managed by controlling the volume of spoil removal with respect to the advance rate (earth pressure balance method) and the application of compressed air to counterbalance earth pressure and underground water.

Pipe jacking equipment. The main jacks are mounted in a jacking frame and are located in the drive (starting) shaft. The jacking frame

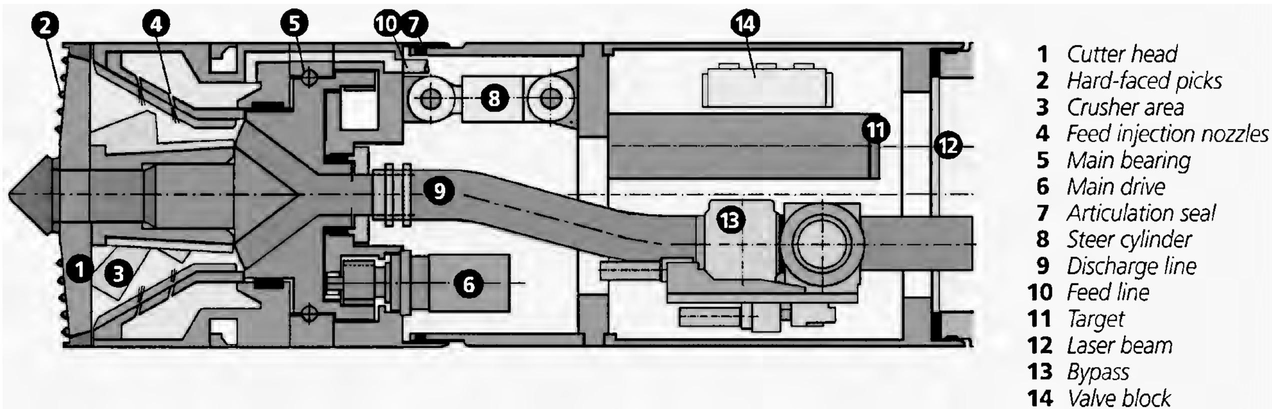

Figure 8.19 Microtunneling machine with slurry material removal. (*Courtesy of Herrenknecht GmbH, Germany.*)

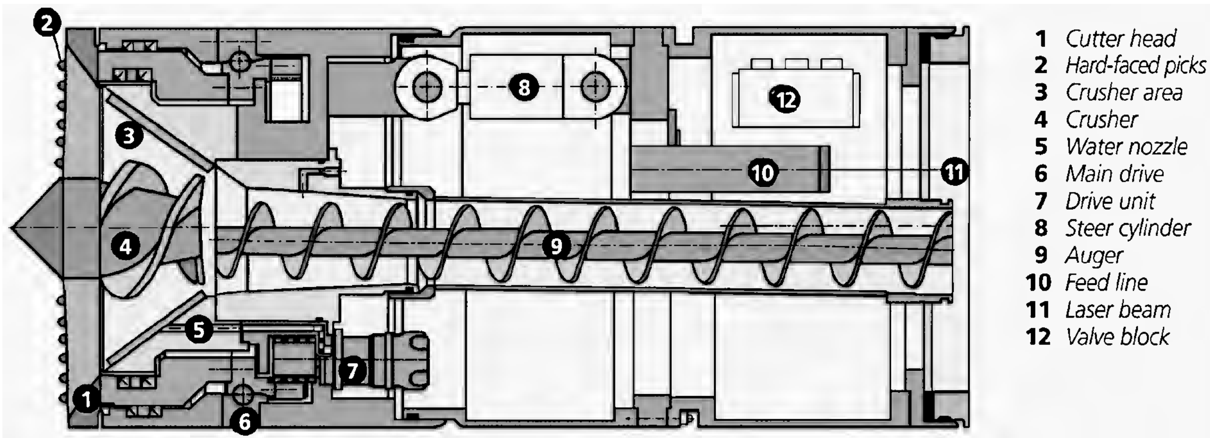

Figure 8.20 Microtunneling machine with auger material removal. (*Courtesy of Herrenknecht GmbH, Germany.*)

Figure 8.21 Completely unnoticed by the constant air traffic, microtunneling takes place directly under the active runway at the Honolulu International Airport. (*Courtesy of Herrenknecht GmbH, Germany.*)

successively pushes the MTBM along with a string of connected pipes toward a receiving shaft (see Fig. 8.21). The jacking capacity of the system must be sufficient to push the MTBM and the string of pipes through the ground. Calculations must be made in advance to determine (1) face excavation forces, (2) frictional forces, and (3) the weight of the MTBM and pipes. The jacking equipment installed must have a capacity greater than the calculated theoretical jacking load, to allow for a safety factor. The hydraulic cylinder extension rate must be synchronized with the excavation rate of the MTBM which is determined by the soil conditions.

Intermediate jacking stations are usually provided for diameters larger than 900 mm (36 in) and when the calculation of the total jacking force needed to complete the installation exceeds 80 percent of the capacity of the main jacks or the designed working compressive loads allowed for the pipe. The jacking system must develop a uniform distribution of jacking forces on the end of the pipe by the use of spreader rings and packing.

If the calculated jacking forces on the pipe are expected to exceed the pipe design strength with a 2.5:1 safety factor, a pipe lubrication system can be utilized. An approved lubricant is injected at the rear of the MTBM and, if necessary, through the pipe walls to lower the friction developed on the surface of the pipe during jacking.

Remote control system. A remote control system is provided to allow for the operation of the system without the need for personnel to enter the microtunnel. The control equipment must integrate the system of excavation and removal of soil and its simultaneous replacement by a pipe. As each pipe section is jacked forward, the control system will synchronize all the operational functions of the system. The system provides complete and adequate ground support at all times.

Active direction control. Line and grade are controlled by a guidance system that relates the actual position of the MTBM to a design reference by a laser beam transmitted from the jacking shaft along the centerline of the pipe to a target mounted in the shield. The MTBM is capable of maintaining grade to within ±25 mm (±1 in) and line to within ±38 mm (±1.5 in). The line and grade tolerances are subject to project and ground conditions.

The active steering information is monitored and transmitted to the operation console. The minimum steering information available to the operator on the control console usually includes the position relative to the reference, role, inclination, attitude, rate of advance, installed length, thrust force, and cutter head torque (see Fig. 8.22).

Jacking pipe. As mentioned previously, pipe used for jacking generally must be round, have a smooth, uniform outer surface, and have watertight joints that also allow for easy connections between pipes. Pipe lengths must be within specified tolerances, and pipe ends must be square and smooth so that jacking loads are evenly distributed around the entire pipe joint and such that point loads will not occur when the pipe is jacked in a reasonably straight alignment. Pipe used for pipe jacking is capable of withstanding all forces that will be imposed by the process of installation, as well as the final in-place loading conditions. The driving end of the pipe and intermediate joints is protected against damage as specified by the manufacturer. The detailed method proposed to cushion and distribute the jacking forces is specified for each particular pipe material.

Any pipe showing signs of failure may be required to be jacked through to the reception shaft and removed. The pipe manufacturer's design jacking loads should not be exceeded during the installation process. Following industry practice, the ultimate axial compressive strength of the pipe must be a minimum of 2.5 times the design jacking loads of the pipe. At present, the following pipe materials specially manufactured for microtunneling operations are available: glassfiber-reinforced polyester mortar (GRP) pipe, reinforced-concrete

Figure 8.22 Parallel-drive microtunneling machines are right on target as they enter the receiving pit in Dubai. (*Courtesy of Herrenknecht GmbH, Germany.*)

pipe (RCP), vitrified clay pipe (VCP), steel pipe, resin concrete pipe, ductile iron pipe, and polyvinyl chloride pipe.

Minidisc cutter development. On large-diameter cutter heads, the disc cutter has been most effective for rock excavations. Friant and Ozdemir[11] reported the development of a high-thrust-capability 5-in-diameter cutter. Since the minidisc is a cantilever design, the shaft can be built as an integral part of the cutter head. A well is burned out in the forward plate of the cutter head, and the cutter shaft is welded into the cutter head structure. In this way, the cutter is both recessed and protected. Rocks or boulders cannot wedge between the cutters and damage the mounts. The tests described in this study are only a few of an extensive testing program. Both the carbide insert and the steel cutters have been extensively tested in various types of rocks with no failures. Only one cutter, a carbide insert type, was tested to destruction. It finally failed at 50,000-lb thrust load. In actual practice, the penetration of the minidisc is so great that no more than an average of 15,000 lb maximum should ever be required. The minidisc has many advantages over conventional tools for drilling, reaming, and microtunneling applications. These advantages include flexible spacing, true rolling, higher performance, single tracking, longer wear, ground condition tolerance, low-cost replacement, and lower initial cost.

Conclusions

1. Renewal of existing buried pipelines is an attractive alternative to traditional dig-up and replace. Liners are a successful means of renewal. Plastic liners stop leaks, resist corrosion and abrasion, and contribute some support to the casing for resisting soil loads. There are several important means of classifying the renewal technologies: design methodology, applicable size range, type of material (indicative of chemical resistance), types and degree of disruption, method of installation, and whether or not bypass pumping is required. It should be noted that pipeline renewal technologies are advancing rapidly and that utility owners, design engineers, and contractors need to stay current with new capabilities and product developments. Design engineers and utility owners should consider technologies and products offered by entrepreneurs who do not have established product histories but whose products may provide new capabilities unlisted in any published book or industry literature.
2. In quick tests, plastic liners in good casings resist external hydrostatic pressure to nearly the yield stress of the plastic. Quick tests are easy to perform and provide a check on the compressive yield strength of the plastic liners.
3. In the long term (50 years), the maximum persistent external pressure on Insitupipe liners is not less than one-half the quick test pressure. Maximum pressure in service is greater than one-half the quick test pressure because pressure on buried pipes is not usually persistent, but fluctuates. Tests should be required to predict long-term performance of all types of liners.

4. Design of liners based on quick tests in good casings should include a safety factor to cover bad casings, high-temperature excursions, dynamic forces, etc. Experience with Insitupipe liners tends toward a safety factor of 2 at the present state of the art. Quick test pressure will increase as the temperature decreases. Quick test pressure will decrease as the casing is deflected out of round, or broken, or corroded, etc.

5. From tests on Insitupipe and Nupipe, the long-term maximum allowable external pressure is greater than the water table head encountered in most buried pipe installations. Most buried pipes have less than 35 ft of soil cover and, consequently, less than the allowable 35 ft of head for Insitupipe at 50 years with a safety factor of 2. See Insitupipe long-term test results.

6. In November 1995, the first microtunneling system completely designed and built in the United States, by Akkerman Inc. of Brownsdale, Minnesota, successfully completed 3250 ft (990 m) of tunneling in very difficult ground conditions. The average jacking advancement rate for the project was 7.5 ft per machine hour. The microtunneling technique and trenchless technology industry, as a whole, have experienced tremendous growth over the past few years. The market will expand more once the design professionals, municipalities, and other decision makers begin to realize that trenchless technology can be cost-competitive with open-trench construction. The selection of a pipe installation method for a particular project will be greatly affected by many factors, such as the size of the borehole, accuracy required, depth of water table, local soil conditions, and availability of funds. Since no one installation method is best suited for all conditions and since some methods provide greater flexibility than others, it is important that the owner, contractor, designer, and regulatory agencies involved with trenchless methods be familiar with the capabilities and limitations of the available methods.

7. Due to the increasingly critical nature of installation or renewal of utility systems in congested areas and aging underground infrastructure, the need for inspection, monitoring, assessment, evaluation, and documentation of underground utility systems has increased. Closed-circuit television (CCTV) and the newly developed sewer scanner and evaluation technology (SSET) provide the means for condition assessment and decision making on the specific type and method of trenchless technology to use. The technology is advancing very rapidly, and project participants must keep pace. There is a need to develop standard guidelines on trenchless construction, to develop standard specifications, and to train the workforce for these advancing technologies.

References

1. American Society of Civil Engineers. 1999. Standard Construction Guidelines for Microtunneling—Draft 1998. *ASCE Standards.* Reston, Va.
2. Atalah, A., and A. Hadala. 1996. Microtunneling Database for the United States and Canada. *No-Dig Engineering* 3(3):18–20, May/June.
3. Bennett, R. D., L. K. Guice, S. Khan, and K. Staheli. 1995. Guidelines for Trenchless Technology. Vicksburg, Miss.: Construction Productivity Advancement Research (CPAR) Program, U.S. Army Corps of Engineers, Waterways Experiment Station.
4. Bennett, D., and P. A. Taylor. 1993. Construction of Microtunneling Test Facility at WES and Preliminary Test Results. In *Proceedings of the Trenchless Technology Advanced Technical Seminar.* Ruston, LA: Trenchless Technology Center.
5. Boyce, G. M., and E. M. Bried. 1994. Estimating the Social Cost Savings of Trenchless Techniques. *No-Dig Engineering* 1(2), December.
6. Cruz, E., Jr. 1993. Microtunneling under Difficult Conditions in New York City. In *Proceedings of Trenchless Technology: An Advanced Technical Seminar.* January. Ruston, LA: Trenchless Technology Center.
7. Das, B. M. 1994. *Principles of Geotechnical Engineering.* Boston: PWS Publishing Company.
8. Doherty, D. J. 1997. Design and Administration of Utility Projects Utilizing Multiple Trenchless Technology Methods. *No-Dig Engineering* 4(3), May/June.
9. Duncan, I. C., Jr. 1992. *Soils and Foundations for Architects and Engineers.* New York: Van Nostrand Reinhold.
10. Essex, R. J. 1997. Geotechnical Baseline Reports for Underground Construction. In *Proceedings of the Construction Congress V,* pp. 219–225. Reston, Va: American Society of Civil Engineers.
11. Friant, J. E., and L. Ozdemir. 1994. Development of the High Thrust Mini-Disc Cutter for Microtunneling Applications. *No-Dig Engineering* 1(1), June.
12. Gilman, B., D. Bennett, and K. Staheli. 1995. Preliminary Results of the 1994 CPAR Microtunneling Testing Project. In *Proceedings of the New Advances in Trenchless Technology.* St. Joseph: Missouri Western State College.
13. Hinze, J. 1997. Risk Assessment in Underground Construction: Uncertainty Is Certain. *No-Dig Engineering,* 4(3), May/June.
14. Iseley, D. T., and M. Najafi, eds. 1995. *Trenchless Pipeline Rehabilitation.* Arlington, VA: The National Utility Contractors Association.
15. Iseley, D. T., and R. Tanwani, eds. 1992. *Trenchless Construction Methods.* Arlington, VA: The National Utility Contractors Association.
16. Iseley, D. T., and M. Najafi. 1998. An Introduction to Microtunneling. Paper presented at Biannual Conference for the Advancement of Trenchless Technology, University of Waterloo, Ontario, Canada.
17. Iseley, D. T., M. Najafi, and R. Tanwani, eds. 1999. *Trenchless Construction Methods and Soil Compatibility Manual,* 3d ed. Arlington, Va.: The National Utility Contractors Association.
18. Iseley, D. T., and S. B. Gokhale. 1997. Synthesis of Highway Practice 242: Trenchless Installations of Conduits Beneath Roadways. Washington: Transportation Research Board, National Research Council.
19. Iseley, D. T. 2000. Recent Advances in Sewer System Assessment Technology. In *Proceedings of Trenchless Technology Symposium at Iowa State University*. Conducted by Midwest Society for Trenchless Technology. October 2–3.
20. Liu, C., and J. B. Evett. 1998. *Soils and Foundations.* Upper Saddle River, N.J.: Prentice-Hall.
21. McCarthy, D. F. 1993. *Essentials of Soil Mechanics and Foundations.* Upper Saddle River, N.J.: Prentice-Hall.
22. Mickie, J. L. 1996. Recognizing Different Soil Classification Systems. *Trenchless Technology,* January.
23. Najafi, M. 1994. *Trenchless Pipeline Rehabilitation: State-of-the-Art Review.* Ruston, La.: Trenchless Technology Center.
24. Najafi, M., and V. K. Varma. 1996. Two Firsts for Iowa—Microtunneling and RCCP. *Trenchless Technology* 5(12):36–37, December.

25. Najafi, M., and D. T. Iseley. 1998. An Overview of Pipeline Renewal Methods. In *1st Trenchless Technology Symposium Proceedings*. Indianapolis: Indiana University and Purdue University.
26. Najafi, M., and D. T. Iseley. 1994. Evaluation of PVC Pipe for Microtunneling. In *Proceedings of the Symposium on Buried Plastic Pipe Technology*. Philadelphia: American Society for Testing and Materials.
27. Schroeder, W. L., and S. E. Dickenson. 1996. *Soils in Construction*. Upper Saddle River, N.J.: Prentice-Hall.
28. Singh, B. K. 1997. Significance of Total Quality Management in Trenchless Technology. *No-Dig Engineering* 4(2), March/April.
29. Terzaghi, K. 1950. Geologic Aspects of Soft Ground Tunneling. In *Applied Sedimentation,* Ed. P. Trask. New York: Wiley.
30. Terzaghi, K., R. B. Peck, and G. Mesri. 1996. *Soil Mechanics in Engineering Practice*. New York: Wiley.
31. Tomforde, Larry. 1996. Pleasant Hill Relief Interceptor (Phase 3): U.S. Manufacturers' First MTBM Project. *No-Dig Engineering* 3(5), September/October.

Index

ABOUT THE AUTHOR

A. P. Moser, Ph.D., is professor and associate dean at Utah State University. He is also founder and director of the Piping Systems Institute, which is a short course that helps train practicing engineers in the design of buried piping systems. He serves on piping committees of the Transportation Research Board and is the past chairman of the committee on culverts and hydraulic structures. He is a consultant to many municipalities, pipe manufacturing companies, and engineering firms. He serves on many bodies that develop codes and specifications for buried piping systems.